



**Michigan  
Technological  
University**

Michigan Technological University  
**Digital Commons @ Michigan Tech**

---

Dissertations, Master's Theses and Master's Reports

---

2020

# EXPLORING SUBSTRATE SPECIFICITY OF FRUCTOSE TRANSPORTERS EN ROUTE TO GLUT SPECIFIC PROBES FOR BIOCHEMICAL AND BIOMEDICAL APPLICATIONS

Vagarshak Vigenovich Begoyan  
*Michigan Technological University, vbegoyan@mtu.edu*


Copyright 2020 Vagarshak Vigenovich Begoyan

---

## Recommended Citation

Begoyan, Vagarshak Vigenovich, "EXPLORING SUBSTRATE SPECIFICITY OF FRUCTOSE TRANSPORTERS EN ROUTE TO GLUT SPECIFIC PROBES FOR BIOCHEMICAL AND BIOMEDICAL APPLICATIONS", Open Access Dissertation, Michigan Technological University, 2020.  
<https://doi.org/10.37099/mtu.dc.etr/1130>

Follow this and additional works at: <https://digitalcommons.mtu.edu/etr>

 Part of the [Biochemistry Commons](#), and the [Organic Chemistry Commons](#)

EXPLORING SUBSTRATE SPECIFICITY OF FRUCTOSE TRANSPORTERS EN  
ROUTE TO GLUT SPECIFIC PROBES FOR BIOCHEMICAL AND BIOMEDICAL  
APPLICATIONS

By

Vagarshak Vigenovich Begoyan

A DISSERTATION

Submitted in partial fulfillment of the requirements for the degree of

DOCTOR OF PHILOSOPHY

In Chemistry

MICHIGAN TECHNOLOGICAL UNIVERSITY

2020

© 2020 Vagarshak Vigenovich Begoyan

This dissertation has been approved in partial fulfillment of the requirements for the Degree of DOCTOR OF PHILOSOPHY in Chemistry.

Department of Chemistry

Dissertation Advisor: *Dr. Marina Tanasova*

Committee Member: *Dr. Shiyue Fang*

Committee Member: *Dr. Tarun Dam*

Committee Member: *Dr. Smitha Rao*

Department Chair: *Dr. Sarah Green*

# Table of Contents

Preface.....	vi
Acknowledgements.....	vii
Abstract.....	x
1 Introduction.....	1
1.1 Sugar Uptake and Metabolism in Health and Disease .....	1
1.2 Sugar Transport Mechanism .....	2
1.3 Structural Requirements for Substrate Recognition by GLUTs.....	6
Glucose 6	
1.4 Carbohydrate Uptake and Metabolic Disorders .....	9
1.5 GLUTs as Biological Targets.....	10
1.5.1 Imaging Agents.....	10
1.5.2 Drug Delivery Agents.....	12
References.....	15
2 ManCous.....	17
2.1 Introduction .....	17
2.2 Development of GLUT5 Specific Probes .....	24
2.3 Exploring the Structural Basis for ManCou-GLUT5 Binding .....	32
2.4 Development of Multicolor GLUT5 Probes .....	35
2.5 Conclusion.....	42
2.6 Materials and Methods .....	43
2.6.1 Synthesis of ManCous 1-14.....	45
References.....	64
3 Metabolism-driven High Throughput Cancer Identification with GLUT5-specific Molecular Probes .....	70
3.1 Introduction .....	70
3.2 Materials and Methods .....	73
3.2.1 Synthesis of ManCou Conjugates.....	74
3.2.2 Tissue culture.....	75
3.2.3 Microplate uptake and inhibition assays.....	76
3.2.4 Immunostaining .....	76
3.2.5 Imaging .....	77

3.3	Results and Discussion.....	78
3.3.1	Design and evaluation of fluorescent fructose mimic as GLUT5-specific probes.....	78
3.3.2	Profiling fructose uptake efficiency and GLUT5 in cells for cancer detection. ....	81
3.4	Conclusion.....	87
	References.....	88
4	Coumarins: Spectroscopic Measurements and First Principles Calculations of C4-substituted 7-Aminocoumarins .....	94
4.1	Introduction .....	94
4.2	Methods.....	95
4.3	Results and Discussion.....	97
4.3.1	Synthesis and spectroscopic properties of C4-substituted coumarins 97	
4.3.2	Theory: Electronic Properties .....	98
4.3.3	Theory: Optical Properties.....	99
4.3.4	Absorption: DFT calculations.....	100
4.3.5	Absorption: TD-DFT calculations .....	100
4.3.6	Fluorescence: TD-DFT calculations .....	104
4.4	Conclusion.....	108
5	Tuning Cross-Coupling Approaches to C3 Modification of 3- Deazaurines .....	110
5.1	Introduction .....	110
5.2	Results and Discussion.....	111
5.3	Conclusions .....	118
5.4	Experimental Section .....	119
	References.....	147
	Appendix A Supporting Info for Chapter 2 .....	152
	Multicolor GLUT5-Permeable Fluorescent Probes for Fructose Transport Analysis 152	
A.1	Supplementary Tables and Figures .....	152
A.2	Materials and Methods .....	160
A.3	Synthesis of ManCous 1-14 .....	162
A.4	Synthesis of Coumarins.....	167
A.5	Cell Imaging .....	172

A.6	Microplate uptake and inhibition assays .....	172
A.7	References .....	173
A.8	Copies of $^1\text{H}$ and $^{13}\text{C}$ NMR spectra.....	174
A.9	HRMS data for ManCou3. ....	223
Appendix B Supporting Info for Chapter 5 .....		230
B.1	General Methods .....	230
B.2	Synthesis and Characterization Data.....	231
B.3	Copies of $^1\text{H}$ and $^{13}\text{C}$ NMR spectra.....	265

## Preface

The initial ideas of all research projects in this dissertation were directed under the supervision of Dr. Marina Tanasova. All of the writing of this dissertation (Chapter 1 – 5) was carried out by Mr. Vagarshak V. Begoyan and revised by Dr. Marina Tanasova.

In Chapter 2, the content was published in *Chemical Communications* **2018**, *54*, 3855-3858.

In Chapter 3, the content was published in *BioSensors* **2018**, *8*, 39. This work was done in collaboration with the lab of Dr. Rao from Biomedical Engineering department at Michigan Technological University.

In Chapter 4, the content was published *Journal of Physical Organic Chemistry* **2018**, *31*, 3852. This work was done in collaboration with the lab of Dr. Pandey from the Physics department at Michigan Technological University.

In Chapter 5, the content was published in *The American Chemical Society Omega* **2017**, *10*, 7002-7015.

## Acknowledgements

I am forever indebted and grateful to my advisor Dr. Marina Tanasova for the patience, teaching, and support she has shown me throughout my journey to obtain my PhD. I cannot express in words how thankful I am for having you on my side all these years, for it would not have been possible without you.

I wish to thank the support I have had from my former and current laboratory members, Joseph Fedie, Dr. Shuai Xia, Avik Ghosh, Andrew Cooper, Jacob Mohar, Alexis Ferrier, and Shleby McGuire. Your presence in the laboratory made it feel very welcoming and somewhere I wanted to be every day.

I want to give a special thank you to Dr. Lukasz Weselinski who beyond being a friend was an additional mentor from who I learned a great deal. I cannot never repay the help you gave me to become a better researcher, but I will always be grateful.

I would like to thank my committee members, Dr. Shiyue Fang, Dr. Tarun Dam, and Dr. Smitha Rao for their time, support, and input regarding my dissertation and defense.

I want to thank the Department of Chemistry for providing financial assistance throughout my PhD. Additional financial sources were also appreciated such as the Portage Health Foundation Graduate Fellowship, Graduate Student Government, and funding from NIH.



To the friends I made along this long journey who were there to share in the pain, joy, and laughter, I thank you. There are too many names to name, but I would be remiss to not mention Dr. Chelsea Nikula, Dr. Christina Welch, and of course Ms. Adikari Mudiyansele Dhananjani Nisansala Eriyagama (DJ).

I want to say thanks and express great gratitude for the assistance from the staff from the Department of Chemistry, especially Charlene Page, Jerry Lutz, Joel Smith, and Dean Seppala. As I said your help was greatly appreciated.

I would like to a special thanks to my family, for who without their love and support I would not have made it to this PhD program let alone made it through. My parents Anna & Vigen have been the shoulders upon which I have leaned heavy on for my whole life, I do not know how I would have made it thus far without them. To that I also wish to thank my brother William who has also been a guiding and protecting hand throughout my life. While not my family by blood, Shahien Shawn Shahsavari is as a brother to me as one can be. He is my closest and dearest friend, I cannot imagine my life without you in it, thank you for everything.

Finally, I wish to thank the one person who contributed most to making me who I am today, my grandmother Svetlana Mirzoyan. My grandmother had sacrificed more for her family in her lifetime than I could in a hundred of my own, this I know without a doubt. As such it deeply saddens me that she alone among these acknowledgments who did not get to see me reach the finish line, for

I lost her to due to cancer in my final year. While you may not have been there to see it, you will always be apart of it. With that I wish to dedicate this dissertation to my grandmother, Svetlana Mirzoyan, for without her none of this would have been possible for me.

## **Abstract**

Carbohydrate Transporters (GLUTs) are responsible for the transportation of sugars into the cell and have been of great interest in research for decades. Alterations or mutations that result in overexpression of GLUTs have been linked to a great number of diseases including, obesity, diabetes, and cancer. Differentiation between transporters has been shown to be incredibly difficult due to the highly conserved nature of the transporter structure, and thus specific targeting of transporters has proven a difficult challenge. Additionally, the GLUTs have been shown to high flexibility in their conformations, so it is difficult to determine what can or cannot pass through the transporter, which has led to many failed attempts at targeting these transporters. So in an attempt to gain a better understanding of one transporter specifically, GLUT 5, a transporter known to be responsible for fructose transporter, new probes were created by conjugating 1-amino-2,5-anhydro-D-mannitol and various fluorescent coumarins. The probes were tested in both normal and cancerous cell lines in order to determine their uptake kinetics and transport specificity. To establish transport specificity the probes were tested in the presence of various competitive and noncompetitive inhibitors. The probe transport was analyzed through various meanings including microplate setting, immunostaining, and confocal microscopy. The combined analysis of the probes has shown to be GLUT5 specific which allows for their use as for biochemical and biomedical imaging an analysis of GLUT5 transporter in cells.

# 1 Introduction

## 1.1 Sugar Uptake and Metabolism in Health and Disease

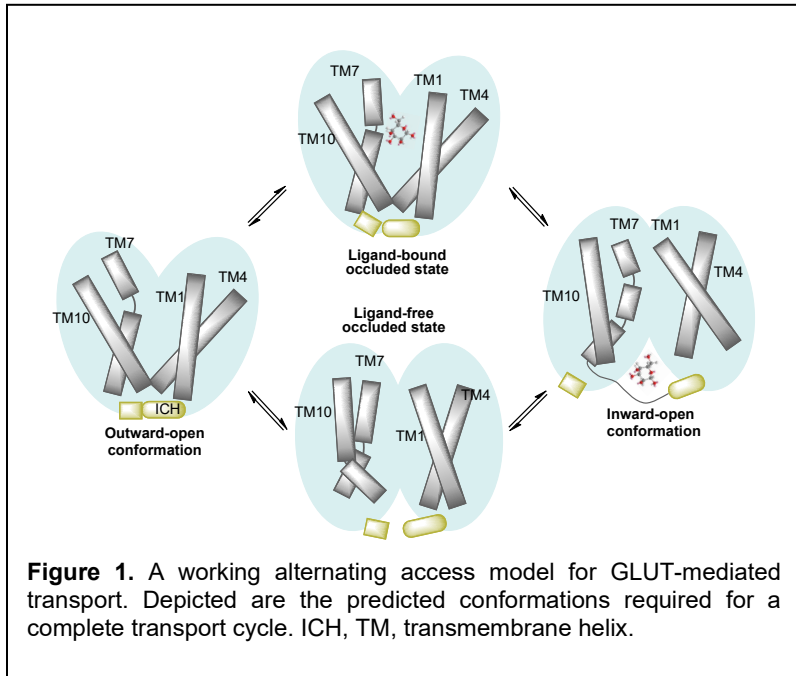
There are currently over one hundred known cancer types that can affect the human body, and they all share the common traits of rapid and uncontrolled proliferation. Sustain a rapid state of proliferation requires an increased uptake of nutrients and cancer cells have developed a way to rapidly uptake larger amounts of the nutrients available in their microenvironment. In normal cells both nutrient uptake and proliferation are controlled by growth factors, whereas cancer cells have overcome this dependence through the alteration of receptor-initiated signaling pathways. Certain pathways are responsible for the activation of nutrient uptake and metabolism. This phenomenon of enhanced nutrient glucose uptake by cancer cells was first described by Otto Warburg, which has established aberrant metabolism as a cancer characteristic for over 70 years. The increased nutrient uptake is then consumed in cancer cells with a system which shifts the metabolism from the standard and efficient oxidative phosphorylation to the much less effective aerobic glycolysis, even while there is sufficient oxygen present. This shift is attributed to defects in the mitochondria leading to impaired respiration in cancers, creating a need for an alternative pathway for energy generation. Advances in the understanding of cancer metabolism has shown that cancers can actively utilize both parts, glycolysis in the cytosol and oxidative phosphorylation in the mitochondria, simultaneously. The notable increase in the nutrient uptake in cancer vs normal cells provided the foundation for targeting cellular metabolism to diagnose, treat, and monitor cancer. For example, the enhanced

glucose uptake in cancers provided a base for targeting cancers with radiolabeled glucose and the development of tumor positron emission topography (PET) imaging with  $^{18}\text{F}$ -fluro-2-deoxy-D-glucose (FDG).<sup>1</sup> Additionally, enhanced nutrient uptake has been used to direct chemotherapeutic agents to cancers through glycoconjugatation.<sup>2</sup> Taking advantage of the increased nutrient uptake in cancers will be further discussed in later sections.

## **1.2 Sugar Transport Mechanism**

Sugars transport across the eukaryotic cellular membrane is mediated by two families of glucose transporters, sodium-dependent glucose transporters (SGLTS) and facilitative glucose transporters (GLUTS). Sugar transport by GLUTs is facilitated by a concentration gradient while SGLTs use sodium ion co-transportation to deliver glucose against a gradient into the cell. The mechanistic difference in transport is vital due to the one of the primary differences in purpose between GLUTs and SGLTS, being that SGLTs are solely responsible for glucose reabsorption through the kidneys. Once reabsorbed from the bloodstream through SGLTs the sugars are then redistributed through the body via GLUTs. As SGLTs were not the focus of the work discussed in this document, there will be no in-depth analysis of those transporters.

GLUTs are... The structures of GLUTs are highly conserved and usually consist of twelve transmembrane helices (TMs) split into two clusters of six. Additionally, they usually have from four to five intercellular helices



(ICs) that are responsible for stabilization. The transport of sugar substrates through a GLUT is concentration gradient dependent, i.e. substrates are moved from areas of high concentration, usually outside the cell in the blood stream, to areas of low concentration, commonly the inside of the cell. The transport process starts with the GLUT protein being in the outward open conformation, where a substrate is capable of binding to the active site. With the binding of the substrate to the active site, interactions between the TM's trigger a conformational change within the protein that results in the substrate translocation inside the cell. The transport of the sugar through the GLUT can proceed in either directions (uniporter), and some GLUTs are also considered to support simultaneous transport of a substrate in both directions (antiporter). However, in the condition of active sugar phosphorylation, the concentration of sugar inside the cell remains low, resulting in minimal sugar excretion. This is due to the fact that GLUTs transport sugars but not their

phosphorylated counterparts. Thus, overall, transport of a sugar through a GLUTs can be considered constant as long as the phosphorylation is being maintained.

**Table 1.** GLUT transporter expression in healthy tissues and substrate preferences

Transporter and Class	Expression in Normal Cells	Substrate
I: GLUT1	erythrocytes	glucose, galactose
GLUT2	renal tubular, intestinal epithelial, liver and pancreatic $\beta$ cells	glucose, galactose, fructose, glucosamine
GLUT3	neurons and placenta	glucose, galactose, mannose
GLUT4	adipose tissue and striated muscle	glucose, glucosamine, galactose, mannose, xylose
GLUT14	testis	glucose, galactose
II: GLUT5	intestinal epithelial, erythrocytes, sperm	fructose
GLUT7	apical membrane in small and large intestine	glucose, fructose
GLUT9	liver, kidney and intestine	glucose, fructose
GLUT11	muscle, heart, fat, placenta, kidney, and pancreas	glucose, fructose
III: GLUT 6	renal tubular, intestinal epithelial, liver and pancreatic $\beta$ cells	glucose
GLUT 8	testis, brain, fat, liver, and spleen	glucose, fructose
GLUT 10	heart and lung	glucose, galactose
GLUT 12	insulin-sensitive tissues	glucose, galactose, fructose
GLUT 13	brain	myoinositol

There are currently fourteen known variants of GLUTs which are grouped into three classes based upon on their structural, substrate, and genetic sequence similarities (Table 1). Class I consist of GLUTs 1-4 and 14 and are primarily responsible for glucose and galactose transport. Class II includes GLUTs 5, 7, 9, and 11, which are primarily fructose transporters. Class III includes GLUTs 6, 8, 10, 12, and 13, which are all unusual members of the facilitative transport family. The binding of glucose is highly conserved in the Class I transporters, due in part to the fact that GLUTs 2-4 all have high sequence similarity to GLUT 1, with them being 83%, 93%, and 85% respectively for GLUTs 2-4. The minor

alterations in residue result in the passage of other substrates, in addition to glucose. The crystal structure of the human GLUT1, hGLUT1, has shown that helices 1 and 7 as the major constituents of the extracellular gate in the inward open conformation. In this state TM1 and TM7 are in contact with one and another on the extracellular side, representing the major constituents of the extracellular gate. The current proposed interaction that facilitate conformational change involve the interactions between the C and N domains, and once the substrate is released because of the concentration gradient, the interactions between the C and N residues equilibrate and following deprotonation GLUT 1 returns to its original extracellular state. GLUT 1 is the most studied and targeted of the GLUT transporters as of writing this dissertation and as previously mentioned is currently the key target in the use of PET imaging. GLUTs 2, 3, and 4 all share many of the same key hydrogen bonding interactions when transporting glucose as GLUTs 2 and 3 both require the presence of the C1, C3, and C4 hydroxyls to have effective glucose transport. As was shown in GLUT1, C2 substitution is tolerated in GLUTs 2-4 but has negative impact on uptake, with GLUT2 being the most impacted by this substitution. Unlike GLUT1, GLUTs 2-4, are capable of transporting other sugars in addition to glucose, such as D-mannose. Some other examples of these variances are that GLUT3 and GLUT4 are both capable transporting 3-flouro-D-glucose, GLUT 2 shows marginal transport activity, while not transport is observed for GLUT1. These variations in substrate preferences highlight the differences within the binding pocket, sensitive towards the alterations in hydrophobicity, size, and hydrogen bonding ability of the substrate.



## 1.3 Structural Requirements for Substrate Recognition by GLUTs

### Glucose

At an early stage of GLUT research, it was determined that GLUT1 favored D-glucose over L-glucose. This observation identified the first bias in substrate selection by GLUTs. Two researchers, Kahlenberg and Barnett, independently showed that the GLUT preference towards glucose relied primarily on hydrogen bonding with the C1, C3, and C4 hydroxyl groups, and a hydrophobic interaction with C6. Later, Rees and co-workers established the importance of the oxygen atom on C5 for glucose uptake. The binding of glucose to GLUTs 1 and 4 was found to be sensitive to alterations in stereochemistry and the substitution-induced steric encumbrance at these critical sites. From the various sugars tested as inhibitors of  $^3\text{H}$ -D-glucose uptake, only 2-deoxy-D-glucose and 6-deoxy-D-glucose proved to be recognized by the protein. These findings suggested the minimal role of C2 and C6 hydroxyl groups in the glucose-transporter interaction. It was also found that the C2 site of glucose was suitable for substitution or epimerization, which was proven by the uptake of 2-chloro-2-deoxy-D-glucose, 2,2-dichloro-2-deoxy-D-glucose, and D-mannose. However the substitution or stereochemical alterations at the C3 position of D-glucose led to a significant decrease in the uptake (D-allose, 3-O-alkyl-, 3-chloro-D-glucose, and 3-deoxy-D-glucose), suggesting a low tolerance from the transporter towards any change in steric at the C3 position or loss of the C3 hydroxyl group as a possible hydrogen bond acceptor (3-deoxy-D-glucose vs. 3-fluoro-D-glucose). Compared to the C3-OH modifications, the chemical changes to the C4-OH group were far better tolerated (D-galactose vs D-glucose), implying that the C3-OH group was vital for binding.

<b>Table 1. Effect of hydroxy groups on glucose affinity towards Gluts 1–4.</b> <sup>[7a–d,12–14]</sup>				
Substrate	Transport rate [%]			
	Glut 1 <sup>[a]</sup>	Glut 2 <sup>[b]</sup>	Glut 3 <sup>[b]</sup>	Glut 4 <sup>[b]</sup>
<b>Controls</b>				
D-glucose	1	20 ± 6	10 ± 2	12 ± 3
L-glucose	95	100	100	100
<b>C1 analogues</b>				
1-deoxy-D-glucose	82	109 ± 10	104 ± 12	79 ± 12
<b>C2 analogues</b>				
2-deoxy-D-glucose	1	20 ± 2	12 ± 2	14 ± 9
D-mannose	33	29 ± 3	14 ± 2	13 ± 7
2-chloro-D-glucose	n.d.	76 ± 5	42 ± 3	40 ± 7
<b>C3 analogues</b>				
3-O-methyl-D-glucose	30	73 ± 6	17 ± 3	41 ± 7
3-O-propyl-D-glucose	n.d.	100 ± 12	80 ± 7	72 ± 8
3-deoxy-D-glucose	67	103 ± 12	85 ± 7	106 ± 12
3-bromo-D-glucose	n.d.	95 ± 10	75 ± 4	79 ± 12
3-fluoro-D-glucose		85 ± 5	14 ± 2	40 ± 6
D-allose	75	59 ± 6	96 ± 7	96 ± 7
<b>C4 analogues</b>				
D-galactose	48	110 ± 12	57 ± 5	96 ± 12
<b>C5/C6 analogues</b>				
6-deoxy-D-glucose	8	33 ± 9	46 ± 7	44 ± 7
D-xylose	n.d.	106 ± 9	78 ± 6	75 ± 6
L-arabinose	n.d.	138 ± 22	63 ± 7	<u>90 ± 8</u>
6-O-methyl-D-galactose	95	57 ± 10	109 ± 11	59 ± 6
6-fluoro-D-galactose	n.d.	50 ± 12	30 ± 9	48 ± 12

Transport rates determined relative to the uptake of [a] D-[<sup>3</sup>H]glucose, [b] [2,6-<sup>3</sup>H]-2-deoxyglucose, n.d., not determined.

Glucose recognition by the transporter has also been shown to depend strongly on the C1-OH group as an H-acceptor and on the hydrophobic interactions with the protein through C6. The loss of uptake observed from methylation (methyl  $\alpha$ -D-glucose and methyl  $\beta$ -D-glucose), removal (1-deoxy-D-glucose) or substitution (1-thio- $\beta$ -D-glucose) of the C1-OH group but not for the 1-fluoro-D-glucose analog suggest the vital importance

of the C1 site as a hydrogen bond acceptor. Additionally, the transporter was found to favor the beta-anomer of glucose, but a recent crystal structure report shows the transporter being capable of accommodating both anomers, although the relative affinities for these substrates are currently unclear. Likewise, increasing the bulk around the C6 position through methylation (6-O-methyl-D-galactose) negatively impacted the uptake. In contrast, the uptake of 6-deoxy-D-glucose was comparable with that of D-glucose, indicating that C6 site does not serve as a hydrogen-bonding site. Colville discovered that other class I transporters - Gluts 2 and 3 - employ a model of glucose recognition similar to that of Glut 1: that is, they require the presence of the C1-, C3-, and C4-OH groups. The presence of the C2-OH group was not needed for high affinity, but substitution at C2 diminished the uptake, with the Glut 2 transporter being least tolerant to such substitution. Gluts 2–4 also appear to be less substrate-specific than Glut 1. Thus, Gluts 2–4 bind d-mannose (C2-epimer of d-glucose) as efficiently as they do d-glucose or 2-deoxy-d-glucose. Additionally, there is an apparent difference in substrate recognition between Glut 2 and Gluts 1, 3, and 4. The loss of affinity observed with 3-deoxy-d-glucose can be restored by 3-fluoro-d-glucose for Gluts 1, 3, and 4, but not for Glut 2, thus suggesting that for Glut 2 the C3-OH group plays the role of an H-donor. Another notable difference amongst Gluts 1–4 is the affinity of 6-O-methyl-d-galactose towards Gluts 2 and 4, but not Glut 3, whereas all three transporters similarly accept the 6-fluoro analogue. This observation suggested more extended hydrophobic interactions favorable for binding within Gluts 2 and 4, and putatively low tolerance for steric interactions for Glut 3. The structure–affinity relationship data provided the basis for a simplified schematic of glucose–transporter interaction. It was proposed that the sugar enters the binding site of the

membrane transporter through initial coordination of the ring oxygen atom and the anomeric hydroxy group. For all isoforms, some degree of H-bonding was suggested for the C1, C3, and C4 hydroxy groups, with the nature of H-bonding at C4 changing from H-acceptor in Glut 1 to H-donor in Glut 2. For Glut 3, H-bonding at the C4-position was proposed to play a relatively minor role, due to the efficient uptake of both glucose and galactose. It was also suggested that binding was stabilized by hydrophobic interaction with C6 and independent of the C6-OH group.

#### **1.4 Carbohydrate Uptake and Metabolic Disorders**

Increased carbohydrate consumption is shown to be implicated in diseases, such as obesity, type II diabetes, fatty liver disease, gout, sclerosis, and Alzheimer's. It has also been shown that either high glucose or fructose consumption is linked with cancer growth and metastasis. Changes in the GLUT expression and composition were observed upon the increased nutritional needs for the uncontrolled growth and division of cancer cells. Examples of this phenomena include changes in the expression of the ubiquitous glucose transporter GLUT1, with it found to be either overexpressed or downregulated in different cancers. Alterations have been noted not only in the levels of GLUT expression but also in the GLUT content. Thus, certain epithelial cancer types gain expression of GLUT13, whereas it is normally found being expressed in the brain tissue. The overexpression of GLUTs 5 and 12 are established for the early and late stage breast carcinoma cell lines, MCF-7 and MDA-MB-21 respectively. It has also been found that GLUT5 expression is active in leukemia, pancreatic, ovarian, and lung cancers. It is noteworthy that despite a substantial bulk of literature on GLUTs, the impact of sugars and sugar consumption on

cancer development is still not well understood, and that some data are contradicting. For example, a high fat and sugar diet have been shown to contribute to the reoccurrence of cancer in stage III colon cancer patients. Whereas high sugar consumption has not shown to have any effect at all on the risk of colon or any other type of cancer or showed increased risk in only a narrow portion of the population. Alternatively, high sugar consumption has been definitively linked with obesity and there is a strong connection between this metabolic disorder and the formation cancer. Also increased circulation of insulin and insulin-like growth factors levels have also been linked with cancer progression, suggesting that both obesity and insulin resistance can promote cancer through the activation of signaling pathways that drive cell growth. Although some links have been established, mapping the road to all sugar-disease connections is long from being complete.

## **1.5 GLUTs as Biological Targets**

### **1.5.1 Imaging Agents**

The discrimination between cancer and normal cells on their differences in sugar uptake has been shown to be a practical approach to induce selectivity in imaging application. As previously mentioned, position emission tomography (PET) has been very successful in taking advantage of this difference in activity in GLUT expression and sugar transport in diseased cells, mainly cancer, for beneficial use. PET imaging uses the  $^{18}\text{F}$ -labeled analog of 2-flouro-2-deoxy-D-glucose (FDG) as a reporter of the enhanced glucose uptake seen in cancer cells and as a predictor of tumorigenesis and tumor aggressiveness.<sup>1</sup>  $2\text{-}^{18}\text{F}\text{-FDG}$  is readily internalized by the cell through multiple GLUTs and then phosphorylated. The phosphorylation of FDG promotes the continuous gradient uptake through the transporter

which then reflects the metabolism coupled glucose uptake in cells, with those with higher metabolic activity having a higher accumulation. It should be mentioned however that this technique is not without faults, as there has been shown for various sites to have a high accumulation of the probe, such as inflamed tissues, that are not related to having any cancerous activity, leading to false positives.<sup>3-4</sup> As FDG uptake is dependent on two metabolism coupled factors, sugar uptake and phosphorylation, it has been considered that direct evaluation of sugar uptake (independent of phosphorylation) could provide an alternate approach for cancer imaging. Among the uptake reporters that have been shown not to be phosphorylated, 6-deoxy-6-iodo-D-glucose allowed for the accurate measurement of glucose transport rates in insulin-responsive tissues.<sup>5-6</sup> However, the rapid efflux from the cell limited the application of this tracer. Rapid excretion was also observed for 6-deoxy-6-flouro-D-glucose, although the probe did provide an important tool for reflecting the glucose uptake not only insulin responsive tissues, but also those that are non-responsive. Overall, there is still room for exploring new GLUT-targeting probes that could carry a radiotracer into the cells and remain in the cell by phosphorylation-unrelated mechanisms.

Development of fluorescent GLUT-targeting probes provided means to recognize cancer cells in vitro. While the stringency of GLUTs in substrate selection poses significant challenges in transporting modified sugars, several sugar fluorophore combinations were shown to produce effective GLUT-targeting probes. Among those, the green-fluorescent 7-Nitrobenzofurazan (NBD) has been shown to pass efficiently through GLUTs in the form of D-glucose (NBDG). Targeting of fructose GLUTs has also gathered attention due to the

recent understanding of direct links between high fructose uptake and cancer. Respectively, D-fructose (NBDF) and 2,5-anhydro-D-mannitol (NBDM) conjugates of NBD were developed for targeting fructose transport.<sup>7-8</sup> Other sugar analogs have also been tested as carriers of NBD, with alterations in stereochemistry shifting the uptake between fructose and glucose transporters.<sup>9</sup> Recent developments also highlight the applicability of coumarins and resorufin as fluorophores for GLUT probes. Glucose conjugates of 7-aminocoumarins (CDGs, Fig. 2) are taken up by the cells through glucose-dependent transport.<sup>10</sup> However, a significant drop in the uptake with increase in fluorophore size poses a new aspect to consider for designing GLUT-specific reporters.

### **1.5.2 Drug Delivery Agents**

Alterations in the expression levels of various GLUTs in cancer has highlighted sugar transporters for potential targeted drug delivery. Consequently, glycoconjugation has emerged as a strategy to direct chemotherapeutic agents to cancerous cells for achieving enhanced cancer specificity and improved drug safety. With higher glucose uptake in cancers becoming clearly evident, glucose transporters became the target of various sugar drug conjugates, particularly for targeting glucose transporter GLUT1. One of the pioneer compounds was glufosfamide, a glucose conjugate of the DNA alkylating agent ifosamide mustard. Following glufosfamide, conjugation to different sugars has been used to improve the cytotoxic properties of chlorambucil. The studies included the development of the 63-member library of compounds (conjugates of glucose, mannose, galactose, xylose and other), among which D-threose conjugate showed the most significant improvement in potency (8-fold more potent in reducing cell growth than chlorambucil). However,

whether the improved cytotoxicity was a result of alterations in mechanism of action or was induced by enhanced cellular accumulation of the probe, or whether glycoconjugation resulted in GLUT-mediated uptake was not addressed. Since then, the glycoconjugation strategy has been widely applied to various anticancer drugs and imaging agents (chlorambucil, azinomycin, clioquinol, adriamycin, warfarin, cyclophosphamide, platinum and palladium-based chemotherapy drugs, and nano materials).<sup>2</sup> The C2-glucose conjugates of platinum and palladium complexes of glucose were tested in cisplatin-sensitive and cisplatin resistant gastric cancer cell lines and in vivo models.<sup>11</sup> Tested in the gastric cancer cell lines, both Pd and Pt conjugates were found to induced DNA double strand breaks similarly to cisplatin but have lesser cytotoxicity. The preference of GLUTs towards C2 glucose-platinum conjugation was established for oxaliplatin-glucose conjugates. In addition, conjugation of glucose to oxaliplatin through C6 was also observed to be tolerated by the GLUT1. The corresponding conjugates varied in the length of the linker between oxaliplatin and glucose showed cytotoxicity comparable to that of an aglycone, with ovarian cancer cells showing the highest sensitivity. All compounds were found to platinate DNA leading to cell apoptosis, with the number of platinated residues relatively similar to oxaliplatin. Glycoconjugation has also been explored with inhibitors of lactate dehydrogenase (LHD) in an attempt to improve the anticancer efficiency of photosensitizers, as well as to deliver drugs to the brain through GLUT1 expressing brain barriers. In particular among the latter, the conjugation of glucose to ibuprofen resulted in a three-fold higher concentrating of the drug in the brain that maintained stability for 4h. All of these findings highlight the possibility of using pro-drugs as a delivery strategy to the brain. While multiple efforts have been made to target GLUTs in biomedical research,



the majority of studies (or conjugates made) failed to provide a significant levels of discrimination between normal and metabolically-compromised cells. These outcomes further underlined the sensitivity of GLUTs towards their substrates

## References

1. Almuhaideb, A.; Papathanasiou, N.; Bomanji, J., 18F-FDG PET/CT imaging in oncology. *Ann. Saudi Med.* **2011**, *31* (1), 3-13.
2. Tanasova, M.; Begoyan, V. V.; Weselinski, L. J., Targeting Sugar Uptake and Metabolism for Cancer Identification and Therapy: An Overview. *Curr. Top. Med. Chem.* **2018**, *18* (6), 467-483.
3. Carter, K. R.; Kotlyarov, E., Common causes of false positive F(18)FDG PET/CT scans in oncology. *Braz. Arch. Biol. Techn.* **2007**, *50*, 29-35.
4. Miljic, D.; Manojlovic-Gacic, E.; Skender-Gazibara, M.; Milojevic, T.; Bogosavljevic, V.; Kozarevic, N.; Petrovic, N.; Stojanovic, M.; Pekic, S.; Doknic, M.; Petakov, M.; Popovic, V., All that glitters on PET is not cancer! F-18-deoxy-glucose avidity versus tumor biology: pituitary incidentaloma in a survivor of two previous unrelated malignancies. *Endokrynol. Pol.* **2017**, *68* (3), 352-357.
5. Grauzam, S.; Moro, C.; Toufektsian, M.; Jouan, M.; Vollaire, J.; de Leiris, J.; Ghezzi, C.; Boucher, F., Early transient cardiac insulin resistance after myocardial infarction in rats: study by nuclear imaging with 125i-6-deoxy-6-iodo-d-glucose (6dig). *Fund. Clin. Pharmacol.* **2011**, *25*, 71-71.
6. Henry, C.; Koumanov, F.; Ghezzi, C.; Morin, C.; Mathieu, J. P.; Vidal, M.; deLeiris, J.; Comet, M.; Fagret, D., [I-123]-6-deoxy-6-iodo-D-glucose (6DIG): A potential tracer of glucose transport. *Nucl. Med. Biol.* **1997**, *24* (6), 527-534.

7. Levi, J.; Cheng, Z.; Gheysens, O.; Patel, M.; Chan, C. T.; Wang, Y. B.; Namavari, M.; Gambhir, S. S., Fluorescent fructose derivatives for imaging breast cancer cells. *Bioconjugate Chem.* **2007**, *18* (3), 628-634.
8. Tanasova, M.; Plutschack, M.; Muroski, M. E.; Sturla, S. J.; Strouse, G. F.; McQuade, D. T., Fluorescent THF-Based Fructose Analogue Exhibits Fructose-Dependent Uptake. *ChemBioChem* **2013**, *14* (10), 1263-1270.
9. Kumar Kondapi, V. P.; Soueidan, O. M.; Cheeseman, C. I.; West, F. G., Tunable GLUT-Hexose Binding and Transport via Modulation of Hexose C-3 Hydrogen-Bonding Capabilities. *Chem. Eur. J.* **2017**, *23* (33), 8073-8081.
10. Otsuka, Y.; Sasaki, A.; Teshima, T.; Yamada, K.; Yamamoto, T., Syntheses of D-Glucose Derivatives Emitting Blue Fluorescence through Pd-Catalyzed C-N Coupling. *Org. Lett.* **2016**, *18* (6), 1338-41.
11. Tanaka, M.; Kataoka, H.; Yano, S.; Ohi, H.; Kawamoto, K.; Shibahara, T.; Mizoshita, T.; Mori, Y.; Tanida, S.; Kamiya, T.; Joh, T., Anti-cancer effects of newly developed chemotherapeutic agent, glycoconjugated palladium (II) complex, against cisplatin-resistant gastric cancer cells. *BMC Cancer* **2013**, *13*, 237-245.

## 2 ManCous

### 2.1 Introduction

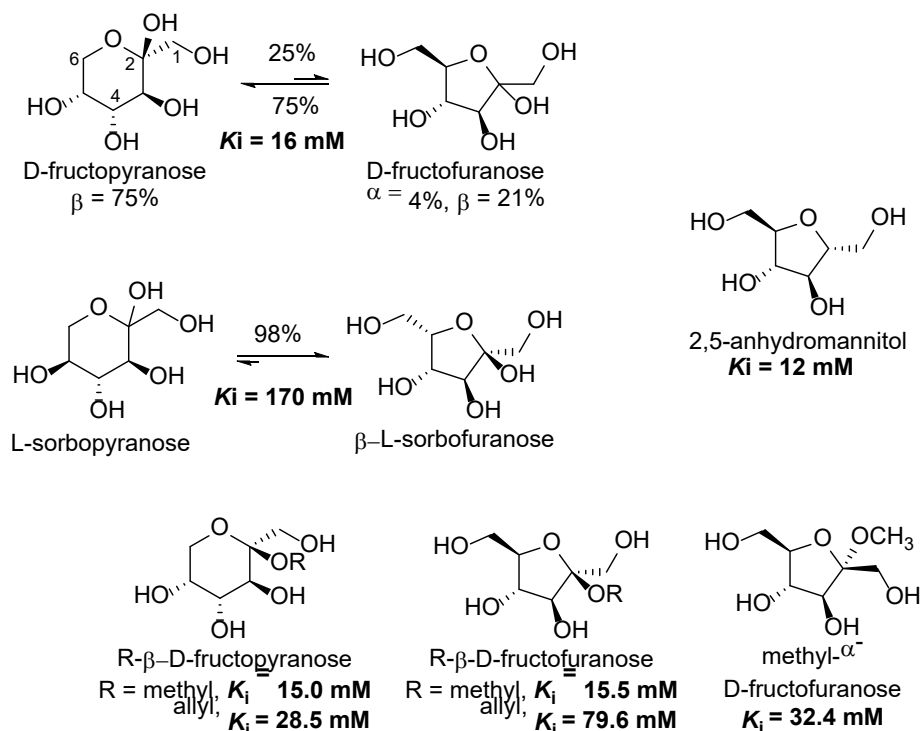
Facilitative glucose transporters (GLUTs) perform gradient dependent influx and efflux of carbohydrates to sustain the nutritional needs for cell proliferation. Metabolic deregulations in cells induce alterations in the cellular GLUT composition, resulting in overexpression of intrinsic or expression of extrinsic GLUTs. Among GLUTs, glucose-transporting GLUT1 attracted attention for half a century as a target for cancer therapy and diagnostics, and other GLUTs started to gather much interest recently because of their direct relationship with cancer.<sup>1</sup> Particular attention is drawn by fructose-transporting GLUTs and the fructose-specific transporter GLUT5 due to the links between fructose uptake and cancer development, progression, and metastasis.<sup>2</sup> Consequently, the fructose transport-targeting probes are of interest as biochemical and biomedical tools.

Analyses of GLUT expression and activity as means to assess the metabolic state of the cell have been approached through the development of GLUT-targeting radiolabeled sugar analogs, as well as affinity labels.<sup>3</sup> Among radiolabeled analogs, halogenated sugar derivatives were accessed to evaluate glucose and fructose transport efficiency in conjunction with and independently of phosphorylation. The development of fluorescently labeled GLUT probes has been approached to alleviate the practical limitations associated with radiolabeling and to obtain high affinity probes. Among fluorescent GLUT probes, 7-nitrobenzofurazan (NBD) has been utilized for GLUT transport analysis in the form of sugar conjugates. Among those, fructose and 2,5-anhydro-D-mannitol were accessed as probes to target fructose transport providing a precedent for distinguishing GLUT5-

expressing vs. GLUT5-deficient cell lines. Recently, coumarin and resorufin conjugates of glucose have been evaluated as probes for glucose GLUTs. The probes showed a limited passage through GLUTs, and accumulated in cells through non-GLUT-mediated transport. The challenge in passing a non-natural moiety through GLUTs is also reflected by the loss of GLUT-mediated uptake for glucose–drug conjugates, with the position of functionalization and possible change in transporter–probe interaction due to alterations in H-bonding being key players. Considering the need in GLUT-specific molecular tools, we have explored the feasibility to develop such tools using GLUT5 as model transporter. The choice of GLUT5 has been prompted by the unique specificity of this protein to one substrate (majority of other GLUTs are promiscuous). A direct link between GLUT5 and various diseases provided additional reasoning to targeting this transporter.

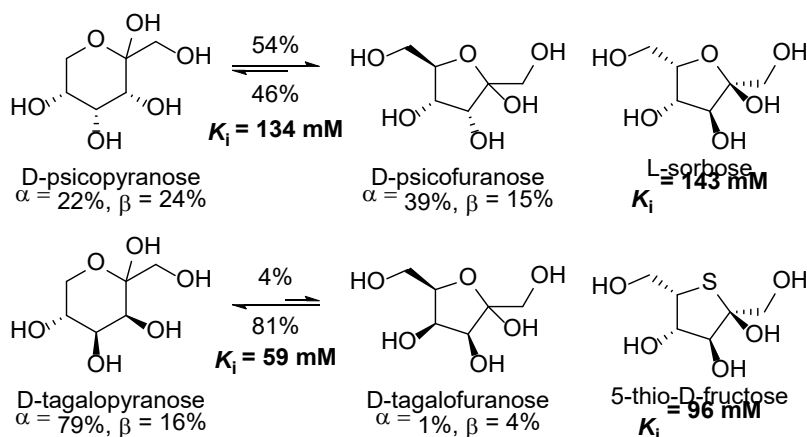
It should be noted that structural requirements for fructose transport are not thoroughly understood, primarily due to the existence of the natural fructose as a mixture of structural isomers – furanose and pyranose. In early studies by Colville et al.,<sup>4,5</sup> selectivity of GLUT2 towards the furanose form of fructose has been proposed based on the ability of L-sorbose (C5-epimer of fructofuranose) and 2,5-anhydromannitol (C2-deoxy analog of fructofuranose) to inhibit 2-deoxy-D-glucose uptake (Scheme 1).<sup>5</sup> Inhibition constant for 2,5-anhydromannitol ( $K_i = 26$  mM) was relatively similar to that of 2-deoxyglucose ( $K_i = 26$  mM) and 6-8 times lower than  $K_i$  for L-sorbose or D-fructose. However, considering that in aqueous solutions D-fructose exists predominantly in pyranose form and that GLUT2 takes up other pyranoses, the plausibility of fructose uptake in both forms is to be verified.

Series of studies by Holman and coworkers<sup>6-9</sup> have focused on designing carbohydrate probes to reveal structural features responsible for fructose-specificity of GLUT5 in view of accessing GLUT5-specific affinity probes. Studies were based on evaluating competitive inhibition of fructose uptake in the presence of fructose analogs and derivatives and, in analogy to other GLUTs, revealed the dependence of uptake via GLUT5 on the presence and the stereochemistry of hydroxyls.



**Scheme 2.1.** Conformer ratios and inhibitory constants for 2-deoxyglucose uptake via GLUT2 for D-fructose, D-sorbose and 2,5-anhydromannitol. Comparison of interaction of C2-derivatives of furanose and pyranose ring forms of fructose with GLUT5. Inhibitory constants were derived by monitoring inhibitory effect of analogs on the uptake of [<sup>14</sup>C]-D-fructose into CHO cells expressing GLUT5.

The uptake of fructose via GLUT5 was found to favor  $\beta$ -anomers over  $\alpha$ -anomer, as was shown by testing C2-methylated fructopyranose and fructofuranose analogs (Scheme 1).<sup>6</sup> Small changes in the sterics around C2 induced by methyl group did not impact the uptake. In contrast, increase in the size of C2-substitution, tested with allyl derivatives, significantly diminished the affinity of a furanose analog, while had a minor impact on the affinity of the pyranose analog. Further testing of 2,5-anhydro-D-mannitol revealed that anomeric hydroxyl does not play any role in fructofuranose uptake and confirmed that GLUT5 effectively takes up fructose in its furanose form.<sup>7</sup> Fructose uptake also requires the presence of cyclic oxygen as H-acceptor, since 6-fold loss in the uptake was observed for 5-thio-D-fructose (Scheme 2).<sup>10</sup>



**Scheme 2.2.** Conformer ratios and inhibitory constants for fructose uptake via GLUT5 for D-fructose, D-psicose and D-tagalose.

The affinity of fructose to GLUT5 also diminishes upon alteration in stereochemistry of ring hydroxyls or their alkylation (except for C2-OH).<sup>6</sup> Thus, the affinity of fructose epimers D-psicose (C3-epimer), D-tagalose (C4-epimer) and L-sorbose

(C5-epimer) was up to 9-fold lower than that of fructose (Scheme 2). Alkylation of C1, C3-5 hydroxyls of fructose resulted in 7-9-fold drop in affinity compared to fructose (Table 4). The observed loss in affinity upon alkylation could suggest the importance of these hydroxyls as H-donors or the data could reflect the impact of steric interaction on uptake. The observed sensitivity of fructose analog binding towards sterics is reminiscent of that observed with glucose analogs.

**Table 2.1.** Effect of hydroxyl alkylation on fructose uptake via GLUT5<sup>a</sup>

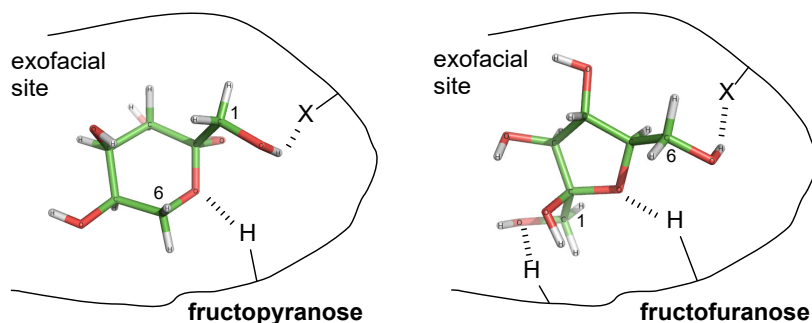
Substrate	Pyranose/furanose ratio		$K_i$ , mM
	$\alpha$ P, $\beta$ P	$\alpha$ F, $\beta$ F	
1-O-allyl-D-fructose	14, 67	Trace, 19	106±19
3-O-allyl-D-fructose	15, 38	12, 35	90±31
4-O-allyl-D-fructose	55, 18	18, 9	106±20
5-O-allyl-D-fructose	73, 27	no F	153±37
6-O-allyl-D-fructose	no P	100, 0	20±8

<sup>a</sup>Uptake determined relative to the uptake of [14C]-D-fructose. The  $K_i$  values calculated by least square fitting to Eqn:  $V_0/V_1 = 1 + I/K_i$ , where  $V_0$  and  $V_1$  are tracer uptake rates in the absence and presence of inhibitor, respectively,  $I$  is the inhibitor concentration and  $K_i$  is the half maximal inhibition constant of affinity constant.

Deriving more complete understanding of binding requirements for fructose is somewhat complicated by the fact that allylated fructose analogs exist as a mixture of conformers and anomers and ratios of those differ (Table 1). Thus, C1-O-allyl and C3-O-allyl analogs are predominately in the  $\beta$ -anomer form (86% and 72%, respectively), while C4 or C5 analogs exist prevalently as  $\alpha$ -anomers (72% and 73%, respectively). Alterations in pyranose/furanose ratios could also influence affinities of analogs. Overall, the heterogeneity of the probes limits interpretation of the data, leaving room for further



studies. Probes where hydroxyls are substituted with H-acceptors, such as fluorine, and analogs with altered size of substituents could be of interest to assess whether diminished uptake is a result of lack of H-donor or excessive steric interaction.

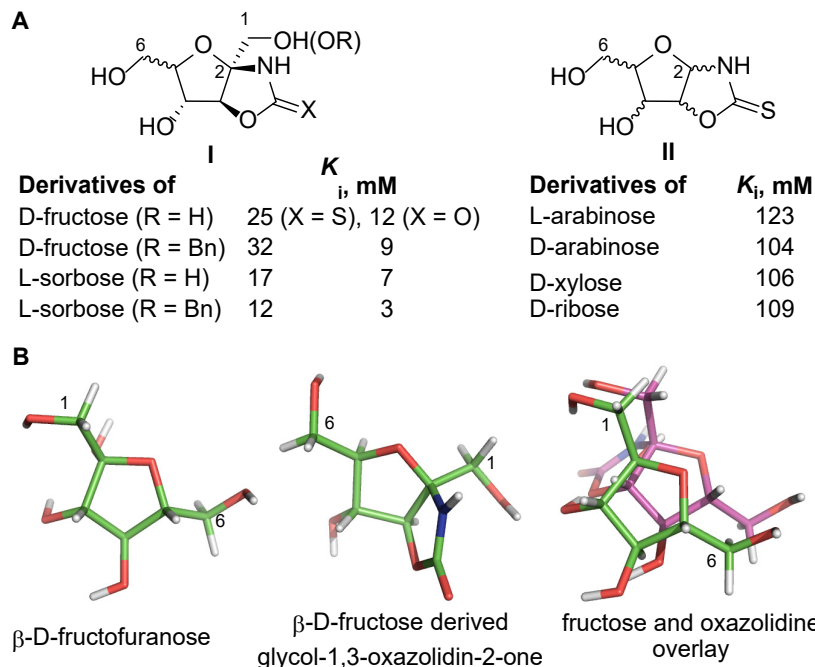


**Figure 2.1.** Simplified diagram of fructose binding to GLUT5. Fructose conformers modeled in Spartan '14 (Molecular Mechanics, MMFF). Visualization was carried out in PyMol. Red, oxygen; green, carbon; white, hydrogen.

Structure-affinity studies carried out by Holman and coworkers led to tentative binding models for fructofuranose and fructopyranose (Figure 1). For fructopyranose, effective binding and uptake relies on H-bonding of the C1-OH (as H-donor) and cyclic oxygen with the exofacial binding site of GLUT5. Binding mode for fructofuranose relies on H-bonding interaction between one of the primary hydroxyls (also as H-donor) and the cyclic oxygen and, in addition, involves a stabilizing interaction with the transporter from the second primary hydroxyls (as H-acceptor). The orientation of hydroxymethylene groups at C2 and C5 stereocenters appears to favor *anti* relationship for effective uptake (based on the loss of GLUT5-mediated uptake of L-sorbose). Due to C<sub>2</sub> pseudo-symmetry and the lack of binding interactions between C2-OH and GLUT5, fructofuranose could

interact with exofacial binding site either by *C1* or *C6*, as long as the binding proton is present.

The Holman team further speculated that analogs locked in a favored for uptake conformation can result in a new class of compounds that interact with GLUT5. Several glycol-1,3-oxazolidin-2-thiones and oxazolidin-2-ones were prepared to test this hypothesis.<sup>9</sup> Two major scaffolds were evaluated: one included compounds maintaining both *C1* and *C6* hydroxyls (**I**, Figure 4) and the other lacked *C1*-OH (**II**, Figure 2). All substrates of scaffold **I** were active as inhibitors of [<sup>14</sup>C]-D-fructose uptake via GLUT5 in CHO cells regardless of whether *C1* was a free hydroxyl or an ether.<sup>9</sup> GLUT5 affinities were ~4-fold higher for carbonyl than thiocarbohyll derivatives, suggesting an additional binding interaction of the carbonyl oxygen with the transporter. In addition, while L-sorbose was a poor GLUT5 substrate,<sup>6</sup> bicyclic derivatives of L-sorbose were more effective GLUT5 probes than derivatives of fructose, plausibly due to the better positioning of the *C6*-OH and the amide of the cycle in the active site for H-bonding. In contrast, substrates of scaffold **II** did not impact the uptake of [<sup>14</sup>C]-D-fructose regardless of the stereochemistry, further supporting the importance of complimentary *C1* and *C6* bonding for the effective uptake.<sup>9</sup> Whether the entry of fructofuranose or derivatives **I** into the binding site occurs with *C1* or *C6* remains elusive, due to the absence of the probes testing H-bonding role of each hydroxyls exclusively.



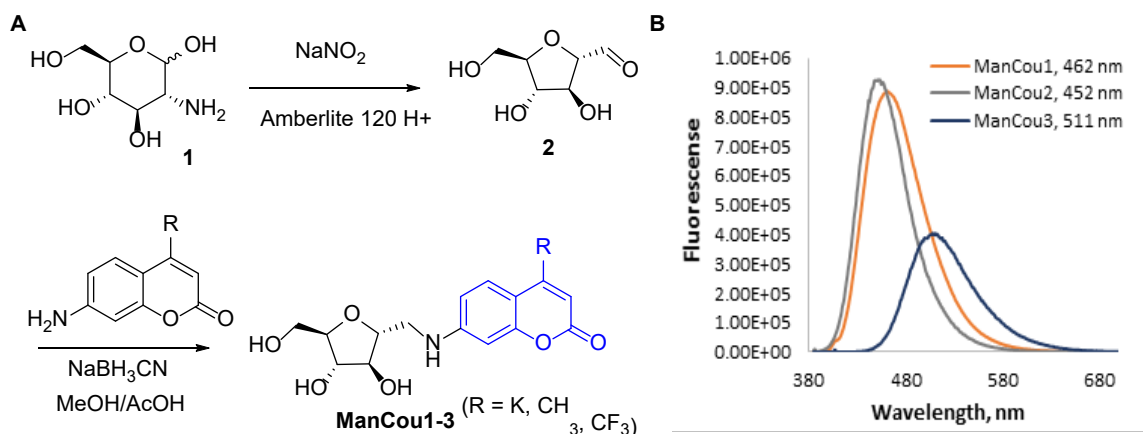
**Figure 2.2.** A. Bicyclic furanose analogs as GLUT5-mediated uptake probes. B. 3-D structures of  $\beta$ -D-fructofuranose and 1,3-oxazolidin-2-one derivative of  $\beta$ -D-fructofuranose (MMFF, Spatran'14). Graphical data visualization by PyMol. Red, oxygen; green or magenta, carbon; white, hydrogen.

The obtained understanding of substrate election by GLUT5 provided the basis for us to explore new molecular probes for specific targeting of this transporter for biochemical and biomedical applications.

## 2.2 Development of GLUT5 Specific Probes

To approach the development of GLUT5 probes we have explored 2,5-anhydro-D-mannitol<sup>8</sup> as a sugar template that can be specifically recognized by GLUT5. With the goal of developing tools for real-time monitoring and assessment of GLUT5 activity, we have explored the ability of GLUT5 to transport fluorescent moieties. Coumarins have been

selected due to their relatively small size and good fluorescent properties. Furthermore, the reported ability to tune fluorescence color for coumarins through functionalization provided additional points of attraction and added the feasibility to produce probes of different fluorescent color.

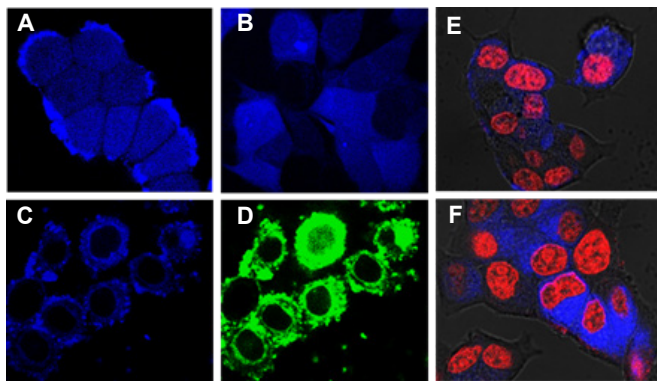


**Scheme 2.3.** Synthesis (A) and fluorescence properties (B) of mannitol-coumarin conjugates ManCou1-3.

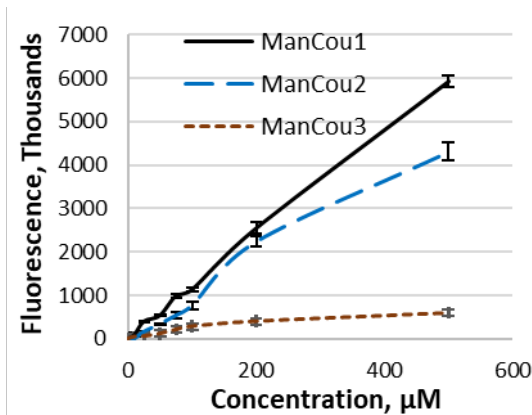
The passage of 7-aminocoumarin in the form of a glucosamine conjugate through glucose GLUTs has been demonstrated,<sup>11</sup> providing a basis for testing this fluorophore as a substrate for GLUT5. Thus, as a proof-of-principle, we have investigated the uptake of a 7-aminocoumarin as a conjugate of GLUT5-targeting 2,5-anhydro-D-mannose. We have targeted three coumarins that differed in the substitution at C4. The 7-aminocoumarin (Cou1) was synthesized from 7-hydroxycoumarin according to the established procedure.<sup>12</sup> The 7-amino-4-methylcoumarin and 7-amino-4-trifluoromethyl coumarin were purchased (Sigma Aldrich). These three fluorophores were then conjugated to 2,5-anhydro-

D-mannitol (Man) through reductive amination with 2,5-anhydro-2-carbaldehyde-D-mannitol to produce the fluorescent-D-mannitol–coumarin conjugates ManCous (Scheme 1, ManCou 1, R = H; ManCou2, R = CH<sub>3</sub>; ManCou3, R = CF<sub>3</sub>).

Fluorescence measurements (Scheme 3B) have shown that ManCous 1 has a strong emission in the “blue” region of the spectrum ( $\lambda_{\text{max}} = 461$  nm). The fluorescence data has clearly reflected the impact of substitution on coumarin fluorescence. Thus, the electron-withdrawing effect of fluorine atoms induced a red-shift in the emission for ManCou3 towards the “green” region of the spectrum ( $\lambda_{\text{max}} = 511$  nm). The electron-donating effect of the methyl group, in turn, induced a blue-shift in the fluorescence emission of a coumarin for ManCou2.



**Figure 2.3.** ManCou probes induce fluorescence in MCF7 cells. ManCou1 (A) and ManCou2 (B) can be observed under the blue filter (exc/em 405 nm/560 nm); ManCou3 (C and D) can be observed under blue or green (exc/em 405 nm/525 nm) filter. E) Co-staining of cells with nuclear dye (Red Dot, exc/em 635/ 655 nm) and ManCou1; D) co-staining of cells with RedDot and ManCou3. Images taken with 60X objective after treating cells with 20  $\mu\text{M}$  ManCous over 10 min. Images recorded at the same laser intensity and exposure time.



**Figure 2.4.** Concentration-dependent uptake of ManCous 1-3 at 37 °C. Data obtained using fluorescent plate reader exc/em 385 nm/460 nm. All uptake data are measured in triplicates in 96-well plate after 10 min incubation of cells, removal of the probe and repeated cell wash.

With new ManCou conjugates in hand, we moved into testing them as GLUT5 probes. For this part, we have used breast cancer MCF7 cells known to express GLUT5. After treating MCF7 cells with various concentrations of ManCou1, a significant accumulation of the coumarin-induced blue fluorescence was observed after a short 10 min incubation. We found that concentrations of 20 μM were sufficient to monitor the probe accumulation through microscopy (Figure 3A). Accumulation of ManCous 1 and 2 could be easily detected under blue filter. In contrast, ManCou3 could be imaged under both, blue and green filter, which fits the observed red-shift in the corresponding emission spectrum (Scheme 3B). Interestingly, the Z-stack images have shown that there is a significant difference in the cellular distribution between three probes. Thus, while ManCou1 and ManCou2 are distributed throughout the cell (including cell nucleus),

ManCou3 accumulates preferentially in the cytosol. The nuclear accumulation was confirmed through co-staining the cell with the nuclear dye (Figure 3, E and D).

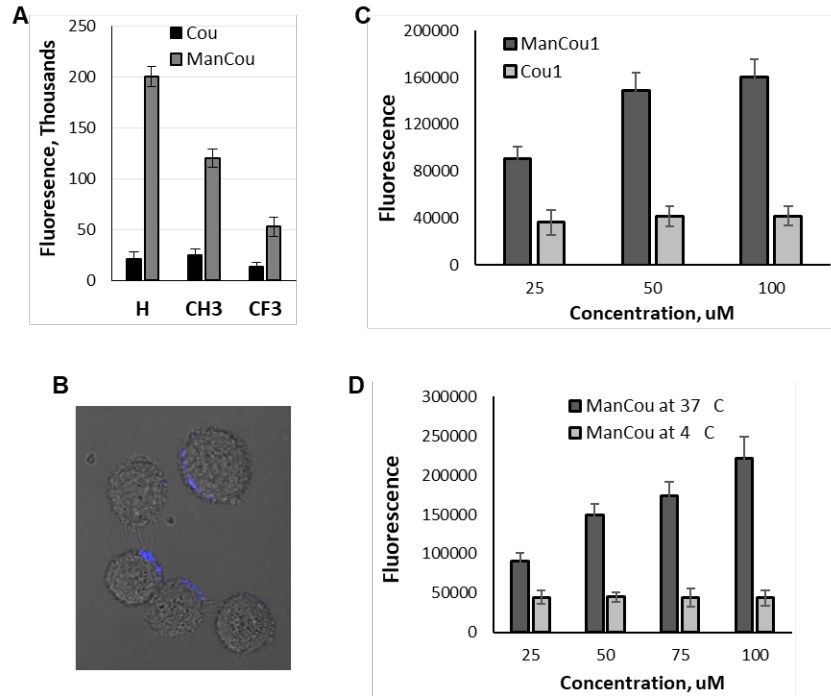
Further evaluations of probe uptake in cells revealed additional differences between probes. Thus, we have observed that increase in probe concentration has differential impact on probe's accumulation in the cell. For example, while linear-type uptake has been measured for ManCou1 probes at 10-500  $\mu\text{M}$  concentrations, the uptake of ManCou2 deviated from the linear trend and the uptake of ManCou3 completely saturated after 200  $\mu\text{M}$  (Figure 4). The differences in accumulation of probes parallel the differences in their cellular distribution. Considering that GLUT-mediated uptake is coupled with sugar phosphorylation, it is feasible to surmise that the observed saturation reflects the lack of phosphorylation for ManCou3 probe. Hence, cellular distribution also appears to depend on phosphorylation status of the probe, reflecting that ability of the cell nucleus to absorb only phosphorylates ManCou conjugates.

With the uptake of ManCou probes in MCF7 cells confirmed, we have moved towards assessing their particular uptake pathway. Considering that the ManCou conjugate represents a merging of a hydrophilic sugar and a hydrophobic fluorophore, we have investigated the contribution from GLUTs vs. passive diffusion to the observed cellular accumulation of this probe. For the analysis, MCF7 cells were incubated with the unconjugated 7-aminocoumarin at 37 °C and fluorescence was recorded. Two major differences were observed between ManCous and unconjugated coumarins. First, unconjugated coumarin showed >10-fold lower accumulation in cells, highlighting a significant contribution from the sugar moiety to the observed ManCou uptake. Analysis

of coumarin-treated cells through microscopy has revealed that the acquired fluorescence was primarily from the coumarin association with the cell membrane (Figure 5, Z-stack images).

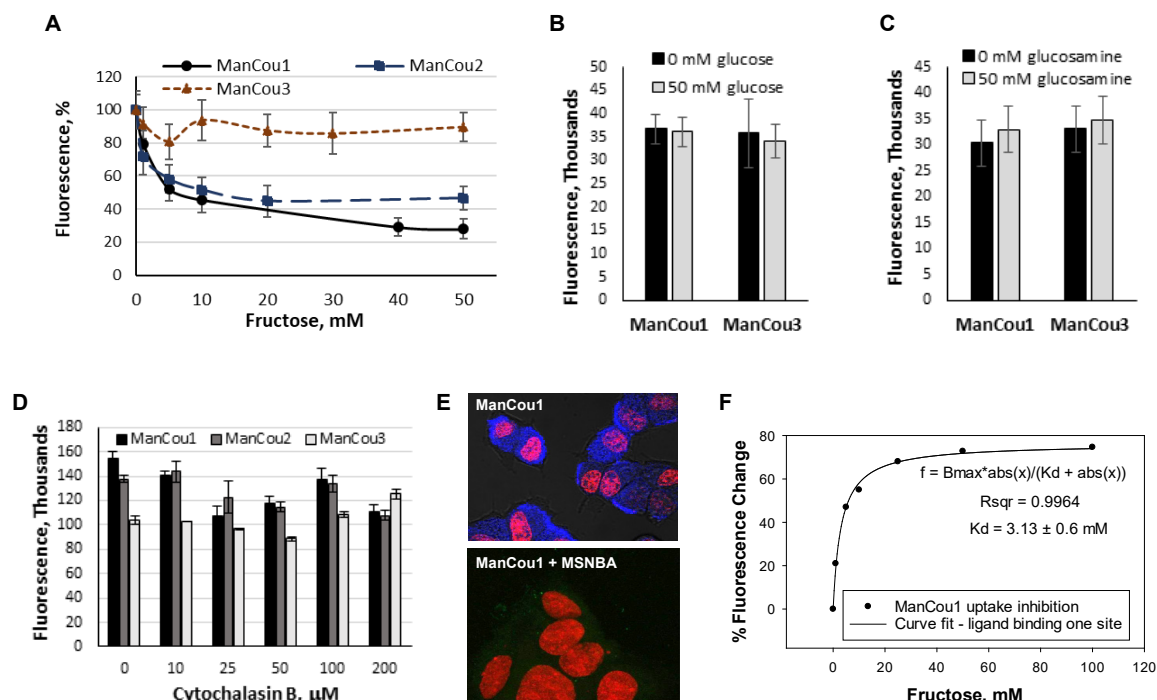
While the ManCou1 uptake was concentration-dependent, the uptake levels for the unconjugated coumarin Cou1 were not affected by the concentration. The concentration-dependent uptake and the unambiguous contribution from the sugar moiety to the enhanced uptake provided a basis to consider the GLUT-mediated transport as a primary uptake mechanism for ManCou1. The GLUT participation became further evident from the loss of ManCou1 uptake after incubating MCF7 cells at 4 °C conditions known to decrease cell metabolism and thereby GLUT-mediated uptake. In contrast, low temperatures did not impact the uptake of Cou1, highlighting its passive diffusion through the membrane into the cell. The loss of the uptake at low temperature was also observed for higher concentrations of ManCou1, suggesting the involvement of GLUT uptake even at elevated concentrations.





**Figure 2.5.** Assessing participation of passive diffusion on ManCou uptake. A) Comparative uptake of ManCou vs. corresponding coumarins (Cou) at 20 μM concentration (37 °C); B) Z-stack image of MCF7 cells treated with 7-aminocoumarin (Cou1) at 37 °C; C) Comparative analysis of ManCou1 vs. Cou1 uptake at varied concentrations (37 °C); D) Comparative analysis of ManCou1 uptake at 37 °C vs. 4 °C. All uptake data are measured in triplicates in 96-well plate after 10 min incubation of cells, removal of the probe and repeated cell wash. Data represents the Gained Fluorescence measured exc/em 385 nm/460 nm. Confocal images obtained with 60X objective using exc/em 405 nm/461 nm.

We have further used a series of competitive uptake and inhibition analyses to verify the uptake of ManCou1 through GLUTs, and particularly through GLUT5. We have observed that the uptake of ManCou1 and ManCou2 is effectively inhibited by fructose (Figure 6A) suggesting the probe to be taken through fructose-transporting GLUT(s). When glucose (Figure 6B) or glucosamine (specific for GLUT2<sup>13</sup>, Figure 6C) were used as competitive inhibitors, no alterations in the ManCou1 uptake were observed, indicating the lack of contribution from glucose or non-specific fructose GLUTs, including GLUT2.



**Figure 2.6.** Analysis of ManCou uptake in the presence of fructose (A); glucose (B); glucosamine (C); cytochalasin B (D); and MSNBA (E). Data in graphs was obtained for 20  $\mu\text{M}$  ManCou1-3 probes in triplicates. Plots represents average data, error bars represent standard deviation. Data are collected after 10 min incubation of cells with ManCou in 96-well plates, removal of the probe, and cell wash (exc. 360 nm, em. 430 nm for ManCous 1 and 2, and em. 500 nm for ManCou3 and 4). Cell imaging (Z-stack) was done with confocal microscope using 60X objective exc/em 405 nm/461 nm. Blue/green correspond for ManCou1; Red corresponds to nuclear RedDot stain. F) Analysis of binding affinity for fructose in the presence of 20  $\mu\text{M}$  ManCou1. Data analyzed by Sigmaplot13 using uptake values from (A). Competitive inhibition of 20  $\mu\text{M}$  ManCou1 uptake with fructose in concentrations 10-50 mM allowed to derive the  $K_d = 3.1 \text{ mM}$  measured for fructose (Figure 6F). This data relates well with other reported binding affinity values between GLUT5 and fructose ranging from 6-9 mM.<sup>8, 15</sup> Considering that no saturation was observed for ManCou1 uptake even at elevated 500 mM concentrations, we used a fructose:ManCou1 ratio measured to induce 50% ManCou1 uptake inhibition to estimate that ManCou1 bind GLUT5 ~9-fold stronger than fructose, allowing us to derive  $K_d \sim 330 \mu\text{M}$ . Interestingly,

the impact of fructose on ManCou3 was minimal. Using the concentration-dependent uptake data (Figure 4), we have found that ManCou3 exhibits ~20-fold higher affinity ( $K_d = 52.45$  mM) than ManCou1. Significant enhancement in affinity suggests that additional interactions with the protein are presented by the presence of potentially H-binding fluorides on the coumarin.

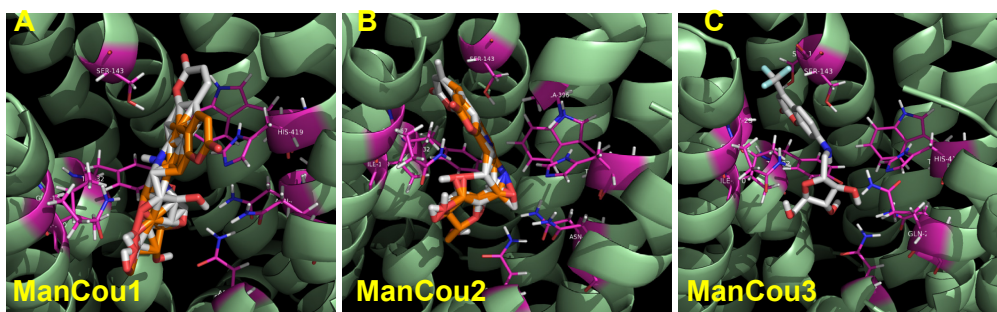
The lack of ManCou1 inhibition in the presence of cytochalasin B (Figure 6D), the established inhibitor of the uptake through GLUTs 1–4 ( $IC_{50} = 2–6$  mM) but not GLUT5, further ruled out non-specific transport, highlighting GLUT5-mediated uptake. The results further highlighted high fructose-dependence for the uptake of these probes, allowing us to indicate fructose-specific transporter GLUT5 as the mode of ManCou transport. Further the complete inhibition of ManCou1 uptake in the presence of GLUT5-specific inhibitor MSNBA<sup>14</sup> (Figure 6E) have validated the specificity of these conjugates to GLUT5.

### **2.3 Exploring the Structural Basis for ManCou-GLUT5 Binding**

To gain insight into the ManCou interaction with GLUT5, molecular docking of DFT-optimized structures of coumarin conjugates into the exofacial cavity of a mammalian fructose transporter GLUT5 (PDB code: 4YB9) using Autodock4<sup>15</sup> was carried out. For each ManCou probe, the resulting complexes were ranked, and the complexes were analyzed to identify the position/binding of conformers.

Overall, the analysis of complexes showed the ManCous to bind with the uptake relevant residues through the 1-AM moiety but accommodate different orientations of the fluorophore (Figure 2.7). All three probes were found to H-bond with Tyr32, Gln167, Gln289, and the GLUT5-specific Asn294 – residues also found to be involved in fructose

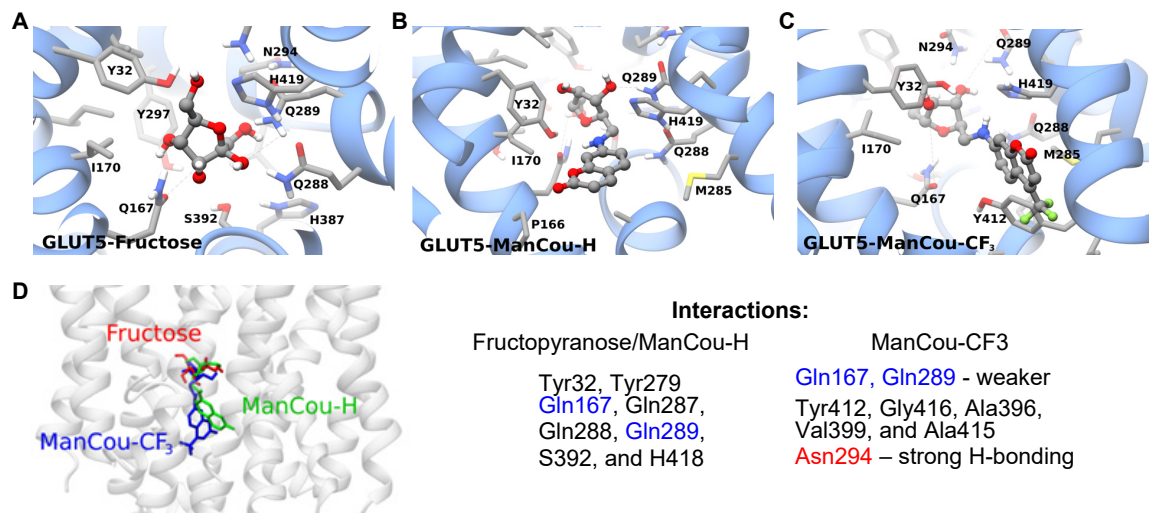
uptake through GLUT5.<sup>15</sup> While the binding of 1-AM between three complexes involved the same residues, the H-bonding sites at 1-AM were altered to accommodate the change in the position of the fluorophore. For ManCou1, the large population of conformers was found to orient the coumarin moiety towards His419 and Trp420 – residues found to be critical for fructose uptake (Figure 2.7A).<sup>15</sup> For ManCou3, nine out of ten conformational isomers had the coumarin moiety oriented away from these residues into the more open space (Figure 2.7C). Interestingly, for ManCou2 (Figure 2.7B), conformations similar to those of ManCou1 and ManCou3 were detected, suggesting the probe to have duality, as sensed by malignant cells. However, a higher level modeling would be required to assess a true binding site(s) for these probes and further identifying key interactions contributing to the differences in their uptake behavior and cellular impact.



**Figure 2.7.** Docking analysis of ManCou1-3. Docking analysis performed with Autodock4. Models visualized with PyMol.

Following these preliminary assessment, the analysis of GLUT5-ManCou interactions was carried out using molecular dynamics. In addition, simulations were run to assess the correlations between GLUT5 binding to ManCous vs fructose in a furanose conformer. The work was done in collaboration with Dr. Christov (MTU).<sup>16</sup> For MD simulations, the inward-open conformation of GLUT5 from *Bob Taurus* (pdb code 4YB9<sup>15</sup>) was used and calculations were carried out using AMBER16 code<sup>17</sup> and ff14SB

forcefield.<sup>18</sup> The substrates were docked within the central binding site of GLUT5 and the impact of ligands on protein conformation was evaluated.



**Figure 2.8.** Molecular dynamic simulation of GLUT5-ManCou interactions. Images represent MD snapshots.

Docked fructose was used as control and has shown stable interactions with Tyr32, Gln167, Q287, S392, and H418. These interactions have been previously observed within the crystal structure reported by Nomura et al<sup>19</sup> and conformed through fluorescence and mutagenesis studies. Additional weak interactions with residues Tyr279 and Gln288 are also seen. Gln167 was experimentally suggested to contribute to the fructose-specificity of GLUT5 as its substitution to glutamate seems to add the capacity to transport glucose for GLUT7.<sup>15, 19</sup> The interaction with Gln167 has also been found essential for the conformational change allowing the substrate translocation through the protein.<sup>15</sup>

Comparative analysis of fructofuranose vs. ManCous revealed a significant impact of the hydrophobic fluorophore moiety on the ligand binding geometry (Figure. 2.8.). The

simulations indicated that interactions with Gln167, and Gln289 are also present for the sugar moiety of ManCou-H, although the ligand is positioned differently from fructofuranose (Figure 2.8). The change in the ligand position appears to be driven by additional interaction between the C=O of coumarin and Asn325, plausibly contributing to the experimentally observed higher affinity of ManCou-H to GLUT5.<sup>20</sup>

The binding of ManCou-CF<sub>3</sub> is accompanied by the additional change in the position of the fluorophore, while the interactions of the sugar with Gln167, and Gln289 are conserved. This change appears to be due to F-H-C and F-H-N interactions with Tyr412, Gly416, Ala396, Val399, and Ala415 residues (Figure 2.8) and could be contributing to stronger binding of ManCou-CF<sub>3</sub> to GLUT5.<sup>20</sup> Furthermore, ManCou-CF<sub>3</sub> appears to induce specific interaction with Asn294 that is not present for ManCou-H or fructofuranose complexes. It should be noted that the interaction with Asn294 has been previously suggested to contribute to inhibition of GLUT5.<sup>14</sup>

Overall, the average number of hydrogen bonds during 1  $\mu$ sec MD simulations was found highest in the ManCou-CF<sub>3</sub> complex (1.7) followed by the ManCou-H complex (1.2) and then by the fructose complex (1.1). The differences in binding interactions were in a good agreement with the free energies of binding. Thus, -43.3 kcal/mol, -39.7 kcal/mol, and -19.6 kcal/mol calculated for GLUT5 complexes with ManCou-CF<sub>3</sub>, ManCou-H, and fructose, respectively, agree with the experimental binding affinity trend.<sup>20</sup>

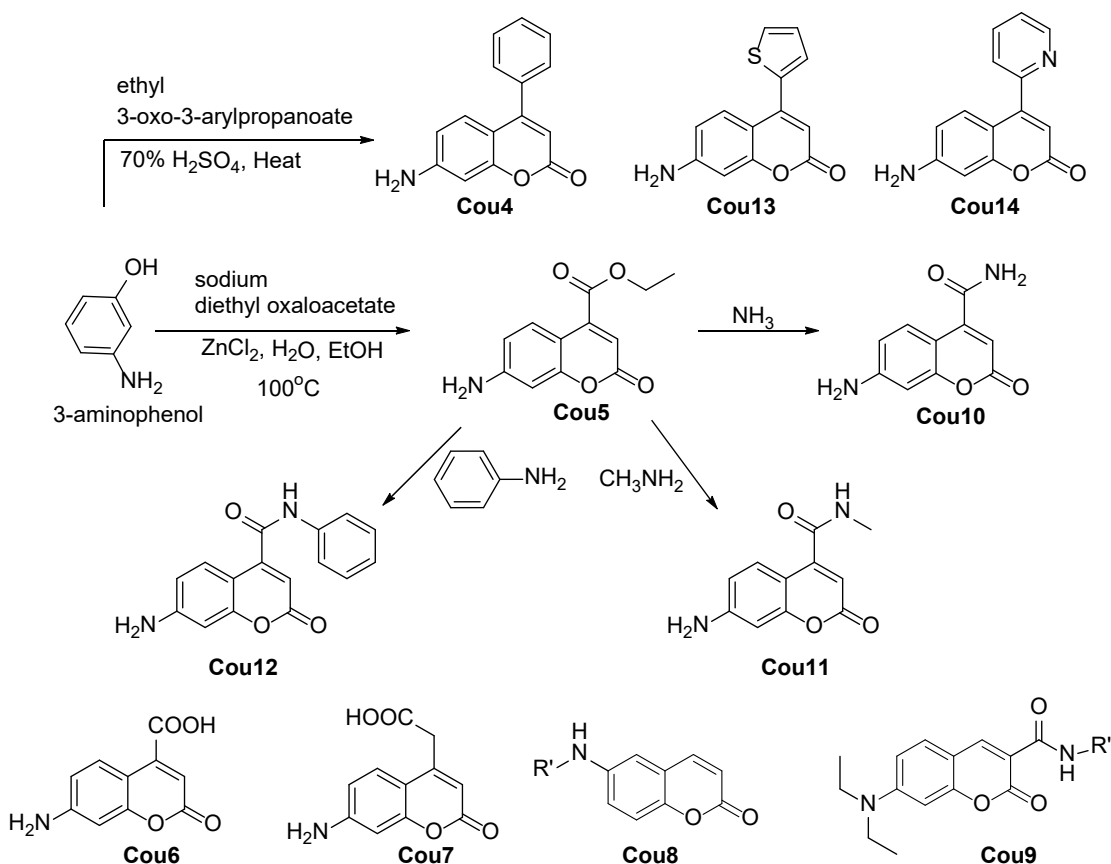
## 2.4 Development of Multicolor GLUT5 Probes

With the successful delivery of a blue-fluorescent 7-aminocoumarin into the cell through GLUT5, we moved forward to testing ManCou analogues to gauge the tolerance

of GLUT5 to coumarin fluorophores and gain access to probes of different fluorescence colors. The substitution at the C4 position of the 7-aminocoumarin had been shown to impact the fluorescence emission.<sup>21</sup> Thus, we constructed a focused library of ManCous by synthesizing Cous bearing various electron withdrawing groups at C4 (C4-EWG),<sup>22-24</sup> including new amides (Cou10-12), 2-furyl (Cou13), and 2-pyridyl (Cou14) C4-analogs. We have completed the library by adding 6-aminocoumarin (Cou8) and the C3-substituted analogue of 7-aminocoumarin Cou9 to assess the impact of alterations in the position of sugar conjugation on the ManCou uptake.

The Cous 5, 13 and 14 were synthesized through Pechmann condensation,<sup>22-23, 25</sup> and Cous 10–12 were obtained from Cou5 through amidation with the corresponding amine.<sup>22</sup> Except for ManCou9, all ManCous were obtained through reductive amination of the corresponding Cous with 2,5-anhydro-2-carbaldehyde-D-mannitol. ManCou9 was obtained through EDCI/HOBt-mediated amidation with 1-amino-2,5-anhydro-D-mannitol.

Fluorescent analysis of the obtained coumarins has shown that C4-substitution indeed highly impacts fluorescence emission while allowing to maintain the excitation at a low wavelength (405 nm). Overall, C4-substitution allowed to shift the emission maxima from 462 nm (ManCOu1) to 564 nm (ManCou10). The fluorescence intensity of ManCous varies with the substitution position and type, with ManCou13 and ManCou8 showing the highest and the lowest fluorescence intensity, respectively. The absolute quantum efficiency for all ManCou conjugates reflects the quenching effect of electron delocalization from the coumarin scaffold into the electron withdrawing substituent.



**Scheme 2.4.** C-4 functionalized coumarins as fluorophores for multi-color GLUT5 probes.

We have also observed that the absorption maxima of ManCou conjugates have red-shifted 8–22 nm compared to the unconjugated coumarin. In an effort to explain the changes in the absorption, density functional theory was employed. The structures of 7-aminocoumarins and the corresponding ManCou conjugates were first geometrically relaxed, and then single point energy calculations were performed. The analysis of the HOMO and LUMO energies revealed a reduction of the energy gap upon alkylation of the exocyclic amine expectedly contributing to the shift of the max to the lesser energy.



<b>ManCou</b>	<b>Absorbance,<sup>a</sup> <math>\lambda_{\text{max}}</math>, nm</b>	<b>Fluorescence,<sup>a</sup> <math>\lambda_{\text{max}}</math>, nm</b>	<b>Stock Shift, nm</b>	<b>Absolute Quantum Yield,<sup>b</sup> <math>\Phi_F</math></b>
1	366	452	86	0.26
2	360	461	101	0.30
3	387	508	121	0.1
4	376	506	130	0.44
5	398	558	160	0.09
6	371	538	167	0.21
7	365	460	95	0.37
8	384	459	75	0.08
9	430	481	51	0.27
10	382	564	182	0.06
11	385	549	164	0.22
12	383	554	171	0.12
13 (2-furyl)	368	531	163	0.29
14 (2-pyridyl)	374	535	161	0.21

<sup>a</sup>All data measured in water/ethanol (70:30 v/v) mixture. <sup>b</sup>Absolute quantum yield was derived with respect to the anthracene as fluorescence standard.

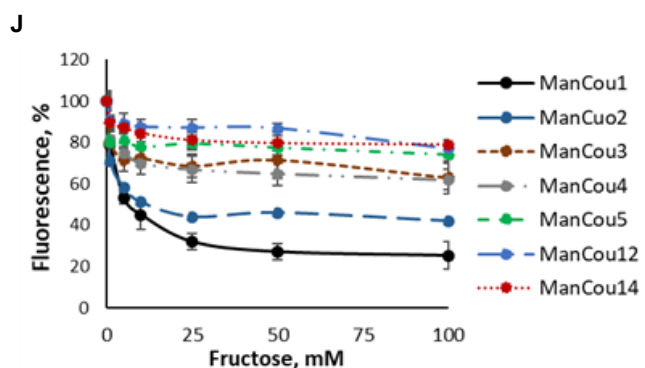
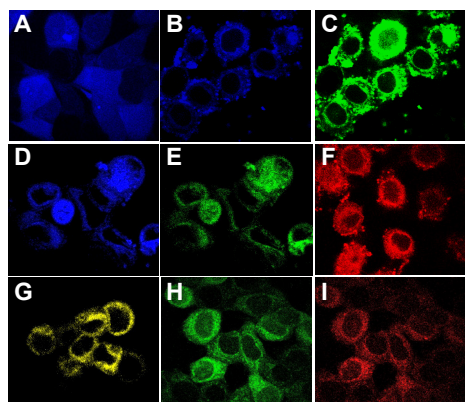
Through confocal imaging, we have observed that MCF7 cells gained fluorescence after treatment with all ManCous except for ManCous 6 and 7 – both bearing carboxylic acid moieties. The gained cell fluorescence for ManCous 2, 8 and 9 (blue filter) highlighted the tolerance of GLUT5 towards positional isomers of coumarin–mannitol conjugates. ManCous 3 and 4 were visible under both green and blue filters; ManCou5 was visible under orange/red filters and ManCous 10–14 were visible under red, yellow, and green filters (Figure 2.9). The GLUT5-specificity of these new analogs was supported by the lack of uptake inhibition in the presence of cytochalasin B, and decline in the uptake in the presence of fructose (Figure 2.9.J). The inhibitory effect of fructose was strong for ManCous 2, but decreased for EWG-substituted ManCous.

**Table 2.3.** Comparative analysis of UV  $\lambda_{\max}$  and HOMO/LUMO contribution for selected C4-substituted Cou and ManCous.<sup>a</sup>

ManCou	UV, $\lambda_{\max}$ , nm	HOMO/LUMO <sup>b</sup>	$\Delta_{\text{HOMO/LUMO}}$	Cou	UV, $\lambda_{\max}$ , nm	HOMO/LUMO	$\Delta_{\text{HOMO/LUMO}}$
1	366	-445/-186	259	1	352	-459/-190	269
2	360	-440/-177	263	2	347	-453/-180	273
3	387	-468/-232	236	3	372	-486/-253	233
4	376	-441/-193	248	4	358	-453/-196	257
5	398	-467/-217	250	5	377	-482/-223	259
13	374	-438/-209	219	13	366	-449/-213	236

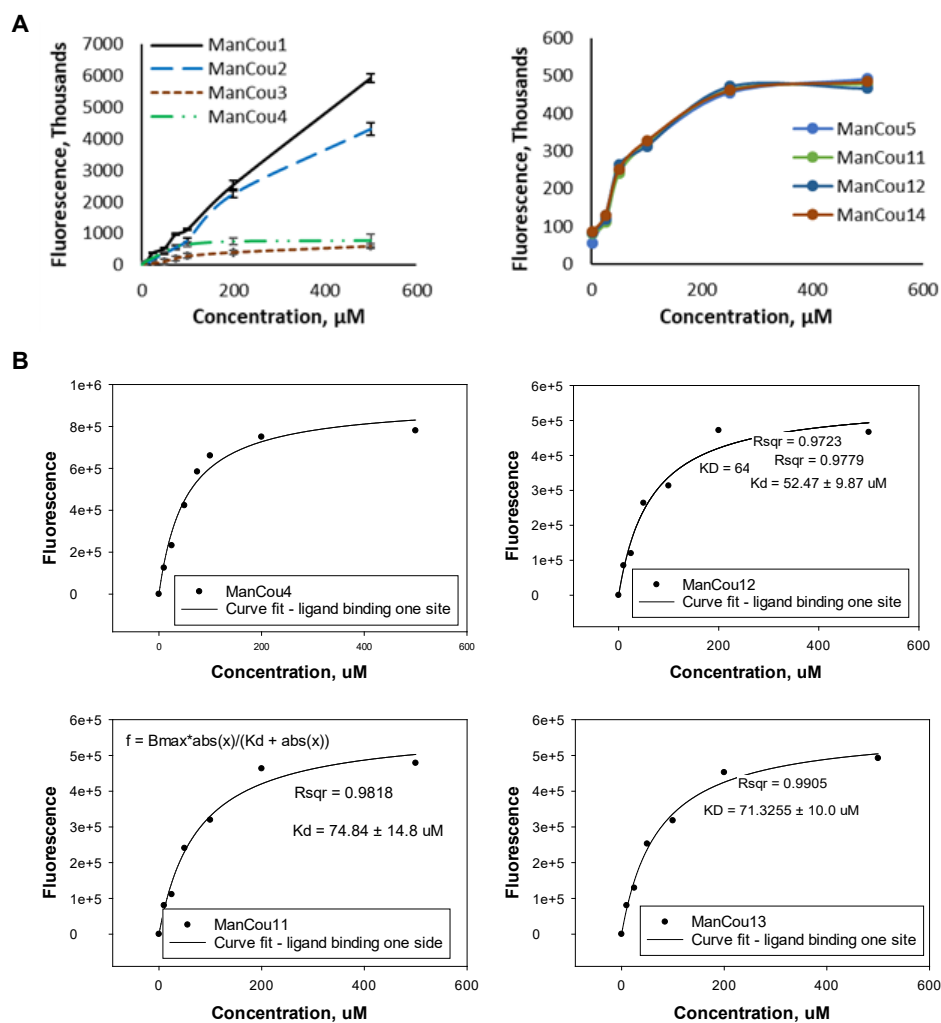
<sup>a</sup>Data provided for probes showing the uptake through GLUT5; <sup>b</sup>HOMO/LUMO orbital energies were calculated with Spartan '14 V1.1.2 (Wavefunction Inc.) using Density Functional, BLYP, 6-31G\*

The Z-stack analysis of ManCou-treated MCF7 cells revealed an apparent impact of coumarin substitution on the cellular distribution of the probe. Namely, while ManCous 1 and 2 were distributed throughout the cell, C4-EWG ManCous and ManCous 8 and 9 accumulated in the cytosol (Figure 2.9). The cytosolic distribution could be readily delineated through the labelling of the cell nucleus and the cell membrane with dyes of contrast fluorescence color.



**Figure 2.9.** Fluorescence confocal Z-stack images of MCF7 cells treated with: A) ManCou2; B) and C) ManCou3; D) ManCou4 (blue and green merge); E) ManCou5; F) ManCou9; G-I) ManCou 11. Blue fluorescence measured at 461 nm; green fluorescence measured at 525 nm; red fluorescence measured at 585 nm. ManCous were excited with 405 nm laser. Yellow color assigned considering the fluorescence maxima for ManCous 10-12. Images taken with 60X objective after treating cells with 20  $\mu$ M ManCous over 10 min. Images recorded at the same laser intensity and exposure time.

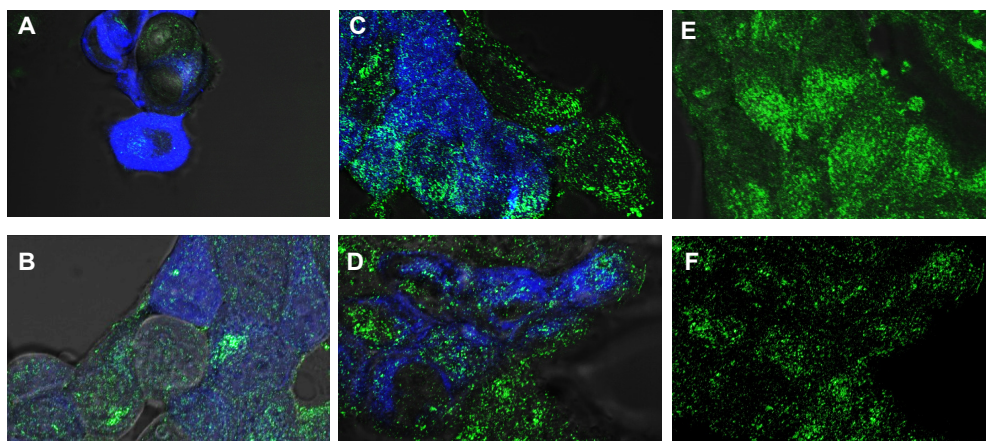
The differences in cellular accumulation of ManCous paralleled the differences in their uptake. Thus, while linear uptake was observed for ManCous 1 and 2 at 1–500 mM concentrations, the uptake for all other ManCous saturated after 200 mM (Figure 2.10, A). Considering that the continuity of the uptake through GLUTs is coupled with phosphorylation, it is feasible that the differences in the uptake behavior between ManCous could be reflecting the impact of coumarin substitution on the phosphorylation of 2,5-anhydro-D-mannitol by cellular kinases. All saturable ManCous showed  $K_d$  in the 54–75 mM range (Figure 2.10, B).



**Figure 2.10.** Uptake (A) and binding affinity (B) for C4-functionalized ManCou probes.

Overall, the presence of EWG groups at the coumarin appears to contribute to the strength of the ManCou–GLUT5 interaction as well as uptake rates. This contribution is manifested by the apparent inhibition of ManCou1 uptake in the presence of ManCou3. Namely, incubating MCF7 cells with the equimolar mixture of ManCous 1 and 3 resulted in the loss of nuclear accumulation of the blue fluorescence, a feature characteristic for ManCou1. To explore this effect further, we have employed the GLUT5-targeting green fluorescent NBDM probe ( $K_D = 22 \text{ mM}$ ).<sup>26</sup> After incubating MCF7 cells with the

equimolar mixture of ManCou3 and NBDM, a trace of NBDM-induced green fluorescence was observed inside the cell. In contrast, ManCou3-induced blue fluorescence was abundant. For the ManCou1–NBDM mixture, the uptake of both was observed, although the total fluorescence intensities were significantly diminished.



**Figure 2.11.** ManCous as competitors for NBDM and NBDG uptake in MCF7 cells (Confocal, Z-stack images). A) Equimolar NBDM and ManCou3; B) Equimolar NBDM and ManCou1; C) Equimolar ManCou1 and NBDG; D) Equimolar ManCou3 and NBDG; E) NBDM; F) NBDG. Z-stack images taken after 10 min treatment and cell wash. Cells imaged with 60X objective using exc/em. 405 nm/425-525 nm for ManCous, and exc/em 450 nm/565 nm for NBDM and NBDG (eGFP, green fluorescence). All images obtained at the same laser intensity and exposure time. Overall, the differential effect of ManCous 1 and 3 on NBDM appears to reflect the differences in the strength of the GLUT5–ManCou interaction. It should be noted that the uptake of the glucose-GLUT-targeting green fluorescent NBDG probe (NBD conjugate of glucose<sup>7</sup>) was not impacted by any of the ManCou conjugates. This observation further validates the GLUT5-specificity of ManCou conjugates. It should be noted that the uptake of glucose-GLUT-targeting green fluorescent NBDG probe (NBD conjugate of glucose<sup>7</sup>) was not impacted by any of the ManCou conjugates (Figure 2.10, C and D). This observations further validates the GLUT5-specificity of ManCou conjugates.

## 2.5 Conclusion

In conclusion, we have shown that fructose-specific transporter GLUT5 is capable of passing coumarins as an imaging cargo, emphasising a capacity for these facilitative

transporters to pass non-native moieties in the form of a proper sugar or sugar mimic conjugate. The focused coumarin library conjugated to the 1-amino-2,5-anhydro-D-mannitol (ManCous) includes fluorescent probes that emit at different parts of the fluorescence spectrum, while maintaining the same excitation. As GLUT5 reporters, the probes allow for a visual discrimination between GLUT5-proficient and GLUT5-deficient cells. The structure-uptake relationship established with ManCou analogs revealed that the presence of a carboxylate moiety compromises GLUT5-mediated uptake, while ester, amide, and free amine functionalities are well tolerated. Also, a strict relationship of uptake saturation and cytosolic accumulation with coumarin substitution was observed. The spectral versatility of ManCou probes allows for combination studies through mismatching fluorescence colors of different reporters, such as nuclear and membrane dyes. Furthermore, variations of fluorescent colors within the ManCou library provides an opportunity for co-analysis of GLUT5 and other GLUTs (or other cellular targets). Considering a direct impact from ManCous on fructose uptake, further evaluation is in work to identify the cellular fate of ManCous and reveal their processivity by cellular kinases and their potential role as kinase inhibitors.

## **2.6 Materials and Methods**

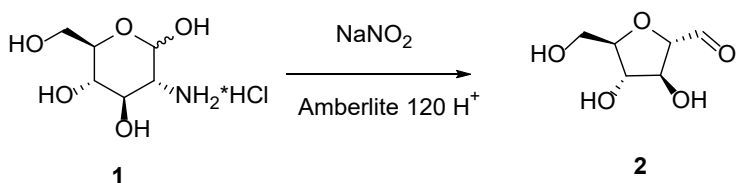
All reagents were used as received unless otherwise stated from Sigma-Aldrich, TCI America, Alfa Aesar, Ark Pharm, AK Scientific, Combi-Blocks or Chem-Impex International. Commercially available coumarins were purchased from: 7-amino-4-methylcoumarin (Cou2), Sigma-Aldrich; 7- amino-4-(trifluoromethyl)coumarin (Cou3), Alfa Aesar; 2-(7-amino-2-oxo-2H-chromen-4-yl)acetic acid (Cou7), Ark Pharm; 6-amino-

2H-chromen-2-one (Cou8), Enamine; 7-(diethylamino)-2-oxo-2H-chromene-3-carboxylic acid (Cou9), Combi-Blocks. N,N-Dimethylformamide (DMF) was dried and stored over CaH<sub>2</sub> before use. Dry tetrahydrofuran was dispensed from an automated Innovative Technology Pure-Solv 400 Solvent Purification System. Analytical TLC was carried out on commercial SiliCycle SiliaPlate® 0.2 mm F254 plates. Preparative silica chromatography was performed using SiliCycle SiliaFlash® F60 40-63 µm (230-400 mesh). Final purification of compounds was achieved with Agilent-1200 HPLC (high-pressure liquid chromatography) using reversed phase semi-preparative column (Phenomenex® Luna® 10 µm C18(2) 100 Å, LC Column 100 x 10 mm, Ea). <sup>1</sup>H and <sup>13</sup>C NMR spectra were recorded at room temperature with a Varian Unity Inova 400 MHz spectrometer. CD<sub>3</sub>OD, DMSO-d<sub>6</sub>, and D<sub>2</sub>O were used as solvents and referenced to the corresponding residual solvent peaks (3.31 and 49.0 ppm for CD<sub>3</sub>OD, respectively; 2.50 and 39.52 ppm for DMSO-d<sub>6</sub>, respectively; 4.79 ppm for D<sub>2</sub>O). The following abbreviations are used to indicate the multiplicity: s - singlet; d - doublet; t - triplet; q - quartet; m - multiplet; b - broad signal; app - approximate. The coupling constants are expressed in Hertz (Hz). The high-resolution (HR) MS data (ESI) were obtained using a Thermo Fisher Orbitrap Elite™ Hybrid Ion Trap-Orbitrap Mass Spectrometer at Chemical Advanced Resolution Methods (ChARM) Laboratory at Michigan Technological University. UV-vis spectra were recorded on a Cary 100 Bio-spectrophotometer from Agilent Technologies. Fluorescence spectra were obtained with FluoroMax-4 spectrophotometer. 96-well plate analysis of cell fluorescence was carried out with Victor3 fluorescence plate reader (excitation at 385 nm). Confocal images were taken with

Olympus FluoView<sup>TM</sup> FV1000 using the FluoView software. Fluorescence imaging was done with EVOS FL Auto inverted microscope

RPMI-1640, Penicillin/Streptomycin, FBS (Fetal Bovine Serum), 25% Trypsin-EDTA (1X), and PBS (phosphate buffered saline solution) were purchased from Life Technologies, USA. MEM Non-Essential Amino Acids 100X were purchased from Quality Biological, USA. Sterile DMSO (25-950-CQC, 250mL) was purchased from Sigma. MCF7 and Hep G2 cells were purchased from ATCC, USA and cultured according to the suggested growth methods.

### 2.6.1 Synthesis of ManCous 1-14



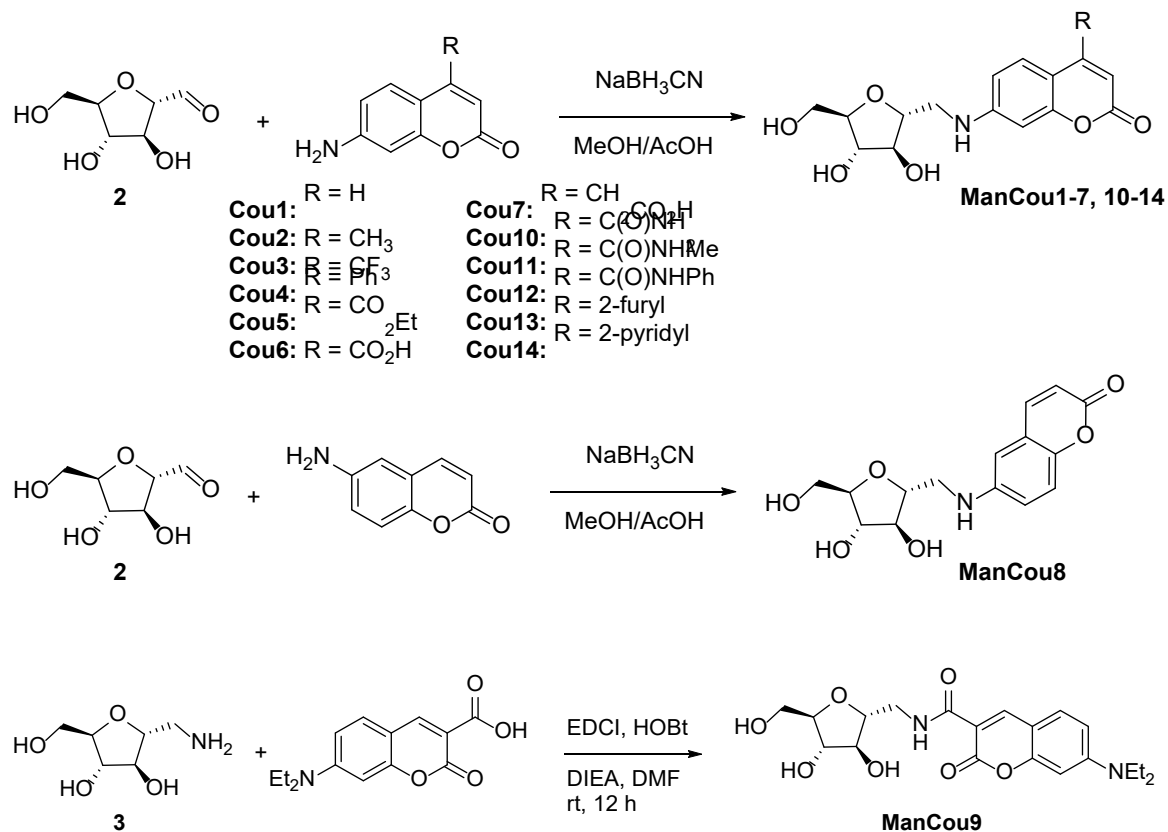
**Scheme S1:** Synthesis of 2,5-anhydro-2-carbaldehyde-D-mannitol **2**.

#### **(2*S*,3*S*,4*S*,5*R*)-3,4-dihydroxy-5-(hydroxymethyl)tetrahydrofuran-2-carbaldehyde**

**(2):**<sup>26</sup> D-Glucosamine hydrochloride **1** (4.00 g, 18.5 mmol) was dissolved in water (100 ml) and stirred at room temperature for 5 h. Sodium nitrite (3.19 g, 45.3 mmol) was then added, followed by cautious addition of Amberlite 120 H<sup>+</sup> resin (90 g) by portion, maintaining the temperature of ice bath for 4 h. After the reaction, the resin was removed by filtration and the solution was then neutralized by adding sodium carbonate. The remaining solution was vacuum dried and then methanol was added to the residue to



precipitate the inorganic salts. After removing the salts by filtration, the solution was vacuum dried to get the compound **2** as a yellow sticky solid (2.49 g, 70%) that was used directly without further purification.



**Scheme S2:** Synthesis of **ManCous1-14**.

**General procedure for the synthesis of ManCous1-8, 10-14:**<sup>27</sup> Typically, (2*S*,3*S*,4*S*,5*R*)-3,4-dihydroxy-5-(hydroxymethyl)tetrahydrofuran-2-carbaldehyde<sup>26</sup> (up to 1 mmol) and the corresponding coumarin (0.8 equiv.) were dissolved in methanol (10 ml). AcOH (1 ml) was used to adjust the pH to <6, followed by portionwise addition of NaBH<sub>3</sub>CN to the reaction mixture (3 X 0.8 equiv, every 20-30 minutes). Water could also be added to

improve solubility of some coumarin substrates (up to 20% v/v). The solutions were stirred at room temperature for up to 24 h. The mixtures were then concentrated to dryness under reduced pressure and purified by column chromatography on silica gel using CH<sub>2</sub>Cl<sub>2</sub> : MeOH (up to 90 : 10), EtOAc : MeOH (up to 80 : 20) or water : isopropanol : EtOAc (1 : 2 : 7 up to 2 : 4 : 4) mixtures. The final purification was achieved by semi-preparative HPLC using water-acetonitrile gradient starting with 2-20% acetonitrile to obtain the final products as yellow solids or semi-solids, 10-30 mg samples. No attempts were made to optimize the yields of the products, which could be estimated as 30-40% average. The composition and purity of the final products was confirmed by HRMS, <sup>1</sup>H-NMR, and <sup>13</sup>C-NMR.

**7-((((2R,3S,4S,5R)-3,4-Dihydroxy-5-(hydroxymethyl)tetrahydrofuran-2-yl)methyl)amino)-2H-chromen-2-one (ManCou1):** <sup>1</sup>H-NMR (400 MHz, CD<sub>3</sub>OD): δ, 7.76-7.36 (d, *J* = 9.2, 1H), 7.32-7.30 (d, *J* = 8.4, 1H), 6.68-6.65 (dd, *J*<sub>1</sub> = 2.4, *J*<sub>2</sub> = 8.4, 1H), 6.53 (d, *J* = 2.4, 1H), 6.01-5.99 (d, *J* = 9.2, 1H), 4.02-3.98 (m, 2H), 3.95-3.92 (m, 1H), 3.88-3.85 (m, 1H), 3.73-3.69 (app dd, *J*<sub>1</sub> = 3.2, *J*<sub>2</sub> = 12.0, 1H), 3.66-3.61 (app dd, *J*<sub>1</sub> = 5.6, *J*<sub>2</sub> = 12.0, 1H), 3.48-3.44 (app dd, *J*<sub>1</sub> = 3.6, *J*<sub>2</sub> = 13.6, 1H), 3.38-3.32 (app dd, *J*<sub>1</sub> = 6.8, *J*<sub>2</sub> = 13.6, 1H) ppm. <sup>13</sup>C-NMR (100 MHz, CD<sub>3</sub>OD): δ, 164.7, 158.1, 154.5, 146.5, 130.2, 112.3, 110.6, 109.1, 98.0, 85.3, 83.2, 80.3, 78.9, 63.3, 46.2 ppm. HRMS (ESI): *m/z* [M + Na]<sup>+</sup> calcd for C<sub>15</sub>H<sub>17</sub>NNaO<sub>6</sub>: 330.09539; found 330.09434.

**7-((((2R,3S,4S,5R)-3,4-Dihydroxy-5-(hydroxymethyl)tetrahydrofuran-2-yl)methyl)amino)-4-methyl-2H-chromen-2-one (ManCou2):** <sup>1</sup>H-NMR (400 MHz, CD<sub>3</sub>OD): δ, 7.48-7.45 (dd, *J*<sub>1</sub> = 3.2, *J*<sub>2</sub> = 8.8, 1H), 6.71-6.67 (dt, *J*<sub>1</sub> = 2.4, *J*<sub>2</sub> = 8.8, 1H),

6.52-6.51 (t,  $J = 2.4$ , 1H), 5.93 (m, 1H), 4.02-3.98 (m, 2H), 3.96-3.93 (m, 1H), 3.88-3.85 (m, 1H), 3.73-3.69 (app dd,  $J_1 = 3.6$ ,  $J_2 = 11.6$ , 1H), 3.66-3.61 (app dd,  $J_1 = 5.6$ ,  $J_2 = 12.0$ , 1H), 3.48-3.43 (app dd,  $J_1 = 3.6$ ,  $J_2 = 13.6$ , 1H), 3.37-3.32 (app dd,  $J_1 = 6.8$ ,  $J_2 = 13.6$ , 1H), 2.38 (d,  $J = 0.8$ , 3H) ppm.  $^{13}\text{C}$ -NMR (100 MHz,  $\text{CD}_3\text{OD}$ ):  $\delta$ , 164.7, 157.3, 156.5, 154.4, 126.9, 112.1, 111.1, 108.6, 98.2, 85.3, 83.2, 80.3, 78.9, 63.3, 46.2, 18.5 ppm. HRMS (ESI):  $m/z$   $[\text{M} + \text{Na}]^+$  calcd for  $\text{C}_{16}\text{H}_{19}\text{NNaO}_6$ : 344.11104; found 344.11043.

**7-((((2R,3S,4S,5R)-3,4-Dihydroxy-5-(hydroxymethyl)tetrahydrofuran-2-yl)methyl)amino)-4-(trifluoromethyl)-2H-chromen-2-one (ManCou3):**  $^1\text{H}$ -NMR (400 MHz,  $\text{CD}_3\text{OD}$ ):  $\delta$ , 7.44-7.41 (dd,  $J_1 = 2.0$ ,  $J_2 = 9.2$ , 1H), 6.74-6.71 (dt,  $J_1 = 2.4$ ,  $J_2 = 9.2$ , 1H), 6.60-6.59 (d,  $J = 2.4$ , 1H), 6.37 (s, 1H), 4.02-3.98 (m, 2H), 3.95-3.92 (m, 1H), 3.89-3.85 (m, 1H), 3.73-3.69 (app dd,  $J_1 = 3.6$ ,  $J_2 = 11.6$ , 1H), 3.66-3.61 (app dd,  $J_1 = 5.6$ ,  $J_2 = 12.0$ , 1H), 3.50-3.46 (app dd,  $J_1 = 3.6$ ,  $J_2 = 14.0$ , 1H), 3.40-3.35 (app dd,  $J_1 = 6.4$ ,  $J_2 = 13.6$ , 1H) ppm.  $^{13}\text{C}$ -NMR (100 MHz,  $\text{CD}_3\text{OD}$ ):  $\delta$ , 162.2, 158.6, 155.0, 143.3, 143.0, 124.8, 122.1, 112.8, 108.3, 104.1, 98.5, 85.4, 83.2, 80.2, 78.8, 63.3, 46.1 ppm. HRMS (ESI):  $m/z$   $[\text{M} + \text{H}]^+$  calcd for  $\text{C}_{16}\text{H}_{17}\text{F}_3\text{NO}_6$ : 376.10082; found 376.09955.

**7-((((2R,3S,4S,5R)-3,4-Dihydroxy-5-(hydroxymethyl)tetrahydrofuran-2-yl)methyl)amino)-4-phenyl-2H-chromen-2-one (ManCou4):**  $^1\text{H}$ -NMR (400 MHz,  $\text{CD}_3\text{OD}$ ):  $\delta$ , 7.50-7.48 (m, 3H), 7.42-7.39 (m, 2H), 7.15-7.13 (d,  $J = 8.8$ , 1H), 6.59-6.56 (m, 2H), 5.90 (s, 1H), 4.03-3.99 (m, 2H), 3.97-3.94 (m, 1H), 3.90-3.86 (m, 1H), 3.74-3.70 (app dd,  $J_1 = 3.6$ ,  $J_2 = 11.6$ , 1H), 3.66-3.61 (app dd,  $J_1 = 5.6$ ,  $J_2 = 12.0$ , 1H), 3.47-3.43 (app dd,  $J_1 = 3.6$ ,  $J_2 = 14.0$ , 1H), 3.37-3.32 (app dd,  $J_1 = 6.8$ ,  $J_2 = 13.6$ , 1H) ppm.  $^{13}\text{C}$ -NMR (100 MHz,  $\text{CD}_3\text{OD}$ ):  $\delta$ , 164.2, 158.7, 157.9, 154.2, 137.2, 130.4, 129.7, 129.3, 128.8, 112.0,

109.6, 108.2, 98.4, 85.2, 83.1, 80.2, 78.8, 63.2, 46.2 ppm. HRMS (ESI):  $m/z$   $[M + Na]^+$  calcd for  $C_{21}H_{21}NNaO_6$ : 406.12669; found 406.12520.

**Ethyl 7-((((2R,3S,4S,5R)-3,4-dihydroxy-5-(hydroxymethyl)tetrahydrofuran-2-yl)methyl)amino)-2-oxo-2H-chromene-4-carboxylate (ManCou5):**  $^1H$ -NMR (400 MHz,  $CD_3OD$ ):  $\delta$ , 7.84-7.82 (d,  $J = 8.8$ , 1H), 6.64-6.61 (dd,  $J_1 = 2.4$ ,  $J_2 = 8.8$ , 1H), 6.49-6.48 (d,  $J = 2.4$ , 1H), 6.36 (s, 1H), 4.43-4.38 (q,  $J = 7.2$ , 2H), 4.03-3.99 (m, 2H), 3.96-3.94 (m, 1H), 3.90-3.86 (m, 1H), 3.74-3.70 (app dd,  $J_1 = 3.6$ ,  $J_2 = 11.6$ , 1H), 3.66-3.62 (app dd,  $J_1 = 5.6$ ,  $J_2 = 12.0$ , 1H), 3.47-3.43 (app dd,  $J_1 = 3.6$ ,  $J_2 = 14.0$ , 1H), 3.38-3.32 (app dd,  $J_1 = 6.8$ ,  $J_2 = 14.0$ , 1H), 1.42-1.38 (t,  $J = 7.2$ , 2H) ppm.  $^{13}C$ -NMR (100 MHz,  $CD_3OD$ ):  $\delta$ , 165.8, 163.6, 158.3, 154.5, 145.3, 128.6, 112.5, 111.0, 106.9, 98.2, 85.3, 83.1, 80.3, 78.8, 63.30, 63.25, 46.1, 14.4 ppm. HRMS (ESI):  $m/z$   $[M + H]^+$  calcd for  $C_{18}H_{22}NO_8$ : 380.13458; found 380.13345.

**7-((((2R,3S,4S,5R)-3,4-Dihydroxy-5-(hydroxymethyl)tetrahydrofuran-2-yl)methyl)amino)-2-oxo-2H-chromene-4-carboxylic acid (ManCou6):**  $^1H$ -NMR (400 MHz,  $D_2O$ ):  $\delta$ , 7.47-7.45 (d,  $J = 8.8$ , 1H), 6.73-6.70 (d,  $J = 8.8$ , 1H), 6.53 (s, 1H), 6.07 (m, 1H), 4.07 (bs, 3H), 3.96-3.93 (m, 1H), 3.80-3.76 (app dd,  $J_1 = 3.2$ ,  $J_2 = 12.4$ , 1H), 3.73-3.68 (app dd,  $J_1 = 6.0$ ,  $J_2 = 12.0$ , 1H), 3.48-3.36 (m, 2H) ppm.  $^{13}C$ -NMR (100 MHz,  $D_2O$ ):  $\delta$ , 172.6, 165.9, 156.4, 155.4, 152.8, 127.7, 112.1, 106.7, 103.4, 97.7, 82.7, 81.0, 78.4, 76.8, 61.4, 44.6 ppm. HRMS (ESI):  $m/z$   $[M + H]^+$  calcd for  $C_{16}H_{18}NO_8$ : 352.10328; found 352.10300.

**2-(7-((((2R,3S,4S,5R)-3,4-Dihydroxy-5-(hydroxymethyl)tetrahydrofuran-2-yl)methyl)amino)-2-oxo-2H-chromen-4-yl)acetic acid (ManCou7):** <sup>1</sup>H-NMR (400 MHz, D<sub>2</sub>O):  $\delta$ , 7.48-7.45 (d,  $J$  = 8.8, 1H), 6.77-6.74 (dd,  $J_1$  = 2.4,  $J_2$  = 8.8, 1H), 6.59 (d,  $J$  = 2.4, 1H), 6.06 (s, 1H), 4.10 (bs, 2H), 3.98-3.94 (m, 1H), 3.81-3.65 (m, 5H), 3.54-3.46 (m, 2H) ppm. We were not able to obtain satisfactory <sup>13</sup>C-NMR data in D<sub>2</sub>O. HRMS (ESI):  $m/z$  [M + H]<sup>+</sup> calcd for C<sub>17</sub>H<sub>20</sub>NO<sub>8</sub>: 366.11893; found 366.11771.

**6-((((2R,3S,4S,5R)-3,4-Dihydroxy-5-(hydroxymethyl)tetrahydrofuran-2-yl)methyl)amino)-2H-chromen-2-one (ManCou8):** <sup>1</sup>H-NMR (400 MHz, CD<sub>3</sub>OD):  $\delta$ , 7.84-7.82 (d,  $J$  = 9.2, 1H), 7.13-7.11 (d,  $J$  = 8.8, 1H), 6.99-6.96 (dd,  $J_1$  = 2.4,  $J_2$  = 9.2, 1H), 6.80-6.79 (d,  $J$  = 2.4, 1H), 6.36-6.33 (d,  $J$  = 9.2, 1H), 4.03-3.96 (m, 3H), 3.89-3.85 (m, 1H), 3.74-3.70 (app dd,  $J_1$  = 3.6,  $J_2$  = 12.0, 1H), 3.66-3.62 (app dd,  $J_1$  = 5.6,  $J_2$  = 11.6, 1H), 3.42-3.38 (app dd,  $J_1$  = 3.6,  $J_2$  = 13.6, 1H), 3.30-3.32 (app dd,  $J_1$  = 6.4,  $J_2$  = 13.6, 1H) ppm. <sup>13</sup>C-NMR (100 MHz, CD<sub>3</sub>OD):  $\delta$ , 163.7, 147.59, 147.56, 146.1, 120.8, 119.9, 118.0, 116.7, 109.4, 85.2, 83.2, 80.4, 78.9, 63.3, 47.3 ppm. HRMS (ESI):  $m/z$  [M + H]<sup>+</sup> calcd for C<sub>15</sub>H<sub>18</sub>NO<sub>6</sub>: 308.11344; found 308.11234.

**7-(Diethylamino)-N-((((2R,3S,4S,5R)-3,4-dihydroxy-5-(hydroxymethyl)tetrahydrofuran-2-yl)methyl)-2-oxo-2H-chromene-3-carboxamide (ManCou9):** This compound was synthesized according to the reported general procedure.<sup>28</sup> To a solution of 1-amino-2,5-anhydro-D-mannitol<sup>26</sup> (100 mg, 0.61 mmol), 7-(diethylamino)-2-oxo-2H-chromene-3-carboxylic acid (120 mg, 0.46 mmol), 1-

hydroxybenzotriazole monohydrate (HOBt; 93 mg, 0.69 mmol) and diisopropylethylamine (DIEA; 0.24 ml, 1.4 mmol) in dry DMF (4 ml), *N*-(3-dimethylaminopropyl)-*N'*-ethylcarbodiimide hydrochloride (EDCI; 132 mg, 0.69 mmol) was added and the mixture was stirred at room temperature for 12 h. It was diluted with EtOAc (100 ml), washed with brine (3 X 20 ml), and dried with MgSO<sub>4</sub>. After filtration and concentration, the residue was purified by column chromatography on silica gel, eluting with 0-100% EtOAc in hexanes, followed by 20% MeOH in EtOAc. The final purification was achieved by semi-preparative HPLC using water-acetonitrile gradient starting with 50% acetonitrile. A sample of compound was obtained as a yellow semi-solid (~20 mg). <sup>1</sup>H-NMR (400 MHz, CD<sub>3</sub>OD): δ, 8.60 (s, 1H), 7.53-7.51 (d, *J* = 9.2, 1H), 6.81-6.78 (dd, *J*<sub>1</sub> = 2.4, *J*<sub>2</sub> = 9.2, 1H), 6.54-6.53 (d, *J* = 2.4, 1H), 4.04-3.86 (m, 4H), 3.75-3.62 (m, 4H), 3.54-3.49 (q, *J* = 7.2, 4H), 1.25-1.21 (t, *J* = 7.2, 6H) ppm. <sup>13</sup>C-NMR (100 MHz, CD<sub>3</sub>OD): δ, 165.4, 163.8, 159.0, 154.4, 149.2, 132.5, 111.6, 109.9, 109.4, 97.2, 85.0, 82.7, 79.8, 78.4, 63.2, 46.0, 42.3, 12.8 ppm. HRMS (ESI): *m/z* [M + H]<sup>+</sup> calcd for C<sub>20</sub>H<sub>27</sub>N<sub>2</sub>O<sub>7</sub>: 407.18187; found 407.18109.

**7-((((2*R*,3*S*,4*S*,5*R*)-3,4-Dihydroxy-5-(hydroxymethyl)tetrahydrofuran-2-yl)methyl)amino)-2-oxo-2*H*-chromene-4-carboxamide (ManCou10):** <sup>1</sup>H-NMR (400 MHz, CD<sub>3</sub>OD): δ, 7.52-7.50 (d, *J* = 8.8, 1H), 6.70-6.68 (dd, *J*<sub>1</sub> = 2.4, *J*<sub>2</sub> = 8.8, 1H), 6.57-6.56 (d, *J* = 2.4, 1H), 6.08 (s, 1H), 4.02-3.98 (m, 2H), 3.95-3.92 (m, 1H), 3.88-3.84 (m, 1H), 3.73-3.69 (app dd, *J*<sub>1</sub> = 3.6, *J*<sub>2</sub> = 12.0, 1H), 3.65-3.61 (app dd, *J*<sub>1</sub> = 5.6, *J*<sub>2</sub> = 12.0, 1H), 3.49-3.45 (app dd, *J*<sub>1</sub> = 4.0, *J*<sub>2</sub> = 13.6, 1H), 3.39-3.34 (app dd, *J*<sub>1</sub> = 6.4, *J*<sub>2</sub> = 13.6, 1H) ppm. <sup>13</sup>C-NMR (100 MHz, CD<sub>3</sub>OD): δ, 170.0, 163.8, 158.3, 154.7, 151.7, 128.2, 112.4, 106.9,

98.2, 85.3, 83.1, 80.2, 78.8, 63.2, 46.2 ppm. HRMS (ESI):  $m/z$   $[M + H]^+$  calcd for  $C_{16}H_{19}N_2O_7$ : 351.11927; found 351.11826.

**7-((((2R,3S,4S,5R)-3,4-Dihydroxy-5-(hydroxymethyl)tetrahydrofuran-2-yl)methyl)amino)-N-methyl-2-oxo-2H-chromene-4-carboxamide (ManCou11):**  $^1H$ -NMR (400 MHz,  $CD_3OD$ ):  $\delta$ , 7.46-7.44 (d,  $J = 8.8$ , 1H), 6.69-6.66 (dd,  $J_1 = 2.4$ ,  $J_2 = 8.8$ , 1H), 6.56 (d,  $J = 2.4$ , 1H), 6.04 (s, 1H), 4.02-3.92 (m, 3H), 3.88-3.84 (m, 1H), 3.73-3.69 (app dd,  $J_1 = 3.6$ ,  $J_2 = 11.6$ , 1H), 3.65-3.61 (app dd,  $J_1 = 5.6$ ,  $J_2 = 11.6$ , 1H), 3.49-3.45 (app dd,  $J_1 = 3.6$ ,  $J_2 = 13.6$ , 1H), 3.39-3.33 (app dd,  $J_1 = 6.4$ ,  $J_2 = 13.6$ , 1H), 2.92 (s, 3H) ppm.  $^{13}C$ -NMR (100 MHz,  $CD_3OD$ ):  $\delta$ , 168.4, 163.9, 158.4, 154.8, 151.9, 128.3, 112.4, 107.1, 98.3, 85.3, 83.2, 80.3, 78.8, 63.3, 46.2, 26.5 ppm. HRMS (ESI):  $m/z$   $[M + H]^+$  calcd for  $C_{17}H_{21}N_2O_7$ : 365.13492; found 365.13368.

**7-((((2R,3S,4S,5R)-3,4-Dihydroxy-5-(hydroxymethyl)tetrahydrofuran-2-yl)methyl)amino)-2-oxo-N-phenyl-2H-chromene-4-carboxamide (ManCou12):**  $^1H$ -NMR (400 MHz,  $CD_3OD$ ):  $\delta$ , 7.70-7.67 (m, 2H), 7.50-7.47 (d,  $J = 9.2$ , 1H), 7.40-7.35 (m, 2H), 7.21-7.16 (m, 1H), 6.71-6.68 (dd,  $J_1 = 2.4$ ,  $J_2 = 8.8$ , 1H), 6.59-6.58 (d,  $J = 2.4$ , 1H), 6.18 (s, 1H), 4.02-3.98 (m, 2H), 3.95-3.93 (app dd,  $J_1 = 5.2$ ,  $J_2 = 6.0$ , 1H), 3.88-3.85 (m, 1H), 3.73-3.69 (app dd,  $J_1 = 3.6$ ,  $J_2 = 12.0$ , 1H), 3.65-3.61 (app dd,  $J_1 = 5.6$ ,  $J_2 = 12.0$ , 1H), 3.50-3.45 (app dd,  $J_1 = 3.6$ ,  $J_2 = 14.0$ , 1H), 3.40-3.34 (app dd,  $J_1 = 6.8$ ,  $J_2 = 14.0$ , 1H) ppm.  $^{13}C$ -NMR (100 MHz,  $CD_3OD$ ):  $\delta$ , 165.7, 163.7, 158.3, 154.7, 151.7, 139.0, 129.9, 128.0, 126.0, 121.6, 112.4, 107.01, 106.95, 98.3, 85.3, 83.1, 80.2, 78.8, 63.2, 46.2 ppm. HRMS (ESI):  $m/z$   $[M + H]^+$  calcd for  $C_{23}H_{23}N_2O_7$ : 427.15057; found 427.15000.

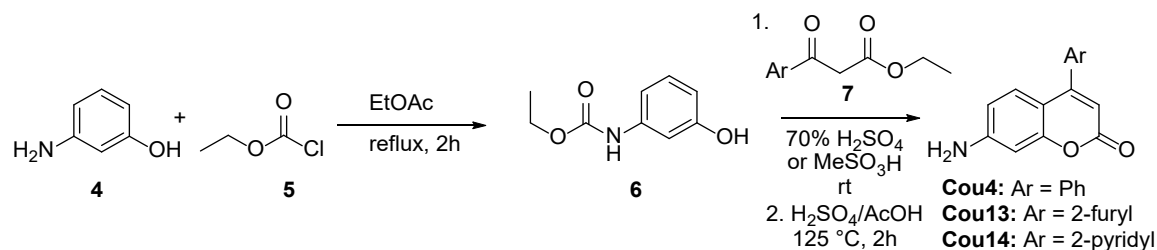
**7-((((2R,3S,4S,5R)-3,4-Dihydroxy-5-(hydroxymethyl)tetrahydrofuran-2-yl)methyl)amino)-4-(furan-2-yl)-2H-chromen-2-one (ManCou13):** <sup>1</sup>H-NMR (400 MHz, CD<sub>3</sub>OD): δ, 7.92-7.90 (d, *J* = 8.8, 1H), 7.81-7.80 (dd, *J*<sub>1</sub> = 0.4, *J*<sub>2</sub> = 1.6, 1H), 7.17-7.16 (dd, *J*<sub>1</sub> = 0.4, *J*<sub>2</sub> = 3.6, 1H), 6.70-6.67 (m, 2H), 6.54-6.53 (d, *J* = 2.4, 1H), 6.24 (s, 1H), 4.04-4.00 (m, 2H), 3.97-3.44 (app dd, *J*<sub>1</sub> = 5.2, *J*<sub>2</sub> = 6.0, 1H), 3.90-3.87 (m, 1H), 3.74-3.70 (app dd, *J*<sub>1</sub> = 3.6, *J*<sub>2</sub> = 12.0, 1H), 3.67-3.62 (app dd, *J*<sub>1</sub> = 5.6, *J*<sub>2</sub> = 12.0, 1H), 3.49-3.44 (app dd, *J*<sub>1</sub> = 3.6, *J*<sub>2</sub> = 14.0, 1H), 3.39-3.34 (app dd, *J*<sub>1</sub> = 6.8, *J*<sub>2</sub> = 14.0, 1H) ppm. <sup>13</sup>C-NMR (100 MHz, CD<sub>3</sub>OD): δ, 164.5, 158.1, 154.1, 150.2, 146.5, 144.6, 128.4, 115.5, 113.3, 112.3, 107.0, 104.3, 98.5, 85.3, 83.1, 80.2, 78.8, 63.3, 46.2 ppm. HRMS (ESI): *m/z* [M + H]<sup>+</sup> calcd for C<sub>19</sub>H<sub>20</sub>NO<sub>7</sub>: 374.12401; found 374.12338.

**7-((((2R,3S,4S,5R)-3,4-Dihydroxy-5-(hydroxymethyl)tetrahydrofuran-2-yl)methyl)amino)-4-(pyridin-2-yl)-2H-chromen-2-one (ManCou14):** <sup>1</sup>H-NMR (400 MHz, CD<sub>3</sub>OD): δ, 8.71-8.69 (ddd, *J*<sub>1</sub> = 1.2, *J*<sub>2</sub> = 1.6, *J*<sub>3</sub> = 5.2, 1H), 8.02-7.98 (dt, *J*<sub>1</sub> = 1.6, *J*<sub>2</sub> = 8.0, 1H), 7.66-7.64 (d, *J* = 8.0, 1H), 7.56-7.53 (ddd, *J*<sub>1</sub> = 0.8, *J*<sub>2</sub> = 5.2, *J*<sub>3</sub> = 8.0, 1H), 7.30-7.28 (d, *J* = 8.8, 1H), 6.63-6.60 (app dd, *J*<sub>1</sub> = 2.4, *J*<sub>2</sub> = 8.8, 1H), 6.59 (d, *J* = 2.4, 1H), 6.09 (s, 1H), 4.02-3.99 (m, 2H), 3.96-3.93 (m, 1H), 3.89-3.85 (m, 1H), 3.73-3.69 (app dd, *J*<sub>1</sub> = 3.6, *J*<sub>2</sub> = 12.0, 1H), 3.66-3.61 (app dd, *J*<sub>1</sub> = 5.6, *J*<sub>2</sub> = 12.0, 1H), 3.48-3.44 (app dd, *J*<sub>1</sub> = 3.6, *J*<sub>2</sub> = 14.0, 1H), 3.38-3.33 (app dd, *J*<sub>1</sub> = 6.8, *J*<sub>2</sub> = 14.0, 1H) ppm. <sup>13</sup>C-NMR (100 MHz, CD<sub>3</sub>OD): δ, 164.0, 158.2, 155.7, 155.6, 154.3, 150.3, 139.0, 128.8, 125.6, 125.5, 112.2, 109.0, 108.8, 98.3, 85.2, 83.1, 80.2, 78.8, 63.2, 46.2 ppm. HRMS (ESI): *m/z* [M + H]<sup>+</sup> calcd for C<sub>20</sub>H<sub>21</sub>N<sub>2</sub>O<sub>6</sub>: 385.14000; found 385.13907.

## Synthesis of Coumarins



7-Aminocoumarin (**Cou1**) was synthesized according to the reported procedure.<sup>12</sup>



**Scheme S3:** Synthesis of C4-aryl coumarins **Cou4** and **Cou13-14**.

**(3-Hydroxyphenyl)carbamic acid ethyl ester (6):**<sup>29</sup> This compound was synthesized according to the reported procedure.<sup>29</sup> 3-Aminophenol **4** (10.0 g, 91.6 mmol) and ethyl acetate (350 ml) were refluxed for 1 hour with vigorous stirring. Ethyl chloroformate **5** (11.92 g, 109.9 mmol) was then added via addition funnel over a 30 minute period. The reaction mixture was refluxed for an additional hour and then allowed to cool to room temperature. Upon cooling a grey/white precipitate formed within the flask. The precipitate was removed via filtration, and washed with ethyl acetate (3 x 150 ml). The combined filtrates were concentrated to afford **6** as a grey solid (9.46 g, 57%) that was used without further purification. <sup>1</sup>H-NMR (400 MHz, DMSO-d<sub>6</sub>): δ, 9.45 (s, 1H), 9.29 (bs, 1H), 7.04-7.00 (m, 2H), 6.86-6.84 (m, 1H), 6.39-6.36 (ddd,  $J_1 = 1.2, J_2 = 2.4, J_3 = 8.0$ , 1H), 4.12-4.07 (q,  $J = 7.2$ , 2H), 1.24-1.21 (t,  $J = 7.2$ , 3H) ppm.

**7-Amino-4-phenyl-2H-chromen-2-one (Cou4):**<sup>23</sup> This compound was synthesized according to the reported procedure.<sup>23</sup> **6** (1.00 g, 5.52 mmol) and ethyl benzoylacetate (1.27g, 6.62 mmol) were added to a 100 ml round-bottom flask equipped with a stir bar. 70% H<sub>2</sub>SO<sub>4</sub> (30 ml) was added and the mixture was stirred at room

temperature. More 70% H<sub>2</sub>SO<sub>4</sub> was added until the reaction mixture turned from yellow/cloudy to amber/clear and then stirring was maintained overnight at room temperature. The reaction mixture was then poured over 100 ml of crushed ice to give a bright yellow precipitate. The solid was filtered and recrystallized from hot methanol to afford clear large crystals of **Cou4-precursor** (0.717g, 42%). <sup>1</sup>H-NMR (400 MHz, DMSO-d<sub>6</sub>): δ, 10.14 (s, 1H), 7.62-7.61 (d, *J* = 2.4, 1H), 7.54-7.48 (m, 5H), 7.36-7.30 (m, 2H), 6.20 (s, 1H), 4.18-4.13 (q, *J* = 7.2, 2H), 1.27-1.24 (t, *J* = 7.2, 3H) ppm.

**Cou4-precursor** (0.408 g, 1.32 mmol) was added to a 50 ml round-bottom flask, followed by H<sub>2</sub>SO<sub>4</sub> conc. (5 ml) and glacial AcOH (5 ml). The reaction mixture was heated to 125 °C for 2 hours under reflux condenser, after which it was cooled to room temperature and poured over 50 ml of crushed ice. The resulting suspension was neutralized till weakly basic using 4M NaOH, affording a yellow precipitate. The precipitate was filtered and recrystallized from hot methanol to give **Cou4** as a fine yellow powder (0.175 g, 56%). <sup>1</sup>H-NMR (400 MHz, DMSO-d<sub>6</sub>): δ, 7.54-7.46 (m, 5H), 7.09-7.07 (d, *J* = 8.8, 1H), 6.54-6.51 (app dd, *J*<sub>1</sub> = 2.0, *J*<sub>2</sub> = 8.8, 1H), 6.50 (d, *J* = 2.0, 1H), 6.24 (bs, 2H), 5.90 (s, 1H) ppm. <sup>13</sup>C-NMR (100 MHz, DMSO-d<sub>6</sub>): δ, 160.3, 156.0, 155.6, 153.1, 135.5, 129.2, 128.6, 128.1, 127.6, 111.3, 107.2, 107.0, 98.8 ppm. HRMS (ESI): *m/z* [M + H]<sup>+</sup> calcd for C<sub>15</sub>H<sub>12</sub>NO<sub>2</sub>: 238.08681; found 238.08597.

**7-Amino-4-(furan-2-yl)-2H-chromen-2-one (Cou13)**: This compound was synthesized according to the reported general procedure.<sup>30</sup> **6** (1.00g, 5.52 mmol) and 3-furan-2-yl-3-oxo-propionic acid ethyl ester (1.27 g, 6.62 mmol) were added to a 50 ml round-bottom flask equipped with a stir bar. Methanesulfonic acid (10 ml) was added and

the mixture was stirred at room temperature for overnight while the colour turned from clear/amber to black. The reaction mixture was then poured over 50 ml of ice water. It was then extracted with ethyl acetate (3 x 75 ml), and the combined organics were washed with brine (2 x 50 ml) and dried over Na<sub>2</sub>SO<sub>4</sub>. After filtration and concentration, a brown solid was obtained which was then recrystallized from hot methanol to afford **Cou13-precursor** as grey-black crystals (0.446 g, 27 %). <sup>1</sup>H-NMR (400 MHz, DMSO-d<sub>6</sub>): δ, 10.18 (s, 1H), 8.16-8.14 (d, *J* = 8.8, 1H), 8.05-8.04 (d, *J* = 1.6, 1H), 7.59 (d, *J* = 2.0, 1H), 7.47-7.46 (d, *J* = 3.6, 1H), 7.44-7.42 (dd, *J*<sub>1</sub> = 2.0, *J*<sub>2</sub> = 8.8, 1H), 6.80-6.78 (dd, *J*<sub>1</sub> = 1.6, *J*<sub>2</sub> = 3.6, 1H), 6.53 (s, 1H), 4.20-4.14 (q, *J* = 7.2, 2H), 1.28-1.25 (t, *J* = 7.2, 3H) ppm. <sup>13</sup>C-NMR (100 MHz, DMSO-d<sub>6</sub>): δ, 159.8, 154.6, 153.1, 147.6, 146.2, 142.8, 140.9, 127.0, 115.3, 114.3, 112.7, 110.0, 107.6, 104.7, 60.7, 14.4 ppm.

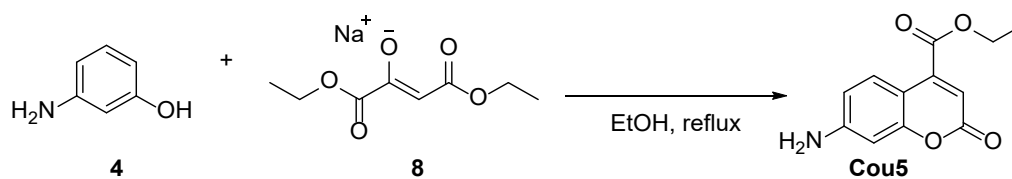
**Cou13-precursor** (1.00 g, 3.34 mmol) was added to a 50 ml round-bottom flask, followed by H<sub>2</sub>SO<sub>4</sub> conc. (5 ml) and glacial AcOH (5 ml). The reaction mixture was heated to 125 °C for 2 hours under reflux condenser, after which it was cooled to room temperature and poured over 50 ml of crushed ice. The resulting suspension was neutralized till weakly basic using 4M NaOH, extracted with ethyl acetate (3 x 75 ml) and dried over Na<sub>2</sub>SO<sub>4</sub>. After filtration and concentration, the residue was purified by column chromatography on silica gel (dry loading), eluting with 40-100% EtOAc in hexanes, followed by 5% MeOH in EtOAc. The residue was triturated with hexanes containing little CH<sub>2</sub>Cl<sub>2</sub>. The product was filtered, washed with hexanes and dried in air to obtain **Cou13** as a yellow-brown powder (0.11 g, 14%). <sup>1</sup>H-NMR (400 MHz, DMSO-d<sub>6</sub>): δ, 8.02 (s, 1H), 7.92-7.90 (d, *J* = 8.4, 1H), 7.36 (s, 1H), 6.76 (s, 1H), 6.63-6.61 (d, *J* = 8.4, 1H), 6.48 (s, 1H), 6.26 (bs, 2H),

6.24 (s, 1H) ppm.  $^{13}\text{C}$ -NMR (100 MHz, DMSO- $d_6$ ):  $\delta$ , 160.7, 156.4, 153.2, 148.6, 145.9, 142.0, 127.5, 114.7, 112.6, 111.6, 104.6, 103.3, 99.1 ppm. HRMS (ESI):  $m/z$   $[\text{M} + \text{H}]^+$  calcd for  $\text{C}_{13}\text{H}_{10}\text{NO}_3$ : 228.06608; found 228.06500.

**7-Amino-4-(pyridin-2-yl)-2H-chromen-2-one (Cou14):** This compound was synthesized according to the reported general procedure.<sup>30</sup> **6** (2.00 g, 11.03 mmol) and ethyl 3-oxo-3-(pyridin-2-yl)propanoate (2.56 g, 13.24 mmol) were added to a 50 ml round-bottom flask with a stir bar. Methanesulfonic acid (10 ml) was added and the mixture was stirred at room temperature for overnight while the color turned from clear/amber to black. The reaction mixture was then poured over 50 ml of ice water. It was then extracted with ethyl acetate (3 x 75 ml), and the combined organics were washed with brine (2 x 50 ml) and dried over  $\text{Na}_2\text{SO}_4$ . After filtration and concentration, a grey solid was obtained which was then recrystallized from hot methanol to afford **Cou14-precursor** as fine white crystals of 1 : 1 MeOH solvate (1.403 g, 41 %).  $^1\text{H}$ -NMR (400 MHz, DMSO- $d_6$ ):  $\delta$ , 10.17 (s, 1H), 8.78-8.76 (ddd,  $J_1 = 1.2$ ,  $J_2 = 2.0$ ,  $J_3 = 8.8$ , 1H), 8.03-8.00 (dt,  $J_1 = 2.0$ ,  $J_2 = 8.0$ , 1H), 7.77-7.75 (m, 1H), 7.70-7.68 (d,  $J = 8.8$ , 1H), 7.64-7.63 (d,  $J = 2.0$ , 1H), 7.58-7.54 (m, 1H), 7.36-7.34 (dd,  $J_1 = 2.0$ ,  $J_2 = 8.8$ , 1H), 4.19-4.14 (q,  $J = 7.2$ , 2H), 4.11-4.07 (q,  $J = 5.2$ , 1H), 3.18-3.16 (d,  $J = 5.2$ , 3H), 1.28-1.24 (t,  $J = 7.2$ , 3H) ppm.  $^{13}\text{C}$ -NMR (100 MHz, DMSO- $d_6$ ):  $\delta$ , 159.8, 154.6, 153.3, 153.1, 152.2, 149.3, 142.8, 137.5, 127.8, 124.4, 124.2, 114.1, 112.7, 112.0, 104.6, 60.7, 48.6, 14.4 ppm.

**Cou14-precursor** (0.50 g, 1.61 mmol) was added to a 50 ml round-bottom flask, followed by  $\text{H}_2\text{SO}_4$  conc. (5 ml) and glacial AcOH (5 ml). The reaction mixture was heated to 125 °C for 2 hours under reflux condenser, after which it was cooled to room temperature

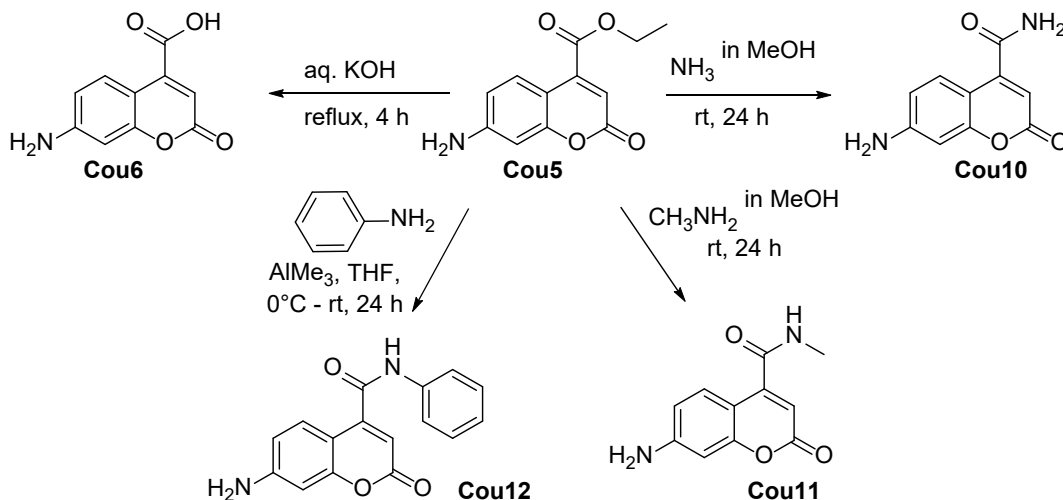
and poured over 50 ml of crushed ice. The resulting suspension was neutralized till weakly basic using 4M NaOH, affording a beige precipitate. The precipitate was filtered and recrystallized from hot methanol to give **Cou14** as fine yellow crystals (0.162 g, 68%). <sup>1</sup>H-NMR (400 MHz, CD<sub>3</sub>OD):  $\delta$ , 8.72-8.70 (ddd,  $J_1 = 1.2$ ,  $J_2 = 1.6$ ,  $J_3 = 4.8$ , 1H), 8.04-8.00 (dt,  $J_1 = 2.0$ ,  $J_2 = 8.0$ , 1H), 7.69-7.66 (dt,  $J_1 = 1.2$ ,  $J_2 = 8.0$ , 1H), 7.58-7.54 (ddd,  $J_1 = 0.8$ ,  $J_2 = 4.8$ ,  $J_3 = 8.0$ , 1H), 7.29-7.26 (app dd,  $J_1 = 3.2$ ,  $J_2 = 6.4$ , 1H), 6.60-6.57 (m, 2H), 6.11 (s, 1H) ppm. <sup>13</sup>C-NMR (100 MHz, CD<sub>3</sub>OD):  $\delta$ , 164.1, 158.2, 156.0, 155.8, 155.0, 150.5, 139.2, 129.2, 125.7, 125.6, 113.2, 109.2, 109.1, 100.7 ppm. HRMS (ESI):  $m/z$  [M + H]<sup>+</sup> calcd for C<sub>14</sub>H<sub>11</sub>N<sub>2</sub>O<sub>2</sub>: 239.08207; found 239.08078.



**Scheme 4:** Synthesis of **Cou5**.

**Ethyl 7-amino-2-oxo-2H-chromene-4-carboxylate (Cou5):**<sup>31</sup> 3-Aminophenol (**4**) (5.00 g, 45.8 mmol), diethyl oxaloacetate sodium salt (**8**) (14.4 g, 68.7 mmol) and EtOH (20 ml) were heated at reflux overnight. The mixture was cooled and concentrated to dryness and the residue was purified by silica gel chromatography (50% EtOAc in hexanes). **Cou5** was obtained as a yellow-orange solid (4.17 g, 39%). <sup>1</sup>H-NMR (400 MHz, DMSO-d<sub>6</sub>):  $\delta$ , 7.69-7.66 (d,  $J = 8.8$ , 1H), 6.60-6.57 (dd,  $J_1 = 2.4$ ,  $J_2 = 8.8$ , 1H), 6.46-6.45 (d,  $J = 2.4$ , 1H), 6.37 (bs, 2H), 6.31 (s, 1H), 4.39-4.33 (q,  $J = 7.2$ , 1H), 1.35-1.31 (t,  $J = 7.2$ , 1H) ppm. <sup>13</sup>C-NMR (100 MHz, DMSO-d<sub>6</sub>):  $\delta$ , 164.3, 160.3, 156.5, 153.6, 143.8,

127.4, 111.8, 109.2, 104.4, 98.8, 62.0, 13.9 ppm. HRMS (ESI):  $m/z$   $[M + H]^+$  calcd for  $C_{12}H_{12}NO_4$ : 234.07665; found 234.07600.



**Scheme 5:** Synthesis of **Cou6** and **Cou10-12**.

**7-Amino-2-oxo-2H-chromene-4-carboxylic acid (Cou6):** Ethyl 7-amino-2-oxo-2H-chromene-4-carboxylate (**Cou5**) (1.00 g, 4.30 mmol) and 2M KOH solution (25 ml) were added to the flask and refluxed for 4 h. After cooling, the reaction mixture was washed with AcOEt (25 ml, discarded). AcOH was used to neutralize the solution that was concentrated to dryness. The residue was purified by column chromatography on silica gel, eluting with water: isopropanol: EtOAc mixtures (1 : 2 : 7 to 2 : 4 : 4). The residue was triturated with  $CH_2Cl_2$  containing little EtOH, and then refluxed in  $CHCl_3$  overnight. The product was filtered, washed with  $CHCl_3$  and dried in air to obtain orange solid (0.38 g, 43%) in satisfying purity.  $^1H$ -NMR (400 MHz, DMSO- $d_6$ ):  $\delta$ , 7.73-7.70 (d,  $J = 8.8$ , 1H), 6.53-6.50 (dd,  $J_1 = 2.0$ ,  $J_2 = 8.8$ , 1H), 6.40 (d,  $J = 2.0$ , 1H), 5.93 (s, 1H) ppm.  $^{13}C$ -NMR

(100 MHz, DMSO- $d_6$ ):  $\delta$ , 167.1, 161.6, 156.3, 152.6, 128.6, 111.0, 106.2, 104.8, 98.4 ppm.

HRMS (ESI):  $m/z$   $[M + H]^+$  calcd for  $C_{10}H_8NO_4$ : 206.04535; found 206.04487.

**7-Amino-2-oxo-2H-chromene-4-carboxamide (Cou10):** This compound was synthesized according to the modified general procedure.<sup>32</sup> **Cou5** (1.00 g, 4.30 mmol) was placed in the flame-dried flask under the flow of Ar. Then 7N  $NH_3$  in absolute MeOH (20 ml) was added and the mixture was allowed to react at room temperature under Ar for 24 h. Then the mixture was concentrated to dryness. The residue was purified by column chromatography on silica gel, eluting with 100%  $CH_2Cl_2$  to 100% EtOAc, followed by 10-40% MeOH in EtOAc. The residue was triturated with  $CH_2Cl_2$ , and filtered washing sequentially with  $CH_2Cl_2$ , water, ethanol, again  $CH_2Cl_2$  and dried in air. The product was obtained as a yellow solid (0.12 g, 14%).  $^1H$ -NMR (400 MHz, DMSO- $d_6$ ):  $\delta$ , 8.16 (bs, 1H), 7.83 (bs, 1H), 7.43-7.41 (d,  $J = 8.8$ , 1H), 6.57-6.55 (dd,  $J_1 = 2.0$ ,  $J_2 = 8.8$ , 1H), 6.44 (d,  $J = 2.0$ , 1H), 6.27 (bs, 2H), 5.99 (s, 1H) ppm.  $^{13}C$ -NMR (100 MHz, DMSO- $d_6$ ):  $\delta$ , 166.8, 160.8, 156.4, 153.5, 150.2, 127.6, 111.6, 105.5, 105.0, 98.7 ppm. HRMS (ESI):  $m/z$   $[M + H]^+$  calcd for  $C_{10}H_9N_2O_3$ : 205.06134; found 205.06064.

**7-Amino-N-methyl-2-oxo-2H-chromene-4-carboxamide (Cou11):** This compound was synthesized according to the modified general procedure.<sup>32</sup> **Cou5** (1.00 g, 4.30 mmol) was placed in the flame-dried flask under the flow of Ar. 33 wt. %  $CH_3NH_2$  in MeOH (20 ml) was added and the mixture was allowed to react at room temperature under Ar for 24 h. Then the mixture was concentrated to dryness. The residue was purified by column chromatography on silica gel, eluting with 50-100% EtOAc in hexanes, followed by 10% MeOH in EtOAc. The residue was stirred overnight in  $CH_2Cl_2$ /EtOAc, filtered,

washed with CH<sub>2</sub>Cl<sub>2</sub> and dried in air. The product was obtained as a yellow solid (0.08 g, 9%). <sup>1</sup>H-NMR (400 MHz, DMSO-d<sub>6</sub>): δ, 8.66 (d, *J* = 4.0, 1H), 7.38-7.36 (d, *J* = 8.8, 1H), 6.56-6.54 (d, *J* = 8.8, 1H), 6.44 (s, 1H), 6.28 (bs, 2H), 5.98 (s, 1H), 2.77 (d, *J* = 4.0, 3H) ppm. <sup>13</sup>C-NMR (100 MHz, DMSO-d<sub>6</sub>): δ, 165.0, 160.5, 156.2, 153.4, 150.0, 127.5, 111.5, 105.6, 105.0, 98.6, 25.8 ppm. HRMS (ESI): *m/z* [M + H]<sup>+</sup> calcd for C<sub>11</sub>H<sub>11</sub>N<sub>2</sub>O<sub>3</sub>: 219.07699; found 219.07602.

**7-Amino-2-oxo-*N*-phenyl-2*H*-chromene-4-carboxamide (Cou12):** This compound was synthesized according to the modified general procedure.<sup>33</sup> A solution of aniline (0.729 ml, 8 mmol) in dry THF (20 ml) was cooled to 0 °C under Ar and a commercial 2.0 M solution of trimethylaluminum in hexanes (10 ml, 20 mmol) was added dropwise over 10 minutes. Then, to the resulting mixture a solution of **Cou5** (0.932 g, 4 mmol) in dry THF (40 ml) was added dropwise over 20 minutes at 0 °C. The mixture was allowed to warm to rt and stirred for overall 22 h. It was diluted with EtOAc (100 ml) and carefully neutralized with aq. NH<sub>4</sub>Cl (100 ml) with vigorous stirring. The phases were separated, and the aqueous phase was additionally extracted with EtOAc (100 ml). The combined organic extracts were washed with brine (50 ml) and dried over MgSO<sub>4</sub>. After filtration and concentration, the residue was purified by column chromatography on silica gel, eluting with 0-80% EtOAc in hexanes. The product was further purified by recrystallization from EtOAc and filtered washing copiously with CH<sub>2</sub>Cl<sub>2</sub> to obtain an orange solid (0.165 g, 14%). <sup>1</sup>H-NMR (400 MHz, DMSO-d<sub>6</sub>): δ, 10.7 (bs, 1H), 7.74-7.72 (d, *J* = 8.0, 2H), 7.39-7.36 (m, 3H), 7.16-7.13 (t, *J* = 7.2, 1H), 6.60-6.58 (d, *J* = 8.0, 1H), 6.49 (s, 1H), 6.34 (bs, 2H), 6.20 (s, 1H) ppm. <sup>13</sup>C-NMR (100 MHz, DMSO-d<sub>6</sub>): δ, 163.2,



160.5, 156.2, 153.5, 149.6, 138.2, 128.7, 127.2, 124.2, 119.9, 111.7, 105.8, 104.8, 98.6 ppm. HRMS (ESI):  $m/z$   $[M + H]^+$  calcd for  $C_{16}H_{13}N_2O_3$ : 281.09264; found 281.09189.

### **Cell Imaging**

For confocal microscopy cells were plated (100,000/plate) in 35 mm glass-bottom confocal dishes (MatTek) and allowed to grow in their respective growth media for 24 hours. For optical microscope analysis cells were plated in a 6-well plates (3 x 10<sup>5</sup>) and allowed to adhere and grow for 24 h. For treatment, cell media was removed and ManCou solution in PBS (1 ml) was added. Cells were incubated with ManCous at 37 °C for 10 min. After incubation, probe solution was removed, and cells were washed with warmed PBS (3 x 1 ml) and leaving 1 ml of PBS for imaging. Cell images were taken using Olympus FluoView™ FV1000 using the FluoView software. 60X oil suspended lens was used to observe fluorescent activity with the following conditions: DAPI (ManCous) and eGFP (NBDM and NBDG) filters; lasers 405 nm (45% intensity), 450/490 nm (30% intensity); 10 μs/pixel. Z-stacking was done using FluoView software and depth command.

### **Microplate uptake and inhibition assays**

For microplate assays, at ~80% confluence cells were collected and plated in 96-well flat bottom plates (20,000 cells/well) and allowed to grow for 24 hours. Cells were then washed with warmed (37 °C) PBS solution, treated with ManCou probes (concentration varies) in PBS and incubated at 37 °C and 5% CO<sub>2</sub> for 10 min. After incubation, cells were carefully washed with warmed PBS (3 x 100 μl). Fluorescent data were immediately collected using

Victor3 plate reader and using Wallac™ umbelliferone (excitation 355 nm, emission 460 nm, 1.0 s) protocol. All trials were done in triplicate on each plate.

Uptake Inhibition studies were carried out in microplate format. Using 96-well plate method fluorescence of ManCou probes in cells was measured in the presence of varying concentrations of fructose, glucose, glucosamine, and cytochalasin B. For this part, PBS solution containing 20  $\mu$ M ManCou and the specific concentration of a sugar were prepared and introduced to cells. Separately, complete culture media were used to establish the impact of nutrients on ManCou uptake. Cell incubation, and data collection were conducted as stated above.

## References

1. Tanasova, M.; Begoyan, V. V.; Weselinski, L. J., Targeting Sugar Uptake and Metabolism for Cancer Identification and Therapy: An Overview. *Curr. Top. Med. Chem.* **2018**, *18* (6), 467-483.
2. McQuade, D. T.; Plutschack, M. B.; Seeberger, P. H., Passive fructose transporters in disease: a molecular overview of their structural specificity. *Org. Biomol. Chem.* **2013**, *11* (30), 4909-4920.
3. Tanasova, M.; Fedie, J. R., Molecular Tools for Facilitative Carbohydrate Transporters (Gluts). *ChemBioChem* **2017**, *18* (18), 1774-1788.
4. Colville, C. A.; Seatter, M. J.; Jess, T. J.; Gould, G. W.; Thomas, H. M., Kinetic-Analysis of the Liver-Type (Glut2) and Brain-Type (Glut3) Glucose Transporters in *Xenopus* Oocytes - Substrate Specificities and Effects of Transport Inhibitors. *Biochem. J.* **1993**, *290*, 701-706.
5. Colville, C. A.; Seatter, M. J.; Gould, G. W., Analysis of the Structural Requirements of Sugar Binding to the Liver, Brain and Insulin-Responsive Glucose Transporters Expressed in Oocytes. *Biochem. J.* **1993**, *294*, 753-760.
6. Tatibouet, A.; Yang, J.; Morin, C.; Holman, G. D., Synthesis and evaluation of fructose analogues as inhibitors of the D-fructose transporter GLUT5. *Bioorgan. Med. Chem.* **2000**, *8* (7), 1825-1833.
7. Yang, J.; Tatibouet, A.; Hatanaka, Y.; Holman, G. D., Fructose analogues with enhanced affinity for GLUT5. *Diabetes* **2001**, *50*, A277-A277.

8. Yang, J.; Dowden, J.; Tatibouet, A.; Hatanaka, Y.; Holman, G. D., Development of high-affinity ligands and photoaffinity labels for the D-fructose transporter GLUT5. *Biochem. J.* **2002**, *367*, 533-539.
9. Girniene, J.; Tatibouet, A.; Sackus, A.; Yang, J.; Holman, G. D.; Rollin, P., Inhibition of the D-fructose transporter protein GLUT5 by fused-ring glyco-1,3-oxazolidin-2-thiones and -oxazolidin-2-ones. *Carbohydr. Res.* **2003**, *338* (8), 711-719.
10. Tatibouet, A.; Lefoix, M.; Nadolny, J.; Martin, O. R.; Rollin, P.; Yang, J.; Holman, G. D., D-Fructose-L-sorbose interconversions. Access to 5-thio-D-fructose and interaction with the D-fructose transporter, GLUT5. *Carbohydr. Res.* **2001**, *333* (4), 327-334.
11. Otsuka, Y.; Sasaki, A.; Teshima, T.; Yamada, K.; Yamamoto, T., Syntheses of D-Glucose Derivatives Emitting Blue Fluorescence through Pd-Catalyzed C-N Coupling. *Org. Lett.* **2016**, *18* (6), 1338-41.
12. Yu, J. Z.; Wang, Y. T.; Zhang, P. Z.; Wu, J., Direct Amination of Phenols under Metal-Free Conditions. *Synlett* **2013**, *24* (11), 1448-1454.
13. Uldry, M.; Ibberson, M.; Hosokawa, M.; Thorens, B., GLUT2 is a high affinity glucosamine transporter. *FEBS Lett.* **2002**, *524* (1-3), 199-203.
14. Thompson, G.; M., A.; Ursu, O.; Babkin, P.; Iancu, C. V.; Whang, A.; Oprea, T. I.; Choe, J.-Y., Discovery of a specific inhibitor of human GLUT5 by virtual screening and in vitro transport evaluation. *Sci. Rep.* **2016**, *6*, 24240-24248.

15. Nomura, N.; Verdon, G.; Kang, H. J.; Shimamura, T.; Nomura, Y.; Sonoda, Y.; Hussien, S. A.; Qureshi, A. A.; Coincon, M.; Sato, Y.; Abe, H.; Nakada-Nakura, Y.; Hino, T.; Arakawa, T.; Kusano-Arai, O.; Iwanari, H.; Murata, T.; Kobayashi, T.; Hamakubo, T.; Kasahara, M.; Iwata, S.; Drew, D., Structure and mechanism of the mammalian fructose transporter GLUT5. *Nature* **2015**, *526* (7573), 397-401.
16. Ainsley, J.; Chaturvedi, S. S.; Karabancheva-Christova, T. G.; Tanasova, M.; Christov, C. Z., Integrating molecular probes and molecular dynamics to reveal binding modes of GLUT5 activatory and inhibitory ligands. *Chem. Commun.* **2018**, *54* (71), 9917-9920.
17. Case, D. A.; Babin, V.; Berryman, J. T.; Betz, R. M.; Cai, Q.; Cerutti, D. S.; Cheatham, T. E. I.; Darden, T. A.; Duke, R. E.; Gohlke, H.; Goetz, A. W.; Gusarov, S.; Homeyer, N.; Janowski, P.; Kaus, J.; Kolossváry, I.; Kovalenko, A.; Lee, T. S.; LeGrand, S.; Luchko, T.; Luo, R.; Madej, B.; Merz, K. M.; Paesani, F.; Roe, D. R.; Roitberg, A.; Sagui, C.; Salomon Ferrer, R.; Seabra, G.; Simmerling, C. L.; Smith, W.; Swails, J.; Walker, R. C.; Wang, J.; Wolf, R. M.; Wu, X.; Kollman, P. A., Amber 14. University of California, San Francisco, 2014.
18. Maier, J. A.; Martinez, C.; Kasavajhala, K.; Wickstrom, L.; Hauser, K. E.; Simmerling, C., ff14SB: Improving the Accuracy of Protein Side Chain and Backbone Parameters from ff99SB. *J. Chem. Theory Comput.* **2015**, *11* (8), 3696-713.
19. Li, Q.; Manolescu, A.; Ritzel, M.; Yao, S.; Slugoski, M.; Young, J. D.; Chen, X. Z.; Cheeseman, C. I., Cloning and functional characterization of the human GLUT7

- isoform SLC2A7 from the small intestine. *Am. J. Physiol. Gastrointest. Liver Physiol.* **2004**, *287* (1), G236-G242.
20. Begoyan, V. V.; Weselinski, L. J.; Xia, S.; Fedie, J.; Kannan, S.; Ferrier, A.; Rao, S.; Tanasova, M., Multicolor GLUT5-permeable fluorescent probes for fructose transport analysis. *Chem. Commun.* **2018**, *54* (31), 3855-3858.
21. Liu, X. G.; Xu, Z. C.; Cole, J. M., Molecular Design of UV-vis Absorption and Emission Properties in Organic Fluorophores: Toward Larger Bathochromic Shifts, Enhanced Molar Extinction Coefficients, and Greater Stokes Shifts. *J. Phys. Chem. C* **2013**, *117* (32), 16584-16595.
22. see Supporting Information for details. *see Supporting Information for details.*
23. Reszka, P.; Schulz, R.; Methling, K.; Lalk, M.; Bednarski, P. J., Synthesis, Enzymatic Evaluation, and Docking Studies of Fluorogenic Caspase 8 Tetrapeptide Substrates. *ChemMedChem* **2010**, *5* (1), 103-117.
24. Kanaoka, Y.; Kobayashi, A.; Sato, E.; Nakayama, H.; Ueno, T.; Muno, D.; Sekine, T., Multifunctional cross-linking reagents. I. Synthesis and properties of novel photoactivable, thiol-directed fluorescent reagents. *Chem. Pharm. Bull.* **1984**, *32* (10), 3926-33.
25. Tasiar, M.; Deperasinska, I.; Morawska, K.; Banasiewicz, M.; Vakuliuk, O.; Kozankiewicz, B.; Gryko, D. T., Vertically [small pi]-expanded coumarin - synthesis via the Scholl reaction and photophysical properties. *Phys. Chem. Chem. Phys.* **2014**, *16* (34), 18268-18275.

26. Tanasova, M.; Plutschack, M.; Muroski, M. E.; Sturla, S. J.; Strouse, G. F.; McQuade, D. T., Fluorescent THF-Based Fructose Analogue Exhibits Fructose-Dependent Uptake. *ChemBioChem* **2013**, *14* (10), 1263-1270.
27. Cardona, F.; La Ferla, B., Synthesis of C-Glycoconjugates from Readily Available Unprotected C-Allyl Glycosides by Chemoselective Ligation. *J. Carbohydr. Chem.* **2008**, *27* (4), 203-213.
28. Beck, H. P.; Booker, S. K.; Bregman, H.; Cee, V. J.; Chakka, N.; Cushing, T. D.; Epstein, O.; Fox, B. M.; Geuns-Meyer, S.; Hao, X.; Hibiya, K.; Hirata, J.; Hua, Z.; Human, J.; Kakuda, S.; Lopez, P.; Nakajima, R.; Okada, K.; Olson, S. H.; Oono, H.; Pennington, L.; Sasaki, K.; Shimada, K.; Shin, Y.; White, R. D.; Wurz, R. P.; Yi, S.; Zheng, X. M. Pyrazole Amide Derivative. World Pat. Appl. 2015129926A1, 2015, 2015, 2015.
29. Maly, D. J.; Leonetti, F.; Backes, B. J.; Dauber, D. S.; Harris, J. L.; Craik, C. S.; Ellman, J. A., Expedient solid-phase synthesis of fluorogenic protease substrates using the 7-amino-4-carbamoylmethylcoumarin (ACC) fluorophore. *J. Org. Chem.* **2002**, *67* (3), 910-915.
30. Tasiar, M.; Deperasinska, I.; Morawska, K.; Banasiewicz, M.; Vakuliuk, O.; Kozankiewicz, B.; Gryko, D. T., Vertically pi-expanded coumarin - synthesis via the Scholl reaction and photophysical properties. *Phys. Chem. Chem. Phys.* **2014**, *16* (34), 18268-18275.

31. Sinev, M.; Landsmann, P.; Sineva, E.; Ittah, V.; Haas, E., Design consideration and probes for fluorescence resonance energy transfer studies. *Bioconjugate Chem.* **2000**, *11* (3), 352-362.
32. Pisani, L.; Barletta, M.; Soto-Otero, R.; Nicolotti, O.; Mendez-Alvarez, E.; Catto, M.; Introcaso, A.; Stefanachi, A.; Cellamare, S.; Altomare, C.; Carotti, A., Discovery, Biological Evaluation, and Structure–Activity and –Selectivity Relationships of 6'-Substituted (E)-2-(Benzofuran-3(2H)-ylidene)-N-methylacetamides, a Novel Class of Potent and Selective Monoamine Oxidase Inhibitors. *J. Med. Chem.* **2013**, *56* (6), 2651-2664.
33. Pelcman, B.; Sanin, A.; Nilsson, P.; Boesen, T.; Vogensen, S. B.; Kromann, H.; Groth, T. Pyrazoles Useful in the Treatment of Inflammation. World Pat. Appl. 2007045868A1, 2007, 2007, 2007.



### **3 Metabolism-driven High Throughput Cancer Identification with GLUT5-specific Molecular Probes**

#### **3.1 Introduction**

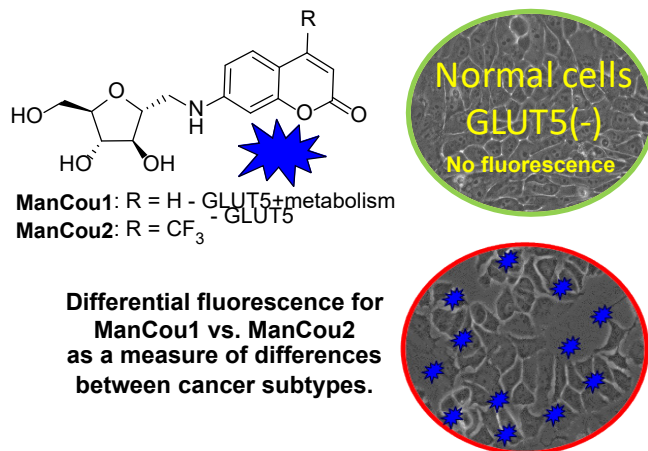
Point of care (POC) and POC-healthcare technologies (POCHT) that monitor changes in the intracellular mechanisms to report disease development have gained prominence in clinical and consumer implementations owing to the ease of access to information, low cost and self-management of health and wellbeing [1-5]. The marked improvement in microfluidics, molecular diagnostics, and nucleic acid chemistries [6-8] to identify cancer-relevant biomarkers [9] has led to an increased interest in POC/POCHT for cancer. However, the relatively low concentration of the biomarkers poses constraints on sensing, limiting the identification of the metastatic capability of the tumor, when present. The diagnosis currently heavily relies on various radiological techniques. Despite the advances to improve the resolution of radiological approaches, pathology reports of biopsy samples remain the sole means to identify cancer type and stage [10]. There exist discrepancies in diagnosis for the same sample owing to the highly heterogeneous nature of the tissue, subtle morphological changes, and the interpretation by the observer particularly when the sample deviates from key criteria used to classify breast tumors [11]. Any approach capable of identification of cancer cell population in the heterogeneous environment of the tumor is expected to be based on error-free cancer detection and diagnosis for development of cancer relevant POC technologies. Within this communication, a metabolism-driven approach for detection and identification of breast cancers is described. The difference in carbohydrate demands among different cells and cancer sub-populations forms the basis for the approach presented here.

The long-recognized higher energy demands in cancer cells [12,13] have led to the development of metabolism-based approach to detect cancer, with <sup>18</sup>F-2-deoxy-glucose being a widely used as PET-imaging cancer agent [14]. Until recently the major efforts in identifying cancer through metabolism changes have focused on targeting glucose uptake and the facilitative glucose transporter GLUT1 [15,16]. However, the global physiological need for glucose and ubiquitous presence of GLUT1 limits this strategy in sensitivity, selectivity, and specificity [17]. Targeting glucose transport is in particular limited for breast cancers, known to exhibit insignificant changes in glucose uptake with respect to their normal counterparts [18-20]. Recently, strong links between cancer and enhanced fructose uptake have been established, bringing forth fructose transport as a promising target to identify cancer on the basis of fructose uptake and metabolism [21]. For example, triple-negative breast cancer phenotypes have been reported to exhibit 8-10-fold higher fructose uptake than other phenotypes, with minimal fructose uptake measured for normal breast cells [22-24]. A particular dependence of cancer cells on fructose for growth and progression identified for breast cancers [25-27] has justified targeting fructose uptake as means to detect breast cancer. Moreover, the possibility to achieve high levels of specificity in detection is provided by the specific expression of fructose transporter GLUT5 in breast cancer cells but not normal breast cells [28], owing the availability of proper detection tools.

Targeting GLUTs has led to only a few molecular probes showing transporter-specificity [16,29]. Fructose transporters have been specifically targeted with fluorescent 7-nitrobenzofurazan conjugates of fructose (NBDF) and 1-amino-2,5-deoxy-D-mannitol (NBDM) [30,31], with NBDM showing unique specificity towards GLUT5. Interestingly, epimers or regio-isomers of NBDM were shown to gain uptake through glucose GLUTs with loss of uptake through the fructose GLUTs [32,33]. Among various fructose analogs, 1-amino-2,5-anhydro-D-mannitol (1-AM) has shown specificity towards GLUT5 and high affinity could be achieved upon functionalization of 1-AM with aromatic moieties [30,34,35]. Among those, NBD conjugate (NBDM) provided fluorescent GLUT-specific probes for direct analysis of GLUT5 activity in different cell lines. While NBDM provided feasibility for discriminating between normal and cancer cells on the basis of the uptake through GLUT5 [30], the probe had limited accumulation in cells (uptake saturation at 50  $\mu$ M concentration measured), resulting in the unfavorable background fluorescence. Here

we report GLUT5-targeting probes with improved cancer detection capability. The two probes described, differ in their uptake profile and reflect the metabolic capacity of the cell and GLUT5 activity. Considering the recognized differences between cells in their metabolic efficiency

as well as GLUT5 expression, the probes enable two-point characterization of cells and



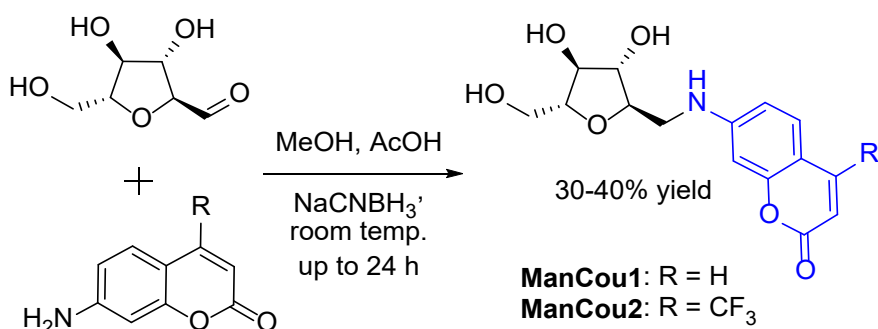
**Figure 3.1.** Fluorescence-based identification of breast cancer cells and discrimination of cancer phenotypes through GLUT5.

allow for discrimination of pre-malignant cells from differentiated epithelial cells and normal cells under in vitro setting (Figure 1).

### 3.2 Materials and Methods

All reagents were used as received unless otherwise stated from Sigma-Aldrich. The 7-aminocoumarin was synthesized according to the reported literature [36] and 7-amino-4-(trifluoromethyl)coumarin was procured from Alfa Aesar. Analytical TLC was carried out on commercial SiliCycle SiliaPlate® 0.2 mm F254 plates. Preparative silica chromatography was performed using SiliCycle SiliaFlash® F60 40-63  $\mu\text{m}$  (230-400 mesh). Final purification of compounds was achieved with Agilent-1200 HPLC (high-pressure liquid chromatography) using reversed phase semi-preparative column (Phenomenex® Luna® 10  $\mu\text{m}$  C18(2) 100 Å, LC Column 100 x 10 mm, Ea).  $^1\text{H}$  and  $^{13}\text{C}$  NMR spectra were recorded at room temperature with a Varian Unity Inova 400 MHz spectrometer.  $\text{CD}_3\text{OD}$  was used as a solvent and referenced to the corresponding residual solvent peaks (3.31 and 49.0 ppm, respectively) The following abbreviations are used to indicate the multiplicity: s - singlet; d - doublet; t - triplet; q - quartet; m - multiplet; b - broad signal; app - approximate. The coupling constants are expressed in Hertz (Hz). The high-resolution (HR) MS data (ESI) were obtained using a Thermo Fisher Orbitrap Elite™ Hybrid Ion Trap-Orbitrap Mass Spectrometer at Chemical Advanced Resolution Methods (ChARM) Laboratory at Michigan Technological University. 96-well plate analysis of cell fluorescence was carried out with Victor3 fluorescence plate reader (excitation at 385 nm). Confocal images were taken with Olympus FluoView™ FV1000 using the FluoView software. Fluorescence imaging was done with EVOS FL Auto inverted microscope.

### 3.2.1 Synthesis of ManCou Conjugates



**Figure 3.2:** Synthesis of ManCou analogs.

General procedure: (2S,3S,4S,5R)-3,4-dihydroxy-5-(hydroxymethyl)tetrahydrofuran-2-carbaldehyde [30] (up to 1 mmol) and the corresponding coumarin (0.8 equiv.) were dissolved in methanol (10 ml). The pH of the solutions was adjusted to <6 by acetic acid (1 ml), and NaBH<sub>3</sub>CN was added portion-wise to the reaction mixture (3 X 0.8 equiv., every 20-30 minutes). The reaction solutions were stirred at room temperature for up to 24 h. The mixtures were then concentrated to dryness under reduced pressure and purified by column chromatography on silica gel using methanol in dichloromethane (0-10%) mixtures. The final purification was achieved by semi-preparative HPLC using water-acetonitrile (2-20%) gradient, with the 30-40% average yield after final purification. Structures of ManCous were verified through spectroscopic analysis.

7-(((2R,3S,4S,5R)-3,4-dihydroxy-5-(hydroxymethyl)tetrahydrofuran-2-yl)methyl)amino)-2H-chromen-2-one (ManCou1): <sup>1</sup>H NMR (400 MHz, CD<sub>3</sub>OD): δ, 7.76-7.36 (d, J = 9.2, 1H), 7.32-7.30 (d, J = 8.4, 1H), 6.68-6.65 (dd, J<sub>1</sub> = 2.4, J<sub>2</sub> = 8.4, 1H), 6.53 (d, J = 2.4, 1H), 6.01-5.99 (d, J = 9.2, 1H), 4.02-3.98 (m, 2H), 3.95-3.92 (m, 1H), 3.88-3.85 (m, 1H), 3.73-3.69 (app dd, J<sub>1</sub> = 3.2, J<sub>2</sub> = 12.0, 1H), 3.66-3.61 (app dd, J<sub>1</sub> = 5.6, J<sub>2</sub> =

12.0, 1H), 3.48-3.44 (app dd, J1 = 3.6, J2 = 13.6, 1H), 3.38-3.32 (app dd, J1 = 6.8, J2 = 13.6, 1H) ppm. <sup>13</sup>C NMR (100 MHz, CD<sub>3</sub>OD): δ, 164.7, 158.1, 154.5, 146.5, 130.2, 112.3, 110.6, 109.1, 98.0, 85.3, 83.2, 80.3, 78.9, 63.3, 46.2 ppm. HRMS (ESI): m/z [M + Na]<sup>+</sup> calc'd for C<sub>15</sub>H<sub>17</sub>NNaO<sub>6</sub>: 330.09539; found 330.09434.

7-((((2R,3S,4S,5R)-3,4-Dihydroxy-5-(hydroxymethyl)tetrahydrofuran-2-yl)methyl)amino)-4-(trifluoromethyl)-2H-chromen-2-one (ManCou2): <sup>1</sup>H NMR (400 MHz, CD<sub>3</sub>OD): δ, 7.44-7.41 (dd, J1 = 2.0, J2 = 9.2, 1H), 6.74-6.71 (dt, J1 = 2.4, J2 = 9.2, 1H), 6.60-6.59 (d, J = 2.4, 1H), 6.37 (s, 1H), 4.02-3.98 (m, 2H), 3.95-3.92 (m, 1H), 3.89-3.85 (m, 1H), 3.73-3.69 (app dd, J1 = 3.6, J2 = 11.6, 1H), 3.66-3.61 (app dd, J1 = 5.6, J2 = 12.0, 1H), 3.50-3.46 (app dd, J1 = 3.6, J2 = 14.0, 1H), 3.40-3.35 (app dd, J1 = 6.4, J2 = 13.6, 1H) ppm. <sup>13</sup>C NMR (100 MHz, CD<sub>3</sub>OD): δ, 162.2, 158.6, 155.0, 143.3, 143.0, 124.8, 122.1, 112.8, 108.3, 104.1, 98.5, 85.4, 83.2, 80.2, 78.8, 63.3, 46.1 ppm. HRMS (ESI): m/z [M + H]<sup>+</sup> calc'd for C<sub>16</sub>H<sub>17</sub>F<sub>3</sub>NO<sub>6</sub>: 376.10082; found 376.09955.

### 3.2.2 Tissue culture

Normal breast cells (MCF 10A/ ATCC® CRL-10317™), adenocarcinoma (MCF-7/ATCC® HTB-22™) cells and hepatocellular carcinoma (Hep G2/ ATCC® CRL-10317™) cells were procured from American Type Cell Culture. The pre-malignant breast cancer cells MCF10AneoT was purchased from the Animal Model and Therapeutics Evaluation Core (AMTEC) Karmanos Cancer Institute, Wayne State University. All cells were maintained at 37°C, at 65% relative humidity and under 5% CO<sub>2</sub> in their respective culture medium (see Appendix A). All cultures were supplemented with 10,000 I.U./mL Penicillin and 10,000 μg/mL Streptomycin to lower chances of bacterial contamination.

### **3.2.3 Microplate uptake and inhibition assays**

For microplate assays, cells at ~80% confluence were collected and plated in 96-well flat bottom plates (20,000 cells/well) and allowed to grow for 24 hours. Cells were then washed with warm (37 °C) PBS solution, treated with ManCou probes (concentration varies) in PBS and incubated at 37 °C and 5% CO<sub>2</sub> for 10 min. After incubation, cells were carefully washed with warm PBS (3 x 100 µl). Fluorescent data was immediately collected using Victor3 plate reader and using Wallac™ umbelliferone (excitation 355 nm, emission 460 nm, 1.0 s) protocol. All trials were done in triplicates. The corresponding errors were derived as standard deviation. Uptake inhibition studies were carried using 96-well plate. Fluorescence of ManCou probes in cells was measured in the presence of varying concentrations of fructose and glucose. For this part, PBS solution containing 20 µM ManCou and the specific concentration of a sugar was prepared and introduced with the cells. In parallel, complete culture media was used to establish the impact of nutrients on ManCou uptake. Cell incubation, and data collection were conducted as stated above.

### **3.2.4 Immunostaining**

The GLUT5 (Slc2a5) primary antibody (sc-271055) was obtained from Santa Cruz Biotechnology, Inc and the secondary antibody (ab6787) was obtained from Abcam, plc. The primary antibody was used with incubation buffer at a 1:200 dilution while the secondary antibody was used at a dilution of 1:1000 as recommended. All the cells were fixed in 4% paraformaldehyde and blocked for 1 hour at room temperature. Incubation for primary and secondary antibodies was 2 hours and 1 hour respectively, at room

temperature. PBS rinse was carried out between each step. Imaging was carried out immediately.

### **3.2.5 Imaging**

The individual cell lines in culture were incubated with ManCou1 and 2 for 10 minutes at a concentration of 20 $\mu$ M across all tests. The test concentration was established after evaluation of the imaging efficiency within a range of concentrations (5-100  $\mu$ M). 20  $\mu$ M concentration was selected as the lowest at which steady fluorescence readout was achieved using a confocal microscope (Olympus FluoView<sup>TM</sup> FV1000). Imaging was carried out using EVOS FL Autoimaging with the EVOS software (Figure 2). All images were taken at a constant gain setting. From the grayscale images, the corrected total cell fluorescence (CTCF) was calculated as described in our previous work [35]. Briefly, using ImageJ, comparing the average fluorescence with the background of the same image, the fluorescence signal only in the region of interest was obtained as described here [37]. The process was repeated five times for each image captured to obtain an average fluorescence. The average CTCF obtained was then normalized to the average CTCF obtained for the normal control sample. The normalized average CTCF (with respect to MCF10A) was then plotted in Microsoft Excel (Figure 4B). The advantage of using CTCF for images obtained along a z-plane with best focus as presented by McCloy et al [37] demonstrates that the information thus obtained eliminates errors due to localized higher levels.



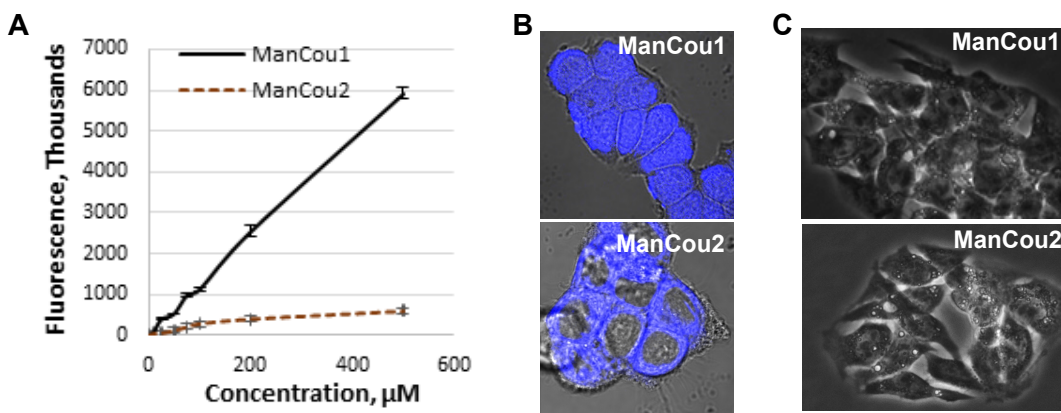
### 3.3 Results and Discussion

#### 3.3.1 Design and evaluation of fluorescent fructose mimic as GLUT5-specific probes

Two blue-fluorescent GLUT5 probes were designed on the basis of the established GLUT5 preference for 1-amino-2,5-anhydro-D-mannitol (Man) [30,34] and the capacity of GLUTs to pass coumarin (Cou) fluorophores [38], to enable significant accumulation in the cell through GLUT5. The resulting sugar-coumarin conjugates – ManCous – bearing H or CF3 at the C4 position of the coumarin ring (ManCou1 and ManCou2, respectively, Figure 2A) were evaluated for the uptake and GLUT5 specificity in cell culture. For this part, MCF-7 cells, previously studied for GLUT5-mediated uptake [22,24,31] and Hep G2 cells which lack GLUT5 [39] were used.

For the initial uptake analysis, MCF7 cells were treated in a 96-well plate with ManCou probes at different concentrations and the cell fluorescence was measured with a fluorescence plate reader. At concentrations exceeding 100  $\mu\text{M}$ , the fluorescence readout for ManCou2 showed signs of saturations and leveled off at 200  $\mu\text{M}$  concentration (Figure 3A). The fluorescence signal from ManCou1 gradually increased and showed no saturation even at 500  $\mu\text{M}$  concentration. The Z-stack analysis of ManCou-treated cells showed a prominent accumulation of probes inside the cell. While both probes are internalized by the cell, they show a marked difference in cellular distribution. ManCou1 is evenly distributed throughout the cell, including the nucleus, while ManCou2 is localized in the cytosol (Figure 3B). The differences in the cell distribution parallel those in the ManCou uptake profile. To delineate the contribution of the sugar in the uptake of ManCous a direct

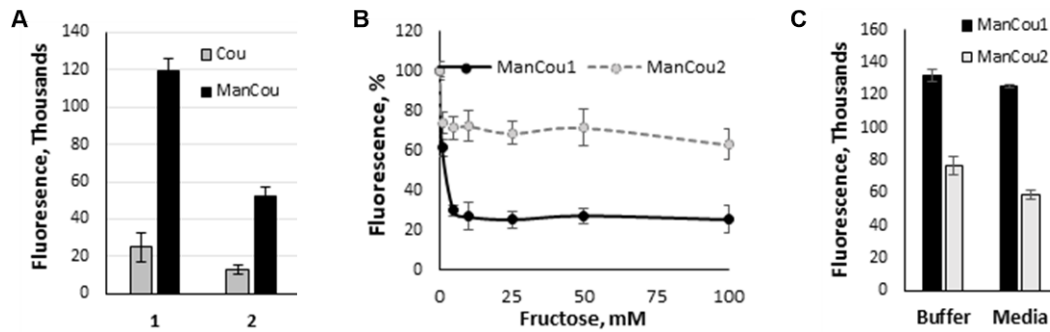
comparison of ManCou uptake with that of the non-conjugated coumarin was carried out. At the same concentrations, we have observed up to 6-fold and 5-fold lesser uptake for unconjugated coumarins (Cou1 is coumarin of ManCou1, Cou2 is coumarin of ManCou2, Figure 4A), implying the sugar-driven uptake of ManCous.



**Figure 3.3.** ManCou uptake analysis. A) concentration-dependent uptake in MCF-7 cells in 96-well plate; B) Brightfield and fluorescence (DAPI) overlay of Confocal Z-stack images of MCF7 with ManCou1 and ManCou2 C) Brightfield and fluorescence (DAPI) overlay of Confocal Z-stack images of Hep G2 cells with ManCaou1 and ManCou2. Images taken for 20  $\mu\text{M}$  ManCous at 405 nm excitation, 461 nm emission, (60X for MCF7 cells and 40X for HepG2 cells).

It also appears that the uptake of ManCou1 is nearly twice as much as ManCou2. The uptake of both ManCous was inhibited by fructose (Figure 4B), although to a greater extent in the case of ManCou1. Glucose, however, had no effect on the uptake as evident from the equally efficient internalization of the probes in buffer and complete high glucose culture medium (Figure 4C). Finally, we have tested ManCou uptake in GLUT5-deficient

HepG2 cells to delineate any contribution from non-specific binding to the observed gained fluorescence. While some basal fluorescence has been observed for whole cell images, the Z-stack analysis (Figure 3C) showed no internalization of the probe, suggesting no active uptake of ManCous. Overall, the lack of inhibition from glucose in conjunction with the lack of uptake observed with Hep G2 cells supports the GLUT5 specificity of ManCous.



**Figure 3.4.** Analysis of sugar impact on ManCou uptake. A) Comparative uptake of ManCous (black bars) vs. non-conjugated (grey bars) coumarins; B) Fructose-induced inhibition of ManCou uptake; C) ManCou uptake is independent of glucose concentration and is equally effective in the buffer and complete culture medium. All data obtained in 96-well plate format. Each data point constitutes an average of two independent experiments in triplicate. Error bars represent standard deviation.

It is noteworthy that the uptake through GLUTs is loosely coupled with phosphorylation. In the uptake of sugars through GLUTs, phosphorylation promotes removal of the sugar buildup in the cell, thus facilitating continuous uptake. With the GLUT-mediated uptake for ManCou established, the apparent differences in the uptake between ManCou1 and ManCous appear to suggest the difference in their connection with

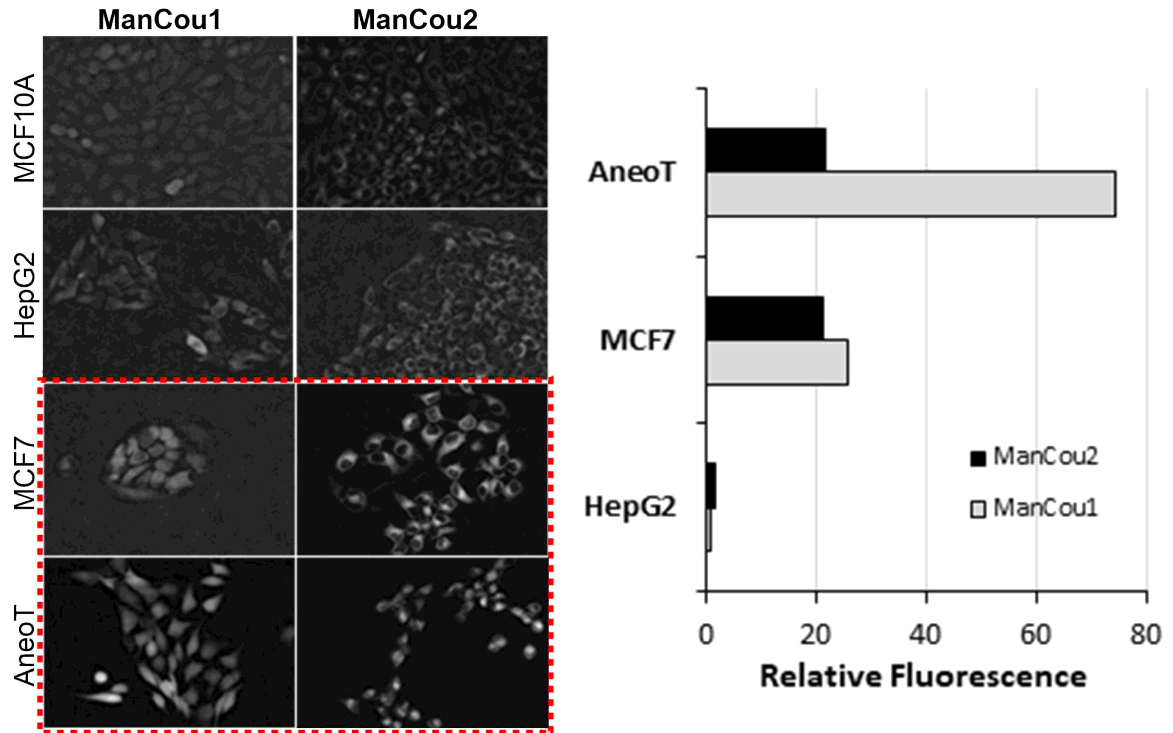
cell metabolism. Thus, is it plausible that the linearity in the uptake of ManCou1 through GLUT5 is promoted by the efficient removal of the probe gradient through phosphorylation, considering an effective phosphorylation of the base 2,5-anhydro-D-mannitol [40-43]. On the other hand, saturable uptake for ManCou2 implies gradient build-up, precluding continuous uptake of the probe, and thus, the lack of phosphorylation. It is then plausible that only phosphorylated species are further taken up by the cell nucleus. While the established mannitol phosphorylation allows to consider a direct connection between ManCou1 and cell metabolism, alternations in the coumarin structure appear to alter the cellular processing of ManCous (as reflected by the change induced by the CF3 group of ManCou2). Further analyses are needed to establish cellular fate of ManCou probes and link nuclear accumulation with ManCou phosphorylation.

### **3.3.2 Profiling fructose uptake efficiency and GLUT5 in cells for cancer detection.**

We analyzed ManCou uptake in normal and cancer cell lines to evaluate the feasibility of cancer cell detection on the basis of the probe uptake through GLUT5. The comparative analysis of normal MCF10A, adenocarcinoma MCF7 and premalignant MCF10AneoT (ANeoT) cells was carried out through imaging. After treating cells with 20  $\mu$ M concentration of ManCous for 10 min, the accumulated fluorescence was recorded and fluorescence intensity analyzed. We have observed minimal to no accumulation of probes in the normal MCF10A breast cells (comparable to that in HepG2 cells). The ManCous have excitation and emission maxima of 405 nm/465 nm respectively. The fluorescent images were captured in the blue channel.

As indicated by the grayscale fluorescent images in Figure 5A, the level of probe-induced fluorescence in the normal MCF10A cells is comparable to that of the Hep G2 cells. The background fluorescence appears to originate from the residual association of probes with the membrane as no fluorescence could be detected inside of MCF10A or Hep G2 cells by Z-stack analysis. Thus, the data implicates that the uptake of ManCou probes in MCF7 and AneoT cells proceeds through GLUT5, resulting in a facile imaging of cancer cells. It is important to note that fructose uptake in the healthy tissues is limited to the liver and intestines and fructose-specific GLUT5 is upregulated in cancer cells [23,24,31,44,45] supporting our approach to using fructose-based detection. This was further confirmed by immunostaining the cells treated with probes for GLUT5 as shown in Figure 6.

Using the normalized average CTCF with respect to the control MCF10A, the relative levels for each of the cells lines and treatment conditions can be directly assessed. As shown in Figure 4B, the fluorescence intensity observed for AneoT treated with ManCou1 was nearly 70-times higher than that for MCF10A and Hep G2 cells for the same concentration and incubation period. Under the same conditions, AneoT had nearly 7-times higher response compared to MCF-7 clearly distinguishing the pre-malignant AneoT from the adenocarcinoma cells MCF-7 (statistically significant data). The differences in the uptake of ManCou1 provides a one point discrimination between normal and cancer cells. Under identical conditions, ManCou2 probe had nearly 65-times higher uptake in the MCF-7 than HepG2 cells, and nearly 3-times higher uptake than in AneoT cells. The differences in the uptake of ManCou2 provide a second point for discriminating between cancer and normal cells and add to a better discrimination between cancer subtypes.

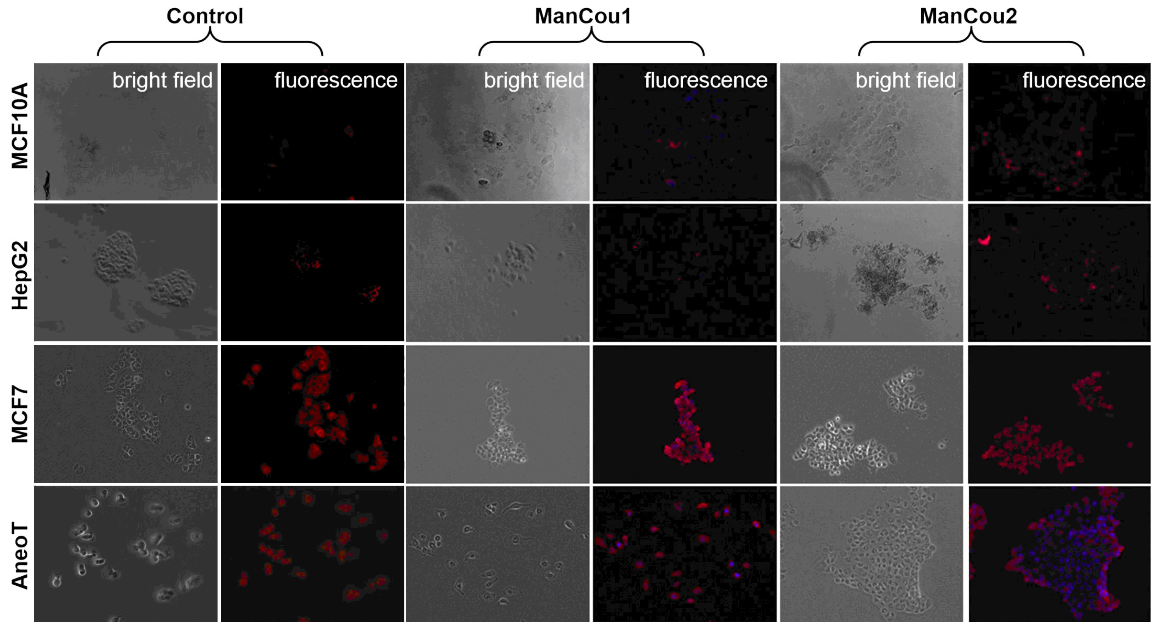


**Figure 3.5** ManCou uptake in cells. A) Grayscale fluorescence images of ManCou uptake in cells used to determine relative fluorescence using EVOS FL Auto at 20X. B) Relative differences in ManCou uptake (normalized for MCF10A cells). Data obtained for normal breast cells MCF 10A, hepatocellular cancer cells Hep G2 (negative control), pre-malignant breast cancer cells AneoT and breast adenocarcinoma cells MCF7 after 10 minutes of incubation with 20 $\mu$ M of ManCous1 and 2. The t-tests ( $p < 0.05$ ) was performed after F-test ( $F \leq F_{critical}$  one-tail). For ManCou1, MCF7 was statistically significant compared to AneoT, HepG2 and MCF10A while AneoT was statistically significant compared to HepG2 and MCF10A. For ManCou2, only MCF7 was statistically significant compared to AneoT, HepG2 and MCF10A.

It should be noted that the ManCou1:ManCou2 ratios increases with the concentration of probes as ManCou2 approaches uptake saturation. Thus, for MCF7 cells, the ratios of 0.9, 1.3, 1.7, and 2.5 were measured for ManCou1:ManCou2 at 20  $\mu$ M, 50  $\mu$ M, 100  $\mu$ M, and 200  $\mu$ M concentrations, respectively. For AneoT, using higher concentration of ManCous induced rapid cell detachment. Overall, the expectations would be that in heterogeneous populations, treating cells with ManCou1 and ManCou2 and analyzing the CTCF will provide a visual discrimination of normal, pre-malignant and adenocarcinoma cells. The two-point analysis would take the form of the analysis shown in Table 1. The disparity in the signal makes this approach also ideal for spectrophotometric analysis in a micro-plate or flow formats.

Reported evidence suggests that Hep G2 cells lack the fructose-specific transporter GLUT5 [39], while breast cancer cells express it in significant levels. In order to assess the relation between uptake of the probe and the presence of the fructose-specific transporter GLUT5 in the cells tested, we carried out immunostaining of the cells for GLUT5 (Texas Red  $\text{\textcircled{R}}$ . Ex: 596nm, Em: 620nm) following a 10-minute incubation with 20 $\mu$ M of the respective probes. Cells without the probes were used as controls. The differential expression of GLUT5 in the cellular membrane is evident from the GLUT5 immunostaining depicted in Figure 5 (control panel). As can be seen, there is little to no GLUT5 in MCF10A and HepG2 cells. In contrast, MCF7 cells and AneoT cells presented detectable levels of GLUT5. The lack of probe uptake (DAPI) in MCF10A and HepG2 is represented well by the absence of GLUT5. Similarly, the probe uptake in MCF7 and AneoT cells are accompanied by the presence of GLUT5 (Figure 5, ManCou panels). The

differences in GLUT5 levels appear to parallel the differences in the accumulation of ManCou probes in the corresponding cells, with the overall levels of uptake increasing with malignancy.






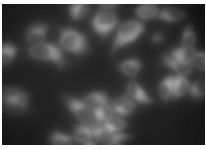
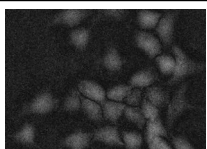
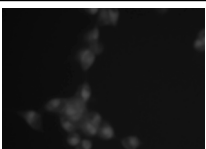
**Figure 3.6** Immunostaining of cells for GLUT5 without and with ManCous. Optical microscopy, 20X. Control panel represents GLUT5 staining. ManCou1 and ManCou2 panels represent GLUT5 staining after 10 min treatment of cells with the respective probes. The red fluorescence represents GLUT5 (Texas Red ®. Ex: 596nm, Em: 620nm) and blue (DAPI) represents the probe. The cells were incubated with 20 $\mu$ M of the respective probes for 10 minutes, fixed in paraformaldehyde before immunostaining. Images were captured using EVOS FL Auto immediately following immunostaining.

The correlation is particularly observable for ManCou1, showing visible difference blue fluorescence between MCF7 and AneoT cells with the latter having higher uptake



despite the lower levels of GLUT5. Overall, the ManCou uptake correlates with the presence of GLUT5, providing further evidence for GLUT5-directed visualization of cancer cells. Further detailed analysis of GLUT5 expression and relation to fructose will be required to develop a better understanding of the relationship between the fructose-specific transporters and uptake of the fructose-like probes.

**Table 3.1:** Example two-point analysis demonstrating identification of normal, adenocarcinoma and pre-malignant cells.

Cell Type	ManCou1 Image	ManCou1 Quantification	ManCou2 Image	ManCou2 Quantification
Control/Normal		Absent (--)		Absent (--)
Adenocarcinoma		Present (++)		Presence (++)
Premalignant		Significant presence (+++)		Less present (+)

Overall, due to the correlations observed for the uptake of the ManCous and the presence of GLUT5 as well as significant differences in accumulation of the ManCous in cancer cells, optical screening of breast cancer using the fluorescent-labeled fructose analogs in a multi-plate format or flow settings is feasible. Further analysis and experimentation is needed to quantify the relative abundance of GLUT5 to establish the

correlations with ManCou uptake, as well as evaluate the contribution from the cell population densities in a given sample to improve the detection system and hence the diagnosis. Combined with fluorescent response, the two-point, two-metric system has the potential to clearly discriminate cancer cells and its subtypes. Future work will involve screening heterogeneous cultures derived from breast cancer biopsy samples for advancing the approach to POC technology.

### **3.4 Conclusion**

We have successfully demonstrated effective discrimination of premalignant and adenocarcinoma cancer cells using fluorescently labeled fructose analogs in vitro. The rapid response from the 10 minutes incubation and the observably different response between the cancer cells with the two fructose analogs highlight the use of this technique in high-throughput point of care healthcare applications.

## References

1. Avcioglu, G.; Nural, C.; Yilmaz, F.M.; Baran, P.; Erel, O.; Yilmaz, G. Comparison of noninvasive and invasive point-of-care testing methods with reference method for hemoglobin measurement. *J Clin Lab Anal* 2017.
2. De Clippel, D.; Van Heddegem, L.; Vandewalle, G.; Vandekerckhove, P.; Compernelle, V. Hemoglobin screening in blood donors: A prospective study assessing the value of an invasive and a noninvasive point-of-care device for donor safety. *Transfusion* 2017, *57*, 938-945.
3. Ekhlaspour, L.; Mondesir, D.; Lautsch, N.; Balliro, C.; Hillard, M.; Magyar, K.; Radocchia, L.G.; Esmaili, A.; Sinha, M.; Russell, S.J. Comparative accuracy of 17 point-of-care glucose meters. *J Diabetes Sci Technol* 2017, *11*, 558-566.
4. Allardet-Servent, J.; Lebsir, M.; Dubroca, C.; Fabrigoule, M.; Jordana, S.; Signouret, T.; Castanier, M.; Thomas, G.; Soundaravelou, R.; Lepidi, A., et al. Point-of-care versus central laboratory measurements of hemoglobin, hematocrit, glucose, bicarbonate and electrolytes: A prospective observational study in critically ill patients. *PLoS One* 2017, *12*, e0169593.
5. Kim, W.H.; Lee, H.C.; Ryu, H.G.; Chung, E.J.; Kim, B.; Jung, H.; Jung, C.W. Reliability of point-of-care hematocrit measurement during liver transplantation. *Anesth Analg* 2017.
6. Bueno, L.; de Araujo, W.R.; Paixão, T.R.L.C. 8 - point of care (poc) medical biosensors for cancer detection a2 - narayan, roger j. In *Medical biosensors for point of care (poc) applications*, Woodhead Publishing: 2017; pp 183-201.
7. Zarei, M. Advances in point-of-care technologies for molecular diagnostics. *Biosensors and Bioelectronics* 2017, *98*, 494-506.
8. Zhang, L.; Ding, B.; Chen, Q.; Feng, Q.; Lin, L.; Sun, J. Point-of-care-testing of nucleic acids by microfluidics. *TrAC Trends in Analytical Chemistry* 2017, *94*, 106-116.

9. Jayanthi, V.S.P.K.Sankara A.; Das, A.B.; Saxena, U. Recent advances in biosensor development for the detection of cancer biomarkers. *Biosensors and Bioelectronics* 2017, 91, 15-23.
10. Science, J.M.E.C.f.C.D.a.C. Having a breast biopsy: A review of the research for women and their families. In Center for Clinical Decisions and Communications Science, Agency for Healthcare Research and Quality (US): Rockville (MD), 2016.
11. Davidson, N.E.; Rimm, D.L. Expertise vs evidence in assessment of breast biopsies: An atypical science. *JAMA* 2015, 313, 1109-1110.
12. Zheng, J. Energy metabolism of cancer: Glycolysis versus oxidative phosphorylation (review). *Oncol Lett* 2012, 4, 1151-1157.
13. Cairns, R.A.; Harris, I.S.; Mak, T.W. Regulation of cancer cell metabolism. *Nat Rev Cancer* 2011, 11, 85-95.
14. Adler, L.P.; Crowe, J.P.; al-Kaisi, N.K.; Sunshine, J.L. Evaluation of breast masses and axillary lymph nodes with [f-18] 2-deoxy-2-fluoro-d-glucose pet. *Radiology* 1993, 187, 743-750.
15. Calvaresi, E.C.; Hergenrother, P.J. Glucose conjugation for the specific targeting and treatment of cancer. *Chem. Sci.* 2013, 4, 2319-2333.
16. Tanasova, M.; Fedie, J. Molecular tools for facilitative carbohydrate transporters *ChemBioChem* 2017, 18, 1774-1788.
17. Alavi, A.; Zhuang, H.M. Finding infection - help from pet. *Lancet* 2001, 358, 1386-1386.
18. Carvalho, K.C.; Cunha, I.W.; Rocha, R.M.; Ayala, F.R.; Cajaiba, M.M.; Begnami, M.D.; Vilela, R.S.; Paiva, G.R.; Andrade, R.G.; Soares, F.A. Glut1 expression in malignant tumors and its use as an immunodiagnostic marker. *Clinics* 2011, 66, 965-972.

19. Kang, S.S.; Chun, Y.K.; Hur, M.H.; Lee, H.K.; Kim, Y.J.; Hong, S.R.; Lee, J.H.; Lee, S.G.; Park, Y.K. Clinical significance of glucose transporter 1 (glut1) expression in human breast carcinoma. *Jpn. J. Cancer Res.* 2002, 93, 1123-1128.
20. Lind, P.; Igerc, I.; Beyer, T.; Reinprecht, P.; Hausegger, K. Advantages and limitations of fdg pet in the follow-up of breast cancer. *Eur. J. Nucl. Med. Mol. I* 2004, 31, S125-S134.
21. McQuade, D.T.; Plutschack, M.B.; Seeberger, P.H. Passive fructose transporters in disease: A molecular overview of their structural specificity. *Org Biomol Chem* 2013, 11, 4909-4920.
22. Gowrishankar, G.; Zitzmann-Kolbe, S.; Junutula, A.; Reeves, R.; Levi, E.; Srinivasan, A.; Bruus-Jensen, K.; Cyr, J.; Dinkelborg, L.; Gambhir, S.S. Glut 5 is not over-expressed in breast cancer cells and patient breast cancer tissues. *PLoS ONE* 2011, 11, e26902-e26909.
23. Trayner, B.J.; Grant, T.N.; West, F.G.; Cheeseman, C.I. Synthesis and characterization of 6-deoxy-6-fluoro-d-fructose as a potential compound for imaging breast cancer with pet. *Bioorgan. Med. Chem.* 2009, 17, 5488-5495.
24. Zamora-Leon, S.P.; Golde, D.W.; Concha, I.I.; Rivas, C.I.; DelgadoLopez, F.; Baselga, J.; Nualart, F.; Vera, J.C. Expression of the fructose transporter glut5 in human breast cancer. *Proc. Natl. Acad. Sci. U.S.A.* 1996, 93, 1847-1852.
25. Mesonero, J.; Matosin, M.; Cambier, D.; Rodriguez-Yoldi, M.J.; Brot-Laroche, E. Sugar-dependent expression of the fructose transporter glut5 in caco-2 cells. *Biochem. J.* 1995, 312 ( Pt 3), 757-762.
26. Baenke, F.; Peck, B.; Miess, H.; Schulze, A. Hooked on fat: The role of lipid synthesis in cancer metabolism and tumour development. *Dis Model Mech* 2013, 6, 1353-1363.
27. Monzavi-Karbassi, B.; Hine, R.J.; Stanley, J.S.; Ramani, V.P.; Carcel-Trullols, J.; Whitehead, T.L.; Kelly, T.; Siegel, E.R.; Artaud, C.; Shaaf, S., et al. Fructose as a carbon source induces an aggressive phenotype in mda-mb-468 breast tumor cells. *Int. J. Oncol.* 2010, 37, 615-622.

28. Manolescu, A.R.; Witkowska, K.; Kinnaird, A.; Cessford, T.; Cheeseman, C. Facilitated hexose transporters: New perspectives on form and function. *Physiology* 2007, 22, 234-240.
29. Granchi, C.; Fortunato, S.; Minutolo, F. Anticancer agents interacting with membrane glucose transporters. *Medchemcomm* 2016, 7, 1716-1729.
30. Tanasova, M.; Plutschack, M.; Muroski, M.E.; Sturla, S.J.; Strouse, G.F.; McQuade, D.T. Fluorescent thf-based fructose analogue exhibits fructose-dependent uptake. *ChemBioChem* 2013, 14, 1263-1270.
31. Levi, J.; Cheng, Z.; Gheysens, O.; Patel, M.; Chan, C.T.; Wang, Y.B.; Namavari, M.; Gambhir, S.S. Fluorescent fructose derivatives for imaging breast cancer cells. *Bioconjugate Chem.* 2007, 18, 628-634.
32. Soueidan, O.M.; Scully, T.W.; Kaur, J.; Panigrahi, R.; Belovodskiy, A.; Do, V.; Matier, C.D.; Lemieux, M.J.; Wuest, F.; Cheeseman, C., et al. Fluorescent hexose conjugates establish stringent stereochemical requirement by glut5 for recognition and transport of monosaccharides. *ACS Chem. Biol.* 2017, 12, 1087-1094.
33. Kumar Kondapi, V.P.; Soueidan, O.M.; Cheeseman, C.I.; West, F.G. Tunable glut-hexose binding and transport via modulation of hexose c-3 hydrogen-bonding capabilities. *Chem. Eur. J.* 2017, 23, 8073-8081.
34. Yang, J.; Dowden, J.; Tatibouet, A.; Hatanaka, Y.; Holman, G.D. Development of high-affinity ligands and photoaffinity labels for the d-fructose transporter glut5. *Biochem. J.* 2002, 367, 533-539.
35. Kannan, S.; Begoyan, V.; Fedie, J.; Xia, S.; Weselinski, L.; Tanasova, M.; Rao, S. In Fructose uptake-based rapid detection of breast cancer, IEEE Life Sciences Conference, Sydney Australia, December 13-15, 2017, 2017; Sydney Australia.
36. Jianzhong Yu; Yongtao Wang; Peizhi Zhang; Wu, J. Direct amination of phenols under metal-free conditions. *Synlett* 2013, 24, 7.

37. McCloy, R.A.; Rogers, S.; Caldon, C.E.; Lorca, T.; Castro, A.; Burgess, A. Partial inhibition of cdk1 in g 2 phase overrides the sac and decouples mitotic events. *Cell Cycle* 2014, 13, 1400-1412.
38. Otsuka, Y.; Sasaki, A.; Teshima, T.; Yamada, K.; Yamamoto, T. Syntheses of d-glucose derivatives emitting blue fluorescence through pd-catalyzed c-n coupling. *Org. Lett.* 2016, 18, 1338-1341.
39. Yamamoto, T.; Seino, Y.; Fukumoto, H.; Koh, G.; Yano, H.; Inagaki, N.; Yamada, Y.; Inoue, K.; Manabe, T.; Imura, H. Over-expression of facilitative glucose transporter genes in human cancer. *Biochem. Biophys. Res. Commun.* 1990, 170, 223-230.
40. Dills, W.L.; Covey, T.R.; Singer, P.; Neal, S.; Rappaport, M.S. 2,5-anhydro-1-deoxy-d-lyxitol, 2,5-anhydro-1-deoxy-d-mannitol, and 2,5-anhydro-1-deoxy-d-talitol - synthesis and enzymic studies. *Carbohydr. Res.* 1982, 99, 23-31.
41. Azema, L.; Claustre, S.; Alric, I.; Blonski, C.; Willson, M.; Perie, J.; Baltz, T.; Tetaud, E.; Bringaud, F.; Cottem, D., et al. Interaction of substituted hexose analogues with the trypanosoma brucei hexose transporter. *Biochem. Pharmacol.* 2004, 67, 459-467.
42. Riquelme, P.T.; Wernette-Hammond, M.E.; Kneer, N.M.; Lardy, H.A. Mechanism of action of 2,5-anhydro-d-mannitol in hepatocytes. Effects of phosphorylated metabolites on enzymes of carbohydrate metabolism. *J. Biol. Chem.* 1984, 259, 5115-5123.
43. Hanson, R.L.; Ho, R.S.; Wiseberg, J.J.; Simpson, R.; Younathan, E.S.; Blair, J.B. Inhibition of gluconeogenesis and glycogenolysis by 2,5-anhydro-d-mannitol. *J. Biol. Chem.* 1984, 259, 218-223.
44. Zamora-Leon, S.P.; Golde, D.W.; Concha, I.I.; Rivas, C.I.; DelgadoLopez, F.; Baselga, J.; Nualart, F.; Vera, J.C. Expression of the fructose transporter glut5 in human breast cancer *Proc. Natl. Acad. Sci. U.S.A.* 1996, 93, 15522-15522.

45. Douard, V.; Ferraris, R.P. Regulation of the fructose transporter glut5 in health and disease. *Am. J. Physiol-Endoc. M.* 2008, 295, E227-E237.



## 4 Coumarins: Spectroscopic Measurements and First Principles Calculations of C4-substituted 7-Aminocoumarins

### 4.1 Introduction

Coumarins are plant metabolites that are known for their biological properties, including antimicrobial, antiviral, anti-inflammatory, antidiabetic, antioxidant, and enzyme inhibitory activity.<sup>1</sup> Among the coumarin family, 7-aminocoumarins have gained the most attention, as evidenced by the extensive study of their fluorescent properties.<sup>2</sup> The large Stokes shifts and emissions in the visible spectral range upon proper functionalization led to the widespread use of 7-aminocoumarins as analytical and biological sensors.<sup>2-5</sup> Recently, application of coumarins as fluorescent sensors was extended to the labeling of proteins,<sup>6</sup> evaluation of sugar transport capacity in mammalian cells,<sup>7-8</sup> and detection of cancer cells.<sup>9</sup> Substitution at coumarins is known to alter their fluorescence and absorption properties. A particular impact on coumarin fluorescence has been observed upon substitution at C4 position. In general, the addition of the electron-withdrawing group at the C4 position induces a strong red-shift in the coumarin fluorescence spectrum, with a relatively small effect on the absorption spectrum.<sup>10</sup> For example, ~50 nm red-shift is measured for the C4-trifluoromethyl and C4-phenyl analogs of 7-aminocoumarin, and ~100 nm red-shift for the C4-methylcarboxy analog.<sup>10</sup> In contrast to the electron withdrawing groups, the presence of an electron donor, such as a methyl group, induces a blue-shift in the fluorescence spectrum. It was suggested that modifications in the fluorescence properties of C4-substituted coumarins depend on the presence of the substituent capable of rotating in the excited state.<sup>10</sup> Considering the variability of the impact that C4-substitution has on the fluorescence properties of coumarins, the task of this investigation was to get an atomistic-level understanding of the electronic interactions that define spectroscopic properties in the coumarin family. Here, we employ the time-dependent (TD) density functional theory (DFT)<sup>11</sup> method to determine the ground state and excited state properties of the coumarin family. Absorption and fluorescence calculations were performed for eight coumarins with substituents including H-, CH<sub>3</sub>-,

CF<sub>3</sub>-, Ph-, COOEt-, CONH<sub>2</sub>-, CONHMe- and the CONHPh- groups at the C4 position of the coumarin aromatic ring. The theoretical findings were correlated to the experimental data produced with chemically-obtained coumarin analogs. Although analysis of few members of this set has been previously investigated,<sup>10, 12-14</sup> this is a systematic experimental/theoretical study of a set of C4-substituted 7-aminocoumarin analogs.

## 4.2 Methods

DFT calculations were performed with GAUSSIAN09<sup>15</sup> using Becke's 3 parameter hybrid functional B3LYP<sup>16-17</sup> with the non-local correlation provided by the Lee, Yang, and Parr (LYP) expression.<sup>16</sup> The 6-311+(2d,p) basis sets were used for C, O, N, and H atoms associated with the coumarin family of molecules. The use of the B3LYP functional is well established in the literature. On the other hand, it is also known that for charge transfer excitations which involve electron-hole separations over larger distances (extended  $\pi$  systems, intermolecular charge transfer) long-range corrected (range-separated) hybrid functional forms like CAM-B3LYP are essential. They give a qualitatively correct description for large charge separations, but usually higher excitation energies than calculated using B3LYP. Comparative test calculations for coumarin 4 showed that the intramolecular charge transfer separation is not large enough to mandate CAM-B3LYP: B3LYP and CAM-B3LYP yield the same qualitative UV spectrum but the B3LYP value of 349 nm is closer to the experimental value of 358 nm than the CAM-B3LYP value of 318 nm for the first excitation energy. Therefore, B3LYP was used for further analysis of the coumarin set. For the optical properties, calculations of the ground state and excited states were performed. Absorption is calculated as the difference between ground and excited state energies at the *optimized ground state geometry*, and the fluorescence is calculated as the difference between ground and excited state energies at the *optimized excited state geometry*. Since the experimental spectra of the coumarin series were taken in solution, the effect of the solvent is approximated by employing the Polarizable Continuum Model (PCM).<sup>18</sup> The total energy of the molecule in solution is calculated by making the solvent reaction field self-consistent with the solute electrostatic potential which is generated from the computed electron density.<sup>15</sup> Dielectric constants for water,

methanol and ethanol ( $\epsilon = 78.35, 24.85$  and  $32.61$ , respectively) were used for a comparative analysis of the solvent effect for coumarin **2** absorption. The calculated results (Table 2) show that the solvent induced red shift is independent whether water, methanol, and ethanol were used, warranting further use of water as a solvent for the calculations.

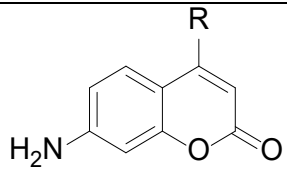
<b>Table 4.2.</b> Calculated first singlet excitation energy ( $\pi \rightarrow \pi^*$ ) for Coumarin <b>2</b> (R = CH <sub>3</sub> ) – solvent effect	
Coumarin <b>2</b> (R = CH <sub>3</sub> )	Singlet S1 excitation (nm)
Gas phase - This work (theory)	314
Gas phase – Ref. 14 (theory)	308
Solvent (water) - This work (theory)	332
Solvent (methanol) - This work (theory)	332
Solvent (methanol) - This work (exp.)	347
Solvent (ethanol) - This work (theory)	332
Solvent (ethanol) – Ref. 14 (theory)	334
Solvent (ethanol) – Ref. 14 (exp.)	353

When calculating the excited state properties of molecules in solution by using PCM as a self-consistent reaction field (SCRF) method, different solvation approaches can be used within GAUSSIAN09. In this paper, we use the vertical absorption and emission PCM approach for which solvation of the excited state is taken into account via a linear response formalism.<sup>15, 19</sup> The absorption and emission results will be labeled PCMa and PCMe, respectively. A summary of the main effects of the solvent on the electronic structure in terms of the difference between the highest occupied molecular orbital (HOMO) and the lowest unoccupied molecular orbital (LUMO) is given in Supplementary Information, Table S1. The inclusion of the solvent effect in calculations leads to a consistent *red shift* of the HOMO-LUMO gap by an average value of 0.18 eV or 15 nm (~5%).

## 4.3 Results and Discussion

### 4.3.1 Synthesis and spectroscopic properties of C4-substituted coumarins

Table 1 lists the members of the coumarin family bearing different substituents at the C4 position in the coumarin aromatic ring (Figure 1). The H-substituted molecule is labeled as Coumarin **1**, CH<sub>3</sub>-substituted as Coumarin **2**, CF<sub>3</sub>-substituted as Coumarin **3**, Ph-substituted as Coumarin **4**, COOEt-substituted as Coumarin **5**, CONH<sub>2</sub>-substituted as Coumarin **6**, CONHMe-substituted as Coumarin **7**, and the CONHPh-substituted molecule is labeled as Coumarin **8**. Coumarins **1**, **2** and **3** were obtained from commercial sources. Coumarins **4** and **5** were synthesized through the established procedure of Pechmann Condensation.<sup>20-21</sup> Coumarin **5** was used as a starting material to access coumarins **6**, **7** and **8** (Figure 1A). The structures of the coumarin molecules were confirmed through standard analytical techniques including nuclear magnetic resonance and mass spectroscopic methods. The absorption (Figure 1B) and fluorescence (Figure 1C) spectra of the coumarin family were measured in methanol and water as solvents. Less than 1 nm difference was

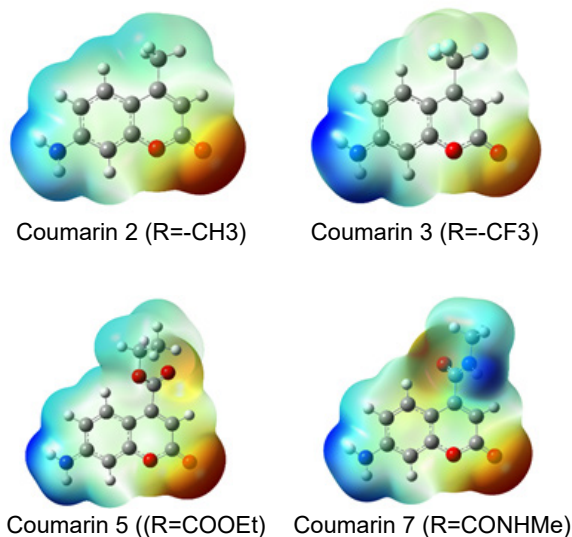
<b>Table 4.1.</b> The experimental absorption and fluorescence maxima of the C4-substituted coumarins.			
 R =	Absorption $\lambda_{\max}$ (nm)	Fluorescence $\lambda_{\max}$ (nm)	Stokes shift (nm)
<b>1</b> (H)	352	463	111
<b>2</b> (CH <sub>3</sub> )**	347	452	105
<b>3</b> (CF <sub>3</sub> )	371	508	136
<b>4</b> (Ph)	358	509	151
<b>5</b> (COOEt)	377	566	189
<b>6</b> (CONH <sub>2</sub> )	364	567	203
<b>7</b> (CONHMe)	362	552	190
<b>8</b> (CONHPh)	362	398, 560	36, 198

observed between aqueous and methanolic samples. In Coumarin **1**, the absorption and fluorescence peaks are located at 352 and 463 nm, respectively. With reference to Coumarin **1**, the methyl substitution in Coumarin **2** is the only substitution that leads to a blue shift of the absorption and fluorescence peaks, all other substitutions lead to a red shift in the corresponding optical spectra. A significant shift ( $\approx 115$  nm) in the fluorescence peak positions is observed in going from H- to CONHPh-group at the C4-position, which is accompanied with a smaller shift ( $\approx 30$  nm) in the absorption peak positions. The calculated Stokes shift (i.e. difference between absorption and fluorescence peak positions) is also noticeable ranging from 105 nm in Coumarin **2** to 203 nm in Coumarin **6** (Table 1).

### 4.3.2 Theory: Electronic Properties

The use of 7-aminocoumarins as sensors of biological processes and protein function brings forth the need of understanding the impact that C4-substitution has on their electron-densities. First, through the Bader charge analysis<sup>22</sup> we identified that altering the type of the functionality at the C4 site does not seem to have a noticeable influence on the electron density of the coumarin family. The Bader's charge associated with the R functional group is calculated to be 0.08e (-H), 0.11e (-CH<sub>3</sub>), -0.12e (-CF<sub>3</sub>), 0.06e (-Ph), -0.09e (-COOEt), 0.01e (-CONH<sub>2</sub>), 0.02e (-CNHMe) and 0e (-CONHPh). Interestingly, subtle changes induced by a specific substituent can be seen in the electrostatic potential surface plots displayed in Figure 2. In contrast to the cases of -CH<sub>3</sub> (i.e. Coumarin **2**) and -CF<sub>3</sub> (i.e. Coumarin **3**), substitution of the carbonyl group (-C=O) for coumarins **5** to **8** induces the electron-excess regions around the carbonyl group which is aligned in the same direction in coumarins **6**, **7**, and **8** but rotated in coumarin **5** with the -OEt group. The relative absence of electrons around the second amino group (-NH-R) creates another high potential area (blue) for coumarin **6**, **7**, and **8**.

**Figure 4.1.** Calculated electrostatic potential maps of the representative C4-substituted coumarins. Regions with the electron-excess density (low potential) and the electron-deficient (high potential) are represented by the red and blue regions with the contours ranging from -0.083 to + 0.083 Hartree/e.



### 4.3.3 Theory: Optical Properties

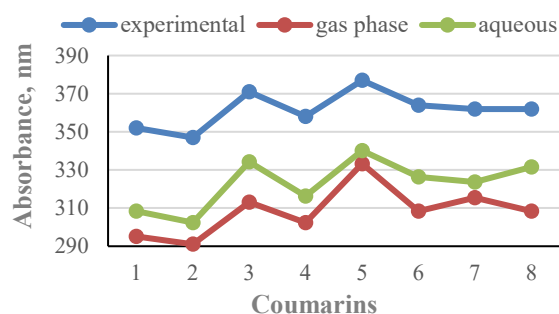
We begin with the calculations of the optimized ground state configurations of the C4-substituted coumarins in gas phase, which are then used as initial configurations for the geometry optimization of the molecules in aqueous-phase using PCM and subsequent TD-DFT calculations to determine the optical properties of the coumarin family. Note that a review and discussion of a large number of benchmark studies about the performance of the TD-DFT method to reproduce vertical (geometry of initial and final states is the same) and adiabatic (geometry of final states differs from initial state) valence electron transitions can be found in a recent analysis of the absorption spectra of four other 7-aminocoumarins.<sup>12</sup> In Table 2 we provide a comparison of our results with the previously reported results for Coumarin 2.

We find that an inclusion of the solvent effect for water with  $\epsilon = 78.35$  induces a red shift of about 18 nm for the first  $1 \rightarrow 1'$  singlet S1 excitation. This red shift is found to be independent of the nature of the solvent. Previous DFT calculations using a Dunning cc-pVDZ basis<sup>23</sup> reported a red shift of 26 nm in ethanol for Coumarin 2.<sup>14</sup>

#### 4.3.4 Absorption: DFT calculations

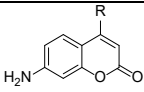
In general, the measured absorption peak of a given molecule can be approximated by the calculated difference between the highest occupied molecular orbital (HOMO) and the lowest unoccupied molecular orbital (LUMO). Interestingly, we find that the relative ordering of the calculated HOMO-LUMO gap values with respect to Coumarin **1** is the same as the relative ordering of the measured absorption peaks (Figure 3). This observation should be an indication that the HOMO-LUMO ( $1 \rightarrow 1'$ ) transition can be expected to be the dominant configuration in the first excited state calculation of the C4-substituted coumarin family.

Figure 2. Calculated HOMO-LUMO gap vs. measured absorption peaks for C4-substituted coumarins. Numbers on x-axis refer to coumarins listed in Table 1. The experimental absorption spectra are measured for coumarin solutions in methanol.



#### 4.3.5 Absorption: TD-DFT calculations

The results of the TD-DFT calculations of the vertical excitation energy of the C4-substituted coumarin family in the aqueous phase are summarized in Table 3.

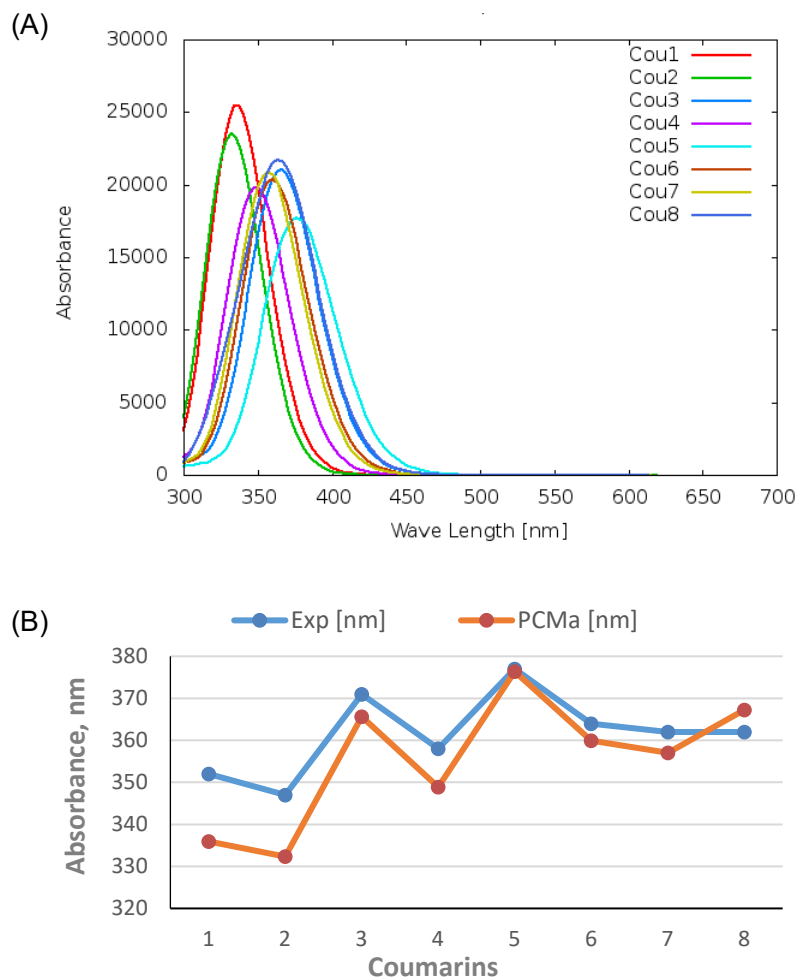
<b>Table 4.3.</b> The calculated vertical excitation energies and the measured absorption peak positions of the C4-substituted coumarins. The orbitals labeled as 1, 2, 1', and 2' are the HOMO, HOMO-1, LUMO and LUMO+1 orbitals, respectively (Figure 5).				
	Transition (weight)	Excitation (Theory) nm	Oscillator Strength	Absorption (Experiment) nm
Coumarin <b>1</b> (R=H)	S1: $1 \rightarrow 1'$ S2: $2 \rightarrow 1'$ (0.59)	336 287	0.4725 0.0047	352

	1→2' (0.37)			
Coumarin <b>2</b> (R=CH <sub>3</sub> )	S1: 1→1' S2: 2→1' (0.59) 1→2' (0.37)	332 284	0.4358 0.0020	347
Coumarin <b>3</b> (R=CF <sub>3</sub> )	S1: 1→1' S2: 2→1' (0.68) 1→2' (0.16)	366 305	0.3903 0.0172	371
Coumarin <b>4</b> (R=Ph)	S1: 1→1' S2: 2→1' (0.63) 1→2' (0.27) 1→4' (0.15)	349 293	0.3671 0.0162	358
Coumarin <b>5</b> (R=COOEt)	S1: 1→1' S2: 2→1' (0.69) 1→2' (0.13)	376 310	0.3281 0.0127	377
Coumarin <b>6</b> (R=CONH <sub>2</sub> )	S1: 1→1' S2: 2→1' (0.67) 1→2' (0.27)	360 300	0.3777 0.0127	364
Coumarin <b>7</b> (R=CONHMe)	S1: 1→1' S2: 2→1' (0.67) 1→2' (0.27)	357 299	0.3864 0.0127	362
Coumarin <b>8</b> (R=CONHPh)	S1: 1→1' S2: 2→1' (0.67)	367 333	0.3734 0.1034	362

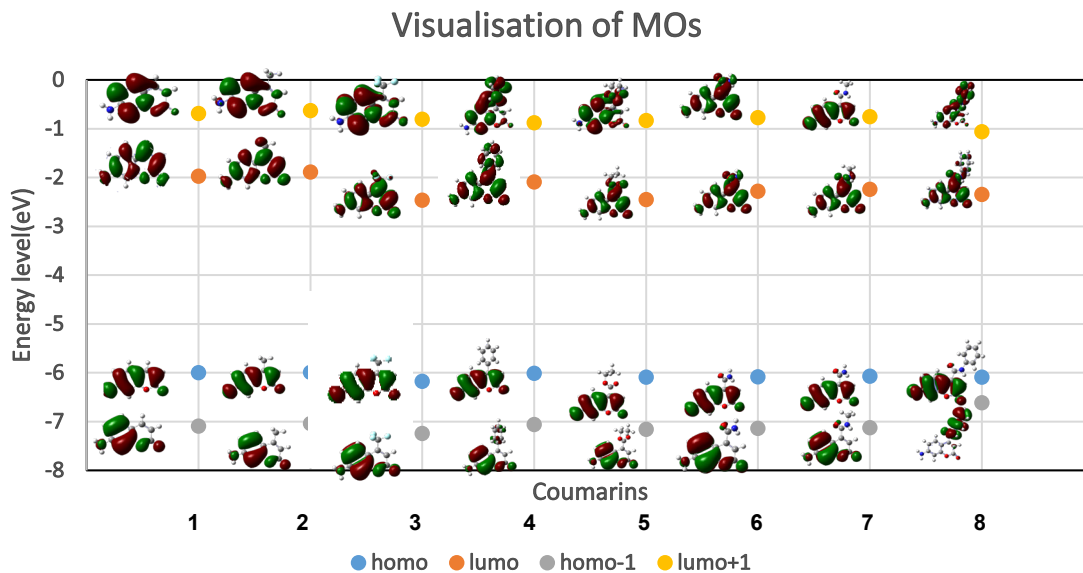
For all eight coumarins, the first few singlet excited states were calculated using the PCM model. The first excited state will be the state of interest whose geometry will be optimized to calculate the emission (fluorescence) spectrum below. The associated absorption spectra obtained with a broadening factor ( $\sigma$ ) of 0.25 eV (peak half-width at half-height) are displayed in Figure 4a. A comparison of the calculated and experimental absorption peak positions is made in Figure 4b showing that the TD-DFT calculations describe the trend observed in experiments very well. For the C4-substituted coumarins, the first excited singlet S1 has the largest oscillator strength (by at least an order of magnitude; the only exception is coumarin **8** where the second singlet excited state S2 has  $\sim 1/3$  of the S1 oscillator strength) as shown in Table 3. S1 is the HOMO→LUMO (1→1') transition between the  $\pi \rightarrow \pi^*$  orbitals that have the same primary character in all eight derivatives (see discussion below and Figure 5). The second singlet excitation S2 also has a similar character in all eight derivatives: it is dominated by the HOMO-1→LUMO (2→1')



transition with some HOMO→LUMO+1 (1→2') admixture. In coumarin **8**, S2 is a pure 2→1' excitation and is associated primarily with an intramolecular state transferring charge from the -CONHPh group at C4 to the coumarin aromatic system (Figure 5). The other exception is coumarin **4** (also a phenyl group at C4) for which S2 has some additional admixture from a 1→4' excitation. To understand the nature of orbitals associated with the optical properties, the frontier molecular orbitals, namely HOMO, HOMO-1, LUMO, and LUMO+1 are displayed in Figure 5. In the ground state of the C4-substituted coumarin family, HOMO is a  $\pi$ -orbital delocalized over the coumarin aromatic system with significant contributions from the benzene rings and the nitrogen atom but not from the carbonyl group and the R-group substitutions at C4. On the other hand, LUMO is a  $\pi^*$ -orbital with contributions from the carbonyl group and the R-group substitutions. A unique feature found only in coumarin **8** is the composition of the HOMO-1: it is completely localized on the -R substitution (-CONHPh) at the C4 site. Here, we restrict ourselves to the lowest excitations in the optical spectra since the experiments do not explore the region below 300 nm. Calculations exploring the <300 nm region have been reported elsewhere for coumarin **2**,<sup>14</sup> showing the next transition with significant oscillator strength to be at 5.4 eV (208 nm).



**Figure 4.2** (A) Calculated absorption spectra of coumarins listed in Table 1. (B) Calculated vs. measured absorption peak positions. Numbers on x-axis refer to coumarins listed in Table 1.



**Figure 3.3** The frontier molecular orbitals associated with the ground states of C4-substituted coumarins. Numbers on the x-axis refer to coumarins listed in Table 1

#### 4.3.6 Fluorescence: TD-DFT calculations

To calculate the fluorescence spectra, the geometry optimization calculations for the first excited singlet state (S1) of coumarins were performed using the PCMe model. The noticeable effects seen in the TD-DFT results can be summarized as follows:

1. Planarity of the amino group: In the ground state configuration, the amino group is pyramidal with the sum of the three C-N-C angles being  $\approx 350^\circ$ . The optimization of the excited state configuration yields the sum to be  $\approx 360^\circ$  making the amino group to be more planar (see Table S2, supplementary information).
2. Rotation of -R group: In the optimized first excited state, the calculated dihedral angle between the coumarin aromatic ring and the side group R is significantly modified relative to its value in the ground state configuration. Figure S1 displays the changes in the dihedral angle for the cases of phenyl ring substitution (e.g. Coumarins **4** and **8**) or the COOEt substitution (e.g. Coumarin **5**). This significant photoexcited rotation can be associated with larger Stokes shifts that was also discussed for a series of 14 fluorophores.<sup>10</sup>

3. Increase in dipole moment: Table 4 shows an enhancement of the dipole moment values in the optimized first excited state configuration relative to the corresponding values in the ground state. This is consistent with the fact that the first excited state is an excitation from HOMO ( $\pi$ -orbital delocalized over the coumarin aromatic system but not on the substituted R-group) to LUMO ( $\pi^*$  orbital with contributions from the R-group and the carbonyl group of the coumarin). Subsequently, this transition yields asymmetric charge distribution in the first excited state leading to higher dipole moments. Our results are similar to the results of *ab initio* excited-state molecular dynamics calculations for Coumarin **3** (or coumarin 151) reporting the significant increase in the gas-phase dipole moment of the excited state.<sup>24</sup>

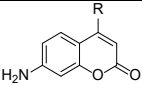
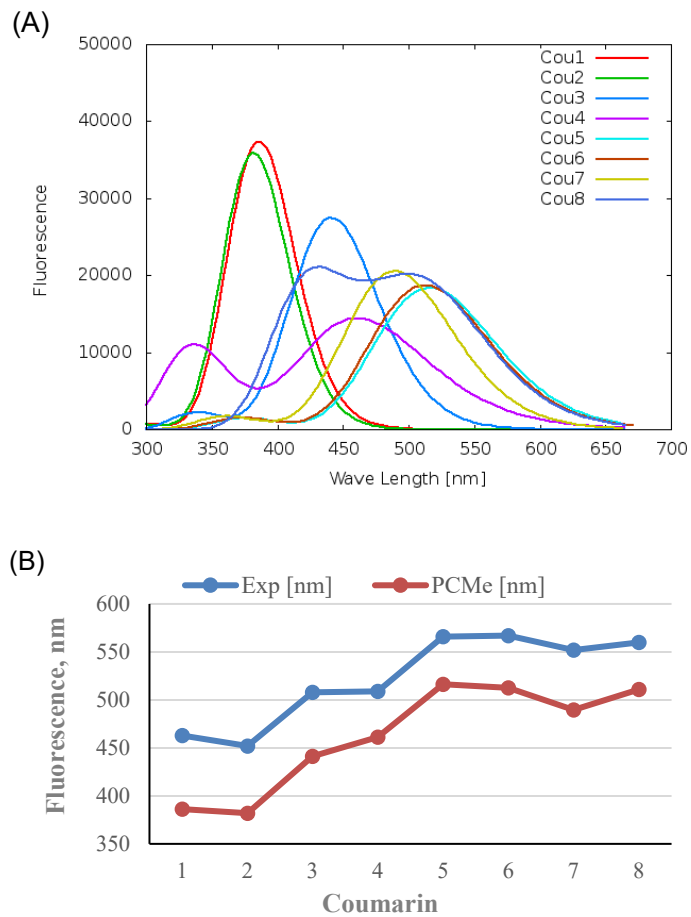
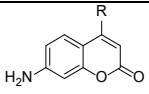
	Dipole Moment (Debye)	
	Ground State	Excited State
Coumarin <b>1</b> (R=H)	9.4	14.9
Coumarin <b>2</b> (R=CH <sub>3</sub> )	9.6	15.0
Coumarin <b>3</b> (R=CF <sub>3</sub> )	9.1	15.6
Coumarin <b>4</b> (R=Ph)	9.7	16.3
Coumarin <b>5</b> (R=COOEt)	11.4	17.9
Coumarin <b>6</b> (R=CONH <sub>2</sub> )	7.4	12.5
Coumarin <b>7</b> (R=CONHMe)	8.4	11.7
Coumarin <b>8</b> (R=CONHPh)	8.2	14.2

Table 5 lists values of the vertical emission energy obtained using the PCMe model for the C4-substituted coumarins in the aqueous phase. Note that most of the S<sub>2</sub> transitions are now associated with single 2 → 1' (HOMO-1 → LUMO) configurations. For Coumarins **4** and **8** with –R group having a phenyl group, significant oscillator strength is found for the second excited state (S<sub>2</sub>) which leads to a double peak structure in their emission spectra (Figure 6a). This is affirmed by the measured fluorescence spectra for Coumarin **8** as shown in Figure 1.



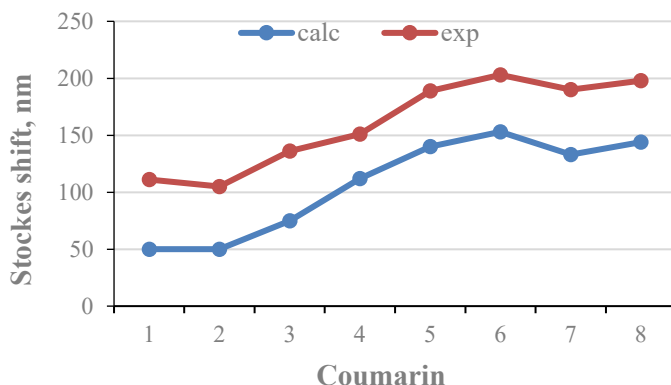
**Figure 4.4** a) Calculated fluorescence spectra. b) Calculated vs. measured fluorescence peak positions. Numbers on x-axis refer to coumarins listed in Table 1

<b>Table 4.5</b> Experimental and Calculated vertical transition energies associated with the fluorescence spectra obtained using the PCMe model for coumarins in the aqueous phase. The transition states are labeled as 1, 2, 1', and 2' for HOMO, HOMO-1, LUMO and LUMO+1 orbital, respectively.				
	Transition (weight)	Fluorescence Theory, nm	Oscillator Strength	Fluorescence Experiment, nm
Coumarin 1 (R=H)	S1: 1→1' S2: 2→1' (0.66) 1→2' (0.24)	386 301	0.6925 0.0132	463
Coumarin 2 (R=CH <sub>3</sub> )	S1: 1→1' S2: 2→1' (0.66) 1→2' (0.25)	382 297	0.6655 0.0122	452
Coumarin 3 (R=CF <sub>3</sub> )	S1: 1→1' S2: 2→1'	441 339	0.5091 0.0412	508
Coumarin 4 (R=Ph)	S1: 1→1' S2: 2→1' (0.48) 3→1' (0.50)	461 336	0.3554 0.2718	509
Coumarin 5 (R=COOEt)	S1: 1→1' S2: 2→1'	516 375	0.3406 0.0272	566
Coumarin 6 (R=CONH <sub>2</sub> )	S1: 1→1' S2: 2→1'	513 374	0.3464 0.0284	567
Coumarin 7 (R=CONHMe)	S1: 1→1' S2: 2→1'	490 361	0.3802 0.0322	552
Coumarin 8 (R=CONHPh)	S1: 1→1' S2: 2→1'	511 424	0.3422 0.3627	560

The theoretical fluorescence spectra for Coumarins 1-8 and the comparative analysis of experimental vs. calculated emission maxima are depicted in Figure 6. The TD-DFT results for the two lowest singlet states compared to the fluorescence peak positions of the experimental spectra suggest that the calculated peak positions follow the experimental trend but with the larger discrepancy: an average shift  $\Delta_e = 60$  nm was found for fluorescence maxima (Figure 6b) vs.  $\Delta_a = 8$  nm for absorption maxima (Figure 4b) between theoretical and experimental results. These larger discrepancies are not due to states crossing during the excited state optimization but seem to indicate that the excited state

optimization in solution using PCM is more sensitive to the specific approach used to describe the solvent-solute interaction: optimization with equilibrium linear response solvation describe the experimental trend; when using the state-specific external iteration solvation approach<sup>19</sup> for the coumarin series we find that it sometimes under- and sometimes overestimate the change in solvent-solute interaction.

The calculated Stokes shifts follow the experimental Stokes shifts (see Table 1) but shifted downwards by ~ 50 nm (see Figure 7).



**Figure 4.5** Comparison of calculated and experimental Stokes shifts.

#### 4.4 Conclusion

Coumarins as fluorescent sensors play an ever-increasing role in many biological applications, including the labeling of proteins, evaluation of sugar transport capacity in mammalian cells, and detection of cancer cells. The aim of this investigation was to get a fundamental understanding of the role of the C4 substitution on the electronic interactions that define coumarin fluorescence. Eight coumarins bearing different substituents at the C4 position were analyzed. Coumarins **1-3** were obtained from commercial sources, coumarins **4 - 8** were synthesized. TD-DFT methods were used to theoretically analyze the measured absorption and fluorescence spectra. We find that the first excited state S1 is the

HOMO→LUMO transition between the  $\pi\rightarrow\pi^*$  orbitals that have the same primary character in all eight derivatives: HOMO is a  $\pi$  orbital delocalized over the coumarin aromatic system with significant contributions from the benzene rings and the nitrogen atom; LUMO is a  $\pi^*$  orbital with contributions from the carbonyl group and the -R-group substitutions. That is, the photoexcitation leads to an asymmetric charge distribution with a large increase in dipole moment and geometry relaxation in the first excited states of coumarins. TD-DFT results for the absorption and emission spectra describe the trend of the experimental spectra well. The larger red shifts for the fluorescence peaks are found if the substituent contains a carbonyl (C=O) group which may be associated with significant change in rotation of the -R group relative to the coumarin rings of these C4-substituted coumarins. Considering the ever-growing interest in fluorescent probes of different colors, the methods provided here could be used for predicting the impacts of various substituents onto coumarin fluorescence.



## 5 Tuning Cross-Coupling Approaches to C3 Modification of 3- Deazaurines

### 5.1 Introduction

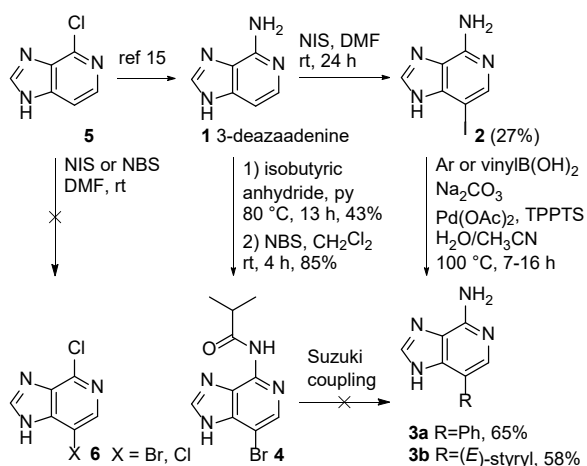
Purines are important building blocks used effectively across various disciplines. Functionalization and modification of purines have been of interest for synthetic organic chemistry, medicinal chemistry, and toxicology as reflected by the half-century application and development of purine-based anticancer or antiviral agents.<sup>1-4</sup> Purines are also of interest as detection probes,<sup>5-9</sup> and as mechanistic probes for understanding cellular responses to DNA and RNA modification.<sup>10,11</sup> Approaching these highly functionalized heterocycles often requires tuning of existing or development of new synthetic routes. Overcoming challenges associated with the reactivity of 3-deazaadenine derivatives, in particular, has been approached through *de novo* construction of 3-deaza-3-substituted purine backbone or functionalization of nucleosides. Several modifications such as 3-methyl, the related protected 3-hydroxymethyl and methylenethiol or nitro groups were reported.<sup>12-15</sup> 3-Deaza-3-fluoroadenosines had to be synthesized stepwise, but other 3-halo derivatives could also be obtained through direct halogenation of the non-substituted 3-deazaadenosines.<sup>16-22</sup> The use of cross-coupling reactions in C3-modification of purines is, however, limited. Examples of palladium-catalyzed methylations of 3-deaza-3-bromoadenosine analogs through Kumada coupling have been demonstrated.<sup>17,20</sup> Recently, the modification of adenosine nucleosides through Sonogashira cross-coupling have been reported, providing access to 3-deaza-3-alkyne adenosine derivatives.<sup>8,9,23</sup> However, the use of nucleosides as substrates for cross-coupling reactions can be challenging due to the presence of potentially labile glycosidic bonds or nucleophilic functional groups that have

to be protected to achieve the compatibility with many organometallic reagents, as reflected by the reported examples of Negishi and Kumada reactions for introduction of alkyl or benzyl substituents.<sup>24-27</sup> Given the importance of modified nucleobases itself, the method that would allow a direct access to C-3 modified purine scaffolds would be therefore of interest. Here we describe a general strategy that allows the deliberate synthesis of various 3-deaza-3-substituted purine analogs through metal-catalyzed cross-coupling reactions.

## 5.2 Results and Discussion

*En route* to 3-deazaadenine analogues of purines we first investigated the reactivity of the readily available 3-deazaadenine **1** (Scheme 1) in cross-coupling reactions.<sup>15</sup> In direct attempts to utilize it as a cross-coupling partner we were able to obtain the 3-iodo-3-deazaadenine **2**, and observe its acceptable reactivity in Suzuki cross-coupling conditions using the Pd(OAc)<sub>2</sub>/TPPTS catalyst system, a general method developed for aqueous coupling reactions of halogenated purine/pyrimidine nucleobases and nucleosides.<sup>4,26,28</sup> The reactions of **2** with phenylboronic acid and *trans*-2-phenylvinylboronic acid afforded compounds **3a** and **3b** with 65 and 58% yield, respectively (Scheme 1).

**Scheme 5.1.** Synthesis of compounds 1-4.



Despite the sufficient results obtained for Suzuki cross-coupling of **2** with model aryl/vinyl boronic acids, this conditions failed in the attempt to produce an alkyl analog with model ethylboronic acid, similarly as reported by other authors.<sup>26</sup> The reactivity of **2** can be hampered by its low solubility in organic solvents and the presence of active nucleophilic nitrogens. When the amino group at C6 was protected as an isobutyryl amide (the established purine protecting group), the more soluble *N*-(7-bromo-1*H*-imidazo[4,5-*c*]pyridin-4-yl)isobutyramide **4** was obtained (Scheme 1).<sup>15</sup> Various Suzuki coupling conditions of **4** with phenyl- and isobutylboronic acids were investigated, involving metal catalysts such as Pd(PPh<sub>3</sub>)<sub>4</sub>, Pd<sub>2</sub>(dba)<sub>3</sub>, PdppfCl<sub>2</sub> and NiCl<sub>2</sub>(dme), ligands such as PCy<sub>3</sub>, (*t*-Bu)<sub>2</sub>PMeHBF<sub>4</sub> and SPhos, and bases such as K<sub>2</sub>CO<sub>3</sub>, Cs<sub>2</sub>CO<sub>3</sub>, K<sub>3</sub>PO<sub>4</sub> and KO*t*-Bu in ethereal or alcoholic solvents.<sup>29-33</sup> Typically, the unreacted starting material was recovered from the reaction mixtures, highlighting the lack of reactivity of **4**. Also, the liability of amide protecting group prohibited the use of aqueous coupling conditions utilizing bases such as carbonates.

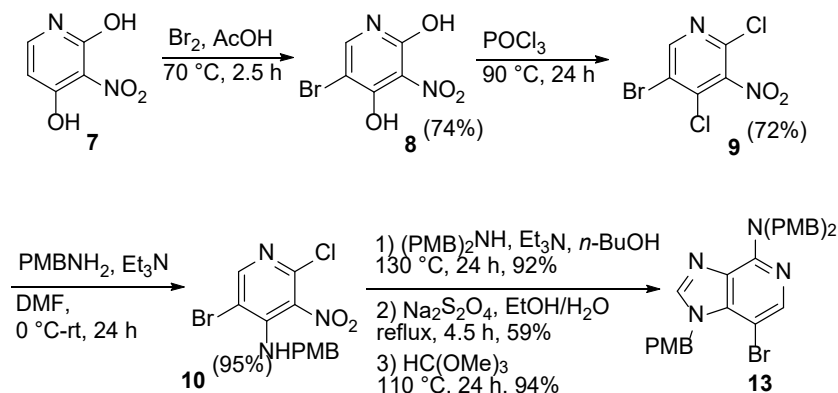
We have also evaluated the possibility to use a commercial C6-chloro (**5**) and the known C6-azide<sup>34</sup> (**5b**) purines as a starting materials amenable for further amination or reduction, respectively, to access 3-deazaadenine. However, the attempts to install a halide at the C3 (Compound **6**, Scheme 1) have failed, precluding further evaluation.

As the electron withdrawing groups at C6 (chloride, amide or azide) were shutting off the reactivity of C3 position, we hypothesized that the use of electronically more neutral protecting groups will promote the solubility of **1**, and retain its reactivity towards cross-coupling reactions. Unfavorably, the direct attempts to react **5** with bisbenzylamines to produce the desired cross-coupling partner of type **13** (Scheme 2) failed even under harsh conditions (e. g., 140 °C, neat or DMF/K<sub>2</sub>CO<sub>3</sub>), reflecting the evident low reactivity of this substrate towards direct displacement of chlorine atom.<sup>12,34</sup> We decided to investigate the catalytic aminations with bis(4-methoxybenzylamine) ((PMB)<sub>2</sub>NH) on **5**. In parallel, the catalytic amination of PMB-protected analog was investigated, considering the reported challenges for modifications of unprotected imidazoles.<sup>35</sup> It should be noted that PMB

protection of **5** (PMBCl, K<sub>2</sub>CO<sub>3</sub>, DMA, 45 °C, 24 h, 96% yield) yielded a ~1.6:1 mixture of N9- and N7-PMB protected products that was used directly.<sup>36</sup> Several literature conditions applicable for chloroarenes, 6-halopurines and their nucleosides were investigated.<sup>37-42</sup> RuPhos and its Pd-bound precatalyst in the presence of NaO*t*-Bu in THF,<sup>41</sup> have been shown to be particularly successful for the reactions of non-activated heteroaryl chlorides with secondary amines. In these conditions, up to 19% of N9-PMB protected product (identical to **13-H**, Experimental Section) was obtained, albeit with higher catalyst loading (6 mol%) and prolonged reaction time (43 h). However, a significant decomposition was observed. The use of LiHMDS instead of NaO*t*-Bu led to the exclusive decomposition of both protected and non-protected **5**. Next, Pd(OAc)<sub>2</sub> was tested in combination with ligands such as BINAP, SPhos and XPhos in the presence of Cs<sub>2</sub>CO<sub>3</sub> or NaO*t*-Bu in solvents such as toluene, THF, dioxane and DMF.<sup>37-40,42</sup> Significant decomposition was observed in the majority of cases, and no product formation. Some level of success was achieved with the combination of Pd(OAc)<sub>2</sub> (0.1 eq.) and SPhos (0.2 eq.) in the presence of NaO*t*-Bu in toluene (110 °C, 22 h). **13-H** was isolated in 21% yield, reflecting the low reactivity of heteroaryl chlorides with secondary amines.<sup>40,41</sup> For practical purposes, we have not investigated this reaction further.

To overcome hurdles posed by the limited reactivity of the tested substrates, we decided to construct the fully protected 3-deazadenenine analog from the cheap, available precursors, using a similar route as reported in the literature.<sup>15,43</sup> The highly regioselective sequential substitutions of 4- and 2-chloro atoms of the known derivative **9**<sup>43</sup> with 4-methoxybenzylamine (PMBNH<sub>2</sub>), followed by (PMB)<sub>2</sub>NH produced the compound **11** (Experimental Section) and upon further reduction of the nitro group and cyclization, we were able to obtain the target 3-deazaadenine precursor (**13**) with the exclusive N9-PMB protection and 26% overall yield in 6 steps from a commercial 3-nitropyridine-2,4-diol **7** (Scheme 2). The length of the synthetic route is similar to that of **1**<sup>15</sup> but offers the access to the fully protected soluble starting material amenable to functionalization.

**Scheme 5.2.** Synthesis of compound **13**.



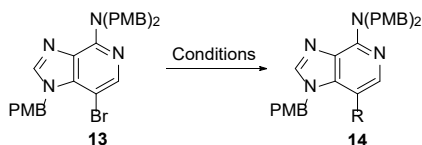
Gratifyingly, a variety of different coupling conditions involving **13** were successfully demonstrated as shown in Table 1, including the examples of reactions such as Suzuki<sup>43,44</sup> (entries 1-5), Heck<sup>45</sup> (entries 6 and 7), Sonogashira<sup>8,23</sup> (entry 8), Kumada<sup>46</sup> (entries 9 and 10), Negishi (entries 11-14)<sup>47</sup> and the nickel-catalyzed reductive couplings of alkyl halides recently developed by the Weix group (entry 15).<sup>48</sup>

The Suzuki couplings could be accomplished with aromatic, alkenyl and alkyl boronic acids (entries 1-5). Both electron-rich and electron-deficient alkenes were tolerated under the Heck conditions (entries 6-7). Sonogashira coupling with phenylacetylene proceeded with high efficiency (89%, entry 8).

The formation of alkyl derivatives, with the challenging substrates containing  $\beta$ -hydrogens, such as alkylboronic acids or ethyl 4-bromobutyrate was less efficient (29-35%, entries 3-5 and 15) and accompanied by a significant hydrodebromination reaction, indicating the extent of the undesired  $\beta$ -H elimination. This byproduct (**13-H**) could be subjected to halogenation, e. g. by the treatment of crude reaction mixtures with NBS/NIS, facilitating a chromatographic separation of the cross-coupled product **14**, while the haloderivative **13/13-I** could be recovered (see Experimental Section). The iodo analog **13-I** obtained this way offered no selectivity enhancement for alkylations using conditions B or F. Propitiously, simple alkyl derivatives could be obtained with improved yields (45-87%)

through Kumada-type couplings with substrates such as trimethylaluminum and benzylmagnesium chloride (entries 9 and 10). Ultimately, modified Negishi conditions allowed the access to a variety of primary alkyl derivatives with notably higher yields than those obtained through Suzuki protocol (entries 11-13 versus 3-5). In the case of challenging isopropyl derivative, we observed up to 20% of the known isopropyl to *n*-propyl isomerization (entry 14).<sup>49</sup> Interestingly, our Negishi protocol provided satisfying and consistent results only when an excess of Grignard reagent against an overstoichiometric amount of zinc chloride was used, which helped to improve the solubility of the intermediate organozinc species. This observation seems to be in accord with the works by the Organ group that unveiled the mechanisms involving organozinc reagents in Negishi cross-couplings.<sup>50,51</sup>

**Table 5.1.** Transformation scope for the metal-catalyzed couplings of **13**.

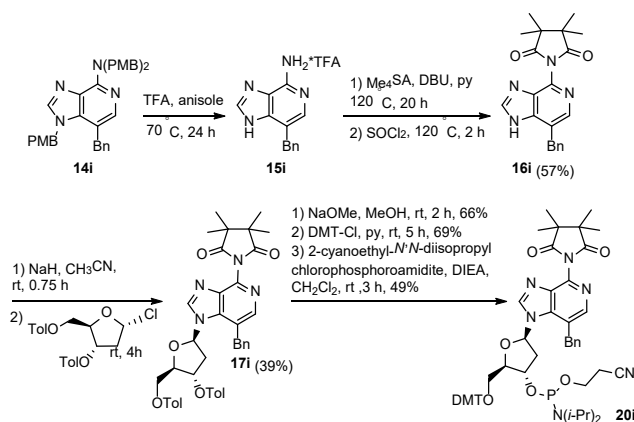


Entry	Substrate	Cond. <sup>a</sup>	Product	Yield (%)
1	PhB(OH) <sub>2</sub>	A	<b>14a</b> , R=Ph	91
2	PhCH=CH <sub>2</sub> B(OH) <sub>2</sub>	A	<b>14b</b> , R=( <i>E</i> )-styryl	79
3	Ph(CH <sub>2</sub> ) <sub>2</sub> B(OH) <sub>2</sub>	B	<b>14c</b> , R=(CH <sub>2</sub> ) <sub>2</sub> Ph	35
4	EtB(OH) <sub>2</sub>	B	<b>14d</b> , R=Et	31
5	<i>i</i> -BuB(OH) <sub>2</sub>	B	<b>14e</b> , R= <i>i</i> -Bu	29
6	PhCH=CH <sub>2</sub>	C	<b>14b</b> , R=( <i>E</i> )-styryl	53
7	CH <sub>2</sub> =CHCO <sub>2</sub> Me	C	<b>14f</b> , R=( <i>E</i> )-acrylate	57 <sup>b</sup>
8	PhC≡CH	D	<b>14g</b> , R=C≡CPh	89
9	Al(Me) <sub>3</sub>	E	<b>14h</b> , R=Me	87
10	BnMgCl	E	<b>14i</b> , R=Bn	45
11	Ph(CH <sub>2</sub> ) <sub>2</sub> ZnX	F	<b>14c</b> , R=(CH <sub>2</sub> ) <sub>2</sub> Ph	77
12	EtZnX	F	<b>14d</b> , R=Et	76
13	<i>i</i> -BuZnX	F	<b>14e</b> , R= <i>i</i> -Bu	85
14	<i>i</i> -PrZnX	F	<b>14j</b> , R= <i>i</i> -Pr	86 <sup>c</sup>
15	Br(CH <sub>2</sub> ) <sub>3</sub> CO <sub>2</sub> Et	G	<b>14k</b> , R=(CH <sub>2</sub> ) <sub>3</sub> CO <sub>2</sub> Et	32 <sup>b</sup>

<sup>a</sup> Conditions A: Ar or vinylB(OH)<sub>2</sub> (1.5 equiv.), Cs<sub>2</sub>CO<sub>3</sub> (2 equiv.), Pd(PPh<sub>3</sub>)<sub>4</sub> (0.1 equiv.), dioxane/H<sub>2</sub>O (2/1), Ar, 90 °C, 6-16 h; Conditions B: AlkylB(OH)<sub>2</sub> (1.1-1.5 equiv.), K<sub>2</sub>CO<sub>3</sub> (3 equiv.), Pd(PPh<sub>3</sub>)<sub>4</sub> (0.1 equiv.), dry dioxane, Ar, 90 °C, 72 h; Conditions C: styrene or methyl acrylate (5 equiv.), Et<sub>3</sub>N (7 equiv.), PPh<sub>3</sub> (0.5 equiv.), Pd(OAc)<sub>2</sub> (0.1 equiv.), dry CH<sub>3</sub>CN, Ar, 90 °C, 36 h; Conditions D: phenylacetylene (1.5 equiv.), Pd(PPh<sub>3</sub>)<sub>2</sub>Cl<sub>2</sub> (0.1 equiv.), CuI (0.1 equiv.), dry DMF/Et<sub>3</sub>N (2/1), Ar, 80 °C, 24 h; Conditions E: Al(Me)<sub>3</sub> or BnMgCl solution (3-3.3 equiv.), Pd(PPh<sub>3</sub>)<sub>4</sub> (0.1 equiv.), dry THF, Ar, 75 °C, 4 h; Conditions F: ZnCl<sub>2</sub> (0.5 M in THF, 5.7 equiv.), AlkylMgX solution (X = Br or Cl, 8.6 eq.), Ar, rt, 1 h, then **13** (1 equiv.), PddppfCl<sub>2</sub> (0.1 eq.), Ar, rt, 21-29 h; Conditions G: Br(CH<sub>2</sub>)<sub>3</sub>CO<sub>2</sub>Et (1.1 equiv.), Zn (2 equiv.), 4,4'-dimethoxy-2,2'-bipyridine (0.1 equiv.), NiI<sub>2</sub> (0.13 equiv.), pyridine (0.1 equiv.), NaI (0.25 equiv.), dry DMA, Ar, rt, 5 min., then 60 °C, 20 h; <sup>b</sup> Yield isolated after treatment of the crude mixture with NIS and separation of **13-I** (for details, see Experimental Section); <sup>c</sup> Contains ~20% of *n*-propyl impurity.

Clearly, the fully protected nucleobase **13** allows the use of a broad scope of coupling conditions with the formation of not only saturated and unsaturated C-C bonds, but also the introduction of functional groups, to access the C3-modified 3-deazaadenine derivatives. These results pinpoint appropriateness of the PMB as a protecting group with suitable electronic and chemical properties that allowed to achieve the desired reactivity of **13** among the other tested 3-deaza-3-halo adenine substrates.

**Scheme 5.3.** Synthesis of phosphoramidite **20i**.



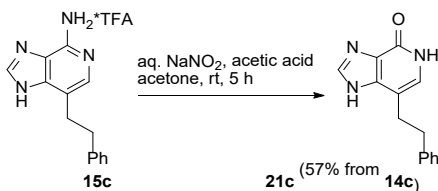
We further aimed to elaborate the products to the protected phosphoramidites to verify their compatibility with producing building blocks for solid phase DNA synthesis. The route to phosphoramidites is exemplified by the synthesis of compound **20i** (Scheme 3). We successfully optimized the procedure for complete deprotection of benzyl derivative **14i** affording modified purine **15i**.<sup>52</sup> The known problem of selectivity for purine glycosylations prompted us to use the tetramethylsuccinimide directing/protecting group, developed by the McLaughlin group<sup>53</sup> in order to increase the selectivity towards the desired N9  $\beta$ -glycosylation. The crude salt **15i** was converted accordingly to the corresponding imide **16i** through the reported two-step procedure using tetramethylsuccinic anhydride (Me<sub>4</sub>SA).<sup>53</sup> The imide **16i** was subjected to glycosylation with 1-( $\alpha$ )-chloro-3,5-di-O-(*p*-toluoyl)-2-deoxy-D-ribose affording the desired N9  $\beta$ -nucleoside **17i** in 39% yield. The configuration of nucleoside **17i** was unambiguously



confirmed by the NOESY experiment (Figure S1, Supporting Information). It was then elaborated to the corresponding phosphoramidite **20i** through standard methods (Scheme 3). Analogously, two other phosphoramidites **20d** and **20e** were prepared from **14d** and **14e**, ethyl and isobutyl analogs, respectively. All three phosphoramidites were successfully used in solid-phase DNA synthesis and further studies are in progress. Interestingly, the preparation of the corresponding phosphoramidite **20a** from phenyl derivative **14a** could not be achieved due to the destabilizing effect of the Ph group on the glycosidic bond (see Experimental Section). We have also considered the possibility of the direct functionalization of nucleosides by an attempt to prepare a bromo analog of **17i** through the halogenation of the reported non-modified 3-deazaadenine phosphoramidite.<sup>13</sup> However, the reactions with NBS in CH<sub>2</sub>Cl<sub>2</sub> or DMF were unsuccessful, likely due to the electronegative effect of the tetramethylsuccinimide group.

Additionally, the modified 3-deazaadenines could be readily converted to the corresponding 3-deazahypoxanthines, purine analogues of interest for medicinal chemistry,<sup>36,54</sup> upon treatment with NaNO<sub>2</sub> as exemplified by the reaction of crude salt **15c** to produce **21c** in 57% yield based on **14c** (Scheme 4).<sup>55,56</sup> This transformation further demonstrates the potential of our synthetic approach towards C3-modified purine scaffold.

**Scheme 5.4.** Synthesis of 3-deazahypoxanthine **21c**.



### 5.3 Conclusions

This study illustrates the merit of a new fully protected 3-bromo-3-deazadenine derivative developed by us as a building block for the deliberate synthesis of 3-substituted 3-deazaadenine and adenosine derivatives through metal-catalyzed cross-coupling reactions

and selective N9  $\beta$ -glycosylations. It should be expected that both modified purines and their nucleosides will be of interest for applications related to chemical biology, DNA studies and medicinal chemistry.

## 5.4 Experimental Section

**General methods:** All reagents were used as received unless otherwise stated from Sigma-Aldrich, TCI America, Alfa Aesar, AK Scientific or Chem-Impex International. 4-Chloro-1*H*-imidazo[4,5*c*]pyridine was obtained from MolBridge. Bis(4-methoxybenzyl)amine and TPPTS were obtained from Ark Pharm. 1-( $\alpha$ )-Chloro-3,5-di-O-(*p*-toluoyl)-2-deoxy-D-ribose was purchased from Berry & Associates. Anhydrous methanol, pyridine, and *N,N*-dimethylacetamide (DMA) were obtained from Sigma-Aldrich. *N,N*-dimethylformamide (DMF) and 1,4-dioxane were dried and stored over CaH<sub>2</sub> before use. Dry acetonitrile, dichloromethane, and tetrahydrofuran were dispensed from an automated Innovative Technology Pure-Solv 400 Solvent Purification System. Analytical TLC was carried out on commercial SiliCycle SiliaPlate® 0.2 mm F254 plates. Preparative silica chromatography was performed using SiliCycle SiliaFlash® F60 40-63  $\mu$ m (230-400 mesh). <sup>1</sup>H, <sup>13</sup>C and <sup>31</sup>P NMR spectra were recorded at room temperature with a Varian Unity Inova 400 MHz spectrometer. CDCl<sub>3</sub>, DMSO-d<sub>6</sub>, CD<sub>3</sub>OD, acetone-d<sub>6</sub> and D<sub>2</sub>O were used as solvents and referenced to the corresponding residual solvent peaks (7.26 and 77.16 ppm for CDCl<sub>3</sub>, respectively; 2.50 and 39.52 ppm for DMSO-d<sub>6</sub>, respectively; 3.31 and 49.0 ppm for CD<sub>3</sub>OD, respectively; 2.05 and 29.84 ppm for acetone-d<sub>6</sub>, respectively; 4.79 ppm for D<sub>2</sub>O).<sup>57</sup> The following abbreviations are used to indicate the multiplicity: s - singlet; d - doublet; t - triplet; q - quartet; m - multiplet; b - broad signal; app - approximate. The coupling constants are expressed in Hertz (Hz). The multiplicity of carbon atoms was determined by DEPT-135 experiment; Cq - quaternary carbon. MS data (ESI) were obtained using a Thermo Finnigan LCQ Advantage Ion-Trap Mass Spectrometer. The high-resolution (HR) MS data (ESI) were obtained using a Thermo Fisher Orbitrap Elite™ Hybrid Ion Trap-Orbitrap Mass Spectrometer at Chemical Advanced Resolution Methods (ChARM) Laboratory at Michigan Technological University.

Synthesis and characterization data.

Compounds **1**,<sup>15</sup> **4**,<sup>15,22</sup> and **5b**<sup>34</sup> were prepared according to the reported procedures.

**7-Iodo-1H-imidazo[4,5c]pyridin-4-amine (2):** To a suspension of amine **1** (536 mg, ca. 4 mmol) in dry DMF (8 ml), *N*-iodosuccinimide (NIS) (1.125 g, 5 mmol) was added in one portion. Slightly exothermic reaction occurred, and the resulting dark solution was stirred at room temperature for 24 h. After 24 h, the solution was added dropwise to EtOAc (100 ml) with vigorous stirring, and the resulting solid was filtered and washed with EtOAc. The solid was then suspended in chloroform (50 ml) and vigorously stirred under reflux condenser at 70 °C overnight. After filtration and drying on air, **2** was obtained as a dark brown solid in 27% yield (0.27 g). HRMS (ESI): *m/z* [M+H]<sup>+</sup> calc'd for C<sub>6</sub>H<sub>4</sub>N<sub>4</sub>I: 260.96373; found: 260.96323. MS (ESI): *m/z*, 261.2 for [M+H]<sup>+</sup>. <sup>1</sup>H NMR (400 MHz, DMSO-*d*<sub>6</sub>): δ, 8.49 (s, 1H), 8.44 (bs, 2H), 7.97 (s, 1H) ppm. We were not able to obtain satisfactory <sup>13</sup>C NMR data in DMSO-*d*<sub>6</sub>.

**7-Phenyl-1H-imidazo[4,5c]pyridin-4-amine (3a):** This compound was synthesized according to the reported general procedures.<sup>4,26</sup> To a vial equipped with septa a mixture of deionized water/acetonitrile (2/1, 9 ml) was added and bubbled with argon for 10 min. **2** (150 mg, 0.58 mmol), phenylboronic acid (88 mg, 0.72 mmol), palladium(II) acetate (7 mg, 0.029 mmol), TPPTS (41 mg; 0.072 mmol) and anhydrous sodium carbonate (183 mg; 1.7 mmol) were added, and the headspace of the vial was flushed with argon for 1 minute. The mixture was vigorously stirred at 100 °C for 7 h. The mixture was then cooled and diluted with ethyl acetate (50 ml) and brine (10 ml). The phases were separated, and the aqueous phase was extracted with additional ethyl acetate (3 x 30 ml). Combined organic extracts were dried with MgSO<sub>4</sub>. After filtration and concentration, the residue was purified by column chromatography on silica gel, eluting with 0-10% MeOH in CH<sub>2</sub>Cl<sub>2</sub> to obtain **3a** as a yellow solid in 65% yield (79 mg). HRMS (ESI): *m/z* [M+H]<sup>+</sup> calc'd for C<sub>12</sub>H<sub>11</sub>N<sub>4</sub>: 211.09838; found: 211.09680. MS (ESI): *m/z*, 211.3 for [M+H]<sup>+</sup>. <sup>1</sup>H NMR (400 MHz,

DMSO-d<sub>6</sub>):  $\delta$ , 8.20 (s, 1H), 7.85 (s, 2H), 7.73 (b, 2H), 7.48-7.44 (m, 2H), 7.34-7.30 (m, 1H), 6.46 (b, 2H) ppm. <sup>13</sup>C NMR (100 MHz, DMSO-d<sub>6</sub>):  $\delta$ , 141.3, 137.5, 136.1, 128.7, 127.3, 126.5 ppm.

**(E)-7-Styryl-1H-imidazo[4,5-c]pyridin-4-amine (3b)**: This compound was synthesized in similar fashion as **3a**. To a vial equipped with septa a mixture of deionized water/acetonitrile (2/1, 6 ml) was added and bubbled with argon for 10 min. **2** (100 mg, 0.38 mmol), *trans*-2-phenylvinylboronic acid (71 mg, 0.48 mmol), palladium(II) acetate (5 mg, 0.019 mmol), TPPTS (28 mg; 0.048 mmol) and anhydrous sodium carbonate (122 mg; 1.2 mmol) were added, and the headspace of the vial was flushed with argon for 1 minute. The mixture was vigorously stirred at 100 °C for 16 h. The mixture was then cooled and diluted with ethyl acetate (40 ml) and brine (10 ml). The phases were separated, and the aqueous phase was extracted with additional ethyl acetate (3 x 20 ml). Combined organic extracts were dried with MgSO<sub>4</sub>. After filtration and concentration, the residue was purified by column chromatography on silica gel, eluting with 0-10% MeOH in CH<sub>2</sub>Cl<sub>2</sub> to obtain **3b** as a cream solid in 58% yield (52 mg). HRMS (ESI): m/z [M+H]<sup>+</sup> calc'd for C<sub>14</sub>H<sub>13</sub>N<sub>4</sub>: 237.11403; found: 211.11269. <sup>1</sup>H NMR (400 MHz, DMSO-d<sub>6</sub>):  $\delta$ , 8.28 (s, 1H), 7.89 (s, 1H), 7.58-7.56 (m, 2H), 7.38-7.31 (m, 4H), 7.23-7.20 (m, 1H), 6.52 (b, 2H) ppm. <sup>13</sup>C NMR (100 MHz, DMSO-d<sub>6</sub>):  $\delta$ , 141.1, 139.7, 138.2, 128.6, 126.8, 125.8, 124.0 ppm.

Synthesis of 13.

Compounds **8** and **9** were prepared by modification of the reported procedures.<sup>43</sup>

**5-Bromo-3-nitropyridine-2,3-diol (8)**: To the suspension of 3-nitropyridine-2,4-diol **7** (10 g, 64.1 mmol) in glacial acetic acid (100 ml), bromine (4.6 ml, 90 mmol) was added in one portion, and the mixture was stirred at 70 °C for 2.5 h. Reaction mixture was then cooled and poured onto 300 ml of crushed ice, stirred vigorously for 30 min., and chilled in the freezer for 1 h. The precipitated solids were filtered on paper, washed with small volume

of ice-cold water several times, then ethanol (3 x 15 ml), and dried on air. **8** was obtained as a yellow solid in 74% yield (11.2 g). <sup>1</sup>H NMR (400 MHz, DMSO-d<sub>6</sub>): δ, 7.86 (s, 1H) ppm. <sup>13</sup>C NMR (100 MHz, DMSO-d<sub>6</sub>): δ, 159.1, 155.6, 138.6, 128.2, 94.0 ppm.

**5-Bromo-2,4-dichloro-3-nitropyridine (9):** A suspension of **8** (11.1 g, 47.4 mmol) in POCl<sub>3</sub> (100 ml) was stirred at 90 °C for 24 h under argon, an excess pressure being released several times within first few hours. Then POCl<sub>3</sub> was carefully distilled off under vacuum. The oily residue was diluted with Et<sub>2</sub>O (100 ml), cooled on an ice bath and crushed ice (200 ml) was carefully added (exothermic reaction). The phases were separated, aqueous phase was additionally extracted with Et<sub>2</sub>O (2 x 50 ml), the combined organics were washed with brine, and dried with MgSO<sub>4</sub>. After filtration and concentration, the residue was purified by column chromatography on silica gel, eluting with 0-10% EtOAc in hexanes to obtain **9** as a yellow oil that slowly solidified (9.27 g, 72% yield). <sup>1</sup>H NMR (400 MHz, CDCl<sub>3</sub>): δ, 8.68 (s, 1H) ppm. <sup>13</sup>C NMR (100 MHz, CDCl<sub>3</sub>): δ, 152.1, 141.5, 137.8, 121.3 ppm.

**5-Bromo-2-chloro-N-(4-methoxybenzyl)-3-nitropyridin-4-amine (10):** To the solution of **9** (9.25 g, 34.3 mmol) in dry DMF (50 ml) at 0 °C under argon, 4-methoxybenzylamine (4.7 ml, 36 mmol) was added in one portion, followed by dropwise addition of Et<sub>3</sub>N (5.5 ml, 36 mmol) over 5 minutes. The mixture was allowed to warm up to room temperature and stirred for 24 h. The mixture was then diluted with EtOAc (300 ml), washed with brine (4 x 100 ml), and dried with MgSO<sub>4</sub>. After filtration, the solution was concentrated in vacuo to give yellow solid that was triturated with hexanes to give **10** as a dark orange solid (12.1 g, 95% yield). HRMS (ESI): m/z [M+H]<sup>+</sup> calc'd for C<sub>13</sub>H<sub>12</sub><sup>79</sup>Br<sup>35</sup>ClN<sub>3</sub>O<sub>3</sub>: 371.97507; found: 371.97488. <sup>1</sup>H NMR (400 MHz, CDCl<sub>3</sub>): δ, 8.23 (s, 1H), 7.24-7.22 (d, J = 8.4, 2H), 6.93-6.91 (d, J = 8.4, 2H), 5.24 (bs, 1H), 4.22-4.21 (d, J = 4.8, 2H), 3.82 (s, 3H) ppm. <sup>13</sup>C NMR (100 MHz, CDCl<sub>3</sub>): δ, 160.1 (Cq), 149.3, 143.4 (Cq), 143.3 (Cq), 129.7, 127.9 (Cq), 114.8, 109.4 (Cq), 55.5, 47.0 (CH<sub>2</sub>) ppm.

**5-Bromo-*N*<sup>2</sup>,*N*<sup>2</sup>,*N*<sup>4</sup>-tris(4-methoxybenzyl)-3-nitropyridine-2,4-diamine (11):** A 250 ml Schlenk tube was charged with **10** (12.1 g, 32.6 mmol), bis(4-methoxybenzyl)amine (10.9 g, 42.4 mmol), *n*-butanol (100 ml) and Et<sub>3</sub>N (6 ml, 43.1 mmol). The mixture was heated at 130 °C for 24 h. It was cooled, diluted with EtOAc (400 ml), washed with brine (200 ml), and dried with MgSO<sub>4</sub>. After filtration, the solution was concentrated to give a dark residue that was purified by column chromatography on silica gel, eluting with 0-15% EtOAc in hexanes to obtain **11** as a red foam (17.6 g, 92% yield). HRMS (ESI): *m/z* [M+H]<sup>+</sup> calc'd for C<sub>29</sub>H<sub>30</sub><sup>79</sup>BrN<sub>4</sub>O<sub>5</sub>: 593.13999; found: 593.13894. <sup>1</sup>H NMR (400 MHz, CDCl<sub>3</sub>): δ, 8.09 (s, 1H), 7.21-7.18 (d, *J* = 8.8, 2H), 7.08-7.05 (d, *J* = 8.8, 4H), 6.88-6.86 (d, *J* = 8.8, 2H), 6.82-6.80 (d, *J* = 8.8, 4H), 6.14-6.12 (t, *J* = 4.8, 1H), 4.46-4.45 (d, *J* = 4.8, 2H), 4.29 (s, 4H), 3.782 (s, 3H), 3.778 (s, 6H) ppm. <sup>13</sup>C NMR (100 MHz, CDCl<sub>3</sub>): δ, 159.6 (Cq), 159.0 (Cq), 155.5 (Cq), 151.1, 146.5 (Cq), 129.7, 129.5 (Cq), 129.4, 129.2 (Cq), 126.0 (Cq), 114.5, 113.9, 99.6 (Cq), 55.4, 55.3, 53.7 (CH<sub>2</sub>), 49.2 (CH<sub>2</sub>) ppm.

**5-Bromo-*N*<sup>2</sup>,*N*<sup>2</sup>,*N*<sup>4</sup>-tris(4-methoxybenzyl)pyridine-2,3,4-triamine (12):** A 1 L round bottom flask was charged with **11** (16.7 g, 28.2 mmol), ethanol (600 ml) and deionized water (300 ml), followed by Na<sub>2</sub>S<sub>2</sub>O<sub>4</sub> (9.81 g, 56.4 mmol, 2 equiv.). The mixture was heated at 85 °C under reflux condenser. Additional sodium hydrosulfite was added at 30 min. intervals (overall, 4 x 2 equiv.) over 2.5 h. The mixture was then concentrated in vacuo to remove most of ethanol, and diluted with EtOAc (200 ml). It was carefully neutralized with solid NaHCO<sub>3</sub> (effervescence!) with vigorous stirring. The organic layer was separated, the aqueous phase was additionally extracted with EtOAc (2 x 150 ml) and the combined organics were washed with brine (100 ml), and dried with MgSO<sub>4</sub>. After filtration and concentration, the residue was purified by column chromatography on silica gel, eluting with 0-60% EtOAc in hexanes, and the product was additionally triturated with hexanes containing some EtOAc to obtain **12** as a cream solid in 59% yield (9.4 g). This compound is somewhat unstable and should be used within few days. HRMS (ESI): *m/z* [M+H]<sup>+</sup> calc'd for C<sub>29</sub>H<sub>32</sub><sup>79</sup>BrN<sub>4</sub>O<sub>3</sub>: 563.1658; found: 563.16396. <sup>1</sup>H NMR (400 MHz, CDCl<sub>3</sub>): δ, 7.77 (s, 1H), 7.22-7.20 (d, *J* = 8.8, 2H), 7.10-7.08 (d, *J* = 8.8, 4H), 6.84-6.82 (d, *J* = 8.8, 2H), 6.81-6.79 (d, *J* = 8.8, 4H), 4.25-4.24 (d, *J* = 6.8, 2H), 4.14 (s, 4H), 4.00 (bs, 2H), 3.78

(s, 9H) ppm.  $^{13}\text{C}$  NMR (100 MHz,  $\text{CDCl}_3$ ):  $\delta$ , 159.1 (Cq), 158.8 (Cq), 150.2 (Cq), 139.8 (Cq), 138.3, 131.6 (Cq), 130.7 (Cq), 130.1, 129.9 (Cq), 129.2, 114.1, 113.7, 110.8 (Cq), 55.36, 55.34, 53.5 ( $\text{CH}_2$ ), 48.7 ( $\text{CH}_2$ ) ppm.

**7-Bromo-*N,N*,1-tris(4-methoxybenzyl)-1*H*-imidazo-[4,5-*c*]pyridin-4-amine (13):** A 250 ml Schlenk tube was charged with **12** (9.4 g, 16.7 mmol) and trimethyl orthoformate (150 ml). The mixture was heated at 110 °C for 24 h, and concentrated in vacuo. The remaining residue was dissolved in the smallest possible volume of EtOAc and hexane was carefully added dropwise with stirring to cause slight turbidity. The mixture was chilled in the freezer at -20 °C overnight and the resulting precipitate was filtered, washed with hexanes and dried on air to give **13** as an off-white to cream solid in 94% yield (8.96 g). HRMS (ESI):  $m/z$   $[\text{M}+\text{H}]^+$  calc'd for  $\text{C}_{30}\text{H}_{30}^{81}\text{BrN}_4\text{O}_3$ : 575.1481; found: 575.14530.  $^1\text{H}$  NMR (399.8 MHz,  $\text{CDCl}_3$ ):  $\delta$ , 7.97 (s, 1H), 7.62 (s, 1H), 7.22-7.20 (d,  $J = 8.8$ , 4H), 7.13-7.10 (d,  $J = 8.8$ , 2H), 6.90-6.87 (d,  $J = 8.8$ , 2H), 6.84-6.82 (d,  $J = 8.8$ , 4H), 5.65 (s, 2H), 5.13 (s, 4H), 3.80 (s, 3H), 3.78 (s, 6H) ppm.  $^{13}\text{C}$  NMR (100 MHz,  $\text{CDCl}_3$ ):  $\delta$ , 159.6 (Cq), 158.7 (Cq), 151.6 (Cq), 143.1, 141.0, 136.6 (Cq), 131.2 (Cq), 129.5 (Cq), 129.2, 128.5, 128.4 (Cq), 114.5, 113.9, 89.0 (Cq), 55.44, 55.38, 49.8 ( $\text{CH}_2$ ), 49.0 ( $\text{CH}_2$ ) ppm.

Cross-coupling reactions of 13.

General conditions A:<sup>43</sup> a solution of 13 (0.25-3.5 mmol, 1 equiv.) in 2/1 dioxane/deionized water mixture (ca. 12 ml per mmol) was placed in a Schlenk tube or a vial equipped with septa. The mixture was bubbled with argon for ca. 1 minute/ml. An aryl or vinylboronic acid (1.5 equiv.), tetrakis(triphenylphosphine)palladium (0) (0.1 equiv.) and anhydrous cesium carbonate (2 equiv.) were added, the mixture was bubbled with argon for few more minutes and heated at 90 °C for 6-16 h with vigorous stirring. It was cooled and diluted with equal volumes of  $\text{CH}_2\text{Cl}_2$  and 1/1 water/brine, the phases were separated and the aqueous phase extracted twice with  $\text{CH}_2\text{Cl}_2$ . The combined organic extracts were dried

with MgSO<sub>4</sub>. After filtration and concentration, the products were purified by column chromatography on silica gel eluting with 0-20% EtOAc in hexanes.

General conditions B:<sup>44</sup> to a flame-dried vial equipped with septa dry dioxane (ca. 7 ml per mmol) was added and bubbled with argon for ca. 1 minute/ml. Compound 13 (0.25-3.5 mmol, 1 equiv.), alkylboronic acid (1.1-1.5 equiv.), tetrakis(triphenylphosphine)palladium(0) (0.1 equiv.), and anhydrous potassium carbonate (3 equiv.) were added. The mixture was bubbled with argon for few more minutes and heated at 90 °C for 72 h with vigorous stirring. It was cooled and filtered through Celite®, washing with CH<sub>2</sub>Cl<sub>2</sub>. After concentration, the products were purified by column chromatography on silica gel eluting with 0-20% EtOAc in hexanes.

General conditions C:<sup>45</sup> to a flame dried vial equipped with septa dry acetonitrile (3.5 ml) was added and bubbled with argon for ca. 1 minute/ml. Compound 13 (0.25 mmol, 1 equiv.), triphenylphosphine (0.5 equiv.) and palladium(II) acetate (0.1 equiv.) were added, followed by an olefin (5 equiv.) and triethylamine (7 equiv.) and the mixture was bubbled with argon for few more minutes and heated at 90 °C for 36 h with vigorous stirring. It was cooled, diluted with CH<sub>2</sub>Cl<sub>2</sub> (50 ml), washed with aqueous NH<sub>4</sub>Cl (2 x 25 ml), and dried with MgSO<sub>4</sub>. After filtration and concentration, the products were purified by column chromatography on silica gel eluting with 0-40% EtOAc in hexanes. The procedure for separation of dehalogenated byproduct: the crude mixture obtained after the extractive workup was redissolved in CH<sub>2</sub>Cl<sub>2</sub> (10 ml) and NIS (ca. 0.6 equiv.) was added. After stirring at room temperature for 2 h, the mixture was diluted with CH<sub>2</sub>Cl<sub>2</sub> (50 ml), washed with brine containing sodium thiosulfate (25 ml), and dried with MgSO<sub>4</sub>. After filtration and concentration, the products were purified by column chromatography on silica gel eluting with 0-40% EtOAc in hexanes. 13-I eluted first.

General conditions D:<sup>23</sup> to a flame dried vial equipped with septa dry DMF (5 ml) and triethylamine (2.5 ml) were added and bubbled with argon for ca. 1 minute/ml. Compound



13 (0.25 mmol, 1 equiv.), CuI (0.1 equiv.) and bis(triphenylphosphine)palladium(II) dichloride (0.1 equiv.) were added, followed by phenylacetylene (1.5 equiv.). The mixture was bubbled with argon for few more minutes and heated at 80 °C for 24 h with vigorous stirring. It was cooled, quenched with saturated aqueous NH<sub>4</sub>Cl (10 ml), diluted with EtOAc (10 ml), washed with brine (3 x 10 ml), and dried with MgSO<sub>4</sub>. After filtration and concentration, the products were purified by column chromatography on silica gel eluting with 0-20% EtOAc in hexanes.

General conditions E:<sup>46</sup> to a flame dried vial equipped with septa dry THF (6 ml) was added and bubbled with argon for ca. 1 minute/ml. Compound 13 (0.25 mmol, 1 equiv.) and tetrakis(triphenylphosphine)palladium(0) (0.1 equiv.) were added, followed by trimethylaluminum or benzylmagnesium chloride solutions (3-3.3 equiv.) and the mixture was stirred at room temperature for 15 minutes and then heated at 80 °C for 4 h with vigorous stirring. It was cooled, carefully quenched with Et<sub>2</sub>O (30 ml), washed with saturated aqueous NH<sub>4</sub>Cl (30 ml), and dried with MgSO<sub>4</sub>. After filtration and concentration, the products were purified by column chromatography on silica gel eluting with 0-40% EtOAc in hexanes.

General conditions F:<sup>58</sup> to a flame dried vial equipped with septa was added a solution of ZnCl<sub>2</sub> (0.5 M in THF, 5.7 eq.), followed by dropwise addition of Grignard reagent solution (8.6 eq.) and the mixture was allowed to stir under argon for 1 h. Then, compound 13 (0.175-0.7 mmol, 1 eq.) and [1,1'-bis(diphenylphosphino)ferrocene]-dichloropalladium(II) (0.1 equiv.) were added, and the mixture was stirred at room temperature under argon for overall 21-29 h. It was carefully quenched with Et<sub>2</sub>O (30-50 ml), washed with equal volume of saturated aqueous NH<sub>4</sub>Cl, and dried with MgSO<sub>4</sub>. After filtration and concentration, the products were purified by column chromatography on silica gel eluting with 0-20% EtOAc in hexanes.

General conditions G:<sup>48</sup> to a flame dried vial equipped with septa were added sequentially: NiI<sub>2</sub> (0.065 mmol, 0.13 equiv.), 4,4'-dimethoxy-2,2'-bipyridine (0.05 mmol, 0.1 equiv.), NaI (0.125 mmol, 0.25 equiv.), 13 (0.5 mmol, 1 equiv.), dry DMA (2 ml), pyridine (5  $\mu$ l), ethyl 4-bromobutyrate (0.55 mmol, 1.1 equiv.), and Zn powder (1 mmol, 2 equiv.). The headspace of the vial was flushed with argon for 1 minute. The reaction mixture was stirred at room temperature for 5 minutes and then heated at 60 °C for 20 h with vigorous stirring. It was cooled, diluted with EtOAc (50 ml), washed with brine (3 x 25 ml), and dried with MgSO<sub>4</sub>. The crude mixtures were subjected to the same procedure of dehalogenated by-product separation as described under general conditions C. The products were purified by column chromatography on silica gel eluting with 0-40% EtOAc in hexanes. 13-I eluted first.

Characterization data for compounds from Table 1.

***N,N*,1-Tris(4-methoxybenzyl)-7-phenyl-1*H*-imidazo[4,5-*c*]pyridin-4-amine (14a):**

General conditions A, 6 h, 335 mg, 91%. Yellowish syrup. HRMS (ESI): *m/z* [M+H]<sup>+</sup> calc'd for C<sub>36</sub>H<sub>35</sub>N<sub>4</sub>O<sub>3</sub>: 571.27093; found: 571.26842. <sup>1</sup>H NMR (400 MHz, CDCl<sub>3</sub>):  $\delta$ , 7.78 (s, 1H), 7.68 (s, 1H), 7.36-7.34 (m, 3H), 7.29-7.27 (d, *J* = 8.8, 4H), 7.27-7.25 (m, 2H), 6.87-6.85 (d, *J* = 8.8, 2H), 6.71-6.69 (d, *J* = 8.8, 2H), 6.56-6.54 (d, *J* = 8.8, 2H), 5.23 (s, 4H), 4.94 (s, 2H), 3.80 (s, 6H), 3.76 (s, 3H) ppm. <sup>13</sup>C NMR (100 MHz, CDCl<sub>3</sub>):  $\delta$ , 159.6 (Cq), 158.7 (Cq), 151.6 (Cq), 141.8, 141.0, 137.7 (Cq), 136.7 (Cq), 131.6 (Cq), 130.4, 129.3, 128.2, 128.10, 128.06 (Cq), 128.0 (Cq), 127.4, 114.1, 113.9, 113.8 (Cq), 55.40, 55.38, 49.64 (CH<sub>2</sub>), 49.55 (CH<sub>2</sub>) ppm.

***(E)*-N,N,1-Tris(4-methoxybenzyl)-7-styryl-1*H*-imid-azo[4,5-*c*]pyridin-4-amine (14b):**

General conditions A, 16 h, 123 mg, 79%. General conditions C, 36 h, 83 mg, 53%. Tan solid. HRMS (ESI): *m/z* [M+H]<sup>+</sup> calc'd for C<sub>38</sub>H<sub>37</sub>N<sub>4</sub>O<sub>3</sub>: 597.28658; found: 597.28453. <sup>1</sup>H NMR (400 MHz, CDCl<sub>3</sub>):  $\delta$ , 8.10 (s, 1H). 7.69 (s, 1H), 7.32-7.23 (m, 8H), 7.20-7.16 (d, *J* = 15.6, 1H), 7.06-7.04 (d, *J* = 8.8, 2H), 6.92-6.89 (d, *J* = 8.8, 2H), 6.86-6.82 (m, 5H), 5.46

(s, 2H), 5.22 (s, 4H), 3.804 (s, 3H), 3.796 (s, 6H) ppm. <sup>13</sup>C NMR (100 MHz, CDCl<sub>3</sub>): δ, 159.6 (Cq), 158.7 (Cq), 151.7 (Cq), 141.0, 139.6, 138.1 (Cq), 137.8 (Cq), 131.5 (Cq), 129.3, 129.0, 128.8, 128.6 (Cq), 127.8 (Cq), 127.6, 127.4, 126.4, 122.2, 114.7, 113.9, 110.8 (Cq), 55.5, 55.4, 49.8 (CH<sub>2</sub>), 49.7 (CH<sub>2</sub>) ppm.

***N,N*,1-Tris(4-methoxybenzyl)-7-phenethyl-1*H*-imidazo[4,5-*c*]pyridin-4-amine (14c):**

General conditions B, 72 h, 55 mg, 35%. General conditions F, 29 h, 327 mg, 77%. Colorless syrup. HRMS (ESI): *m/z* [M+H]<sup>+</sup> calc'd for C<sub>38</sub>H<sub>39</sub>N<sub>4</sub>O<sub>3</sub>: 599.30224; found: 599.29971. <sup>1</sup>H NMR (400 MHz, CDCl<sub>3</sub>): δ, 7.76 (s, 1H), 7.63 (s, 1H), 7.31 -7.20 (m, 3H), 7.26-7.24 (d, *J* = 8.8, 4H), 7.10-7.08 (d, *J* = 8.8, 4H), 6.94-6.92 (d, *J* = 8.8, 2H), 6.87-6.84 (m, 2H), 6.86-6.83 (d, *J* = 8.8, 2H), 5.34 (s, 2H), 5.18 (s, 4H), 3.80 (s, 6H), 3.79 (s, 3H), 3.02-2.88 (m, 4H) ppm. <sup>13</sup>C NMR (100 MHz, CDCl<sub>3</sub>): δ, 159.6 (Cq), 158.6 (Cq), 151.4 (Cq), 141.4, 141.3 (Cq), 141.0, 138.8 (Cq), 131.7 (Cq), 129.3, 128.59, 128.56 (Cq), 128.48, 127.6, 126.3, 114.7, 113.8, 110.9 (Cq), 55.44, 55.36, 49.7 (CH<sub>2</sub>), 49.4 (CH<sub>2</sub>), 38.5 (CH<sub>2</sub>), 30.7 (CH<sub>2</sub>) ppm. For other conditions tested, see Supporting Information.

***N,N*,1-Tris(4-methoxybenzyl)-1*H*-imidazo[4,5-*c*]pyridin-4-amine (13-H):**

General conditions B, 72 h, 34 mg, 30%. Yellowish syrup. HRMS (ESI): *m/z* [M+H]<sup>+</sup> calc'd for C<sub>30</sub>H<sub>31</sub>N<sub>4</sub>O<sub>3</sub>: 495.23964; found: 495.23722. <sup>1</sup>H NMR (400 MHz, CDCl<sub>3</sub>): δ, 7.96-7.94 (d, *J* = 5.6, 1H), 7.70 (s, 1H), 7.25-7.23 (d, *J* = 8.8, 4H), 7.16-7.14 (d, *J* = 8.8, 2H), 6.90-6.87 (d, *J* = 8.8, 2H), 6.84-6.82 (d, *J* = 8.8, 4H), 6.64-6.62 (d, *J* = 5.6, 1H), 5.21 (s, 2H), 5.17 (s, 4H), 3.80 (s, 3H), 3.78 (s, 6H) ppm. <sup>13</sup>C NMR (100 MHz, CDCl<sub>3</sub>): δ, 159.8 (Cq), 158.6 (Cq), 152.3 (Cq), 141.1, 140.5 (Cq), 139.2, 131.5 (Cq), 129.2, 129.0, 127.9 (Cq), 127.3 (Cq), 114.6, 113.9, 96.2, 55.45, 55.36, 49.4 (CH<sub>2</sub>), 48.6 (CH<sub>2</sub>) ppm.

**7-Iodo-*N,N*,1-tris(4-methoxybenzyl)-1*H*-imidazo[4,5-*c*]pyridin-4-amine (13-I):**

General conditions C, 36 h, 50 mg, 31%. General conditions G, 20 h, 110 mg, 36%. Yellowish foam. HRMS (ESI): *m/z* [M+H]<sup>+</sup> calc'd for C<sub>30</sub>H<sub>30</sub>IN<sub>4</sub>O<sub>3</sub>: 621.13629; found: 621.13419. <sup>1</sup>H NMR (400 MHz, CDCl<sub>3</sub>): δ, 8.17 (s, 1H), 7.62 (s, 1H), 7.23-7.20 (d, *J* =

8.8, 4H), 7.08-7.06 (d,  $J = 8.8$ , 2H), 6.90-6.88 (d,  $J = 8.8$ , 2H), 6.84-6.82 (d,  $J = 8.8$ , 4H), 5.67 (s, 2H), 5.15 (s, 4H), 3.80 (s, 3H), 3.79 (s, 6H) ppm.  $^{13}\text{C}$  NMR (100 MHz,  $\text{CDCl}_3$ ):  $\delta$ , 159.6 (Cq), 158.7 (Cq), 152.3 (Cq), 149.2, 141.4, 138.5 (Cq), 131.2 (Cq), 129.8 (Cq), 129.2, 128.5, 128.4 (Cq), 114.5, 113.9, 56.0 (Cq), 55.44, 55.38, 49.8 ( $\text{CH}_2$ ), 48.5 ( $\text{CH}_2$ ) ppm.

**7-Ethyl-*N,N*,1-tris(4-methoxybenzyl)-1*H*-imidazo[4,5-*c*]pyridin-4-amine (14d):**

General conditions B, 72 h, 284 mg, 31%. General conditions F, 25 h, 69 mg, 76%. Colorless syrup. HRMS (ESI):  $m/z$   $[\text{M}+\text{H}]^+$  calc'd for  $\text{C}_{32}\text{H}_{35}\text{N}_4\text{O}_3$ : 523.27093; found: 523.26894.  $^1\text{H}$  NMR (400 MHz,  $\text{CDCl}_3$ ):  $\delta$ , 7.73 (s, 1H), 7.64 (s, 1H), 7.24-7.21 (d,  $J = 8.8$ , 4H), 6.99-6.97 (d,  $J = 8.8$ , 2H), 6.88-6.86 (d,  $J = 8.8$ , 2H), 6.83-6.81 (d,  $J = 8.8$ , 4H), 5.44 (s, 2H), 5.15 (s, 4H), 3.79 (s, 3H), 3.78 (s, 6H), 2.77-2.71 (q,  $J = 7.6$ , 2H), 1.25-1.21 (t,  $J = 7.6$ , 3H) ppm.  $^{13}\text{C}$  NMR (100 MHz,  $\text{CDCl}_3$ ):  $\delta$ , 159.6 (Cq), 158.6 (Cq), 151.3 (Cq), 141.0, 140.5, 138.8 (Cq), 131.8 (Cq), 129.3, 128.8 (Cq), 128.6 (Cq), 127.6, 114.6, 113.8, 113.2 (Cq), 55.5, 55.4, 49.7 ( $\text{CH}_2$ ), 49.6 ( $\text{CH}_2$ ), 22.0 ( $\text{CH}_2$ ), 16.2 ppm.

**7-Isobutyl-*N,N*,1-tris(4-methoxybenzyl)-1*H*-imid-azo[4,5-*c*]pyridin-4-amine (14e):**

General conditions B, 72 h, 658 mg, 29%. General conditions F, 21 h, 327 mg, 85%. Yellowish syrup. HRMS (ESI):  $m/z$   $[\text{M}+\text{H}]^+$  calc'd for  $\text{C}_{34}\text{H}_{39}\text{N}_4\text{O}_3$ : 551.30224; found: 551.29987.  $^1\text{H}$  NMR (400 MHz,  $\text{CDCl}_3$ ):  $\delta$ , 7.67 (s, 1H), 7.63 (s, 1H), 7.24-7.21 (d,  $J = 8.8$ , 4H), 6.98-6.95 (d,  $J = 8.8$ , 2H), 6.88-6.86 (d,  $J = 8.8$ , 2H), 6.84-6.82 (d,  $J = 8.8$ , 4H), 5.40 (s, 2H), 5.15 (s, 4H), 3.79 (s, 3H), 3.78 (s, 6H), 2.51-2.49 (d,  $J = 7.2$ , 2H), 1.84-1.74 (septet,  $J = 6.4$ , 1H), 0.95-0.94 (d,  $J = 6.4$ , 6H) ppm.  $^{13}\text{C}$  NMR (100 MHz,  $\text{CDCl}_3$ ):  $\delta$ , 159.6 (Cq), 158.6 (Cq), 151.4 (Cq), 142.3, 140.9, 139.0 (Cq), 131.8 (Cq), 129.3, 128.8 (Cq), 128.7 (Cq), 127.6, 114.7, 113.8, 110.6 (Cq), 55.5, 55.4, 49.6 ( $\text{CH}_2$ ), 49.5 ( $\text{CH}_2$ ), 38.2 ( $\text{CH}_2$ ), 30.7, 22.4 ppm.

**Methyl (*E*)-3-(4-(bis(4-methoxybenzyl)amino)-1-(4-methoxybenzyl)-1*H*-imidazo[4,5-*c*]pyridin-7-yl)acrylate (14f):** General conditions C, 36 h, 86 mg, 57%. Yellowish syrup.

HRMS (ESI):  $m/z$   $[M+H]^+$  calc'd for  $C_{34}H_{35}N_4O_5$ : 579.26077; found: 579.25862.  $^1H$  NMR (400 MHz,  $CDCl_3$ ):  $\delta$ , 8.23 (s, 1H), 8.05-8.01 (d,  $J = 15.6$ , 1H), 7.69 (s, 1H), 7.24-7.22 (d,  $J = 8.8$ , 4H), 7.12-7.09 (d,  $J = 8.8$ , 2H), 6.90-6.88 (d,  $J = 8.8$ , 2H), 6.85-6.83 (d,  $J = 8.8$ , 4H), 6.26-6.22 (d,  $J = 15.6$ , 1H), 5.44 (s, 2H), 5.23 (s, 4H), 3.79-3.78 (overlapped s, 12H) ppm.  $^{13}C$  NMR (100 MHz,  $CDCl_3$ ):  $\delta$ , 167.8 (Cq), 159.8 (Cq), 158.8 (Cq), 152.8 (Cq), 141.3, 138.8, 138.0 (Cq), 130.9 (Cq), 129.4, 129.2, 128.2 (Cq), 127.6 (Cq), 127.3 (Cq), 114.6, 114.5, 114.0, 107.6 (Cq), 55.41, 55.36, 51.6, 50.4 ( $CH_2$ ), 49.7 ( $CH_2$ ) ppm.

***N,N*,1-Tris(4-methoxybenzyl)-7-(phenylethynyl)-1*H*-imidazo[4,5-*c*]pyridin-4-amine (14g)**: General conditions D, 20 h, 138 mg, 89%. Brown syrup. HRMS (ESI):  $m/z$   $[M+H]^+$  calc'd for  $C_{38}H_{35}N_4O_3$ : 595.27093; found: 595.26894.  $^1H$  NMR (400 MHz,  $CDCl_3$ ):  $\delta$ , 8.22 (s, 1H), 7.67 (s, 1H), 7.39-7.37 (m, 2H), 7.33-7.30 (m, 3H), 7.26-7.24 (d,  $J = 8.4$ , 2H), 7.25-7.23 (d,  $J = 8.4$ , 4H), 6.89-6.87 (d,  $J = 8.4$ , 2H), 6.86-6.84 (d,  $J = 8.4$ , 4H), 5.75 (s, 2H), 5.21 (s, 4H), 3.80 (s, 9H) ppm.  $^{13}C$  NMR (100 MHz,  $CDCl_3$ ):  $\delta$ , 159.6 (Cq), 158.8 (Cq), 151.9 (Cq), 146.7, 140.3, 138.3 (Cq), 131.1, 129.3, 128.9, 128.8 (Cq), 128.5, 128.0, 127.0 (Cq), 123.7 (Cq), 114.5, 113.9, 93.6 (Cq), 85.1 (Cq), 55.44, 55.38, 49.6 ( $CH_2$ ), 48.5 ( $CH_2$ ) ppm.

***N,N*,1-Tris(4-methoxybenzyl)-7-methyl-1*H*-imid-azo[4,5-*c*]pyridin-4-amine (14h)**: General conditions E, 4 h, 115 mg, 87%. Yellow syrup. HRMS (ESI):  $m/z$   $[M+H]^+$  calc'd for  $C_{31}H_{33}N_4O_3$ : 509.25528; found: 509.25341.  $^1H$  NMR (400 MHz,  $CDCl_3$ ):  $\delta$ , 7.66 (s, 1H), 7.65 (s, 1H), 7.24-7.21 (d,  $J = 8.4$ , 4H), 7.00-6.97 (d,  $J = 8.4$ , 2H), 6.88-6.86 (d,  $J = 8.4$ , 2H), 6.83-6.81 (d,  $J = 8.4$ , 2H), 5.45 (s, 2H), 5.15 (s, 4H), 3.79 (s, 3H), 3.78 (s, 6H), 2.35 (s, 3H) ppm.  $^{13}C$  NMR (100 MHz,  $CDCl_3$ ):  $\delta$ , 159.5 (Cq), 158.6 (Cq), 151.4 (Cq), 141.5, 140.8, 139.5 (Cq), 131.8 (Cq), 129.3, 129.0, 128.5 (Cq), 127.5, 114.6, 113.8, 106.6 (Cq), 55.44, 55.36, 49.7 ( $CH_2$ ), 49.3 ( $CH_2$ ), 15.1 ppm.

**7-Benzyl-*N,N*,1-tris(4-methoxybenzyl)-1*H*-imid-azo[4,5-*c*]pyridin-4-amine (14i)**: General conditions E, 4 h, 69 mg, 45%. Brown syrup. HRMS (ESI):  $m/z$   $[M+H]^+$  calc'd

for C<sub>37</sub>H<sub>37</sub>N<sub>4</sub>O<sub>3</sub>: 585.286588; found: 585.28433. <sup>1</sup>H NMR (400 MHz, CDCl<sub>3</sub>): δ, 7.76 (s, 1H), 7.59 (s, 1H), 7.32-7.23 (m, 7H), 7.09–7.08 (d, *J* = 8.8, 2H), 6.87–6.82 (m, 8H), 5.22 (s, 4H), 5.05 (s, 2H), 4.00 (s, 2H), 3.80 (s, 9H) ppm. <sup>13</sup>C NMR (100 MHz, CDCl<sub>3</sub>): δ, 159.5 (Cq), 158.6 (Cq), 151.8 (Cq), 142.9, 141.4 (Cq), 140.9, 139.2 (Cq), 131.6 (Cq), 129.3, 129.0 (Cq), 128.9 (Cq), 128.8, 128.0, 127.2, 126.5, 114.6, 113.8, 108.5 (Cq), 55.42, 55.35, 49.7 (CH<sub>2</sub>), 49.0 (CH<sub>2</sub>), 35.0 (CH<sub>2</sub>) ppm.

**7-Isopropyl-*N,N*,1-tris(4-methoxybenzyl)-1*H*-imid-azo[4,5-*c*]pyridin-4-amine (14j):**

General conditions F, 27 h, 80 mg, 86%. Contains ~20% of *n*-propyl impurity. Colorless syrup. HRMS (ESI): *m/z* [M+H]<sup>+</sup> calc'd for C<sub>33</sub>H<sub>37</sub>N<sub>4</sub>O<sub>3</sub>: 537.28658; found: 537.28573. <sup>1</sup>H NMR (400 MHz, CDCl<sub>3</sub>): δ, 7.89 (s, 1H), 7.63 (s, 1H), 7.25-7.22 (d, *J* = 8.8, 4H), 6.98-6.96 (d, *J* = 8.8, 2H), 6.88-6.86 (d, *J* = 8.8, 2H), 6.84-6.82 (d, *J* = 8.8, 4H), 5.44 (s, 2H), 5.16 (s, 4H), 3.79 (s, 3H), 3.78 (s, 6H), 3.30-3.20 (septet, *J* = 6.8, 1H), 1.25-1.24 (d, *J* = 6.4, 6H) ppm. <sup>13</sup>C NMR (100 MHz, CDCl<sub>3</sub>): δ, 159.6 (Cq), 158.6 (Cq), 151.0 (Cq), 141.4, 138.1 (Cq), 138.0, 131.8 (Cq), 129.3, 128.7 (Cq), 128.6 (Cq), 127.6, 118.3 (Cq), 114.6, 113.8, 55.45, 55.36, 50.0 (CH<sub>2</sub>), 49.7 (CH<sub>2</sub>), 26.3, 24.3 ppm.

**Ethyl 4-(4-(bis(4-methoxybenzyl)amino)-1-(4-methoxybenzyl)-1*H*-imidazo[4,5-*c*]pyridin-7-yl)butanoate (14k):**

General conditions G, 20 h, 100 mg, 32%. Colorless syrup. HRMS (ESI): *m/z* [M+H]<sup>+</sup> calc'd for C<sub>36</sub>H<sub>41</sub>N<sub>4</sub>O<sub>5</sub>: 609.30773; found: 609.30580. <sup>1</sup>H NMR (400 MHz, CDCl<sub>3</sub>): δ, 7.69 (s, 1H), 7.65 (s, 1H), 7.24-7.22 (d, *J* = 8.8, 4H), 6.98-6.96 (d, *J* = 8.8, 2H), 6.87-6.85 (d, *J* = 8.8, 2H), 6.84-6.82 (d, *J* = 8.8, 4H), 5.47 (s, 2H), 5.16 (s, 4H), 4.14-4.08 (q, *J* = 7.2, 2H), 3.78 (overlapped s, 9H), 2.71-2.68 (m, 2H), 2.37-2.33 (t, *J* = 7.2, 2H), 1.91-1.86 (m, 2H), 1.26-1.22 (t, *J* = 7.2, 3H) ppm. <sup>13</sup>C NMR (100 MHz, CDCl<sub>3</sub>): δ, 173.5 (Cq), 159.5 (Cq), 158.6 (Cq), 151.4 (Cq), 141.6, 141.1, 138.7 (Cq), 131.7 (Cq), 129.3, 128.8 (Cq), 128.7 (Cq), 127.5, 114.6, 113.8, 110.6 (Cq), 60.5 (CH<sub>2</sub>), 55.42, 55.36, 49.6 (CH<sub>2</sub>), 49.4 (CH<sub>2</sub>), 33.7 (CH<sub>2</sub>), 28.4 (CH<sub>2</sub>), 27.4 (CH<sub>2</sub>), 14.4 ppm.

Synthesis of phosphoramidites 20i, 20d, 20e and attempted synthesis of 20a.

**7-Benzyl-1*H*-imidazo[4,5*c*]pyridin-4-amine, trifluoro-acetic acid salt (15i):** This compound was synthesized according to the modified general procedure.<sup>52</sup> A solution of **14i** (589 mg, 1 mmol) in TFA (6 ml) was placed in a 100 ml pressure tube, anisole (0.65 ml, 6 equiv.) was added, and the mixture was heated at 70 °C for 24 h with vigorous stirring. It was cooled and concentrated under reduced pressure. The residue was coevaporated with toluene (3 x 25 ml) to obtain **15i** (ca. 0.34 g, quantitative) as an oil that was taken into next step without further purification.

**1-(7-Benzyl-1*H*-imidazo[4,5-*c*]pyridin-4-yl)-3,3,4,4-tetramethylpyrrolidine-2,5-dione (16i):** This compound was synthesized according to the reported general procedure.<sup>53</sup> A solution of **15i** (0.34 g, 1 mmol) in pyridine (10 ml) was placed in a 100 ml Schlenk flask. Tetramethylsuccinic anhydride (M<sub>4</sub>SA)<sup>59</sup> (0.312 g, 2 mmol) and DBU (0.6 ml, 4 mmol) were added, and the mixture was heated at 120 °C under argon for 20 h with vigorous stirring. It was cooled and concentrated under reduced pressure. The residue was coevaporated with toluene (3 x 25 ml). The product was purified by column chromatography on silica gel eluting with 0-5% MeOH in CH<sub>2</sub>Cl<sub>2</sub> to give a cream foam. It was taken in SOCl<sub>2</sub> (10 ml), heated at 80 °C for 2 h, cooled and concentrated under reduced pressure. The residue was coevaporated with EtOAc (3 x 25 ml). The product was purified by column chromatography on silica gel eluting with 0-5% MeOH in CH<sub>2</sub>Cl<sub>2</sub> to give **16i** as a cream foam in 57% yield (0.208 g). HRMS (ESI): *m/z* [M+H]<sup>+</sup> calc'd for C<sub>21</sub>H<sub>23</sub>N<sub>4</sub>O<sub>2</sub>: 363.18212; found: 363.18045. <sup>1</sup>H NMR (400 MHz, CD<sub>3</sub>OD): δ, 8.36 (s, 1H), 8.12 (s, 1H), 7.29-7.20 (m, 5H), 4.35 (s, 2H), 1.37 (bs, 12H) ppm. <sup>13</sup>C NMR (100 MHz, CD<sub>3</sub>OD): δ, 183.4, 146.2, 141.8, 139.7, 137.5, 129.8, 127.7, 124.7, 118.3, 35.5, 21.8 ppm.

(2*R*,3*S*,5*R*)-5-(7-Benzyl-4-(3,3,4,4-tetramethyl-2,5-dioxopyrrolidin-1-yl)-1*H*-imidazo[4,5-*c*]pyridin-1-yl)-2-(((4-methylbenzoyl)oxy)methyl)tetrahydrofuran-3-yl 4-methylbenzoate (17i): This compound was synthesized according to the reported general procedure.<sup>53</sup> To a solution of **16i** (0.19 g, 0.52 mmol) in dry CH<sub>3</sub>CN (25 ml) in a 100 ml round bottom flask, 60% NaH in oil (42 mg, 1.05 mmol) was added, and the mixture was vigorously stirred at room temperature under argon for 45 min. 1-( $\alpha$ )-Chloro-3,5-di-*O*-(*p*-

toluoyl)-2-deoxy-D-ribose (0.368 g, 0.94 mmol) was subsequently added in one portion, and the stirring was continued at room temperature for 4.5 h. The mixture was filtered through Celite® and concentrated. The product was purified by column chromatography on silica gel eluting with 50% EtOAc in hexanes. 17i was obtained as a yellowish syrup in 39% yield (0.145 g). HRMS (ESI):  $m/z$   $[M+H]^+$  calc'd for  $C_{42}H_{43}N_4O_7$ : 715.31322; found: 715.31184.  $^1H$  NMR (400 MHz,  $CDCl_3$ ):  $\delta$ , 8.32 (s, 1H), 8.19 (s, 1H), 7.92-7.90 (d,  $J = 8.4$ , 2H), 7.87-7.85 (d,  $J = 8.4$ , 2H), 7.34-7.32 (d,  $J = 8.4$ , 2H), 7.92-7.90 (d,  $J = 8.4$ , 2H), 7.14-7.11 (m, 3H), 7.06-7.04 (m, 2H), 6.20-6.17 (dd,  $J_1 = 5.2$ ,  $J_2 = 9.2$ , 1H), 5.54-5.53 (m, 1H), 4.60-4.49 (m, 4H), 4.38-4.34 (AB/2,  $J = 16.8$ , 1H), 2.49 (s, 3H), 2.46-2.42 (m, 1H), 2.40 (s, 3H), 2.06-2.01 (m, 1H), 1.39 (bs, 1H) ppm.  $^{13}C$  NMR (100 MHz,  $CDCl_3$ ):  $\delta$ , 181.6 (Cq), 166.2 (Cq), 165.8 (Cq), 144.8 (Cq), 144.6, 144.4 (Cq), 142.3, 139.6 (Cq), 138.7 (Cq), 138.6 (Cq), 137.5 (Cq), 130.0, 129.8, 129.54, 129.47, 129.2, 128.1, 127.1, 126.6 (Cq), 126.5 (Cq), 120.0 (Cq), 85.8, 82.7, 74.8, 64.3 ( $CH_2$ ), 48.1 (Cq), 39.4 ( $CH_2$ ), 35.8 ( $CH_2$ ), 21.9, 21.8, 21.7, 21.5 ppm. For the critical NOESY correlations, see Figure S1 and copies of spectra (Supporting Information).

1-(7-Benzyl-1-((2*R*,4*S*,5*R*)-4-hydroxy-5-(hydroxymethyl)tetrahydrofuran-2-yl)-1*H*-imidazo[4,5-*c*]pyridin-4-yl)-3,3,4,4-tetramethylpyrrolidine-2,5-dione (18i): This compound was synthesized according to the general procedure.<sup>53</sup> To a solution of 17i (0.14 g, 0.20 mmol) in dry MeOH (4 ml) in a 25 ml round bottom flask, NaOMe (32 mg, 0.60 mmol) was added. The mixture was stirred at room temperature under argon for 2 h and concentrated in vacuo. The product was purified by column chromatography on silica gel eluting with 0-10% MeOH in dichloromethane to obtain 18i as an off-white solid in 66% yield (62 mg). HRMS (ESI):  $m/z$   $[M+H]^+$  calc'd for  $C_{26}H_{31}N_4O_5$ : 479.22948; found: 479.22931.  $^1H$  NMR (400 MHz,  $CD_3OD$ ):  $\delta$ , 8.69 (s, 1H), 8.14 (s, 1H), 7.32-7.14 (m, 5H), 6.35-6.32 (dd,  $J_1 = 6.4$ ,  $J_2 = 12.8$ , 1H), 4.61-4.57 (AB/2,  $J = 16.8$ , 1H), 4.47-4.30 (AB/2,  $J = 16.8$ , 1H), 4.46-4.44 (m, 1H), 3.95-3.92 (app q,  $J = 3.6$ , 1H), 3.73-3.69 (app dd,  $J_1 = 3.6$ ,  $J_2 = 12.0$ , 1H), 3.66-3.62 (app dd,  $J_1 = 3.6$ ,  $J_2 = 12.0$ , 1H), 2.52-2.46 (ddd,  $J_1 = J_2 = 6.0$ ,  $J_3 = 12.8$ , 1H), 2.14-2.08 (ddd,  $J_1 = 4.4$ ,  $J_2 = 6.0$ ,  $J_3 = 10.4$ , 1H), 1.37 (bs, 12H) ppm.  $^{13}C$  NMR (100 MHz,  $CD_3OD$ ):  $\delta$ , 183.4 (Cq), 145.9 (Cq), 144.3, 141.0 (Cq), 140.1 (Cq), 138.6 (Cq),



138.4 (Cq), 130.1, 129.5, 127.9, 123.5 (Cq), 89.2, 87.1, 71.7, 62.6 (CH<sub>2</sub>), 48.9 (Cq), 42.0 (CH<sub>2</sub>), 35.9 (CH<sub>2</sub>), 21.88, 21.84 ppm.

1-(7-Benzyl-1-((2*R*,4*S*,5*R*)-5-((bis(4-methoxyphenyl)-(phenyl)methoxy)methyl)-4-hydroxytetrahydrofuran-2-yl)-1*H*-imidazo[4,5-*c*]pyridin-4-yl)-3,3,4,4-tetramethylpyrrolidine-2,5-dione (19i): This compound was synthesized according to the reported general procedure.<sup>53</sup> To a solution of 18i (56 mg, 0.12 mmol) in pyridine (2 ml), 4,4'-dimethoxytrityl chloride (DMT-Cl) (155 mg, 0.457 mmol) was added in one portion and the mixture was stirred at room temperature under argon for 5 h (TLC showed complete conversion). MeOH (0.2 ml) was then added, and the mixture was concentrated in vacuo. The product was purified by column chromatography on silica gel (neutralized with triethylamine) eluting with 5-20% acetone in dichloromethane to obtain 19i as a colorless solid in 69% yield (63 mg). HRMS (ESI): *m/z* [M+H]<sup>+</sup> calc'd for C<sub>47</sub>H<sub>49</sub>N<sub>4</sub>O<sub>7</sub>: 781.36017; found: 781.35738. <sup>1</sup>H NMR (400 MHz, CDCl<sub>3</sub>): δ, 8.24 (s, 1H), 8.10 (s, 1H), 7.38-7.10 (m, 14H), 6.82-6.80 (d, *J* = 8.4, 4H), 6.16-6.12 (dd, *J*<sub>1</sub> = 6.4, *J*<sub>2</sub> = 12.4, 1H), 4.50-4.46 (AB/2, *J* = 16.8, 1H), 4.43-4.38 (m, 1H), 4.36-4.32 (AB/2, *J* = 16.8, 1H), 4.01-3.98 (app q, *J* = 4.4, 1H), 3.78 (s, 6H), 3.36-3.32 (app dd, *J*<sub>1</sub> = 4.4, *J*<sub>2</sub> = 10.4, 1H), 3.28-3.24 (app dd, *J*<sub>1</sub> = 4.8, *J*<sub>2</sub> = 10.4, 1H), 2.6 (bs, 1H), 2.28-2.22 (ddd, *J*<sub>1</sub> = *J*<sub>2</sub> = 6.0, *J*<sub>3</sub> = 13.2, 1H), 1.90-1.84 (ddd, *J*<sub>1</sub> = *J*<sub>2</sub> = 5.6, *J*<sub>3</sub> = 9.6, 1H), 1.39-1.38 (overlapped s, 12H) ppm. <sup>13</sup>C NMR (100 MHz, CDCl<sub>3</sub>): δ, 181.7 (Cq), 158.7 (Cq), 144.5 (Cq), 144.1, 142.6, 139.4 (Cq), 138.8 (Cq), 138.2 (Cq), 137.6 (Cq), 135.63 (Cq), 135.55 (Cq), 130.12, 130.09, 129.1, 128.6, 128.13, 128.10, 127.11, 127.07, 120.6 (Cq), 113.4, 86.8 (Cq), 85.7, 85.2, 72.0, 63.7 (CH<sub>2</sub>), 55.3, 48.0 (Cq), 41.4 (CH<sub>2</sub>), 35.6 (CH<sub>2</sub>), 21.8, 21.4 ppm.

(2*R*,3*S*,5*R*)-5-(7-Benzyl-4-(3,3,4,4-tetramethyl-2,5-dioxopyrrolidin-1-yl)-1*H*-imidazo[4,5-*c*]pyridin-1-yl)-2-((bis(4-methoxyphenyl)(phenyl)methoxy)methyl)tetrahydrofuran-3-yl (2-cyanoethyl) diisopropylphosphoramidite (20i): This compound was synthesized according to the reported general procedure.<sup>60</sup> To a solution of 19i (62 mg, 0.080 mmol) in dry CH<sub>2</sub>Cl<sub>2</sub> (2 ml) containing *N,N*-diisopropylethylamine (DIEA) (70 μl, 0.4 mmol), 2-cyanoethyl-*N,N*-

diisopropyl chlorophosphoramidite (40  $\mu$ l, 0.175 mmol) was added in one portion and the mixture was stirred at room temperature under argon for 3 h (TLC showed complete conversion). The mixture was concentrated in vacuo at rt and the product was purified by column chromatography on silica gel (neutralized with triethylamine) eluting with 50% EtOAc in hexanes containing 1% triethylamine, to obtain **20i** as a mixture of diastereomers (colorless solid,  $R_f$  ~0.5 in 5% acetone/ $\text{CH}_2\text{Cl}_2$ , two close spots visible on TLC) in 49% yield (38 mg). HRMS (ESI):  $m/z$   $[\text{M}+\text{H}]^+$  calc'd for  $\text{C}_{56}\text{H}_{66}\text{N}_6\text{O}_8\text{P}$ : 981.46801; found: 981.46481.  $^1\text{H}$  NMR (400 MHz, acetone- $d_6$ ):  $\delta$ , 8.40, 8.39 (s, 1H), 8.21, 8.19 (s, 1H), 7.45-7.18 (m, 14H), 6.84-6.80 (m, 4H), 6.40-6.35 (dd,  $J_1 = 7.0$ ,  $J_2 = 12.8$ , 1H), 4.68-4.78 (m, 2H), 4.56-4.52, 4.53-4.49 (AB/2,  $J = 16.4$ , 1H), 4.28-4.26, 4.24-4.21 (app q,  $J = 4.4$ , 1H), 3.763, 3.757 (s, 6H), 3.67-3.58 (m, 2H), 3.36-3.32 (m, 2H), 2.91-2.78 (m, 3H), 2.76-2.73 (t,  $J = 6.0$ , 1H), 2.68-2.65 (t,  $J = 6.0$ , 1H), 1.35, 1.31 (bs, 12H), 1.21-1.19 (m, 6H), 1.15-1.14, 1.13-1.11 (d,  $J = 6.8$ , 6H) ppm.  $^{13}\text{C}$  NMR (100 MHz, acetone- $d_6$ ):  $\delta$ , 181.7, 159.6, 145.9, 144.36, 144.27, 144.02, 143.97, 140.4, 140.08, 140.05, 139.2, 138.8, 136.64, 136.58, 136.52, 130.96, 130.93, 129.7, 129.34, 129.31, 128.97, 128.91, 128.6, 127.6, 127.50, 127.47, 122.3, 122.2, 119.0, 114.0, 87.22, 87.18, 86.6, 86.4, 86.3, 86.2, 74.4, 74.0, 73.8, 64.3, 64.3, 59.7, 59.6, 59.4, 55.5, 55.0, 48.3, 44.06, 43.99, 43.94, 43.86, 40.4, 40.3, 35.5, 24.94, 24.86, 24.82, 22.0, 21.7, 21.4, 20.8, 20.7 ppm.  $^{31}\text{P}$  NMR (162 MHz, acetone- $d_6$ ):  $\delta$ , 149.8, 149.6 ppm.

**7-Ethyl-1*H*-imidazo[4,5*c*]pyridin-4-amine, trifluoro-acetic acid salt (15d):** This compound was synthesized in similar fashion as **15i**. A solution of **14d** (750 mg, 1.4 mmol) in TFA (10 ml) was placed in a 100 ml pressure tube, anisole (ca. 1 ml, 6 equiv.) was added, and the mixture was heated at 70  $^\circ\text{C}$  for 24 h with vigorous stirring. It was cooled and concentrated under reduced pressure. The residue was coevaporated with toluene (3 x 20 ml) to obtain **15d** (ca. 0.4 g, quantitative) as an oil that was taken into next step without further purification.

**1-(7-Ethyl-1*H*-imidazo[4,5-*c*]pyridin-4-yl)-3,3,4,4-tetramethylpyrrolidine-2,5-dione (16d):** This compound was synthesized in similar fashion as **16i**. A solution of **15d** (0.4 g,

1.4 mmol) in pyridine (15 ml) was placed in a 100 ml Schlenk flask. Tetramethylsuccinic anhydride (M<sub>4</sub>SA) (0.5 g, 3.2 mmol) and DBU (1 ml, 6.7 mmol) were added, and the mixture was heated at 120 °C under argon for 22 h with vigorous stirring. It was cooled and concentrated under reduced pressure. The residue was coevaporated with toluene (3 x 20 ml). The product was purified by column chromatography on silica gel eluting with 0-5% MeOH in CH<sub>2</sub>Cl<sub>2</sub> to give a cream solid. It was taken in SOCl<sub>2</sub> (12 ml), heated at 80 °C for 2 h, cooled and concentrated under reduced pressure. The residue was coevaporated with EtOAc (3 x 20 ml). The product was purified by column chromatography on silica gel eluting with 0-8% MeOH in CH<sub>2</sub>Cl<sub>2</sub> to give **16d** as a cream solid in 88% yield (0.37 g). HRMS (ESI): m/z [M+H]<sup>+</sup> calc'd for C<sub>16</sub>H<sub>21</sub>N<sub>4</sub>O<sub>2</sub>: 301.16647; found: 301.16501. <sup>1</sup>H NMR (400 MHz, CD<sub>3</sub>OD): δ, 8.52 (s, 1H), 8.24 (s, 1H), 3.07-3.01 (q, *J* = 7.2, 2H), 1.41-1.37 (t, *J* = 7.2, 3H), 1.37 (bs, 12H) ppm. <sup>13</sup>C NMR (100 MHz, CD<sub>3</sub>OD): δ, 182.9, 146.9, 143.5, 139.6, 135.4, 135.1, 128.7, 48.9, 23.2, 21.8, 14.5 ppm.

(2*R*,3*S*,5*R*)-5-(7-Ethyl-4-(3,3,4,4-tetramethyl-2,5-dioxopyrrolidin-1-yl)-1*H*-imidazo[4,5-*c*]pyridin-1-yl)-2-(((4-methylbenzoyl)oxy)methyl)tetrahydrofuran-3-yl 4-methylbenzoate (17d): This compound was synthesized in similar fashion as 17i. To a solution of 16i (0.35 g, 1.17 mmol) in dry CH<sub>3</sub>CN (60 ml) in a 250 ml round bottom flask, 60% NaH in oil (100 mg, 2.5 mmol) was added, and the mixture was vigorously stirred at room temperature under argon for 45 min. 1-(α)-Chloro-3,5-di-*O*-(*p*-toluoyl)-2-deoxy-D-ribose (0.817 g, 2.1 mmol) was subsequently added portionwise over 1 h, and the stirring was continued at room temperature for overall 5 h. The mixture was filtered through Celite® and concentrated. The product was purified by column chromatography on silica gel eluting with 0-50% EtOAc in hexanes, and concentrated repeatedly with dichloromethane. 17d was obtained as a yellowish syrup in 65% yield (0.494 g). HRMS (ESI): m/z [M+H]<sup>+</sup> calc'd for C<sub>37</sub>H<sub>41</sub>N<sub>4</sub>O<sub>7</sub>: 653.29757; found: 653.29654. <sup>1</sup>H NMR (400 MHz, CDCl<sub>3</sub>): δ, 8.27 (s, 1H), 8.25 (s, 1H), 7.92-7.90 (d, *J* = 8.0, 2H), 7.88-7.86 (d, *J* = 8.0, 2H), 7.30-7.28 (d, *J* = 8.4, 2H), 7.24-7.22 (d, *J* = 8.4, 2H), 6.60-6.57 (dd, *J*<sub>1</sub> = 6.4, *J*<sub>2</sub> = 12.8, 1H), 5.72-5.68 (m, 1H), 4.67-4.59 (m, 3H), 3.16-3.00 (m, 2H), 2.82-2.79 (dd, *J*<sub>1</sub> = 4.4, *J*<sub>2</sub> = 6.8, 2H), 2.44 (s, 3H), 2.40 (s, 3H), 1.43-1.40 (t, *J* = 7.6, 3H), 1.37 (bs, 1H) ppm. <sup>13</sup>C NMR (100 MHz,

CDCl<sub>3</sub>):  $\delta$ , 181.7 (Cq), 166.3 (Cq), 165.9 (Cq), 144.9 (Cq), 144.4 (Cq), 142.6, 142.0, 138.9 (Cq), 137.6 (Cq), 137.3 (Cq), 130.0, 129.9, 129.8, 129.5, 126.6 (Cq), 126.4 (Cq), 124.2 (Cq), 85.5, 82.7, 74.6, 64.0 (CH<sub>2</sub>), 48.0 (Cq), 39.7 (CH<sub>2</sub>), 22.9 (CH<sub>2</sub>), 21.9, 21.8, 21.7, 21.5, 15.4 ppm. For the critical NOESY correlations, see Figure S2 and copies of spectra (Supporting Information).

1-(7-Ethyl-1-((2*R*,4*S*,5*R*)-4-hydroxy-5-(hydroxymethyl)tetrahydrofuran-2-yl)-1*H*-imidazo[4,5-*c*]pyridin-4-yl)-3,3,4,4-tetramethylpyrrolidine-2,5-dione (18d): This compound was synthesized in similar fashion as 18i. To a solution of 17d (0.46 g, 0.7 mmol) in dry MeOH (6 ml) in a 25 ml round bottom flask, NaOMe (114 mg, 2.11 mmol) was added. The mixture was stirred at room temperature under argon for 2 h and concentrated in vacuo. The product was purified by column chromatography on silica gel eluting with 0-10% MeOH in dichloromethane to obtain 18d as an off-white solid in 74% yield (218 mg). HRMS (ESI):  $m/z$  [M+H]<sup>+</sup> calc'd for C<sub>21</sub>H<sub>29</sub>N<sub>4</sub>O<sub>5</sub>: 417.21383; found: 417.21265. <sup>1</sup>H NMR (400 MHz, CD<sub>3</sub>OD):  $\delta$ , 8.74 (s, 1H), 8.20 (s, 1H), 6.63-6.60 (dd,  $J_1 = 6.4$ ,  $J_2 = 12.8$ , 1H), 4.58-4.55 (m, 1H), 4.06-4.03 (app q,  $J = 3.6$ , 1H), 3.78-3.65 (m, 2H), 3.23-3.12 (app septet,  $J = 3.6$ , 2H), 2.78-2.72 (m, 1H), 2.60-2.54 (ddd,  $J_1 = 3.6$ ,  $J_2 = 6.0$ ,  $J_3 = 10.4$ , 1H), 1.44-1.40 (t,  $J = 7.6$ , 3H), 1.37 (bs, 12H) ppm. <sup>13</sup>C NMR (100 MHz, CD<sub>3</sub>OD):  $\delta$ , 183.4 (Cq), 145.8 (Cq), 142.4, 140.4 (Cq), 138.4 (Cq), 137.8 (Cq), 127.2 (Cq), 89.4, 87.2, 72.1, 62.7 (CH<sub>2</sub>), 48.8 (Cq), 42.2 (CH<sub>2</sub>), 23.5 (CH<sub>2</sub>), 21.9, 21.8, 15.7 ppm.

1-(1-((2*R*,4*S*,5*R*)-5-((Bis(4-methoxyphenyl)(phenyl)methoxy)methyl)-4-hydroxytetrahydrofuran-2-yl)-7-ethyl-1*H*-imidazo[4,5-*c*]pyridin-4-yl)-3,3,4,4-tetramethylpyrrolidine-2,5-dione (19d): This compound was synthesized in similar fashion as 19i. To a solution of 18d (190 mg, 0.457 mmol) in pyridine (3 ml), 4,4'-dimethoxytrityl chloride (DMT-Cl) (217 mg, 0.639 mmol) was added in one portion and the mixture was stirred at room temperature under argon for 4 h. The mixture was concentrated in vacuo. The product was purified by column chromatography on silica gel (neutralized with triethylamine) eluting with 0-20% acetone in dichloromethane to obtain 19d as a colorless solid in 33% yield (110 mg). HRMS (ESI):  $m/z$  [M+H]<sup>+</sup> calc'd for C<sub>42</sub>H<sub>47</sub>N<sub>4</sub>O<sub>7</sub>: 719.34452;

found: 719.34247. <sup>1</sup>H NMR (400 MHz, CDCl<sub>3</sub>): δ, 8.21 (s, 1H), 8.16 (s, 1H), 7.40-7.38 (d, *J* = 7.2, 2H), 7.30-7.20 (m, 7H), 6.82-6.80 (d, *J* = 9.2, 4H), 6.42-6.39 (dd, *J*<sub>1</sub> = 6.4, *J*<sub>2</sub> = 12.4, 1H), 4.54-4.48 (m, 1H), 4.11-4.08 (app q, *J* = 4.4, 1H), 3.77 (s, 6H), 3.38-3.34 (app dd, *J*<sub>1</sub> = 4.4, *J*<sub>2</sub> = 10.4, 1H), 3.32-3.29 (app dd, *J*<sub>1</sub> = 4.8, *J*<sub>2</sub> = 10.4, 1H), 3.17 (bs, 1H), 3.03-3.00 (app dd, *J*<sub>1</sub> = 3.2, *J*<sub>2</sub> = 7.6, 1H), 2.99-2.96 (app dd, *J*<sub>1</sub> = 3.2, *J*<sub>2</sub> = 7.6, 1H), 2.46-2.44 (app t, *J* = 6.0, 2H), 1.38-1.37 (overlapped s, 12H), 1.36-1.32 (t, *J* = 7.2, 3H) ppm. <sup>13</sup>C NMR (100 MHz, CDCl<sub>3</sub>): δ, 181.8 (Cq), 158.7 (Cq), 144.5 (Cq), 142.6, 141.9, 138.9 (Cq), 137.3 (Cq), 137.2 (Cq), 135.63 (Cq), 135.58 (Cq), 130.1, 128.13, 128.06, 127.1, 124.6 (Cq), 113.4, 86.8 (Cq), 86.0, 85.2, 71.9, 63.7 (CH<sub>2</sub>), 55.3, 48.0 (Cq), 41.7 (CH<sub>2</sub>), 22.7 (CH<sub>2</sub>), 21.8, 21.4, 15.3 ppm.

(2*R*,3*S*,5*R*)-2-((Bis(4-methoxyphenyl)(phenyl)methoxy)methyl)-5-(7-ethyl-4-(3,3,4,4-tetramethyl-2,5-dioxopyrrolidin-1-yl)-1*H*-imidazo[4,5-*c*]pyridin-1-yl)tetrahydrofuran-3-yl (2-cyanoethyl) diisopropylphosphoramidite (20d): This compound was synthesized in similar fashion as 20i. To a solution of 19d (105 mg, 0.146 mmol) in dry CH<sub>2</sub>Cl<sub>2</sub> (4 ml) containing *N,N*-diisopropylethylamine (DIEA) (127 μl, 0.731 mmol), 2-cyanoethyl-*N,N*-diisopropyl chloro-phosphoramidite (40 μl, 0.175 mmol) was added in one portion and the mixture was stirred at room temperature under argon for 4 h (TLC showed complete conversion). The mixture was concentrated in vacuo at rt and the product was purified by column chromatography on silica gel (neutralized with triethylamine) eluting with 40-60% EtOAc in hexanes containing 1% triethylamine, to obtain 20d as a mixture of diastereomers (white foam, *R*<sub>f</sub> ~0.5 in 5% acetone/CH<sub>2</sub>Cl<sub>2</sub>, two close spots visible on TLC) in 67% yield (90 mg). HRMS (ESI): *m/z* [M+H]<sup>+</sup> calc'd for C<sub>51</sub>H<sub>64</sub>N<sub>6</sub>O<sub>8</sub>P: 919.45236; found: 919.45047. <sup>1</sup>H NMR (400 MHz, CDCl<sub>3</sub>): δ, 8.25 (s, 1H), 8.23, 8.19 (s, 1H), 7.40-7.38 (m, 2H), 7.30-7.20 (m, 7H), 6.83-6.79 (m, 4H), 6.49-6.46 (dd, *J*<sub>1</sub> = 6.8, *J*<sub>2</sub> = 13.6, 1H), 4.70-4.59 (m, 1H), 4.32-4.24 (m, 1H), 3.78, 3.77 (s, 6H), 3.70-3.53 (m, 3H), 3.32-3.31 (m, 1H), 3.13-2.99 (m, 2H), 2.62-2.59 (t, *J* = 6.4, 1H), 2.57-2.55 (m, 1H), 2.44-2.41 (t, *J* = 6.4, 1H), 1.38, 1.37 (bs, 12H), 1.20-1.17 (m, 9H), 1.13-1.12 (d, *J* = 6.8, 3H) ppm. <sup>13</sup>C NMR (100 MHz, CDCl<sub>3</sub>): δ, 181.7, 158.7, 144.5, 142.5, 142.4, 139.0, 137.4, 135.63, 135.56, 130.2, 128.3, 128.2, 128.1, 127.1, 124.5, 124.4, 117.5, 113.4, 86.7, 85.8, 85.5, 85.4, 74.1, 73.9,

63.4, 63.2, 58.4, 58.2, 55.38, 55.36, 48.0, 43.61, 43.55, 43.4, 41.0, 24.7, 24.6, 22.9, 21.8, 21.5, 15.6 ppm.  $^{31}\text{P}$  NMR (162 MHz,  $\text{CDCl}_3$ ):  $\delta$ , 150.8, 150.2 ppm.

**7-Isobutyl-1*H*-imidazo[4,5*c*]pyridin-4-amine, trifluoroacetic acid salt (15e):** This compound was synthesized in similar fashion as **15i**. A solution of **14e** (1.3 g, 2.4 mmol) in TFA (20 ml) was placed in a 100 ml pressure tube, anisole (1.6 ml, 6 equiv.) was added, and the mixture was heated at 70 °C for 24 h with vigorous stirring. It was cooled and concentrated under reduced pressure. The residue was coevaporated with toluene (3 x 20 ml) to obtain **15e** (ca. 0.8 g, quantitative) as an oil that was taken into next step without further purification.

**1-(7-Isobutyl-1*H*-imidazo[4,5-*c*]pyridin-4-yl)-3,3,4,4-tetramethylpyrrolidine-2,5-dione (16e):** This compound was synthesized in similar fashion as **16i**. A solution of **15e** (ca. 0.8 g, 2.4 mmol) in pyridine (20 ml) was placed in a 100 ml Schlenk flask. Tetramethylsuccinic anhydride ( $\text{M}_4\text{SA}$ ) (0.8 g, 5.1 mmol) and DBU (1.5 ml, 10.0 mmol) were added, and the mixture was heated at 120 °C under argon for 22 h with vigorous stirring. It was cooled and concentrated under reduced pressure. The residue was coevaporated with toluene (3 x 20 ml). The product was purified by column chromatography on silica gel eluting with 0-5% MeOH in  $\text{CH}_2\text{Cl}_2$  to give a cream foam. It was taken in  $\text{SOCl}_2$  (20 ml), heated at 80 °C for 2 h, cooled and concentrated under reduced pressure. The residue was coevaporated with EtOAc (3 x 20 ml). The product was purified by column chromatography on silica gel eluting with 0-8% MeOH in  $\text{CH}_2\text{Cl}_2$  to give **16e** as a cream foam in 79% yield (0.61 g). HRMS (ESI):  $m/z$   $[\text{M}+\text{H}]^+$  calc'd for  $\text{C}_{18}\text{H}_{25}\text{N}_4\text{O}_2$ : 329.19777; found: 329.19608.  $^1\text{H}$  NMR (400 MHz,  $\text{CD}_3\text{OD}$ ):  $\delta$ , 8.43 (s, 1H), 8.16 (s, 1H), 2.87-2.85 (d,  $J = 7.6$ , 2H), 2.11-2.05 (app septet,  $J = 6.8$ , 1H), 1.37 (bs, 12H), 0.99-0.97 (d,  $J = 6.4$ , 6H) ppm.  $^{13}\text{C}$  NMR (100 MHz,  $\text{CD}_3\text{OD}$ ):  $\delta$ , 183.2, 146.4, 143.7, 141.6, 135.8, 135.4, 126.0, 38.9, 30.4, 22.6, 21.9 ppm.

(2*R*,3*S*,5*R*)-5-(7-Isobutyl-4-(3,3,4,4-tetramethyl-2,5-dioxopyrrolidin-1-yl)-1*H*-imidazo[4,5-*c*]pyridin-1-yl)-2-(((4-methylbenzoyl)oxy)methyl)tetrahydrofuran-3-yl 4-methylbenzoate (17e): This compound was synthesized in similar fashion as 17i. To a solution of 16e (0.585 g, 1.78 mmol) in dry CH<sub>3</sub>CN (60 ml) in a 250 ml round bottom flask, 60% NaH in oil (143 mg, 3.57 mmol) was added, and the mixture was vigorously stirred at room temperature under argon for 35 min. 1-( $\alpha$ )-Chloro-3,5-di-*O*-(*p*-toluoyl)-2-deoxy-D-ribose (1.25 g, 3.21 mmol) was subsequently added portionwise over 1 h, and the stirring was continued at room temperature for overall 4.5 h. The mixture was filtered through Celite® and concentrated. The product was purified by column chromatography on silica gel eluting with 0-50% EtOAc in hexanes, and concentrated repeatedly with dichloromethane. 17e was obtained as a yellowish solid in 38% yield (0.465 g). HRMS (ESI): *m/z* [M+H]<sup>+</sup> calc'd for C<sub>39</sub>H<sub>45</sub>N<sub>4</sub>O<sub>7</sub>: 681.32887; found: 681.32697. <sup>1</sup>H NMR (400 MHz, CDCl<sub>3</sub>):  $\delta$ , 8.27 (s, 1H), 8.20 (s, 1H), 7.97-7.95 (d, *J* = 8.0, 2H), 7.92-7.90 (d, *J* = 8.0, 2H), 7.30-7.28 (d, *J* = 8.4, 2H), 7.27-7.25 (d, *J* = 8.4, 2H), 6.59-6.55 (dd, *J*<sub>1</sub> = 5.2, *J*<sub>2</sub> = 8.8, 1H), 5.73-5.72 (m, 1H), 4.70-4.61 (m, 3H), 2.98-2.92 (dd, *J*<sub>1</sub> = 7.2, *J*<sub>2</sub> = 14.4, 1H), 2.84-2.72 (m, 3H), 2.45 (s, 3H), 2.42 (s, 3H), 1.98-1.88 (app septet, *J* = 6.4, 1H), 1.38 (bs, 1H), 1.05-1.03 (d, *J* = 6.8, 6H) ppm. <sup>13</sup>C NMR (100 MHz, CDCl<sub>3</sub>):  $\delta$ , 181.6 (Cq), 166.3 (Cq), 165.9 (Cq), 144.9 (Cq), 144.4 (Cq), 144.1, 142.2, 139.2 (Cq), 137.7 (Cq), 137.4 (Cq), 129.9, 129.8, 129.54, 129.47, 126.6 (Cq), 126.3 (Cq), 121.8 (Cq), 85.4, 82.9, 74.9, 64.2 (CH<sub>2</sub>), 48.0 (Cq), 39.9 (CH<sub>2</sub>), 39.1 (CH<sub>2</sub>), 30.2, 22.5, 21.9, 21.8, 21.7, 21.5 ppm. For the critical NOESY correlations, see Figure S3 and copies of spectra (Supporting Information).

1-(1-((2*R*,4*S*,5*R*)-4-Hydroxy-5-(hydroxymethyl)tetrahydrofuran-2-yl)-7-isobutyl-1*H*-imidazo[4,5-*c*]pyridin-4-yl)-3,3,4,4-tetramethylpyrrolidine-2,5-dione (18e): This compound was synthesized in similar fashion as 18i. To a solution of 17e (0.46 g, 0.68 mmol) in dry MeOH (7 ml) in a 25 ml round bottom flask, NaOMe (110 mg, 2.03 mmol) was added. The mixture was stirred at room temperature under argon for 2 h and concentrated in vacuo. The product was purified by column chromatography on silica gel eluting with 0-10% MeOH in dichloromethane to obtain 18e as an off-white foam in 85% yield (256 mg). HRMS (ESI): *m/z* [M+H]<sup>+</sup> calc'd for C<sub>23</sub>H<sub>33</sub>N<sub>4</sub>O<sub>5</sub>: 445.24512; found:

445.24381. <sup>1</sup>H NMR (400 MHz, CD<sub>3</sub>OD): δ, 8.74 (s, 1H), 8.14 (s, 1H), 6.58-6.55 (dd, *J*<sub>1</sub> = 6.4, *J*<sub>2</sub> = 12.8, 1H), 4.58-4.55 (dt, *J*<sub>1</sub> = 3.2, *J*<sub>2</sub> = 6.8, 1H), 4.06-4.04 (app q, *J* = 3.2, 1H), 3.77-3.73 (app dd, *J*<sub>1</sub> = 3.6, *J*<sub>2</sub> = 12.0, 1H), 3.72-3.68 (app dd, *J*<sub>1</sub> = 3.6, *J*<sub>2</sub> = 12.0, 1H), 3.06-3.01 (app dd, *J*<sub>1</sub> = 6.8, *J*<sub>2</sub> = 14.4, 1H), 2.92-2.86 (app dd, *J*<sub>1</sub> = 7.2, *J*<sub>2</sub> = 14.0, 1H), 2.76-2.69 (ddd, *J*<sub>1</sub> = 5.6, *J*<sub>2</sub> = 6.8, *J*<sub>3</sub> = 13.2, 1H), 2.56-2.51 (ddd, *J*<sub>1</sub> = 3.6, *J*<sub>2</sub> = 6.0, *J*<sub>3</sub> = 9.6, 1H), 2.04-1.94 (app septet, *J* = 6.8, 1H), 1.37 (bs, 12H), 1.05-1.03 (d, *J* = 6.8, 6H) ppm. <sup>13</sup>C NMR (100 MHz, CD<sub>3</sub>OD): δ, 183.4 (Cq), 146.0 (Cq), 144.0, 140.7 (Cq), 138.5 (Cq), 137.9 (Cq), 124.6 (Cq), 89.4, 87.0, 72.3, 62.8 (CH<sub>2</sub>), 48.9 (Cq), 42.3 (CH<sub>2</sub>), 39.4 (CH<sub>2</sub>), 31.1, 22.6, 22.5, 21.9, 21.8 ppm.

1-(1-((2*R*,4*S*,5*R*)-5-((Bis(4-methoxyphenyl)(phenyl)methoxy)methyl)-4-hydroxytetrahydrofuran-2-yl)-7-isobutyl-1*H*-imidazo[4,5-*c*]pyridin-4-yl)-3,3,4,4-tetramethylpyrrolidine-2,5-dione (19e): This compound was synthesized in similar fashion as 19i. To a solution of 18e (225 mg, 0.507 mmol) in dry pyridine (4 ml), 4,4'-dimethoxytrityl chloride (DMT-Cl) (240 mg, 0.709 mmol) was added in one portion and the mixture was stirred at room temperature under argon for 4 h. TLC analysis indicated that a lot of starting material remained and then additional DMT-Cl (0.120 g, 0.355 mmol) and cat. DMAP (10 mg) were added. After 14 h more DMT-Cl (0.120 g, 0.350 mmol), triethylamine (85 μl, 0.608 mmol), and cat. DMAP (10 mg) were added. After 8 h, another portion as above was added, and after 16 h TLC showed no further conversion (overall 42 h). The mixture was quenched with 200 μl of MeOH, concentrated in vacuo, the residue was taken in AcOEt and filtered, and the filtrate was concentrated in vacuo. The product was purified by column chromatography on silica gel (neutralized with triethylamine) eluting with 0-25% acetone in dichloromethane to obtain 19e as a colorless foam in 46% yield (175 mg). Further elution with 10% MeOH in dichloromethane yielded the recovered starting material 18e as a colorless syrup in 45% yield (102 mg). HRMS (ESI): *m/z* [M+H]<sup>+</sup> calc'd for C<sub>44</sub>H<sub>51</sub>N<sub>4</sub>O<sub>7</sub>: 747.37582; found: 747.37412. <sup>1</sup>H NMR (400 MHz, CDCl<sub>3</sub>): δ, 8.17 (s, 1H), 8.14 (s, 1H), 7.40-7.38 (d, *J* = 8.8, 2H), 7.30-7.20 (m, 7H), 6.82-6.80 (d, *J* = 8.8, 4H), 6.42-6.38 (dd, *J*<sub>1</sub> = 6.4, *J*<sub>2</sub> = 12.8, 1H), 4.52-4.51 (m, 1H), 4.10-4.07 (app q, *J* = 4.4, 1H), 3.77 (s, 6H), 3.38-3.35 (app dd, *J*<sub>1</sub> = 4.4, *J*<sub>2</sub> = 10.4, 1H), 3.33-3.29 (app dd, *J*<sub>1</sub> = 4.8,



$J_2 = 10.4$ , 1H), 2.88-2.83 (app dd,  $J_1 = 7.2$ ,  $J_2 = 14.4$ , 1H), 2.75-2.70 (app dd,  $J_1 = 6.4$ ,  $J_2 = 14.0$ , 1H), 2.46-2.41 (m, 2H), 1.90-1.84 (app quintet,  $J = 6.4$ , 1H), 1.37-1.36 (overlapped s, 12H), 1.01-0.99 (dd,  $J_1 = 2.4$ ,  $J_2 = 6.4$ , 6H) ppm.  $^{13}\text{C}$  NMR (100 MHz,  $\text{CDCl}_3$ ):  $\delta$ , 181.7 (Cq), 158.7 (Cq), 144.5 (Cq), 143.6, 142.7, 139.2 (Cq), 137.5 (Cq), 137.4 (Cq), 135.63 (Cq), 135.58 (Cq), 130.1, 128.2, 128.1, 127.1, 122.2 (Cq), 113.4, 86.8 (Cq), 86.0, 85.0, 72.0, 63.7 ( $\text{CH}_2$ ), 55.3, 48.0 (Cq), 41.8 ( $\text{CH}_2$ ), 38.8 ( $\text{CH}_2$ ), 30.1, 22.5, 22.4, 21.8, 21.4 ppm.

(2*R*,3*S*,5*R*)-2-((Bis(4-methoxyphenyl)(phenyl)methoxy)methyl)-5-(7-isobutyl-4-(3,3,4,4-tetramethyl-2,5-dioxopyrrolidin-1-yl)-1*H*-imidazo[4,5-*c*]pyridin-1-yl)tetrahydrofuran-3-yl (2-cyanoethyl) diisopropylphosphoramidite (20e): This compound was synthesized in similar fashion as 20i. To a solution of 19e (105 mg, 0.146 mmol) in dry  $\text{CH}_2\text{Cl}_2$  (5 ml) containing *N,N*-diisopropylethylamine (DIEA) (185  $\mu\text{l}$ , 1.07 mmol), 2-cyanoethyl-*N,N*-diisopropyl chloro-phosphoramidite (105  $\mu\text{l}$ , 0.472 mmol) was added in one portion and the mixture was stirred at room temperature under argon for 4 h (TLC showed complete conversion). The mixture was concentrated in vacuo at rt and the product was purified by column chromatography on silica gel (neutralized with triethylamine) eluting with 40-60% EtOAc in hexanes containing 1% triethylamine, to obtain 20e as a mixture of diastereomers (white foam,  $R_f \sim 0.5$  in 50% EtOAc in hexanes, two close spots visible on TLC) in 59% yield (120 mg). HRMS (ESI):  $m/z$   $[\text{M}+\text{H}]^+$  calc'd for  $\text{C}_{53}\text{H}_{68}\text{N}_6\text{O}_8\text{P}$ : 947.48366; found: 947.48314.  $^1\text{H}$  NMR (400 MHz, acetone- $d_6$ ):  $\delta$ , 8.43, 8.41 (s, 1H), 8.15 (s, 1H), 7.46-7.41 (m, 2H), 7.33-7.19 (m, 7H), 6.85-6.81 (m, 4H), 6.62-6.58 (dd,  $J_1 = 6.4$ ,  $J_2 = 13.2$ , 1H), 4.86-4.81 (m, 1H), 4.37-4.29 (m, 1H), 3.96-3.82 (m, 1H), 3.77, 3.76 (s, 6H), 3.74-3.66 (m, 2H), 3.39-3.34 (m, 2H), 3.13-3.09 (m, 1H), 3.03-2.96 (m, 1H), 2.94-2.87 (m, 1H), 2.81 (m, 3H), 2.79-2.76 (t,  $J = 6.4$ , 1H), 2.68-2.64 (t,  $J = 6.0$ , 1H), 1.36, 1.35, 1.30 (bs, 12H), 1.23-1.21, 1.22-1.20, 1.17-1.16 (d,  $J = 6.8$ , 12H), 1.08-1.06 (d,  $J = 6.8$ , 3H), 1.05-1.03 (dd,  $J_1 = 1.6$ ,  $J_2 = 6.4$ , 3H) ppm.  $^{13}\text{C}$  NMR (100 MHz, acetone- $d_6$ ):  $\delta$ , 181.8, 159.6, 145.9, 144.1, 144.0, 139.9, 138.7, 136.6, 136.5, 131.0, 130.9, 129.0, 128.9, 128.6, 127.6, 123.32, 123.28, 119.0, 114.0, 87.2, 86.7, 86.1, 86.0, 75.0, 74.9, 74.5, 74.3, 64.5, 59.6, 59.4, 55.5, 48.4, 44.1, 44.0, 40.4, 39.0, 25.0, 24.9, 24.8, 22.9, 22.5, 22.0, 21.7, 21.4, 20.8 ppm.  $^{31}\text{P}$  NMR (162 MHz, acetone- $d_6$ ):  $\delta$ , 149.9, 149.7 ppm.

**7-Phenyl-1*H*-imidazo[4,5*c*]pyridin-4-amine, trifluoroacetic acid salt (15a, 3a\*TFA):**

This compound was synthesized in similar fashion as **15i**. A solution of **14a** (2.09 g, 3.65 mmol) in TFA (20 ml) was placed in a 100 ml pressure tube, anisole (2.4 ml, 6 equiv.) was added, and the mixture was heated at 70 °C for 24 h with vigorous stirring. It was cooled and concentrated under reduced pressure. The residue was coevaporated with toluene (3 x 25 ml) to obtain grey-brown powder. It was taken in toluene (10 ml) and filtered, washing with toluene (2 x 5 ml), then hexane (2 x 5 ml) and dried on air to obtain **15a** as a free flowing, light gray powder, 1.13 g (quantitative). MS (ESI): *m/z*, 211.3 for [M + H]<sup>+</sup>. <sup>1</sup>H NMR (400 MHz, DMSO-*d*<sub>6</sub>): δ, 8.60 (bs, 2H), 8.52 (s, 1H), 7.82 (s, 1H), 7.70-7.69 (m, 2H), 7.56-7.53 (m, 2H), 7.49-7.46 (m, 1H) ppm. <sup>13</sup>C NMR (100 MHz, DMSO-*d*<sub>6</sub>): δ, 159.4, 159.0, 158.7, 158.3, 147.5, 144.3, 132.7, 129.1, 128.5, 128.0, 126.7, 115.2 ppm.

**3,3,4,4-Tetramethyl-1-(7-phenyl-1*H*-imidazo[4,5-*c*]pyridin-4-yl)pyrrolidine-2,5-**

**dione (16a):** This compound was synthesized in similar fashion as **16i**. A solution of **15a** (0.34 g, 1 mmol) in pyridine (10 ml) was placed in a 100 ml Schlenk flask. Tetramethylsuccinic anhydride (M<sub>4</sub>SA) (0.546 g, 3.5 mmol) and DBU (1.05 ml, 7 mmol) were added, and the mixture was heated at 120 °C under argon for 20 h with vigorous stirring. It was cooled and concentrated under reduced pressure. The residue was coevaporated with toluene (3 x 25 ml). The product was purified by column chromatography on silica gel eluting with 0-5% MeOH in CH<sub>2</sub>Cl<sub>2</sub> to give a colorless syrup. It was taken in SOCl<sub>2</sub> (12 ml), heated at 80 °C for 2 h, cooled and concentrated under reduced pressure. The residue was coevaporated with EtOAc (3 x 25 ml). The product was purified by column chromatography on silica gel eluting with 0-5% MeOH in CH<sub>2</sub>Cl<sub>2</sub> to give **16a** as a light brown foam in 92% yield (0.56 g). HRMS (ESI): *m/z* [M+H]<sup>+</sup> calc'd for C<sub>20</sub>H<sub>21</sub>N<sub>4</sub>O<sub>2</sub>: 349.16647; found: 349.16505. <sup>1</sup>H NMR (400 MHz, CD<sub>3</sub>OD): δ, 8.75 (s, 1H), 8.52 (s, 1H), 7.76-7.75 (m, 2H), 7.61-7.51 (m, 3H), 1.40 (bs, 12H) ppm. <sup>13</sup>C NMR (100 MHz, CD<sub>3</sub>OD): δ, 182.5, 147.9, 142.4, 139.6, 135.4, 134.4, 134.3, 130.5, 129.8, 127.0, 49.1, 21.8 ppm.

((2*R*,3*S*,5*R*)-3-((4-methylbenzoyl)oxy)-5-(7-phenyl-4-(3,3,4,4-tetramethyl-2,5-dioxopyrrolidin-1-yl)-1*H*-imidazo[4,5-*c*]pyridin-1-yl)tetrahydrofuran-2-yl)methyl 4-methylbenzoate (17a): This compound was synthesized in similar fashion as 17i. To a solution of 16a (0.51 g, 1.46 mmol) in dry CH<sub>3</sub>CN (60 ml) in a 100 ml round bottom flask, 60% NaH in oil (117 mg, 2.93 mmol) was added, and the mixture was vigorously stirred at room temperature under argon for 45 min. 1-( $\alpha$ )-Chloro-3,5-di-O-(*p*-toluoyl)-2-deoxy-D-ribose (0.368 g, 0.94 mmol) was subsequently added portionwise over 1 h, and the stirring was continued at room temperature for overall 5 h. The mixture was filtered through Celite® and concentrated. The product was purified by column chromatography on silica gel eluting with 0-50% EtOAc in hexanes. 17a was obtained as a yellowish syrup in 64% yield (0.64 g). HRMS (ESI): *m/z* [M+H]<sup>+</sup> calc'd for C<sub>41</sub>H<sub>40</sub>N<sub>4</sub>O<sub>7</sub>: 701.29757; found: 701.29626. <sup>1</sup>H NMR (400 MHz, CDCl<sub>3</sub>):  $\delta$ , 8.33 (s, 1H), 8.31 (s, 1H), 7.86-7.84 (d, *J* = 8.0, 2H), 7.75-7.73 (d, *J* = 8.0, 2H), 7.46 (bs, 4H), 7.32-7.28 (m, 1H), 7.31-7.29 (d, *J* = 8.0, 2H), 7.24-7.22 (d, *J* = 8.0, 2H), 5.96-5.93 (dd, *J*<sub>1</sub> = 5.2, *J*<sub>2</sub> = 8.8, 1H), 5.46-5.44 (m, 1H), 4.62-4.53 (m, 2H), 4.38-4.36 (m, 1H), 2.48 (s, 3H), 2.40 (s, 3H), 2.30-2.16 (m, 2H), 1.40 (bs, 12H) ppm. <sup>13</sup>C NMR (100 MHz, CDCl<sub>3</sub>):  $\delta$ , 181.7 (Cq), 166.2 (Cq), 165.6 (Cq), 144.7 (Cq), 144.5 (Cq), 142.9, 142.7, 138.4 (Cq), 138.0 (Cq), 137.4 (Cq), 134.8 (Cq), 130.0, 129.7, 129.6, 129.3, 129.0, 128.8, 126.6 (Cq), 126.4 (Cq), 123.5 (Cq), 85.9, 82.8, 74.9, 64.2 (CH<sub>2</sub>), 48.1 (Cq), 40.1 (CH<sub>2</sub>), 21.9, 21.8, 21.6 ppm. For the critical NOESY correlations, see Figure S4 and copies of spectra (Supporting Information).

1-(1-((2*R*,4*S*,5*R*)-4-hydroxy-5-(hydroxymethyl)tetrahydrofuran-2-yl)-7-phenyl-1*H*-imidazo[4,5-*c*]pyridin-4-yl)-3,3,4,4-tetramethylpyrrolidine-2,5-dione (18a): This compound was synthesized in similar fashion as 18i. To a solution of 17a (0.44 g, 0.63 mmol) in dry MeOH (6 ml) in a 25 ml round bottom flask, NaOMe (102 mg, 1.89 mmol) was added, and the mixture was stirred at room temperature under argon for 2 h. It was concentrated in vacuo, and the product was purified by column chromatography on silica gel eluting with 0-10% MeOH in CH<sub>2</sub>Cl<sub>2</sub> to obtain 18a as a white foam in 58% yield (0.17 g). HRMS (ESI): *m/z* [M+H]<sup>+</sup> calc'd for C<sub>25</sub>H<sub>29</sub>N<sub>4</sub>O<sub>5</sub>: 465.21383; found: 465.21228. <sup>1</sup>H NMR (400 MHz, CD<sub>3</sub>OD):  $\delta$ , 8.85 (s, 1H), 8.19 (s, 1H), 7.56 (m, 5H), 5.97-5.94 (t, *J*=6.0,

1H), 4.37-4.33 (m, 1H), 3.78-3.65 (m, 3H), 2.35-2.28 (m, 1H), 1.96-1.90 (ddd,  $J_1 = 4.4$ ,  $J_2 = 6.0$ ,  $J_3 = 10.8$ , 1H), 1.39 (bs, 12H) ppm.  $^{13}\text{C}$  NMR (100 MHz,  $\text{CD}_3\text{OD}$ ):  $\delta$ , 183.4 (Cq), 146.5 (Cq), 143.1, 139.4 (Cq), 138.7 (Cq), 138.6 (Cq), 135.6 (Cq), 130.9, 130.2, 129.9, 126.0 (Cq), 88.9, 87.1, 71.2, 62.3 ( $\text{CH}_2$ ), 49.0 (Cq), 42.9 ( $\text{CH}_2$ ), 21.9, 21.8 ppm.

The attempted tritylation of **18a** was carried forward in similar fashion as for **18i**. To a solution of **18a** (0.15 g, 0.323 mmol) in pyridine (3 ml) under Ar, 4,4'-dimethoxytrityl chloride (DMT-Cl) (0.153 g, 0.453 mmol) was added in one portion, and the mixture was stirred at room temperature for 4.5 h. TLC analysis indicated that some starting material remained, and then additional DMT-Cl was added (0.076 g, 0.225 mmol). After 3.5 h, the starting material still remained, and then triethylamine (45  $\mu\text{l}$ , 0.323 mmol), cat. DMAP (10 mg) and additional DMT-Cl (44 mg, 0.129 mmol) were added. After 8 h, most of the starting material was consumed, and the mixture was concentrated in vacuo, the residue was coevaporated with toluene (3 x 10 ml) to remove residual pyridine. A TLC analysis indicated that an extensive deglycosylation occurred, indicating the instability of the compound which may be ascribed to the electronic character of phenyl group at the position 3 as suggested by other reports.<sup>15</sup> Deglycosylation was also observed to occur upon mild heating of the TLC plate in order to remove pyridine before analysis.

Synthesis of 3-deazahypoxanthine 21c.

**7-Phenethyl-1H-imidazo[4,5-c]pyridin-4-amine, tri-fluoroacetic acid salt (15c):** This compound was synthesized in similar fashion as **15i**. A solution of **14c** (0.327 g, 0.55 mmol) in TFA (8 ml) was placed in a 100 ml pressure tube, anisole (0.36 ml, 6 equiv.) was added, and the mixture was heated at 70 °C for 21 h with vigorous stirring. It was cooled and concentrated under reduced pressure. The residue was coevaporated with toluene (3 x 15 ml) to obtain **15c** (ca. 0.2 g, quantitative) as a syrup that was taken into next step without further purification.

**7-Phenethyl-1,5-dihydro-4*H*-imidazo[4,5-*c*]pyridin-4-one (21c):** This compound was synthesized according to the general procedure.<sup>56</sup> A solution of crude **15c** (ca. 0.2 g, 0.55 mmol) in acetone/H<sub>2</sub>O/AcOH (4/2/2 ml) was stirred at room temperature for 5 h in a closed vessel. The pressure was carefully released and the mixture was carefully neutralized with aq. NaHCO<sub>3</sub> and diluted with Et<sub>2</sub>O (50 ml). The phases were shaken, and the precipitated solid was filtered, washing with water and Et<sub>2</sub>O, and dried on air to obtain **21c** as a light yellow solid (75 mg, 57% based on **14c**). HRMS (ESI): m/z [M+H]<sup>+</sup> calc'd for C<sub>14</sub>H<sub>14</sub>N<sub>3</sub>O: 240.11369; found: 240.11281. MS (ESI): m/z, 240.3 for [M+H]<sup>+</sup>, 262.2 for [M+Na]<sup>+</sup>, 501.2 for [2M+Na]<sup>+</sup>; 238.3 for [M-H]<sup>-</sup>. <sup>1</sup>H NMR (400 MHz, DMSO-*d*<sub>6</sub>): δ, 10.9 (bs, 1H), 8.09 (s, 1H), 7.26-7.16 (m, 5H), 6.79 (s, 1H), 2.93-2.89 (m, 4H) ppm. <sup>13</sup>C NMR (100 MHz, DMSO-*d*<sub>6</sub>): δ, 156.1, 141.6, 141.2, 128.4, 128.2, 125.8, 124.9, 110.7, 35.1, 29.7 ppm.

**Purification of salts 15:** TFA salts **15** were used for synthetic purposes typically without further purification. Pure amines could be also isolated as water soluble HCl salts as exemplified below. Free amines could be obtained by neutralization of their aqueous solutions with Na<sub>2</sub>CO<sub>3</sub> followed by extraction with AcOEt.

**7-Phenethyl-1*H*-imidazo[4,5-*c*]pyridin-4-amine, hydrochloric acid salt (15c\*HCl):** A solution of **14c** (0.173 g, 0.29 mmol) in EtOH/H<sub>2</sub>O/HCl conc. (8/8/4 ml) was heated under reflux condenser at 100 °C for 23 h. It was cooled and EtOH was removed under reduced pressure. It was diluted with aq. HCl and washed with Et<sub>2</sub>O (40 ml, discarded) to remove a precipitated oil. The residue was concentrated and dried under vacuum to obtain **15c\*HCl** (ca. 0.08 g, quantitative) as an off-white solid. HRMS (ESI): m/z [M+H]<sup>+</sup> calc'd for C<sub>14</sub>H<sub>15</sub>N<sub>4</sub>: 239.12968; found: 239.12930. MS (ESI): m/z, 239.3 for [M+H]<sup>+</sup>; 237.3 for [M-H]<sup>-</sup>, 273.0 for [M+Cl]<sup>-</sup>. <sup>1</sup>H NMR (400 MHz, D<sub>2</sub>O): δ, 8.35 (s, 1H), 7.28-7.19 (m, 4H), 7.11-7.09 (m, 2H), 3.09-3.05 (m, 2H), 2.99-2.96 (m, 2H) ppm. <sup>13</sup>C NMR (100 MHz, D<sub>2</sub>O): δ, 146.6, 143.6, 140.6, 128.8, 128.6, 127.0, 126.5, 123.8, 114.7, 34.6, 29.3 ppm.

## References

- (1) Jordheim, L. P.; Durantel, D.; Zoulim, F.; Dumontet, C. Advances in the development of nucleoside and nucleotide analogues for cancer and viral diseases. *Nat. Rev. Drug Discov.* **2013**, *12*, 447-464.
- (2) Sharma, S.; Mehndiratta, S.; Kumar, S.; Singh, J.; Bedi, P. M. S.; Nepali, K. Purine analogues as kinase inhibitors: A review. *Recent Pat. Anticancer Drug. Discov.* **2015**, *10*, 308-341.
- (3) Sala, M.; Kogler, M.; Plackova, P.; Mejdrova, I.; Hrebabecky, H.; Prochazkova, E.; Strunin, D.; Lee, G.; Birkus, G.; Weber, J.; Mertlikova-Kaiserova, H.; Nencka, R. Purine analogs as phosphatidylinositol 4-kinase III beta inhibitors. *Bioorg. Med. Chem. Lett.* **2016**, *26*, 2706-2712.
- (4) Shaughnessy, K. H. Palladium-catalyzed modification of unprotected nucleosides, nucleotides, and oligonucleotides. *Molecules* **2015**, *20*, 9419-9454.
- (5) Yang, Y. X.; Cohn, P.; Dyer, A. L.; Eom, S. H.; Reynolds, J. R.; Castellano, R. K.; Xue, J. G. Blue-violet electroluminescence from a highly fluorescent purine. *Chem. Mater.* **2010**, *22*, 3580-3582.
- (6) Venkatesh, V.; Shukla, A.; Sivakumar, S.; Verma, S. Purine-stabilized green fluorescent gold nanoclusters for cell nuclei imaging applications. *ACS Appl. Mater. Inter.* **2014**, *6*, 2185-2191.
- (7) Yang, Y. X.; Cohn, P.; Eom, S. H.; Abboud, K. A.; Castellano, R. K.; Xue, J. G. Ultraviolet-violet electroluminescence from highly fluorescent purines. *J. Mater. Chem. C* **2013**, *1*, 2867-2874.
- (8) Aso, T.; Saito, K.; Suzuki, A.; Saito, Y. Synthesis and photophysical properties of pyrene-labeled 3-deaza-2'-deoxyadenosines comprising a non-pi-conjugated linker: Fluorescence quenching-based oligodeoxynucleotide probes for thymine identification. *Org. Biomol. Chem.* **2015**, *13*, 10540-10547.
- (9) Suzuki, A.; Yanaba, T.; Saito, I.; Saito, Y. Molecular design of an environmentally sensitive fluorescent nucleoside, 3-deaza-2'-deoxyadenosine derivative: Distinguishing thymine by probing the DNA minor groove. *ChemBioChem* **2014**, *15*, 1637-1643.
- (10) Herdewijn, P. *Modified Nucleosides: In Biochemistry, Biotechnology and Medicine*; Wiley-VCH Verlag GmbH & Co. KGaA: Weinheim, Germany, 2008.
- (11) Kornberg, R. The molecular basis of eukaryotic transcription (Nobel lecture). *Angew. Chem. Int. Edit.* **2007**, *46*, 6957-6965.
- (12) Irani, R. J.; SantaLucia, J. The synthesis of anti-fixed 3-methyl-3-deaza-2'-deoxyadenosine and other 3H-imidazo[4,5-c]pyridine analogs. *Nucleosides, Nucleotides Nucleic Acids* **2002**, *21*, 737-751.
- (13) Salandria, K. J.; Arico, J. W.; Calhoun, A. K.; McLaughlin, L. W. Stability of DNA containing a structural water mimic in an A-T rich sequence. *J. Am. Chem. Soc.* **2011**, *133*, 1766-1768.
- (14) Pal, A.; Salandria, K. J.; Arico, J. W.; Schlegel, M. K.; McLaughlin, L. W. 2,3-Dicyclohexylsuccinimide as a directing/protecting group for the regioselective glycosylation or alkylation of purines. *Chem. Commun.* **2013**, *49*, 2936-2938.

- (15) Crey-Desbiolles, C.; Kotera, M. Synthesis of 3-deaza-3-nitro-2'-deoxyadenosine. *Bioorg. Med. Chem.* **2006**, *14*, 1935-1941.
- (16) Minakawa, N.; Kawano, Y.; Murata, S.; Inoue, N.; Matsuda, A. Oligodeoxynucleotides containing 3-bromo-3-deazaadenine and 7-bromo-7-deazaadenine 2'-deoxynucleosides as chemical probes to investigate DNA-protein interactions. *ChemBioChem* **2008**, *9*, 464-470.
- (17) Liu, C.; Chen, Q.; Gorden, J. D.; Schneller, S. W. 2- and 3-Fluoro-3-deazaneplanocins, 2-fluoro-3-deazaaristeromycins, and 3-methyl-3-deazaneplanocin: Synthesis and antiviral properties. *Bioorg. Med. Chem.* **2015**, *23*, 5496-5501.
- (18) Saito-Tarashima, N.; Kira, H.; Wada, T.; Miki, K.; Ide, S.; Yamazaki, N.; Matsuda, A.; Minakawa, N. Groove modification of siRNA duplexes to elucidate siRNA-protein interactions using 7-bromo-7-deazaadenosine and 3-bromo-3-deazaadenosine as chemical probes. *Org. Biomol. Chem.* **2016**, *14*, 11096-11105.
- (19) Liu, C.; Chen, Q.; Schneller, S. W. Enantiomeric 3-deaza-1',6'-isoneplanocin and its 3-bromo analogue: Synthesis by the Ullmann reaction and their antiviral properties. *Bioorg. Med. Chem. Lett.* **2016**, *26*, 928-930.
- (20) Liu, C.; Chen, Q.; Yang, M.; Schneller, S. W. C-3 halo and 3-methyl substituted 5'-nor-3-deazaaristeromycins: Synthesis and antiviral properties. *Bioorg. Med. Chem.* **2013**, *21*, 359-364.
- (21) Liu, C.; Chen, Q.; Schneller, S. W. 3-Bromo-3-deazaneplanocin and 3-bromo-3-deazaaristeromycin: Synthesis and antiviral activity. *Bioorg. Med. Chem. Lett.* **2012**, *22*, 5182-5184.
- (22) Minakawa, N.; Kojima, N.; Matsuda, A. Nucleosides and nucleotides. 184. Synthesis and conformational investigation of anti-fixed 3-deaza-3-halopurine ribonucleosides. *J. Org. Chem.* **1999**, *64*, 7158-7172.
- (23) Malvezzi, S.; Angelov, T.; Sturla, S. J. Minor groove 3-deaza-adenosine analogues: Synthesis and bypass in translesion DNA synthesis. *Chem. Eur. J.* **2017**, *23*, 1101-1109.
- (24) Hocek, M.; Dvorakova, H. An efficient synthesis of 2-substituted 6-methylpurine bases and nucleosides by Fe- or Pd-catalyzed cross-coupling reactions of 2,6-dichloropurines. *J. Org. Chem.* **2003**, *68*, 5773-5776.
- (25) Hocek, M.; Silhar, P.; Shih, I. H.; Mabery, E.; Mackman, R. Cytostatic and antiviral 6-arylpurine ribonucleosides. Part 7: Synthesis and evaluation of 6-substituted purine L-ribonucleosides. *Bioorg. Med. Chem. Lett.* **2006**, *16*, 5290-5293.
- (26) Naus, P.; Kuchar, M.; Hocek, M. Cytostatic and antiviral 6-arylpurine ribonucleosides IX. Synthesis and evaluation of 6-substituted 3-deazapurine ribonucleosides. *Collect. Czech. Chem. Commun.* **2008**, *73*, 665-678.
- (27) Wang, D. C.; Niu, H. Y.; Qu, G. R.; Liang, L.; Wei, X. J.; Zhang, Y.; Guo, H. M. Nickel-catalyzed Negishi cross-couplings of 6-chloropurines with organozinc halides at room temperature. *Org. Biomol. Chem.* **2011**, *9*, 7663-7666.
- (28) Čapek, P.; Vrábek, M.; Hasník, Z.; Pohl, R.; Hocek, M. Aqueous-phase Suzuki-Miyaura cross-coupling reactions of free halopurine bases. *Synthesis* **2006**, 3515-3526.
- (29) Suzuki, A. Cross-coupling reactions of organoboranes: an easy way to construct C-C bonds (Nobel Lecture). *Angew. Chem. Int. Edit.* **2011**, *50*, 6722-6737.

- (30) Netherton, M. R.; Fu, G. C. Air-stable trialkylphosphonium salts: Simple, practical, and versatile replacements for air-sensitive trialkylphosphines. Applications in stoichiometric and catalytic processes. *Org. Lett.* **2001**, *3*, 4295-4298.
- (31) Kudo, N.; Perseghini, M.; Fu, G. C. A versatile method for Suzuki cross-coupling reactions of nitrogen heterocycles. *Angew. Chem. Int. Edit.* **2006**, *45*, 1282-1284.
- (32) Luebke, R.; Belmabkhout, Y.; Weselinski, L. J.; Cairns, A. J.; Alkordi, M.; Norton, G.; Wojtas, L.; Adil, K.; Eddaoudi, M. Versatile rare earth hexanuclear clusters for the design and synthesis of highly-connected ftw-MOFs. *Chem. Sci.* **2015**, *6*, 4095-4102.
- (33) Magano, J.; Monfette, S. Development of an air-stable, broadly applicable nickel source for nickel-catalyzed cross-coupling. *ACS Catalysis* **2015**, *5*, 3120-3123.
- (34) Krenitsky, T. A.; Rideout, J. L.; Chao, E. Y.; Koszalka, G. W.; Gurney, F.; Crouch, R. C.; Cohn, N. K.; Wolberg, G.; Vinegar, R. Imidazo[4,5-c]pyridines (3-deazapurines) and their nucleosides as immunosuppressive and antiinflammatory agents. *J. Med. Chem.* **1986**, *29*, 138-143.
- (35) Su, M.; Hoshiya, N.; Buchwald, S. L. Palladium-catalyzed amination of unprotected five-membered heterocyclic bromides. *Org. Lett.* **2014**, *16*, 832-835.
- (36) Lougiakis, N.; Gavriil, E. S.; Kairis, M.; Sioupouli, G.; Lambrinidis, G.; Benaki, D.; Kryptou, E.; Mikros, E.; Marakos, P.; Pouli, N.; Diallinas, G. Design and synthesis of purine analogues as highly specific ligands for FcyB, a ubiquitous fungal nucleobase transporter. *Bioorg. Med. Chem.* **2016**, *24*, 5941-5952.
- (37) Chida, N.; Suzuki, T.; Tanaka, S.; Yamada, I. Pd-Catalyzed coupling reaction of glycosylamines with 6-chloropurines: Synthesis of 6-(beta-D-mannopyranosylamino)-9H-purine and its beta-D-glucosyl isomer, N-glycoside models for spicamycin and septacidin. *Tetrahedron Lett.* **1999**, *40*, 2573-2576.
- (38) De Riccardis, F.; Johnson, F. Chemical synthesis of cross-linked purine nucleosides. *Org. Lett.* **2000**, *2*, 293-295.
- (39) Lakshman, M. K. Palladium-catalyzed C–N and C–C cross-couplings as versatile, new avenues for modifications of purine 2'-deoxynucleosides. *J. Organomet. Chem.* **2002**, *653*, 234-251.
- (40) Surry, D. S.; Buchwald, S. L. Dialkylbiaryl phosphines in Pd-catalyzed amination: A user's guide. *Chem. Sci.* **2011**, *2*, 27-50.
- (41) Maiti, D.; Fors, B. P.; Henderson, J. L.; Nakamura, Y.; Buchwald, S. L. Palladium-catalyzed coupling of functionalized primary and secondary amines with aryl and heteroaryl halides: Two ligands suffice in most cases. *Chem. Sci.* **2011**, *2*, 57-68.
- (42) Tichy, M.; Pohl, R.; Xu, H. Y.; Chen, Y. L.; Yokokawa, F.; Shi, P. Y.; Hocek, M. Synthesis and antiviral activity of 4,6-disubstituted pyrimido[4,5-b]indole ribonucleosides. *Bioorg. Med. Chem.* **2012**, *20*, 6123-6133.
- (43) Borchardt, A.; Davis, R.; Noble, S. A. Heterocyclic inhibitors of histamine receptors for the treatment of disease. World Pat. Appl. 2011112766A3, 2011.
- (44) Molander, G. A.; Yun, C. S. Cross-coupling reactions of primary alkylboronic acids with aryl triflates and aryl halides. *Tetrahedron* **2002**, *58*, 1465-1470.
- (45) Niu, C. S.; Li, J.; Doyle, T. W.; Chen, S. H. Synthesis of 3-aminopyridine-2-carboxaldehyde thiosemicarbazone (3-AP). *Tetrahedron* **1998**, *54*, 6311-6318.



- (46) Hirota, K.; Kitade, Y.; Kanbe, Y.; Maki, Y. Convenient method for the synthesis of C-alkylated purine nucleosides: Palladium-catalyzed cross-coupling reaction of halogenopurine nucleosides with trialkylaluminums. *J. Org. Chem.* **1992**, *57*, 5268-5270.
- (47) King, A. O.; Okukado, N.; Negishi, E. I. Highly general stereo-, regio-, and chemo-selective synthesis of terminal and internal conjugated enynes by Pd-catalysed reaction of alkynylzinc reagents with alkenyl halides. *J. Chem. Soc., Chem. Commun.* **1977**, 683-684.
- (48) Everson, D. A.; Jones, B. A.; Weix, D. J. Replacing conventional carbon nucleophiles with electrophiles: Nickel-catalyzed reductive alkylation of aryl bromides and chlorides. *J. Am. Chem. Soc.* **2012**, *134*, 6146-6159.
- (49) Sanderson, J. N.; Dominey, A. P.; Percy, J. M. Iron-catalyzed isopropylation of electron-deficient aryl and heteroaryl chlorides. *Adv. Synth. Catal.* **2017**, *359*, 1007-1017.
- (50) McCann, L. C.; Organ, M. G. On the remarkably different role of salt in the cross-coupling of arylzincs from that seen with alkylzincs. *Angew. Chem. Int. Edit.* **2014**, *53*, 4386-4389.
- (51) Hunter, H. N.; Hadei, N.; Blagojevic, V.; Patschinski, P.; Achonduh, G. T.; Avola, S.; Bohme, D. K.; Organ, M. G. Identification of a higher-order organozincate intermediate involved in Negishi cross-coupling reactions by mass spectrometry and NMR spectroscopy. *Chem. Eur. J.* **2011**, *17*, 7845-7851.
- (52) Seiple, I. B.; Su, S.; Young, I. S.; Nakamura, A.; Yamaguchi, J.; Jorgensen, L.; Rodriguez, R. A.; O'Malley, D. P.; Gaich, T.; Kock, M.; Baran, P. S. Enantioselective total syntheses of (-)-palau'amine, (-)-axinellamines, and (-)-massadines. *J. Am. Chem. Soc.* **2011**, *133*, 14710-14726.
- (53) Arico, J. W.; Calhoun, A. K.; Salandria, K. J.; McLaughlin, L. W. Tetramethylsuccinimide as a directing/protecting group in purine glycosylations. *Org. Lett.* **2010**, *12*, 120-122.
- (54) Casimiro-Garcia, A.; Heemstra, R. J.; Bigge, C. F.; Chen, J.; Ciske, F. A.; Davis, J. A.; Ellis, T.; Esmacil, N.; Flynn, D.; Han, S.; Jalaie, M.; Ohren, J. F.; Powell, N. A. Design, synthesis, and evaluation of imidazo[4,5-c]pyridin-4-one derivatives with dual activity at angiotensin II type 1 receptor and peroxisome proliferator-activated receptor-gamma. *Bioorg. Med. Chem. Lett.* **2013**, *23*, 767-772.
- (55) Bae, S.; Lakshman, M. K. Synthetic utility of an isolable nucleoside phosphonium salt. *Org. Lett.* **2008**, *10*, 2203-2206.
- (56) Kodra, J. T.; Benner, S. A. Synthesis of an N-alkyl derivative of 2'-deoxyisoguanosine. *Synlett* **1997**, 939-940.
- (57) Gottlieb, H. E.; Kotlyar, V.; Nudelman, A. NMR chemical shifts of common laboratory solvents as trace impurities. *J. Org. Chem.* **1997**, *62*, 7512-7515.
- (58) Luo, X. C.; Zhang, H.; Duan, H.; Liu, O.; Zhu, W.; Zhang, T.; Lei, A. Superior effect of a pi-acceptor ligand (Phosphine-electron-deficient olefin ligand) in the Negishi coupling involving alkylzinc reagents. *Org. Lett.* **2007**, *9*, 4571-4574.
- (59) Whitesides, G. M.; Hackett, M.; Brainard, R. L.; Lavalleye, J. P. P. M.; Sowinski, A. F.; Izumi, A. N.; Moore, S. S.; Brown, D. W.; Staudt, E. M. Suppression of unwanted heterogeneous platinum(0)-catalyzed reactions by poisoning with mercury(0) in systems involving competing homogeneous reactions of soluble organoplatinum compounds: Thermal-decomposition of bis(triethylphosphine)-3,3,4,4-tetramethylplatinacyclopentane. *Organometallics* **1985**, *4*, 1819-1830.

(60) Gahlon, H. L.; Sturla, S. J. Hydrogen bonding or stacking interactions in differentiating duplex stability in oligonucleotides containing synthetic nucleoside probes for alkylated DNA. *Chem. Eur. J.* **2013**, *19*, 11062-11067

## Appendix A Supporting Info for Chapter 2

Multicolor GLUT5-Permeable Fluorescent Probes for Fructose Transport Analysis

### A.1 Supplementary Tables and Figures

**Table A1.** Spectroscopic properties of ManCous.

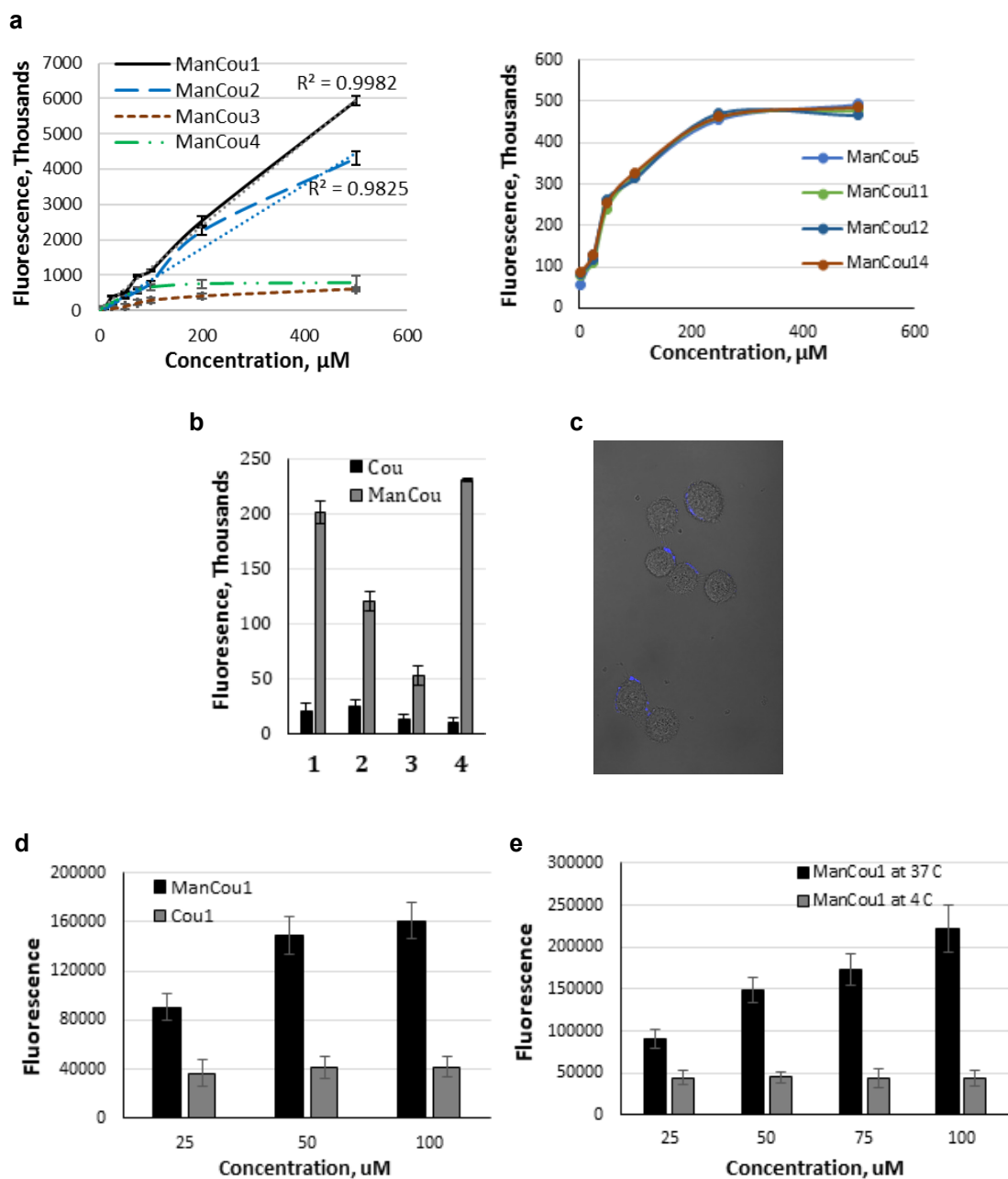
ManCou	Absorbance, <sup>a</sup> $\lambda_{\max}$ , nm	Fluorescence, <sup>a</sup> $\lambda_{\max}$ , nm	Stock Shift, nm	Absolute Quantum Yield, <sup>b</sup> $\Phi_F$
1	366	452	86	0.26
2	360	461	101	0.30
3	387	508	121	0.1
4	376	506	130	0.44
5	398	558	160	0.09
6	371	538	167	0.21
7	365	460	95	0.37
8	384	459	75	0.08
9	430	481	51	0.27
10	382	564	182	0.06
11	385	549	164	0.22
12	383	554	171	0.12
13 (2-furyl)	368	531	163	0.29
14 (2-pyridyl)	374	535	161	0.21

<sup>a</sup>All data measured in water/ethanol (70:30 v/v) mixture. <sup>b</sup>Absolute quantum yield was derived with respect to the anthracene as fluorescence standard.

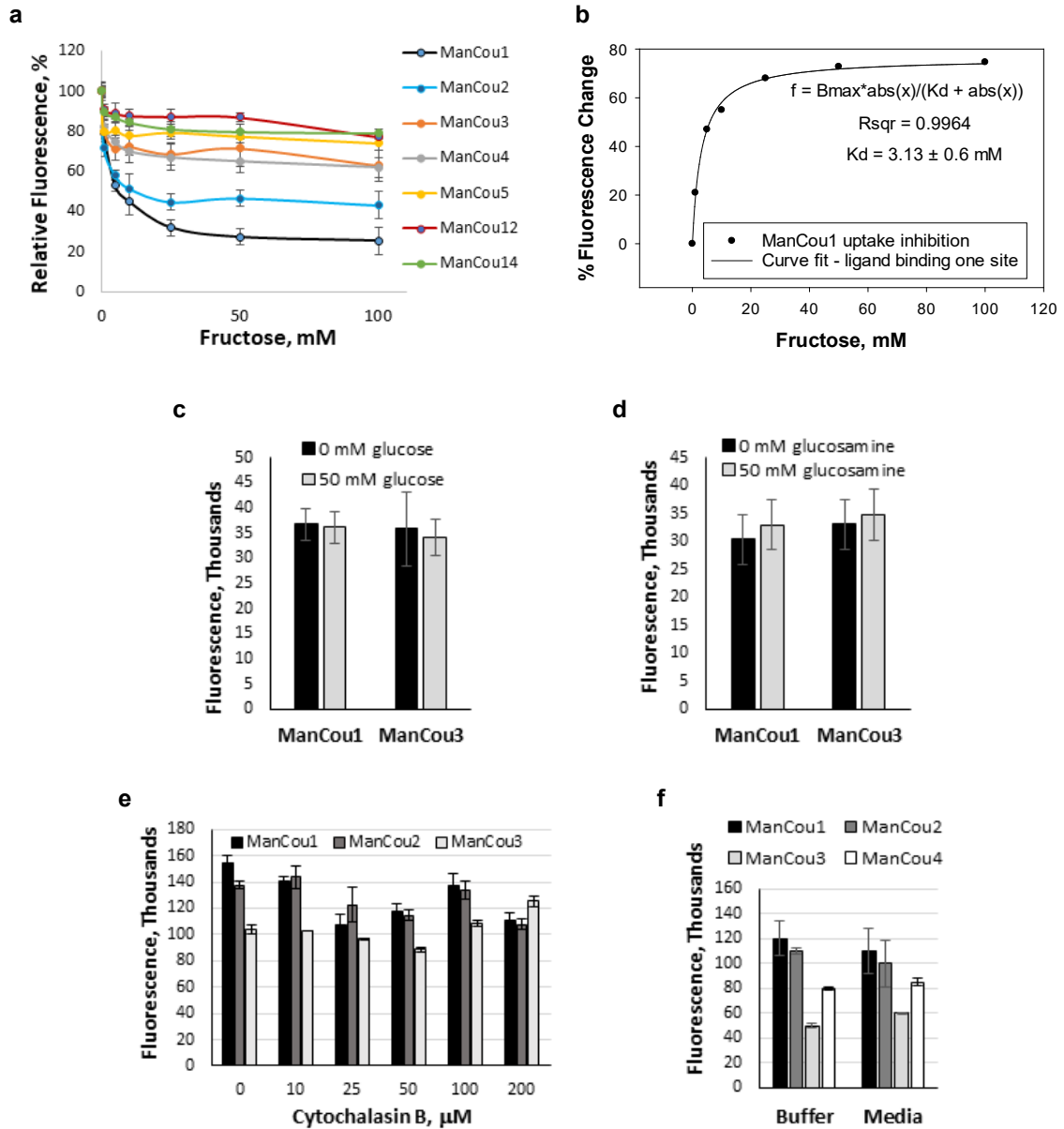
**Table A2.** Comparative analysis of UV  $\lambda_{\text{max}}$  and HOMO/LUMO contribution for selected C4-substituted Cou and ManCou.<sup>a</sup>

ManCou	UV, $\lambda_{\text{max}}$ , nm	HOMO/LUMO <sup>b</sup>	$\Delta_{ \text{HOMO/LUMO} }$	Cou	UV, $\lambda_{\text{max}}$ , nm	HOMO/LUMO	$\Delta_{ \text{HOMO/LUMO} }$
<b>1</b>	366	-445/-186	259	<b>1</b>	352	-459/-190	269
<b>2</b>	360	-440/-177	263	<b>2</b>	347	-453/-180	273
<b>3</b>	387	-468/-232	236	<b>3</b>	372	-486/-253	233
<b>4</b>	376	-441/-193	248	<b>4</b>	358	-453/-196	257
<b>5</b>	398	-467/-217	250	<b>5</b>	377	-482/-223	259
<b>13</b>	374	-438/-209	219	<b>13</b>	366	-449/-213	236

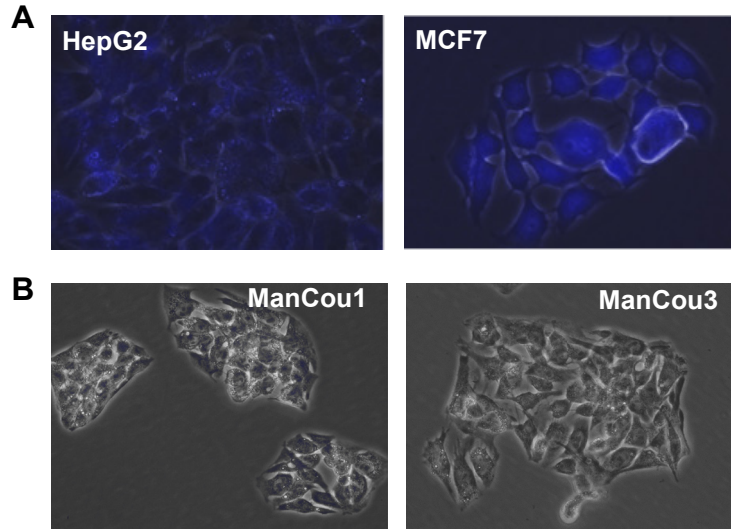
<sup>a</sup>Data provided for probes showing the uptake through GLUT5; <sup>b</sup>HOMO/LUMO orbital energies were calculated with Spartan '14 V1.1.2 (Wavefunction Inc.) using Density Functional, BLYP, 6-31G\*



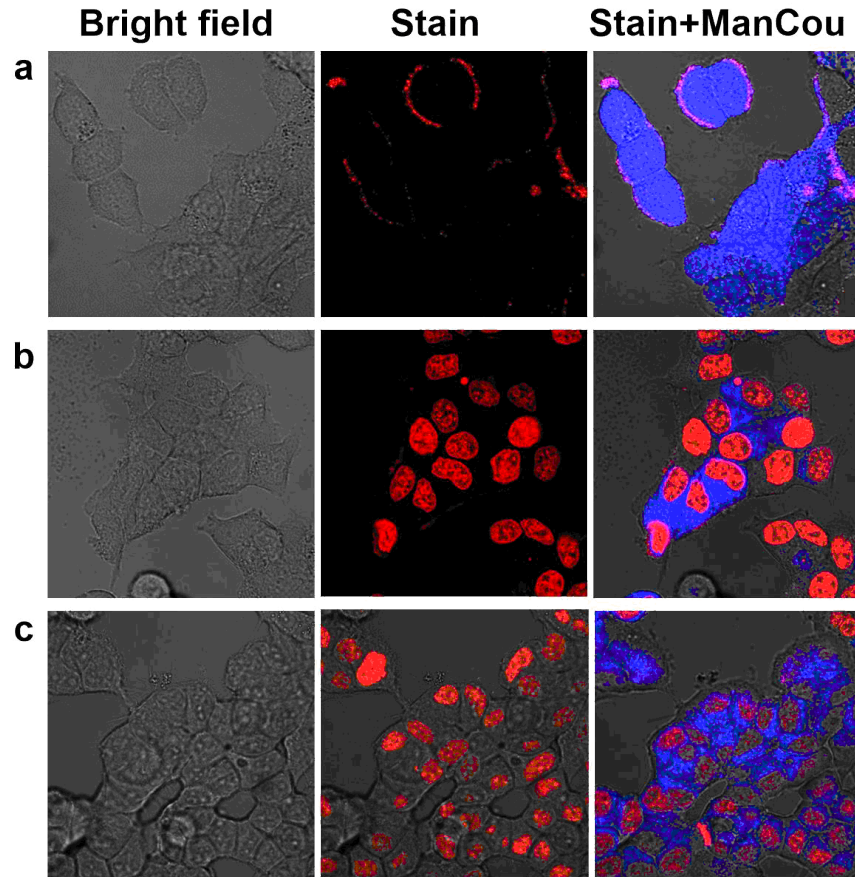
**Figure A1.** ManCous uptake analysis. a) Concentration-dependent uptake of ManCous at 37 °C; b) Comparative uptake of ManCous vs. corresponding coumarins (Cou) at 20  $\mu\text{M}$  concentration (37 °C); c) Z-stack imaged of MCF7 cells treated with 7-aminocoumarin (Cou1) at 37 °C; d) Comparative analysis of ManCou1 vs. Cou1 uptake at varied concentrations (37 °C); e) Comparative analysis of ManCou1 uptake at 37 °C vs. 4 °C. All uptake data are measured in triplicates in 96-well plate after 10 min incubation of cells, removal of the probe and repeated cell wash. Data represents the Gained Fluorescence (exc. 385 nm) measured for 20  $\mu\text{M}$  solutions of probes. Confocal images obtained with 60X objective using exc/em 405 nm/461 nm.



**Figure A2.** Analysis of ManCou uptake in the presence of fructose (a and b); glucose (c); glucosamine (d); cytochalasin B (e); and culture media (f). All data obtained in triplicates. Data collected for 20  $\mu\text{M}$  ManCou probe. Plots represents average data, error bars represent standard deviation. Data are collected after 10 min incubation of cells with ManCou in 96-well plates, removal of the probe, and cell wash (exc. 360 nm, em. 430 nm for ManCous 1 and 2, and em. 500 nm for ManCou3 and 4).

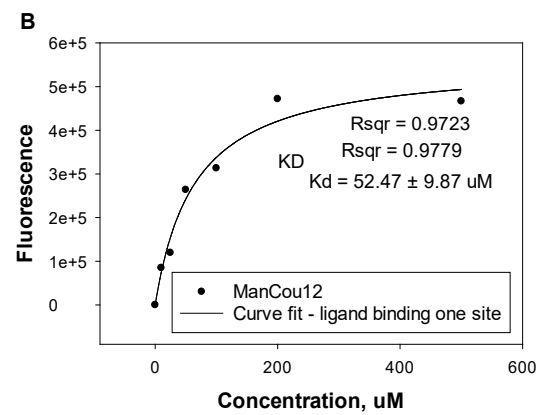
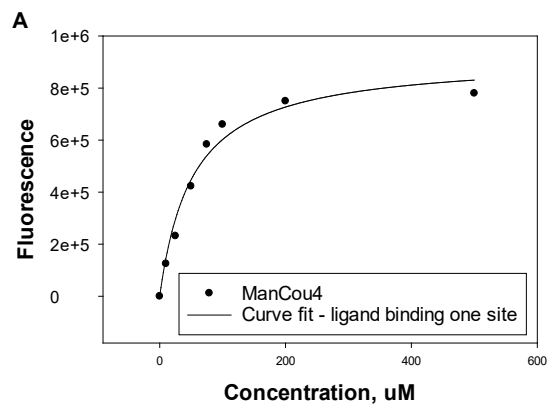


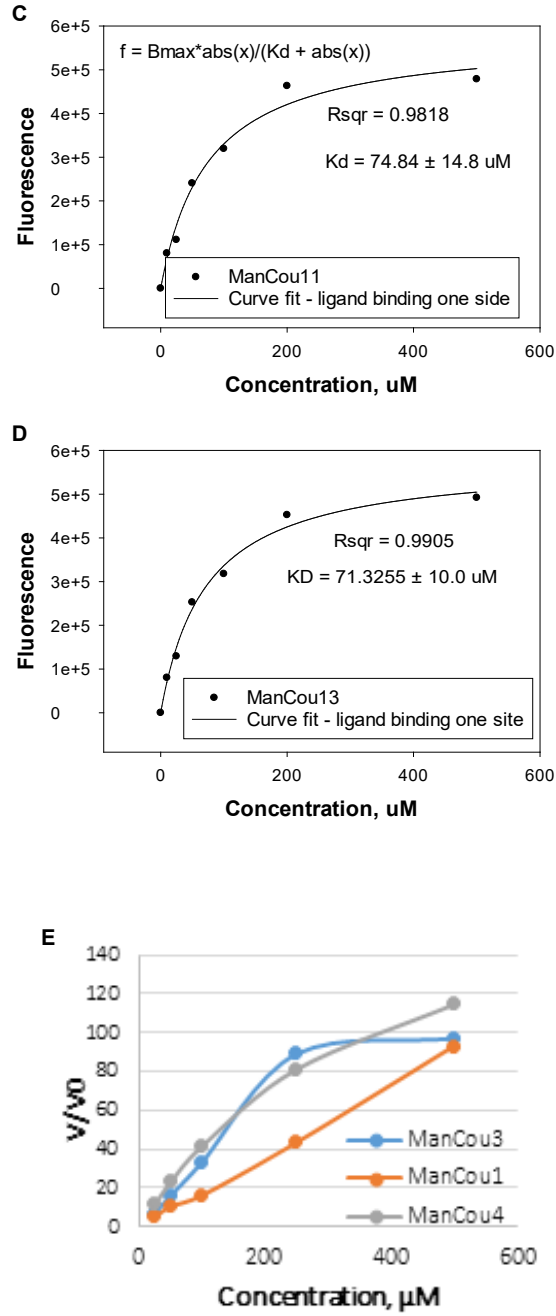
**Figure A3.** Blight-field and fluorescence overlay images of ManCou-treated cells: A) Images of HepG2 and MCF7 cells treated with 20  $\mu$ m ManCou1 (40X objective); B) Z-stack images of HepG2 cells treated with ManCou1 and ManCou3 (20X objective). Images taken with EVOS optical microscope, exc/em 405 nm/461 nm.



**Figure A4.** Fluorescence confocal Z-stack images of MCF7 cells treated with ManCous and established stains. a) ManCou1 with DID membrane staining; b) ManCou3 with RedDot nuclear staining; c) ManCou4 with RedDot nuclear staining. ManCous imaged under exc/em 405 nm/425-525 nm; RedDot and DID imaged under exc/em 635/ 655-755 nm. Images taken with 60X objective.







**Figure A5.** GLUT5-ManCou uptake analysis. A-D) Binding affinity. Data derived after fitting the concentration-dependent change in fluorescence into the ligand binding (one site) curve (SigmaPlot 13). The  $K_d$  values are calculated from the  $f = a/(1+\exp(-(x-x_0)/b))$ . E) Kinetic analysis of uptake.

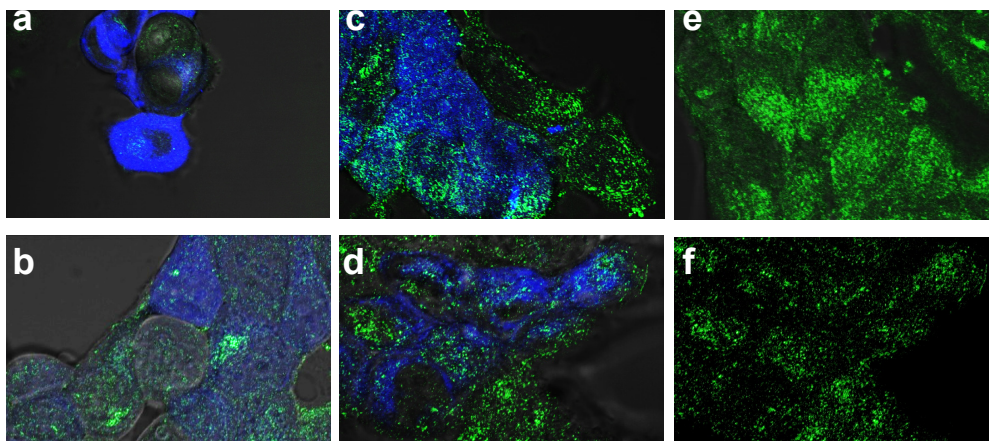


Figure S6. ManCous as competitors for NBDM and NBDG uptake in MCF7 cells (Confocal, Z-stack images). a) equimolar NBDM and ManCou3; b) equimolar NBDM and ManCou1; c) Equimolar ManCou1 and NBDG; d) Equimolar ManCou3 and NBDG; e) NBDM; f) NBDG. Z-stack images taken after 10 min treatment and cell wash. Cells imaged with 60X objective using exc/em. 405 nm/425-525 nm for ManCous, and exc/em 450 nm/565 nm for NBDM and NBDG (eGFP, green fluorescence). All images obtained at the same laser intensity and exposure time.

## A.2 Materials and Methods

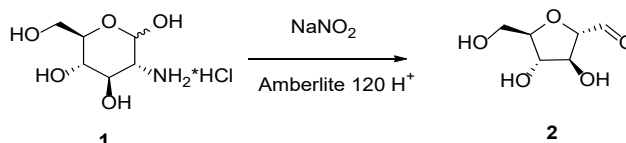
All reagents were used as received unless otherwise stated from Sigma-Aldrich, TCI America, Alfa Aesar, Ark Pharm, AK Scientific, Combi-Blocks or Chem-Impex International. Commercially available coumarins were purchased from: 7-amino-4-methylcoumarin (**Cou2**), Sigma-Aldrich; 7-amino-4-(trifluoromethyl)coumarin (**Cou3**), Alfa Aesar; 2-(7-amino-2-oxo-2*H*-chromen-4-yl)acetic acid (**Cou7**), Ark

Pharm; 6-amino-2*H*-chromen-2-one (**Cou8**), Enamine; 7-(diethylamino)-2-oxo-2*H*-chromene-3-carboxylic acid (**Cou9**), Combi-Blocks. *N,N*-Dimethylformamide (DMF) was dried and stored over CaH<sub>2</sub> before use. Dry tetrahydrofuran was dispensed from an automated Innovative Technology Pure-Solv 400 Solvent Purification System. Analytical TLC was carried out on commercial SiliCycle SiliaPlate® 0.2 mm F254 plates. Preparative silica chromatography was performed using SiliCycle SiliaFlash® F60 40-63 μm (230-400 mesh). Final purification of compounds was achieved with Agilent-1200 HPLC (high-pressure liquid chromatography) using reversed phase semi-preparative column (Phenomenex® Luna® 10 μm C18(2) 100 Å, LC Column 100 x 10 mm, Ea). <sup>1</sup>H and <sup>13</sup>C NMR spectra were recorded at room temperature with a Varian Unity Inova 400 MHz spectrometer. CD<sub>3</sub>OD, DMSO-d<sub>6</sub>, and D<sub>2</sub>O were used as solvents and referenced to the corresponding residual solvent peaks (3.31 and 49.0 ppm for CD<sub>3</sub>OD, respectively; 2.50 and 39.52 ppm for DMSO-d<sub>6</sub>, respectively; 4.79 ppm for D<sub>2</sub>O).<sup>1</sup> The following abbreviations are used to indicate the multiplicity: s - singlet; d - doublet; t - triplet; q - quartet; m - multiplet; b - broad signal; app - approximate. The coupling constants are expressed in Hertz (Hz). The high-resolution (HR) MS data (ESI) were obtained using a Thermo Fisher Orbitrap Elite™ Hybrid Ion Trap-Orbitrap Mass Spectrometer at Chemical Advanced Resolution Methods (ChARM) Laboratory at Michigan Technological University. UV-vis spectra were recorded on a Cary 100 Bio-spectrophotometer from Agilent Technologies. Fluorescence spectra were obtained with FluoroMax-4 spectrophotometer. 96-well plate analysis of cell fluorescence was carried out with Victor3 fluorescence plate reader (excitation at 385 nm). Confocal images were taken with Olympus FluoView™ FV1000 using the FluoView software. Fluorescence imaging was done with EVOS FLAuto inverted microscope.

RPMI-1640, Penicillin/Streptomycin, FBS (Fetal Bovine Serum), 25% Trypsin-EDTA (1X), and PBS (phosphate buffered saline solution) were purchased from Life Technologies, USA. MEM Non-Essential Amino Acids 100X were purchased

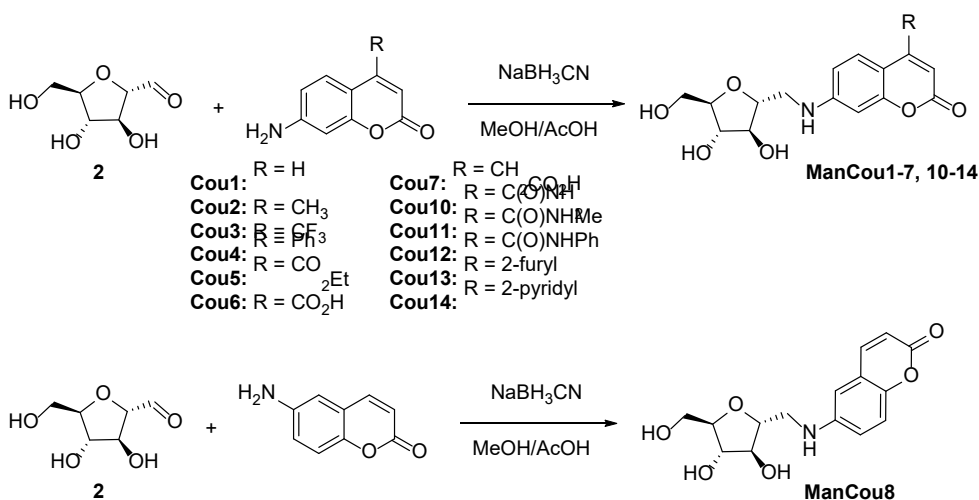
from Quality Biological, USA. Sterile DMSO (25-950-CQC, 250mL) was purchased from Sigma. MCF7 and Hep G2 cells were purchased from ATCC, USA and cultured according to the suggested growth methods.

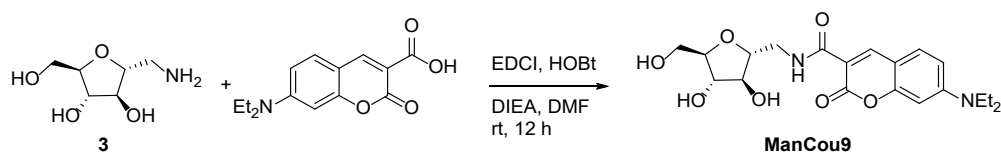
### A.3 Synthesis of ManCous 1-14



**Scheme A1:** Synthesis of 2,5-anhydro-2-carbaldehyde-D-mannitol **2**.

**(2S,3S,4S,5R)-3,4-dihydroxy-5-(hydroxymethyl)tetrahydrofuran-2-carbaldehyde (2):**<sup>2</sup> D-Glucosamine hydrochloride **1** (4.00 g, 18.5 mmol) was dissolved in water (100 ml) and stirred at room temperature for 5 h. Sodium nitrite (3.19 g, 45.3 mmol) was then added, followed by cautious addition of Amberlite 120 H<sup>+</sup> resin (90 g) by portion, maintaining the temperature of ice bath for 4 h. After the reaction, the resin was removed by filtration and the solution was then neutralized by adding sodium carbonate. The remaining solution was vacuum dried and then methanol was added to the residue to precipitate the inorganic salts. After removing the salts by filtration, the solution was vacuum dried to get the compound **2** as a yellow sticky solid (2.49 g, 70%) that was used directly without further purification.





**Scheme A2:** Synthesis of **ManCous1-14**.

**General procedure for the synthesis of ManCous1-8, 10-14:**<sup>3</sup> Typically, (2*S*,3*S*,4*S*,5*R*)-3,4-dihydroxy-5-(hydroxymethyl)tetrahydrofuran-2-carbaldehyde<sup>2</sup> (up to 1 mmol) and the corresponding coumarin (0.8 equiv.) were dissolved in methanol (10 ml). AcOH (1 ml) was used to adjust the pH to <6, followed by portionwise addition of NaBH<sub>3</sub>CN to the reaction mixture (3 X 0.8 equiv, every 20-30 minutes). Water could also be added to improve solubility of some coumarin substrates (up to 20% v/v). The solutions were stirred at room temperature for up to 24 h. The mixtures were then concentrated to dryness under reduced pressure and purified by column chromatography on silica gel using CH<sub>2</sub>Cl<sub>2</sub> : MeOH (up to 90 : 10), EtOAc : MeOH (up to 80 : 20) or water : isopropanol : EtOAc (1 : 2 : 7 up to 2 : 4 : 4) mixtures. The final purification was achieved by semi-preparative HPLC using water-acetonitrile gradient starting with 2-20% acetonitrile to obtain the final products as yellow solids or semi-solids, 10-30 mg samples. No attempts were made to optimize the yields of the products, which could be estimated as 30-40% average. The composition and purity of the final products was confirmed by HRMS, <sup>1</sup>H NMR, and <sup>13</sup>C NMR.

**7-(((2*R*,3*S*,4*S*,5*R*)-3,4-Dihydroxy-5-(hydroxymethyl)tetrahydrofuran-2-yl)methyl)amino)-2*H*-chromen-2-one (ManCou1):** <sup>1</sup>H NMR (400 MHz, CD<sub>3</sub>OD): δ, 7.76-7.36 (d, *J* = 9.2, 1H), 7.32-7.30 (d, *J* = 8.4, 1H), 6.68-6.65 (dd, *J*<sub>1</sub> = 2.4, *J*<sub>2</sub> = 8.4, 1H), 6.53 (d, *J* = 2.4, 1H), 6.01-5.99 (d, *J* = 9.2, 1H), 4.02-3.98 (m, 2H), 3.95-3.92 (m, 1H), 3.88-3.85 (m, 1H), 3.73-3.69 (app dd, *J*<sub>1</sub> = 3.2, *J*<sub>2</sub> = 12.0, 1H), 3.66-3.61 (app dd, *J*<sub>1</sub> = 5.6, *J*<sub>2</sub> = 12.0, 1H), 3.48-3.44 (app dd, *J*<sub>1</sub> = 3.6, *J*<sub>2</sub> = 13.6, 1H), 3.38-3.32 (app dd, *J*<sub>1</sub> = 6.8, *J*<sub>2</sub> = 13.6, 1H) ppm. <sup>13</sup>C NMR (100 MHz, CD<sub>3</sub>OD): δ, 164.7, 158.1, 154.5, 146.5, 130.2, 112.3, 110.6, 109.1, 98.0, 85.3, 83.2, 80.3, 78.9, 63.3, 46.2 ppm. HRMS (ESI): *m/z* [M + Na]<sup>+</sup> calcd for C<sub>15</sub>H<sub>17</sub>NNaO<sub>6</sub>: 330.09539; found 330.09434.

**7-(((2*R*,3*S*,4*S*,5*R*)-3,4-Dihydroxy-5-(hydroxymethyl)tetrahydrofuran-2-yl)methyl)amino)-4-methyl-2*H*-chromen-2-one (ManCou2):** <sup>1</sup>H NMR (400 MHz, CD<sub>3</sub>OD): δ, 7.48-7.45 (dd, *J*<sub>1</sub> = 3.2, *J*<sub>2</sub> = 8.8, 1H), 6.71-6.67 (dt, *J*<sub>1</sub> = 2.4, *J*<sub>2</sub> = 8.8, 1H), 6.52-6.51 (t, *J* = 2.4, 1H), 5.93 (m, 1H), 4.02-3.98 (m, 2H), 3.96-3.93 (m, 1H), 3.88-3.85 (m, 1H), 3.73-3.69 (app dd, *J*<sub>1</sub> = 3.6, *J*<sub>2</sub> = 11.6, 1H), 3.66-3.61 (app dd, *J*<sub>1</sub> = 5.6, *J*<sub>2</sub> = 12.0, 1H), 3.48-3.43 (app dd, *J*<sub>1</sub> = 3.6, *J*<sub>2</sub> = 13.6, 1H), 3.37-3.32 (app dd, *J*<sub>1</sub> = 6.8, *J*<sub>2</sub> = 13.6, 1H), 2.38 (d, *J* = 0.8, 3H) ppm. <sup>13</sup>C NMR (100 MHz, CD<sub>3</sub>OD): δ, 164.7,

157.3, 156.5, 154.4, 126.9, 112.1, 111.1, 108.6, 98.2, 85.3, 83.2, 80.3, 78.9, 63.3, 46.2, 18.5 ppm. HRMS (ESI):  $m/z$  [M + Na]<sup>+</sup> calcd for C<sub>16</sub>H<sub>19</sub>NNaO<sub>6</sub>: 344.11104; found 344.11043.

**7-(((2R,3S,4S,5R)-3,4-Dihydroxy-5-(hydroxymethyl)tetrahydrofuran-2-yl)methylamino)-4-(trifluoromethyl)-2H-chromen-2-one (ManCou3):** <sup>1</sup>H NMR (400 MHz, CD<sub>3</sub>OD): δ, 7.44-7.41 (dd,  $J_1 = 2.0$ ,  $J_2 = 9.2$ , 1H), 6.74-6.71 (dt,  $J_1 = 2.4$ ,  $J_2 = 9.2$ , 1H), 6.60-6.59 (d,  $J = 2.4$ , 1H), 6.37 (s, 1H), 4.02-3.98 (m, 2H), 3.95-3.92 (m, 1H), 3.89-3.85 (m, 1H), 3.73-3.69 (app dd,  $J_1 = 3.6$ ,  $J_2 = 11.6$ , 1H), 3.66-3.61 (app dd,  $J_1 = 5.6$ ,  $J_2 = 12.0$ , 1H), 3.50-3.46 (app dd,  $J_1 = 3.6$ ,  $J_2 = 14.0$ , 1H), 3.40-3.35 (app dd,  $J_1 = 6.4$ ,  $J_2 = 13.6$ , 1H) ppm. <sup>13</sup>C NMR (100 MHz, CD<sub>3</sub>OD): δ, 162.2, 158.6, 155.0, 143.3, 143.0, 124.8, 122.1, 112.8, 108.3, 104.1, 98.5, 85.4, 83.2, 80.2, 78.8, 63.3, 46.1 ppm. HRMS (ESI):  $m/z$  [M + H]<sup>+</sup> calcd for C<sub>16</sub>H<sub>17</sub>F<sub>3</sub>NO<sub>6</sub>: 376.10082; found 376.09955.

**7-(((2R,3S,4S,5R)-3,4-Dihydroxy-5-(hydroxymethyl)tetrahydrofuran-2-yl)methylamino)-4-phenyl-2H-chromen-2-one (ManCou4):** <sup>1</sup>H NMR (400 MHz, CD<sub>3</sub>OD): δ, 7.50-7.48 (m, 3H), 7.42-7.39 (m, 2H), 7.15-7.13 (d,  $J = 8.8$ , 1H), 6.59-6.56 (m, 2H), 5.90 (s, 1H), 4.03-3.99 (m, 2H), 3.97-3.94 (m, 1H), 3.90-3.86 (m, 1H), 3.74-3.70 (app dd,  $J_1 = 3.6$ ,  $J_2 = 11.6$ , 1H), 3.66-3.61 (app dd,  $J_1 = 5.6$ ,  $J_2 = 12.0$ , 1H), 3.47-3.43 (app dd,  $J_1 = 3.6$ ,  $J_2 = 14.0$ , 1H), 3.37-3.32 (app dd,  $J_1 = 6.8$ ,  $J_2 = 13.6$ , 1H) ppm. <sup>13</sup>C NMR (100 MHz, CD<sub>3</sub>OD): δ, 164.2, 158.7, 157.9, 154.2, 137.2, 130.4, 129.7, 129.3, 128.8, 112.0, 109.6, 108.2, 98.4, 85.2, 83.1, 80.2, 78.8, 63.2, 46.2 ppm. HRMS (ESI):  $m/z$  [M + Na]<sup>+</sup> calcd for C<sub>21</sub>H<sub>21</sub>NNaO<sub>6</sub>: 406.12669; found 406.12520.

**Ethyl 7-(((2R,3S,4S,5R)-3,4-dihydroxy-5-(hydroxymethyl)tetrahydrofuran-2-yl)methylamino)-2-oxo-2H-chromene-4-carboxylate (ManCou5):** <sup>1</sup>H NMR (400 MHz, CD<sub>3</sub>OD): δ, 7.84-7.82 (d,  $J = 8.8$ , 1H), 6.64-6.61 (dd,  $J_1 = 2.4$ ,  $J_2 = 8.8$ , 1H), 6.49-6.48 (d,  $J = 2.4$ , 1H), 6.36 (s, 1H), 4.43-4.38 (q,  $J = 7.2$ , 2H), 4.03-3.99 (m, 2H), 3.96-3.94 (m, 1H), 3.90-3.86 (m, 1H), 3.74-3.70 (app dd,  $J_1 = 3.6$ ,  $J_2 = 11.6$ , 1H), 3.66-3.62 (app dd,  $J_1 = 5.6$ ,  $J_2 = 12.0$ , 1H), 3.47-3.43 (app dd,  $J_1 = 3.6$ ,  $J_2 = 14.0$ , 1H), 3.38-3.32 (app dd,  $J_1 = 6.8$ ,  $J_2 = 14.0$ , 1H), 1.42-1.38 (t,  $J = 7.2$ , 2H) ppm. <sup>13</sup>C NMR (100 MHz, CD<sub>3</sub>OD): δ, 165.8, 163.6, 158.3, 154.5, 145.3, 128.6, 112.5, 111.0, 106.9, 98.2, 85.3, 83.1, 80.3, 78.8, 63.30, 63.25, 46.1, 14.4 ppm. HRMS (ESI):  $m/z$  [M + H]<sup>+</sup> calcd for C<sub>18</sub>H<sub>22</sub>NO<sub>8</sub>: 380.13458; found 380.13345.

**7-(((2R,3S,4S,5R)-3,4-Dihydroxy-5-(hydroxymethyl)tetrahydrofuran-2-yl)methylamino)-2-oxo-2H-chromene-4-carboxylic acid (ManCou6):** <sup>1</sup>H NMR (400 MHz, D<sub>2</sub>O): δ, 7.47-7.45 (d,  $J = 8.8$ , 1H), 6.73-6.70 (d,  $J = 8.8$ , 1H), 6.53 (s, 1H), 6.07 (m, 1H), 4.07 (bs, 3H), 3.96-3.93 (m, 1H), 3.80-3.76 (app dd,  $J_1 = 3.2$ ,  $J_2 = 12.4$ , 1H), 3.73-3.68 (app dd,  $J_1 = 6.0$ ,  $J_2 = 12.0$ , 1H), 3.48-3.36 (m, 2H) ppm. <sup>13</sup>C NMR (100 MHz, D<sub>2</sub>O): δ, 172.6, 165.9, 156.4, 155.4, 152.8, 127.7, 112.1, 106.7,

103.4, 97.7, 82.7, 81.0, 78.4, 76.8, 61.4, 44.6 ppm. HRMS (ESI):  $m/z$  [M + H]<sup>+</sup> calcd for C<sub>16</sub>H<sub>18</sub>NO<sub>8</sub>: 352.10328; found 352.10300.

**2-(7-(((2R,3S,4S,5R)-3,4-Dihydroxy-5-(hydroxymethyl)tetrahydrofuran-2-yl)methyl)amino)-2-oxo-2H-chromen-4-yl)acetic acid (ManCou7):** <sup>1</sup>H NMR (400 MHz, D<sub>2</sub>O): δ, 7.48-7.45 (d,  $J$  = 8.8, 1H), 6.77-6.74 (dd,  $J_1$  = 2.4,  $J_2$  = 8.8, 1H), 6.59 (d,  $J$  = 2.4, 1H), 6.06 (s, 1H), 4.10 (bs, 2H), 3.98-3.94 (m, 1H), 3.81-3.65 (m, 5H), 3.54-3.46 (m, 2H) ppm. We were not able to obtain satisfactory <sup>13</sup>C NMR data in D<sub>2</sub>O. HRMS (ESI):  $m/z$  [M + H]<sup>+</sup> calcd for C<sub>17</sub>H<sub>20</sub>NO<sub>8</sub>: 366.11893; found 366.11771.

**6-(((2R,3S,4S,5R)-3,4-Dihydroxy-5-(hydroxymethyl)tetrahydrofuran-2-yl)methyl)amino)-2H-chromen-2-one (ManCou8):** <sup>1</sup>H NMR (400 MHz, CD<sub>3</sub>OD): δ, 7.84-7.82 (d,  $J$  = 9.2, 1H), 7.13-7.11 (d,  $J$  = 8.8, 1H), 6.99-6.96 (dd,  $J_1$  = 2.4,  $J_2$  = 9.2, 1H), 6.80-6.79 (d,  $J$  = 2.4, 1H), 6.36-6.33 (d,  $J$  = 9.2, 1H), 4.03-3.96 (m, 3H), 3.89-3.85 (m, 1H), 3.74-3.70 (app dd,  $J_1$  = 3.6,  $J_2$  = 12.0, 1H), 3.66-3.62 (app dd,  $J_1$  = 5.6,  $J_2$  = 11.6, 1H), 3.42-3.38 (app dd,  $J_1$  = 3.6,  $J_2$  = 13.6, 1H), 3.30-3.32 (app dd,  $J_1$  = 6.4,  $J_2$  = 13.6, 1H) ppm. <sup>13</sup>C NMR (100 MHz, CD<sub>3</sub>OD): δ, 163.7, 147.59, 147.56, 146.1, 120.8, 119.9, 118.0, 116.7, 109.4, 85.2, 83.2, 80.4, 78.9, 63.3, 47.3 ppm. HRMS (ESI):  $m/z$  [M + H]<sup>+</sup> calcd for C<sub>15</sub>H<sub>18</sub>NO<sub>6</sub>: 308.11344; found 308.11234.

**7-(Diethylamino)-N-(((2R,3S,4S,5R)-3,4-dihydroxy-5-(hydroxymethyl)tetrahydrofuran-2-yl)methyl)-2-oxo-2H-chromene-3-carboxamide (ManCou9):** This compound was synthesized according to the reported general procedure.<sup>4</sup> To a solution of 1-amino-2,5-anhydro-D-mannitol<sup>2</sup> (100 mg, 0.61 mmol), 7-(diethylamino)-2-oxo-2H-chromene-3-carboxylic acid (120 mg, 0.46 mmol), 1-hydroxybenzotriazole monohydrate (HOBt; 93 mg, 0.69 mmol) and diisopropylethylamine (DIEA; 0.24 ml, 1.4 mmol) in dry DMF (4 ml), *N*-(3-dimethylaminopropyl)-*N'*-ethylcarbodiimide hydrochloride (EDCI; 132 mg, 0.69 mmol) was added and the mixture was stirred at room temperature for 12 h. It was diluted with EtOAc (100 ml), washed with brine (3 X 20 ml), and dried with MgSO<sub>4</sub>. After filtration and concentration, the residue was purified by column chromatography on silica gel, eluting with 0-100% EtOAc in hexanes, followed by 20% MeOH in EtOAc. The final purification was achieved by semi-preparative HPLC using water-acetonitrile gradient starting with 50% acetonitrile. A sample of compound was obtained as a yellow semi-solid (~20 mg). <sup>1</sup>H NMR (400 MHz, CD<sub>3</sub>OD): δ, 8.60 (s, 1H), 7.53-7.51 (d,  $J$  = 9.2, 1H), 6.81-6.78 (dd,  $J_1$  = 2.4,  $J_2$  = 9.2, 1H), 6.54-6.53 (d,  $J$  = 2.4, 1H), 4.04-3.86 (m, 4H), 3.75-3.62 (m, 4H), 3.54-3.49 (q,  $J$  = 7.2, 4H), 1.25-1.21 (t,  $J$  = 7.2, 6H) ppm. <sup>13</sup>C NMR (100 MHz, CD<sub>3</sub>OD): δ, 165.4, 163.8, 159.0, 154.4, 149.2, 132.5, 111.6, 109.9, 109.4, 97.2, 85.0, 82.7, 79.8, 78.4, 63.2, 46.0, 42.3, 12.8 ppm. HRMS (ESI):  $m/z$  [M + H]<sup>+</sup> calcd for C<sub>20</sub>H<sub>27</sub>N<sub>2</sub>O<sub>7</sub>: 407.18187; found 407.18109.



**7-(((2R,3S,4S,5R)-3,4-Dihydroxy-5-(hydroxymethyl)tetrahydrofuran-2-yl)methyl)amino)-2-oxo-2H-chromene-4-carboxamide (ManCou10):** <sup>1</sup>H NMR (400 MHz, CD<sub>3</sub>OD): δ, 7.52-7.50 (d, *J* = 8.8, 1H), 6.70-6.68 (dd, *J*<sub>1</sub> = 2.4, *J*<sub>2</sub> = 8.8, 1H), 6.57-6.56 (d, *J* = 2.4, 1H), 6.08 (s, 1H), 4.02-3.98 (m, 2H), 3.95-3.92 (m, 1H), 3.88-3.84 (m, 1H), 3.73-3.69 (app dd, *J*<sub>1</sub> = 3.6, *J*<sub>2</sub> = 12.0, 1H), 3.65-3.61 (app dd, *J*<sub>1</sub> = 5.6, *J*<sub>2</sub> = 12.0, 1H), 3.49-3.45 (app dd, *J*<sub>1</sub> = 4.0, *J*<sub>2</sub> = 13.6, 1H), 3.39-3.34 (app dd, *J*<sub>1</sub> = 6.4, *J*<sub>2</sub> = 13.6, 1H) ppm. <sup>13</sup>C NMR (100 MHz, CD<sub>3</sub>OD): δ, 170.0, 163.8, 158.3, 154.7, 151.7, 128.2, 112.4, 106.9, 98.2, 85.3, 83.1, 80.2, 78.8, 63.2, 46.2 ppm. HRMS (ESI): *m/z* [M + H]<sup>+</sup> calcd for C<sub>16</sub>H<sub>19</sub>N<sub>2</sub>O<sub>7</sub>: 351.11927; found 351.11826.

**7-(((2R,3S,4S,5R)-3,4-Dihydroxy-5-(hydroxymethyl)tetrahydrofuran-2-yl)methyl)amino)-N-methyl-2-oxo-2H-chromene-4-carboxamide (ManCou11):** <sup>1</sup>H NMR (400 MHz, CD<sub>3</sub>OD): δ, 7.46-7.44 (d, *J* = 8.8, 1H), 6.69-6.66 (dd, *J*<sub>1</sub> = 2.4, *J*<sub>2</sub> = 8.8, 1H), 6.56 (d, *J* = 2.4, 1H), 6.04 (s, 1H), 4.02-3.92 (m, 3H), 3.88-3.84 (m, 1H), 3.73-3.69 (app dd, *J*<sub>1</sub> = 3.6, *J*<sub>2</sub> = 11.6, 1H), 3.65-3.61 (app dd, *J*<sub>1</sub> = 5.6, *J*<sub>2</sub> = 11.6, 1H), 3.49-3.45 (app dd, *J*<sub>1</sub> = 3.6, *J*<sub>2</sub> = 13.6, 1H), 3.39-3.33 (app dd, *J*<sub>1</sub> = 6.4, *J*<sub>2</sub> = 13.6, 1H), 2.92 (s, 3H) ppm. <sup>13</sup>C NMR (100 MHz, CD<sub>3</sub>OD): δ, 168.4, 163.9, 158.4, 154.8, 151.9, 128.3, 112.4, 107.1, 98.3, 85.3, 83.2, 80.3, 78.8, 63.3, 46.2, 26.5 ppm. HRMS (ESI): *m/z* [M + H]<sup>+</sup> calcd for C<sub>17</sub>H<sub>21</sub>N<sub>2</sub>O<sub>7</sub>: 365.13492; found 365.13368.

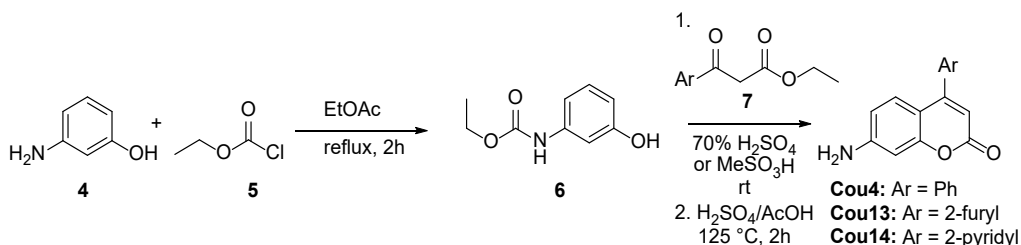
**7-(((2R,3S,4S,5R)-3,4-Dihydroxy-5-(hydroxymethyl)tetrahydrofuran-2-yl)methyl)amino)-2-oxo-N-phenyl-2H-chromene-4-carboxamide (ManCou12):** <sup>1</sup>H NMR (400 MHz, CD<sub>3</sub>OD): δ, 7.70-7.67 (m, 2H), 7.50-7.47 (d, *J* = 9.2, 1H), 7.40-7.35 (m, 2H), 7.21-7.16 (m, 1H), 6.71-6.68 (dd, *J*<sub>1</sub> = 2.4, *J*<sub>2</sub> = 8.8, 1H), 6.59-6.58 (d, *J* = 2.4, 1H), 6.18 (s, 1H), 4.02-3.98 (m, 2H), 3.95-3.93 (app dd, *J*<sub>1</sub> = 5.2, *J*<sub>2</sub> = 6.0, 1H), 3.88-3.85 (m, 1H), 3.73-3.69 (app dd, *J*<sub>1</sub> = 3.6, *J*<sub>2</sub> = 12.0, 1H), 3.65-3.61 (app dd, *J*<sub>1</sub> = 5.6, *J*<sub>2</sub> = 12.0, 1H), 3.50-3.45 (app dd, *J*<sub>1</sub> = 3.6, *J*<sub>2</sub> = 14.0, 1H), 3.40-3.34 (app dd, *J*<sub>1</sub> = 6.8, *J*<sub>2</sub> = 14.0, 1H) ppm. <sup>13</sup>C NMR (100 MHz, CD<sub>3</sub>OD): δ, 165.7, 163.7, 158.3, 154.7, 151.7, 139.0, 129.9, 128.0, 126.0, 121.6, 112.4, 107.01, 106.95, 98.3, 85.3, 83.1, 80.2, 78.8, 63.2, 46.2 ppm. HRMS (ESI): *m/z* [M + H]<sup>+</sup> calcd for C<sub>23</sub>H<sub>23</sub>N<sub>2</sub>O<sub>7</sub>: 427.15057; found 427.15000.

**7-(((2R,3S,4S,5R)-3,4-Dihydroxy-5-(hydroxymethyl)tetrahydrofuran-2-yl)methyl)amino)-4-(furan-2-yl)-2H-chromen-2-one (ManCou13):** <sup>1</sup>H NMR (400 MHz, CD<sub>3</sub>OD): δ, 7.92-7.90 (d, *J* = 8.8, 1H), 7.81-7.80 (dd, *J*<sub>1</sub> = 0.4, *J*<sub>2</sub> = 1.6, 1H), 7.17-7.16 (dd, *J*<sub>1</sub> = 0.4, *J*<sub>2</sub> = 3.6, 1H), 6.70-6.67 (m, 2H), 6.54-6.53 (d, *J* = 2.4, 1H), 6.24 (s, 1H), 4.04-4.00 (m, 2H), 3.97-3.44 (app dd, *J*<sub>1</sub> = 5.2, *J*<sub>2</sub> = 6.0, 1H), 3.90-3.87 (m, 1H), 3.74-3.70 (app dd, *J*<sub>1</sub> = 3.6, *J*<sub>2</sub> = 12.0, 1H), 3.67-3.62 (app dd, *J*<sub>1</sub> = 5.6, *J*<sub>2</sub> = 12.0, 1H), 3.49-3.44 (app dd, *J*<sub>1</sub> = 3.6, *J*<sub>2</sub> = 14.0, 1H), 3.39-3.34 (app dd, *J*<sub>1</sub> = 6.8, *J*<sub>2</sub> = 14.0, 1H) ppm. <sup>13</sup>C NMR (100 MHz, CD<sub>3</sub>OD): δ, 164.5, 158.1, 154.1, 150.2, 146.5, 144.6, 128.4, 115.5, 113.3, 112.3, 107.0, 104.3, 98.5, 85.3, 83.1, 80.2, 78.8, 63.3, 46.2 ppm. HRMS (ESI): *m/z* [M + H]<sup>+</sup> calcd for C<sub>19</sub>H<sub>20</sub>NO<sub>7</sub>: 374.12401; found 374.12338.

**7-((((2R,3S,4S,5R)-3,4-Dihydroxy-5-(hydroxymethyl)tetrahydrofuran-2-yl)methyl)amino)-4-(pyridin-2-yl)-2H-chromen-2-one (ManCou14):** <sup>1</sup>H NMR (400 MHz, CD<sub>3</sub>OD): δ, 8.71-8.69 (ddd,  $J_1 = 1.2$ ,  $J_2 = 1.6$ ,  $J_3 = 5.2$ , 1H), 8.02-7.98 (dt,  $J_1 = 1.6$ ,  $J_2 = 8.0$ , 1H), 7.66-7.64 (d,  $J = 8.0$ , 1H), 7.56-7.53 (ddd,  $J_1 = 0.8$ ,  $J_2 = 5.2$ ,  $J_3 = 8.0$ , 1H), 7.30-7.28 (d,  $J = 8.8$ , 1H), 6.63-6.60 (app dd,  $J_1 = 2.4$ ,  $J_2 = 8.8$ , 1H), 6.59 (d,  $J = 2.4$ , 1H), 6.09 (s, 1H), 4.02-3.99 (m, 2H), 3.96-3.93 (m, 1H), 3.89-3.85 (m, 1H), 3.73-3.69 (app dd,  $J_1 = 3.6$ ,  $J_2 = 12.0$ , 1H), 3.66-3.61 (app dd,  $J_1 = 5.6$ ,  $J_2 = 12.0$ , 1H), 3.48-3.44 (app dd,  $J_1 = 3.6$ ,  $J_2 = 14.0$ , 1H), 3.38-3.33 (app dd,  $J_1 = 6.8$ ,  $J_2 = 14.0$ , 1H) ppm. <sup>13</sup>C NMR (100 MHz, CD<sub>3</sub>OD): δ, 164.0, 158.2, 155.7, 155.6, 154.3, 150.3, 139.0, 128.8, 125.6, 125.5, 112.2, 109.0, 108.8, 98.3, 85.2, 83.1, 80.2, 78.8, 63.2, 46.2 ppm. HRMS (ESI):  $m/z$  [M + H]<sup>+</sup> calcd for C<sub>20</sub>H<sub>21</sub>N<sub>2</sub>O<sub>6</sub>: 385.14000; found 385.13907.

## A.4 Synthesis of Coumarins

7-Aminocoumarin (**Cou1**) was synthesized according to the reported procedure.<sup>5</sup>



**Scheme A3:** Synthesis of C4-aryl coumarins **Cou4** and **Cous13-14**.

**(3-Hydroxyphenyl)carbamic acid ethyl ester (6):**<sup>6</sup> This compound was synthesized according to the reported procedure.<sup>6</sup> 3-Aminophenol **4** (10.0 g, 91.6 mmol) and ethyl acetate (350 ml) were refluxed for 1 hour with vigorous stirring. Ethyl chloroformate **5** (11.92 g, 109.9 mmol) was then added via addition funnel over a 30 minute period. The reaction mixture was refluxed for an additional hour and then allowed to cool to room temperature. Upon cooling a grey/white precipitate formed within the flask. The precipitate was removed via filtration, and washed with ethyl acetate (3 X 150 ml). The combined filtrates were concentrated to afford **6** as a grey solid (9.46 g, 57%) that was used without further purification. <sup>1</sup>H NMR (400 MHz, DMSO-*d*<sub>6</sub>): δ, 9.45 (s, 1H), 9.29 (bs, 1H), 7.04-7.00 (m, 2H), 6.86-6.84 (m, 1H), 6.39-6.36 (ddd,  $J_1 = 1.2$ ,  $J_2 = 2.4$ ,  $J_3 = 8.0$ , 1H), 4.12-4.07 (q,  $J = 7.2$ , 2H), 1.24-1.21 (t,  $J = 7.2$ , 3H) ppm.

**7-Amino-4-phenyl-2H-chromen-2-one (Cou4):**<sup>7</sup> This compound was synthesized according to the reported procedure.<sup>7</sup> **6** (1.00 g, 5.52 mmol) and ethyl benzoylacetate (1.27g, 6.62 mmol) were added to a 100 ml round-bottom flask equipped with a stir bar. 70% H<sub>2</sub>SO<sub>4</sub> (30 ml) was added and the mixture was stirred at room temperature. More 70% H<sub>2</sub>SO<sub>4</sub> was added until the reaction mixture turned from yellow/cloudy to amber/clear and then stirring was maintained overnight at room temperature. The reaction mixture was then poured over 100 ml of crushed ice to give a bright yellow precipitate. The solid was filtered and recrystallized from hot methanol to afford clear large crystals of **Cou4-precursor** (0.717g, 42%). <sup>1</sup>H NMR (400 MHz, DMSO-d<sub>6</sub>): δ, 10.14 (s, 1H), 7.62-7.61 (d, *J* = 2.4, 1H), 7.54-7.48 (m, 5H), 7.36-7.30 (m, 2H), 6.20 (s, 1H), 4.18-4.13 (q, *J* = 7.2, 2H), 1.27-1.24 (t, *J* = 7.2, 3H) ppm.

**Cou4-precursor** (0.408 g, 1.32 mmol) was added to a 50 ml round-bottom flask, followed by H<sub>2</sub>SO<sub>4</sub> conc. (5 ml) and glacial AcOH (5 ml). The reaction mixture was heated to 125 °C for 2 hours under reflux condenser, after which it was cooled to room temperature and poured over 50 ml of crushed ice. The resulting suspension was neutralized till weakly basic using 4M NaOH, affording a yellow precipitate. The precipitate was filtered and recrystallized from hot methanol to give **Cou4** as a fine yellow powder (0.175 g, 56%). <sup>1</sup>H NMR (400 MHz, DMSO-d<sub>6</sub>): δ, 7.54-7.46 (m, 5H), 7.09-7.07 (d, *J* = 8.8, 1H), 6.54-6.51 (app dd, *J*<sub>1</sub> = 2.0, *J*<sub>2</sub> = 8.8, 1H), 6.50 (d, *J* = 2.0, 1H), 6.24 (bs, 2H), 5.90 (s, 1H) ppm. <sup>13</sup>C NMR (100 MHz, DMSO-d<sub>6</sub>): δ, 160.3, 156.0, 155.6, 153.1, 135.5, 129.2, 128.6, 128.1, 127.6, 111.3, 107.2, 107.0, 98.8 ppm. HRMS (ESI): *m/z* [M + H]<sup>+</sup> calcd for C<sub>15</sub>H<sub>12</sub>NO<sub>2</sub>: 238.08681; found 238.08597.

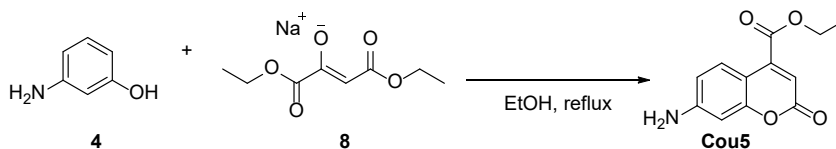
**7-Amino-4-(furan-2-yl)-2H-chromen-2-one (Cou13):** This compound was synthesized according to the reported general procedure.<sup>8</sup> **6** (1.00g, 5.52 mmol) and 3-furan-2-yl-3-oxo-propionic acid ethyl ester (1.27 g, 6.62 mmol) were added to a 50 ml round-bottom flask equipped with a stir bar. Methanesulfonic acid (10 ml) was added and the mixture was stirred at room temperature for overnight while the colour turned from clear/amber to black. The reaction mixture was then poured over 50 ml of ice water. It was then extracted with ethyl acetate (3 X 75 ml), and the combined organics were washed with brine (2 X 50 ml) and dried over Na<sub>2</sub>SO<sub>4</sub>. After filtration and concentration, a brown solid was obtained which was then recrystallized from hot methanol to afford **Cou13-precursor** as grey-black crystals (0.446 g, 27 %). <sup>1</sup>H NMR (400 MHz, DMSO-d<sub>6</sub>): δ, 10.18 (s, 1H), 8.16-8.14 (d, *J* = 8.8, 1H), 8.05-8.04 (d, *J* = 1.6, 1H), 7.59 (d, *J* = 2.0, 1H), 7.47-7.46 (d, *J* = 3.6, 1H), 7.44-7.42 (dd, *J*<sub>1</sub> = 2.0, *J*<sub>2</sub> = 8.8, 1H), 6.80-6.78 (dd, *J*<sub>1</sub> = 1.6, *J*<sub>2</sub> = 3.6, 1H), 6.53 (s, 1H), 4.20-4.14 (q, *J* = 7.2, 2H), 1.28-1.25 (t, *J* = 7.2, 3H) ppm. <sup>13</sup>C NMR (100 MHz, DMSO-d<sub>6</sub>): δ, 159.8, 154.6, 153.1, 147.6, 146.2, 142.8, 140.9, 127.0, 115.3, 114.3, 112.7, 110.0, 107.6, 104.7, 60.7, 14.4 ppm.

**Cou13-precursor** (1.00 g, 3.34 mmol) was added to a 50 ml round-bottom flask, followed by H<sub>2</sub>SO<sub>4</sub> conc. (5 ml) and glacial AcOH (5 ml). The reaction mixture was heated to 125 °C for 2 hours under reflux condenser, after which it was cooled to room temperature and poured over 50 ml of crushed ice. The resulting suspension was neutralized till weakly basic using 4M NaOH, extracted with ethyl acetate (3 X 75 ml) and dried over Na<sub>2</sub>SO<sub>4</sub>. After filtration and concentration, the residue was purified by column chromatography on silica gel (dry loading), eluting with 40-100% EtOAc in hexanes, followed by 5% MeOH in EtOAc. The residue was triturated with hexanes containing little CH<sub>2</sub>Cl<sub>2</sub>. The product was filtered, washed with hexanes and dried in air to obtain **Cou13** as a yellow-brown powder (0.11 g, 14%). <sup>1</sup>H NMR (400 MHz, DMSO-d<sub>6</sub>): δ, 8.02 (s, 1H), 7.92-7.90 (d, *J* = 8.4, 1H), 7.36 (s, 1H), 6.76 (s, 1H), 6.63-6.61 (d, *J* = 8.4, 1H), 6.48 (s, 1H), 6.26 (bs, 2H), 6.24 (s, 1H) ppm. <sup>13</sup>C NMR (100 MHz, DMSO-d<sub>6</sub>): δ, 160.7, 156.4, 153.2, 148.6, 145.9, 142.0, 127.5, 114.7, 112.6, 111.6, 104.6, 103.3, 99.1 ppm. HRMS (ESI): *m/z* [M + H]<sup>+</sup> calcd for C<sub>13</sub>H<sub>10</sub>NO<sub>3</sub>: 228.06608; found 228.06500.

**7-Amino-4-(pyridin-2-yl)-2H-chromen-2-one (Cou14)**: This compound was synthesized according to the reported general procedure.<sup>8</sup> **6** (2.00 g, 11.03 mmol) and ethyl 3-oxo-3-(pyridin-2-yl)propanoate (2.56 g, 13.24 mmol) were added to a 50 ml round-bottom flask with a stir bar. Methanesulfonic acid (10 ml) was added and the mixture was stirred at room temperature for overnight while the colour turned from clear/amber to black. The reaction mixture was then poured over 50 ml of ice water. It was then extracted with ethyl acetate (3 X 75 ml), and the combined organics were washed with brine (2 X 50 ml) and dried over Na<sub>2</sub>SO<sub>4</sub>. After filtration and concentration, a grey solid was obtained which was then recrystallized from hot methanol to afford **Cou14-precursor** as fine white crystals of 1 : 1 MeOH solvate (1.403 g, 41 %). <sup>1</sup>H NMR (400 MHz, DMSO-d<sub>6</sub>): δ, 10.17 (s, 1H), 8.78-8.76 (ddd, *J*<sub>1</sub> = 1.2, *J*<sub>2</sub> = 2.0, *J*<sub>3</sub> = 8.8, 1H), 8.03-8.00 (dt, *J*<sub>1</sub> = 2.0, *J*<sub>2</sub> = 8.0, 1H), 7.77-7.75 (m, 1H), 7.70-7.68 (d, *J* = 8.8, 1H), 7.64-7.63 (d, *J* = 2.0, 1H), 7.58-7.54 (m, 1H), 7.36-7.34 (dd, *J*<sub>1</sub> = 2.0, *J*<sub>2</sub> = 8.8, 1H), 4.19-4.14 (q, *J* = 7.2, 2H), 4.11-4.07 (q, *J* = 5.2, 1H), 3.18-3.16 (d, *J* = 5.2, 3H), 1.28-1.24 (t, *J* = 7.2, 3H) ppm. <sup>13</sup>C NMR (100 MHz, DMSO-d<sub>6</sub>): δ, 159.8, 154.6, 153.3, 153.1, 152.2, 149.3, 142.8, 137.5, 127.8, 124.4, 124.2, 114.1, 112.7, 112.0, 104.6, 60.7, 48.6, 14.4 ppm.

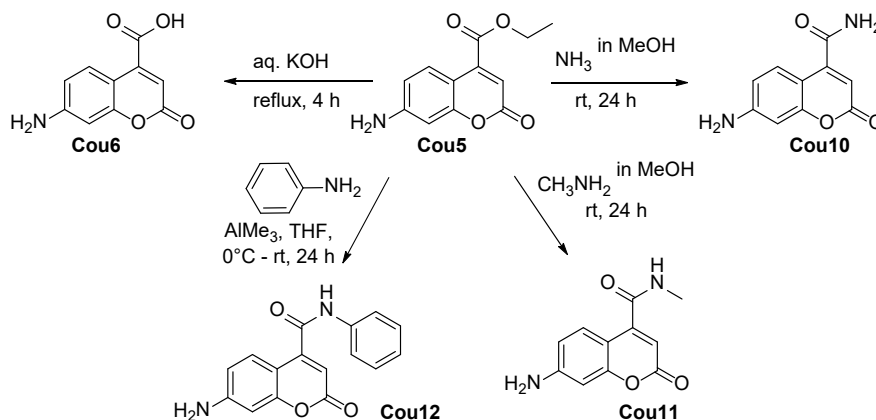
**Cou14-precursor** (0.50 g, 1.61 mmol) was added to a 50 ml round-bottom flask, followed by H<sub>2</sub>SO<sub>4</sub> conc. (5 ml) and glacial AcOH (5 ml). The reaction mixture was heated to 125 °C for 2 hours under reflux condenser, after which it was cooled to room temperature and poured over 50 ml of crushed ice. The resulting suspension was neutralized till weakly basic using 4M NaOH, affording a beige precipitate. The precipitate was filtered and recrystallized from hot methanol to give **Cou14** as fine yellow crystals (0.162 g, 68%). <sup>1</sup>H NMR (400 MHz, CD<sub>3</sub>OD): δ, 8.72-8.70 (ddd, *J*<sub>1</sub> = 1.2, *J*<sub>2</sub>

= 1.6,  $J_2 = 4.8$ , 1H), 8.04-8.00 (dt,  $J_1 = 2.0$ ,  $J_2 = 8.0$ , 1H), 7.69-7.66 (dt,  $J_1 = 1.2$ ,  $J_2 = 8.0$ , 1H), 7.58-7.54 (ddd,  $J_1 = 0.8$ ,  $J_2 = 4.8$ ,  $J_3 = 8.0$ , 1H), 7.29-7.26 (app dd,  $J_1 = 3.2$ ,  $J_2 = 6.4$ , 1H), 6.60-6.57 (m, 2H), 6.11 (s, 1H) ppm.  $^{13}\text{C}$  NMR (100 MHz,  $\text{CD}_3\text{OD}$ ):  $\delta$ , 164.1, 158.2, 156.0, 155.8, 155.0, 150.5, 139.2, 129.2, 125.7, 125.6, 113.2, 109.2, 109.1, 100.7 ppm. HRMS (ESI):  $m/z$   $[\text{M} + \text{H}]^+$  calcd for  $\text{C}_{14}\text{H}_{11}\text{N}_2\text{O}_2$ : 239.08207; found 239.08078.



**Scheme A4:** Synthesis of **Cou5**.

**Ethyl 7-amino-2-oxo-2H-chromene-4-carboxylate (Cou5):**<sup>9</sup> 3-Aminophenol (**4**) (5.00 g, 45.8 mmol), diethyl oxaloacetate sodium salt (**8**) (14.4 g, 68.7 mmol) and EtOH (20 ml) were heated at reflux overnight. The mixture was cooled and concentrated to dryness and the residue was purified by silica gel chromatography (50% EtOAc in hexanes). **Cou5** was obtained as a yellow-orange solid (4.17 g, 39%).  $^1\text{H}$  NMR (400 MHz,  $\text{DMSO-d}_6$ ):  $\delta$ , 7.69-7.66 (d,  $J = 8.8$ , 1H), 6.60-6.57 (dd,  $J_1 = 2.4$ ,  $J_2 = 8.8$ , 1H), 6.46-6.45 (d,  $J = 2.4$ , 1H), 6.37 (bs, 2H), 6.31 (s, 1H), 4.39-4.33 (q,  $J = 7.2$ , 1H), 1.35-1.31 (t,  $J = 7.2$ , 1H) ppm.  $^{13}\text{C}$  NMR (100 MHz,  $\text{DMSO-d}_6$ ):  $\delta$ , 164.3, 160.3, 156.5, 153.6, 143.8, 127.4, 111.8, 109.2, 104.4, 98.8, 62.0, 13.9 ppm. HRMS (ESI):  $m/z$   $[\text{M} + \text{H}]^+$  calcd for  $\text{C}_{12}\text{H}_{12}\text{NO}_4$ : 234.07665; found 234.07600.



**Scheme A5:** Synthesis of **Cou6** and **Cou10-12**.

**7-Amino-2-oxo-2H-chromene-4-carboxylic acid (Cou6):**<sup>9</sup> Ethyl 7-amino-2-oxo-2H-chromene-4-carboxylate (**Cou5**) (1.00 g, 4.30 mmol) and 2M KOH solution (25 ml) were added to the flask and refluxed for 4 h. After cooling, the reaction mixture was washed with AcOEt (25 ml,

discarded). AcOH was used to neutralize the solution that was concentrated to dryness. The residue was purified by column chromatography on silica gel, eluting with water : isopropanol : EtOAc mixtures (1 : 2 : 7 to 2 : 4 : 4). The residue was triturated with CH<sub>2</sub>Cl<sub>2</sub> containing little EtOH, and then refluxed in CHCl<sub>3</sub> overnight. The product was filtered, washed with CHCl<sub>3</sub> and dried in air to obtain orange solid (0.38 g, 43%) in satisfying purity. <sup>1</sup>H NMR (400 MHz, DMSO-d<sub>6</sub>): δ, 7.73-7.70 (d, *J* = 8.8, 1H), 6.53-6.50 (dd, *J*<sub>1</sub> = 2.0, *J*<sub>2</sub> = 8.8, 1H), 6.40 (d, *J* = 2.0, 1H), 5.93 (s, 1H) ppm. <sup>13</sup>C NMR (100 MHz, DMSO-d<sub>6</sub>): δ, 167.1, 161.6, 156.3, 152.6, 128.6, 111.0, 106.2, 104.8, 98.4 ppm. HRMS (ESI): *m/z* [M + H]<sup>+</sup> calcd for C<sub>10</sub>H<sub>8</sub>NO<sub>4</sub>: 206.04535; found 206.04487.

**7-Amino-2-oxo-2H-chromene-4-carboxamide (Cou10):** This compound was synthesized according to the modified general procedure.<sup>10</sup> **Cou5** (1.00 g, 4.30 mmol) was placed in the flame-dried flask under the flow of Ar. Then 7N NH<sub>3</sub> in absolute MeOH (20 ml) was added and the mixture was allowed to react at room temperature under Ar for 24 h. Then the mixture was concentrated to dryness. The residue was purified by column chromatography on silica gel, eluting with 100% CH<sub>2</sub>Cl<sub>2</sub> to 100% EtOAc, followed by 10-40% MeOH in EtOAc. The residue was triturated with CH<sub>2</sub>Cl<sub>2</sub>, and filtered washing sequentially with CH<sub>2</sub>Cl<sub>2</sub>, water, ethanol, again CH<sub>2</sub>Cl<sub>2</sub> and dried in air. The product was obtained as a yellow solid (0.12 g, 14%). <sup>1</sup>H NMR (400 MHz, DMSO-d<sub>6</sub>): δ, 8.16 (bs, 1H), 7.83 (bs, 1H), 7.43-7.41 (d, *J* = 8.8, 1H), 6.57-6.55 (dd, *J*<sub>1</sub> = 2.0, *J*<sub>2</sub> = 8.8, 1H), 6.44 (d, *J* = 2.0, 1H), 6.27 (bs, 2H), 5.99 (s, 1H) ppm. <sup>13</sup>C NMR (100 MHz, DMSO-d<sub>6</sub>): δ, 166.8, 160.8, 156.4, 153.5, 150.2, 127.6, 111.6, 105.5, 105.0, 98.7 ppm. HRMS (ESI): *m/z* [M + H]<sup>+</sup> calcd for C<sub>10</sub>H<sub>9</sub>N<sub>2</sub>O<sub>3</sub>: 205.06134; found 205.06064.

**7-Amino-N-methyl-2-oxo-2H-chromene-4-carboxamide (Cou11):** This compound was synthesized according to the modified general procedure.<sup>10</sup> **Cou5** (1.00 g, 4.30 mmol) was placed in the flame-dried flask under the flow of Ar. 33 wt. % CH<sub>3</sub>NH<sub>2</sub> in MeOH (20 ml) was added and the mixture was allowed to react at room temperature under Ar for 24 h. Then the mixture was concentrated to dryness. The residue was purified by column chromatography on silica gel, eluting with 50-100% EtOAc in hexanes, followed by 10% MeOH in EtOAc. The residue was stirred overnight in CH<sub>2</sub>Cl<sub>2</sub>/EtOAc, filtered, washed with CH<sub>2</sub>Cl<sub>2</sub> and dried in air. The product was obtained as a yellow solid (0.08 g, 9%). <sup>1</sup>H NMR (400 MHz, DMSO-d<sub>6</sub>): δ, 8.66 (d, *J* = 4.0, 1H), 7.38-7.36 (d, *J* = 8.8, 1H), 6.56-6.54 (d, *J* = 8.8, 1H), 6.44 (s, 1H), 6.28 (bs, 2H), 5.98 (s, 1H), 2.77 (d, *J* = 4.0, 3H) ppm. <sup>13</sup>C NMR (100 MHz, DMSO-d<sub>6</sub>): δ, 165.0, 160.5, 156.2, 153.4, 150.0, 127.5, 111.5, 105.6, 105.0, 98.6, 25.8 ppm. HRMS (ESI): *m/z* [M + H]<sup>+</sup> calcd for C<sub>11</sub>H<sub>11</sub>N<sub>2</sub>O<sub>3</sub>: 219.07699; found 219.07602.

**7-Amino-2-oxo-N-phenyl-2H-chromene-4-carboxamide (Cou12):** This compound was synthesized according to the modified general procedure.<sup>11</sup> A solution of aniline (0.729 ml, 8 mmol)

in dry THF (20 ml) was cooled to 0 °C under Ar and a commercial 2.0 M solution of trimethylaluminum in hexanes (10 ml, 20 mmol) was added dropwise over 10 minutes. Then, to the resulting mixture a solution of **Cou5** (0.932 g, 4 mmol) in dry THF (40 ml) was added dropwise over 20 minutes at 0 °C. The mixture was allowed to warm to rt and stirred for overall 22 h. It was diluted with EtOAc (100 ml) and carefully neutralized with aq. NH<sub>4</sub>Cl (100 ml) with vigorous stirring. The phases were separated, and the aqueous phase was additionally extracted with EtOAc (100 ml). The combined organic extracts were washed with brine (50 ml) and dried over MgSO<sub>4</sub>. After filtration and concentration, the residue was purified by column chromatography on silica gel, eluting with 0-80% EtOAc in hexanes. The product was further purified by recrystallization from EtOAc and filtered washing copiously with CH<sub>2</sub>Cl<sub>2</sub> to obtain an orange solid (0.165 g, 14%). <sup>1</sup>H NMR (400 MHz, DMSO-d<sub>6</sub>): δ, 10.7 (bs, 1H), 7.74-7.72 (d, *J* = 8.0, 2H), 7.39-7.36 (m, 3H), 7.16-7.13 (t, *J* = 7.2, 1H), 6.60-6.58 (d, *J* = 8.0, 1H), 6.49 (s, 1H), 6.34 (bs, 2H), 6.20 (s, 1H) ppm. <sup>13</sup>C NMR (100 MHz, DMSO-d<sub>6</sub>): δ, 163.2, 160.5, 156.2, 153.5, 149.6, 138.2, 128.7, 127.2, 124.2, 119.9, 111.7, 105.8, 104.8, 98.6 ppm. HRMS (ESI): *m/z* [M + H]<sup>+</sup> calcd for C<sub>16</sub>H<sub>13</sub>N<sub>2</sub>O<sub>3</sub>: 281.09264; found 281.09189.

## A.5 Cell Imaging

For confocal microscopy cells were plated (100,000/plate) in 35 mm glass-bottom confocal dishes (MatTek) and allowed to grow in their respective growth media for 24 hours. For optical microscope analysis cells were plated in a 6-well plates (3 X 10<sup>5</sup>) and allowed to adhere and grow for 24 h. For treatment, cell media was removed and ManCou solution in PBS (1 ml) was added. Cells were incubated with ManCous at 37 °C for 10 min. After incubation, probe solution was removed, and cells were washed with warmed PBS (3 x 1 ml) and leaving 1 ml of PBS for imaging. Cell images were taken using Olympus FluoView™ FV1000 using the FluoView software. 60X oil suspended lens was used to observe fluorescent activity with the following conditions: DAPI (ManCous) and eGFP (NBDM and NBDG) filters; lasers 405 nm (45% intensity), 450/490 nm (30% intensity); 10 μs/pixel. Z-stacking was done using FluoView software and depth command.

## A.6 Microplate uptake and inhibition assays

For microplate assays, at ~80% confluence cells were collected and plated in 96-well flat bottom plates (20,000 cells/well) and allowed to grow for 24 hours. Cells were then washed with warmed (37 °C) PBS solution, treated with ManCou probes (concentration varies) in PBS and incubated at 37 °C and 5% CO<sub>2</sub> for 10 min. After incubation, cells were carefully washed with warmed PBS (3 X 100 μl). Fluorescent data were immediately collected using Victor3 plate reader

and using Wallac™ umbelliferone (excitation 355 nm, emission 460 nm, 1.0 s) protocol. All trials were done in triplicate on each plate.

Uptake Inhibition studies were carried out in microplate format. Using 96-well plate method fluorescence of ManCou probes in cells was measured in the presence of varying concentrations of fructose, glucose, glucosamine, and cytochalasin B. For this part, PBS solution containing 20  $\mu$ M ManCou and the specific concentration of a sugar were prepared and introduced to cells. Separately, complete culture media were used to establish the impact of nutrients on ManCou uptake. Cell incubation, and data collection were conducted as stated above.

## A.7 References

1. H. E. Gottlieb, V. Kotlyar and A. Nudelman, *J. Org. Chem.*, 1997, **62**, 7512-7515.
2. M. Tanasova, M. Plutschack, M. E. Muroski, S. J. Sturla, G. F. Strouse and D. T. McQuade, *ChemBioChem*, 2013, **14**, 1263-1270.
3. F. Cardona and B. La Ferla, *J. Carbohydr. Chem.*, 2008, **27**, 203-213.
4. H. P. Beck, S. K. Booker, H. Bregman, V. J. Cee, N. Chakka, T. D. Cushing, O. Epstein, B. M. Fox, S. Geuns-Meyer, X. Hao, K. Hibiya, J. Hirata, Z. Hua, J. Human, S. Kakuda, P. Lopez, R. Nakajima, K. Okada, S. H. Olson, H. Oono, L. Pennington, K. Sasaki, K. Shimada, Y. Shin, R. D. White, R. P. Wurz, S. Yi and X. M. Zheng. Pyrazole Amide Derivative. World Pat. Appl. 2015129926A1, 2015.
5. J. Z. Yu, Y. T. Wang, P. Z. Zhang and J. Wu, *Synlett*, 2013, **24**, 1448-1454.
6. D. J. Maly, F. Leonetti, B. J. Backes, D. S. Dauber, J. L. Harris, C. S. Craik and J. A. Ellman, *J. Org. Chem.*, 2002, **67**, 910-915.
7. P. Reszka, R. Schulz, K. Methling, M. Lalk and P. J. Bednarski, *ChemMedChem*, 2010, **5**, 103-117.
8. M. Tasiar, I. Deperasinska, K. Morawska, M. Banasiewicz, O. Vakuliuk, B. Kozankiewicz and D. T. Gryko, *Phys. Chem. Chem. Phys.*, 2014, **16**, 18268-18275.
9. M. Sinev, P. Landsmann, E. Sineva, V. Ittah and E. Haas, *Bioconjugate Chem.*, 2000, **11**, 352-362.
10. L. Pisani, M. Barletta, R. Soto-Otero, O. Nicolotti, E. Mendez-Alvarez, M. Catto, A. Introcaso, A. Stefanachi, S. Cellamare, C. Altomare and A. Carotti, *J. Med. Chem.*, 2013, **56**, 2651-2664.
11. B. Pelcman, A. Sanin, P. Nilsson, T. Boesen, S. B. Vogensen, H. Kromann and T. Groth. Pyrazoles Useful in the Treatment of Inflammation. World Pat. Appl. 2007045868A1, 2007.



## A.8 Copies of $^1\text{H}$ and $^{13}\text{C}$ NMR spectra

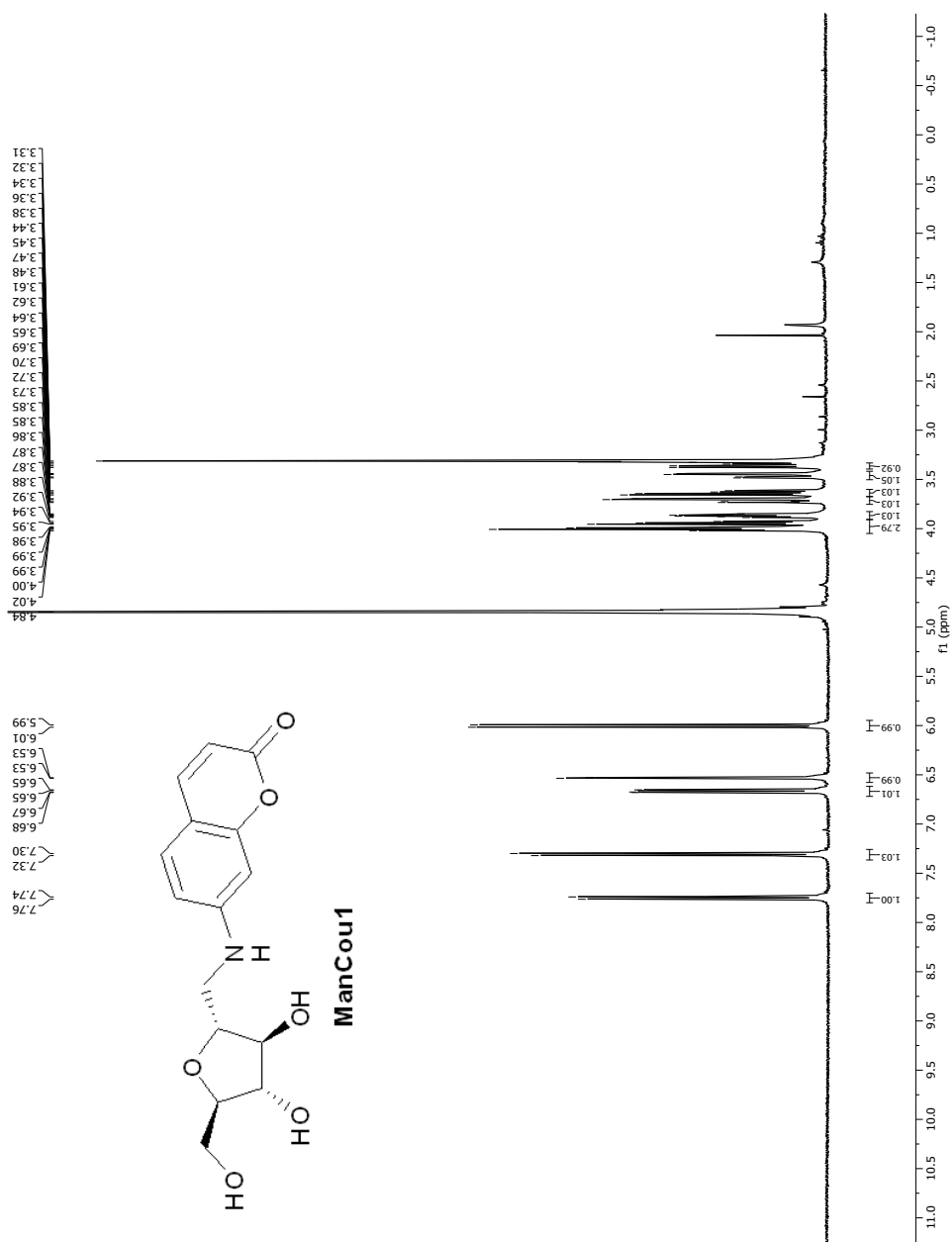
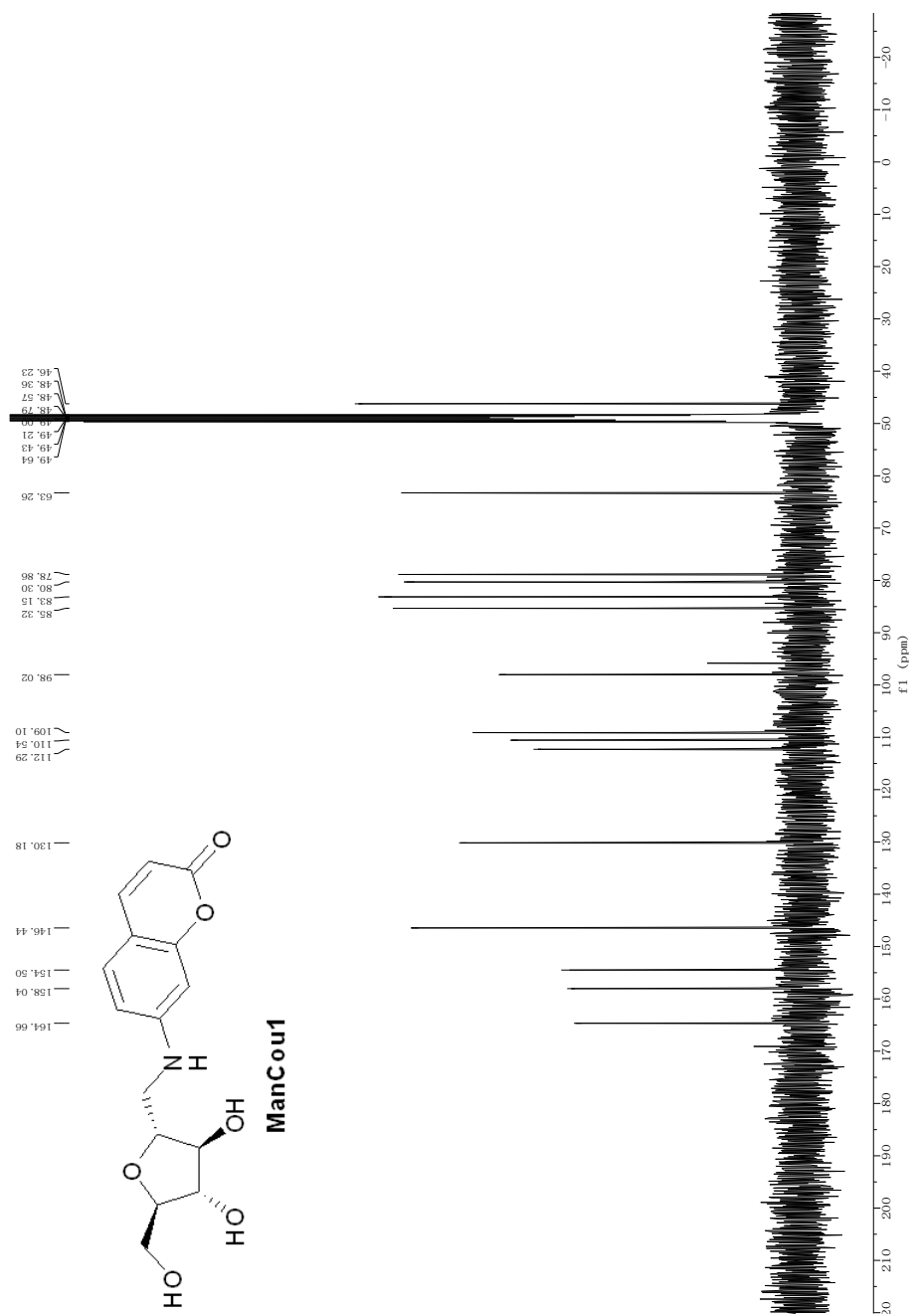
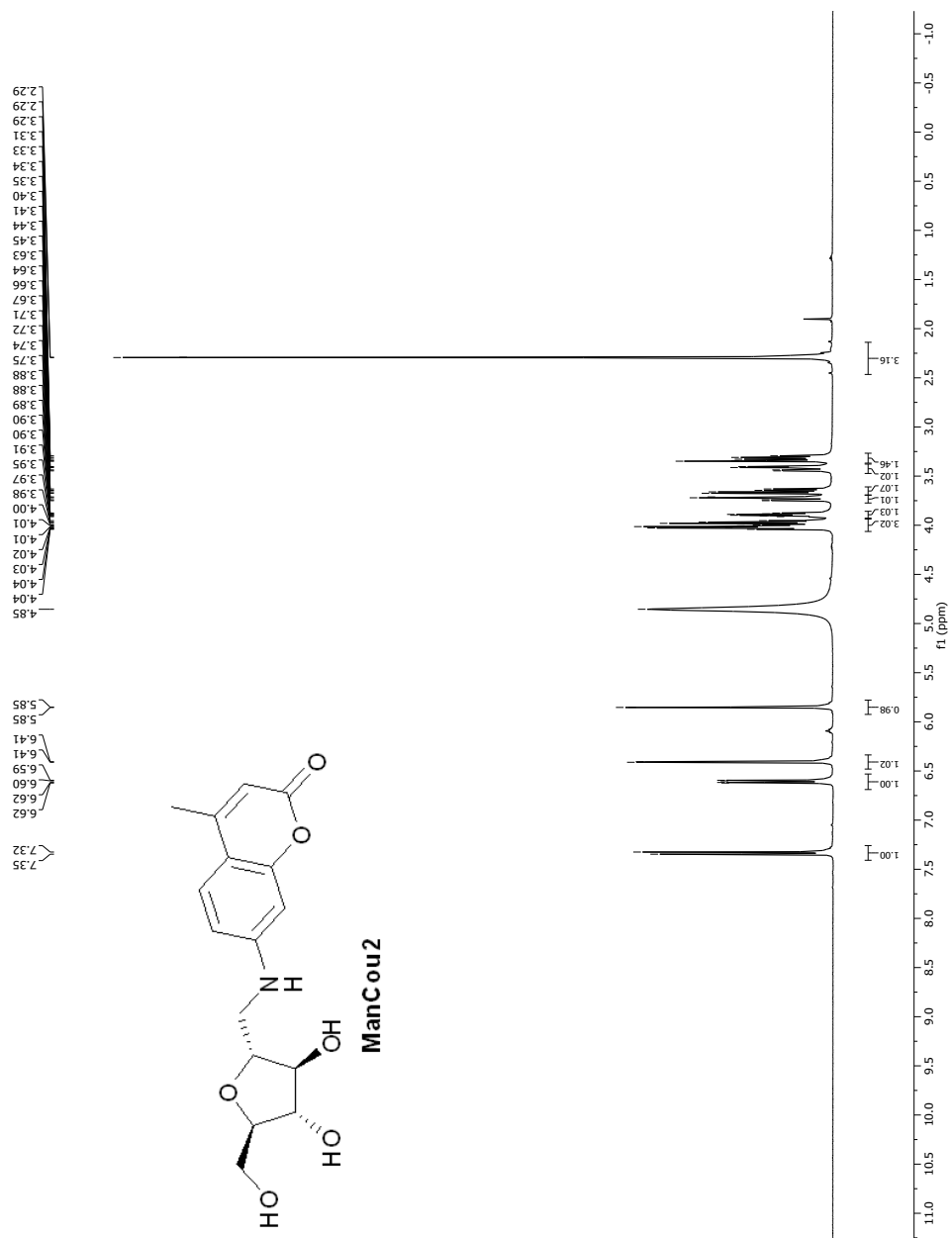


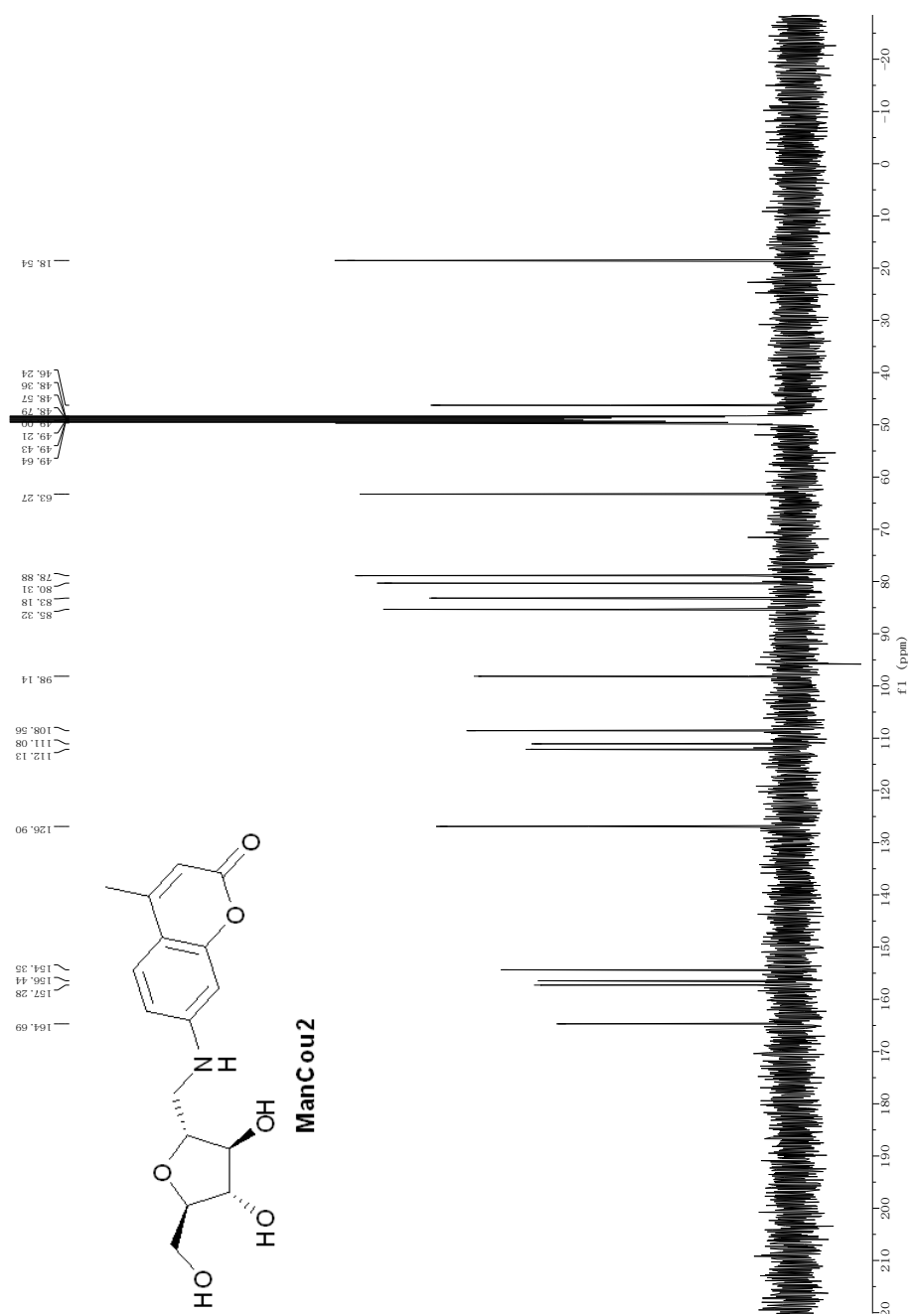
Figure A7.  $^1\text{H}$  NMR spectrum of ManCou1 ( $\text{CD}_3\text{OD}$ , 400 MHz).



**Figure A8.** <sup>13</sup>C NMR spectrum of **ManCou1** (CD<sub>3</sub>OD, 100 MHz).

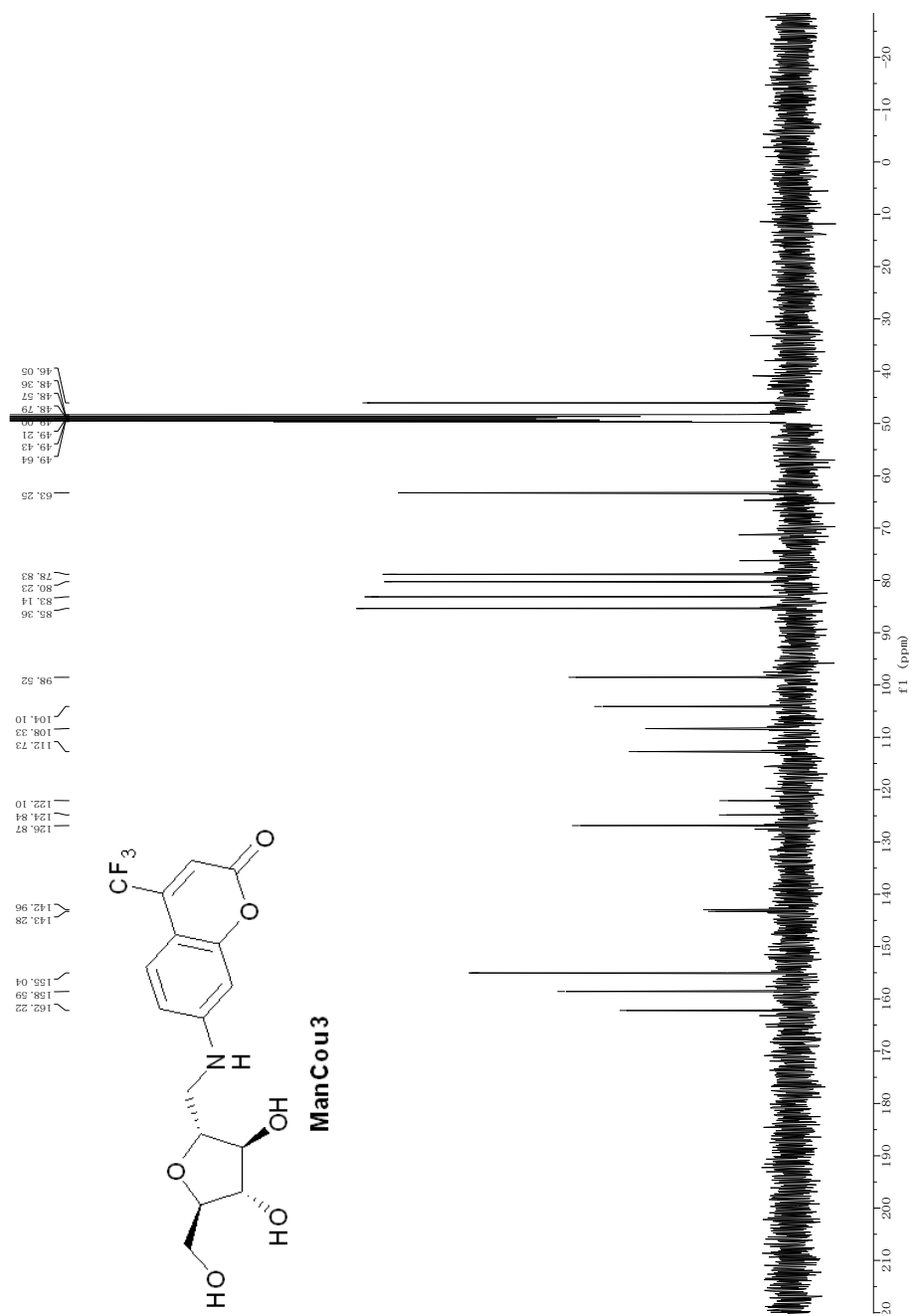


**Figure A9.** <sup>1</sup>H NMR spectrum of **ManCou2** (CD<sub>3</sub>OD, 400 MHz).



**Figure A10.** <sup>13</sup>C NMR spectrum of **ManCou2** (CD<sub>3</sub>OD, 100 MHz).





**Figure A12.** <sup>13</sup>C NMR spectrum of **ManCou3** (CD<sub>3</sub>OD, 100 MHz).

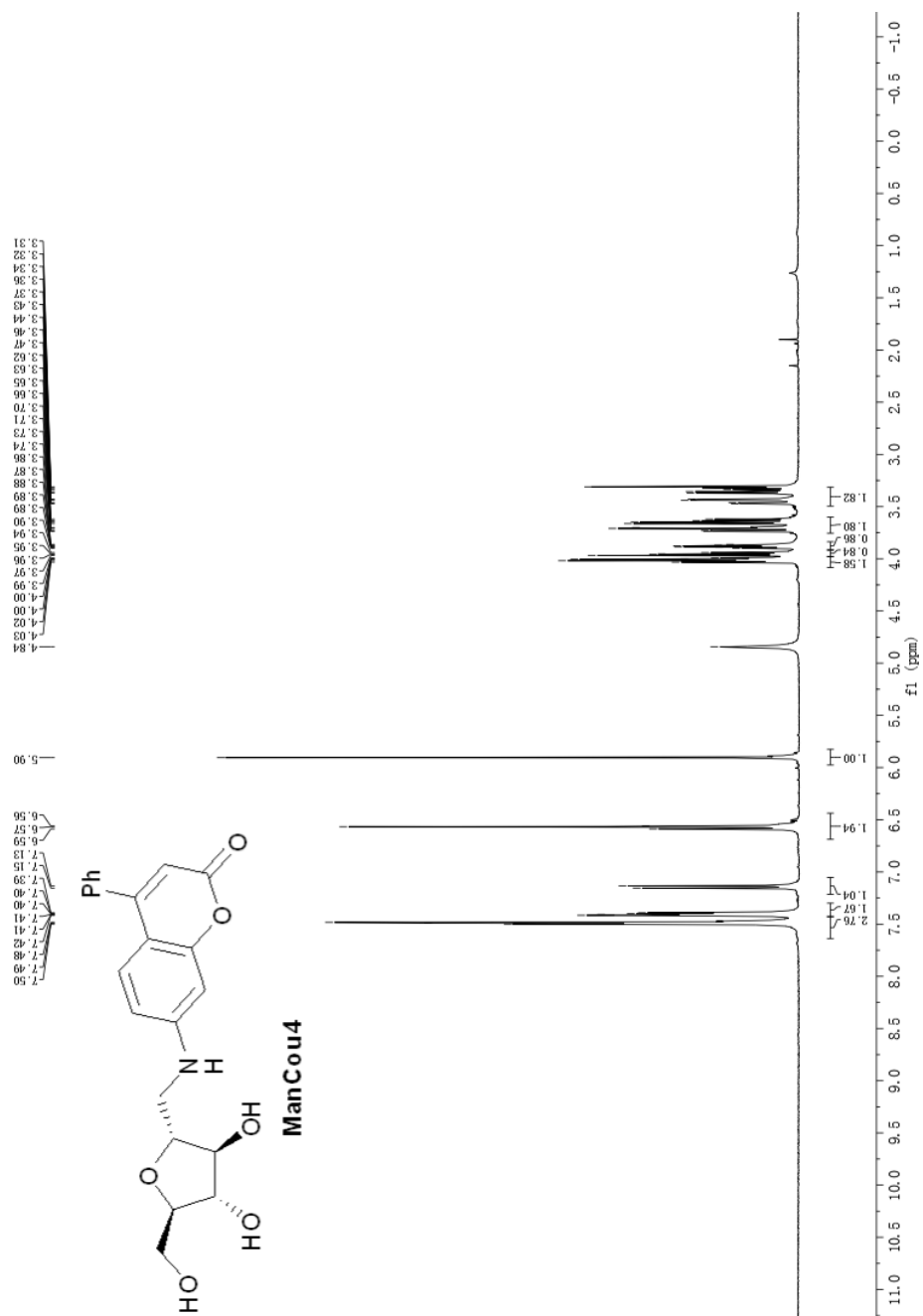
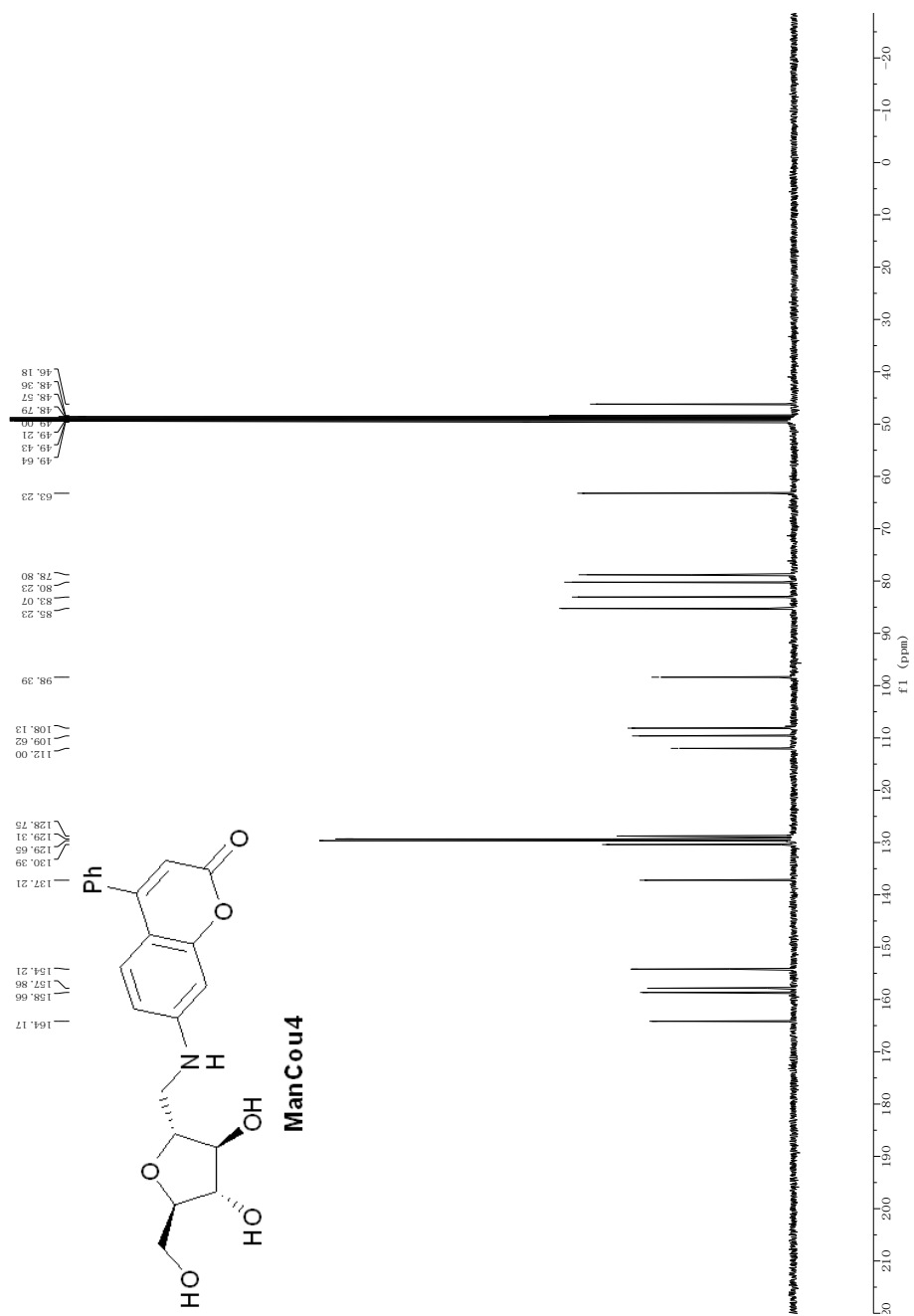
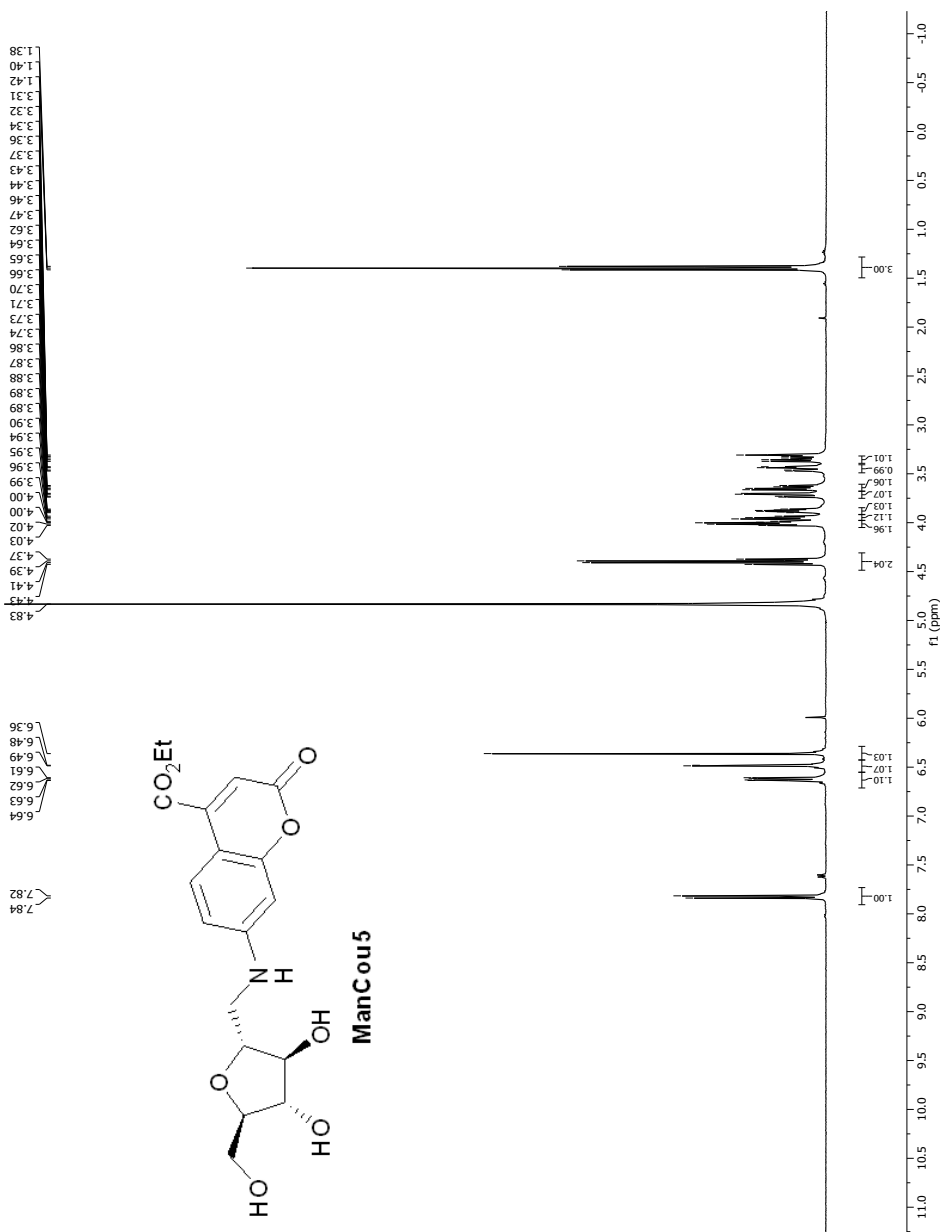


Figure A13. <sup>1</sup>H NMR spectrum of ManCou4 (CD<sub>3</sub>OD, 400 MHz).

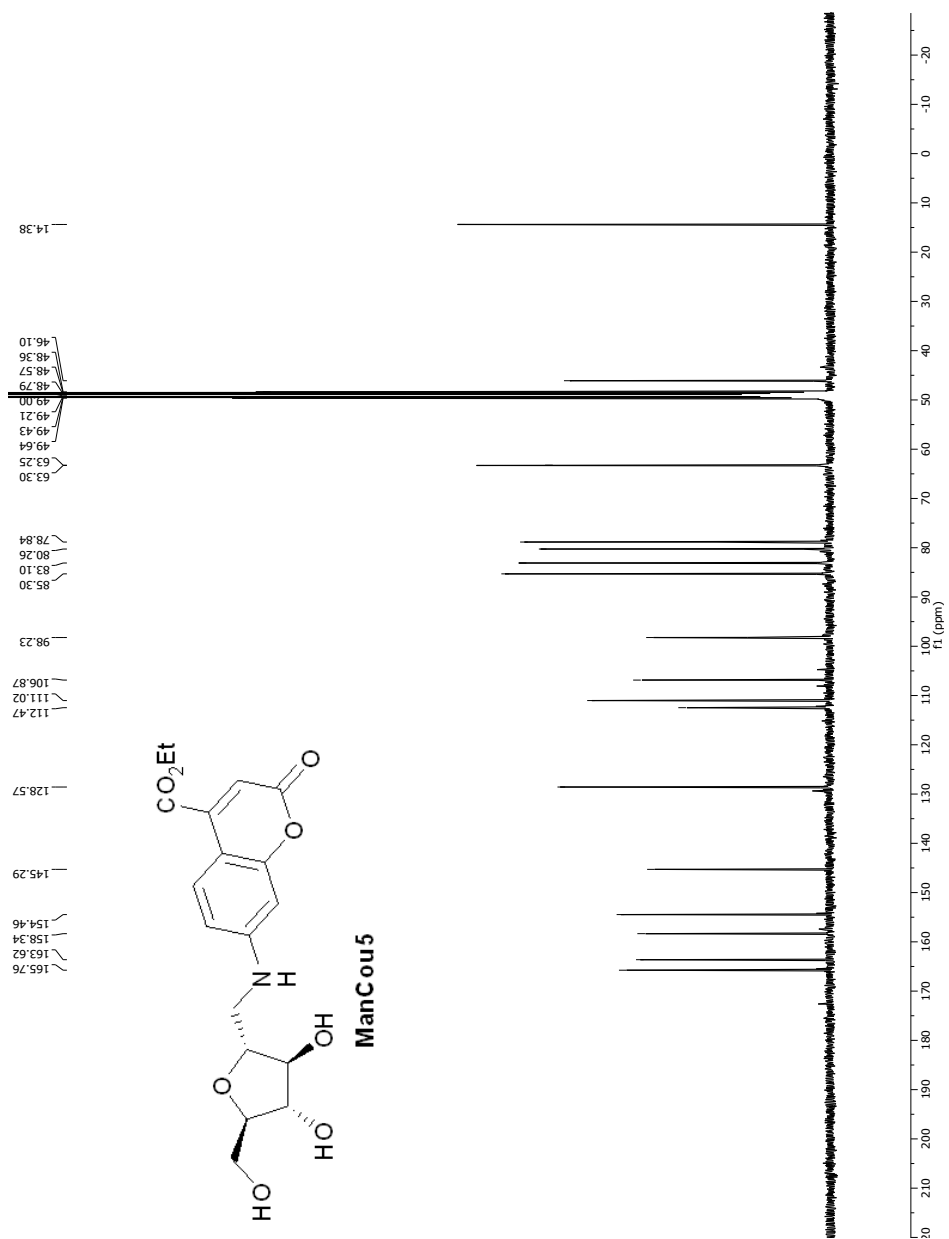


**Figure A14.** <sup>13</sup>C NMR spectrum of **ManCou4** (CD<sub>3</sub>OD, 100 MHz).





**Figure A15.**  $^1\text{H}$  NMR spectrum of **ManCou5** (CD<sub>3</sub>OD, 400 MHz).



**Figure A16.** <sup>13</sup>C NMR spectrum of **ManCou5** (CD<sub>3</sub>OD, 100 MHz).

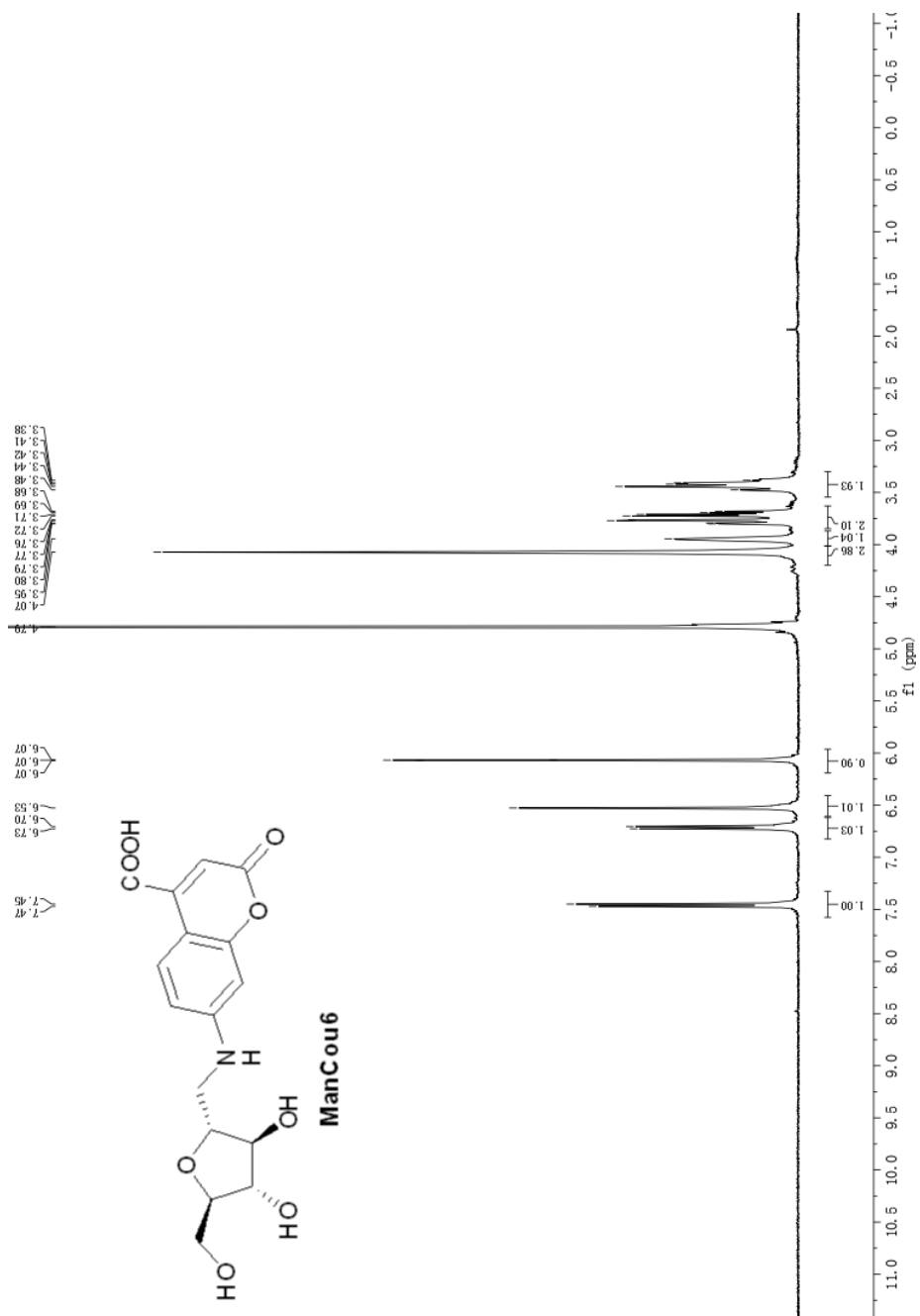
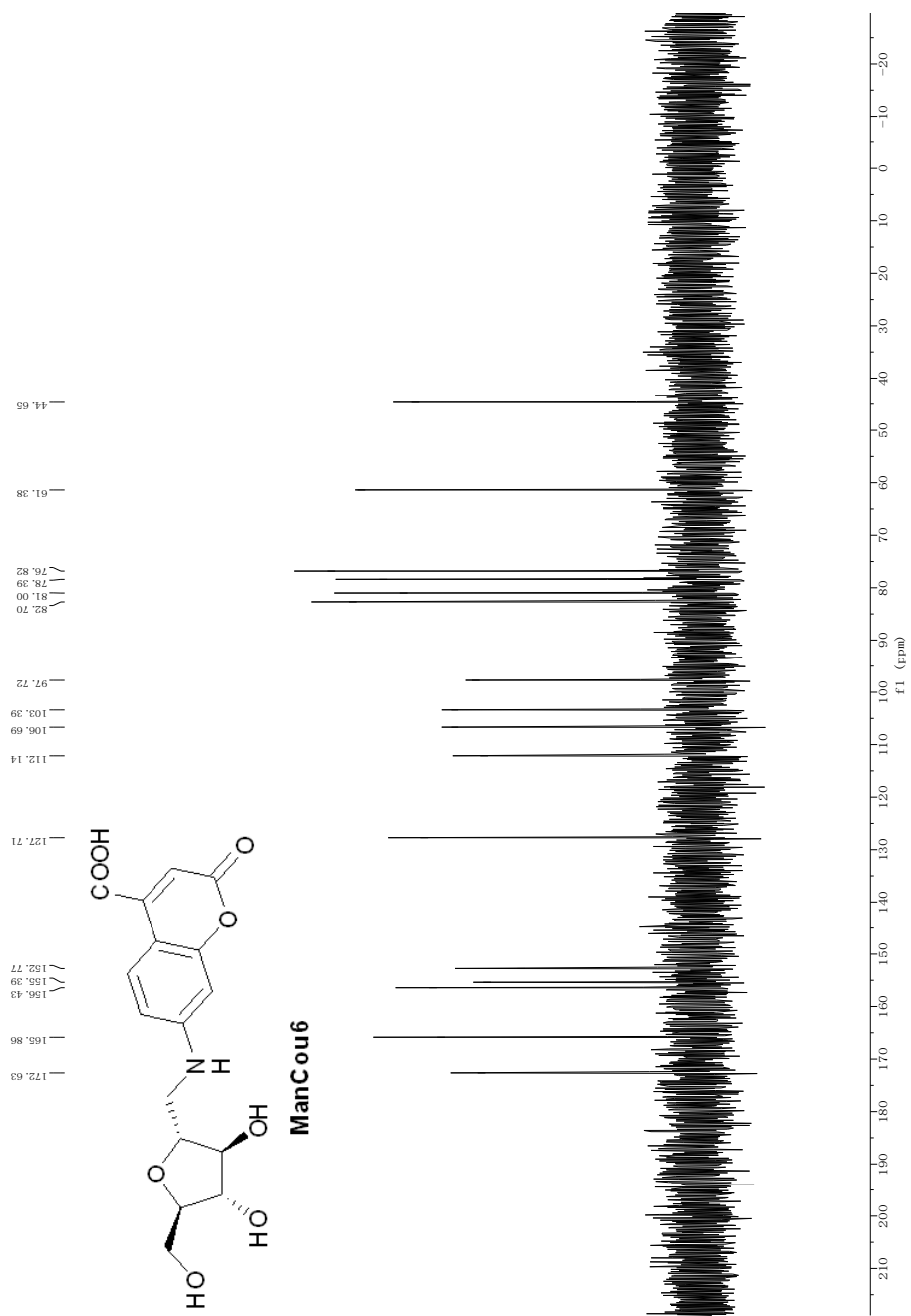
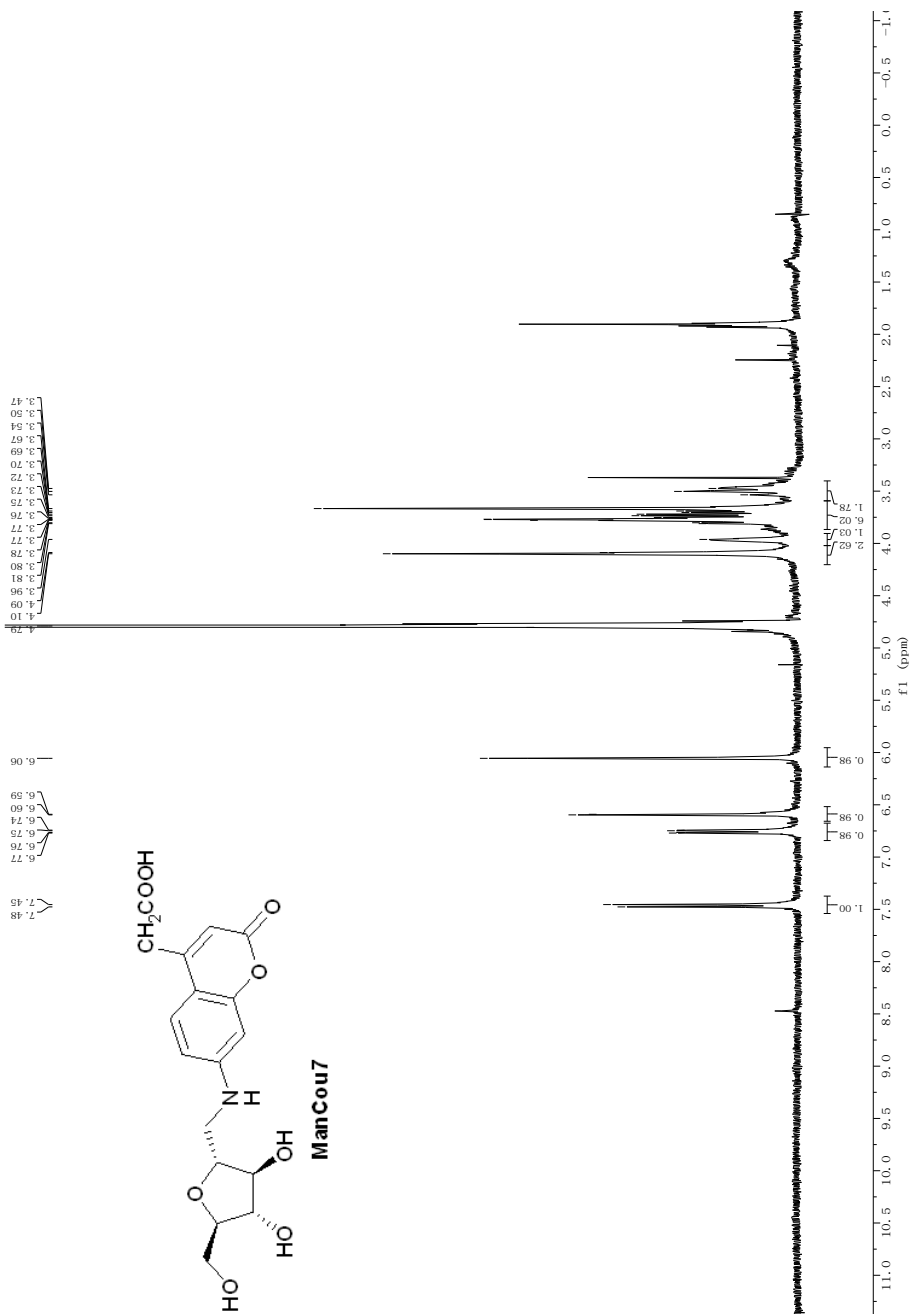


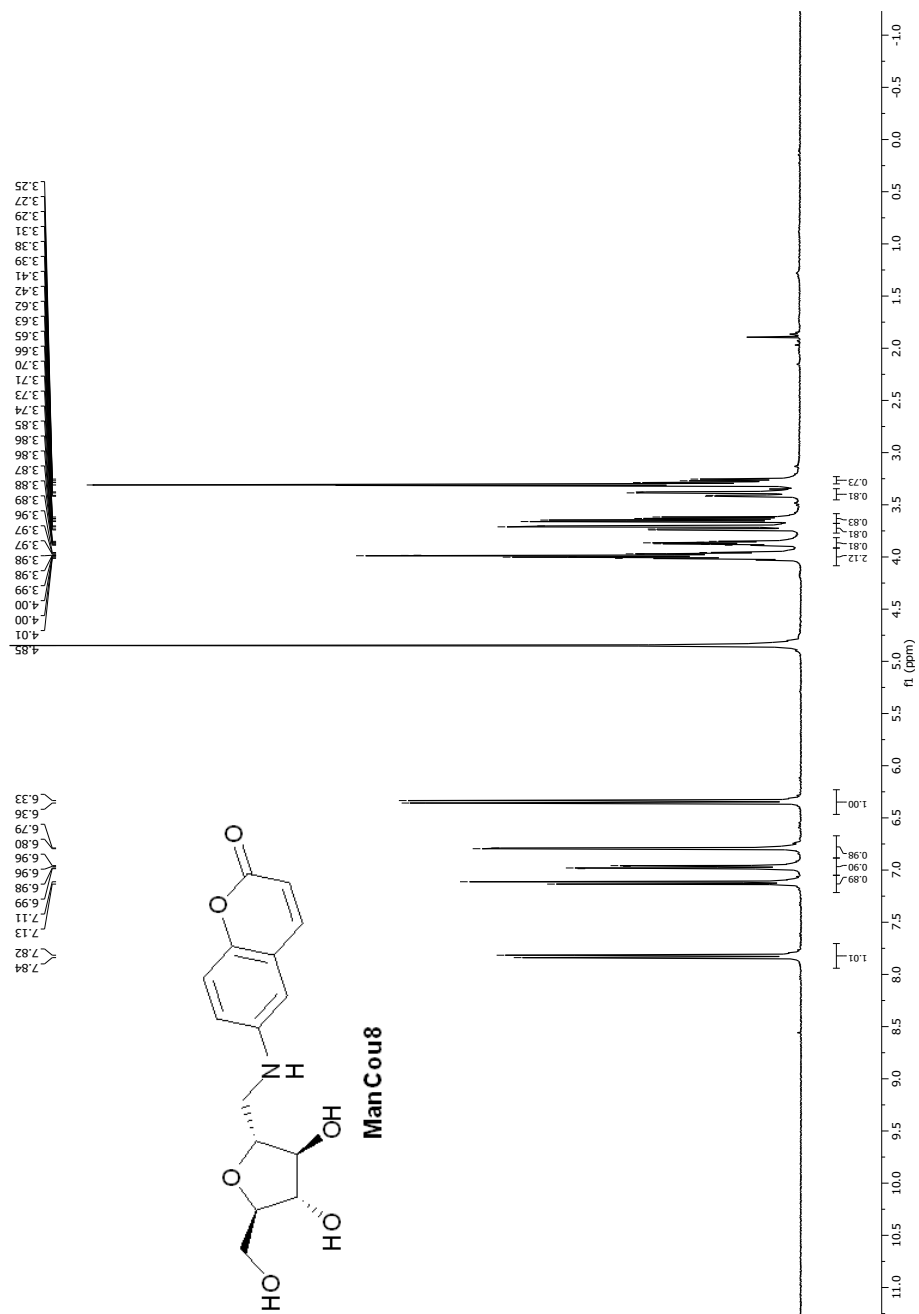
Figure A17. <sup>1</sup>H NMR spectrum of ManCou6 (D<sub>2</sub>O, 400 MHz).



**Figure A18.**  $^{13}\text{C}$  NMR spectrum of **ManCou6** ( $\text{D}_2\text{O}$ , 100 MHz).



**Figure A19.** <sup>1</sup>H NMR spectrum of **ManCou7** (D<sub>2</sub>O, 400 MHz).



**Figure A20.** <sup>1</sup>H NMR spectrum of **ManCou8** (CD<sub>3</sub>OD, 400 MHz).

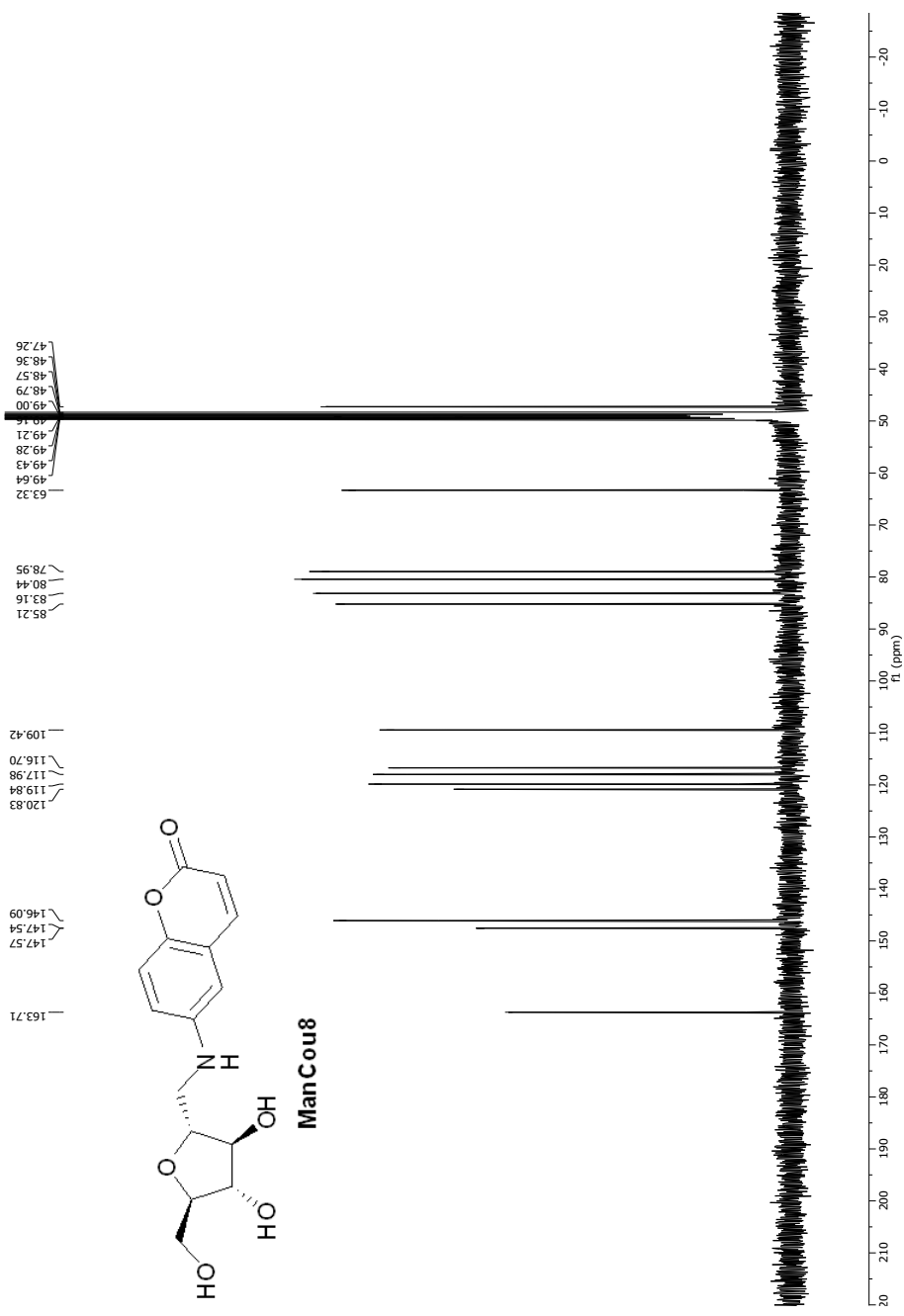
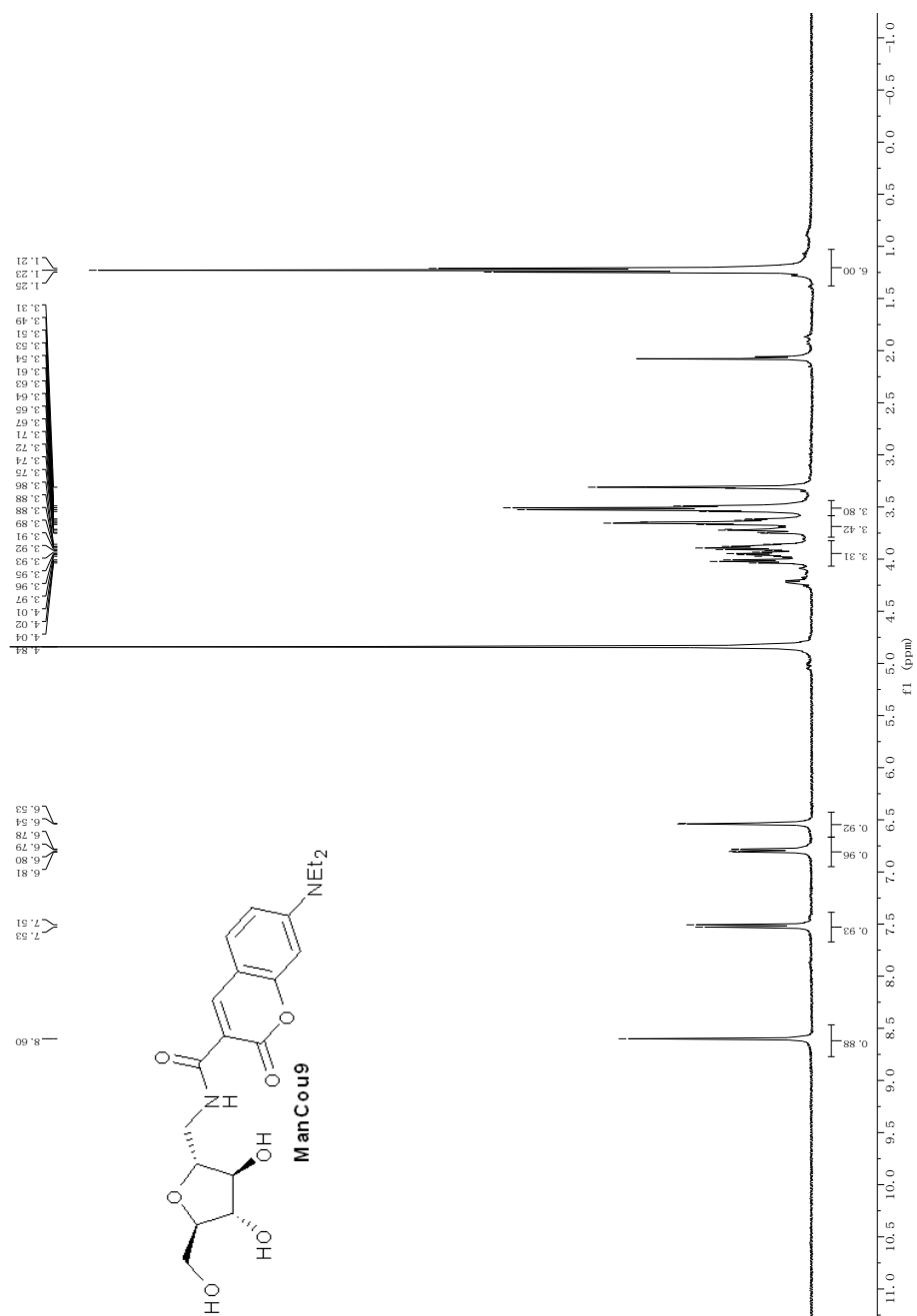


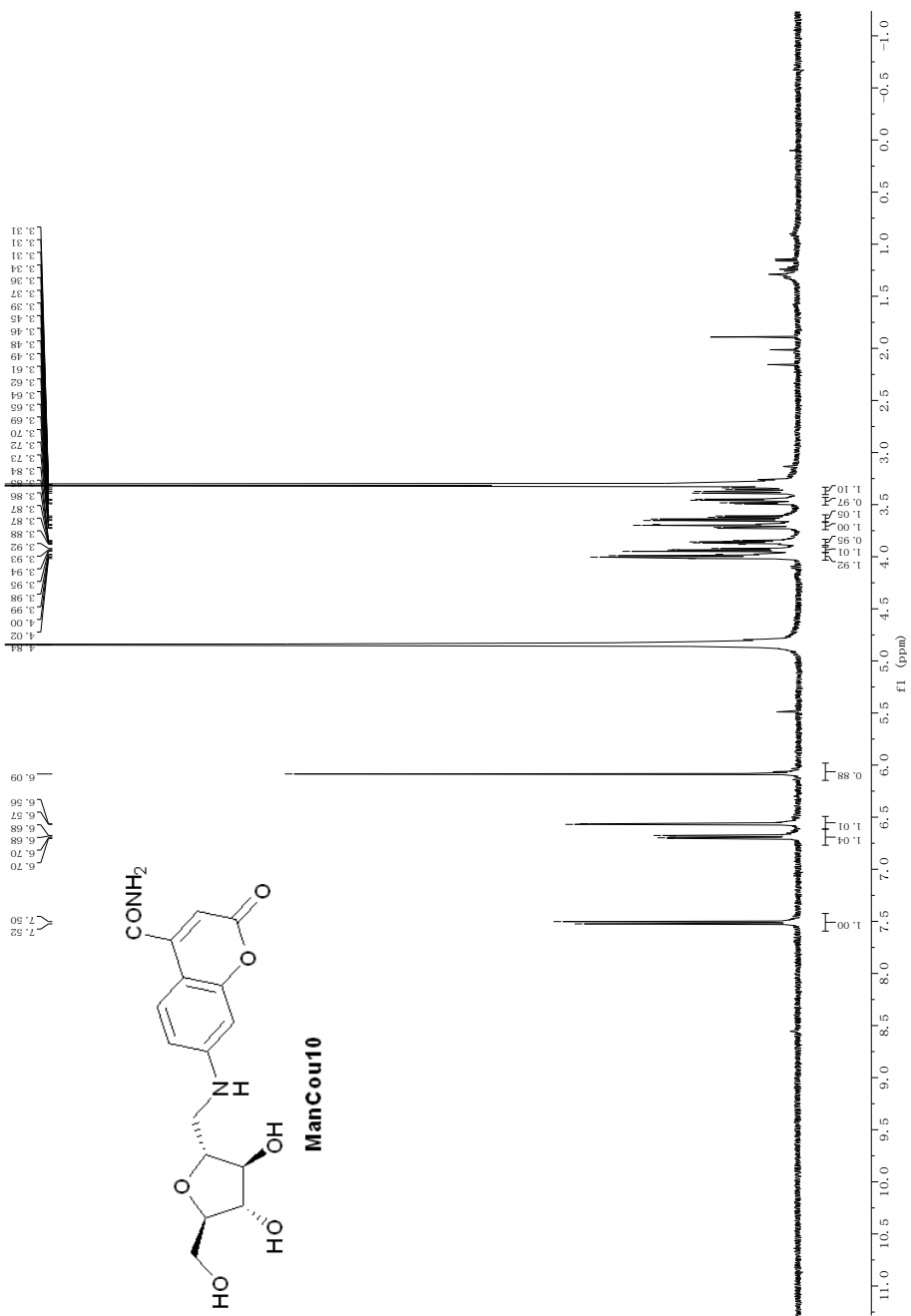
Figure A21. <sup>13</sup>C NMR spectrum of ManCou8 (CD<sub>3</sub>OD, 100 MHz).



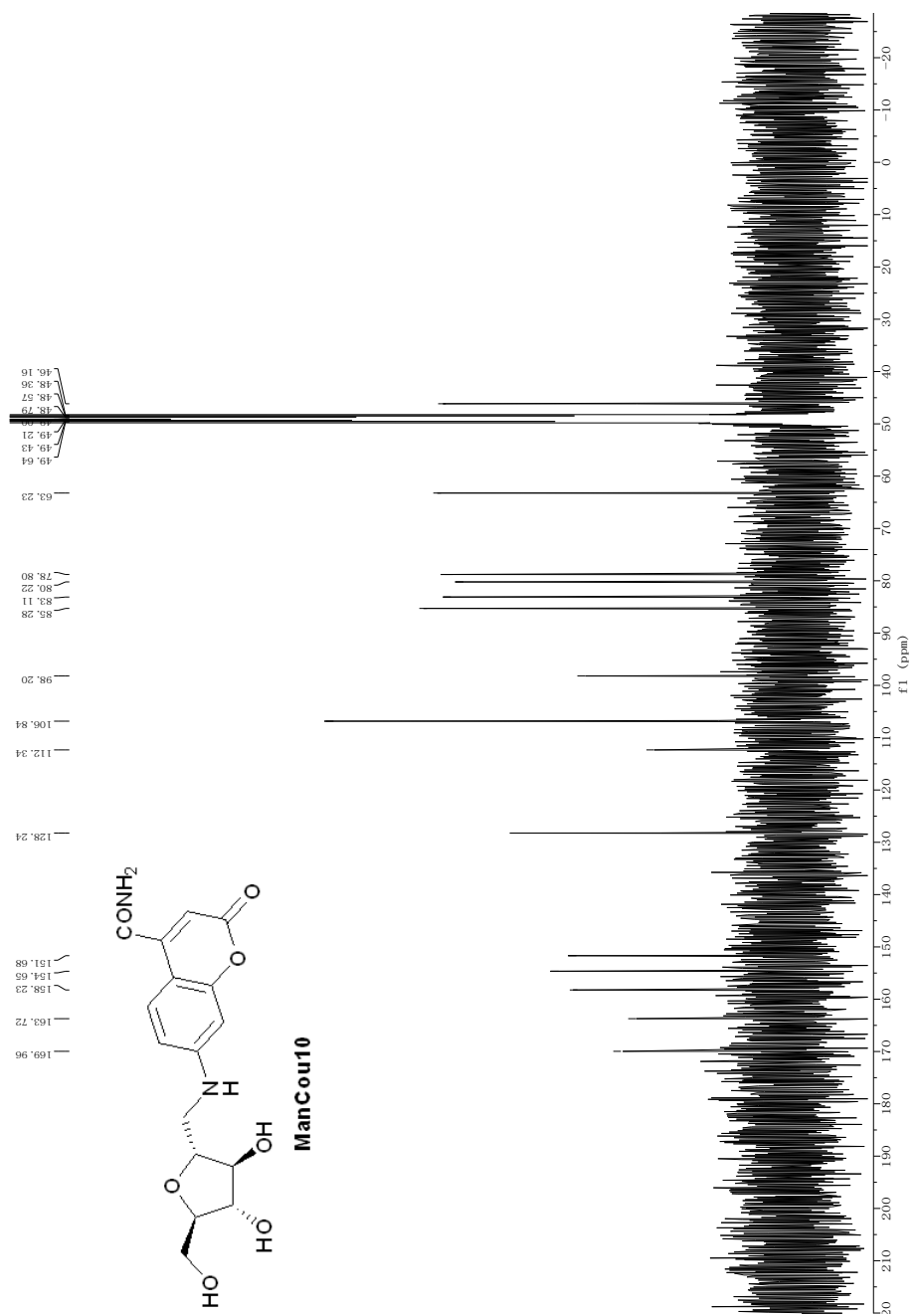
**Figure A22.** <sup>1</sup>H NMR spectrum of **ManCou9** (CD<sub>3</sub>OD, 400 MHz).



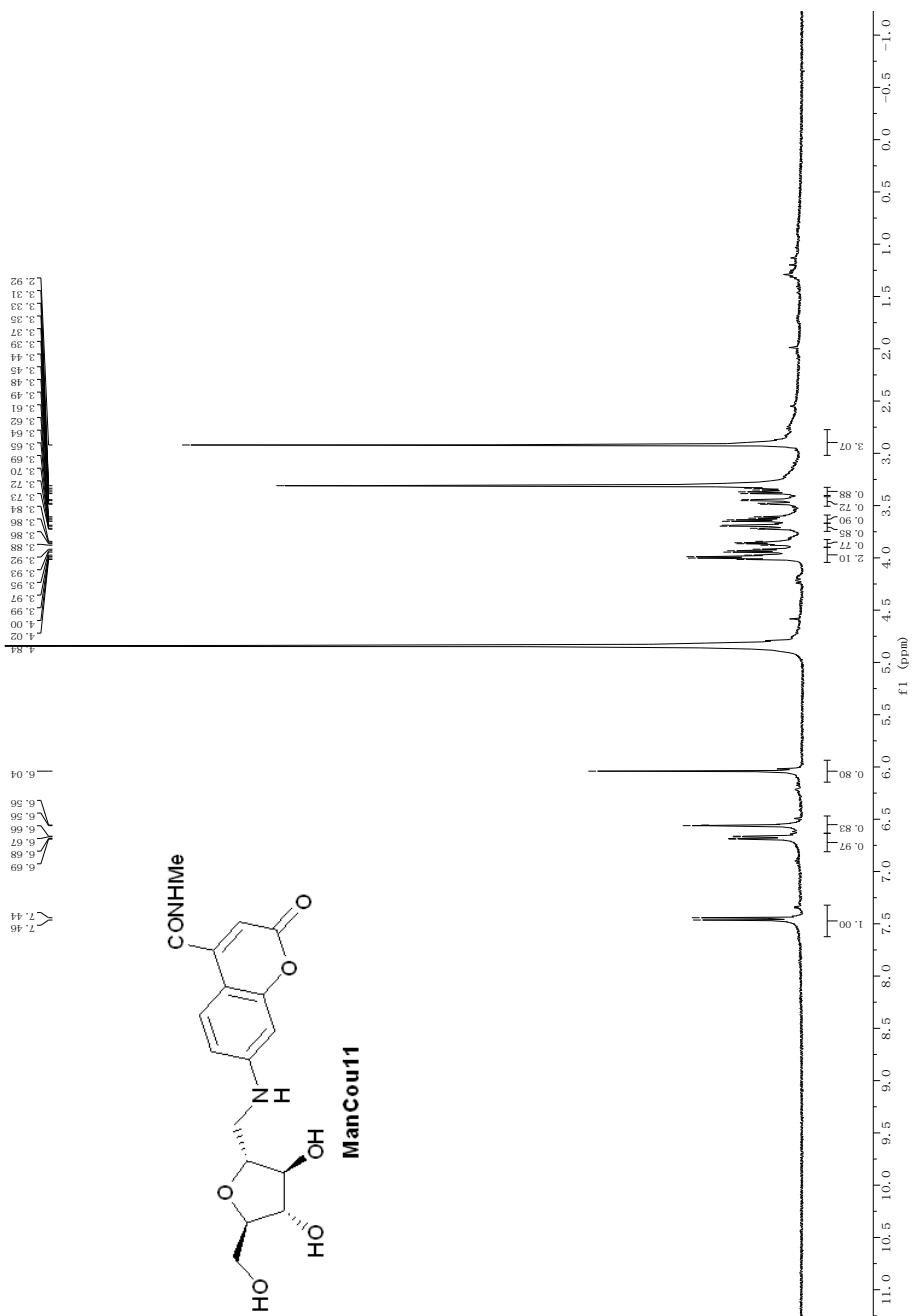




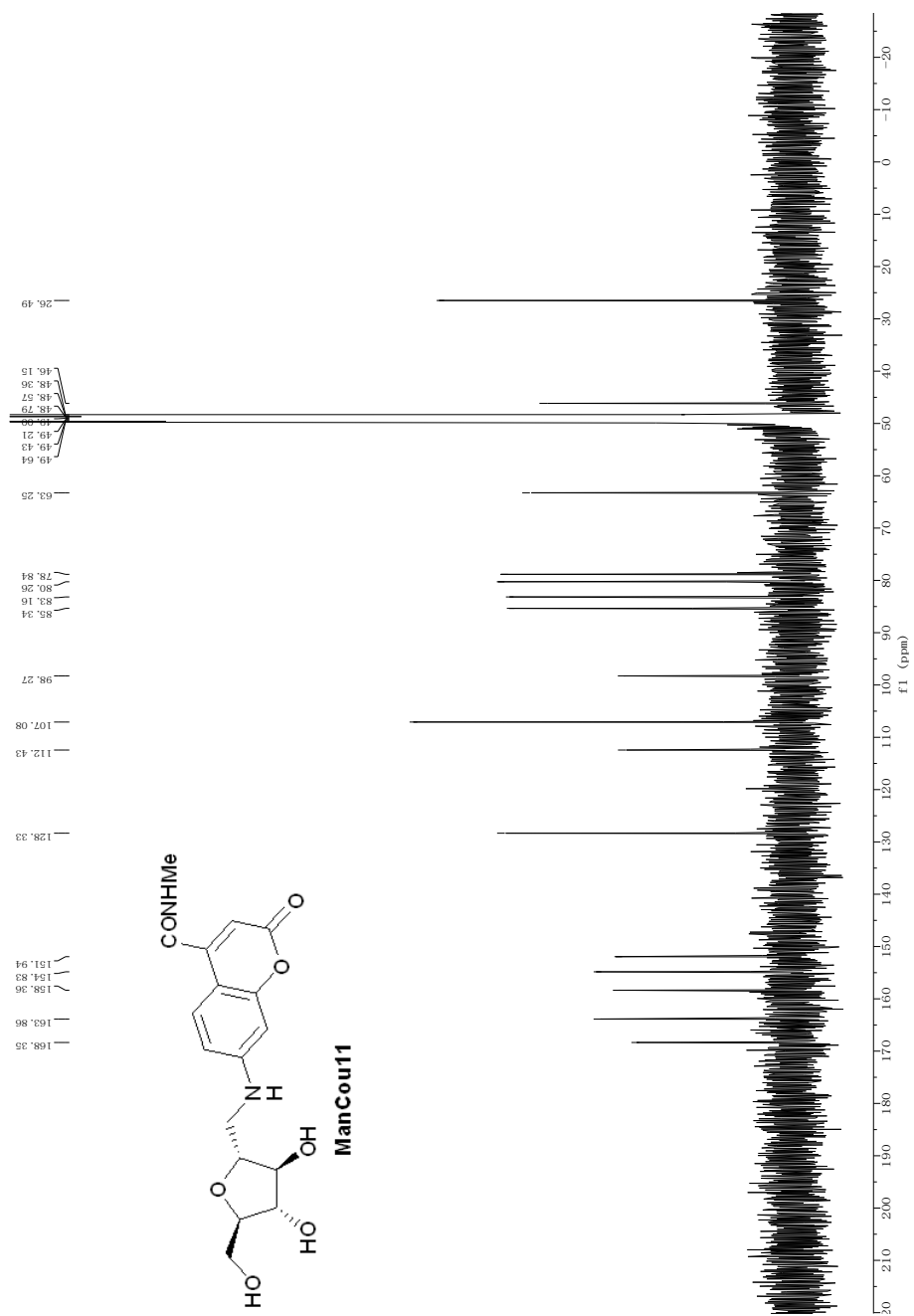
**Figure A24.** <sup>1</sup>H NMR spectrum of **ManCou10** (CD<sub>3</sub>OD, 400 MHz).



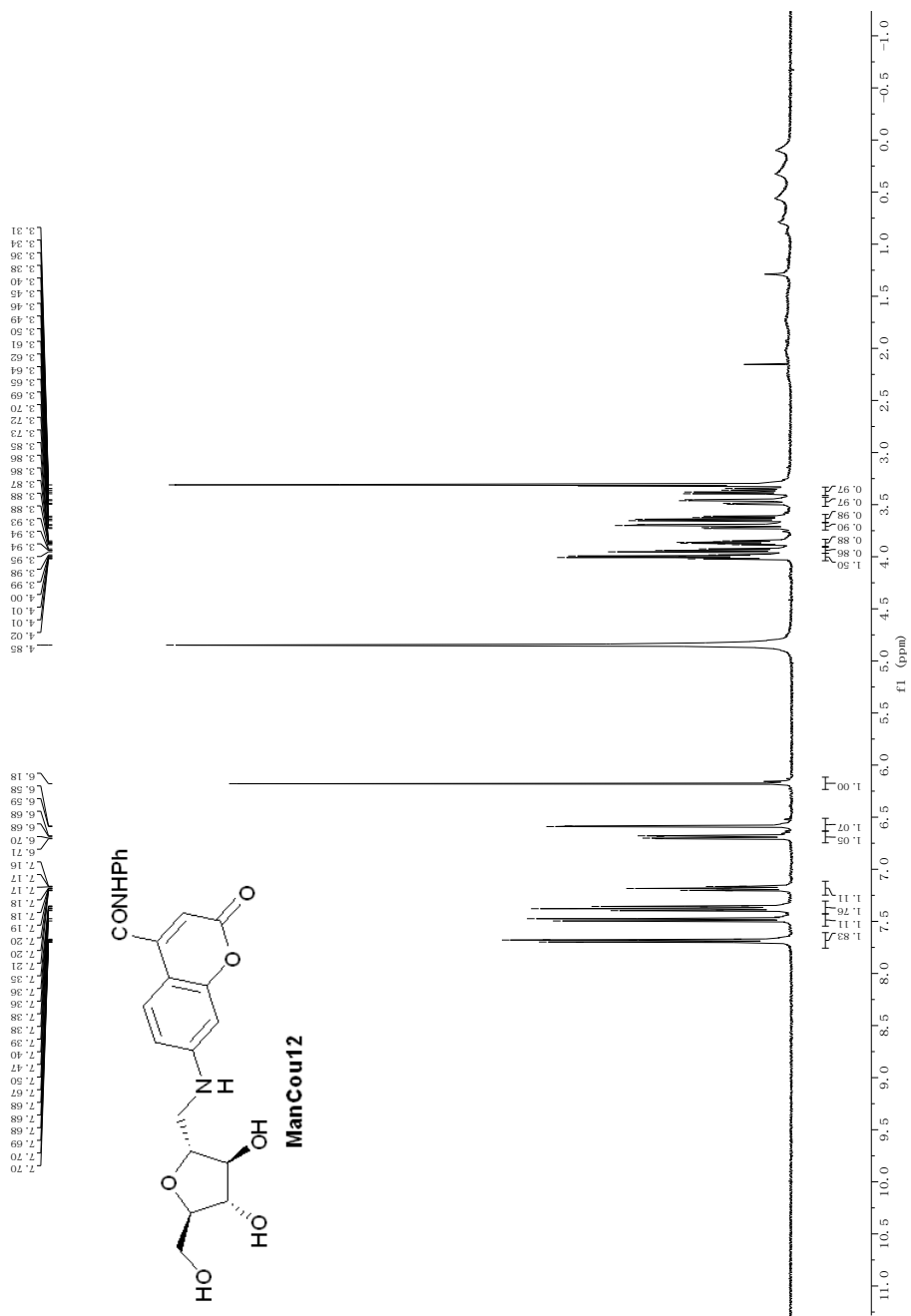
**Figure A25.** <sup>13</sup>C NMR spectrum of **ManCou10** (CD<sub>3</sub>OD, 100 MHz).

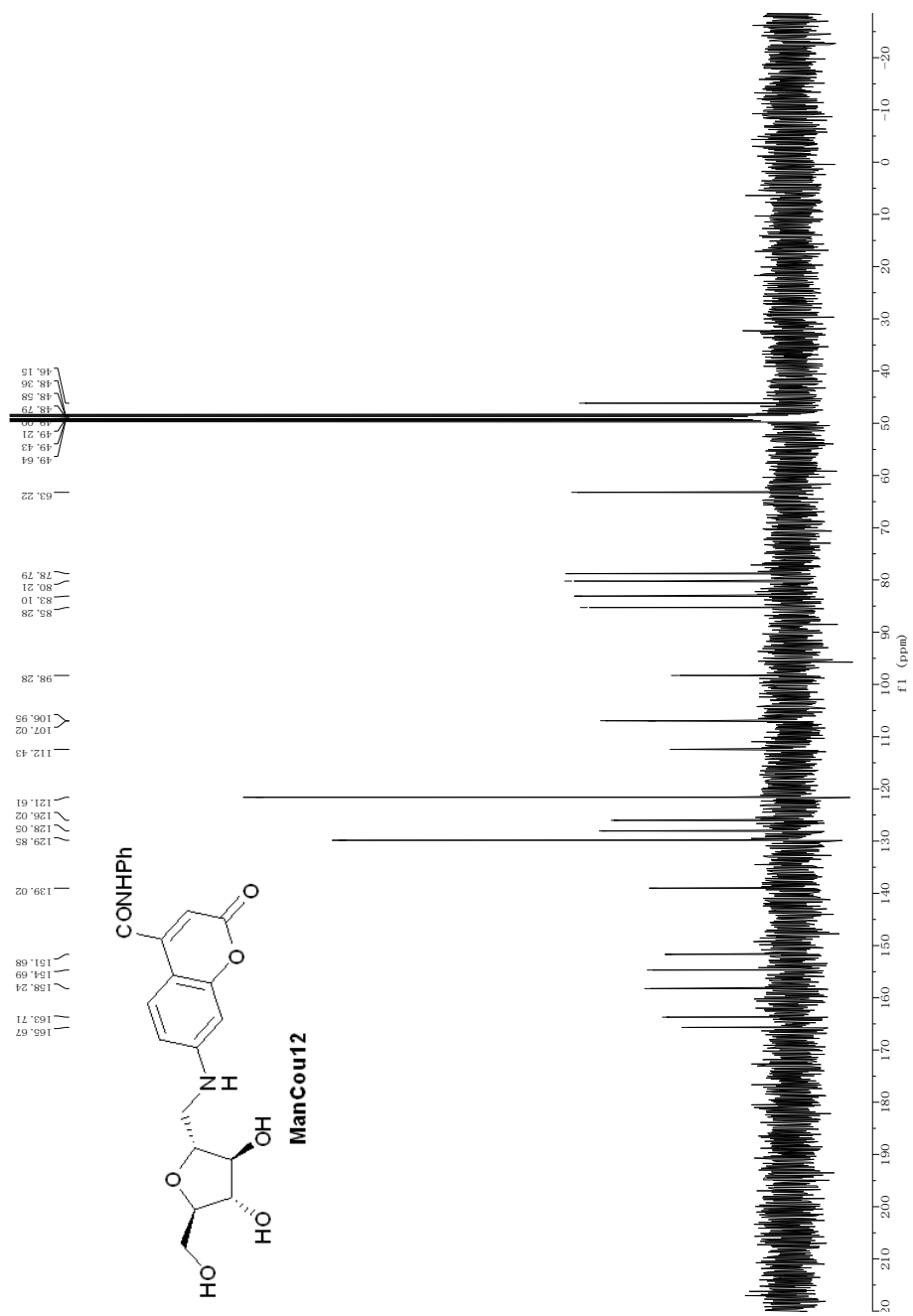


**Figure A26.** <sup>1</sup>H NMR spectrum of **ManCou11** (CD<sub>3</sub>OD, 400 MHz).



**Figure A27.** <sup>13</sup>C NMR spectrum of **ManCou11** (CD<sub>3</sub>OD, 100 MHz).





**Figure A29.**  $^{13}\text{C}$  NMR spectrum of **ManCou12** ( $\text{CD}_3\text{OD}$ , 100 MHz).

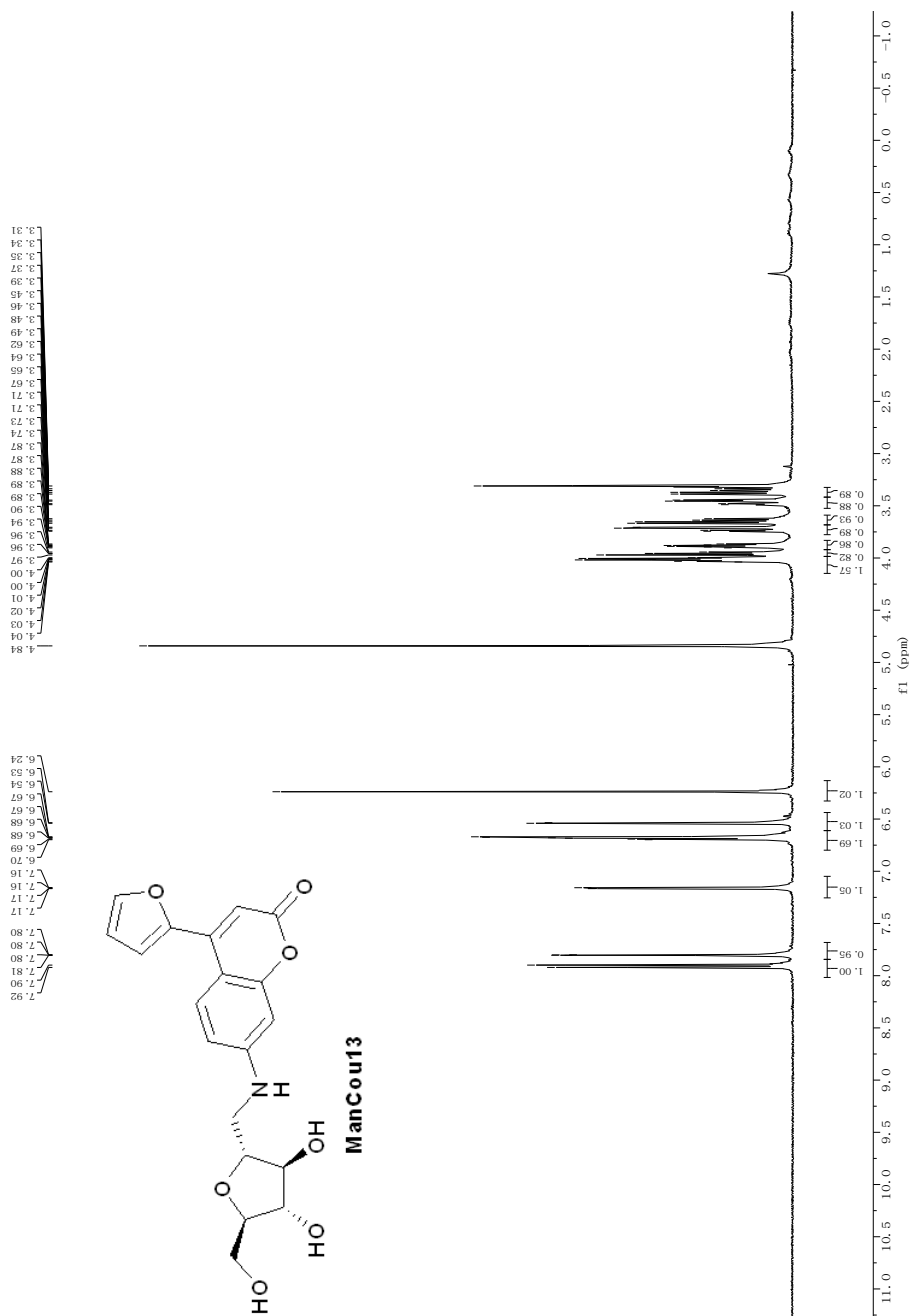
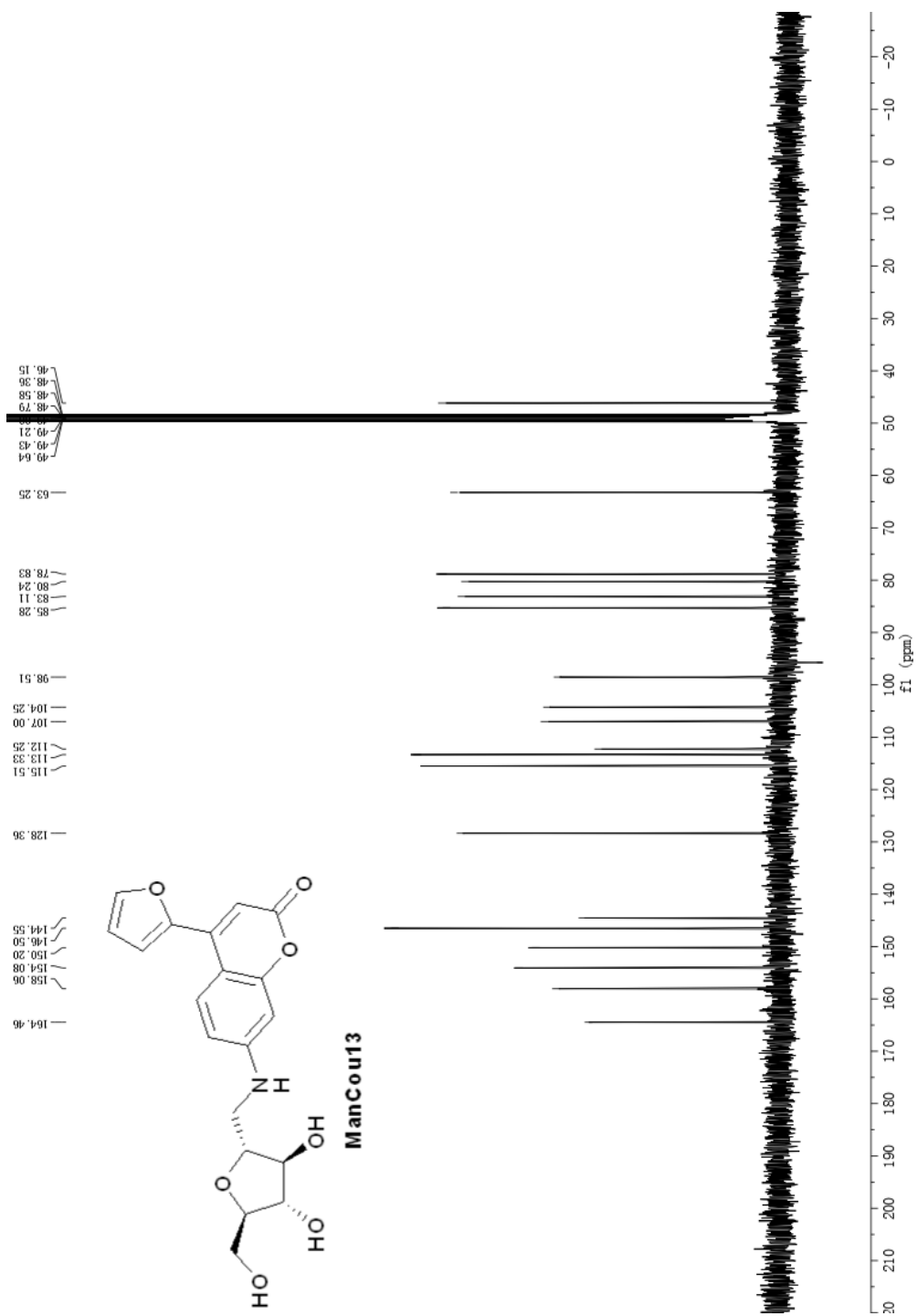
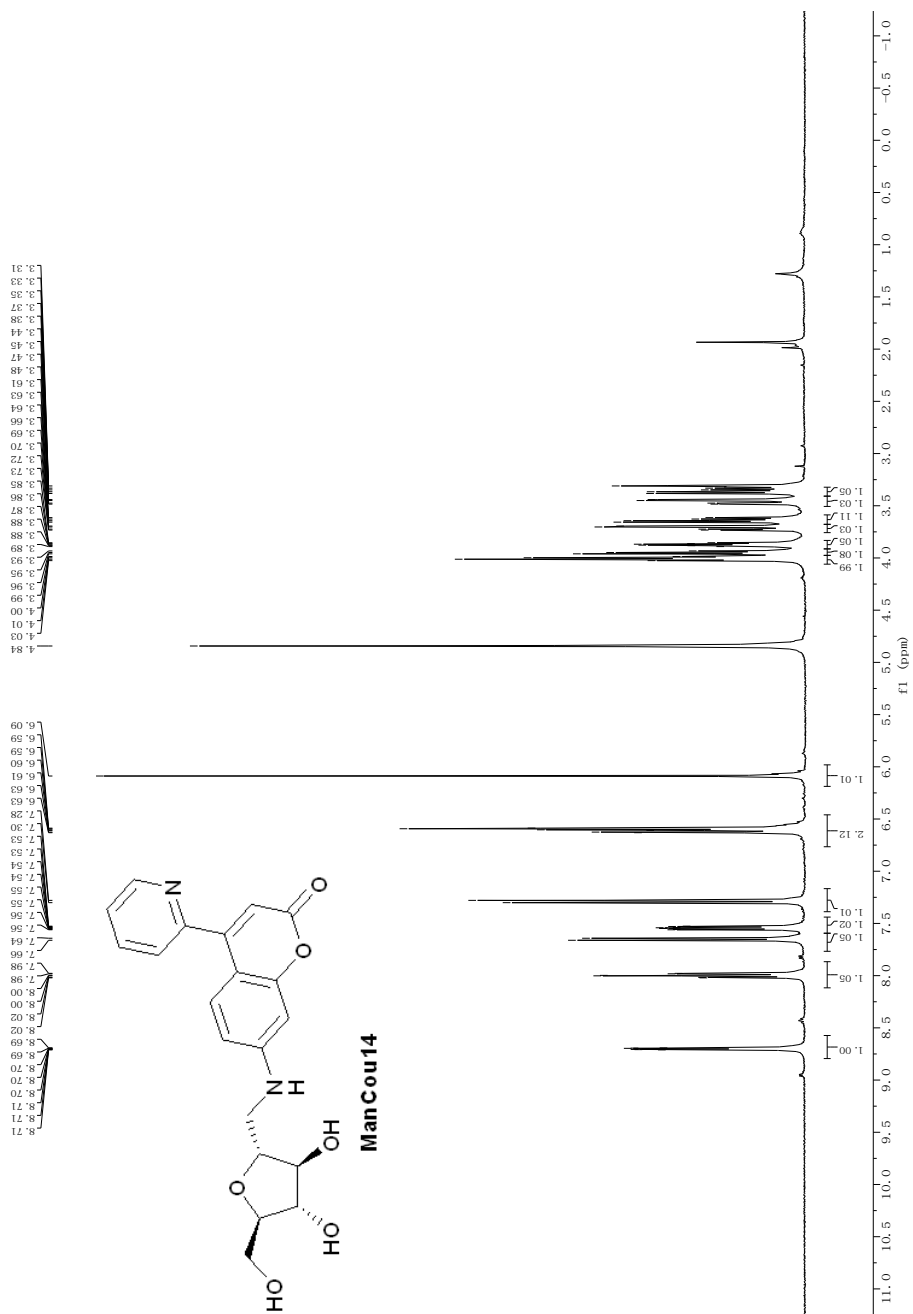


Figure A30. <sup>1</sup>H NMR spectrum of ManCou13 (CD<sub>3</sub>OD, 400 MHz).

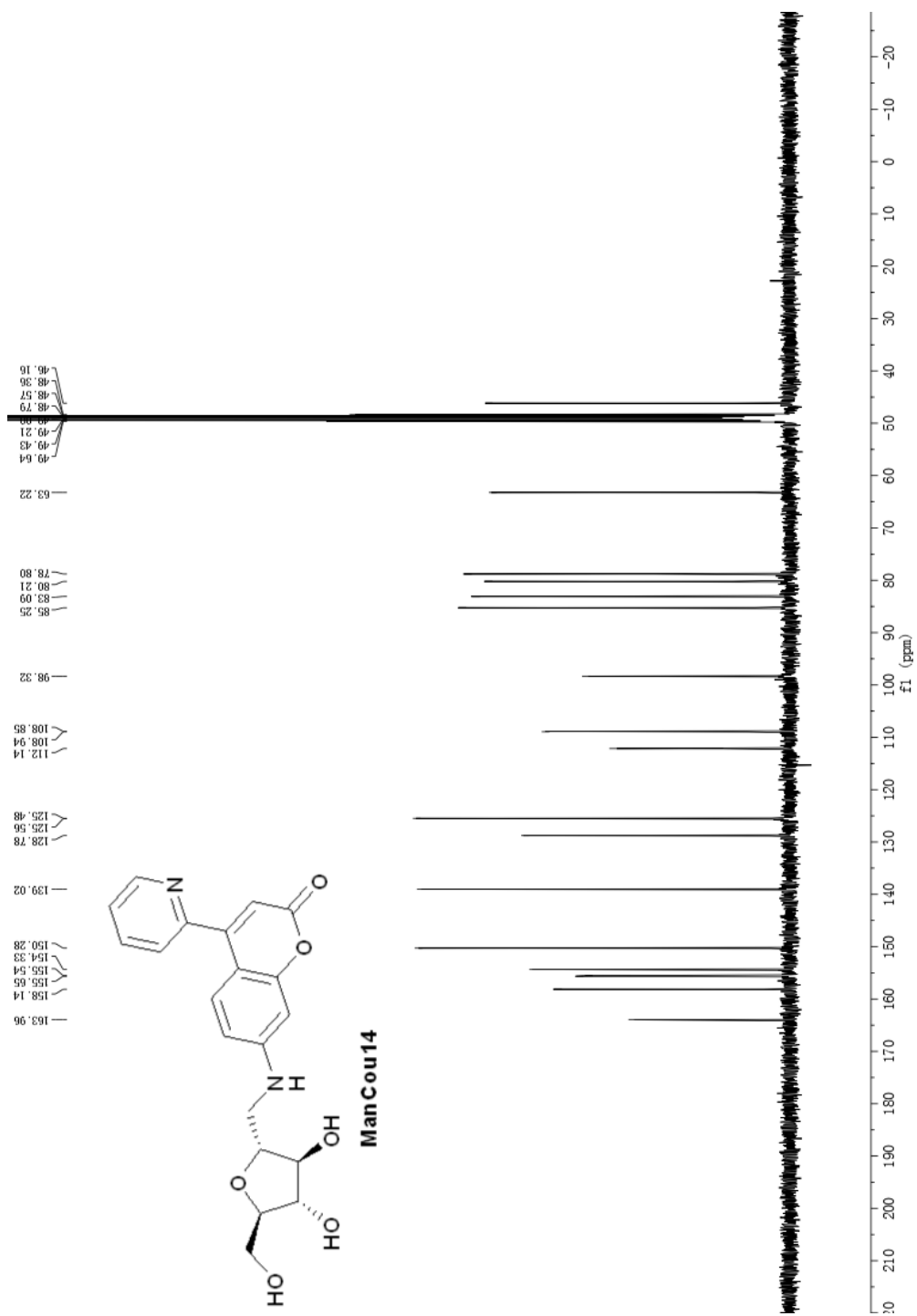




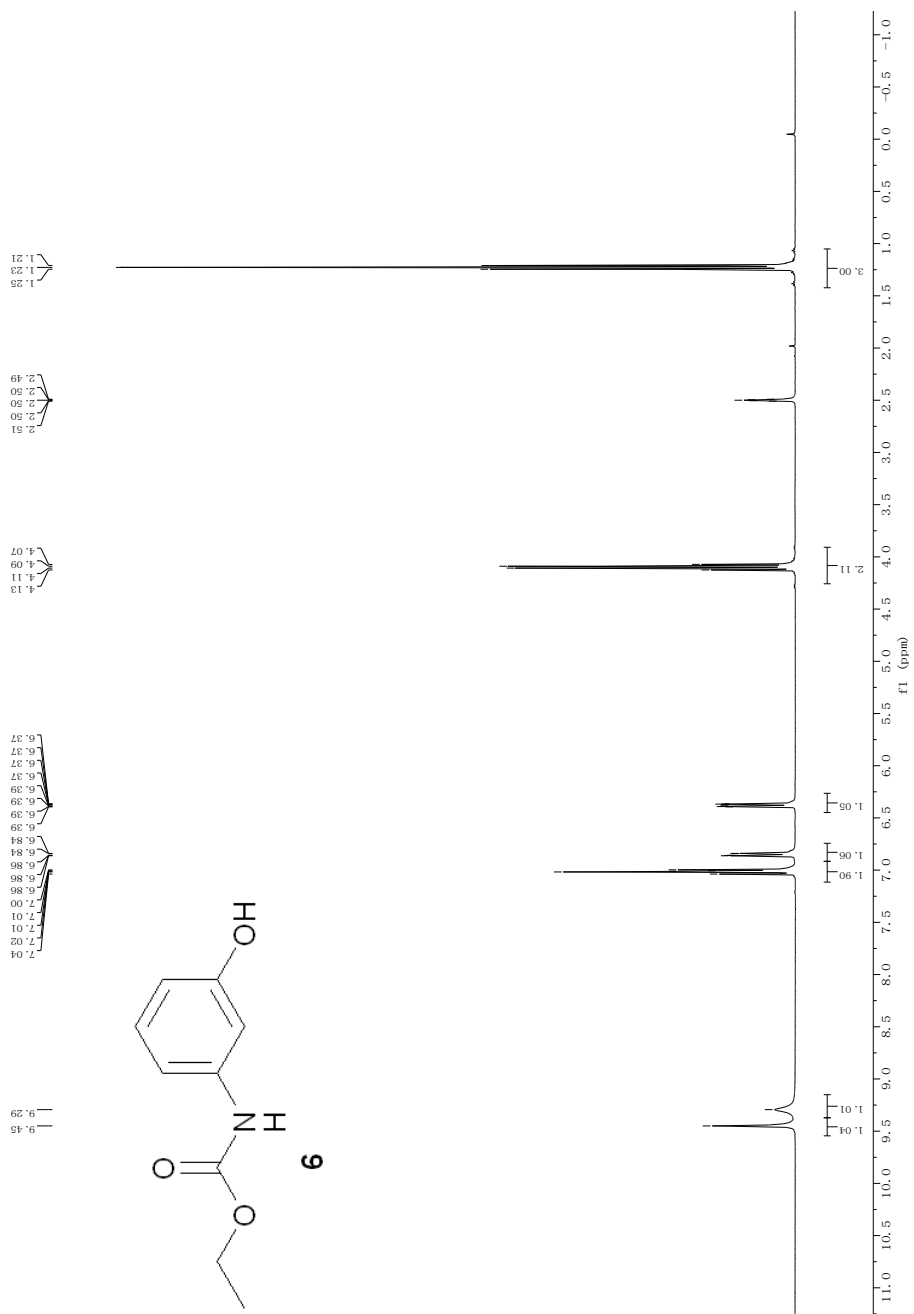
**Figure A31.**  $^{13}\text{C}$  NMR spectrum of **ManCou13** ( $\text{CD}_3\text{OD}$ , 100 MHz).



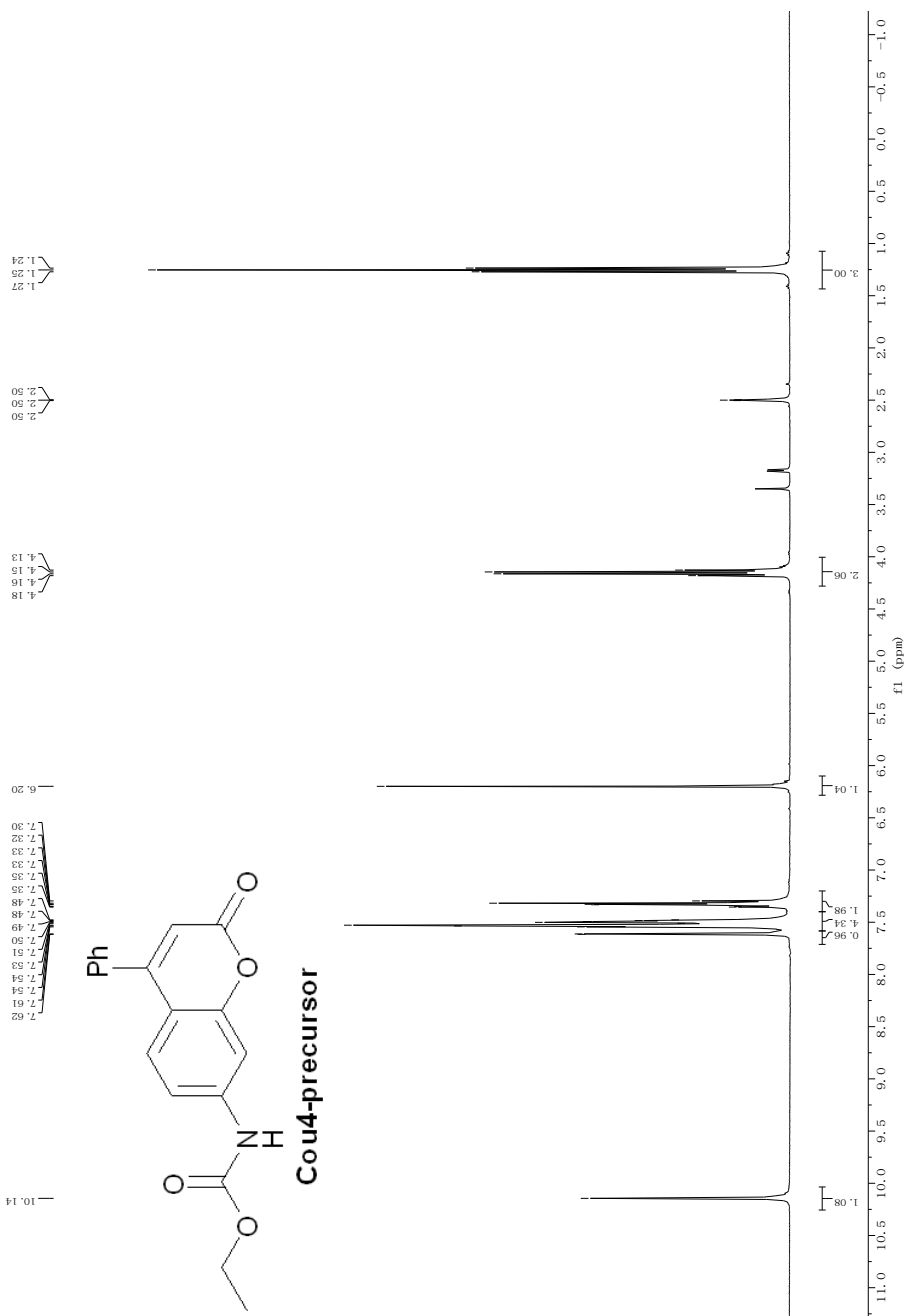
**Figure A32.** <sup>1</sup>H NMR spectrum of **ManCou14** (CD<sub>3</sub>OD, 400 MHz).



**Figure A33.** <sup>13</sup>C NMR spectrum of **ManCou14** (CD<sub>3</sub>OD, 400 MHz).



**Figure A34.** <sup>1</sup>H NMR spectrum of **6** (DMSO-d<sub>6</sub>, 400 MHz).



**Figure A35.** <sup>1</sup>H NMR spectrum of **Cou4-precursor** (DMSO-d<sub>6</sub>, 400 MHz).

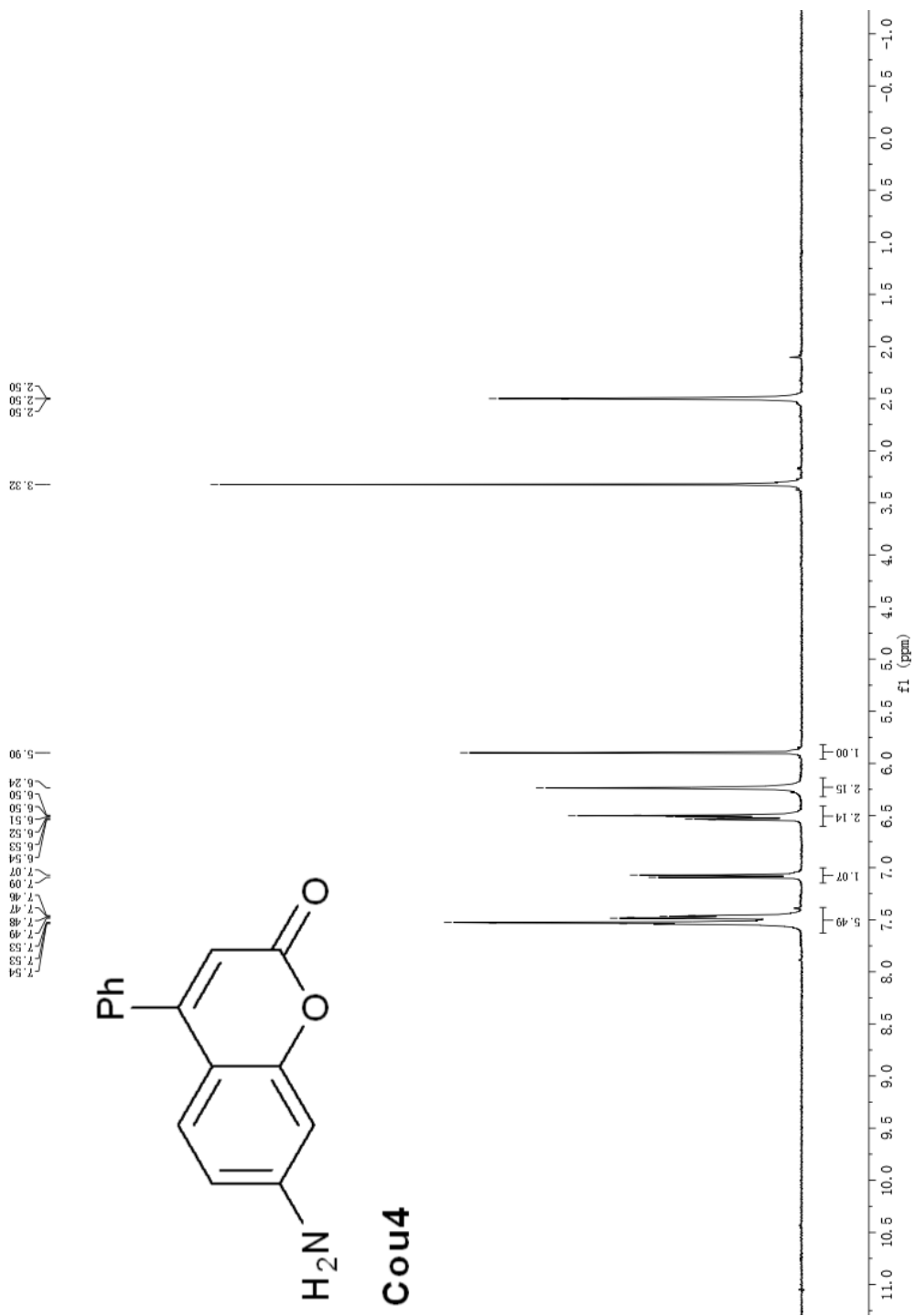
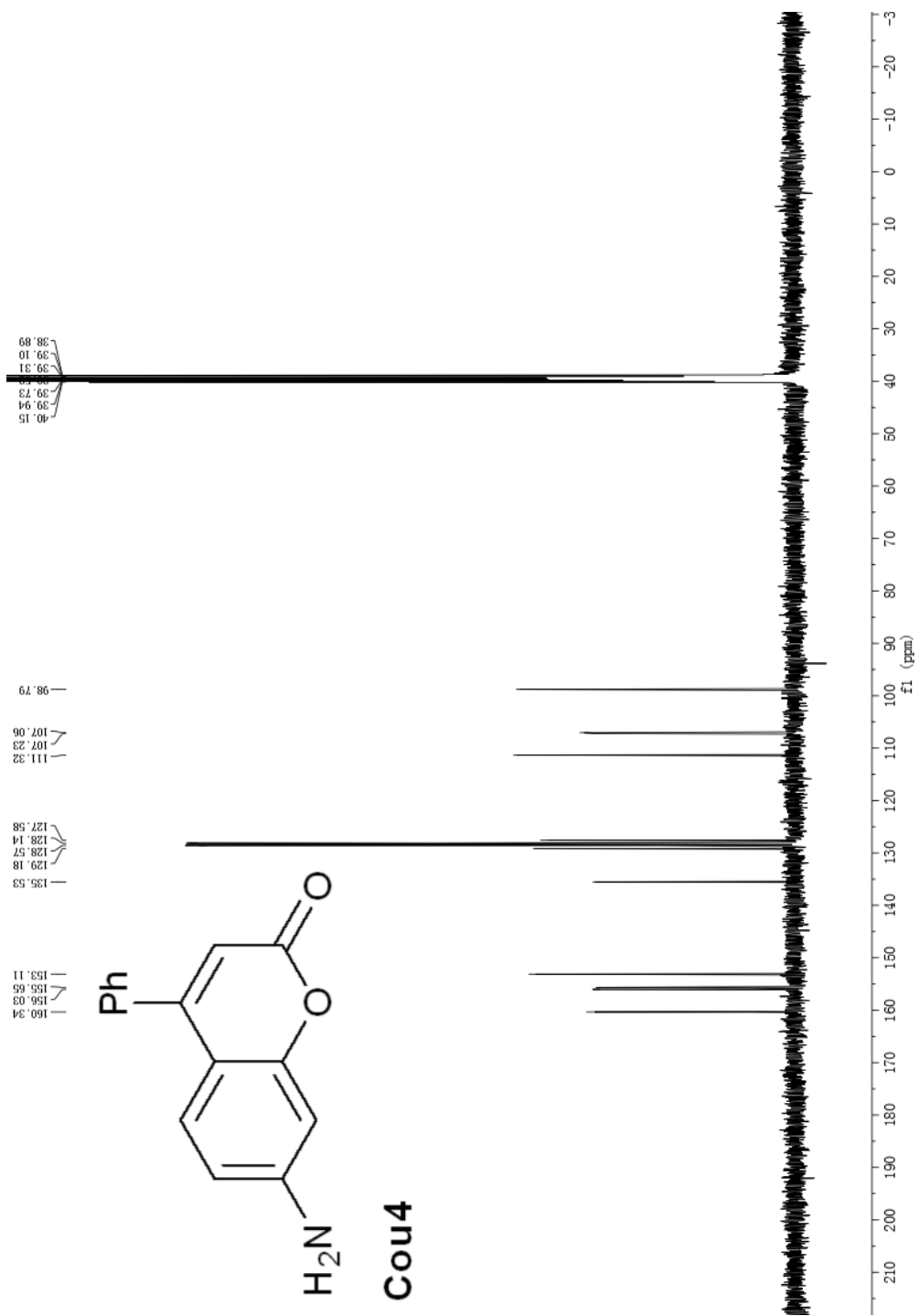
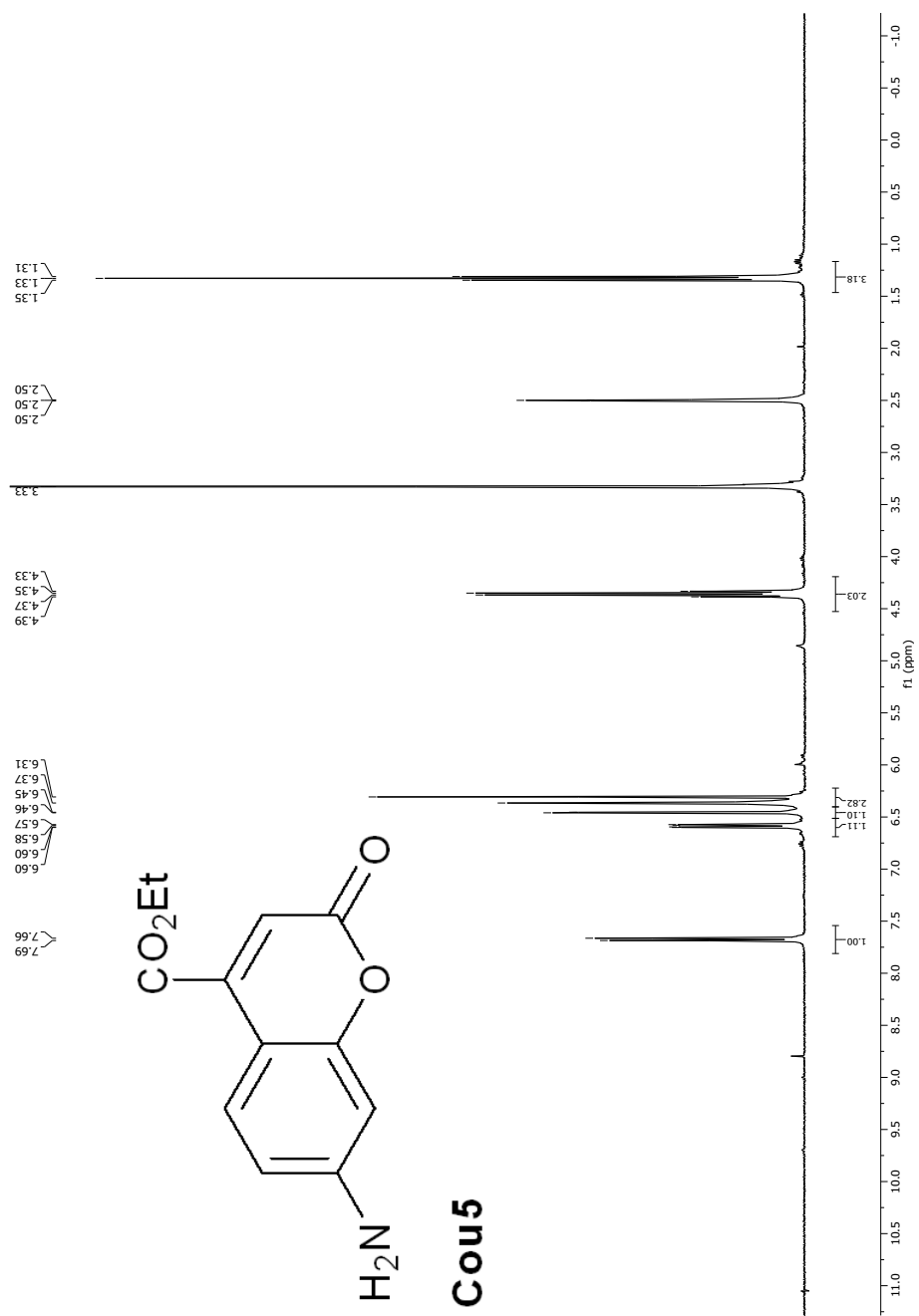


Figure A36. <sup>1</sup>H NMR spectrum of Cou4 (DMSO-d<sub>6</sub>, 400 MHz).

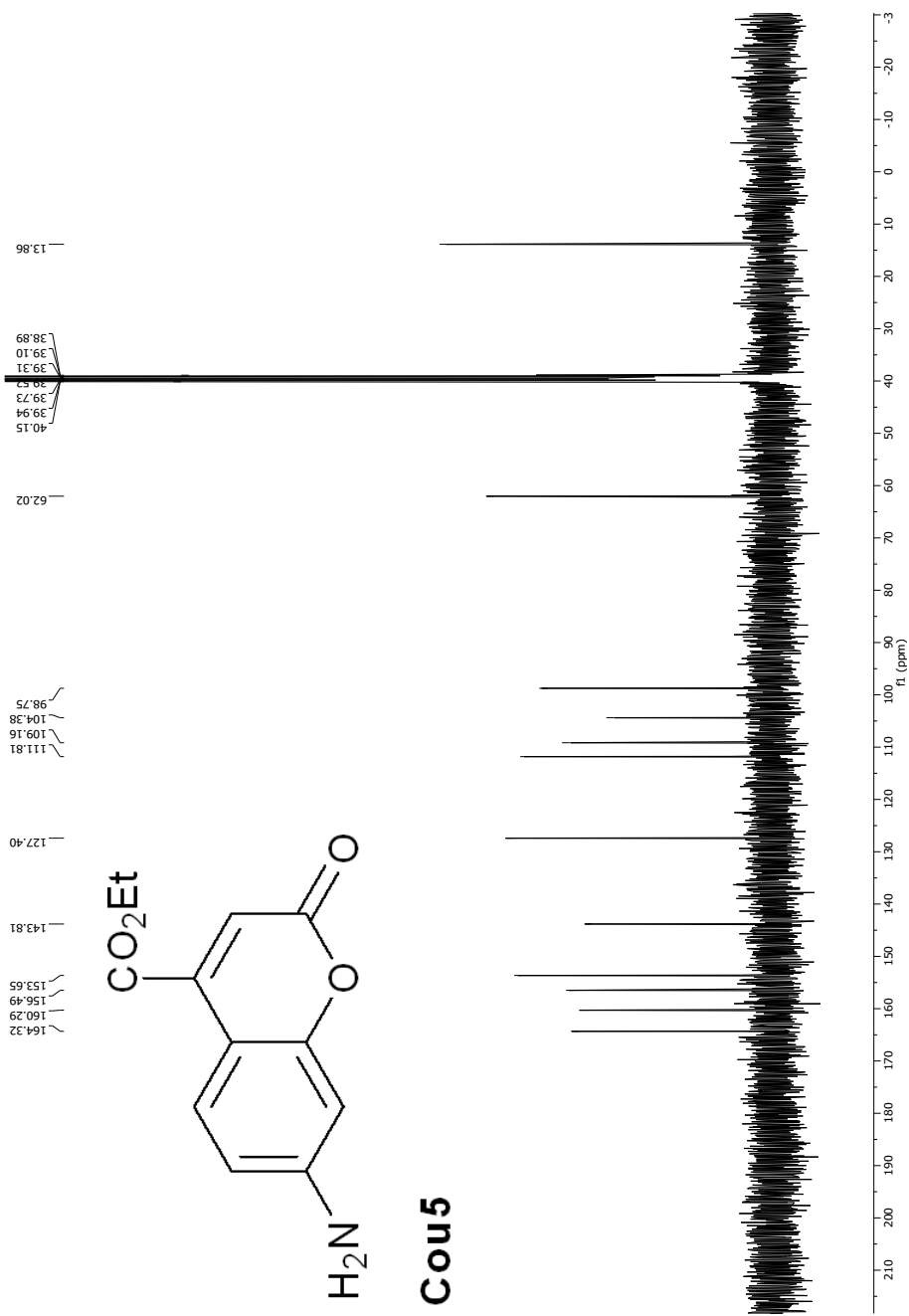


**Figure A37.**  $^{13}\text{C}$  NMR spectrum of **Cou4** (DMSO- $d_6$ , 100 MHz).

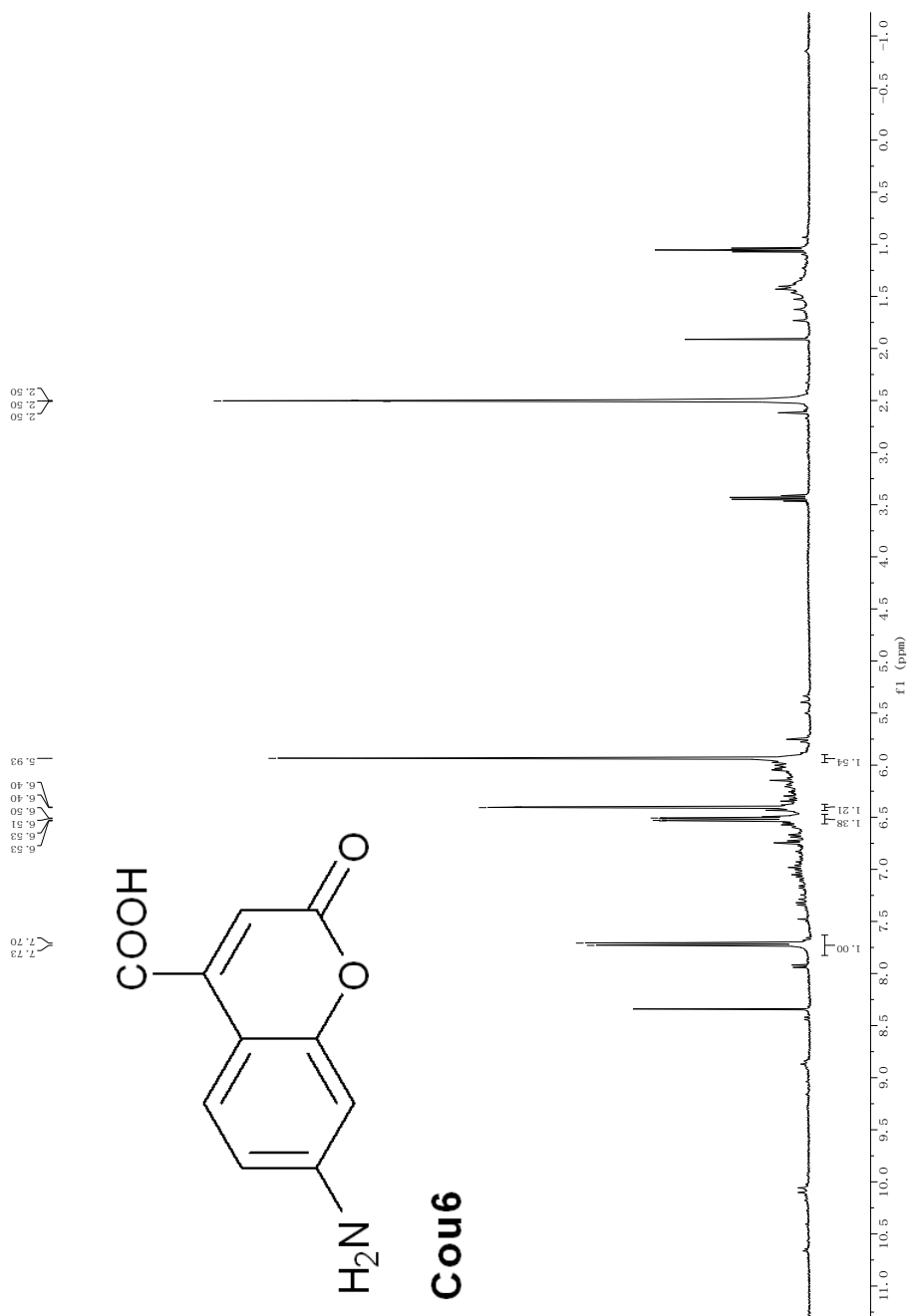


**Figure A38.** <sup>1</sup>H NMR spectrum of **Cou5** (DMSO-d<sub>6</sub>, 400 MHz).

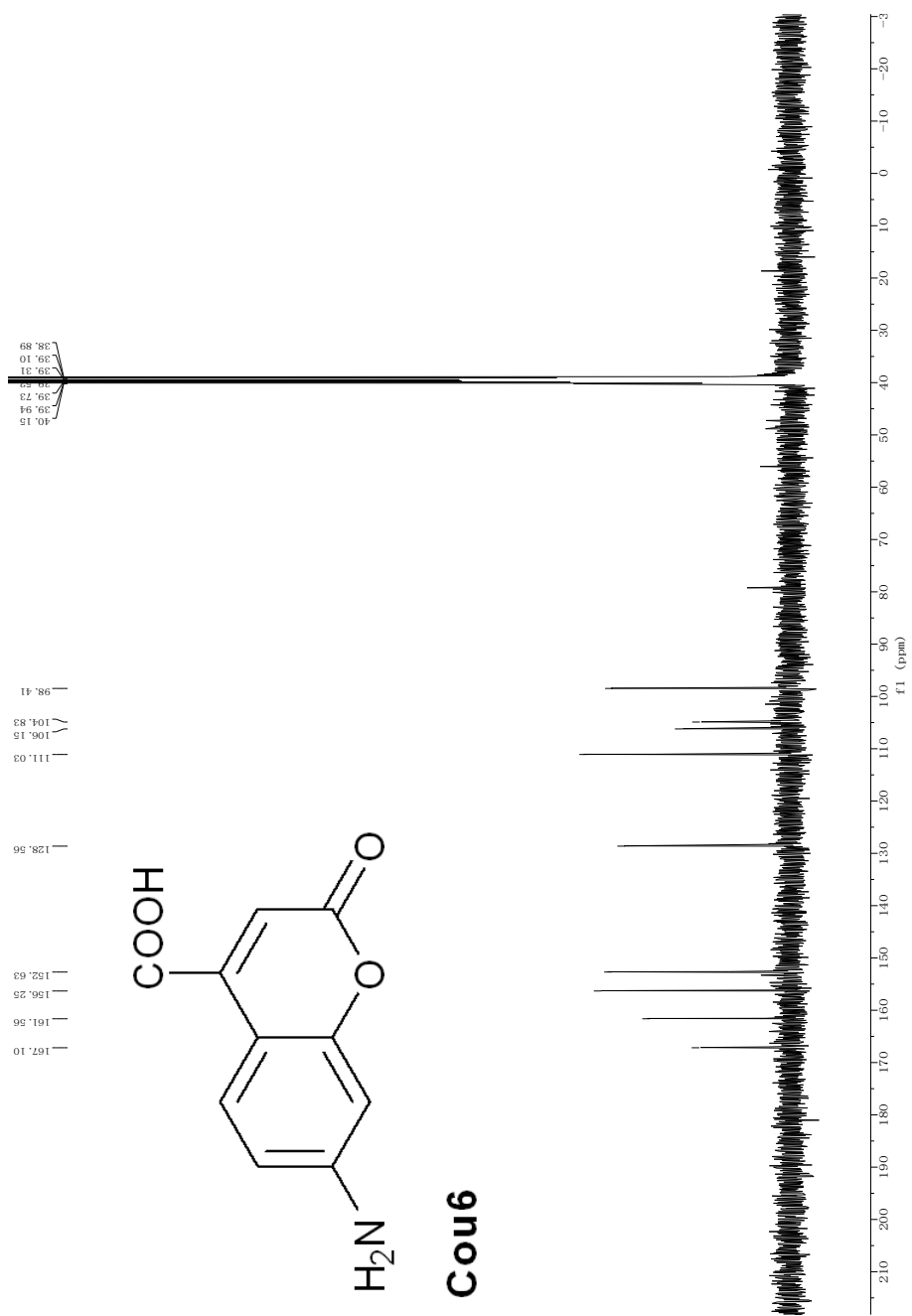




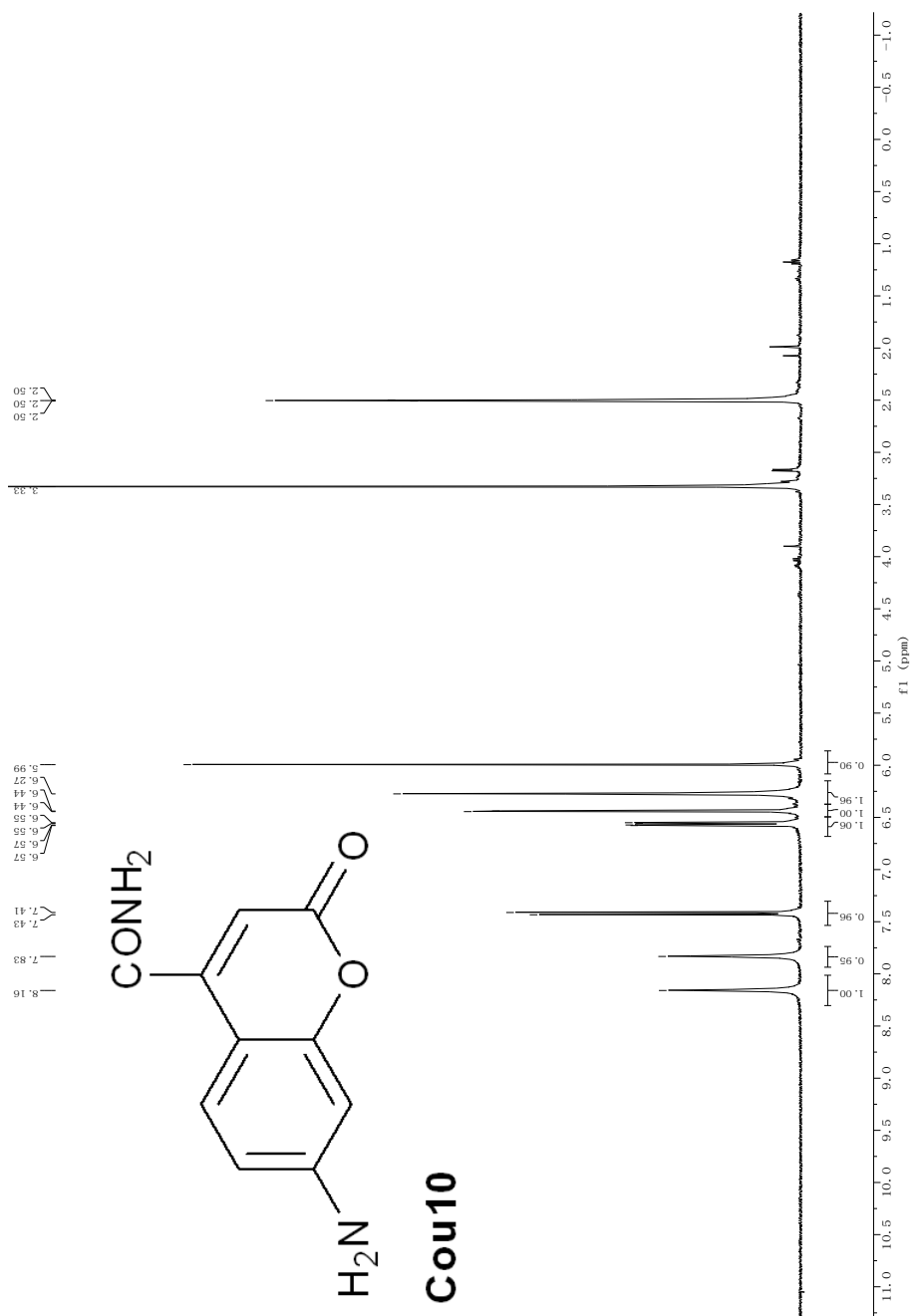
**Figure A39.**  $^{13}\text{C}$  NMR spectrum of **Cou5** (DMSO- $d_6$ , 100 MHz).



**Figure A40.**  $^1\text{H}$  NMR spectrum of **Cou6** (DMSO- $d_6$ , 400 MHz).



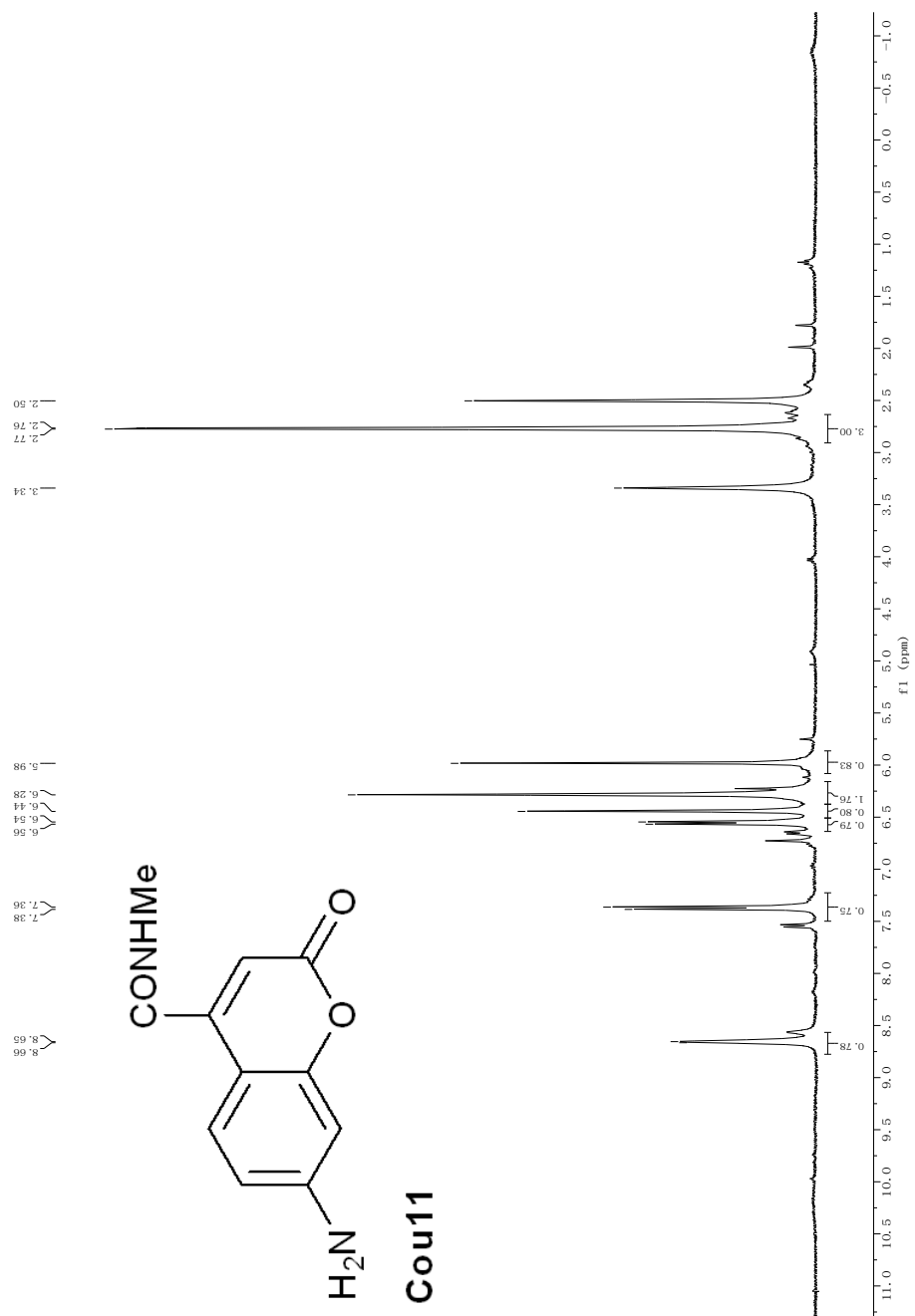
**Figure A41.** <sup>13</sup>C NMR spectrum of **Cou6** (DMSO-d<sub>6</sub>, 100 MHz).



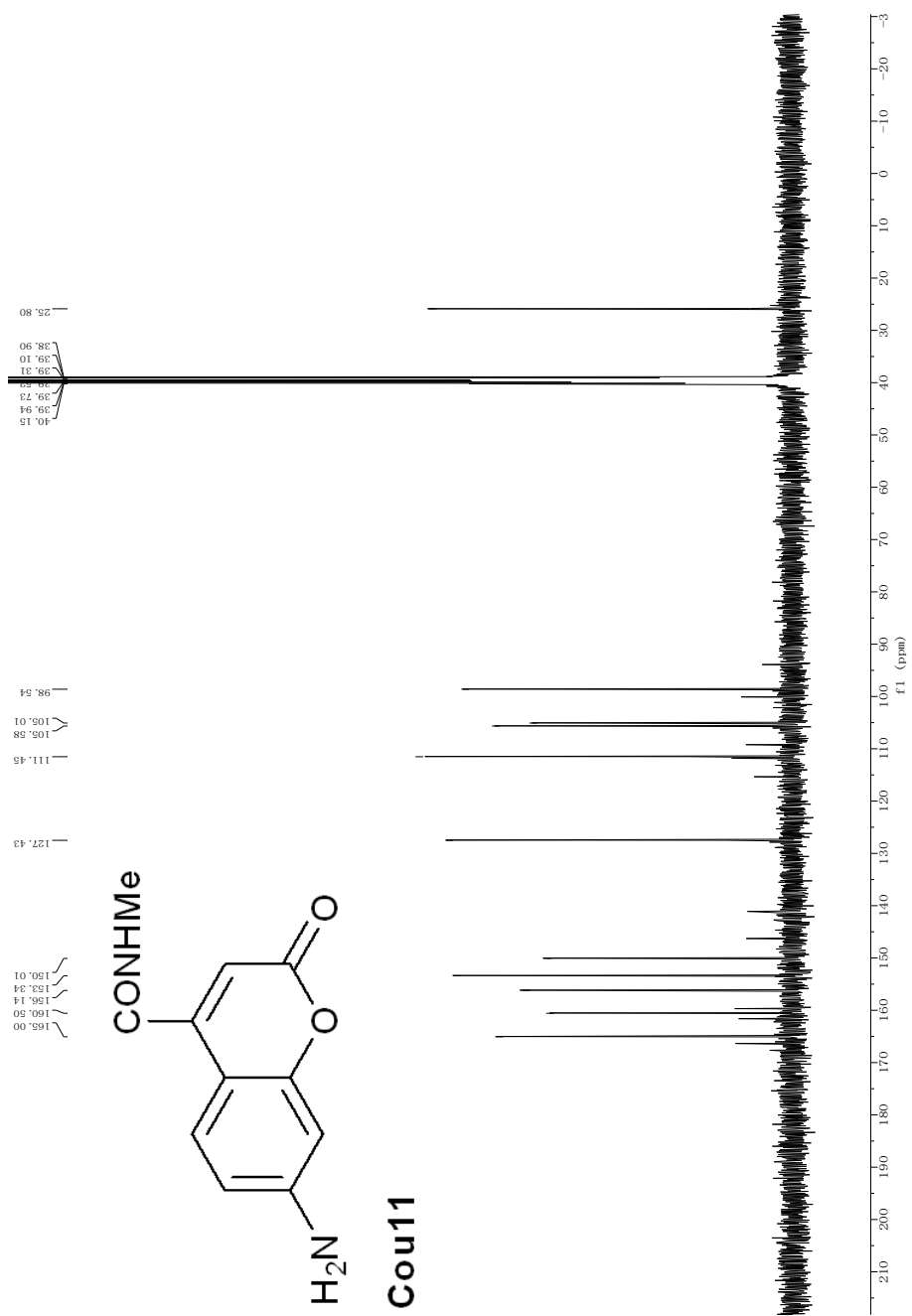
**Figure SA2.** <sup>1</sup>H NMR spectrum of **Cou10** (DMSO-d<sub>6</sub>, 400 MHz).



**Figure A43.** <sup>13</sup>C NMR spectrum of **Cou10** (DMSO-d<sub>6</sub>, 100 MHz).



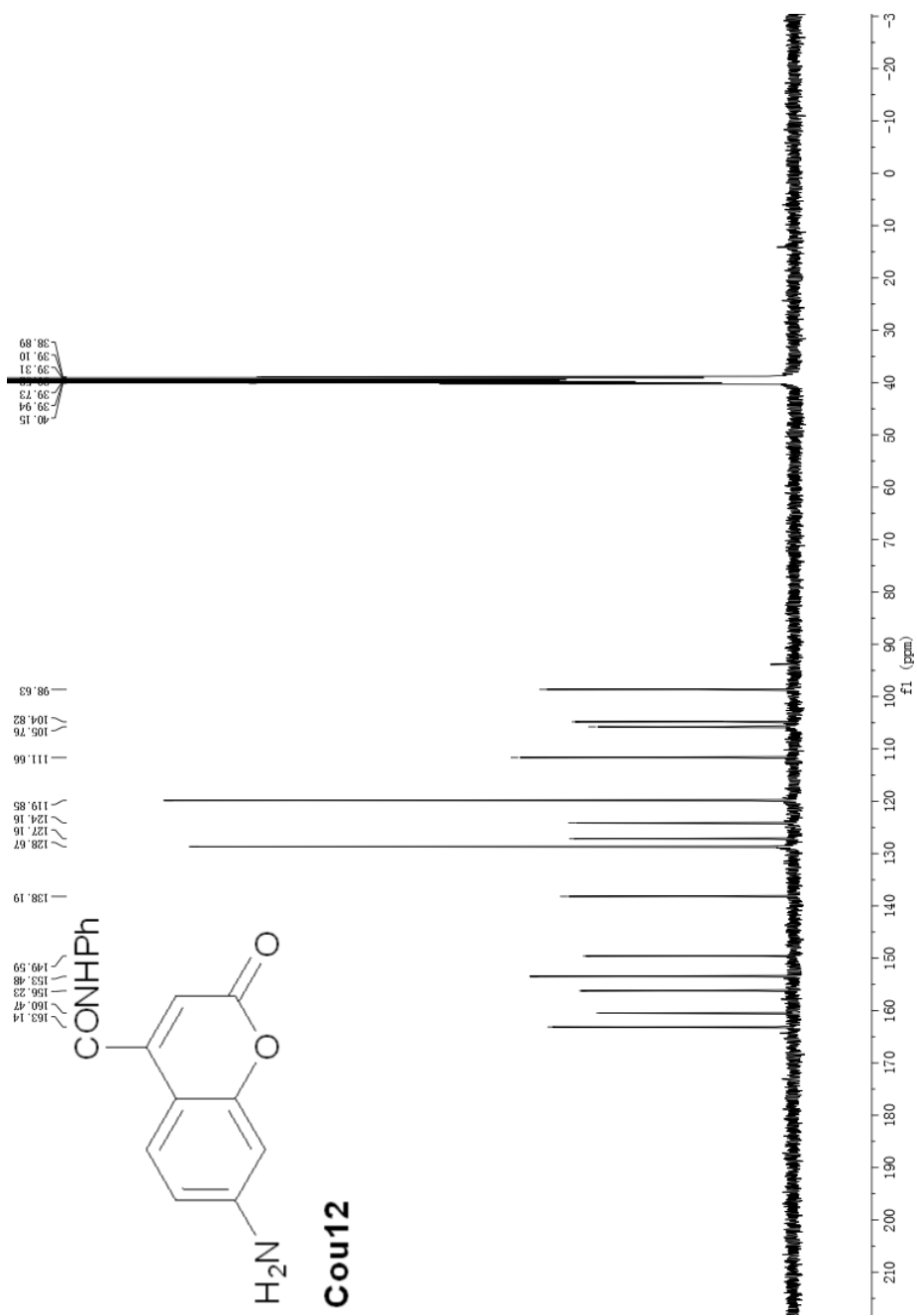
**Figure A44.** <sup>1</sup>H NMR spectrum of **Cou11** (DMSO-d<sub>6</sub>, 400 MHz).



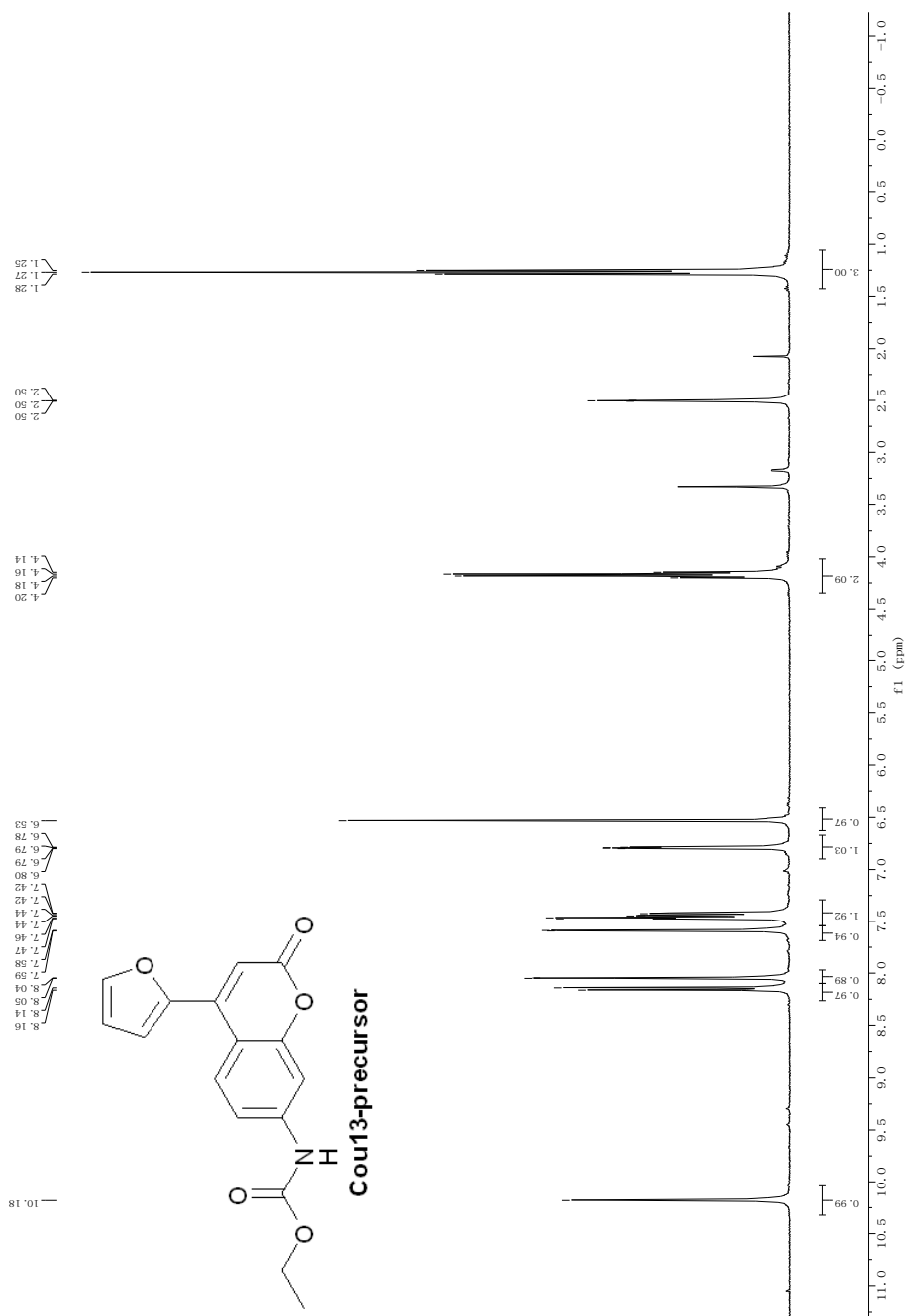
**Figure A45.** <sup>13</sup>C NMR spectrum of **Cou11** (DMSO-d<sub>6</sub>, 100 MHz).



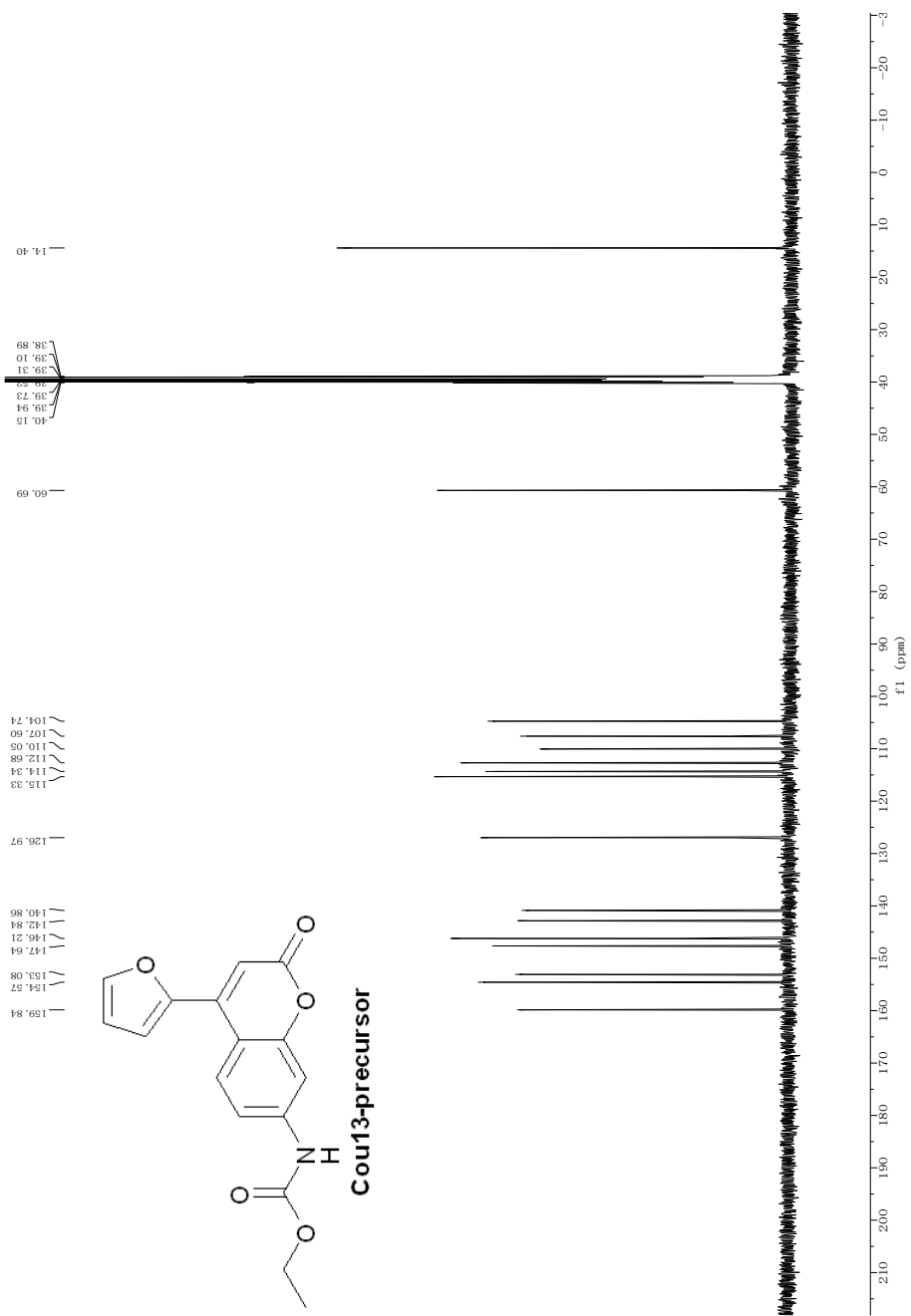




**Figure A47.**  $^{13}\text{C}$  NMR spectrum of **Cou12** (DMSO- $\text{d}_6$ , 100 MHz).



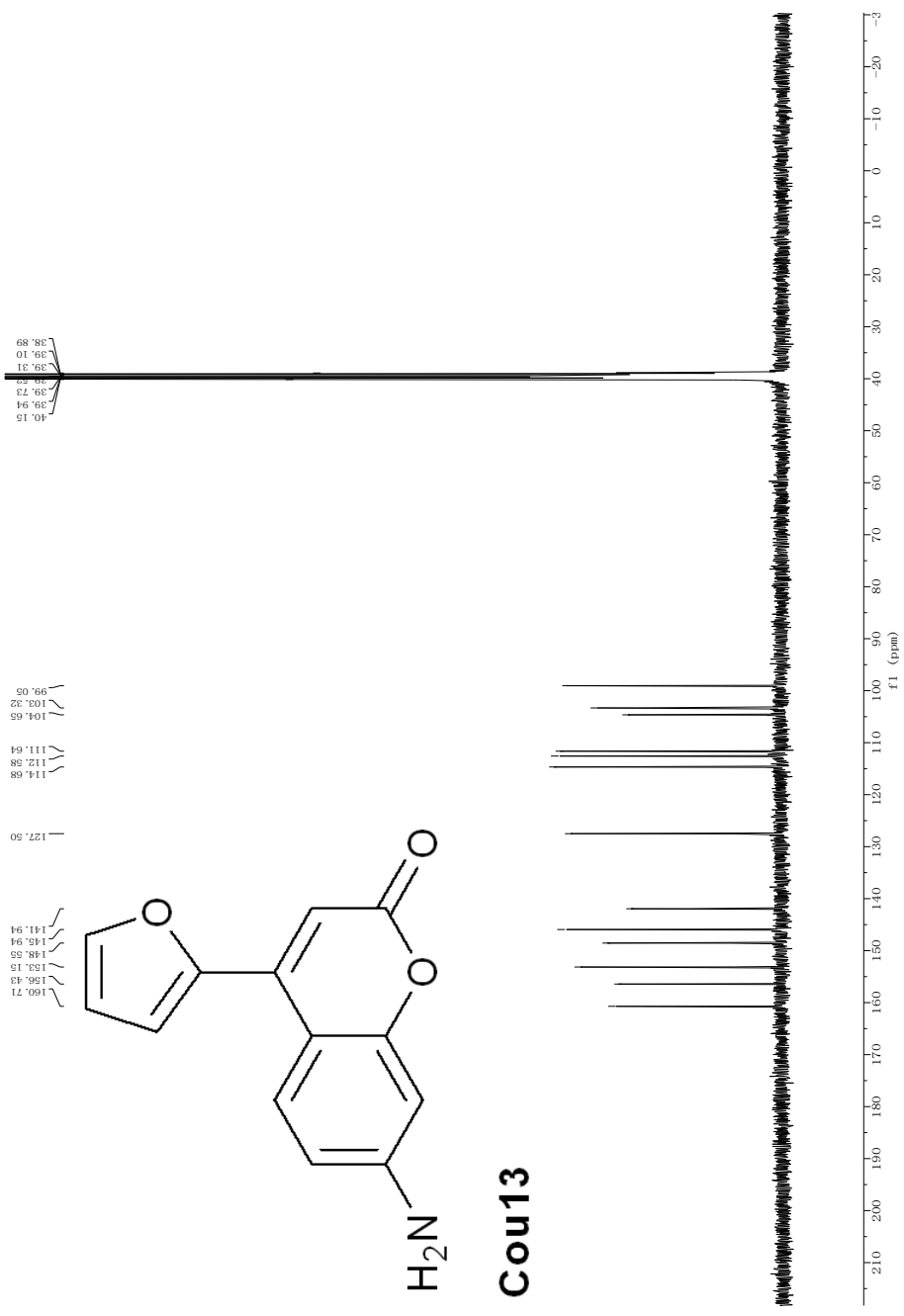
**Figure A48.** <sup>1</sup>H NMR spectrum of **Cou13-precursor** (DMSO-d<sub>6</sub>, 400 MHz).



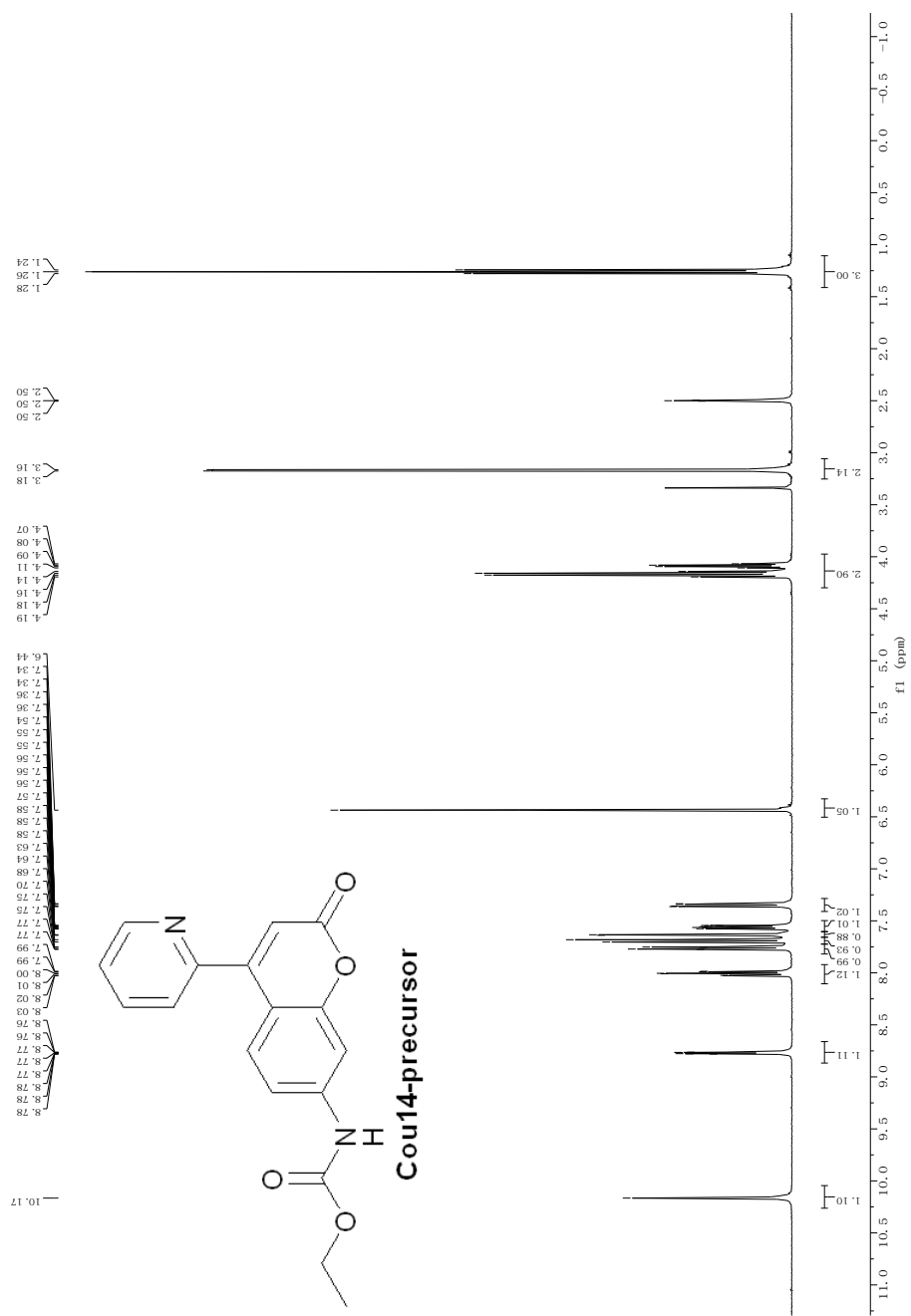
**Figure A49.** <sup>13</sup>C NMR spectrum of **Cou13-precursor** (DMSO-d<sub>6</sub>, 100 MHz).

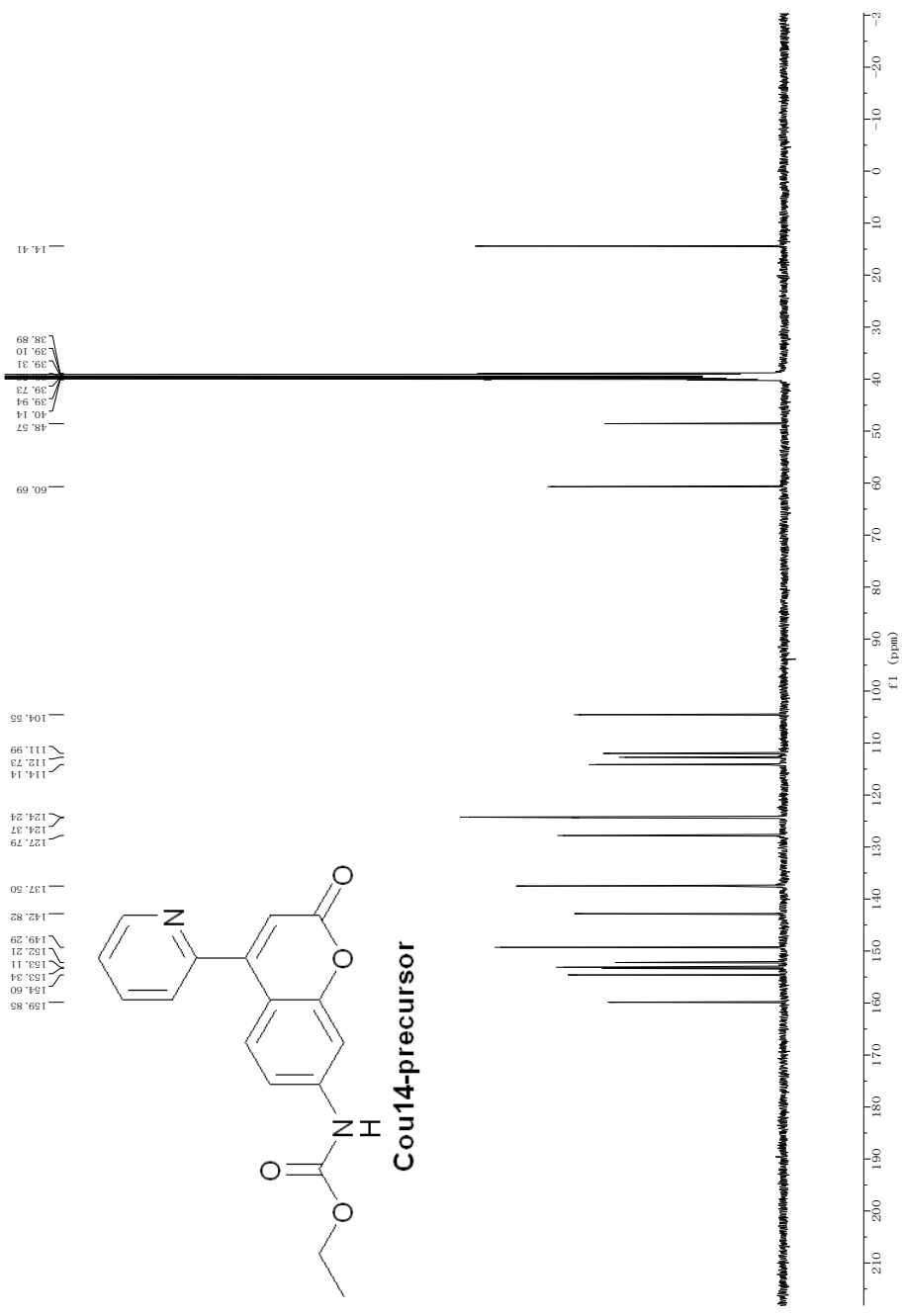


**Figure A50.** <sup>1</sup>H NMR spectrum of **Cou13** (DMSO-d<sub>6</sub>, 400 MHz).



**Figure A51.** <sup>13</sup>C NMR spectrum of **Cou13** (DMSO-d<sub>6</sub>, 100 MHz).

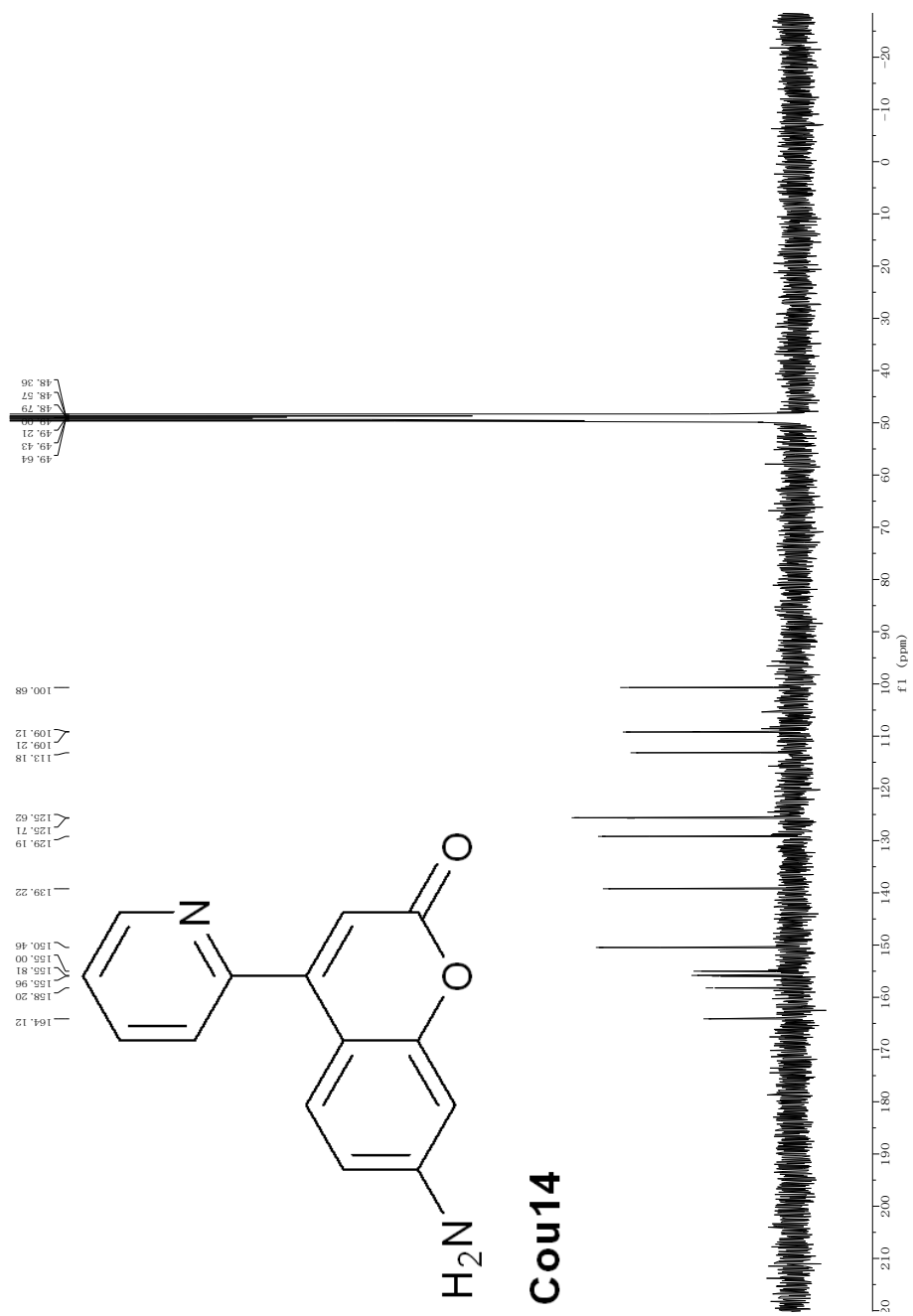




**Figure A53.** <sup>13</sup>C NMR spectrum of **Cou14-precursor** (DMSO-d<sub>6</sub>, 100 MHz).







**Figure A55.** <sup>13</sup>C NMR spectrum of **Cou14** (DMSO-d<sub>6</sub>, 100 MHz).

## A.9 HRMS data for ManCou3.

Figure A56. HRMS data for ManCou1.

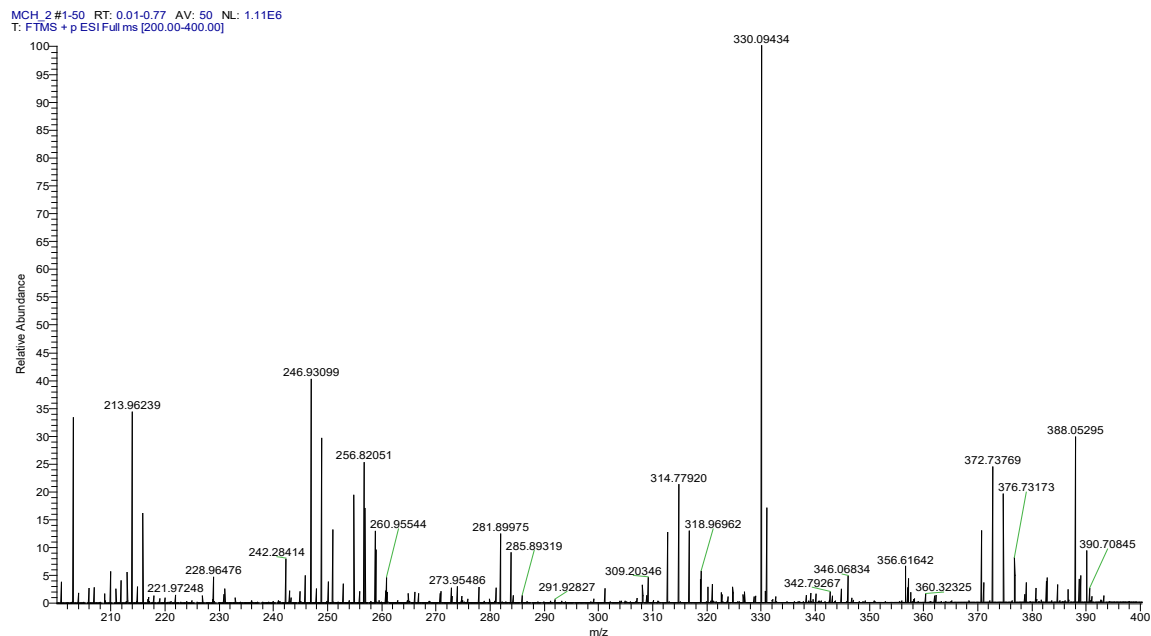
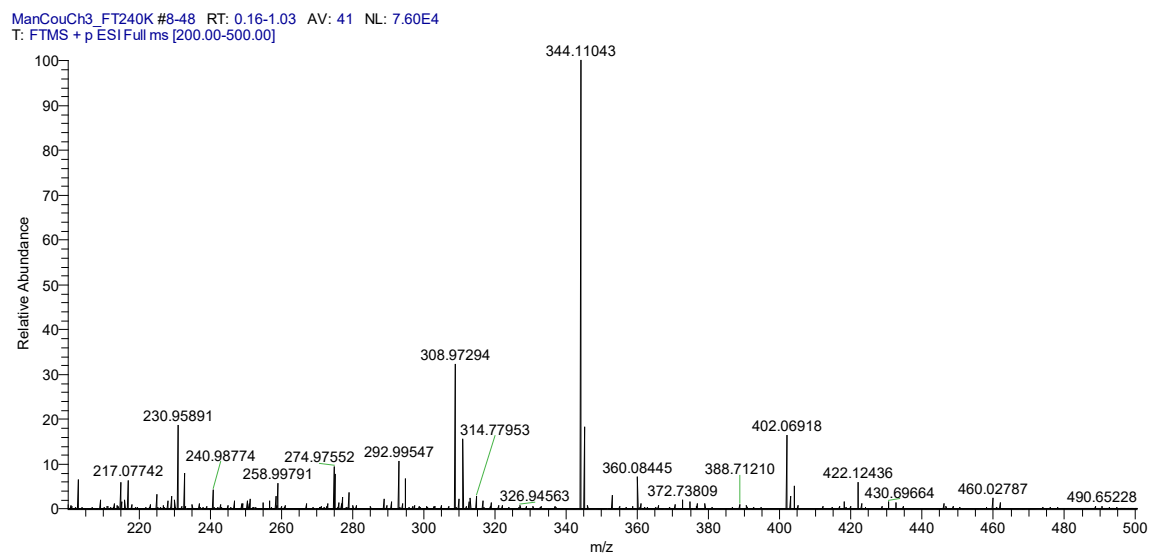
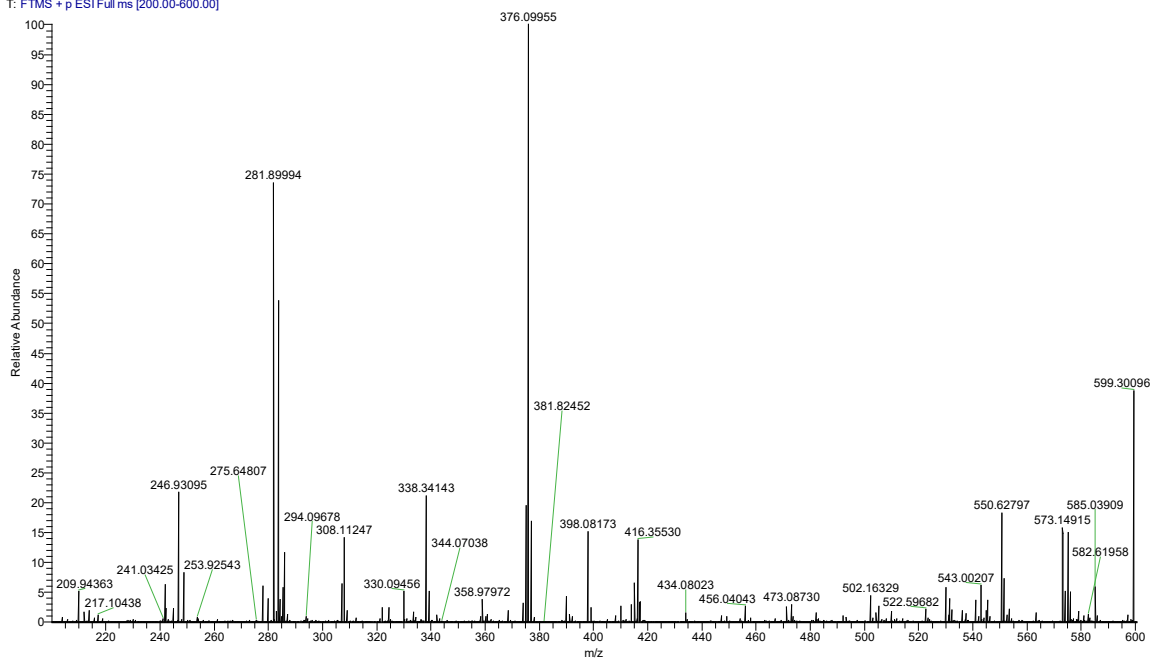


Figure A57. HRMS data for ManCou2.



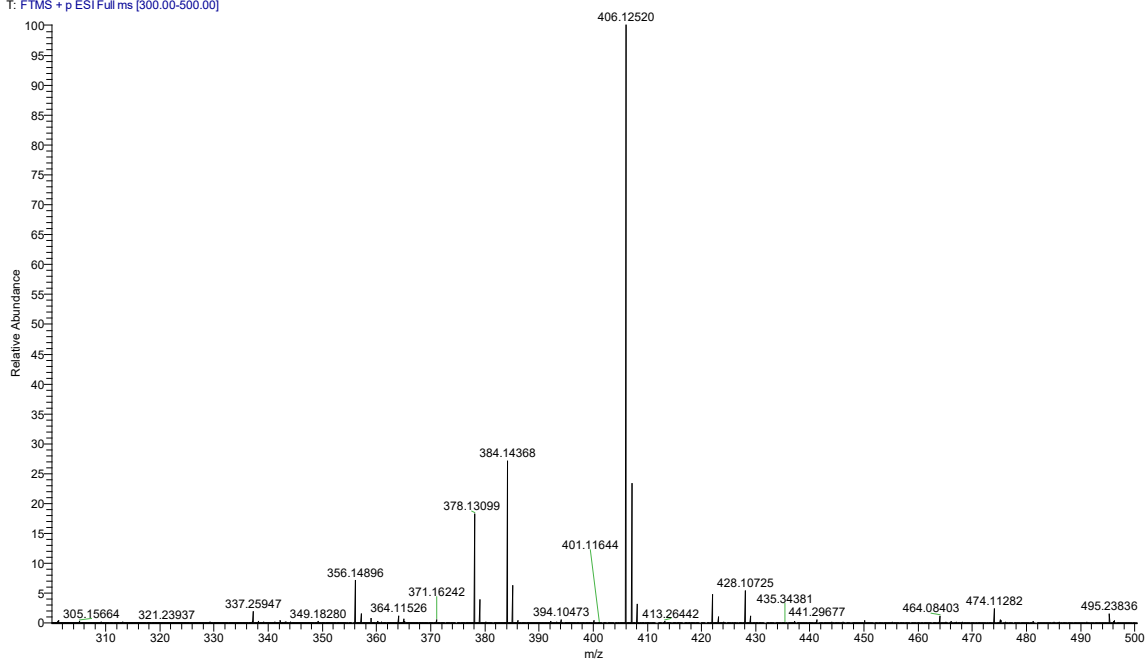
**Figure A58. HRMS data for ManCou3.**

MC3\_240K #1-49 RT: 0.01-0.70 AV: 49 NL: 2.35E6  
T: FTMS + p ESI Full ms [200.00-600.00]

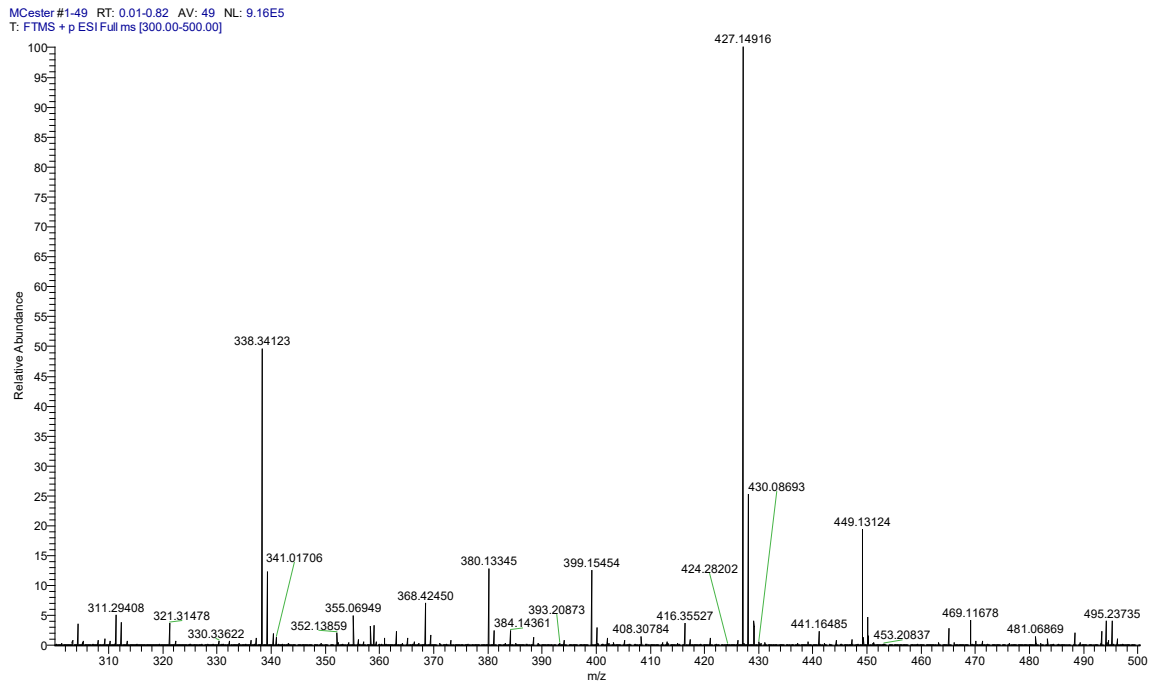


**Figure A59. HRMS data for ManCou4.**

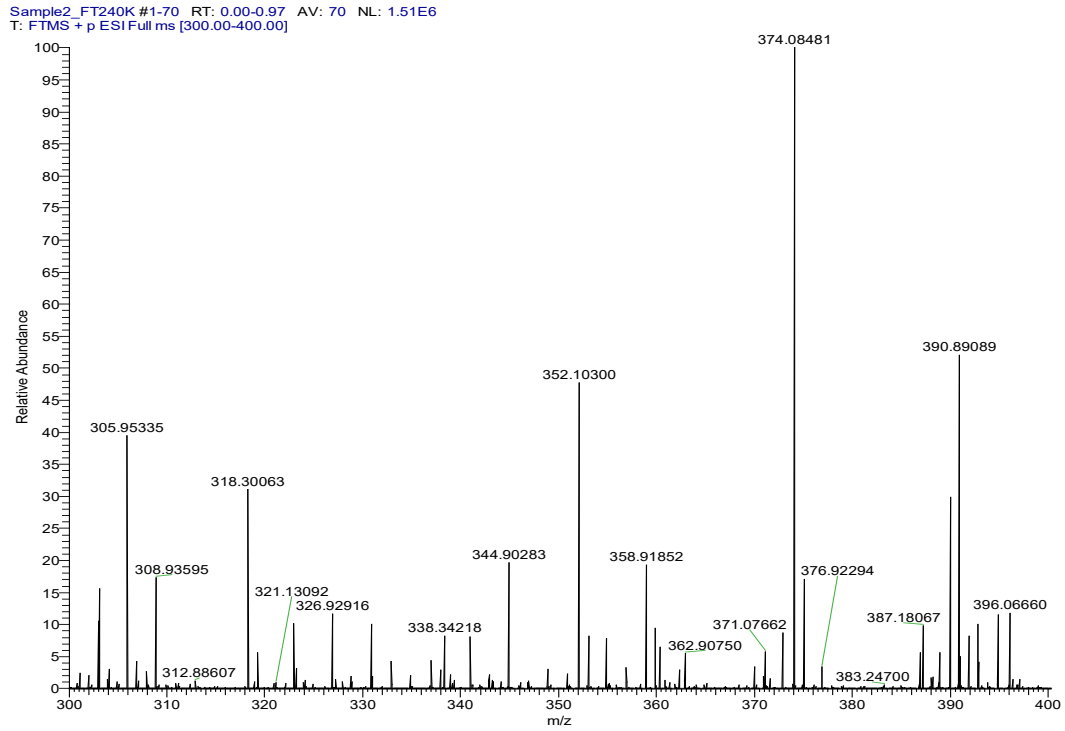
MCP#1-49 RT: 0.00-0.71 AV: 49 NL: 4.96E6  
T: FTMS + p ESI Full ms [300.00-500.00]



**Figure A60.** HRMS data for **ManCou5**.

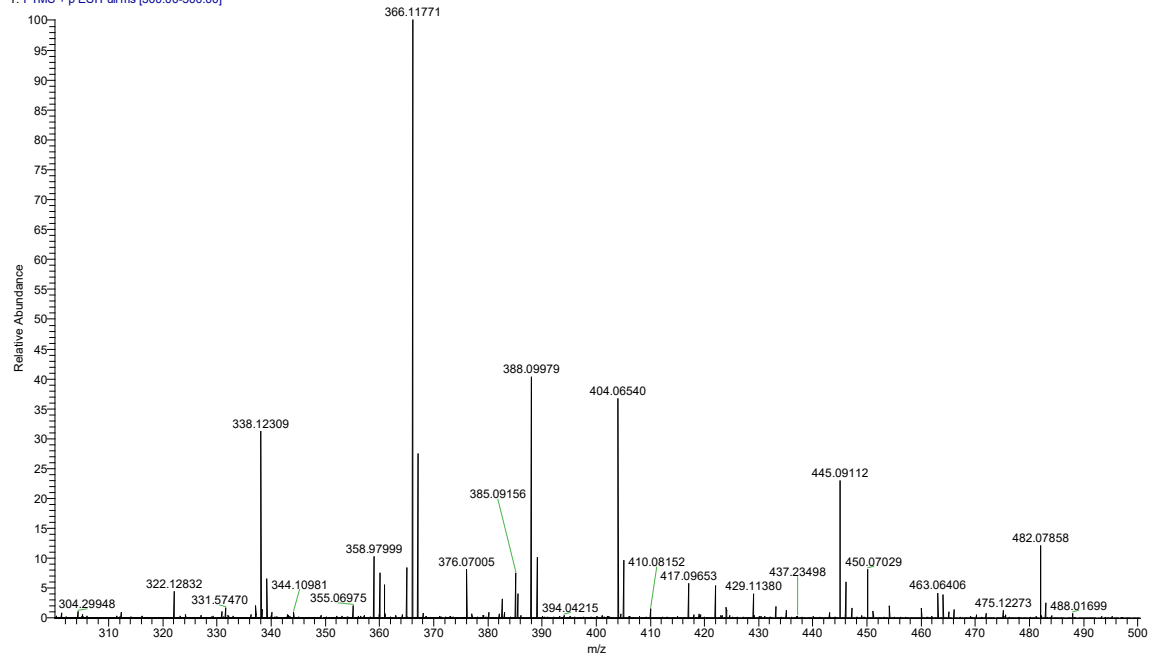


**Figure A61.** HRMS data for **ManCou6**.



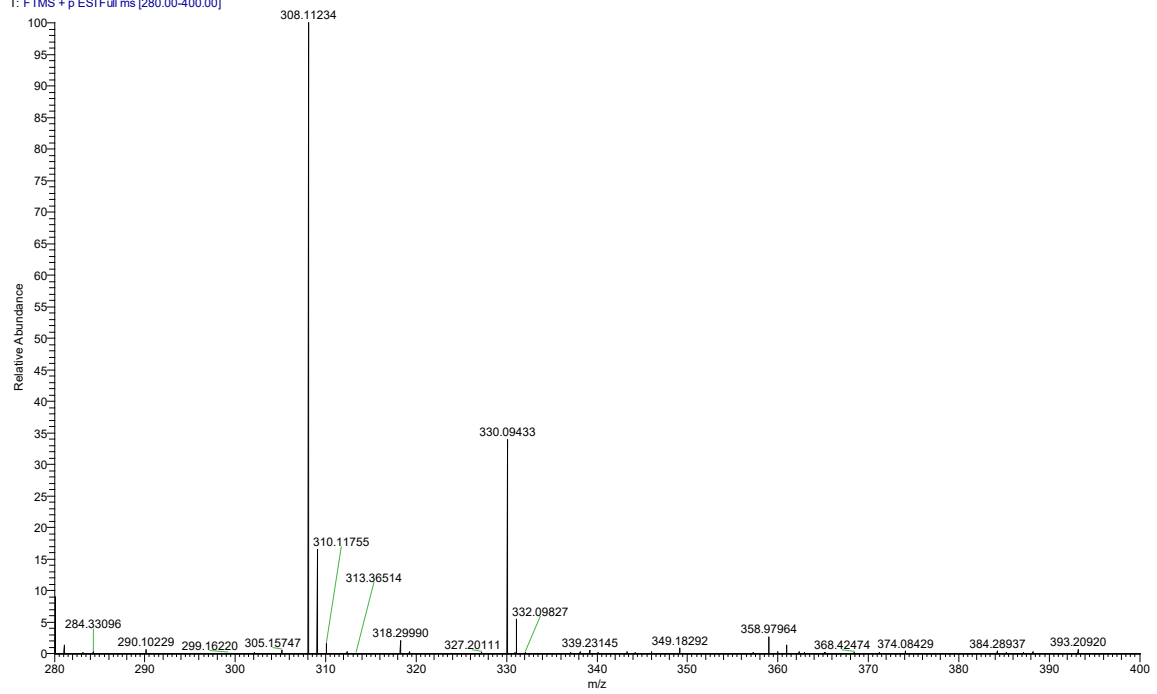
**Figure A62.** HRMS data for **ManCou7**.

ME methylcooh #1-49 RT: 0.01-0.87 AV: 49 NL: 3.88E5  
T: FTMS + p ESI Full ms [300.00-500.00]

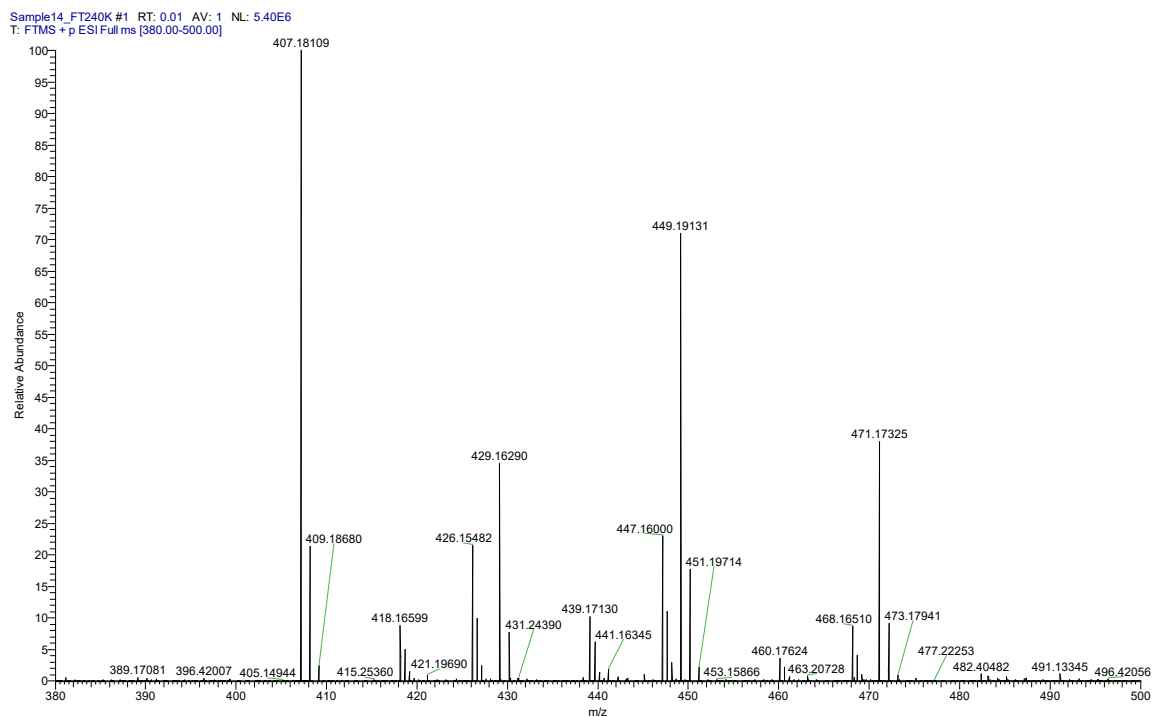


**Figure A63.** HRMS data for **ManCou8**.

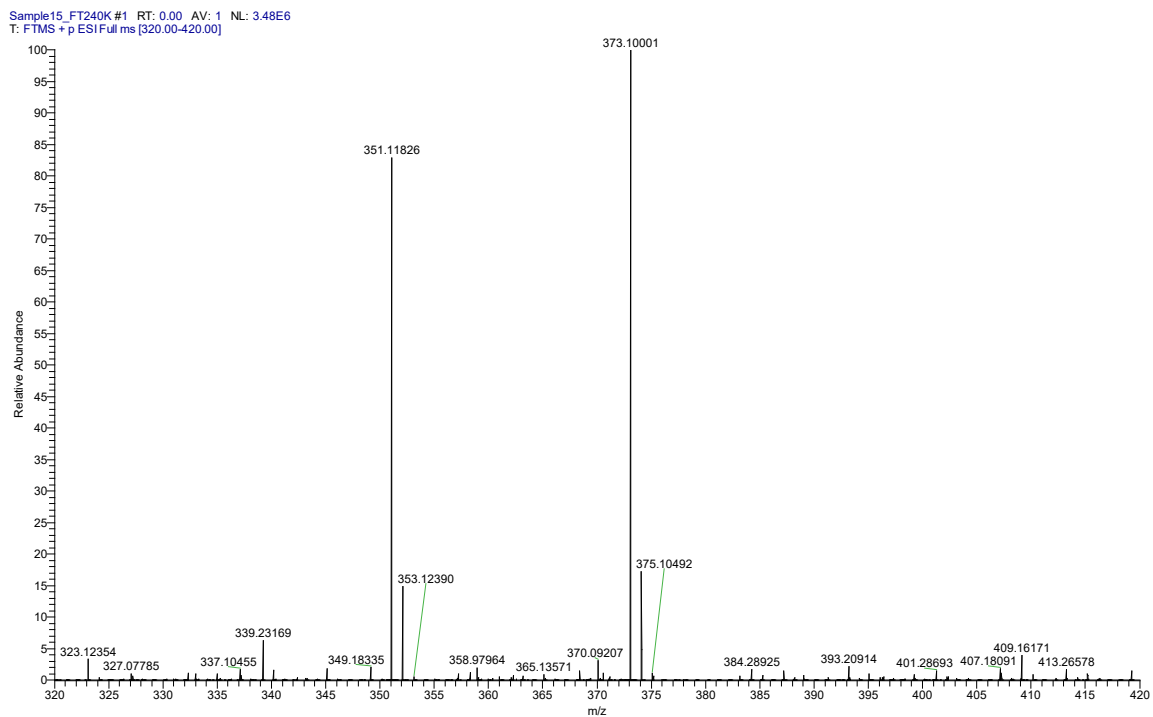
Sample13\_FT240K #1 RT: 0.01 AV: 1 NL: 8.25E6  
T: FTMS + p ESI Full ms [280.00-400.00]



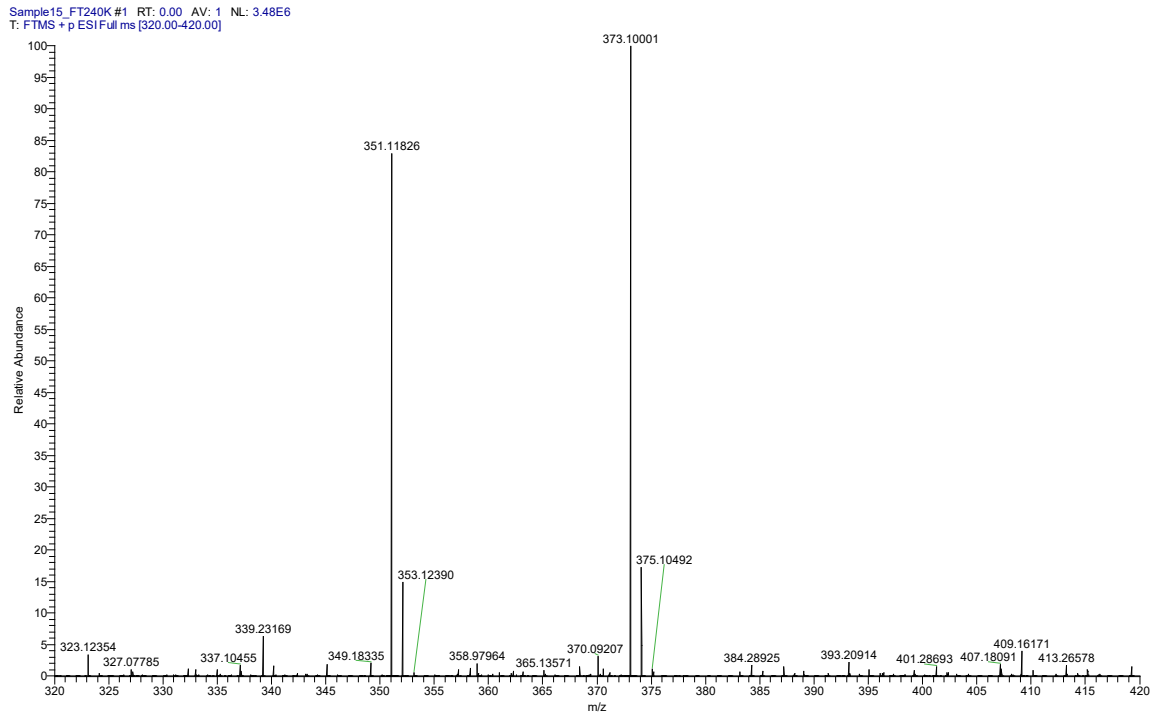
**Figure A64.** HRMS data for **ManCou9**.



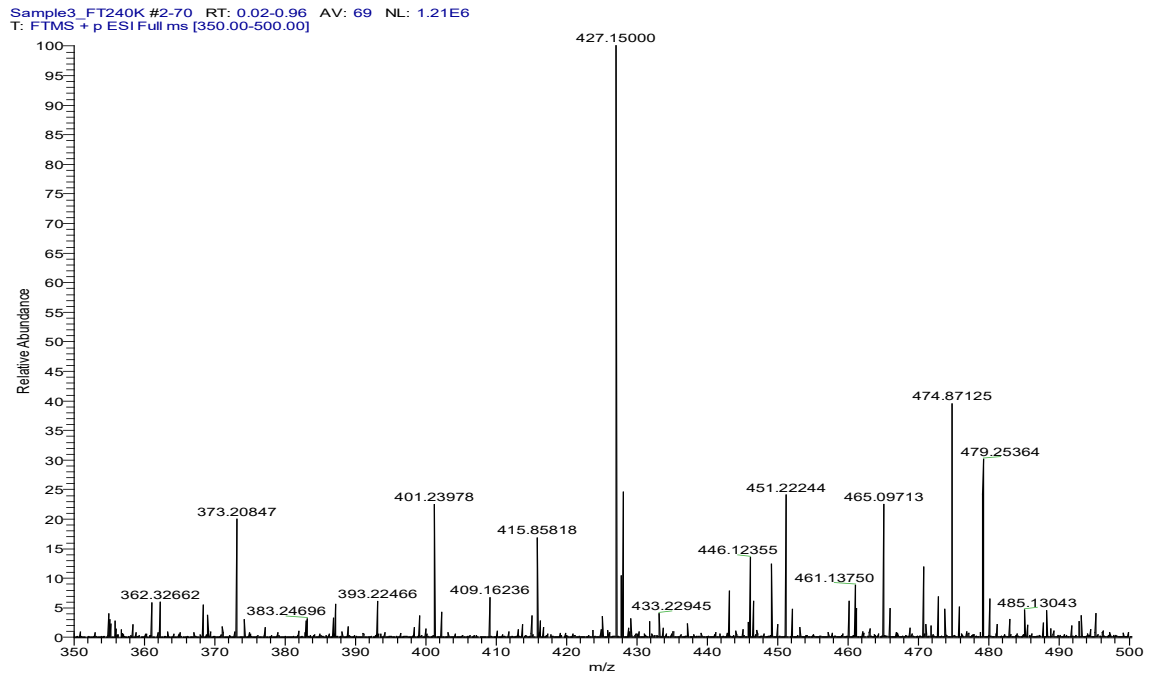
**Figure A65.** HRMS data for **ManCou10**.



**Figure A66.** HRMS data for **ManCou11**.

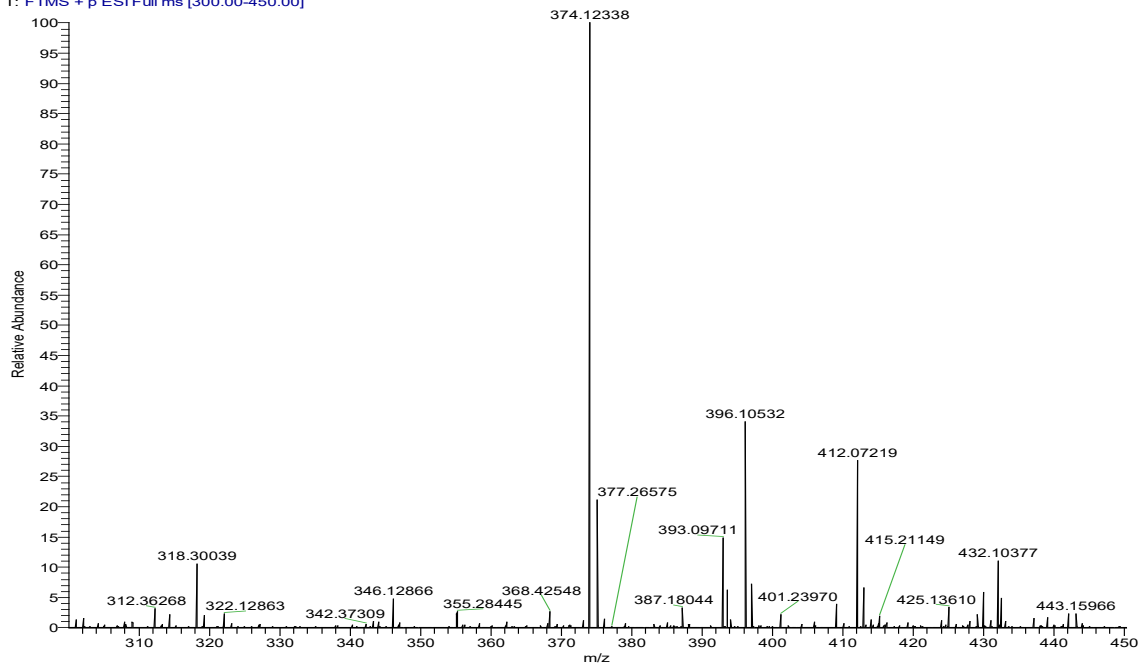


**Figure A67.** HRMS data for **ManCou12**.



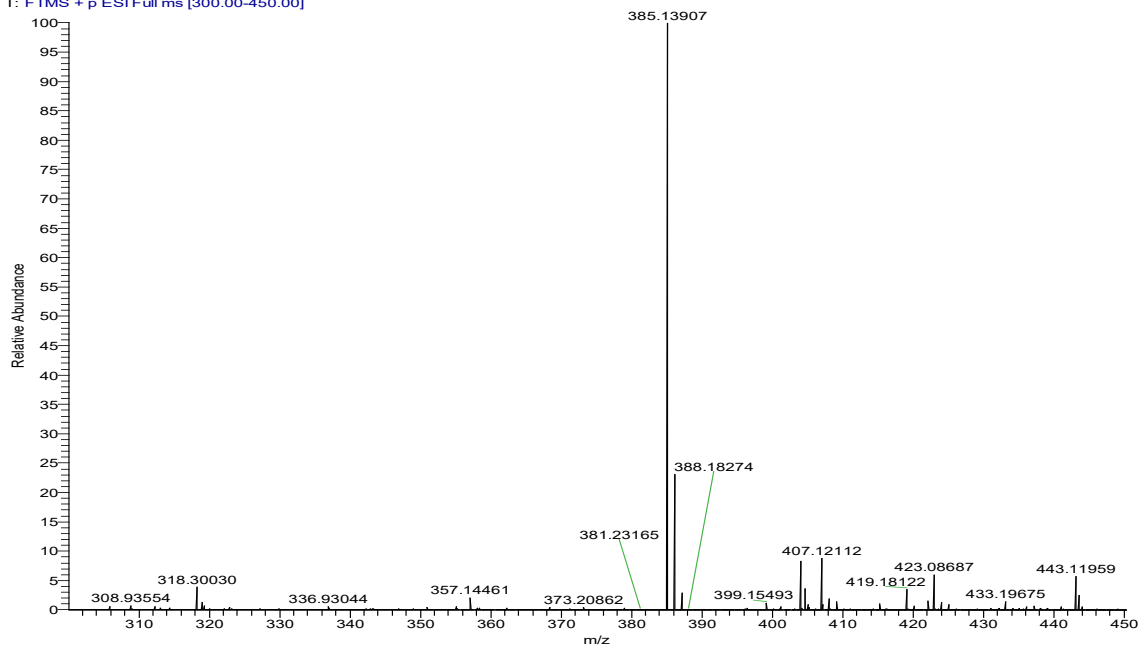
**Figure A68.** HRMS data for **ManCou13.**

Sample4\_FT240K #2-69 RT: 0.02-1.05 AV: 68 NL: 8.05E5  
T: FTMS + p ESI Full ms [300.00-450.00]



**Figure A69.** HRMS data for **ManCou14.**

Sample5\_FT240K\_2 #3-69 RT: 0.04-0.99 AV: 67 NL: 3.80E6  
T: FTMS + p ESI Full ms [300.00-450.00]





## Appendix B Supporting Info for Chapter 5

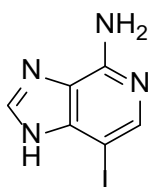
### Tuning Cross-Coupling Approaches to C3-Modification of 3-Deazapurines

#### B.1 General Methods

All reagents were used as received unless otherwise stated from Sigma-Aldrich, TCI America, Alfa Aesar, AK Scientific or Chem-Impex International. 4-Chloro-1*H*-imidazo[4,5*c*]pyridine was obtained from MolBridge. Bis(4-methoxybenzyl)amine and TPPTS were obtained from Ark Pharm. 1-( $\alpha$ )-Chloro-3,5-di-O-(*p*-toluoyl)-2-deoxy-D-ribose was purchased from Berry & Associates. Anhydrous methanol, pyridine, and *N,N*-dimethylacetamide (DMA) were obtained from Sigma-Aldrich. *N,N*-dimethylformamide (DMF) and 1,4-dioxane were dried and stored over CaH<sub>2</sub> before use. Dry acetonitrile, dichloromethane, and tetrahydrofuran were dispensed from an automated Innovative Technology Pure-Solv 400 Solvent Purification System. Analytical TLC was carried out on commercial SiliCycle SiliaPlate® 0.2 mm F254 plates. Preparative silica chromatography was performed using SiliCycle SiliaFlash® F60 40-63  $\mu$ m (230-400 mesh). <sup>1</sup>H, <sup>13</sup>C and <sup>31</sup>P NMR spectra were recorded at room temperature with a Varian Unity Inova 400 MHz spectrometer. CDCl<sub>3</sub>, DMSO-d<sub>6</sub>, CD<sub>3</sub>OD, acetone-d<sub>6</sub> and D<sub>2</sub>O were used as solvents and referenced to the corresponding residual solvent peaks (7.26 and 77.16 ppm for CDCl<sub>3</sub>, respectively; 2.50 and 39.52 ppm for DMSO-d<sub>6</sub>, respectively; 3.31 and 49.0 ppm for CD<sub>3</sub>OD, respectively; 2.05 and 29.84 ppm for acetone-d<sub>6</sub>, respectively; 4.79 ppm for D<sub>2</sub>O).<sup>1</sup> The following abbreviations are used to indicate the multiplicity: s - singlet; d - doublet; t - triplet; q - quartet; m - multiplet; b - broad signal; app - approximate. The coupling constants are expressed in Hertz (Hz). The multiplicity of carbon atoms was determined by DEPT-135 experiment; Cq - quaternary carbon. MS data (ESI) were obtained using a Thermo Finnigan LCQ Advantage Ion-Trap Mass Spectrometer. The high-resolution (HR) MS data (ESI) were obtained using a Thermo Fisher Orbitrap Elite™ Hybrid Ion Trap-Orbitrap Mass Spectrometer at Chemical Advanced Resolution Methods (ChARM) Laboratory at Michigan Technological University.

## B.2 Synthesis and Characterization Data

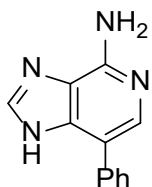
Compounds **1**,<sup>2</sup> **4**,<sup>1,3</sup> and **5b**<sup>4</sup> were prepared according to the reported procedures.



### 7-Iodo-1*H*-imidazo[4,5c]pyridin-4-amine (**2**)

To a suspension of crude amine **1** (536 mg, ca. 4 mmol) in dry DMF (8 ml), *N*-iodosuccinimide (NIS) (1.125 g, 5 mmol) was added in one portion. Slightly exothermic reaction occurred, and the resulting dark solution was stirred at room temperature for 24 h. After 24 h, the solution was added dropwise to EtOAc (100 ml) with vigorous stirring, and the resulting solid was filtered and washed with EtOAc. The solid was then suspended in chloroform (50 ml) and vigorously stirred under reflux condenser at 70 °C overnight. After filtration and drying on air, **2** was obtained as a dark brown solid in 27% yield (0.27 g). HRMS (ESI): *m/z* [M+H]<sup>+</sup> calc'd for C<sub>6</sub>H<sub>4</sub>N<sub>4</sub>I: 260.96373; found: 260.96323. MS (ESI): *m/z*, 261.2 for [M+H]<sup>+</sup>. <sup>1</sup>H NMR (400 MHz, DMSO-*d*<sub>6</sub>): δ, 8.49 (s, 1H), 8.44 (bs, 2H), 7.97 (s, 1H) ppm. We were not able to obtain satisfactory <sup>13</sup>C NMR data in DMSO-*d*<sub>6</sub>.

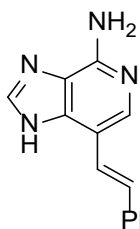
### 7-Phenyl-1*H*-imidazo[4,5c]pyridin-4-amine (**3a**)



This compound was synthesized according to the reported general procedures.<sup>5-7</sup> To a vial equipped with septa a mixture of deionized water/acetonitrile (2/1, 9 ml) was added and bubbled with argon for 10 min. **2** (150 mg, 0.58 mmol), phenylboronic acid (88 mg, 0.72 mmol), palladium(II) acetate (7 mg, 0.029 mmol), TPPTS (41 mg; 0.072 mmol) and anhydrous sodium carbonate (183 mg; 1.7 mmol) were added, and the headspace of the vial was flushed with argon for 1 minute. The mixture was vigorously stirred at 100 °C for 7 h. The mixture was then cooled and diluted with ethyl acetate (50 ml) and brine (10 ml). The phases were separated, and the aqueous phase was extracted with additional ethyl acetate (3 x 30 ml). Combined organic extracts were dried with MgSO<sub>4</sub>. After filtration and concentration, the residue was purified by column chromatography on silica gel, eluting with 0-10% MeOH in CH<sub>2</sub>Cl<sub>2</sub> to obtain

**3a** as a yellow solid in 65% yield (79 mg). HRMS (ESI):  $m/z$   $[M+H]^+$  calc'd for  $C_{12}H_{11}N_4$ : 211.09838; found: 211.09680. MS (ESI):  $m/z$ , 211.3 for  $[M+H]^+$ .  $^1H$  NMR (400 MHz, DMSO- $d_6$ ):  $\delta$ , 8.20 (s, 1H), 7.85 (s, 2H), 7.73 (b, 2H), 7.48-7.44 (m, 2H), 7.34-7.30 (m, 1H), 6.46 (b, 2H) ppm.  $^{13}C$  NMR (100 MHz, DMSO- $d_6$ ):  $\delta$ , 141.3, 137.5, 136.1, 128.7, 127.3, 126.5 ppm.

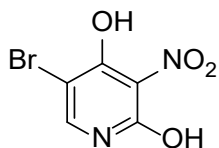
### (*E*)-7-Styryl-1*H*-imidazo[4,5-*c*]pyridin-4-amine (**3b**)



This compound was synthesized in similar fashion as **3a**. To a vial equipped with septa a mixture of deionized water/acetonitrile (2/1, 6 ml) was added and bubbled with argon for 10 min. **2** (100 mg, 0.38 mmol), *trans*-2-phenylvinylboronic acid (71 mg, 0.48 mmol), palladium(II) acetate (5 mg, 0.019 mmol), TPPTS (28 mg; 0.048 mmol) and anhydrous sodium carbonate (122 mg; 1.2 mmol) were added, and the headspace of the vial was flushed with argon for 1 minute. The mixture was vigorously stirred at 100 °C for 16 h. The mixture was then cooled and diluted with ethyl acetate (40 ml) and brine (10 ml). The phases were separated, and the aqueous phase was extracted with additional ethyl acetate (3 x 20 ml). Combined organic extracts were dried with  $MgSO_4$ . After filtration and concentration, the residue was purified by column chromatography on silica gel, eluting with 0-10% MeOH in  $CH_2Cl_2$  to obtain **3b** as a cream solid in 58% yield (52 mg). HRMS (ESI):  $m/z$   $[M+H]^+$  calc'd for  $C_{14}H_{13}N_4$ : 237.11403; found: 211.11269.  $^1H$  NMR (400 MHz, DMSO- $d_6$ ):  $\delta$ , 8.28 (s, 1H), 7.89 (s, 1H), 7.58-7.56 (m, 2H), 7.38-7.31 (m, 4H), 7.23-7.20 (m, 1H), 6.52 (b, 2H) ppm.  $^{13}C$  NMR (100 MHz, DMSO- $d_6$ ):  $\delta$ , 141.1, 139.7, 138.2, 128.6, 126.8, 125.8, 124.0 ppm.

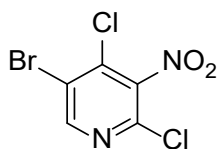
Compounds **8** and **9** were prepared by modification of the reported procedures.<sup>8</sup>

### 5-Bromo-3-nitropyridine-2,3-diol (**8**)



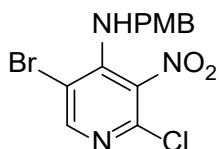
To the suspension of 3-nitropyridine-2,4-diol **7** (10 g, 64.1 mmol) in glacial acetic acid (100 ml), bromine (4.6 ml, 90 mmol) was added in one portion, and the mixture was stirred at 70 °C for 2.5 h. Reaction mixture was then cooled and poured onto 300 ml of crushed ice, stirred vigorously for 30 min., and chilled in the freezer for 1 h. The precipitated solids were filtered on paper, washed with small volume of ice-cold water several times, then ethanol (3 x 15 ml), and dried on air. **8** was obtained as a yellow solid in 74% yield (11.2 g). <sup>1</sup>H NMR (400 MHz, DMSO-d<sub>6</sub>): δ, 7.86 (s, 1H) ppm. <sup>13</sup>C NMR (100 MHz, DMSO-d<sub>6</sub>): δ, 159.1, 155.6, 138.6, 128.2, 94.0 ppm.

### 5-Bromo-2,4-dichloro-3-nitropyridine (**9**)



A suspension of **8** (11.1 g, 47.4 mmol) in POCl<sub>3</sub> (100 ml) was stirred at 90 °C for 24 h under argon, an excess pressure being released several times within first few hours. Then POCl<sub>3</sub> was carefully distilled off under vacuum. The oily residue was diluted with Et<sub>2</sub>O (100 ml), cooled on an ice bath and crushed ice (200 ml) was carefully added (exothermic reaction). The phases were separated, aqueous phase was additionally extracted with Et<sub>2</sub>O (2 x 50 ml), the combined organics were washed with brine, and dried with MgSO<sub>4</sub>. After filtration and concentration, the residue was purified by column chromatography on silica gel, eluting with 0-10% EtOAc in hexanes to obtain **9** as a yellow oil that slowly solidified (9.27 g, 72% yield). <sup>1</sup>H NMR (400 MHz, CDCl<sub>3</sub>): δ, 8.68 (s, 1H) ppm. <sup>13</sup>C NMR (100 MHz, CDCl<sub>3</sub>): δ, 152.1, 141.5, 137.8, 121.3 ppm.

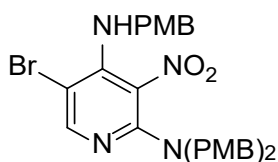
### 5-Bromo-2-chloro-N-(4-methoxybenzyl)-3-nitropyridin-4-amine (**10**)



To the solution of **9** (9.25 g, 34.3 mmol) in dry DMF (50 ml) at 0 °C under argon, 4-methoxybenzylamine (4.7 ml, 36 mmol) was added in one portion, followed by dropwise addition of Et<sub>3</sub>N (5.5 ml, 36 mmol) over 5 minutes. The mixture was allowed to warm up to room temperature and stirred for 24 h. The mixture was then diluted with EtOAc (300 ml), washed with brine (4 x 100 ml), and dried with MgSO<sub>4</sub>. After filtration, the solution was concentrated in vacuo to give

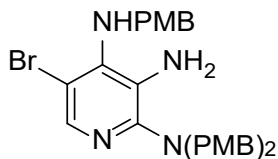
yellow solid that was triturated with hexanes to give **10** as a dark orange solid (12.1 g, 95% yield). HRMS (ESI):  $m/z$   $[M+H]^+$  calc'd for  $C_{13}H_{12}^{79}Br^{35}ClN_3O_3$ : 371.97507; found: 371.97488.  $^1H$  NMR (400 MHz,  $CDCl_3$ ):  $\delta$ , 8.23 (s, 1H), 7.24-7.22 (d,  $J = 8.4$ , 2H), 6.93-6.91 (d,  $J = 8.4$ , 2H), 5.24 (bs, 1H), 4.22-4.21 (d,  $J = 4.8$ , 2H), 3.82 (s, 3H) ppm.  $^{13}C$  NMR (100 MHz,  $CDCl_3$ ):  $\delta$ , 160.1 (Cq), 149.3, 143.4 (Cq), 143.3 (Cq), 129.7, 127.9 (Cq), 114.8, 109.4 (Cq), 55.5, 47.0 ( $CH_2$ ) ppm.

### 5-Bromo- $N^2,N^2,N^4$ -tris(4-methoxybenzyl)-3-nitropyridine-2,4-diamine (**11**)



A 250 ml Schlenk tube was charged with **10** (12.1 g, 32.6 mmol), bis(4-methoxybenzyl)amine (10.9 g, 42.4 mmol), *n*-butanol (100 ml) and  $Et_3N$  (6 ml, 43.1 mmol). The mixture was heated at 130 °C for 24 h. It was cooled, diluted with EtOAc (400 ml), washed with brine (200 ml), and dried with  $MgSO_4$ . After filtration, the solution was concentrated to give a dark residue that was purified by column chromatography on silica gel, eluting with 0-15% EtOAc in hexanes to obtain **11** as a red foam (17.6 g, 92% yield). HRMS (ESI):  $m/z$   $[M+H]^+$  calc'd for  $C_{29}H_{30}^{79}BrN_4O_5$ : 593.13999; found: 593.13894.  $^1H$  NMR (400 MHz,  $CDCl_3$ ):  $\delta$ , 8.09 (s, 1H), 7.21-7.18 (d,  $J = 8.8$ , 2H), 7.08-7.05 (d,  $J = 8.8$ , 4H), 6.88-6.86 (d,  $J = 8.8$ , 2H), 6.82-6.80 (d,  $J = 8.8$ , 4H), 6.14-6.12 (t,  $J = 4.8$ , 1H), 4.46-4.45 (d,  $J = 4.8$ , 2H), 4.29 (s, 4H), 3.782 (s, 3H), 3.778 (s, 6H) ppm.  $^{13}C$  NMR (100 MHz,  $CDCl_3$ ):  $\delta$ , 159.6 (Cq), 159.0 (Cq), 155.5 (Cq), 151.1, 146.5 (Cq), 129.7, 129.5 (Cq), 129.4, 129.2 (Cq), 126.0 (Cq), 114.5, 113.9, 99.6 (Cq), 55.4, 55.3, 53.7 ( $CH_2$ ), 49.2 ( $CH_2$ ) ppm.

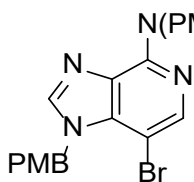
### 5-Bromo- $N^2,N^2,N^4$ -tris(4-methoxybenzyl)pyridine-2,3,4-triamine (**12**)



A 1 L round bottom flask was charged with **11** (16.7 g, 28.2 mmol), ethanol (600 ml) and deionized water (300 ml), followed by  $Na_2S_2O_4$  (9.81 g, 56.4 mmol, 2 equiv.). The mixture was heated at

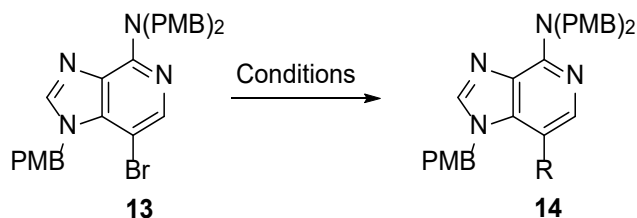
85 °C under reflux condenser. Additional sodium hydrosulfite was added at 30 min. intervals (overall, 4 x 2 equiv.) over 2.5 h. The mixture was then concentrated in vacuo to remove most of ethanol, and diluted with EtOAc (200 ml). It was carefully neutralized with solid NaHCO<sub>3</sub> (effervescence!) with vigorous stirring. The organic layer was separated, the aqueous phase was additionally extracted with EtOAc (2 x 150 ml) and the combined organics were washed with brine (100 ml), and dried with MgSO<sub>4</sub>. After filtration and concentration, the residue was purified by column chromatography on silica gel, eluting with 0-60% EtOAc in hexanes, and the product was additionally triturated with hexanes containing some EtOAc to obtain **12** as a cream solid in 59% yield (9.4 g). This compound is somewhat unstable and should be used within few days. HRMS (ESI): *m/z* [M+H]<sup>+</sup> calc'd for C<sub>29</sub>H<sub>32</sub><sup>79</sup>BrN<sub>4</sub>O<sub>3</sub>: 563.1658; found: 563.16396. <sup>1</sup>H NMR (400 MHz, CDCl<sub>3</sub>): δ, 7.77 (s, 1H), 7.22-7.20 (d, *J* = 8.8, 2H), 7.10-7.08 (d, *J* = 8.8, 4H), 6.84-6.82 (d, *J* = 8.8, 2H), 6.81-6.79 (d, *J* = 8.8, 4H), 4.25-4.24 (d, *J* = 6.8, 2H), 4.14 (s, 4H), 4.00 (bs, 2H), 3.78 (s, 9H) ppm. <sup>13</sup>C NMR (100 MHz, CDCl<sub>3</sub>): δ, 159.1 (Cq), 158.8 (Cq), 150.2 (Cq), 139.8 (Cq), 138.3, 131.6 (Cq), 130.7 (Cq), 130.1, 129.9 (Cq), 129.2, 114.1, 113.7, 110.8 (Cq), 55.36, 55.34, 53.5 (CH<sub>2</sub>), 48.7 (CH<sub>2</sub>) ppm.

### 7-Bromo-*N,N*,1-tris(4-methoxybenzyl)-1*H*-imidazo[4,5-*c*]pyridin-4-amine (**13**)



A 250 ml Schlenk tube was charged with **12** (9.4 g, 16.7 mmol) and trimethyl orthoformate (150 ml). The mixture was heated at 110 °C for 24 h, and concentrated in vacuo. The remaining residue was dissolved in the smallest possible volume of EtOAc and hexane was carefully added dropwise with stirring to cause slight turbidity. The mixture was chilled in the freezer at -20 °C overnight and the resulting precipitate was filtered, washed with hexanes and dried on air to give **13** as an off-white to cream solid in 94% yield (8.96 g). HRMS (ESI): *m/z* [M+H]<sup>+</sup> calc'd for C<sub>30</sub>H<sub>30</sub><sup>81</sup>BrN<sub>4</sub>O<sub>3</sub>: 575.1481; found: 575.14530. <sup>1</sup>H NMR (399.8 MHz, CDCl<sub>3</sub>): δ, 7.97 (s, 1H), 7.62 (s, 1H), 7.22-7.20 (d, *J* = 8.8, 4H), 7.13-7.10 (d, *J* = 8.8, 2H), 6.90-6.87 (d, *J* = 8.8, 2H), 6.84-6.82 (d, *J* = 8.8, 4H), 5.65 (s, 2H), 5.13 (s, 4H), 3.80 (s,

3H), 3.78 (s, 6H) ppm.  $^{13}\text{C}$  NMR (100 MHz,  $\text{CDCl}_3$ ):  $\delta$ , 159.6 (Cq), 158.7 (Cq), 151.6 (Cq), 143.1, 141.0, 136.6 (Cq), 131.2 (Cq), 129.5 (Cq), 129.2, 128.5, 128.4 (Cq), 114.5, 113.9, 89.0 (Cq), 55.44, 55.38, 49.8 ( $\text{CH}_2$ ), 49.0 ( $\text{CH}_2$ ) ppm.



**General conditions A:**<sup>8</sup> a solution of **13** (0.25-3.5 mmol, 1 equiv.) in 2/1 dioxane/deionized water mixture (ca. 12 ml per mmol) was placed in a Schlenk tube or a vial equipped with septa. The mixture was bubbled with argon for ca. 1 minute/ml. An aryl or vinylboronic acid (1.5 equiv.), tetrakis(triphenylphosphine)palladium (0) (0.1 equiv.) and anhydrous cesium carbonate (2 equiv.) were added, the mixture was bubbled with argon for few more minutes and heated at 90 °C for 6-16 h with vigorous stirring. It was cooled and diluted with equal volumes of  $\text{CH}_2\text{Cl}_2$  and 1/1 water/brine, the phases were separated and the aqueous phase extracted twice with  $\text{CH}_2\text{Cl}_2$ . The combined organic extracts were dried with  $\text{MgSO}_4$ . After filtration and concentration, the products were purified by column chromatography on silica gel eluting with 0-20% EtOAc in hexanes.

**General conditions B:**<sup>9</sup> to a flame-dried vial equipped with septa dry dioxane (ca. 7 ml per mmol) was added and bubbled with argon for ca. 1 minute/ml. Compound **13** (0.25-3.5 mmol, 1 equiv.), alkylboronic acid (1.1-1.5 equiv.), tetrakis(triphenylphosphine)palladium(0) (0.1 equiv.), and anhydrous potassium carbonate (3 equiv.) were added. The mixture was bubbled with argon for few more minutes and heated at 90 °C for 72 h with vigorous stirring. It was cooled and filtered through Celite®, washing with  $\text{CH}_2\text{Cl}_2$ . After concentration, the products were purified by column chromatography on silica gel eluting with 0-20% EtOAc in hexanes.

**General conditions C:**<sup>10</sup> to a flame dried vial equipped with septa dry acetonitrile (3.5 ml) was added and bubbled with argon for ca. 1 minute/ml. Compound **13** (0.25 mmol, 1 equiv.), triphenylphosphine (0.5 equiv.) and palladium(II) acetate (0.1 equiv.) were added, followed by an olefin (5 equiv.) and triethylamine (7 equiv.) and the mixture was bubbled with argon for few more minutes and heated at 90 °C for 36 h with vigorous stirring. It was cooled, diluted with CH<sub>2</sub>Cl<sub>2</sub> (50 ml), washed with aqueous NH<sub>4</sub>Cl (2 x 25 ml), and dried with MgSO<sub>4</sub>. After filtration and concentration, the products were purified by column chromatography on silica gel eluting with 0-40% EtOAc in hexanes. **The procedure for separation of dehalogenated byproduct:** the crude mixture obtained after the extractive workup was redissolved in CH<sub>2</sub>Cl<sub>2</sub> (10 ml) and NIS (ca. 0.6 equiv.) was added. After stirring at room temperature for 2 h, the mixture was diluted with CH<sub>2</sub>Cl<sub>2</sub> (50 ml), washed with brine containing sodium thiosulfate (25 ml), and dried with MgSO<sub>4</sub>. After filtration and concentration, the products were purified by column chromatography on silica gel eluting with 0-40% EtOAc in hexanes. **13-I** eluted first.

**General conditions D:**<sup>11</sup> to a flame dried vial equipped with septa dry DMF (5 ml) and triethylamine (2.5 ml) were added and bubbled with argon for ca. 1 minute/ml. Compound **13** (0.25 mmol, 1 equiv.), CuI (0.1 equiv.) and bis(triphenylphosphine)palladium(II) dichloride (0.1 equiv.) were added, followed by phenylacetylene (1.5 equiv.). The mixture was bubbled with argon for few more minutes and heated at 80 °C for 24 h with vigorous stirring. It was cooled, quenched with saturated aqueous NH<sub>4</sub>Cl (10 ml), diluted with EtOAc (10 ml), washed with brine (3 x 10 ml), and dried with MgSO<sub>4</sub>. After filtration and concentration, the products were purified by column chromatography on silica gel eluting with 0-20% EtOAc in hexanes.

**General conditions E:**<sup>12</sup> to a flame dried vial equipped with septa dry THF (6 ml) was added and bubbled with argon for ca. 1 minute/ml. Compound **13** (0.25 mmol, 1 equiv.) and tetrakis(triphenylphosphine)palladium(0) (0.1 equiv.) were added, followed by trimethylaluminum or benzylmagnesium chloride solutions (3-3.3 equiv.) and the mixture was stirred at room temperature for 15 minutes and then heated at 80 °C for 4 h with vigorous stirring. It was cooled, carefully quenched with Et<sub>2</sub>O (30 ml), washed with

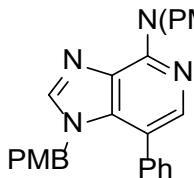


saturated aqueous NH<sub>4</sub>Cl (30 ml), and dried with MgSO<sub>4</sub>. After filtration and concentration, the products were purified by column chromatography on silica gel eluting with 0-40% EtOAc in hexanes.

**General conditions F:**<sup>13</sup> to a flame dried vial equipped with septa was added a solution of ZnCl<sub>2</sub> (0.5 M in THF, 5.7 eq.), followed by dropwise addition of Grignard reagent solution (8.6 eq.) and the mixture was allowed to stir under argon for 1 h. Then, compound **13** (0.175-0.7 mmol, 1 eq.) and [1,1'-bis(diphenylphosphino)ferrocene]dichloropalladium(II) (0.1 equiv.) were added, and the mixture was stirred at room temperature under argon for overall 21-29 h. It was carefully quenched with Et<sub>2</sub>O (30-50 ml), washed with equal volume of saturated aqueous NH<sub>4</sub>Cl, and dried with MgSO<sub>4</sub>. After filtration and concentration, the products were purified by column chromatography on silica gel eluting with 0-20% EtOAc in hexanes.

**General conditions G:**<sup>14</sup> to a flame dried vial equipped with septa were added sequentially: NiI<sub>2</sub> (0.065 mmol, 0.13 equiv.), 4,4'-dimethoxy-2,2'-bipyridine (0.05 mmol, 0.1 equiv.), NaI (0.125 mmol, 0.25 equiv.), **13** (0.5 mmol, 1 equiv.), dry DMA (2 ml), pyridine (5 μl), ethyl 4-bromobutyrate (0.55 mmol, 1.1 equiv.), and Zn powder (1 mmol, 2 equiv.). The headspace of the vial was flushed with argon for 1 minute. The reaction mixture was stirred at room temperature for 5 minutes and then heated at 60 °C for 20 h with vigorous stirring. It was cooled, diluted with EtOAc (50 ml), washed with brine (3 x 25 ml), and dried with MgSO<sub>4</sub>. The crude mixtures were subjected to the same procedure of dehalogenated by-product separation as described under general conditions C. The products were purified by column chromatography on silica gel eluting with 0-40% EtOAc in hexanes. **13-I** eluted first.

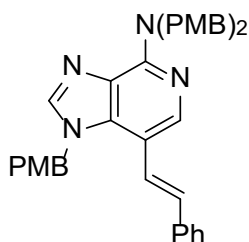
***N,N*,1-Tris(4-methoxybenzyl)-7-phenyl-1*H*-imidazo[4,5-*c*]pyridin-4-amine (14a)**



General conditions A, 6 h, 335 mg, 91%. Yellowish syrup. HRMS (ESI): m/z [M+H]<sup>+</sup> calc'd for C<sub>36</sub>H<sub>35</sub>N<sub>4</sub>O<sub>3</sub>: 571.27093; found: 571.26842. <sup>1</sup>H NMR (400 MHz, CDCl<sub>3</sub>): δ, 7.78 (s, 1H), 7.68 (s, 1H), 7.36-7.34 (m, 3H), 7.29-7.27 (d, *J* = 8.8, 4H), 7.27-7.25 (m, 2H), 6.87-6.85 (d, *J* =

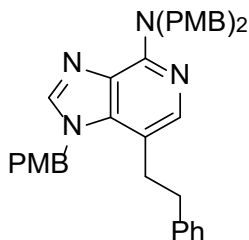
8.8, 2H), 6.71-6.69 (d,  $J = 8.8$ , 2H), 6.56-6.54 (d,  $J = 8.8$ , 2H), 5.23 (s, 4H), 4.94 (s, 2H), 3.80 (s, 6H), 3.76 (s, 3H) ppm.  $^{13}\text{C}$  NMR (100 MHz,  $\text{CDCl}_3$ ):  $\delta$ , 159.6 (Cq), 158.7 (Cq), 151.6 (Cq), 141.8, 141.0, 137.7 (Cq), 136.7 (Cq), 131.6 (Cq), 130.4, 129.3, 128.2, 128.10, 128.06 (Cq), 128.0 (Cq), 127.4, 114.1, 113.9, 113.8 (Cq), 55.40, 55.38, 49.64 ( $\text{CH}_2$ ), 49.55 ( $\text{CH}_2$ ) ppm.

**(E)-N,N,1-Tris(4-methoxybenzyl)-7-styryl-1H-imidazo[4,5-c]pyridin-4-amine (14b)**



General conditions A, 16 h, 123 mg, 79%. General conditions C, 36 h, 83 mg, 53%. Tan solid. HRMS (ESI):  $m/z$   $[\text{M}+\text{H}]^+$  calc'd for  $\text{C}_{38}\text{H}_{37}\text{N}_4\text{O}_3$ : 597.28658; found: 597.28453.  $^1\text{H}$  NMR (400 MHz,  $\text{CDCl}_3$ ):  $\delta$ , 8.10 (s, 1H), 7.69 (s, 1H), 7.32-7.23 (m, 8H), 7.20-7.16 (d,  $J = 15.6$ , 1H), 7.06-7.04 (d,  $J = 8.8$ , 2H), 6.92-6.89 (d,  $J = 8.8$ , 2H), 6.86-6.82 (m, 5H), 5.46 (s, 2H), 5.22 (s, 4H), 3.804 (s, 3H), 3.796 (s, 6H) ppm.  $^{13}\text{C}$  NMR (100 MHz,  $\text{CDCl}_3$ ):  $\delta$ , 159.6 (Cq), 158.7 (Cq), 151.7 (Cq), 141.0, 139.6, 138.1 (Cq), 137.8 (Cq), 131.5 (Cq), 129.3, 129.0, 128.8, 128.6 (Cq), 127.8 (Cq), 127.6, 127.4, 126.4, 122.2, 114.7, 113.9, 110.8 (Cq), 55.5, 55.4, 49.8 ( $\text{CH}_2$ ), 49.7 ( $\text{CH}_2$ ) ppm.

**N,N,1-Tris(4-methoxybenzyl)-7-phenethyl-1H-imidazo[4,5-c]pyridin-4-amine (14c)**

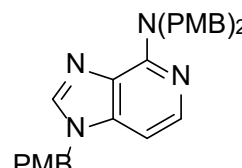


General conditions B, 72 h, 55 mg, 35%. General conditions F, 29 h, 327 mg, 77%. Colorless syrup. HRMS (ESI):  $m/z$   $[\text{M}+\text{H}]^+$  calc'd for  $\text{C}_{38}\text{H}_{39}\text{N}_4\text{O}_3$ : 599.30224; found: 599.29971.  $^1\text{H}$  NMR (400 MHz,  $\text{CDCl}_3$ ):  $\delta$ , 7.76 (s, 1H), 7.63 (s, 1H), 7.31-7.20 (m, 3H), 7.26-7.24 (d,  $J = 8.8$ , 4H), 7.10-7.08 (d,  $J = 8.8$ , 4H), 6.94-6.92 (d,  $J = 8.8$ , 2H), 6.87-6.84 (m, 2H), 6.86-6.83 (d,  $J = 8.8$ , 2H), 5.34 (s, 2H), 5.18 (s, 4H), 3.80 (s, 6H), 3.79 (s, 3H), 3.02-2.88 (m, 4H) ppm.  $^{13}\text{C}$  NMR (100 MHz,  $\text{CDCl}_3$ ):  $\delta$ , 159.6 (Cq), 158.6 (Cq), 151.4 (Cq), 141.4, 141.3 (Cq), 141.0, 138.8 (Cq), 131.7 (Cq), 129.3, 128.59, 128.56 (Cq), 128.48, 127.6,

126.3, 114.7, 113.8, 110.9 (Cq), 55.44, 55.36, 49.7 (CH<sub>2</sub>), 49.4 (CH<sub>2</sub>), 38.5 (CH<sub>2</sub>), 30.7 (CH<sub>2</sub>) ppm.

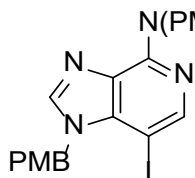
**Note:** Extensive optimization studies were conducted to improve the synthesis of **14c** through the Suzuki method. Among the most important variables tested were solvents and bases. The crude reaction mixtures were routinely analyzed by <sup>1</sup>H NMR. The reaction performed best in dry dioxane with K<sub>2</sub>CO<sub>3</sub> as a base at 90 °C for 72 h to give ~ 1:1 mixture of the cross-coupled and hydrodebrominated products **14c** and **13-H**, respectively, corresponding with up to 35% isolated yields of **14c**. Similar results could be obtained using K<sub>3</sub>PO<sub>4</sub> in dry dioxane. Other bases such as CaCO<sub>3</sub>, Na<sub>2</sub>CO<sub>3</sub> or Et<sub>3</sub>N did not promote the reaction at all, while Cs<sub>2</sub>CO<sub>3</sub> afforded **13-H** as a major product. CsF was inferior. Dioxane performed best as a solvent, while THF, toluene or DMA were inferior. The addition of water led to complicated mixtures and the formation of styryl derivatives. Shortening the time or lowering the temperature of the reaction led to incomplete conversions. Additives such as Ag<sub>2</sub>O or 18-C-6 were detrimental. When **13-I** was used as a substrate, **13-H** was a major product. When phenethylboronic acid pinacol ester was used instead of the free boronic acid, an unreacted **13** was recovered with no trace of **14c** formation. Also, the use of more soluble carbonates such as Cs<sub>2</sub>CO<sub>3</sub> (or increasing the solubility of K<sub>2</sub>CO<sub>3</sub> by addition of 18-C-6 or the use of DMA as a solvent) led predominantly to hydrodebromination and often the substantial amounts of recovered **13**. Hence, we believe that the activation of boronic acid is occurring on the surface of potassium carbonate. However, increasing the amount of a solid base to 20-100 equiv. did not improve the isolated yields of **14c**.

***N,N*,1-Tris(4-methoxybenzyl)-1*H*-imidazo[4,5-*c*]pyridin-4-amine (13-H)**

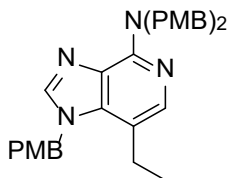
  
General conditions B, 72 h, 34 mg, 30%. Yellowish syrup. HRMS (ESI): m/z [M+H]<sup>+</sup> calc'd for C<sub>30</sub>H<sub>31</sub>N<sub>4</sub>O<sub>3</sub>: 495.23964; found: 495.23722. <sup>1</sup>H NMR (400 MHz, CDCl<sub>3</sub>): δ, 7.96-7.94 (d, *J* = 5.6, 1H), 7.70 (s, 1H), 7.25-7.23 (d, *J* = 8.8, 4H), 7.16-7.14 (d, *J* = 8.8, 2H), 6.90-6.87 (d, *J* = 8.8, 2H), 6.84-6.82 (d, *J* = 8.8, 4H), 6.64-6.62 (d, *J* = 5.6, 1H), 5.21 (s, 2H), 5.17 (s, 4H), 3.80

(s, 3H), 3.78 (s, 6H) ppm.  $^{13}\text{C}$  NMR (100 MHz,  $\text{CDCl}_3$ ):  $\delta$ , 159.8 (Cq), 158.6 (Cq), 152.3 (Cq), 141.1, 140.5 (Cq), 139.2, 131.5 (Cq), 129.2, 129.0, 127.9 (Cq), 127.3 (Cq), 114.6, 113.9, 96.2, 55.45, 55.36, 49.4 ( $\text{CH}_2$ ), 48.6 ( $\text{CH}_2$ ) ppm.

**7-Iodo-*N,N*,1-tris(4-methoxybenzyl)-1*H*-imidazo[4,5-*c*]pyridin-4-amine (13-I)**



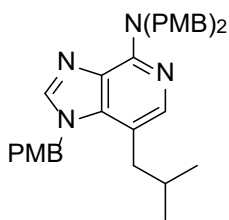
General conditions C, 36 h, 50 mg, 31%. General conditions G, 20 h, 110 mg, 36%. Yellowish foam. HRMS (ESI):  $m/z$   $[\text{M}+\text{H}]^+$  calc'd for  $\text{C}_{30}\text{H}_{30}\text{IN}_4\text{O}_3$ : 621.13629; found: 621.13419.  $^1\text{H}$  NMR (400 MHz,  $\text{CDCl}_3$ ):  $\delta$ , 8.17 (s, 1H), 7.62 (s, 1H), 7.23-7.20 (d,  $J = 8.8$ , 4H), 7.08-7.06 (d,  $J = 8.8$ , 2H), 6.90-6.88 (d,  $J = 8.8$ , 2H), 6.84-6.82 (d,  $J = 8.8$ , 4H), 5.67 (s, 2H), 5.15 (s, 4H), 3.80 (s, 3H), 3.79 (s, 6H) ppm.  $^{13}\text{C}$  NMR (100 MHz,  $\text{CDCl}_3$ ):  $\delta$ , 159.6 (Cq), 158.7 (Cq), 152.3 (Cq), 149.2, 141.4, 138.5 (Cq), 131.2 (Cq), 129.8 (Cq), 129.2, 128.5, 128.4 (Cq), 114.5, 113.9, 56.0 (Cq), 55.44, 55.38, 49.8 ( $\text{CH}_2$ ), 48.5 ( $\text{CH}_2$ ) ppm.



**7-Ethyl-*N,N*,1-tris(4-methoxybenzyl)-1*H*-imidazo[4,5-*c*]pyridin-4-amine (14d)**

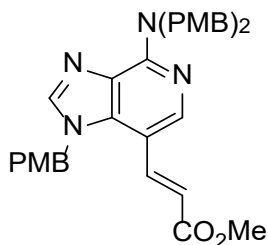
General conditions B, 72 h, 284 mg, 31%. General conditions F, 25 h, 69 mg, 76%. Colorless syrup. HRMS (ESI):  $m/z$   $[\text{M}+\text{H}]^+$  calc'd for  $\text{C}_{32}\text{H}_{35}\text{N}_4\text{O}_3$ : 523.27093; found: 523.26894.  $^1\text{H}$  NMR (400 MHz,  $\text{CDCl}_3$ ):  $\delta$ , 7.73 (s, 1H), 7.64 (s, 1H), 7.24-7.21 (d,  $J = 8.8$ , 4H), 6.99-6.97 (d,  $J = 8.8$ , 2H), 6.88-6.86 (d,  $J = 8.8$ , 2H), 6.83-6.81 (d,  $J = 8.8$ , 4H), 5.44 (s, 2H), 5.15 (s, 4H), 3.79 (s, 3H), 3.78 (s, 6H), 2.77-2.71 (q,  $J = 7.6$ , 2H), 1.25-1.21 (t,  $J = 7.6$ , 3H) ppm.  $^{13}\text{C}$  NMR (100 MHz,  $\text{CDCl}_3$ ):  $\delta$ , 159.6 (Cq), 158.6 (Cq), 151.3 (Cq), 141.0, 140.5, 138.8 (Cq), 131.8 (Cq), 129.3, 128.8 (Cq), 128.6 (Cq), 127.6, 114.6, 113.8, 113.2 (Cq), 55.5, 55.4, 49.7 ( $\text{CH}_2$ ), 49.6 ( $\text{CH}_2$ ), 22.0 ( $\text{CH}_2$ ), 16.2 ppm.

**7-Isobutyl-*N,N*,1-tris(4-methoxybenzyl)-1*H*-imidazo[4,5-*c*]pyridin-4-amine (14e)**

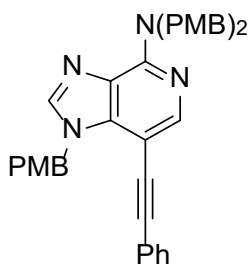


General conditions B, 72 h, 658 mg, 29%. General conditions F, 21 h, 327 mg, 85%. Yellowish syrup. HRMS (ESI):  $m/z$   $[M+H]^+$  calc'd for  $C_{34}H_{39}N_4O_3$ : 551.30224; found: 551.29987.  $^1H$  NMR (400 MHz,  $CDCl_3$ ):  $\delta$ , 7.67 (s, 1H), 7.63 (s, 1H), 7.24-7.21 (d,  $J = 8.8$ , 4H), 6.98-6.95 (d,  $J = 8.8$ , 2H), 6.88-6.86 (d,  $J = 8.8$ , 2H), 6.84-6.82 (d,  $J = 8.8$ , 4H), 5.40 (s, 2H), 5.15 (s, 4H), 3.79 (s, 3H), 3.78 (s, 6H), 2.51-2.49 (d,  $J = 7.2$ , 2H), 1.84-1.74 (septet,  $J = 6.4$ , 1H), 0.95-0.94 (d,  $J = 6.4$ , 6H) ppm.  $^{13}C$  NMR (100 MHz,  $CDCl_3$ ):  $\delta$ , 159.6 (Cq), 158.6 (Cq), 151.4 (Cq), 142.3, 140.9, 139.0 (Cq), 131.8 (Cq), 129.3, 128.8 (Cq), 128.7 (Cq), 127.6, 114.7, 113.8, 110.6 (Cq), 55.5, 55.4, 49.6 ( $CH_2$ ), 49.5 ( $CH_2$ ), 38.2 ( $CH_2$ ), 30.7, 22.4 ppm.

**Methyl (*E*)-3-(4-(bis(4-methoxybenzyl)amino)-1-(4-methoxybenzyl)-1*H*-imidazo[4,5-*c*]pyridin-7-yl)acrylate (14f)**



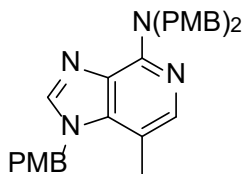
General conditions C, 36 h, 86 mg, 57%. Yellowish syrup. HRMS (ESI):  $m/z$   $[M+H]^+$  calc'd for  $C_{34}H_{35}N_4O_5$ : 579.26077; found: 579.25862.  $^1H$  NMR (400 MHz,  $CDCl_3$ ):  $\delta$ , 8.23 (s, 1H), 8.05-8.01 (d,  $J = 15.6$ , 1H), 7.69 (s, 1H), 7.24-7.22 (d,  $J = 8.8$ , 4H), 7.12-7.09 (d,  $J = 8.8$ , 2H), 6.90-6.88 (d,  $J = 8.8$ , 2H), 6.85-6.83 (d,  $J = 8.8$ , 4H), 6.26-6.22 (d,  $J = 15.6$ , 1H), 5.44 (s, 2H), 5.23 (s, 4H), 3.79-3.78 (overlapped s, 12H) ppm.  $^{13}C$  NMR (100 MHz,  $CDCl_3$ ):  $\delta$ , 167.8 (Cq), 159.8 (Cq), 158.8 (Cq), 152.8 (Cq), 141.3, 138.8, 138.0 (Cq), 130.9 (Cq), 129.4, 129.2, 128.2 (Cq), 127.6 (Cq), 127.3 (Cq), 114.6, 114.5, 114.0, 107.6 (Cq), 55.41, 55.36, 51.6, 50.4 ( $CH_2$ ), 49.7 ( $CH_2$ ) ppm.



***N,N,1-Tris(4-methoxybenzyl)-7-(phenylethynyl)-1H-imidazo[4,5-c]pyridin-4-amine (14g)***

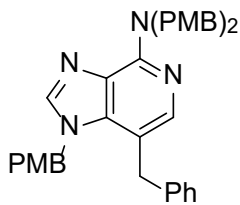
General conditions D, 20 h, 138 mg, 89%. Brown syrup. HRMS (ESI):  $m/z$   $[M+H]^+$  calc'd for  $C_{38}H_{35}N_4O_3$ : 595.27093; found: 595.26894.  $^1H$  NMR (400 MHz,  $CDCl_3$ ):  $\delta$ , 8.22 (s, 1H), 7.67 (s, 1H), 7.39-7.37 (m, 2H), 7.33-7.30 (m, 3H), 7.26-7.24 (d,  $J = 8.4$ , 2H), 7.25-7.23 (d,  $J = 8.4$ , 4H), 6.89-6.87 (d,  $J = 8.4$ , 2H), 6.86-6.84 (d,  $J = 8.4$ , 4H), 5.75 (s, 2H), 5.21 (s, 4H), 3.80 (s, 9H) ppm.  $^{13}C$  NMR (100 MHz,  $CDCl_3$ ):  $\delta$ , 159.6 (Cq), 158.8 (Cq), 151.9 (Cq), 146.7, 140.3, 138.3 (Cq), 131.1, 129.3, 128.9, 128.8 (Cq), 128.5, 128.0, 127.0 (Cq), 123.7 (Cq), 114.5, 113.9, 93.6 (Cq), 85.1 (Cq), 55.44, 55.38, 49.6 ( $CH_2$ ), 48.5 ( $CH_2$ ) ppm.

***N,N,1-Tris(4-methoxybenzyl)-7-methyl-1H-imidazo[4,5-c]pyridin-4-amine (14h)***



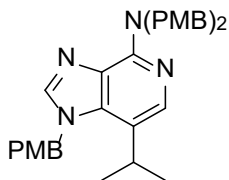
General conditions E, 4 h, 115 mg, 87%. Yellow syrup. HRMS (ESI):  $m/z$   $[M+H]^+$  calc'd for  $C_{31}H_{33}N_4O_3$ : 509.25528; found: 509.25341.  $^1H$  NMR (400 MHz,  $CDCl_3$ ):  $\delta$ , 7.66 (s, 1H), 7.65 (s, 1H), 7.24-7.21 (d,  $J = 8.4$ , 4H), 7.00-6.97 (d,  $J = 8.4$ , 2H), 6.88-6.86 (d,  $J = 8.4$ , 2H), 6.83-6.81 (d,  $J = 8.4$ , 2H), 5.45 (s, 2H), 5.15 (s, 4H), 3.79 (s, 3H), 3.78 (s, 6H), 2.35 (s, 3H) ppm.  $^{13}C$  NMR (100 MHz,  $CDCl_3$ ):  $\delta$ , 159.5 (Cq), 158.6 (Cq), 151.4 (Cq), 141.5, 140.8, 139.5 (Cq), 131.8 (Cq), 129.3, 129.0, 128.5 (Cq), 127.5, 114.6, 113.8, 106.6 (Cq), 55.44, 55.36, 49.7 ( $CH_2$ ), 49.3 ( $CH_2$ ), 15.1 ppm.

***7-Benzyl-N,N,1-tris(4-methoxybenzyl)-1H-imidazo[4,5-c]pyridin-4-amine (14i)***



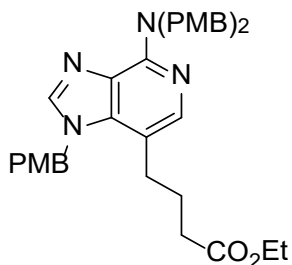
General conditions E, 4 h, 69 mg, 45%. Brown syrup. HRMS (ESI):  $m/z$   $[M+H]^+$  calc'd for  $C_{37}H_{37}N_4O_3$ : 585.286588; found: 585.28433.  $^1H$  NMR (400 MHz,  $CDCl_3$ ):  $\delta$ , 7.76 (s, 1H), 7.59 (s, 1H), 7.32-7.23 (m, 7H), 7.09-7.08 (d,  $J = 8.8$ , 2H), 6.87-6.82 (m, 8H), 5.22 (s, 4H), 5.05 (s, 2H), 4.00 (s, 2H), 3.80 (s, 9H) ppm.  $^{13}C$  NMR (100 MHz,  $CDCl_3$ ):  $\delta$ , 159.5 (Cq), 158.6 (Cq), 151.8 (Cq), 142.9, 141.4 (Cq), 140.9, 139.2 (Cq), 131.6 (Cq), 129.3, 129.0 (Cq), 128.9 (Cq), 128.8, 128.0, 127.2, 126.5, 114.6, 113.8, 108.5 (Cq), 55.42, 55.35, 49.7 (CH<sub>2</sub>), 49.0 (CH<sub>2</sub>), 35.0 (CH<sub>2</sub>) ppm.

#### 7-Isopropyl-*N,N*,1-tris(4-methoxybenzyl)-1*H*-imidazo[4,5-*c*]pyridin-4-amine (14j)



General conditions F, 27 h, 80 mg, 86%. Contains ~20% of *n*-propyl impurity. Colorless syrup. HRMS (ESI):  $m/z$   $[M+H]^+$  calc'd for  $C_{33}H_{37}N_4O_3$ : 537.28658; found: 537.28573.  $^1H$  NMR (400 MHz,  $CDCl_3$ ):  $\delta$ , 7.89 (s, 1H), 7.63 (s, 1H), 7.25-7.22 (d,  $J = 8.8$ , 4H), 6.98-6.96 (d,  $J = 8.8$ , 2H), 6.88-6.86 (d,  $J = 8.8$ , 2H), 6.84-6.82 (d,  $J = 8.8$ , 4H), 5.44 (s, 2H), 5.16 (s, 4H), 3.79 (s, 3H), 3.78 (s, 6H), 3.30-3.20 (septet,  $J = 6.8$ , 1H), 1.25-1.24 (d,  $J = 6.4$ , 6H) ppm.  $^{13}C$  NMR (100 MHz,  $CDCl_3$ ):  $\delta$ , 159.6 (Cq), 158.6 (Cq), 151.0 (Cq), 141.4, 138.1 (Cq), 138.0, 131.8 (Cq), 129.3, 128.7 (Cq), 128.6 (Cq), 127.6, 118.3 (Cq), 114.6, 113.8, 55.45, 55.36, 50.0 (CH<sub>2</sub>), 49.7 (CH<sub>2</sub>), 26.3, 24.3 ppm.

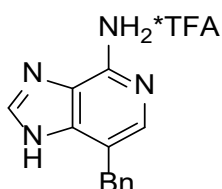
#### Ethyl 4-(4-(bis(4-methoxybenzyl)amino)-1-(4-methoxybenzyl)-1*H*-imidazo[4,5-*c*]pyridin-7-yl)butanoate (14k)



General conditions G, 20 h, 100 mg, 32%. Colorless syrup. HRMS (ESI):  $m/z$   $[M+H]^+$  calc'd for  $C_{36}H_{41}N_4O_5$ : 609.30773; found: 609.30580.  $^1H$  NMR (400 MHz,  $CDCl_3$ ):  $\delta$ , 7.69 (s, 1H), 7.65 (s, 1H), 7.24-7.22 (d,  $J = 8.8$ , 4H), 6.98-6.96 (d,  $J = 8.8$ , 2H), 6.87-

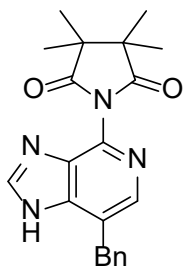
6.85 (d,  $J = 8.8$ , 2H), 6.84-6.82 (d,  $J = 8.8$ , 4H), 5.47 (s, 2H), 5.16 (s, 4H), 4.14-4.08 (q,  $J = 7.2$ , 2H), 3.78 (overlapped s, 9H), 2.71-2.68 (m, 2H), 2.37-2.33 (t,  $J = 7.2$ , 2H), 1.91-1.86 (m, 2H), 1.26-1.22 (t,  $J = 7.2$ , 3H) ppm.  $^{13}\text{C}$  NMR (100 MHz,  $\text{CDCl}_3$ ):  $\delta$ , 173.5 (Cq), 159.5 (Cq), 158.6 (Cq), 151.4 (Cq), 141.6, 141.1, 138.7 (Cq), 131.7 (Cq), 129.3, 128.8 (Cq), 128.7 (Cq), 127.5, 114.6, 113.8, 110.6 (Cq), 60.5 ( $\text{CH}_2$ ), 55.42, 55.36, 49.6 ( $\text{CH}_2$ ), 49.4 ( $\text{CH}_2$ ), 33.7 ( $\text{CH}_2$ ), 28.4 ( $\text{CH}_2$ ), 27.4 ( $\text{CH}_2$ ), 14.4 ppm.

### 7-Benzyl-1*H*-imidazo[4,5*c*]pyridin-4-amine, trifluoroacetic acid salt (**15i**)



This compound was synthesized according to the modified general procedure.<sup>15</sup> A solution of **14i** (589 mg, 1 mmol) in TFA (6 ml) was placed in a 100 ml pressure tube, anisole (0.65 ml, 6 equiv.) was added, and the mixture was heated at 70 °C for 24 h with vigorous stirring. It was cooled and concentrated under reduced pressure. The residue was coevaporated with toluene (3 x 25 ml) to obtain **15i** (ca. 0.34 g, quantitative) as an oil that was taken into next step without further purification.

### 1-(7-Benzyl-1*H*-imidazo[4,5-*c*]pyridin-4-yl)-3,3,4,4-tetramethylpyrrolidine-2,5-dione (**16i**)

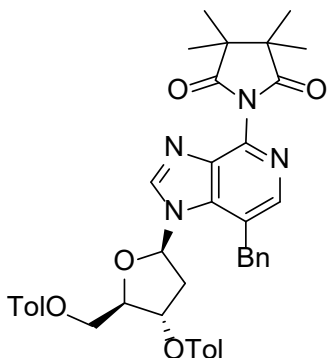


This compound was synthesized according to the reported general procedure.<sup>16</sup> A solution of **15i** (0.34 g, 1 mmol) in pyridine (10 ml) was placed in a 100 ml Schlenk flask. Tetramethylsuccinic anhydride ( $\text{M}_4\text{SA}$ )<sup>17</sup> (0.312 g, 2 mmol) and DBU (0.6 ml, 4 mmol) were added, and the mixture was heated at 120 °C under argon for 20 h with vigorous stirring. It was cooled and concentrated under reduced pressure. The residue was coevaporated with toluene (3 x 25 ml). The product was purified by column chromatography on silica gel eluting with 0-5% MeOH in  $\text{CH}_2\text{Cl}_2$  to give a cream foam. It



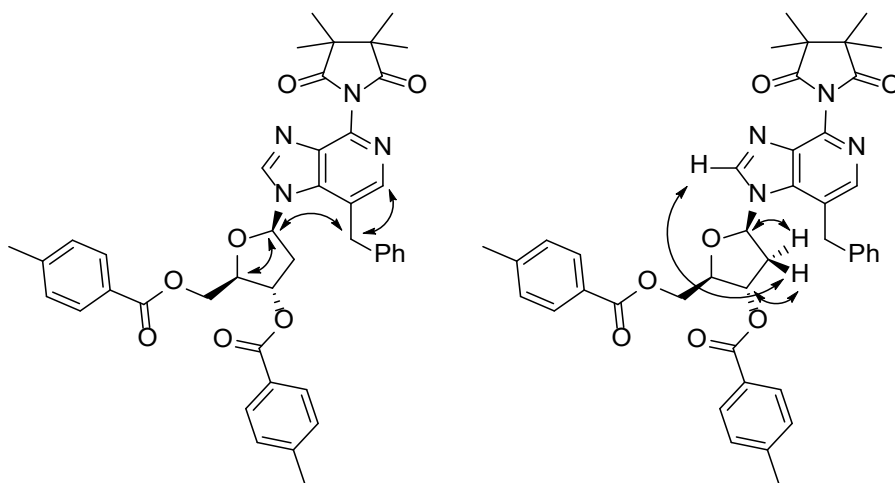
was taken in SOCl<sub>2</sub> (10 ml), heated at 80 °C for 2 h, cooled and concentrated under reduced pressure. The residue was coevaporated with EtOAc (3 x 25 ml). The product was purified by column chromatography on silica gel eluting with 0-5% MeOH in CH<sub>2</sub>Cl<sub>2</sub> to give **16i** as a cream foam in 57% yield (0.208 g). HRMS (ESI): m/z [M+H]<sup>+</sup> calc'd for C<sub>21</sub>H<sub>23</sub>N<sub>4</sub>O<sub>2</sub>: 363.18212; found: 363.18045. <sup>1</sup>H NMR (400 MHz, CD<sub>3</sub>OD): δ, 8.36 (s, 1H), 8.12 (s, 1H), 7.29-7.20 (m, 5H), 4.35 (s, 2H), 1.37 (bs, 12H) ppm. <sup>13</sup>C NMR (100 MHz, CD<sub>3</sub>OD): δ, 183.4, 146.2, 141.8, 139.7, 137.5, 129.8, 127.7, 124.7, 118.3, 35.5, 21.8 ppm.

**(2*R*,3*S*,5*R*)-5-(7-Benzyl-4-(3,3,4,4-tetramethyl-2,5-dioxopyrrolidin-1-yl)-1*H*-imidazo[4,5-*c*]pyridin-1-yl)-2-(((4-methylbenzoyl)oxy)methyl)tetrahydrofuran-3-yl 4-methylbenzoate (**17i**)**



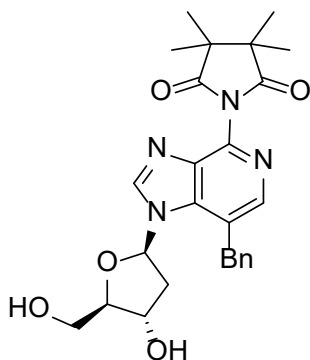
This compound was synthesized according to the reported general procedure.<sup>16</sup> To a solution of **16i** (0.19 g, 0.52 mmol) in dry CH<sub>3</sub>CN (25 ml) in a 100 ml round bottom flask, 60% NaH in oil (42 mg, 1.05 mmol) was added, and the mixture was vigorously stirred at room temperature under argon for 45 min. 1-(α)-Chloro-3,5-di-*O*-(*p*-toluoyl)-2-deoxy-D-ribose (0.368 g, 0.94 mmol) was subsequently added in one portion, and the stirring was continued at room temperature for 4.5 h. The mixture was filtered through Celite® and concentrated. The product was purified by column chromatography on silica gel eluting with 50% EtOAc in hexanes. **17i** was obtained as a yellowish syrup in 39% yield (0.145 g). HRMS (ESI): m/z [M+H]<sup>+</sup> calc'd for C<sub>42</sub>H<sub>43</sub>N<sub>4</sub>O<sub>7</sub>: 715.31322; found: 715.31184. <sup>1</sup>H NMR (400 MHz, CDCl<sub>3</sub>): δ, 8.32 (s, 1H), 8.19 (s, 1H), 7.92-7.90 (d, *J* = 8.4, 2H), 7.87-7.85 (d, *J* = 8.4, 2H), 7.34-7.32 (d, *J* = 8.4, 2H), 7.92-7.90 (d, *J* = 8.4, 2H), 7.14-7.11 (m, 3H), 7.06-7.04 (m, 2H), 6.20-6.17 (dd, *J*<sub>1</sub> = 5.2, *J*<sub>2</sub> = 9.2, 1H), 5.54-5.53 (m, 1H), 4.60-4.49 (m, 4H), 4.38-4.34 (AB/2, *J* = 16.8, 1H), 2.49 (s, 3H), 2.46-2.42 (m, 1H), 2.40 (s, 3H), 2.06-2.01 (m, 1H), 1.39 (bs, 1H) ppm. <sup>13</sup>C NMR (100 MHz, CDCl<sub>3</sub>): δ, 181.6 (Cq), 166.2 (Cq), 165.8 (Cq), 144.8 (Cq), 144.6, 144.4 (Cq), 142.3, 139.6 (Cq), 138.7 (Cq), 138.6 (Cq), 137.5 (Cq), 130.0,

129.8, 129.54, 129.47, 129.2, 128.1, 127.1, 126.6 (Cq), 126.5 (Cq), 120.0 (Cq), 85.8, 82.7, 74.8, 64.3 (CH<sub>2</sub>), 48.1 (Cq), 39.4 (CH<sub>2</sub>), 35.8 (CH<sub>2</sub>), 21.9, 21.8, 21.7, 21.5 ppm.



**Figure S1.** The critical NOESY correlations observed for **17i**.

**1-(7-Benzyl-1-((2*R*,4*S*,5*R*)-4-hydroxy-5-(hydroxymethyl)tetrahydrofuran-2-yl)-1*H*-imidazo[4,5-*c*]pyridin-4-yl)-3,3,4,4-tetramethylpyrrolidine-2,5-dione (**18i**)**

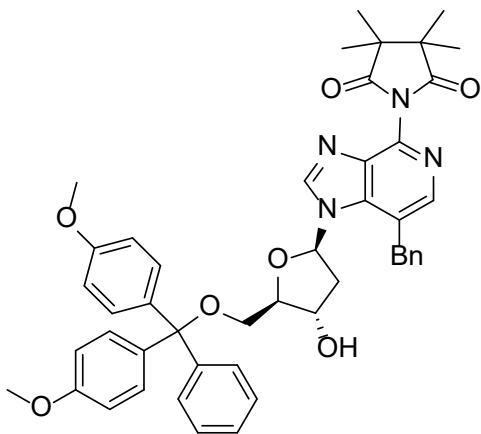


This compound was synthesized according to the general procedure.<sup>16</sup> To a solution of **17i** (0.14 g, 0.20 mmol) in dry MeOH (4 ml) in a 25 ml round bottom flask, NaOMe (32 mg, 0.60 mmol) was added. The mixture was stirred at room temperature under argon for 2 h and concentrated in vacuo. The product was purified by column chromatography on silica gel eluting with 0-10% MeOH in dichloromethane to obtain **18i** as

an off-white solid in 66% yield (62 mg). HRMS (ESI):  $m/z$  [M+H]<sup>+</sup> calc'd for C<sub>26</sub>H<sub>31</sub>N<sub>4</sub>O<sub>5</sub>: 479.22948; found: 479.22931. <sup>1</sup>H NMR (400 MHz, CD<sub>3</sub>OD):  $\delta$ , 8.69 (s, 1H), 8.14 (s, 1H), 7.32-7.14 (m, 5H), 6.35-6.32 (dd,  $J_1 = 6.4$ ,  $J_2 = 12.8$ , 1H), 4.61-4.57 (AB/2,  $J = 16.8$ , 1H), 4.47-4.30 (AB/2,  $J = 16.8$ , 1H), 4.46-4.44 (m, 1H), 3.95-3.92 (app q,  $J = 3.6$ , 1H), 3.73-3.69 (app dd,  $J_1 = 3.6$ ,  $J_2 = 12.0$ , 1H), 3.66-3.62 (app dd,  $J_1 = 3.6$ ,  $J_2 = 12.0$ , 1H), 2.52-2.46 (ddd,  $J_1 = J_2 = 6.0$ ,  $J_3 = 12.8$ , 1H), 2.14-2.08 (ddd,  $J_1 = 4.4$ ,  $J_2 = 6.0$ ,  $J_3 = 10.4$ , 1H), 1.37

(bs, 12H) ppm.  $^{13}\text{C}$  NMR (100 MHz,  $\text{CD}_3\text{OD}$ ):  $\delta$ , 183.4 (Cq), 145.9 (Cq), 144.3, 141.0 (Cq), 140.1 (Cq), 138.6 (Cq), 138.4 (Cq), 130.1, 129.5, 127.9, 123.5 (Cq), 89.2, 87.1, 71.7, 62.6 ( $\text{CH}_2$ ), 48.9 (Cq), 42.0 ( $\text{CH}_2$ ), 35.9 ( $\text{CH}_2$ ), 21.88, 21.84 ppm.

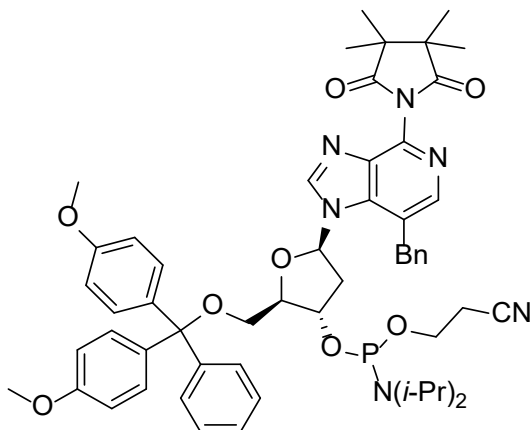
**1-(7-Benzyl-1-((2*R*,4*S*,5*R*)-5-((bis(4-methoxyphenyl)(phenyl)methoxy)methyl)-4-hydroxytetrahydrofuran-2-yl)-1*H*-imidazo[4,5-*c*]pyridin-4-yl)-3,3,4,4-tetramethylpyrrolidine-2,5-dione (19i)**



This compound was synthesized according to the reported general procedure.<sup>16</sup> To a solution of **18i** (56 mg, 0.12 mmol) in pyridine (2 ml), 4,4'-dimethoxytrityl chloride (DMT-Cl) (155 mg, 0.457 mmol) was added in one portion and the mixture was stirred at room temperature under argon for 5 h (TLC showed complete conversion). MeOH (0.2 ml) was then added, and the mixture

was concentrated in vacuo. The product was purified by column chromatography on silica gel (neutralized with triethylamine) eluting with 5-20% acetone in dichloromethane to obtain **19i** as a colorless solid in 69% yield (63 mg). HRMS (ESI):  $m/z$   $[\text{M}+\text{H}]^+$  calc'd for  $\text{C}_{47}\text{H}_{49}\text{N}_4\text{O}_7$ : 781.36017; found: 781.35738.  $^1\text{H}$  NMR (400 MHz,  $\text{CDCl}_3$ ):  $\delta$ , 8.24 (s, 1H), 8.10 (s, 1H), 7.38-7.10 (m, 14H), 6.82-6.80 (d,  $J = 8.4$ , 4H), 6.16-6.12 (dd,  $J_1 = 6.4$ ,  $J_2 = 12.4$ , 1H), 4.50-4.46 (AB/2,  $J = 16.8$ , 1H), 4.43-4.38 (m, 1H), 4.36-4.32 (AB/2,  $J = 16.8$ , 1H), 4.01-3.98 (app q,  $J = 4.4$ , 1H), 3.78 (s, 6H), 3.36-3.32 (app dd,  $J_1 = 4.4$ ,  $J_2 = 10.4$ , 1H), 3.28-3.24 (app dd,  $J_1 = 4.8$ ,  $J_2 = 10.4$ , 1H), 2.6 (bs, 1H), 2.28-2.22 (ddd,  $J_1 = J_2 = 6.0$ ,  $J_3 = 13.2$ , 1H), 1.90-1.84 (ddd,  $J_1 = J_2 = 5.6$ ,  $J_3 = 9.6$ , 1H), 1.39-1.38 (overlapped s, 12H) ppm.  $^{13}\text{C}$  NMR (100 MHz,  $\text{CDCl}_3$ ):  $\delta$ , 181.7 (Cq), 158.7 (Cq), 144.5 (Cq), 144.1, 142.6, 139.4 (Cq), 138.8 (Cq), 138.2 (Cq), 137.6 (Cq), 135.63 (Cq), 135.55 (Cq), 130.12, 130.09, 129.1, 128.6, 128.13, 128.10, 127.11, 127.07, 120.6 (Cq), 113.4, 86.8 (Cq), 85.7, 85.2, 72.0, 63.7 ( $\text{CH}_2$ ), 55.3, 48.0 (Cq), 41.4 ( $\text{CH}_2$ ), 35.6 ( $\text{CH}_2$ ), 21.8, 21.4 ppm.

**(2*R*,3*S*,5*R*)-5-(7-Benzyl-4-(3,3,4,4-tetramethyl-2,5-dioxopyrrolidin-1-yl)-1*H*-imidazo[4,5-*c*]pyridin-1-yl)-2-((bis(4-methoxyphenyl)(phenyl)methoxy)methyl)tetrahydrofuran-3-yl (2-cyanoethyl) diisopropylphosphoramidite (**20i**)**

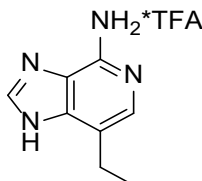


This compound was synthesized according to the reported general procedure.<sup>18</sup> To a solution of **19i** (62 mg, 0.080 mmol) in dry CH<sub>2</sub>Cl<sub>2</sub> (2 ml) containing *N,N*-diisopropylethylamine (DIEA) (70 μl, 0.4 mmol), 2-cyanoethyl-*N,N*-diisopropyl chlorophosphoramidite (40 μl, 0.175 mmol) was added in one portion and the

mixture was stirred at room temperature under argon for 3 h (TLC showed complete conversion). The mixture was concentrated in vacuo at rt and the product was purified by column chromatography on silica gel (neutralized with triethylamine) eluting with 50% EtOAc in hexanes containing 1% triethylamine, to obtain **20i** as a mixture of diastereomers (colorless solid, *R<sub>f</sub>* ~0.5 in 5% acetone/CH<sub>2</sub>Cl<sub>2</sub>, two close spots visible on TLC) in 49% yield (38 mg). HRMS (ESI): *m/z* [M+H]<sup>+</sup> calc'd for C<sub>56</sub>H<sub>66</sub>N<sub>6</sub>O<sub>8</sub>P: 981.46801; found: 981.46481. <sup>1</sup>H NMR (400 MHz, acetone-*d*<sub>6</sub>): δ, 8.40, 8.39 (s, 1H), 8.21, 8.19 (s, 1H), 7.45-7.18 (m, 14H), 6.84-6.80 (m, 4H), 6.40-6.35 (dd, *J*<sub>1</sub> = 7.0, *J*<sub>2</sub> = 12.8, 1H), 4.68-4.78 (m, 2H), 4.56-4.52, 4.53-4.49 (AB/2, *J* = 16.4, 1H), 4.28-4.26, 4.24-4.21 (app q, *J* = 4.4, 1H), 3.763, 3.757 (s, 6H), 3.67-3.58 (m, 2H), 3.36-3.32 (m, 2H), 2.91-2.78 (m, 3H), 2.76-2.73 (t, *J* = 6.0, 1H), 2.68-2.65 (t, *J* = 6.0, 1H), 1.35, 1.31 (bs, 12H), 1.21-1.19 (m, 6H), 1.15-1.14, 1.13-1.11 (d, *J* = 6.8, 6H) ppm. <sup>13</sup>C NMR (100 MHz, acetone-*d*<sub>6</sub>): δ, 181.7, 159.6, 145.9, 144.36, 144.27, 144.02, 143.97, 140.4, 140.08, 140.05, 139.2, 138.8, 136.64, 136.58, 136.52, 130.96, 130.93, 129.7, 129.34, 129.31, 128.97, 128.91, 128.6, 127.6, 127.50, 127.47, 122.3, 122.2, 119.0, 114.0, 87.22, 87.18, 86.6, 86.4, 86.3, 86.2, 74.4, 74.0, 73.8, 64.3, 64.3, 59.7, 59.6, 59.4, 55.5, 55.0, 48.3, 44.06, 43.99, 43.94, 43.86, 40.4, 40.3,

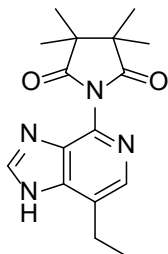
35.5, 24.94, 24.86, 24.82, 22.0, 21.7, 21.4, 20.8, 20.7 ppm.  $^{31}\text{P}$  NMR (162 MHz, acetone- $d_6$ ):  $\delta$ , 149.8, 149.6 ppm.

### 7-Ethyl-1*H*-imidazo[4,5*c*]pyridin-4-amine, trifluoroacetic acid salt (**15d**)



This compound was synthesized in similar fashion as **15i**. A solution of **14d** (750 mg, 1.4 mmol) in TFA (10 ml) was placed in a 100 ml pressure tube, anisole (ca. 1 ml, 6 equiv.) was added, and the mixture was heated at 70 °C for 24 h with vigorous stirring. It was cooled and concentrated under reduced pressure. The residue was coevaporated with toluene (3 x 20 ml) to obtain **15d** (ca. 0.4 g, quantitative) as an oil that was taken into next step without further purification.

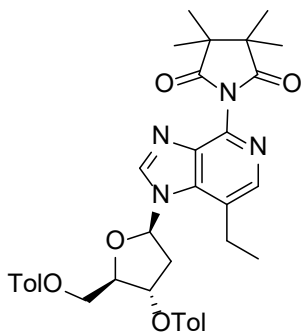
### 1-(7-Ethyl-1*H*-imidazo[4,5-*c*]pyridin-4-yl)-3,3,4,4-tetramethylpyrrolidine-2,5-dione (**16d**)



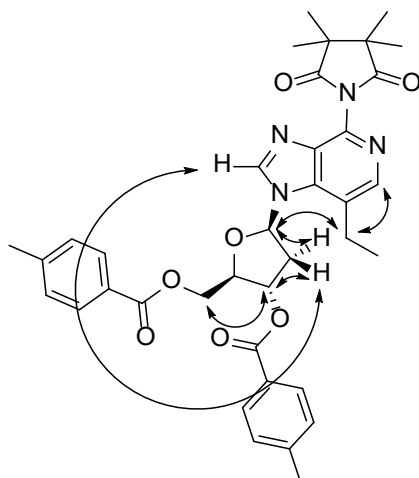
This compound was synthesized in similar fashion as **16i**. A solution of **15d** (0.4 g, 1.4 mmol) in pyridine (15 ml) was placed in a 100 ml Schlenk flask. Tetramethylsuccinic anhydride (M<sub>4</sub>SA) (0.5 g, 3.2 mmol) and DBU (1 ml, 6.7 mmol) were added, and the mixture was heated at 120 °C under argon for 22 h with vigorous stirring. It was cooled and concentrated under reduced pressure. The residue was coevaporated with toluene (3 x 20 ml). The product was purified by column chromatography on silica gel eluting with 0-5% MeOH in CH<sub>2</sub>Cl<sub>2</sub> to give a cream solid. It was taken in SOCl<sub>2</sub> (12 ml), heated at 80 °C for 2 h, cooled and concentrated under reduced pressure. The residue was coevaporated with EtOAc (3 x 20 ml). The product was purified by column chromatography on silica gel eluting with 0-8% MeOH in CH<sub>2</sub>Cl<sub>2</sub> to give **16d** as a cream solid in 88% yield (0.37 g). HRMS (ESI):  $m/z$  [M+H]<sup>+</sup> calc'd for C<sub>16</sub>H<sub>21</sub>N<sub>4</sub>O<sub>2</sub>: 301.16647; found: 301.16501.  $^1\text{H}$  NMR (400 MHz, CD<sub>3</sub>OD):  $\delta$ , 8.52 (s, 1H), 8.24 (s, 1H), 3.07-3.01 (q,  $J$  = 7.2, 2H), 1.41-1.37 (t,  $J$  = 7.2, 3H),

1.37 (bs, 12H) ppm.  $^{13}\text{C}$  NMR (100 MHz,  $\text{CD}_3\text{OD}$ ):  $\delta$ , 182.9, 146.9, 143.5, 139.6, 135.4, 135.1, 128.7, 48.9, 23.2, 21.8, 14.5 ppm.

**(2*R*,3*S*,5*R*)-5-(7-Ethyl-4-(3,3,4,4-tetramethyl-2,5-dioxopyrrolidin-1-yl)-1*H*-imidazo[4,5-*c*]pyridin-1-yl)-2-(((4-methylbenzoyl)oxy)methyl)tetrahydrofuran-3-yl 4-methylbenzoate (17d)**

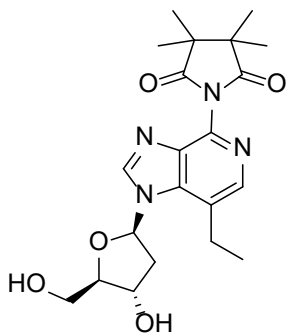


This compound was synthesized in similar fashion as **17i**. To a solution of **16i** (0.35 g, 1.17 mmol) in dry  $\text{CH}_3\text{CN}$  (60 ml) in a 250 ml round bottom flask, 60% NaH in oil (100 mg, 2.5 mmol) was added, and the mixture was vigorously stirred at room temperature under argon for 45 min. 1-( $\alpha$ )-Chloro-3,5-di-*O*-(*p*-toluoyl)-2-deoxy-D-ribose (0.817 g, 2.1 mmol) was subsequently added portionwise over 1 h, and the stirring was continued at room temperature for overall 5 h. The mixture was filtered through Celite® and concentrated. The product was purified by column chromatography on silica gel eluting with 0-50% EtOAc in hexanes, and concentrated repeatedly with dichloromethane. **17d** was obtained as a yellowish syrup in 65% yield (0.494 g). HRMS (ESI):  $m/z$   $[\text{M}+\text{H}]^+$  calc'd for  $\text{C}_{37}\text{H}_{41}\text{N}_4\text{O}_7$ : 653.29757; found: 653.29654.  $^1\text{H}$  NMR (400 MHz,  $\text{CDCl}_3$ ):  $\delta$ , 8.27 (s, 1H), 8.25 (s, 1H), 7.92-7.90 (d,  $J = 8.0$ , 2H), 7.88-7.86 (d,  $J = 8.0$ , 2H), 7.30-7.28 (d,  $J = 8.4$ , 2H), 7.24-7.22 (d,  $J = 8.4$ , 2H), 6.60-6.57 (dd,  $J_1 = 6.4$ ,  $J_2 = 12.8$ , 1H), 5.72-5.68 (m, 1H), 4.67-4.59 (m, 3H), 3.16-3.00 (m, 2H), 2.82-2.79 (dd,  $J_1 = 4.4$ ,  $J_2 = 6.8$ , 2H), 2.44 (s, 3H), 2.40 (s, 3H), 1.43-1.40 (t,  $J = 7.6$ , 3H), 1.37 (bs, 1H) ppm.  $^{13}\text{C}$  NMR (100 MHz,  $\text{CDCl}_3$ ):  $\delta$ , 181.7 (Cq), 166.3 (Cq), 165.9 (Cq), 144.9 (Cq), 144.4 (Cq), 142.6, 142.0, 138.9 (Cq), 137.6 (Cq), 137.3 (Cq), 130.0, 129.9, 129.8, 129.5, 126.6 (Cq), 126.4 (Cq), 124.2 (Cq), 85.5, 82.7, 74.6, 64.0 ( $\text{CH}_2$ ), 48.0 (Cq), 39.7 ( $\text{CH}_2$ ), 22.9 ( $\text{CH}_2$ ), 21.9, 21.8, 21.7, 21.5, 15.4 ppm.



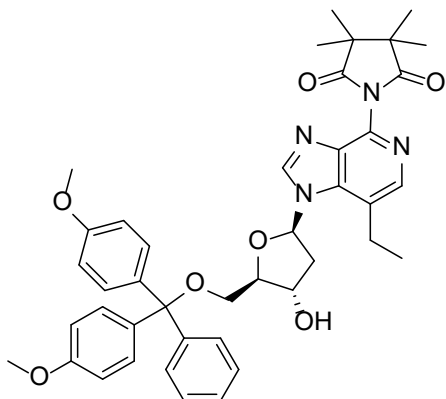
**Figure S2.** The critical NOESY correlations observed for **17d**.

**1-(7-Ethyl-1-((2*R*,4*S*,5*R*)-4-hydroxy-5-(hydroxymethyl)tetrahydrofuran-2-yl)-1*H*-imidazo[4,5-*c*]pyridin-4-yl)-3,3,4,4-tetramethylpyrrolidine-2,5-dione (**18d**)**



This compound was synthesized in similar fashion as **18i**. To a solution of **17d** (0.46 g, 0.7 mmol) in dry MeOH (6 ml) in a 25 ml round bottom flask, NaOMe (114 mg, 2.11 mmol) was added. The mixture was stirred at room temperature under argon for 2 h and concentrated in vacuo. The product was purified by column chromatography on silica gel eluting with 0-10% MeOH in dichloromethane to obtain **18d** as an off-white solid in 74% yield (218 mg). HRMS (ESI):  $m/z$   $[M+H]^+$  calc'd for  $C_{21}H_{29}N_4O_5$ : 417.21383; found: 417.21265.  $^1H$  NMR (400 MHz,  $CD_3OD$ ):  $\delta$ , 8.74 (s, 1H), 8.20 (s, 1H), 6.63-6.60 (dd,  $J_1 = 6.4$ ,  $J_2 = 12.8$ , 1H), 4.58-4.55 (m, 1H), 4.06-4.03 (app q,  $J = 3.6$ , 1H), 3.78-3.65 (m, 2H), 3.23-3.12 (app septet,  $J = 3.6$ , 2H), 2.78-2.72 (m, 1H), 2.60-2.54 (ddd,  $J_1 = 3.6$ ,  $J_2 = 6.0$ ,  $J_3 = 10.4$ , 1H), 1.44-1.40 (t,  $J = 7.6$ , 3H), 1.37 (bs, 12H) ppm.  $^{13}C$  NMR (100 MHz,  $CD_3OD$ ):  $\delta$ , 183.4 (Cq), 145.8 (Cq), 142.4, 140.4 (Cq), 138.4 (Cq), 137.8 (Cq), 127.2 (Cq), 89.4, 87.2, 72.1, 62.7 ( $CH_2$ ), 48.8 (Cq), 42.2 ( $CH_2$ ), 23.5 ( $CH_2$ ), 21.9, 21.8, 15.7 ppm.

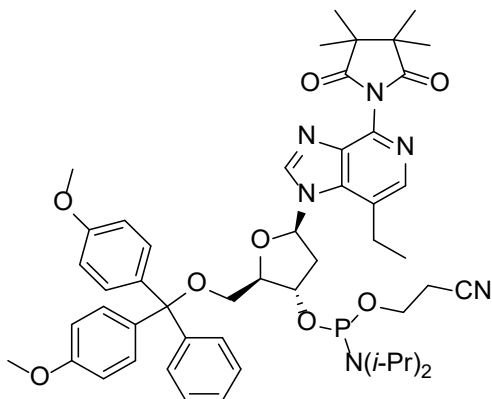
**1-(1-((2*R*,4*S*,5*R*)-5-((Bis(4-methoxyphenyl)(phenyl)methoxy)methyl)-4-hydroxytetrahydro-furan-2-yl)-7-ethyl-1*H*-imidazo[4,5-*c*]pyridin-4-yl)-3,3,4,4-tetramethylpyrrolidine-2,5-dione (19d)**



This compound was synthesized in similar fashion as **19i**. To a solution of **18d** (190 mg, 0.457 mmol) in pyridine (3 ml), 4,4'-dimethoxytrityl chloride (DMT-Cl) (217 mg, 0.639 mmol) was added in one portion and the mixture was stirred at room temperature under argon for 4 h. The mixture was concentrated in vacuo. The product was purified by column chromatography on silica gel (neutralized with triethylamine) eluting with 0-20% acetone in dichloromethane to obtain **19d** as a colorless solid in 33% yield (110 mg). HRMS (ESI):  $m/z$   $[M+H]^+$  calc'd for  $C_{42}H_{47}N_4O_7$ : 719.34452; found: 719.34247.  $^1H$  NMR (400 MHz,  $CDCl_3$ ):  $\delta$ , 8.21 (s, 1H), 8.16 (s, 1H), 7.40-7.38 (d,  $J = 7.2$ , 2H), 7.30-7.20 (m, 7H), 6.82-6.80 (d,  $J = 9.2$ , 4H), 6.42-6.39 (dd,  $J_1 = 6.4$ ,  $J_2 = 12.4$ , 1H), 4.54-4.48 (m, 1H), 4.11-4.08 (app q,  $J = 4.4$ , 1H), 3.77 (s, 6H), 3.38-3.34 (app dd,  $J_1 = 4.4$ ,  $J_2 = 10.4$ , 1H), 3.32-3.29 (app dd,  $J_1 = 4.8$ ,  $J_2 = 10.4$ , 1H), 3.17 (bs, 1H), 3.03-3.00 (app dd,  $J_1 = 3.2$ ,  $J_2 = 7.6$ , 1H), 2.99-2.96 (app dd,  $J_1 = 3.2$ ,  $J_2 = 7.6$ , 1H), 2.46-2.44 (app t,  $J = 6.0$ , 2H), 1.38-1.37 (overlapped s, 12H), 1.36-1.32 (t,  $J = 7.2$ , 3H) ppm.  $^{13}C$  NMR (100 MHz,  $CDCl_3$ ):  $\delta$ , 181.8 (Cq), 158.7 (Cq), 144.5 (Cq), 142.6, 141.9, 138.9 (Cq), 137.3 (Cq), 137.2 (Cq), 135.63 (Cq), 135.58 (Cq), 130.1, 128.13, 128.06, 127.1, 124.6 (Cq), 113.4, 86.8 (Cq), 86.0, 85.2, 71.9, 63.7 ( $CH_2$ ), 55.3, 48.0 (Cq), 41.7 ( $CH_2$ ), 22.7 ( $CH_2$ ), 21.8, 21.4, 15.3 ppm.

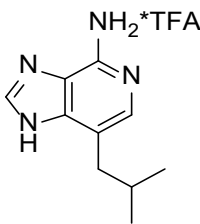
**(2*R*,3*S*,5*R*)-2-((Bis(4-methoxyphenyl)(phenyl)methoxy)methyl)-5-(7-ethyl-4-(3,3,4,4-tetramethyl-2,5-dioxopyrrolidin-1-yl)-1*H*-imidazo[4,5-*c*]pyridin-1-yl)tetrahydrofuran-3-yl (2-cyanoethyl) diisopropylphosphoramidite (20d)**





This compound was synthesized in similar fashion as **20i**. To a solution of **19d** (105 mg, 0.146 mmol) in dry CH<sub>2</sub>Cl<sub>2</sub> (4 ml) containing *N,N*-diisopropylethylamine (DIEA) (127 μl, 0.731 mmol), 2-cyanoethyl-*N,N*-diisopropyl chloro-phosphoramidite (40 μl, 0.175 mmol) was added in one portion and the mixture was stirred at room temperature under argon for 4 h (TLC showed complete conversion). The mixture was concentrated in vacuo at rt and the product was purified by column chromatography on silica gel (neutralized with triethylamine) eluting with 40-60% EtOAc in hexanes containing 1% triethylamine, to obtain **20d** as a mixture of diastereomers (white foam, R<sub>f</sub> ~0.5 in 5% acetone/CH<sub>2</sub>Cl<sub>2</sub>, two close spots visible on TLC) in 67% yield (90 mg). HRMS (ESI): *m/z* [M+H]<sup>+</sup> calc'd for C<sub>51</sub>H<sub>64</sub>N<sub>6</sub>O<sub>8</sub>P: 919.45236; found: 919.45047. <sup>1</sup>H NMR (400 MHz, CDCl<sub>3</sub>): δ, 8.25 (s, 1H), 8.23, 8.19 (s, 1H), 7.40-7.38 (m, 2H), 7.30-7.20 (m, 7H), 6.83-6.79 (m, 4H), 6.49-6.46 (dd, *J*<sub>1</sub> = 6.8, *J*<sub>2</sub> = 13.6, 1H), 4.70-4.59 (m, 1H), 4.32-4.24 (m, 1H), 3.78, 3.77 (s, 6H), 3.70-3.53 (m, 3H), 3.32-3.31 (m, 1H), 3.13-2.99 (m, 2H), 2.62-2.59 (t, *J* = 6.4, 1H), 2.57-2.55 (m, 1H), 2.44-2.41 (t, *J* = 6.4, 1H), 1.38, 1.37 (bs, 12H), 1.20-1.17 (m, 9H), 1.13-1.12 (d, *J* = 6.8, 3H) ppm. <sup>13</sup>C NMR (100 MHz, CDCl<sub>3</sub>): δ, 181.7, 158.7, 144.5, 142.5, 142.4, 139.0, 137.4, 135.63, 135.56, 130.2, 128.3, 128.2, 128.1, 127.1, 124.5, 124.4, 117.5, 113.4, 86.7, 85.8, 85.5, 85.4, 74.1, 73.9, 63.4, 63.2, 58.4, 58.2, 55.38, 55.36, 48.0, 43.61, 43.55, 43.4, 41.0, 24.7, 24.6, 22.9, 21.8, 21.5, 15.6 ppm. <sup>31</sup>P NMR (162 MHz, CDCl<sub>3</sub>): δ, 150.8, 150.2 ppm.

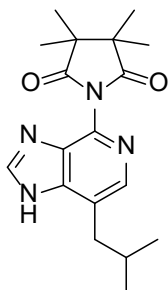
### 7-Isobutyl-1*H*-imidazo[4,5*c*]pyridin-4-amine, trifluoroacetic acid salt (**15e**)



This compound was synthesized in similar fashion as **15i**. A solution of **14e** (1.3 g, 2.4 mmol) in TFA (20 ml) was placed in a 100 ml pressure tube, anisole (1.6 ml, 6 equiv.) was added, and the mixture was heated at 70 °C for 24 h with vigorous stirring. It was cooled and concentrated

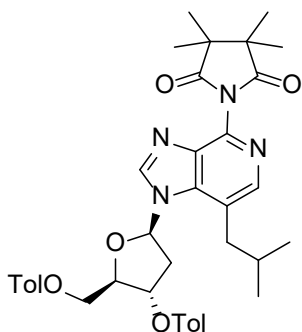
under reduced pressure. The residue was coevaporated with toluene (3 x 20 ml) to obtain **15e** (ca. 0.8 g, quantitative) as an oil that was taken into next step without further purification.

**1-(7-Isobutyl-1*H*-imidazo[4,5-*c*]pyridin-4-yl)-3,3,4,4-tetramethylpyrrolidine-2,5-dione (16e)**

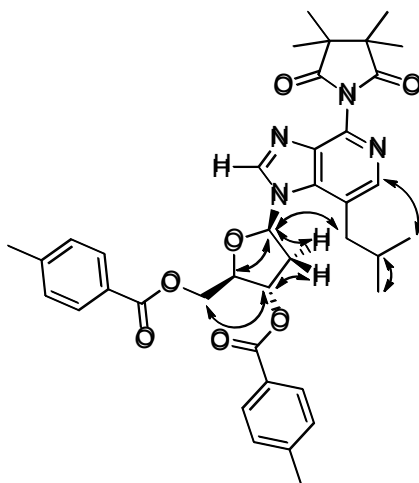


This compound was synthesized in similar fashion as **16i**. A solution of **15e** (ca. 0.8 g, 2.4 mmol) in pyridine (20 ml) was placed in a 100 ml Schlenk flask. Tetramethylsuccinic anhydride (M<sub>4</sub>SA) (0.8 g, 5.1 mmol) and DBU (1.5 ml, 10.0 mmol) were added, and the mixture was heated at 120 °C under argon for 22 h with vigorous stirring. It was cooled and concentrated under reduced pressure. The residue was coevaporated with toluene (3 x 20 ml). The product was purified by column chromatography on silica gel eluting with 0-5% MeOH in CH<sub>2</sub>Cl<sub>2</sub> to give a cream foam. It was taken in SOCl<sub>2</sub> (20 ml), heated at 80 °C for 2 h, cooled and concentrated under reduced pressure. The residue was coevaporated with EtOAc (3 x 20 ml). The product was purified by column chromatography on silica gel eluting with 0-8% MeOH in CH<sub>2</sub>Cl<sub>2</sub> to give **16e** as a cream foam in 79% yield (0.61 g). HRMS (ESI): *m/z* [M+H]<sup>+</sup> calc'd for C<sub>18</sub>H<sub>25</sub>N<sub>4</sub>O<sub>2</sub>: 329.19777; found: 329.19608. <sup>1</sup>H NMR (400 MHz, CD<sub>3</sub>OD): δ, 8.43 (s, 1H), 8.16 (s, 1H), 2.87-2.85 (d, *J* = 7.6, 2H), 2.11-2.05 (app septet, *J* = 6.8, 1H), 1.37 (bs, 12H), 0.99-0.97 (d, *J* = 6.4, 6H) ppm. <sup>13</sup>C NMR (100 MHz, CD<sub>3</sub>OD): δ, 183.2, 146.4, 143.7, 141.6, 135.8, 135.4, 126.0, 38.9, 30.4, 22.6, 21.9 ppm.

**(2*R*,3*S*,5*R*)-5-(7-Isobutyl-4-(3,3,4,4-tetramethyl-2,5-dioxopyrrolidin-1-yl)-1*H*-imidazo[4,5-*c*]pyridin-1-yl)-2-(((4-methylbenzoyl)oxy)methyl)tetrahydrofuran-3-yl 4-methylbenzoate (17e)**

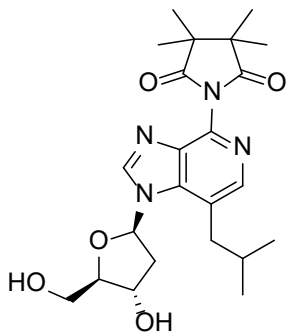


This compound was synthesized in similar fashion as **17i**. To a solution of **16e** (0.585 g, 1.78 mmol) in dry CH<sub>3</sub>CN (60 ml) in a 250 ml round bottom flask, 60% NaH in oil (143 mg, 3.57 mmol) was added, and the mixture was vigorously stirred at room temperature under argon for 35 min. 1-( $\alpha$ )-Chloro-3,5-di-*O*-(*p*-toluoyl)-2-deoxy-D-ribose (1.25 g, 3.21 mmol) was subsequently added portionwise over 1 h, and the stirring was continued at room temperature for overall 4.5 h. The mixture was filtered through Celite® and concentrated. The product was purified by column chromatography on silica gel eluting with 0-50% EtOAc in hexanes, and concentrated repeatedly with dichloromethane. **17e** was obtained as a yellowish solid in 38% yield (0.465 g). HRMS (ESI):  $m/z$  [M+H]<sup>+</sup> calc'd for C<sub>39</sub>H<sub>45</sub>N<sub>4</sub>O<sub>7</sub>: 681.32887; found: 681.32697. <sup>1</sup>H NMR (400 MHz, CDCl<sub>3</sub>):  $\delta$ , 8.27 (s, 1H), 8.20 (s, 1H), 7.97-7.95 (d,  $J$  = 8.0, 2H), 7.92-7.90 (d,  $J$  = 8.0, 2H), 7.30-7.28 (d,  $J$  = 8.4, 2H), 7.27-7.25 (d,  $J$  = 8.4, 2H), 6.59-6.55 (dd,  $J_1$  = 5.2,  $J_2$  = 8.8, 1H), 5.73-5.72 (m, 1H), 4.70-4.61 (m, 3H), 2.98-2.92 (dd,  $J_1$  = 7.2,  $J_2$  = 14.4, 1H), 2.84-2.72 (m, 3H), 2.45 (s, 3H), 2.42 (s, 3H), 1.98-1.88 (app septet,  $J$  = 6.4, 1H), 1.38 (bs, 1H), 1.05-1.03 (d,  $J$  = 6.8, 6H) ppm. <sup>13</sup>C NMR (100 MHz, CDCl<sub>3</sub>):  $\delta$ , 181.6 (Cq), 166.3 (Cq), 165.9 (Cq), 144.9 (Cq), 144.4 (Cq), 144.1, 142.2, 139.2 (Cq), 137.7 (Cq), 137.4 (Cq), 129.9, 129.8, 129.54, 129.47, 126.6 (Cq), 126.3 (Cq), 121.8 (Cq), 85.4, 82.9, 74.9, 64.2 (CH<sub>2</sub>), 48.0 (Cq), 39.9 (CH<sub>2</sub>), 39.1 (CH<sub>2</sub>), 30.2, 22.5, 21.9, 21.8, 21.7, 21.5 ppm.



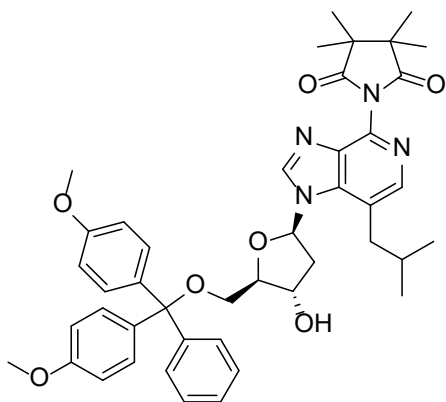
**Figure S3.** The critical NOESY correlations observed for **17e**.

**1-(1-((2*R*,4*S*,5*R*)-4-Hydroxy-5-(hydroxymethyl)tetrahydrofuran-2-yl)-7-isobutyl-1*H*-imidazo[4,5-*c*]pyridin-4-yl)-3,3,4,4-tetramethylpyrrolidine-2,5-dione (**18e**)**



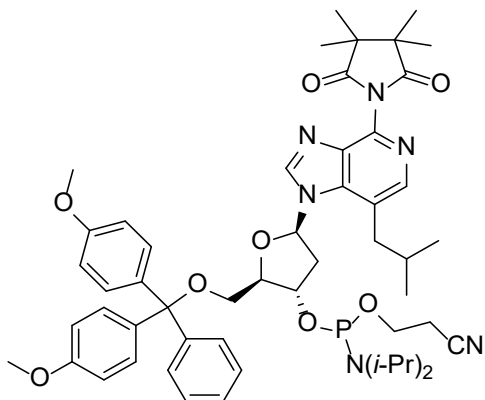
This compound was synthesized in similar fashion as **18i**. To a solution of **17e** (0.46 g, 0.68 mmol) in dry MeOH (7 ml) in a 25 ml round bottom flask, NaOMe (110 mg, 2.03 mmol) was added. The mixture was stirred at room temperature under argon for 2 h and concentrated in vacuo. The product was purified by column chromatography on silica gel eluting with 0-10% MeOH in dichloromethane to obtain **18e** as an off-white foam in 85% yield (256 mg). HRMS (ESI):  $m/z$   $[M+H]^+$  calc'd for  $C_{23}H_{33}N_4O_5$ : 445.24512; found: 445.24381.  $^1H$  NMR (400 MHz,  $CD_3OD$ ):  $\delta$ , 8.74 (s, 1H), 8.14 (s, 1H), 6.58-6.55 (dd,  $J_1 = 6.4$ ,  $J_2 = 12.8$ , 1H), 4.58-4.55 (dt,  $J_1 = 3.2$ ,  $J_2 = 6.8$ , 1H), 4.06-4.04 (app q,  $J = 3.2$ , 1H), 3.77-3.73 (app dd,  $J_1 = 3.6$ ,  $J_2 = 12.0$ , 1H), 3.72-3.68 (app dd,  $J_1 = 3.6$ ,  $J_2 = 12.0$ , 1H), 3.06-3.01 (app dd,  $J_1 = 6.8$ ,  $J_2 = 14.4$ , 1H), 2.92-2.86 (app dd,  $J_1 = 7.2$ ,  $J_2 = 14.0$ , 1H), 2.76-2.69 (ddd,  $J_1 = 5.6$ ,  $J_2 = 6.8$ ,  $J_3 = 13.2$ , 1H), 2.56-2.51 (ddd,  $J_1 = 3.6$ ,  $J_2 = 6.0$ ,  $J_3 = 9.6$ , 1H), 2.04-1.94 (app septet,  $J = 6.8$ , 1H), 1.37 (bs, 12H), 1.05-1.03 (d,  $J = 6.8$ , 6H) ppm.  $^{13}C$  NMR (100 MHz,  $CD_3OD$ ):  $\delta$ , 183.4 (Cq), 146.0 (Cq), 144.0, 140.7 (Cq), 138.5 (Cq), 137.9 (Cq), 124.6 (Cq), 89.4, 87.0, 72.3, 62.8 ( $CH_2$ ), 48.9 (Cq), 42.3 ( $CH_2$ ), 39.4 ( $CH_2$ ), 31.1, 22.6, 22.5, 21.9, 21.8 ppm.

**1-(1-((2*R*,4*S*,5*R*)-5-((Bis(4-methoxyphenyl)(phenyl)methoxy)methyl)-4-hydroxytetrahydrofuran-2-yl)-7-isobutyl-1*H*-imidazo[4,5-*c*]pyridin-4-yl)-3,3,4,4-tetramethylpyrrolidine-2,5-dione (**19e**)**



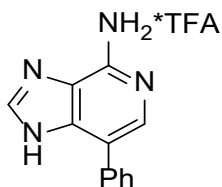
This compound was synthesized in similar fashion as **19i**. To a solution of **18e** (225 mg, 0.507 mmol) in dry pyridine (4 ml), 4,4'-dimethoxytrityl chloride (DMT-Cl) (240 mg, 0.709 mmol) was added in one portion and the mixture was stirred at room temperature under argon for 4 h. TLC analysis indicated that a lot of starting material remained and then additional DMT-Cl (0.120 g, 0.355 mmol) and cat. DMAP (10 mg) were added. After 14 h more DMT-Cl (0.120 g, 0.355 mmol), triethylamine (85  $\mu$ l, 0.608 mmol), and cat. DMAP (10 mg) were added. After 8 h, another portion as above was added, and after 16 h TLC showed no further conversion (overall 42 h). The mixture was quenched with 200  $\mu$ l of MeOH, concentrated in vacuo, the residue was taken in AcOEt and filtered, and the filtrate was concentrated in vacuo. The product was purified by column chromatography on silica gel (neutralized with triethylamine) eluting with 0-25% acetone in dichloromethane to obtain **19e** as a colorless foam in 46% yield (175 mg). Further elution with 10% MeOH in dichloromethane yielded the recovered starting material **18e** as a colorless syrup in 45% yield (102 mg). HRMS (ESI):  $m/z$   $[M+H]^+$  calc'd for  $C_{44}H_{51}N_4O_7$ : 747.37582; found: 747.37412.  $^1H$  NMR (400 MHz,  $CDCl_3$ ):  $\delta$ , 8.17 (s, 1H), 8.14 (s, 1H), 7.40-7.38 (d,  $J$  = 8.8, 2H), 7.30-7.20 (m, 7H), 6.82-6.80 (d,  $J$  = 8.8, 4H), 6.42-6.38 (dd,  $J_1$  = 6.4,  $J_2$  = 12.8, 1H), 4.52-4.51 (m, 1H), 4.10-4.07 (app q,  $J$  = 4.4, 1H), 3.77 (s, 6H), 3.38-3.35 (app dd,  $J_1$  = 4.4,  $J_2$  = 10.4, 1H), 3.33-3.29 (app dd,  $J_1$  = 4.8,  $J_2$  = 10.4, 1H), 2.88-2.83 (app dd,  $J_1$  = 7.2,  $J_2$  = 14.4, 1H), 2.75-2.70 (app dd,  $J_1$  = 6.4,  $J_2$  = 14.0, 1H), 2.46-2.41 (m, 2H), 1.90-1.84 (app quintet,  $J$  = 6.4, 1H), 1.37-1.36 (overlapped s, 12H), 1.01-0.99 (dd,  $J_1$  = 2.4,  $J_2$  = 6.4, 6H) ppm.  $^{13}C$  NMR (100 MHz,  $CDCl_3$ ):  $\delta$ , 181.7 (Cq), 158.7 (Cq), 144.5 (Cq), 143.6, 142.7, 139.2 (Cq), 137.5 (Cq), 137.4 (Cq), 135.63 (Cq), 135.58 (Cq), 130.1, 128.2, 128.1, 127.1, 122.2 (Cq), 113.4, 86.8 (Cq), 86.0, 85.0, 72.0, 63.7 ( $CH_2$ ), 55.3, 48.0 (Cq), 41.8 ( $CH_2$ ), 38.8 ( $CH_2$ ), 30.1, 22.5, 22.4, 21.8, 21.4 ppm.

**(2*R*,3*S*,5*R*)-2-((Bis(4-methoxyphenyl)(phenyl)methoxy)methyl)-5-(7-isobutyl-4-(3,3,4,4-tetramethyl-2,5-dioxopyrrolidin-1-yl)-1*H*-imidazo[4,5-*c*]pyridin-1-yl)tetrahydrofuran-3-yl (2-cyanoethyl) diisopropylphosphoramidite (**20e**)**



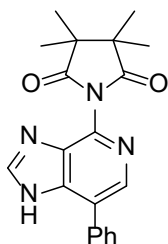
This compound was synthesized in similar fashion as **20i**. To a solution of **19e** (105 mg, 0.146 mmol) in dry CH<sub>2</sub>Cl<sub>2</sub> (5 ml) containing *N,N*-diisopropylethylamine (DIEA) (185 μl, 1.07 mmol), 2-cyanoethyl-*N,N*-diisopropyl chlorophosphoramidite (105 μl, 0.472 mmol) was added in one portion and the mixture was stirred at room temperature under argon for 4 h (TLC showed complete conversion). The mixture was concentrated in vacuo at rt and the product was purified by column chromatography on silica gel (neutralized with triethylamine) eluting with 40-60% EtOAc in hexanes containing 1% triethylamine, to obtain **20e** as a mixture of diastereomers (white foam, R<sub>f</sub> ~0.5 in 50% EtOAc in hexanes, two close spots visible on TLC) in 59% yield (120 mg). HRMS (ESI): *m/z* [M+H]<sup>+</sup> calc'd for C<sub>53</sub>H<sub>68</sub>N<sub>6</sub>O<sub>8</sub>P: 947.48366; found: 947.48314. <sup>1</sup>H NMR (400 MHz, acetone-*d*<sub>6</sub>): δ, 8.43, 8.41 (s, 1H), 8.15 (s, 1H), 7.46-7.41 (m, 2H), 7.33-7.19 (m, 7H), 6.85-6.81 (m, 4H), 6.62-6.58 (dd, *J*<sub>1</sub> = 6.4, *J*<sub>2</sub> = 13.2, 1H), 4.86-4.81 (m, 1H), 4.37-4.29 (m, 1H), 3.96-3.82 (m, 1H), 3.77, 3.76 (s, 6H), 3.74-3.66 (m, 2H), 3.39-3.34 (m, 2H), 3.13-3.09 (m, 1H), 3.03-2.96 (m, 1H), 2.94-2.87 (m, 1H), 2.81 (m, 3H), 2.79-2.76 (t, *J* = 6.4, 1H), 2.68-2.64 (t, *J* = 6.0, 1H), 1.36, 1.35, 1.30 (bs, 12H), 1.23-1.21, 1.22-1.20, 1.17-1.16 (d, *J* = 6.8, 12H), 1.08-1.06 (d, *J* = 6.8, 3H), 1.05-1.03 (dd, *J*<sub>1</sub> = 1.6, *J*<sub>2</sub> = 6.4, 3H) ppm. <sup>13</sup>C NMR (100 MHz, acetone-*d*<sub>6</sub>): δ, 181.8, 159.6, 145.9, 144.1, 144.0, 139.9, 138.7, 136.6, 136.5, 131.0, 130.9, 129.0, 128.9, 128.6, 127.6, 123.32, 123.28, 119.0, 114.0, 87.2, 86.7, 86.1, 86.0, 75.0, 74.9, 74.5, 74.3, 64.5, 59.6, 59.4, 55.5, 48.4, 44.1, 44.0, 40.4, 39.0, 25.0, 24.9, 24.8, 22.9, 22.5, 22.0, 21.7, 21.4, 20.8 ppm. <sup>31</sup>P NMR (162 MHz, acetone-*d*<sub>6</sub>): δ, 149.9, 149.7 ppm.

### 7-Phenyl-1*H*-imidazo[4,5*c*]pyridin-4-amine, trifluoroacetic acid salt (**15a**, **3a**\*TFA)



This compound was synthesized in similar fashion as **15i**. A solution of **14a** (2.09 g, 3.65 mmol) in TFA (20 ml) was placed in a 100 ml pressure tube, anisole (2.4 ml, 6 equiv.) was added, and the mixture was heated at 70 °C for 24 h with vigorous stirring. It was cooled and concentrated under reduced pressure. The residue was coevaporated with toluene (3 x 25 ml) to obtain grey-brown powder. It was taken in toluene (10 ml) and filtered, washing with toluene (2 x 5 ml), then hexane (2 x 5 ml) and dried on air to obtain **15a** as a free flowing, light gray powder, 1.13 g (quantitative). MS (ESI): *m/z*, 211.3 for [M + H]<sup>+</sup>. <sup>1</sup>H NMR (400 MHz, DMSO-*d*<sub>6</sub>): δ, 8.60 (bs, 2H), 8.52 (s, 1H), 7.82 (s, 1H), 7.70-7.69 (m, 2H), 7.56-7.53 (m, 2H), 7.49-7.46 (m, 1H) ppm. <sup>13</sup>C NMR (100 MHz, DMSO-*d*<sub>6</sub>): δ, 159.4, 159.0, 158.7, 158.3, 147.5, 144.3, 132.7, 129.1, 128.5, 128.0, 126.7, 115.2 ppm.

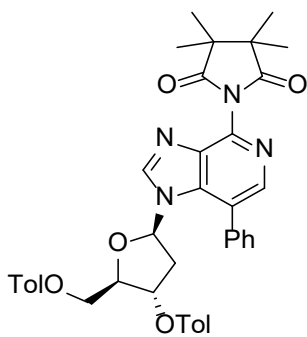
### 3,3,4,4-Tetramethyl-1-(7-phenyl-1*H*-imidazo[4,5-*c*]pyridin-4-yl)pyrrolidine-2,5-dione (**16a**)



This compound was synthesized in similar fashion as **16i**. A solution of **15a** (0.34 g, 1 mmol) in pyridine (10 ml) was placed in a 100 ml Schlenk flask. Tetramethylsuccinic anhydride (M<sub>4</sub>SA) (0.546 g, 3.5 mmol) and DBU (1.05 ml, 7 mmol) were added, and the mixture was heated at 120 °C under argon for 20 h with vigorous stirring. It was cooled and concentrated under reduced pressure. The residue was coevaporated with toluene (3 x 25 ml). The product was purified by column chromatography on silica gel eluting with 0-5% MeOH in CH<sub>2</sub>Cl<sub>2</sub> to give a colorless syrup. It was taken in SOCl<sub>2</sub> (12 ml), heated at 80 °C for 2 h, cooled and concentrated under reduced pressure. The residue was coevaporated with EtOAc (3 x 25 ml). The product was purified by column chromatography on silica gel eluting with 0-5% MeOH in CH<sub>2</sub>Cl<sub>2</sub> to give **16a** as a light brown foam in 92% yield (0.56 g). HRMS (ESI): *m/z* [M+H]<sup>+</sup> calc'd for C<sub>20</sub>H<sub>21</sub>N<sub>4</sub>O<sub>2</sub>: 349.16647; found: 349.16505. <sup>1</sup>H NMR (400 MHz, CD<sub>3</sub>OD): δ, 8.75 (s, 1H), 8.52 (s, 1H), 7.76-7.75 (m, 2H), 7.61-7.51 (m, 3H), 1.40 (bs, 12H) ppm. <sup>13</sup>C NMR

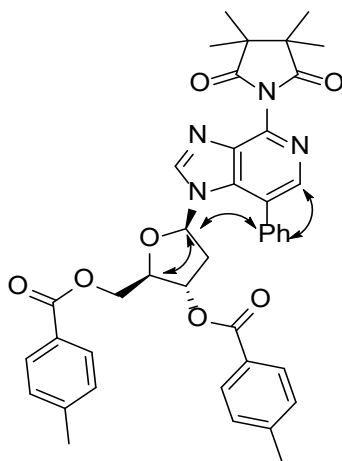
(100 MHz, CD<sub>3</sub>OD):  $\delta$ , 182.5, 147.9, 142.4, 139.6, 135.4, 134.4, 134.3, 130.5, 129.8, 127.0, 49.1, 21.8 ppm.

**((2*R*,3*S*,5*R*)-3-((4-methylbenzoyl)oxy)-5-(7-phenyl-4-(3,3,4,4-tetramethyl-2,5-dioxopyrrolidin-1-yl)-1*H*-imidazo[4,5-*c*]pyridin-1-yl)tetrahydrofuran-2-yl)methyl 4-methylbenzoate (17a)**



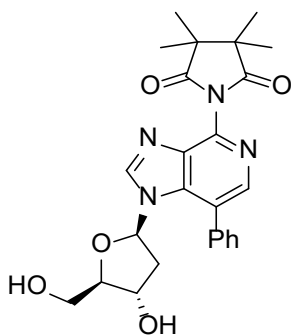
This compound was synthesized in similar fashion as **17i**. To a solution of **16a** (0.51 g, 1.46 mmol) in dry CH<sub>3</sub>CN (60 ml) in a 100 ml round bottom flask, 60% NaH in oil (117 mg, 2.93 mmol) was added, and the mixture was vigorously stirred at room temperature under argon for 45 min. 1-( $\alpha$ )-Chloro-3,5-di-O-(*p*-toluoyl)-2-deoxy-D-ribose (0.368 g, 0.94 mmol) was subsequently added portionwise over 1 h, and the stirring was continued at room temperature for overall 5 h. The mixture was filtered through Celite® and concentrated. The product was purified by column chromatography on silica gel eluting with 0-50% EtOAc in hexanes. **17a** was obtained as a yellowish syrup in 64% yield (0.64 g). HRMS (ESI):  $m/z$  [M+H]<sup>+</sup> calc'd for C<sub>41</sub>H<sub>40</sub>N<sub>4</sub>O<sub>7</sub>: 701.29757; found: 701.29626. <sup>1</sup>H NMR (400 MHz, CDCl<sub>3</sub>):  $\delta$ , 8.33 (s, 1H), 8.31 (s, 1H), 7.86-7.84 (d,  $J$  = 8.0, 2H), 7.75-7.73 (d,  $J$  = 8.0, 2H), 7.46 (bs, 4H), 7.32-7.28 (m, 1H), 7.31-7.29 (d,  $J$  = 8.0, 2H), 7.24-7.22 (d,  $J$  = 8.0, 2H), 5.96-5.93 (dd,  $J_1$  = 5.2,  $J_2$  = 8.8, 1H), 5.46-5.44 (m, 1H), 4.62-4.53 (m, 2H), 4.38-4.36 (m, 1H), 2.48 (s, 3H), 2.40 (s, 3H), 2.30-2.16 (m, 2H), 1.40 (bs, 12H) ppm. <sup>13</sup>C NMR (100 MHz, CDCl<sub>3</sub>):  $\delta$ , 181.7 (Cq), 166.2 (Cq), 165.6 (Cq), 144.7 (Cq), 144.5 (Cq), 142.9, 142.7, 138.4 (Cq), 138.0 (Cq), 137.4 (Cq), 134.8 (Cq), 130.0, 129.7, 129.6, 129.3, 129.0, 128.8, 126.6 (Cq), 126.4 (Cq), 123.5 (Cq), 85.9, 82.8, 74.9, 64.2 (CH<sub>2</sub>), 48.1 (Cq), 40.1 (CH<sub>2</sub>), 21.9, 21.8, 21.6 ppm.





**Figure S4.** The critical NOESY correlations observed for **17a**.

**1-(1-((2*R*,4*S*,5*R*)-4-hydroxy-5-(hydroxymethyl)tetrahydrofuran-2-yl)-7-phenyl-1*H*-imidazo[4,5-*c*]pyridin-4-yl)-3,3,4,4-tetramethylpyrrolidine-2,5-dione (**18a**)**

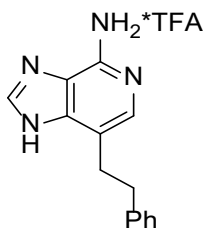


This compound was synthesized in similar fashion as **18i**. To a solution of **17a** (0.44 g, 0.63 mmol) in dry MeOH (6 ml) in a 25 ml round bottom flask, NaOMe (102 mg, 1.89 mmol) was added, and the mixture was stirred at room temperature under argon for 2 h. It was concentrated in vacuo, and the product was purified by column chromatography on silica gel eluting with 0-10% MeOH

in CH<sub>2</sub>Cl<sub>2</sub> to obtain **18a** as a white foam in 58% yield (0.17 g). HRMS (ESI):  $m/z$  [M+H]<sup>+</sup> calc'd for C<sub>25</sub>H<sub>29</sub>N<sub>4</sub>O<sub>5</sub>: 465.21383; found: 465.21228. <sup>1</sup>H NMR (400 MHz, CD<sub>3</sub>OD):  $\delta$ , 8.85 (s, 1H), 8.19 (s, 1H), 7.56 (m, 5H), 5.97-5.94 (t,  $J=6.0$ , 1H), 4.37-4.33 (m, 1H), 3.78-3.65 (m, 3H), 2.35-2.28 (m, 1H), 1.96-1.90 (ddd,  $J_1=4.4$ ,  $J_2=6.0$ ,  $J_3=10.8$ , 1H), 1.39 (bs, 12H) ppm. <sup>13</sup>C NMR (100 MHz, CD<sub>3</sub>OD):  $\delta$ , 183.4 (Cq), 146.5 (Cq), 143.1, 139.4 (Cq), 138.7 (Cq), 138.6 (Cq), 135.6 (Cq), 130.9, 130.2, 129.9, 126.0 (Cq), 88.9, 87.1, 71.2, 62.3 (CH<sub>2</sub>), 49.0 (Cq), 42.9 (CH<sub>2</sub>), 21.9, 21.8 ppm.

The attempted tritylation of **18a** was carried forward in similar fashion as for **18i**. To a solution of **18a** (0.15 g, 0.323 mmol) in pyridine (3 ml) under Ar, 4,4'-dimethoxytrityl chloride (DMT-Cl) (0.153 g, 0.453 mmol) was added in one portion, and the mixture was stirred at room temperature for 4.5 h. TLC analysis indicated that some starting material remained, and then additional DMT-Cl was added (0.076 g, 0.225 mmol). After 3.5 h, the starting material still remained, and then triethylamine (45  $\mu$ l, 0.323 mmol), cat. DMAP (10 mg) and additional DMT-Cl (44 mg, 0.129 mmol) were added. After 8 h, most of the starting material was consumed, and the mixture was concentrated in vacuo, the residue was coevaporated with toluene (3 x 10 ml) to remove residual pyridine. A TLC analysis indicated that an extensive deglycosylation occurred, indicating the instability of the compound which may be ascribed to the electronic character of phenyl group at the position 3 as suggested by other reports.<sup>2</sup> Deglycosylation was also observed to occur upon mild heating of the TLC plate in order to remove pyridine before analysis.

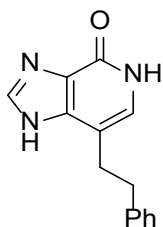
#### 7-Phenethyl-1*H*-imidazo[4,5-*c*]pyridin-4-amine, trifluoroacetic acid salt (**15c**)



This compound was synthesized in similar fashion as **15i**. A solution of **14c** (0.327 g, 0.55 mmol) in TFA (8 ml) was placed in a 100 ml pressure tube, anisole (0.36 ml, 6 equiv.) was added, and the mixture was heated at 70 °C for 21 h with vigorous stirring. It was cooled and concentrated under reduced pressure. The residue was coevaporated with toluene (3 x 15 ml) to obtain **15c** (ca. 0.2 g, quantitative) as a syrup that was taken into next step without further purification.

#### 7-Phenethyl-1,5-dihydro-4*H*-imidazo[4,5-*c*]pyridin-4-one (**21c**)

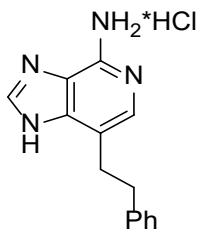
This compound was synthesized according to the general procedure.<sup>19</sup> A solution of crude **15c** (ca. 0.2 g, 0.55 mmol) in acetone/H<sub>2</sub>O/AcOH (4/2/2 ml) was stirred at room



temperature for 5 h in a closed vessel. The pressure was carefully released and the mixture was carefully neutralized with aq. NaHCO<sub>3</sub> and diluted with Et<sub>2</sub>O (50 ml). The phases were shaken, and the precipitated solid was filtered, washing with water and Et<sub>2</sub>O, and dried on air to obtain **21c** as a light yellow solid (75 mg, 57% based on **14c**). HRMS (ESI): m/z [M+H]<sup>+</sup> calc'd for C<sub>14</sub>H<sub>14</sub>N<sub>3</sub>O: 240.11369; found: 240.11281. MS (ESI): m/z, 240.3 for [M+H]<sup>+</sup>, 262.2 for for [M+Na]<sup>+</sup>, 501.2 for for [2M+Na]<sup>+</sup>; 238.3 for [M-H]<sup>-</sup>. <sup>1</sup>H NMR (400 MHz, DMSO-d<sub>6</sub>): δ, 10.9 (bs, 1H), 8.09 (s, 1H), 7.26-7.16 (m, 5H), 6.79 (s, 1H), 2.93-2.89 (m, 4H) ppm. <sup>13</sup>C NMR (100 MHz, DMSO-d<sub>6</sub>): δ, 156.1, 141.6, 141.2, 128.4, 128.2, 125.8, 124.9, 110.7, 35.1, 29.7 ppm.

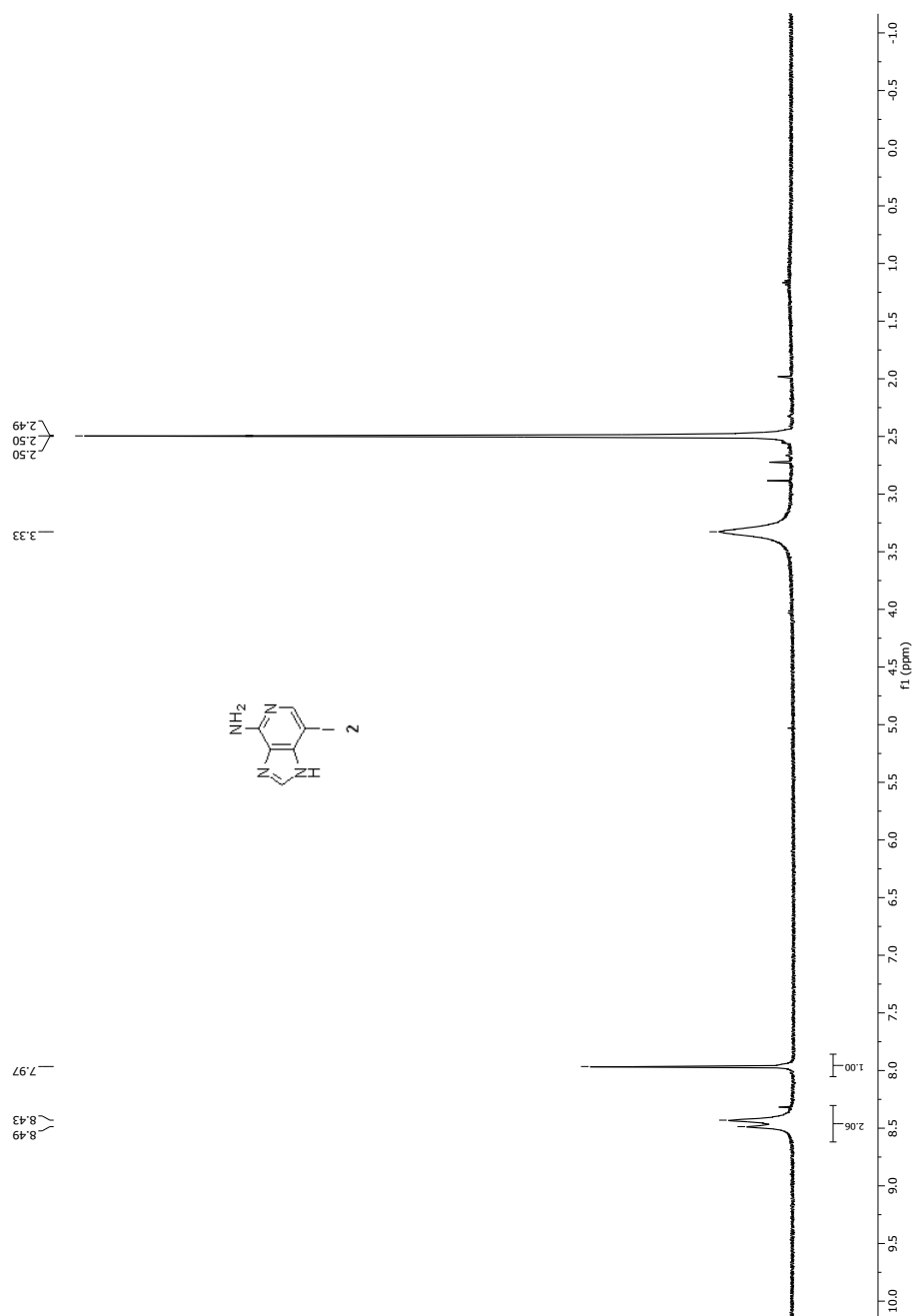
TFA salts **15** were used for synthetic purposes typically without further purification. Pure amines could be also isolated as water soluble HCl salts as exemplified below. Free amines could be obtained by neutralization of their aqueous solutions with Na<sub>2</sub>CO<sub>3</sub> followed by extraction with AcOEt.

#### 7-Phenethyl-1H-imidazo[4,5-c]pyridin-4-amine, hydrochloric acid salt (**15c**\*HCl)

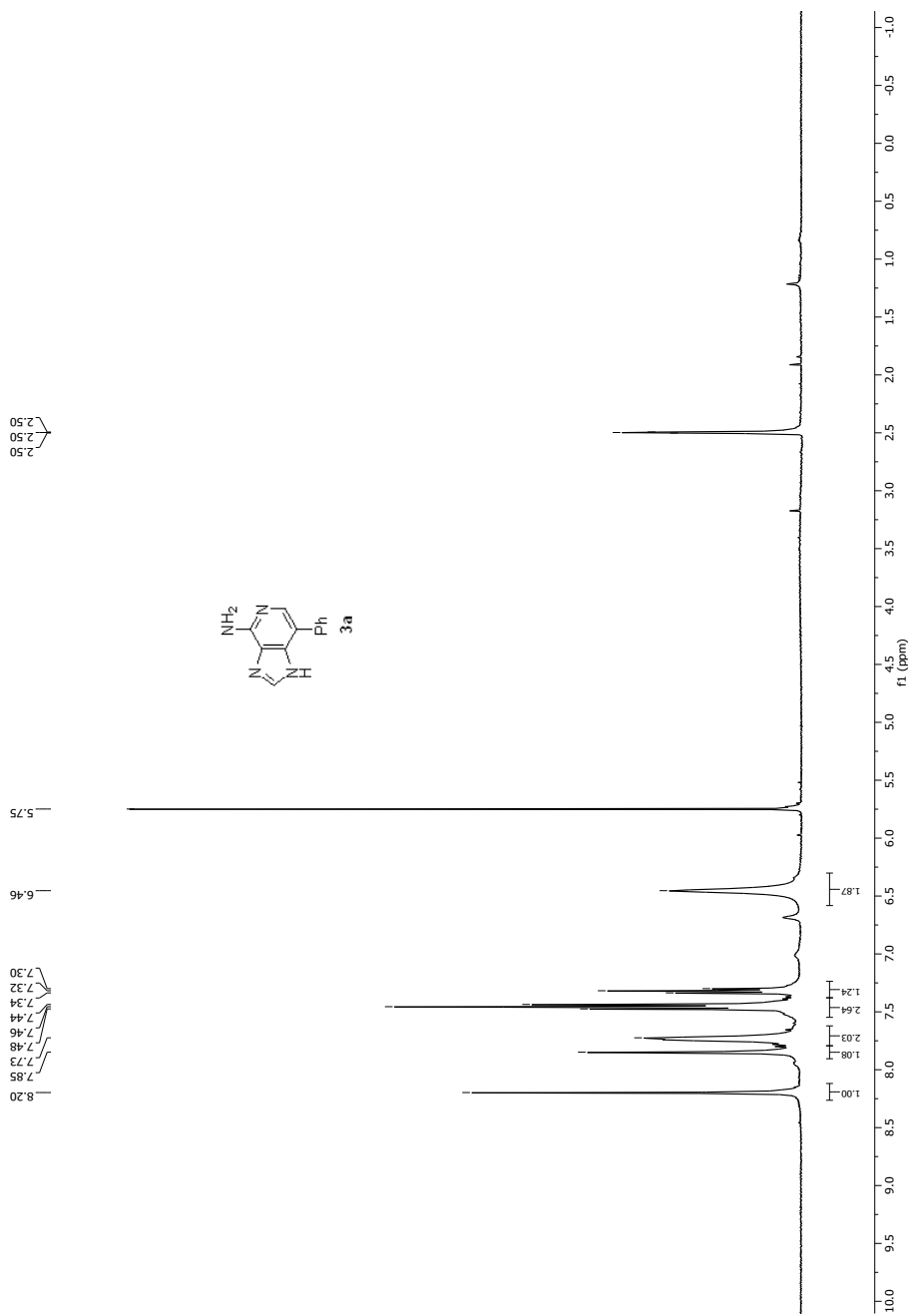


A solution of **14c** (0.173 g, 0.29 mmol) in EtOH/H<sub>2</sub>O/HCl conc. (8/8/4 ml) was heated under reflux condenser at 100 °C for 23 h. It was cooled and EtOH was removed under reduced pressure. It was diluted with aq. HCl and washed with Et<sub>2</sub>O (40 ml, discarded) to remove a precipitated oil. The residue was concentrated and dried under vacuum to obtain **15c**\*HCl (ca. 0.08 g, quantitative) as an off-white solid. HRMS (ESI): m/z [M+H]<sup>+</sup> calc'd for C<sub>14</sub>H<sub>15</sub>N<sub>4</sub>: 239.12968; found: 239.12930. MS (ESI): m/z, 239.3 for [M+H]<sup>+</sup>; 237.3 for [M-H]<sup>-</sup>, 273.0 for [M+Cl]<sup>-</sup>. <sup>1</sup>H NMR (400 MHz, D<sub>2</sub>O): δ, 8.35 (s, 1H), 7.28-7.19 (m, 4H), 7.11-7.09 (m, 2H), 3.09-3.05 (m, 2H), 2.99-2.96 (m, 2H) ppm. <sup>13</sup>C NMR (100 MHz, D<sub>2</sub>O): δ, 146.6, 143.6, 140.6, 128.8, 128.6, 127.0, 126.5, 123.8, 114.7, 34.6, 29.3 ppm.

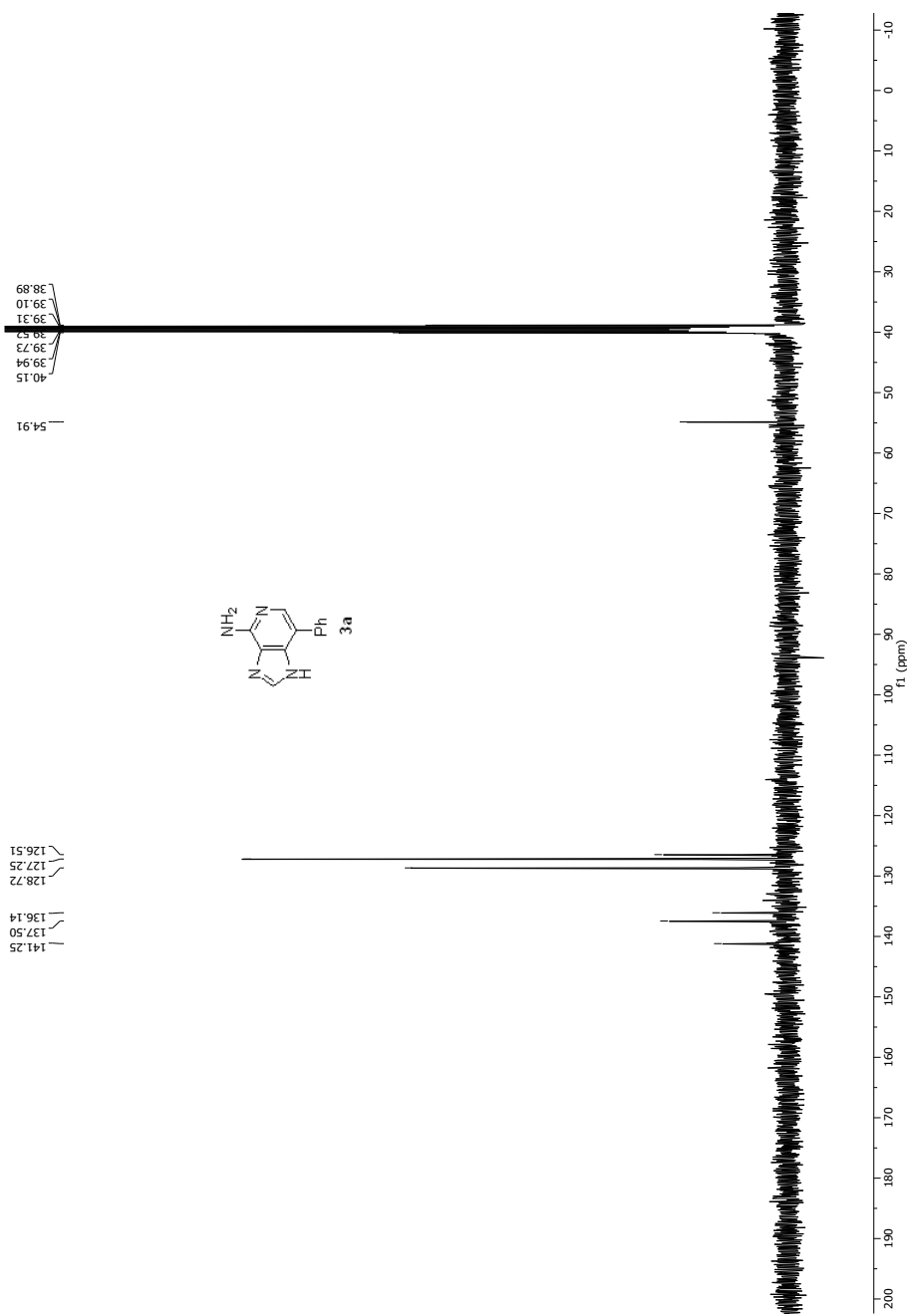
### B.3 Copies of $^1\text{H}$ and $^{13}\text{C}$ NMR spectra



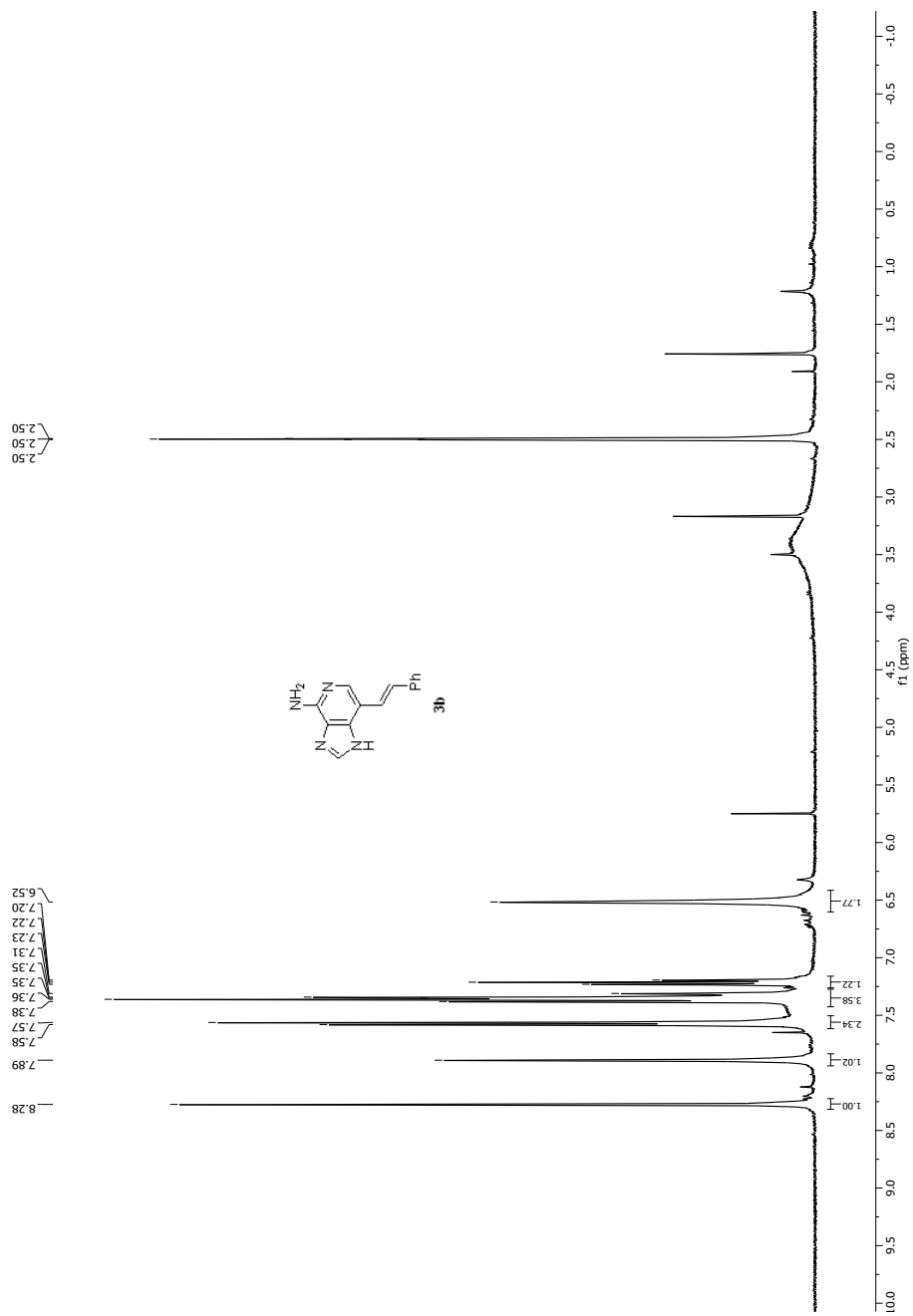
**Figure. B5**  $^1\text{H}$  NMR spectrum of **2** ( $\text{DMSO-d}_6$ , 400 MHz).



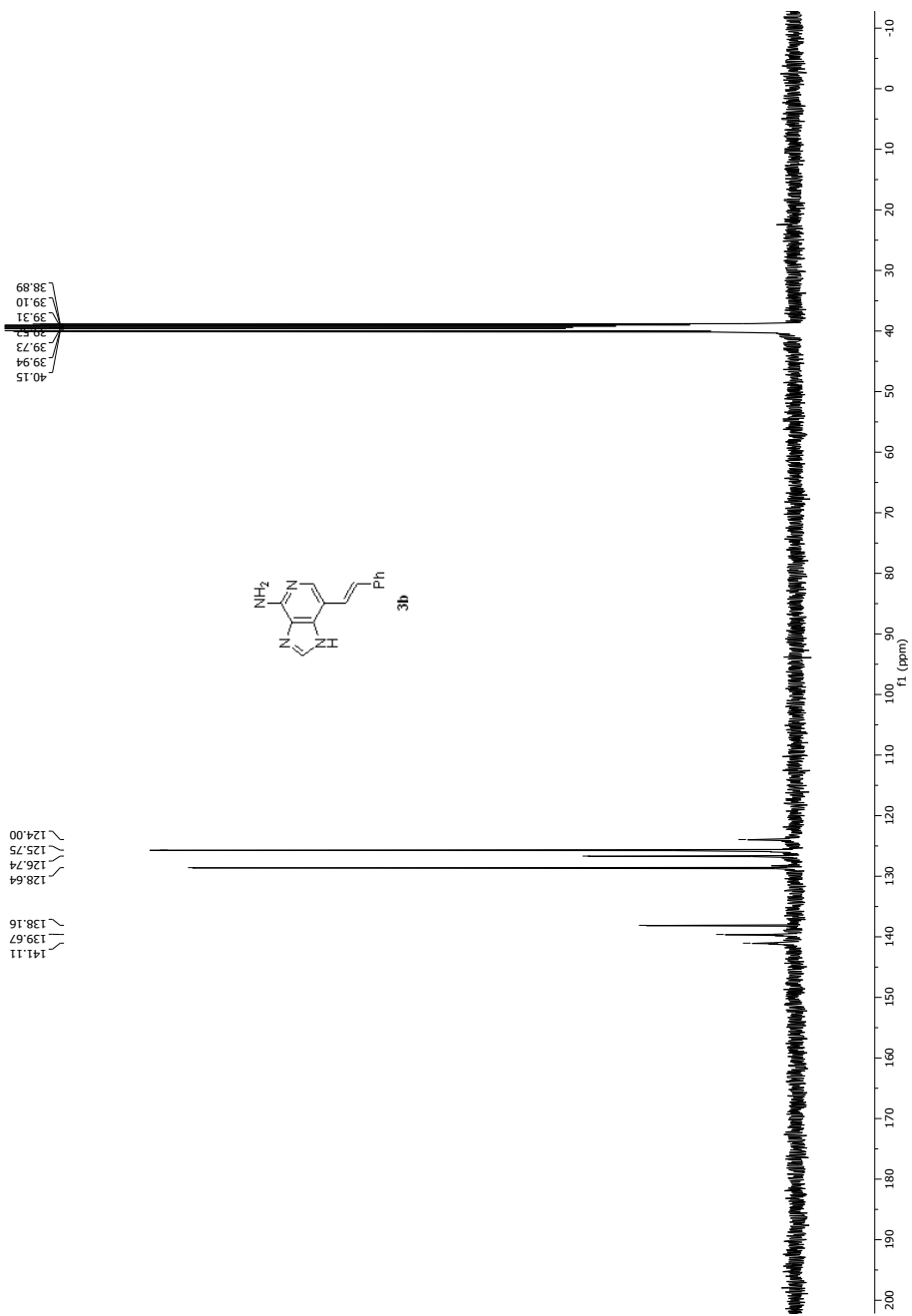
**Figure. B6**  $^1\text{H}$  NMR spectrum of **3a** (DMSO- $d_6$ , 400 MHz).



**Figure. B7** <sup>13</sup>C NMR spectrum of **3a** (DMSO-d<sub>6</sub>, 100 MHz).

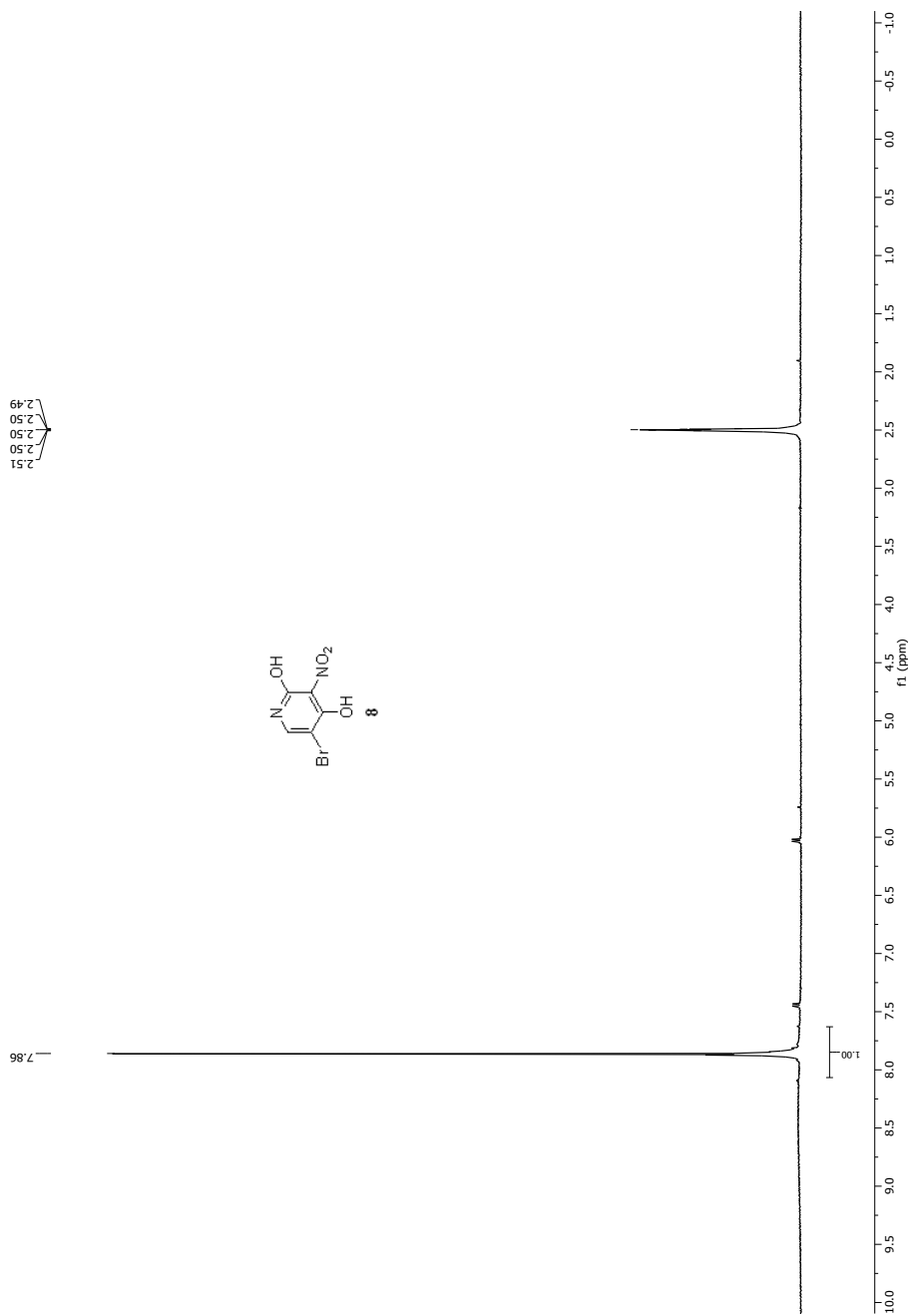


**Figure. B8** <sup>1</sup>H NMR spectrum of **3b** (DMSO-d<sub>6</sub>, 400 MHz).



**Figure. B9**  $^{13}\text{C}$  NMR spectrum of **3b** (DMSO- $d_6$ , 100 MHz).





**Figure. B10**  $^1\text{H}$  NMR spectrum of **8** ( $\text{DMSO-d}_6$ , 400 MHz).

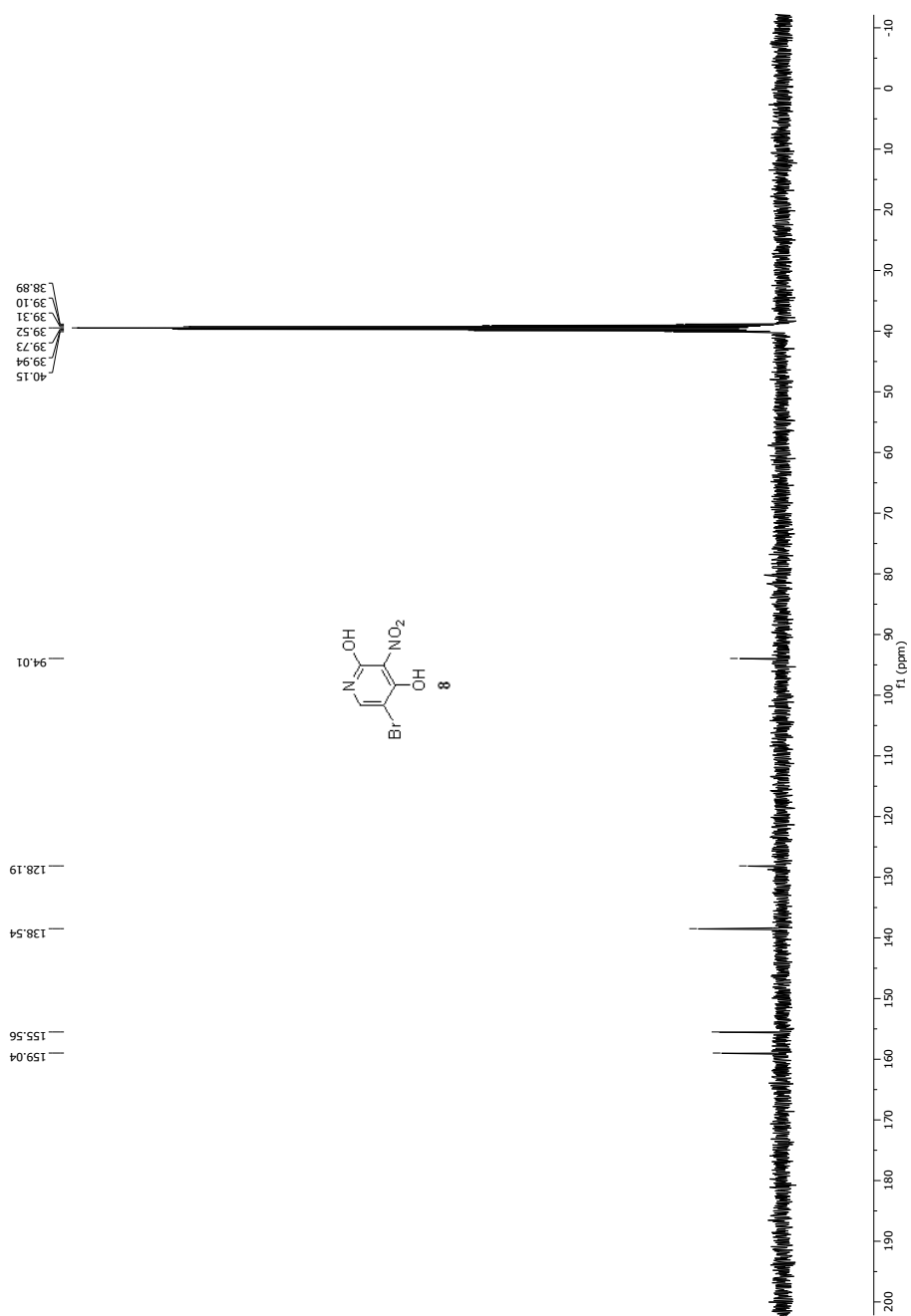


Figure. B11  $^{13}\text{C}$  NMR spectrum of **8** ( $\text{DMSO-d}_6$ , 100 MHz).

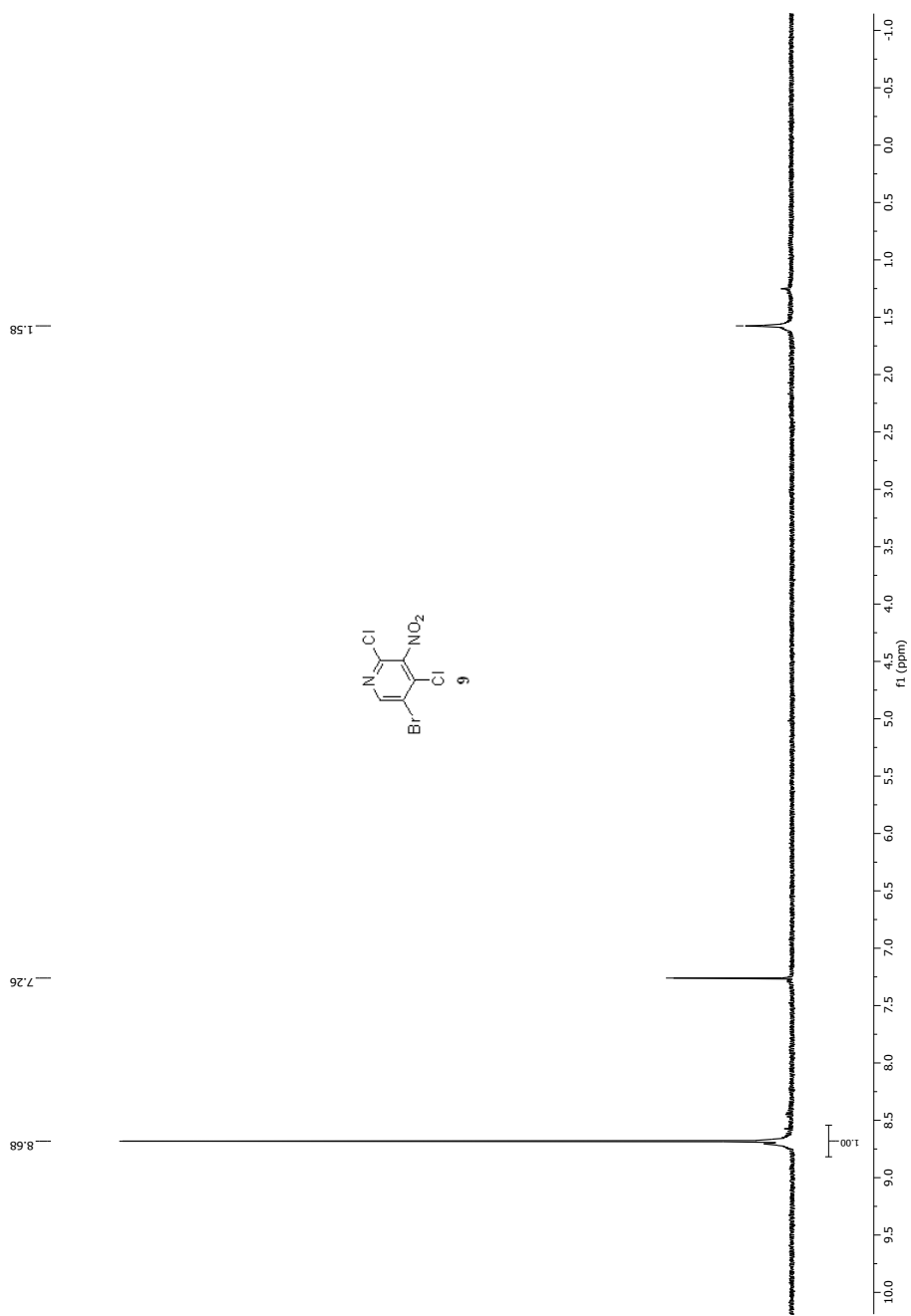
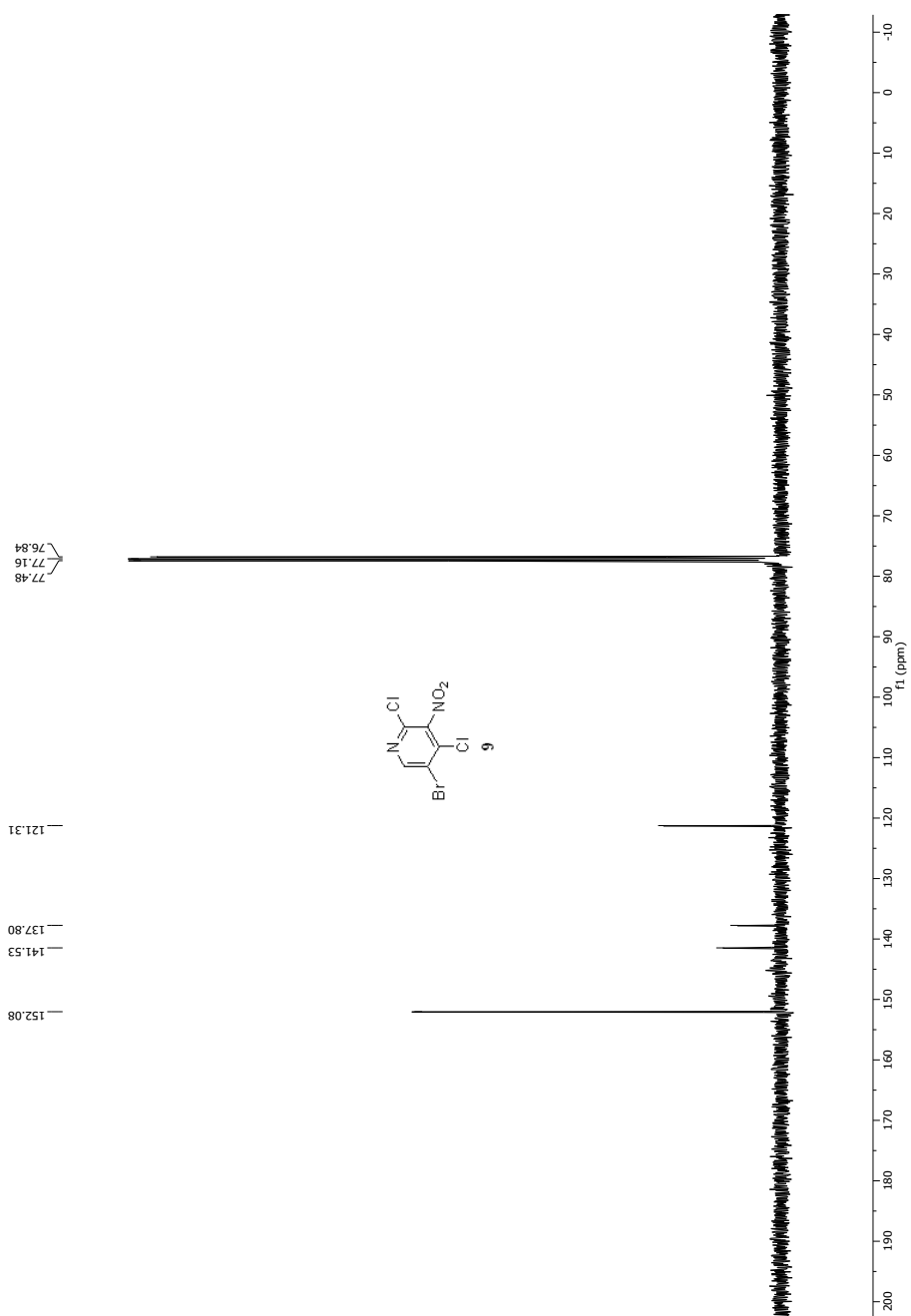
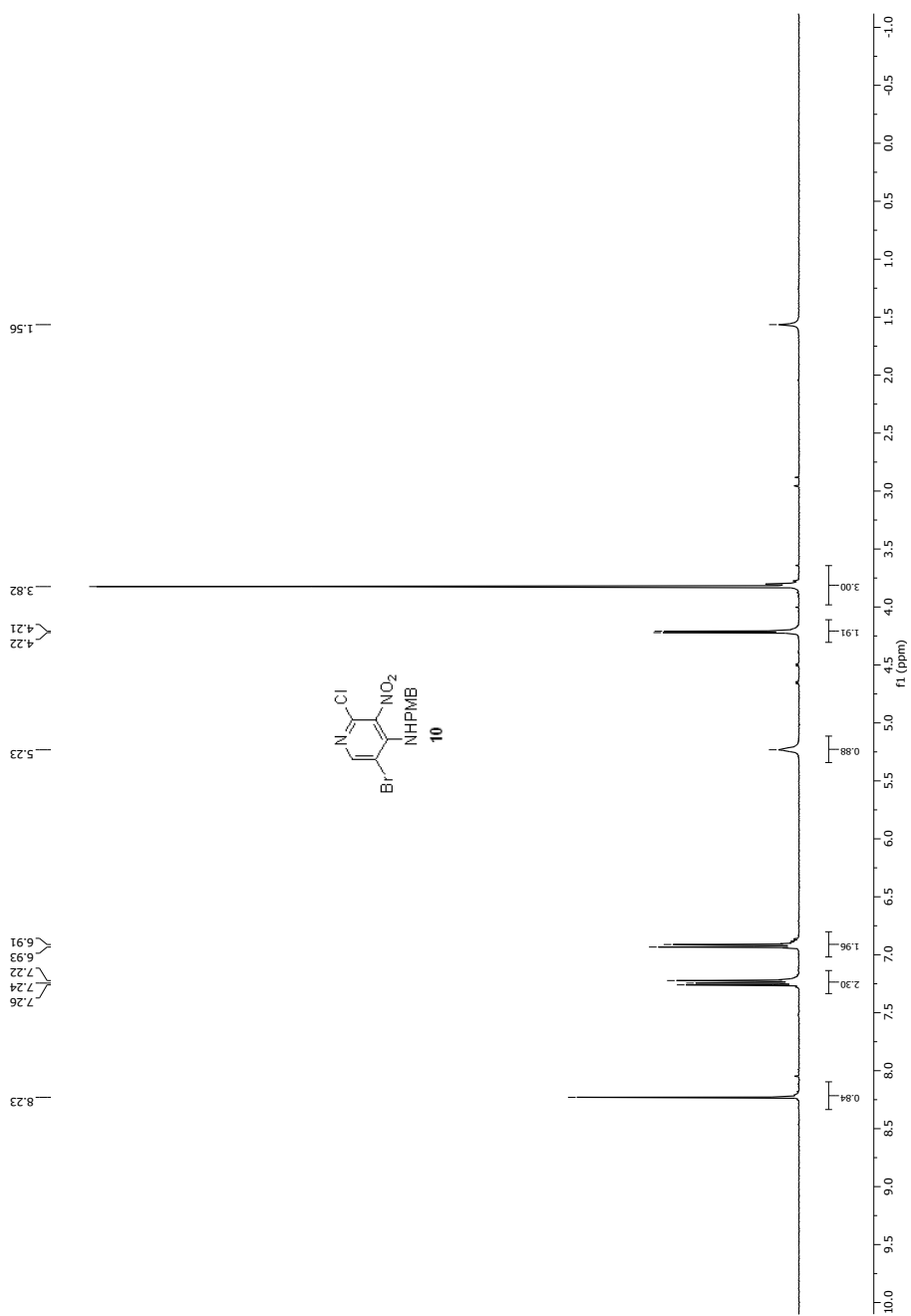


Figure. B12 <sup>1</sup>H NMR spectrum of **9** (CDCl<sub>3</sub>, 400 MHz).



**Figure. B13**  $^{13}\text{C}$  NMR spectrum of **9** ( $\text{CDCl}_3$ , 100 MHz).



**Figure. B14**  $^1\text{H}$  NMR spectrum of **10** ( $\text{CDCl}_3$ , 400 MHz).

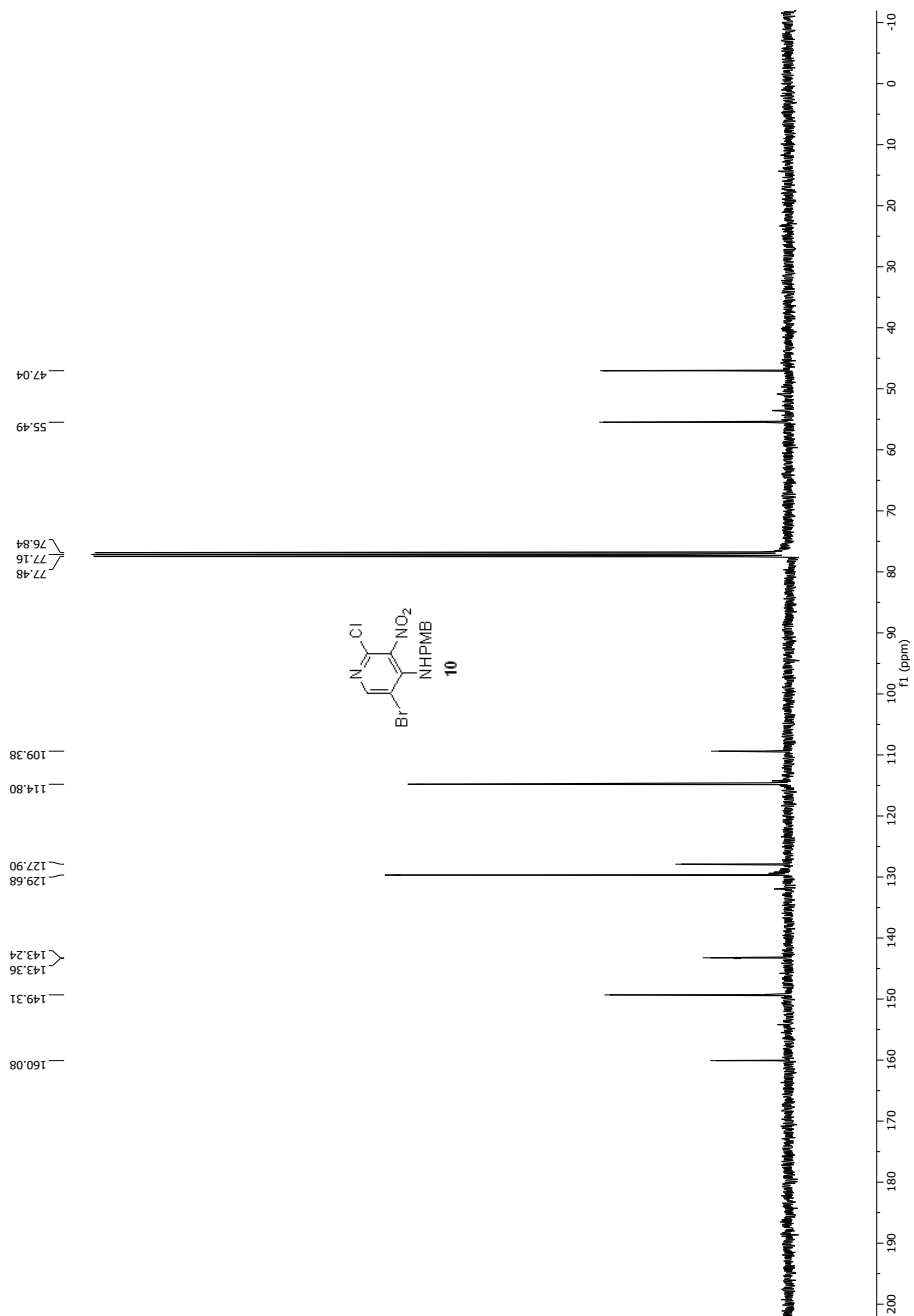
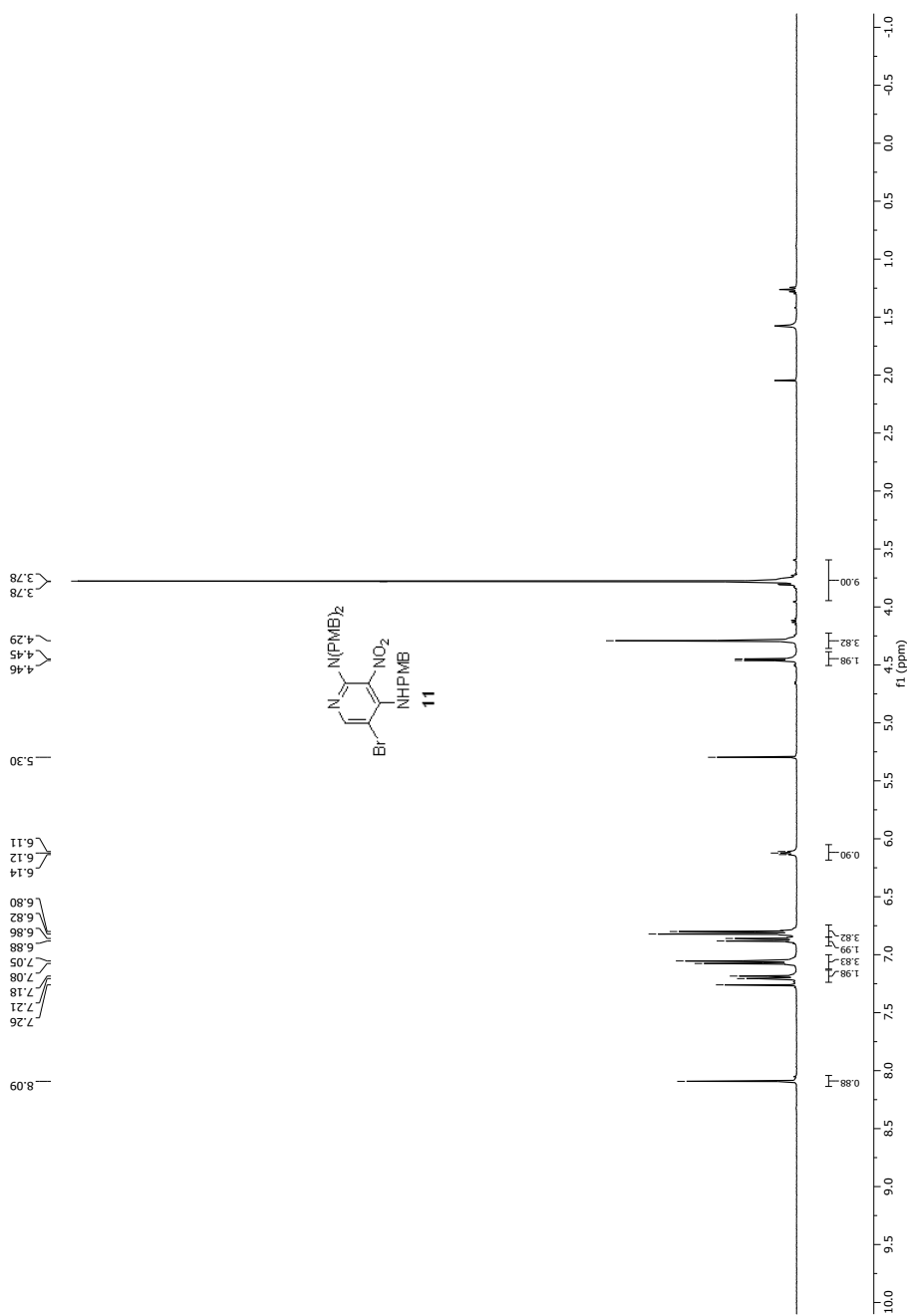


Figure. B15  $^{13}\text{C}$  NMR spectrum of **10** ( $\text{CDCl}_3$ , 100 MHz).



**Figure. B16** <sup>1</sup>H NMR spectrum of **11** (CDCl<sub>3</sub>, 400 MHz).

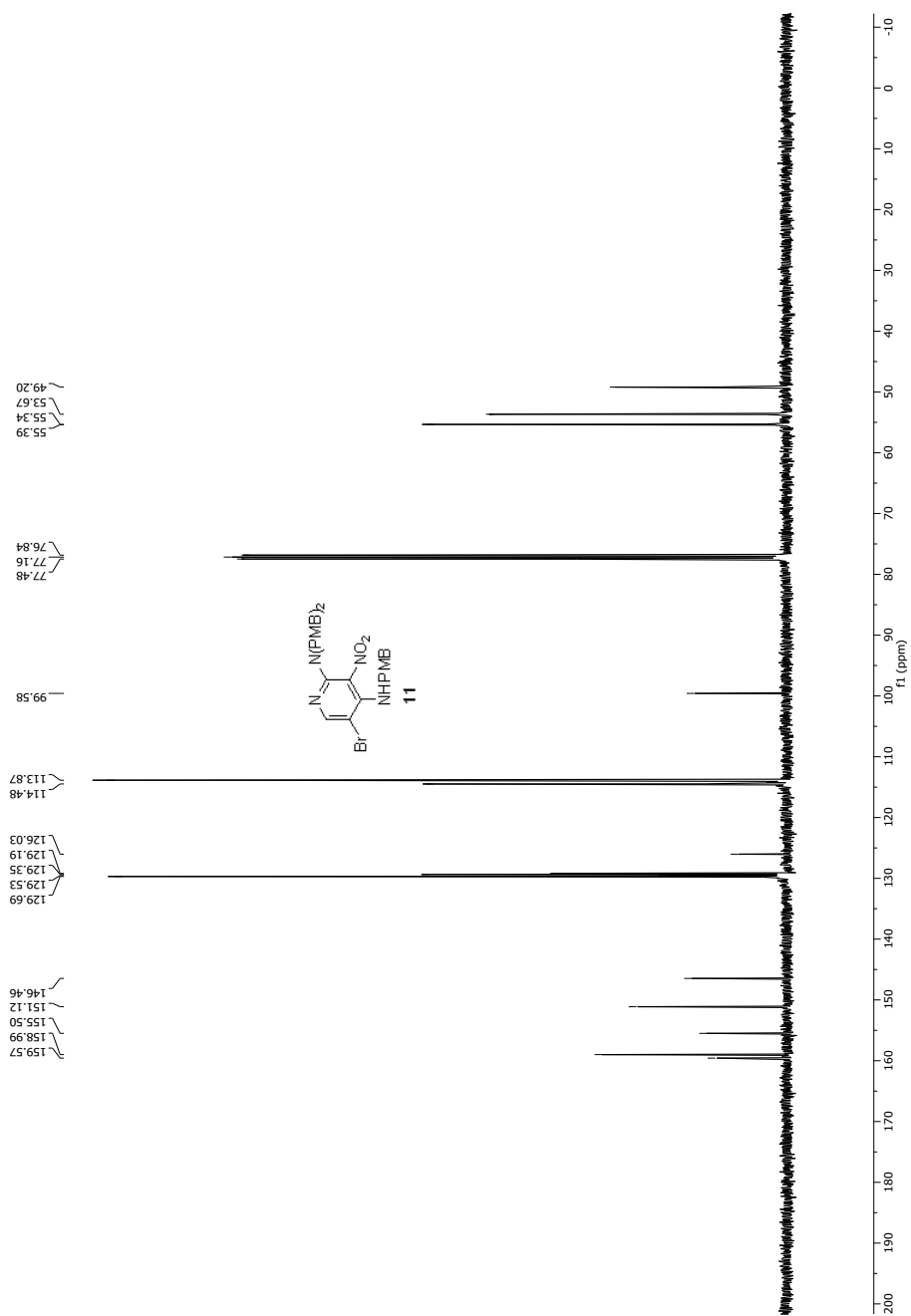
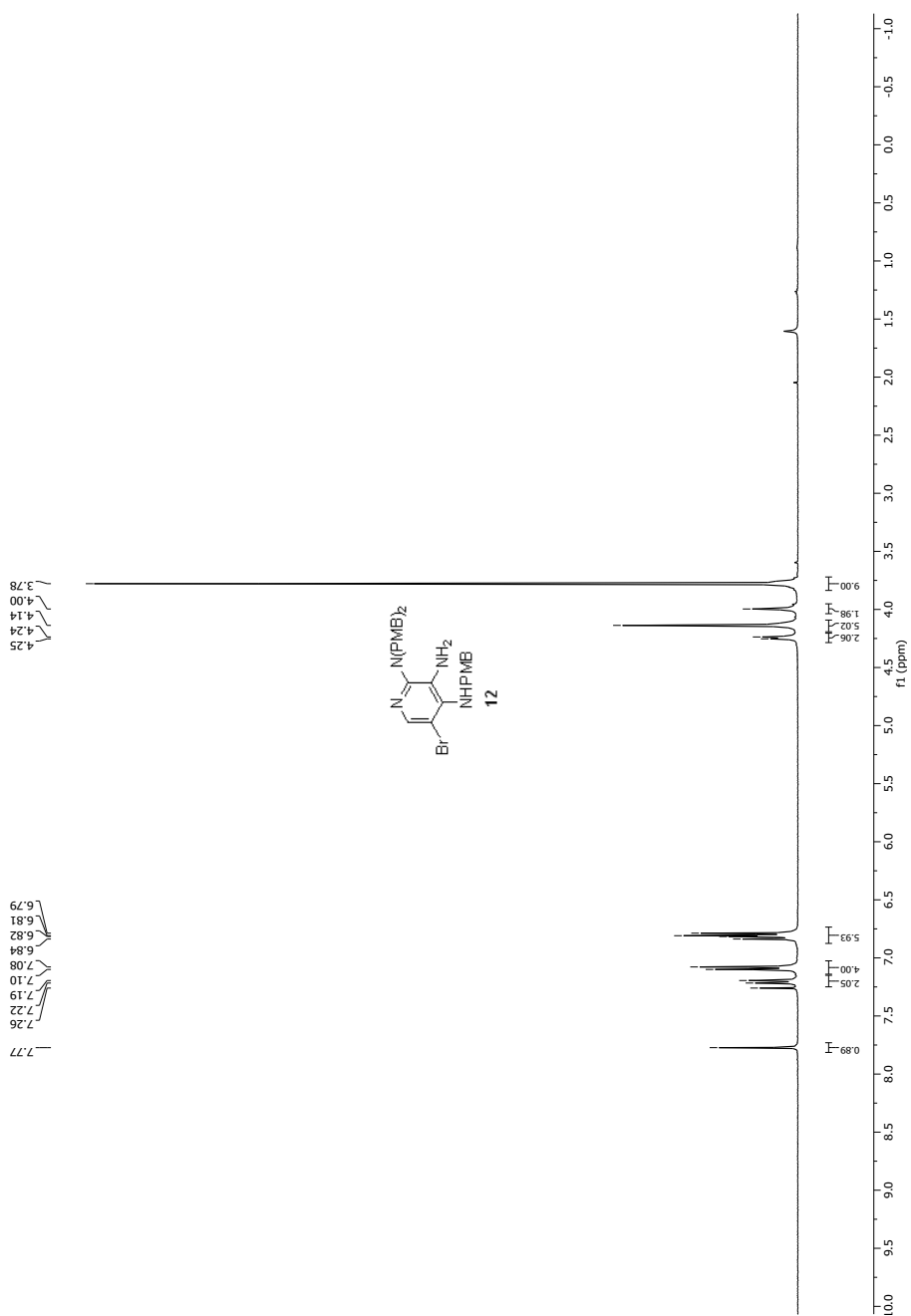


Figure. B17 <sup>13</sup>C NMR spectrum of **11** (CDCl<sub>3</sub>, 100 MHz).





**Figure. B18** <sup>1</sup>H NMR spectrum of **12** (CDCl<sub>3</sub>, 400 MHz).

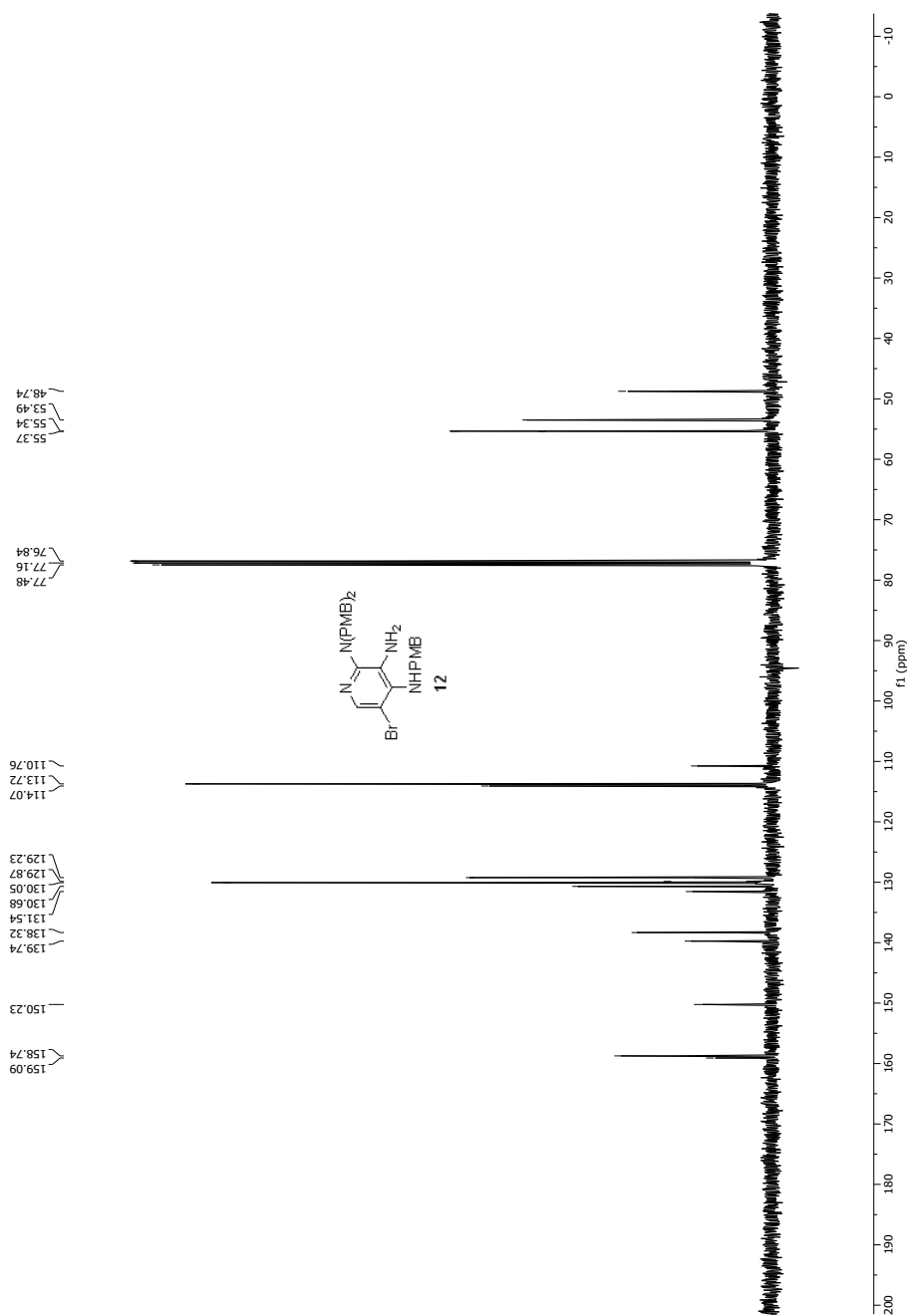
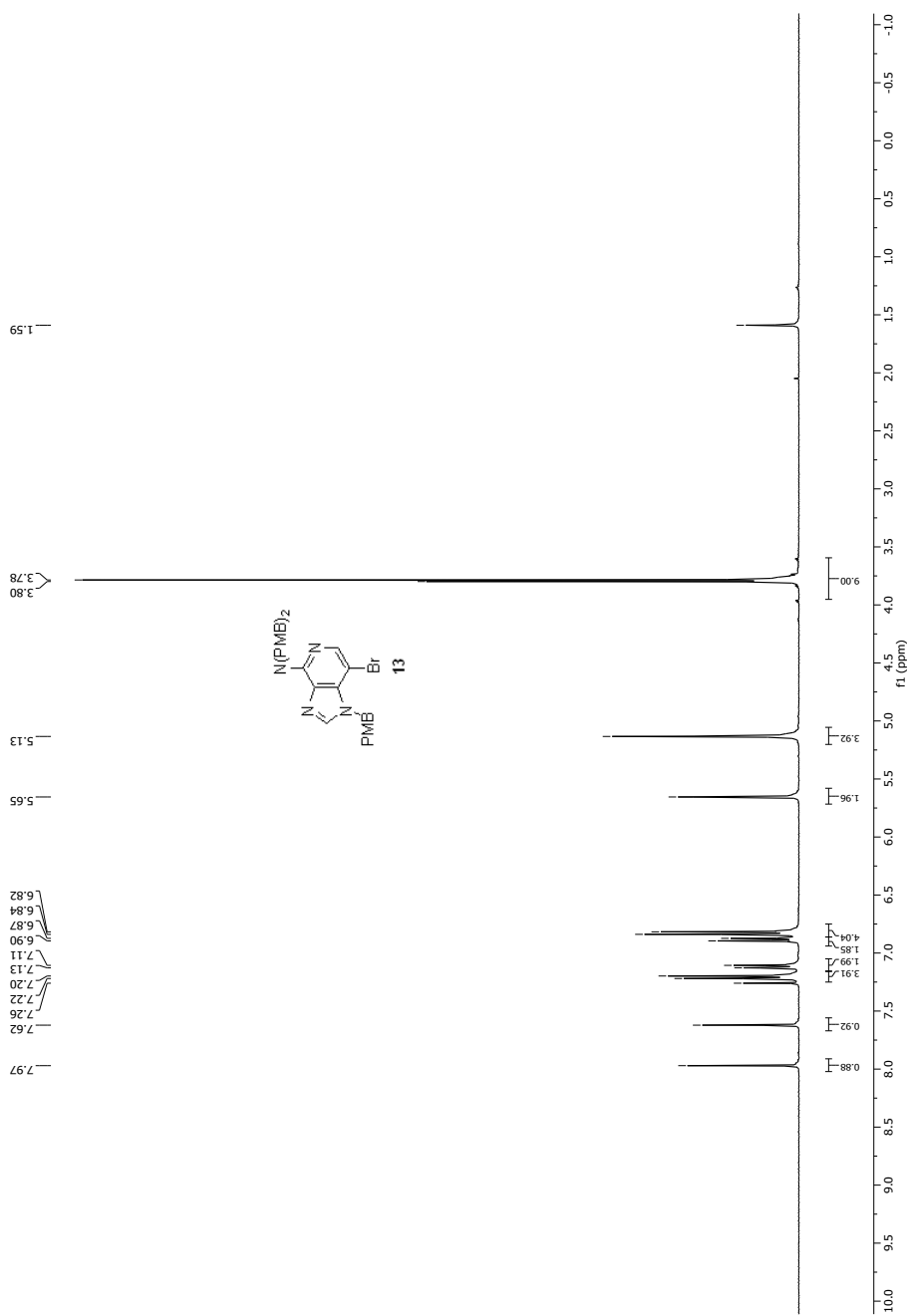


Figure. B19 <sup>13</sup>C NMR spectrum of **12** (CDCl<sub>3</sub>, 100 MHz).



**Figure. B20** <sup>1</sup>H NMR spectrum of **13** (CDCl<sub>3</sub>, 400 MHz).

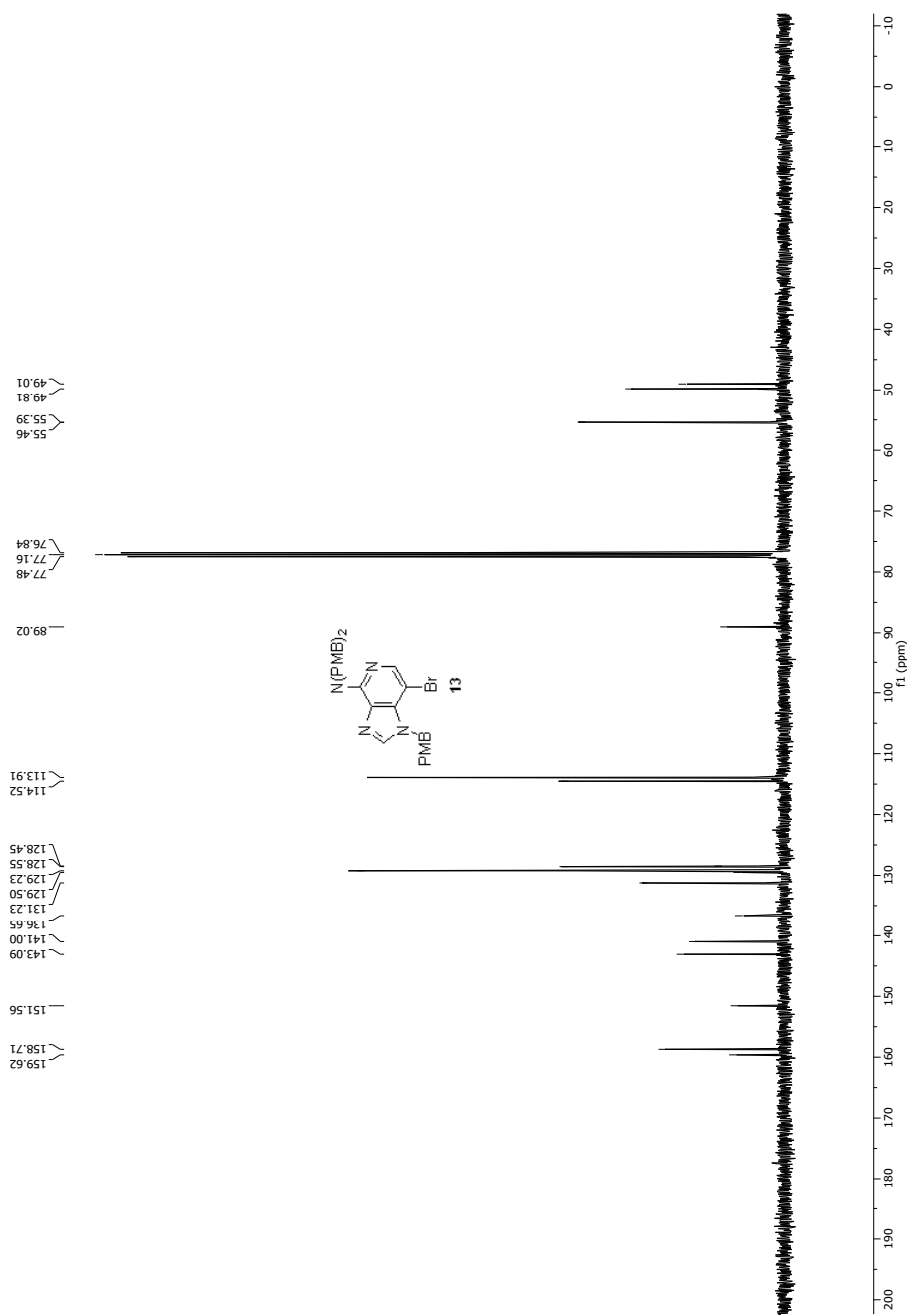
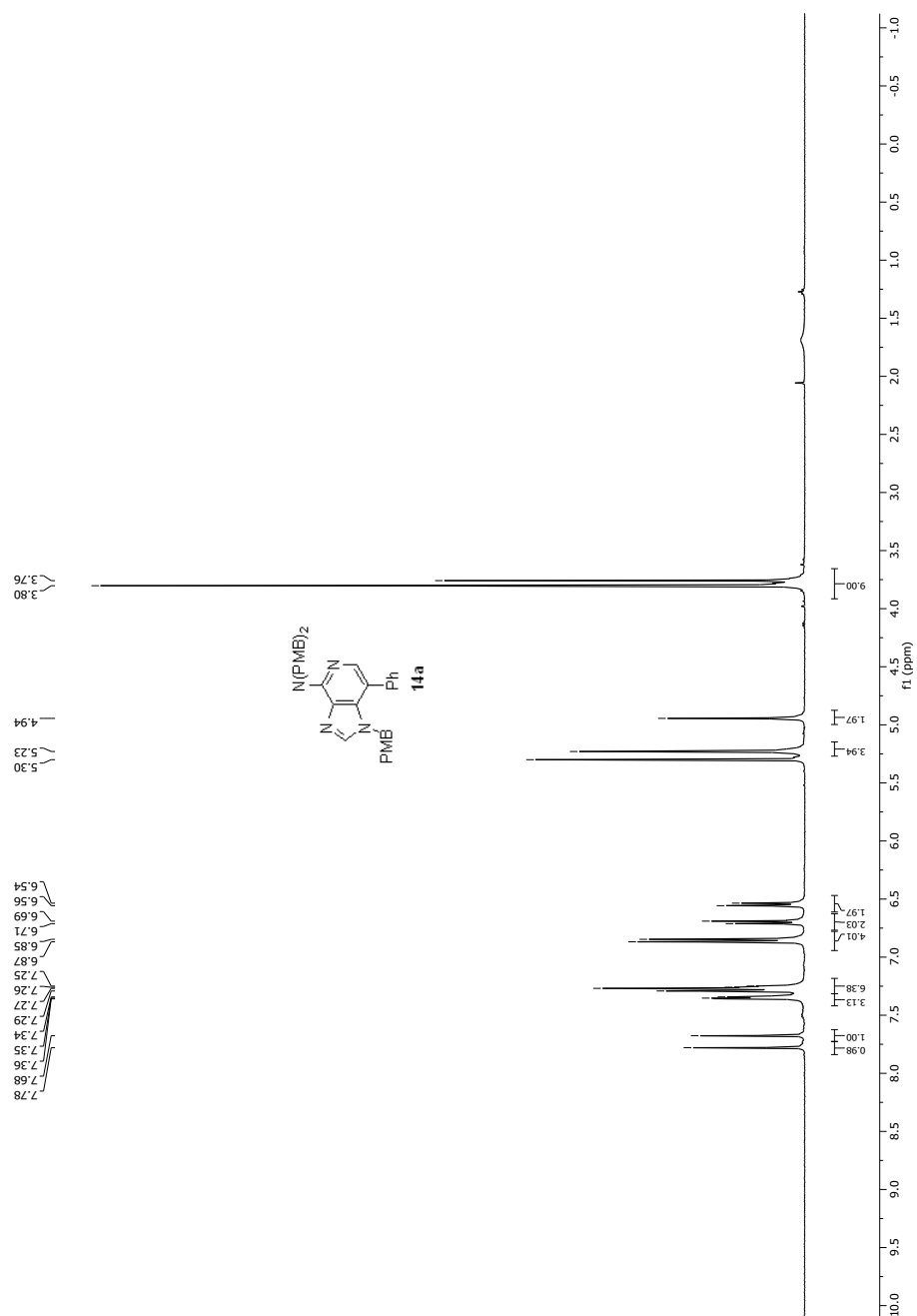


Figure. B21 <sup>13</sup>C NMR spectrum of **13** (CDCl<sub>3</sub>, 100 MHz).



**Figure. B22** <sup>1</sup>H NMR spectrum of **14a** (CDCl<sub>3</sub>, 400 MHz).

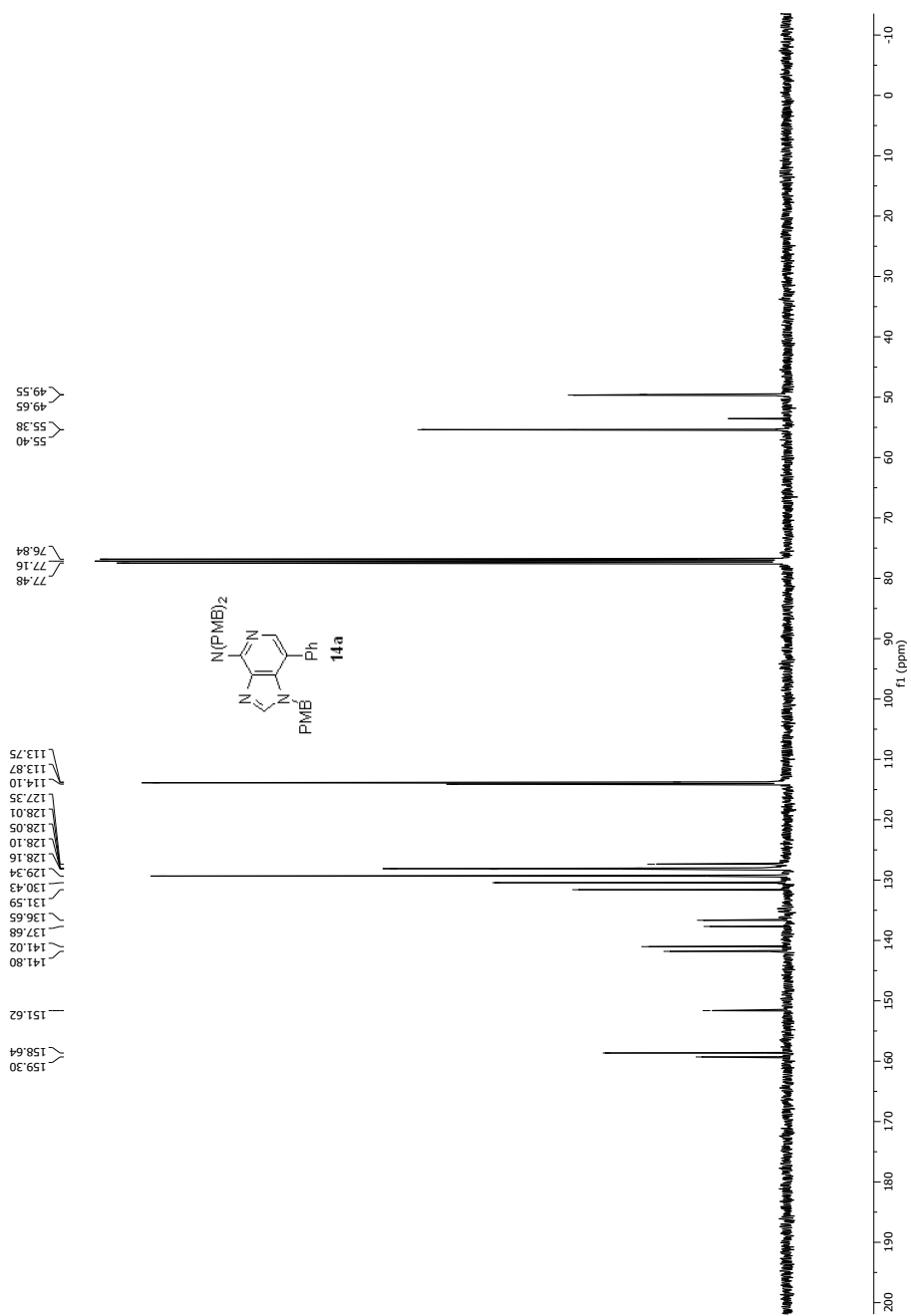
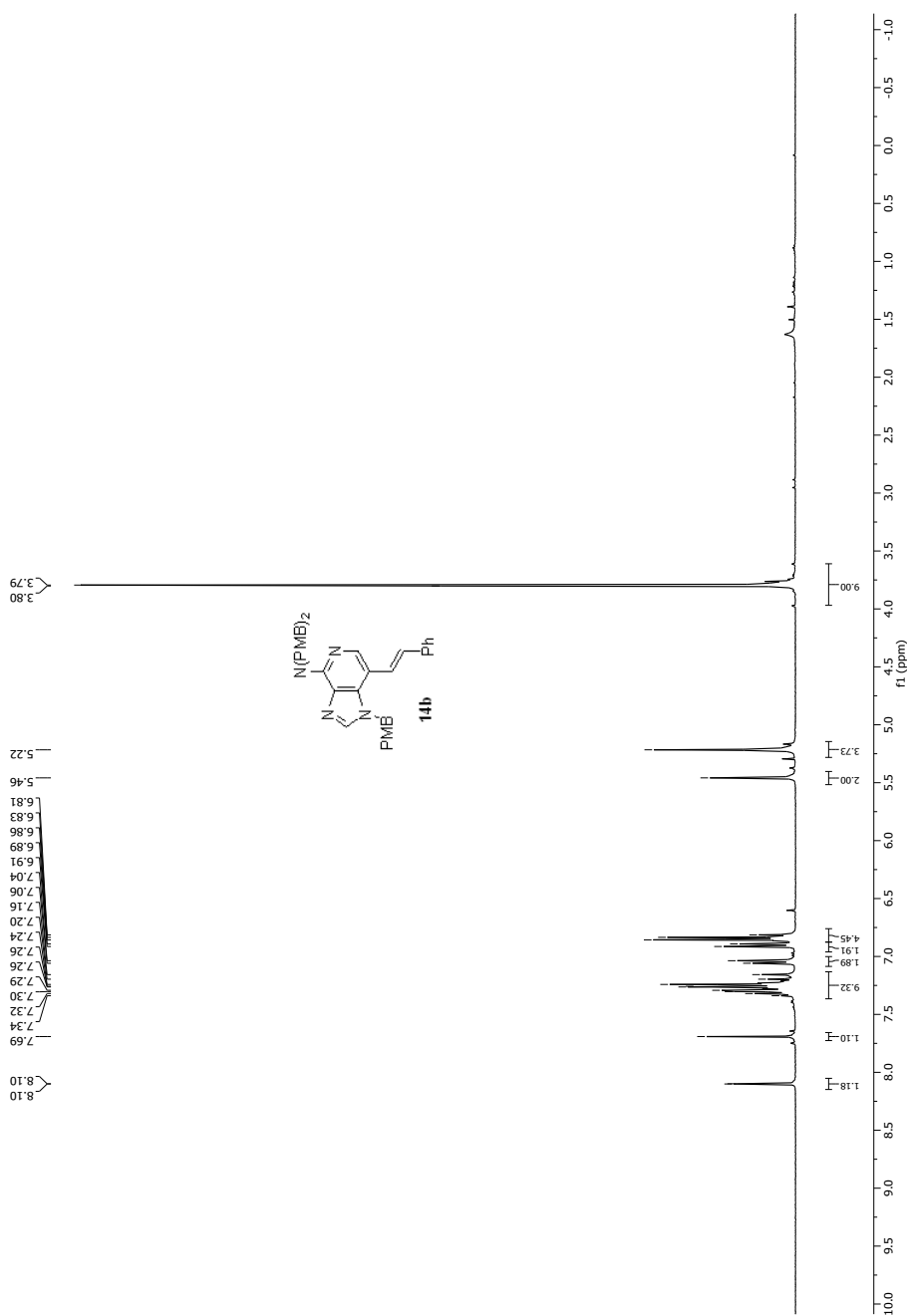


Figure. B23 <sup>13</sup>C NMR spectrum of **14a** (CDCl<sub>3</sub>, 100 MHz).



**Figure. B24**  $^1\text{H}$  NMR spectrum of **14b** ( $\text{CDCl}_3$ , 400 MHz).

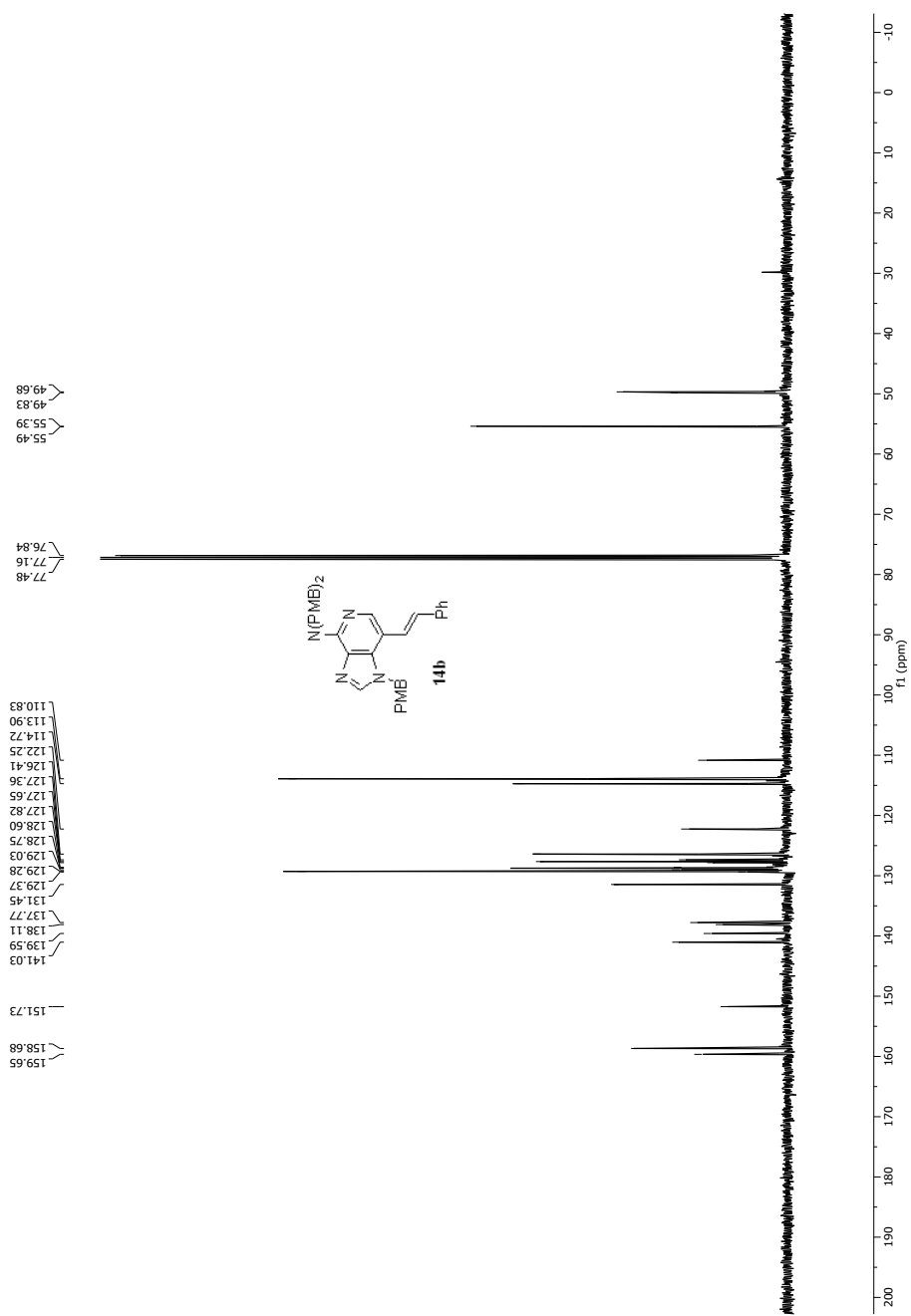
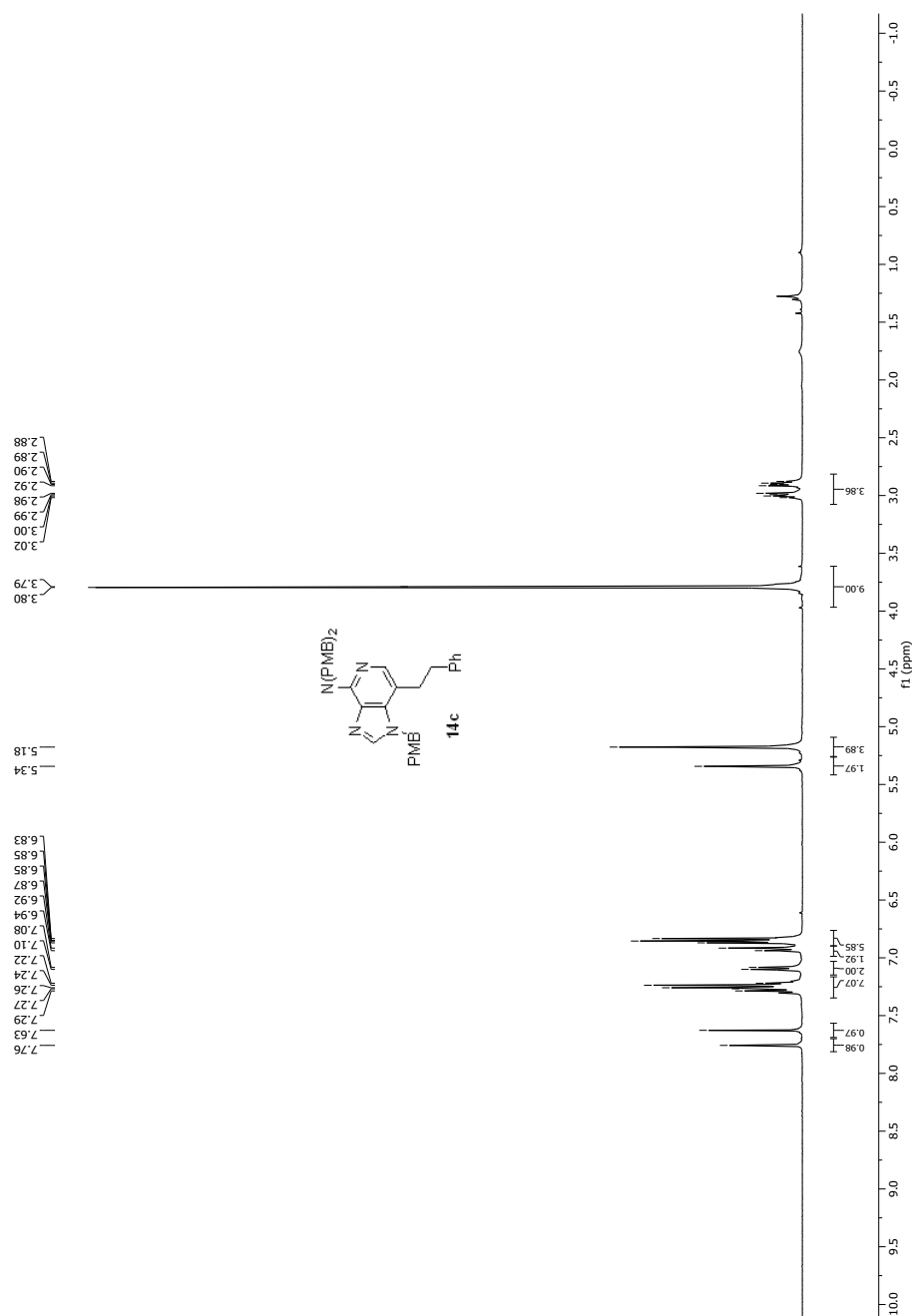
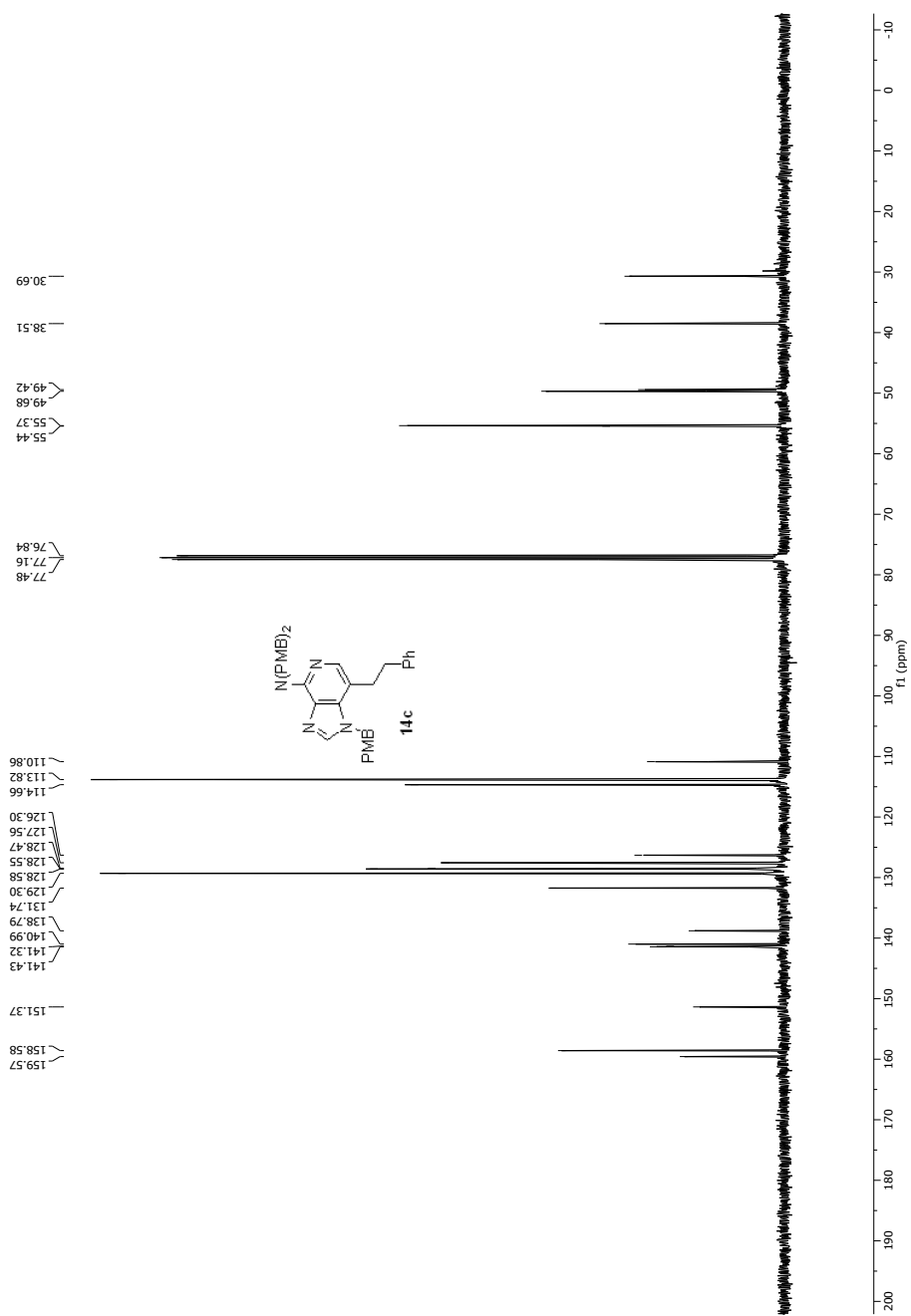


Figure. B25  $^{13}\text{C}$  NMR spectrum of **14b** ( $\text{CDCl}_3$ , 100 MHz).

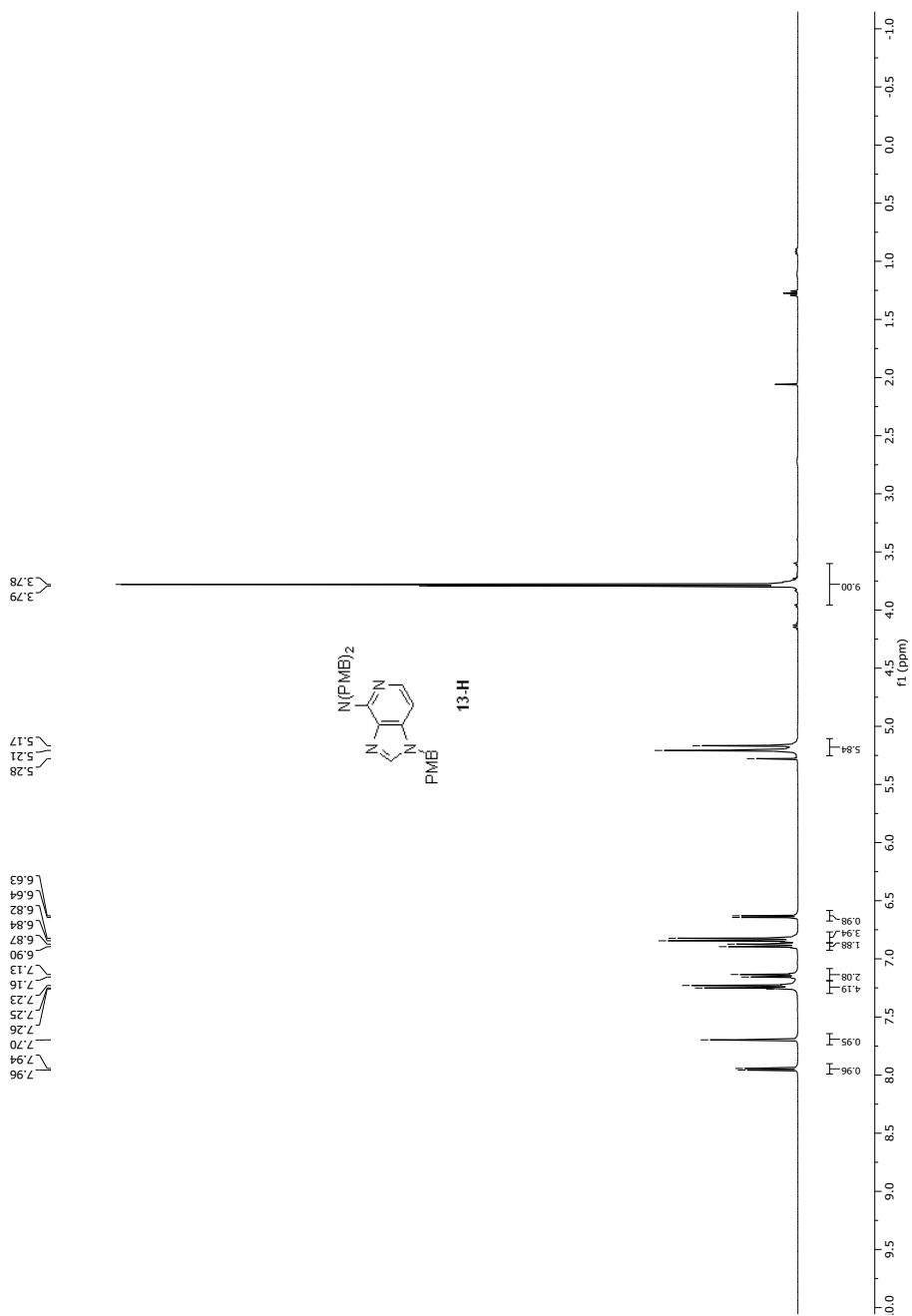




**Figure. B26** <sup>1</sup>H NMR spectrum of **14c** (CDCl<sub>3</sub>, 400 MHz).



**Figure. B27** <sup>13</sup>C NMR spectrum of **14c** (CDCl<sub>3</sub>, 100 MHz).



**Figure. B28** <sup>1</sup>H NMR spectrum of **13-H** (CDCl<sub>3</sub>, 400 MHz).

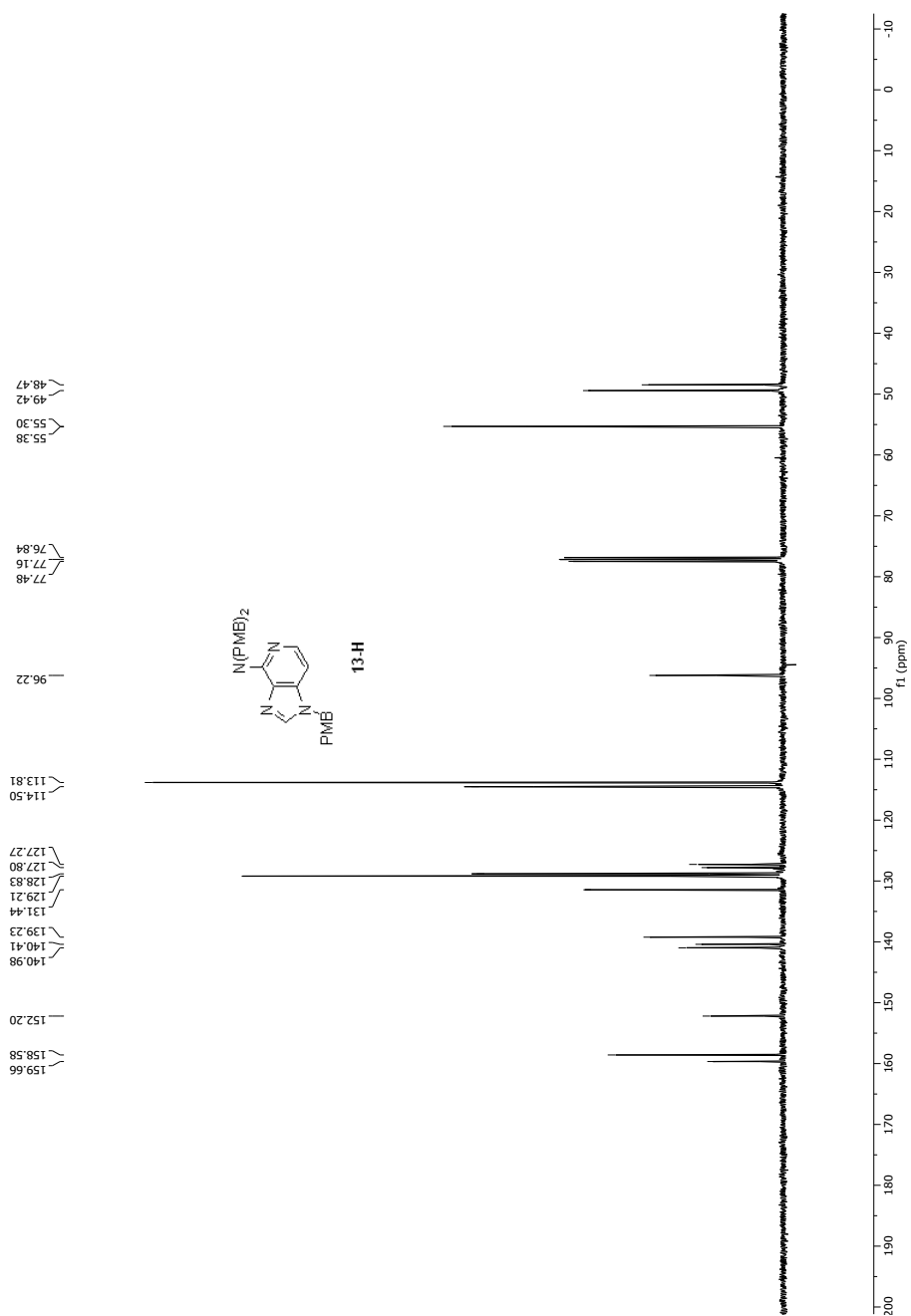
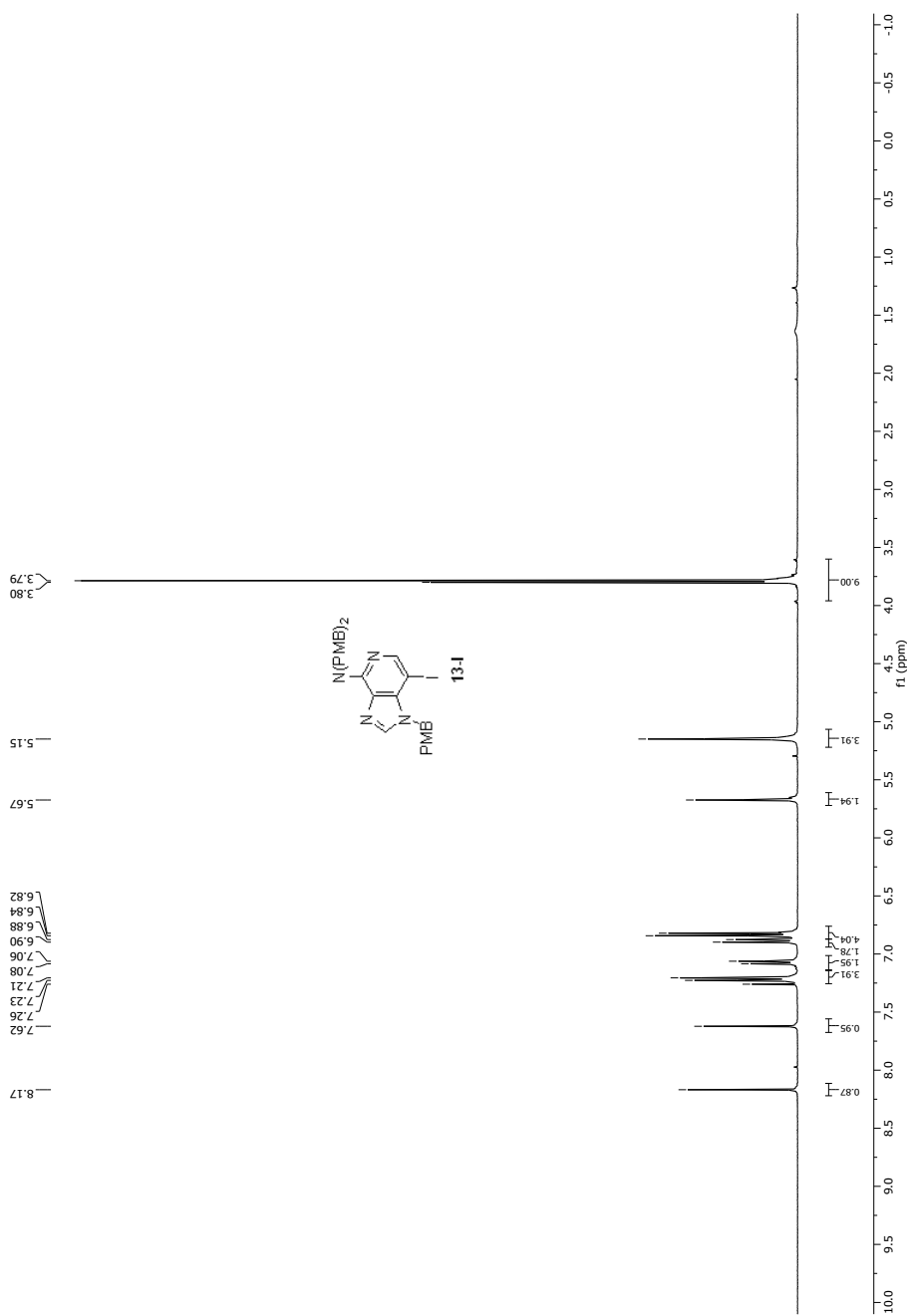


Figure. B29 <sup>13</sup>C NMR spectrum of **13-H** (CDCl<sub>3</sub>, 100 MHz).



**Figure. B30**  $^1\text{H}$  NMR spectrum of **13-I** ( $\text{CDCl}_3$ , 400 MHz).

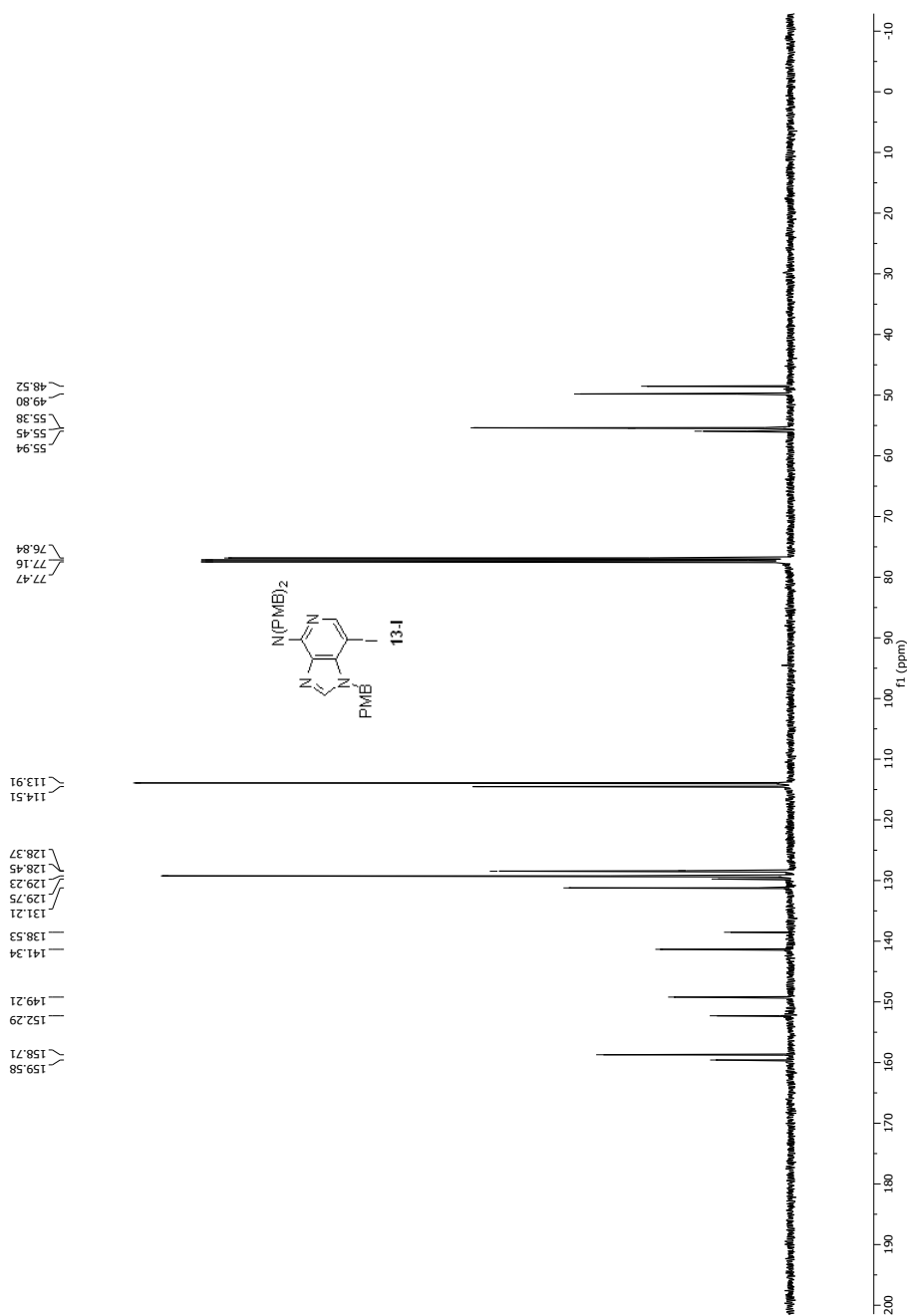
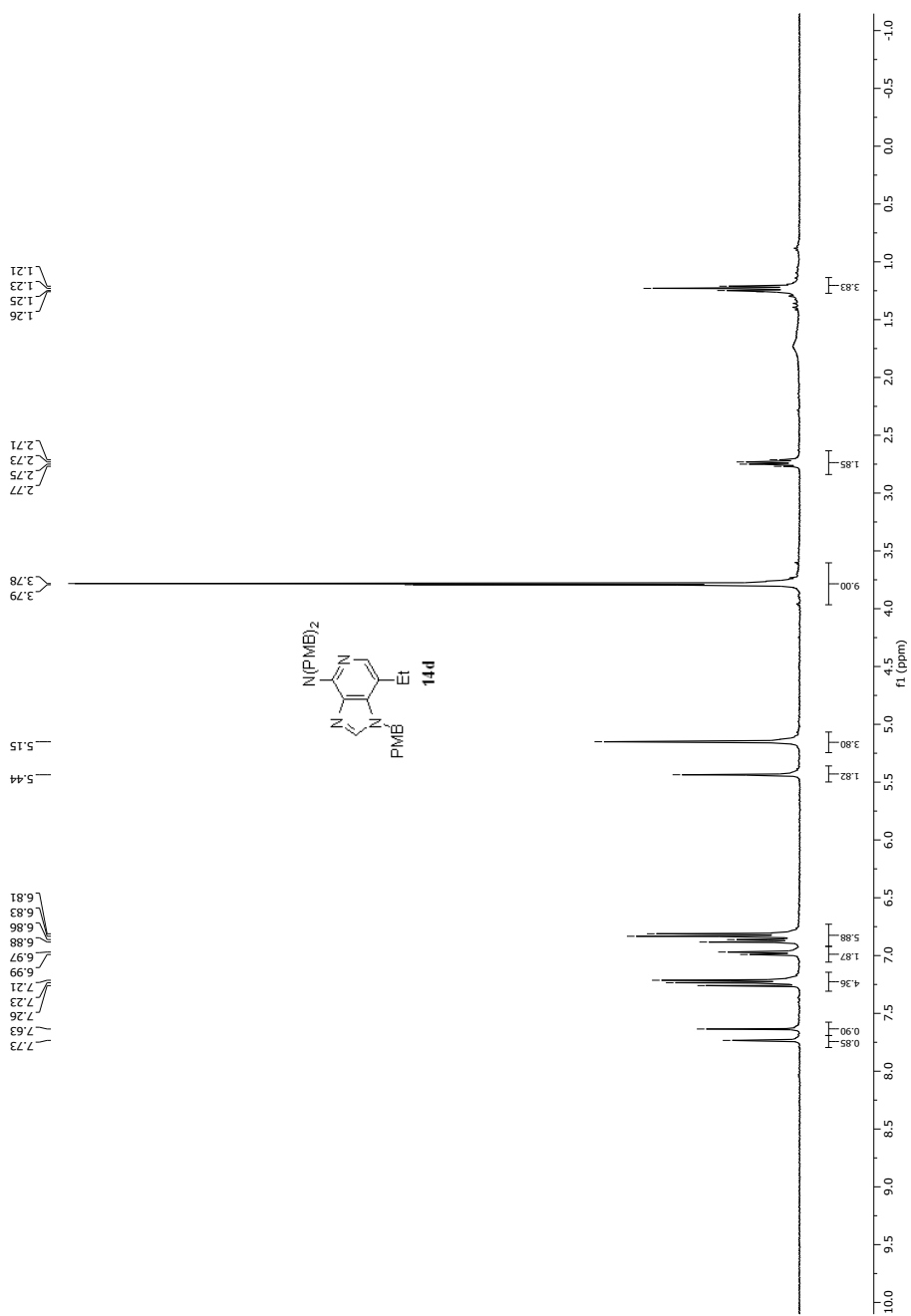


Figure. B31 <sup>13</sup>C NMR spectrum of 13-I (CDCl<sub>3</sub>, 100 MHz).



**Figure. B32** <sup>1</sup>H NMR spectrum of **14d** (CDCl<sub>3</sub>, 400 MHz).

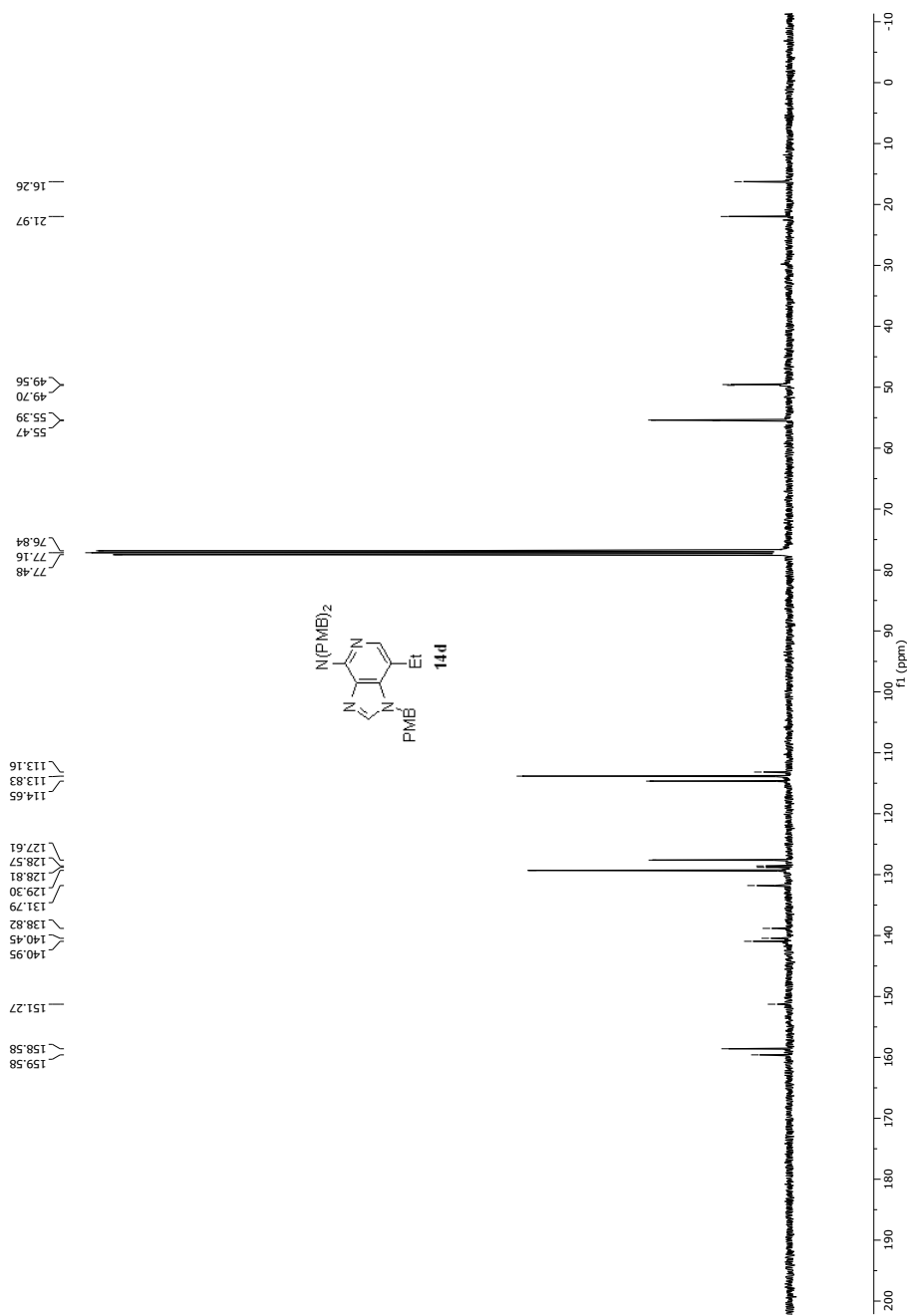
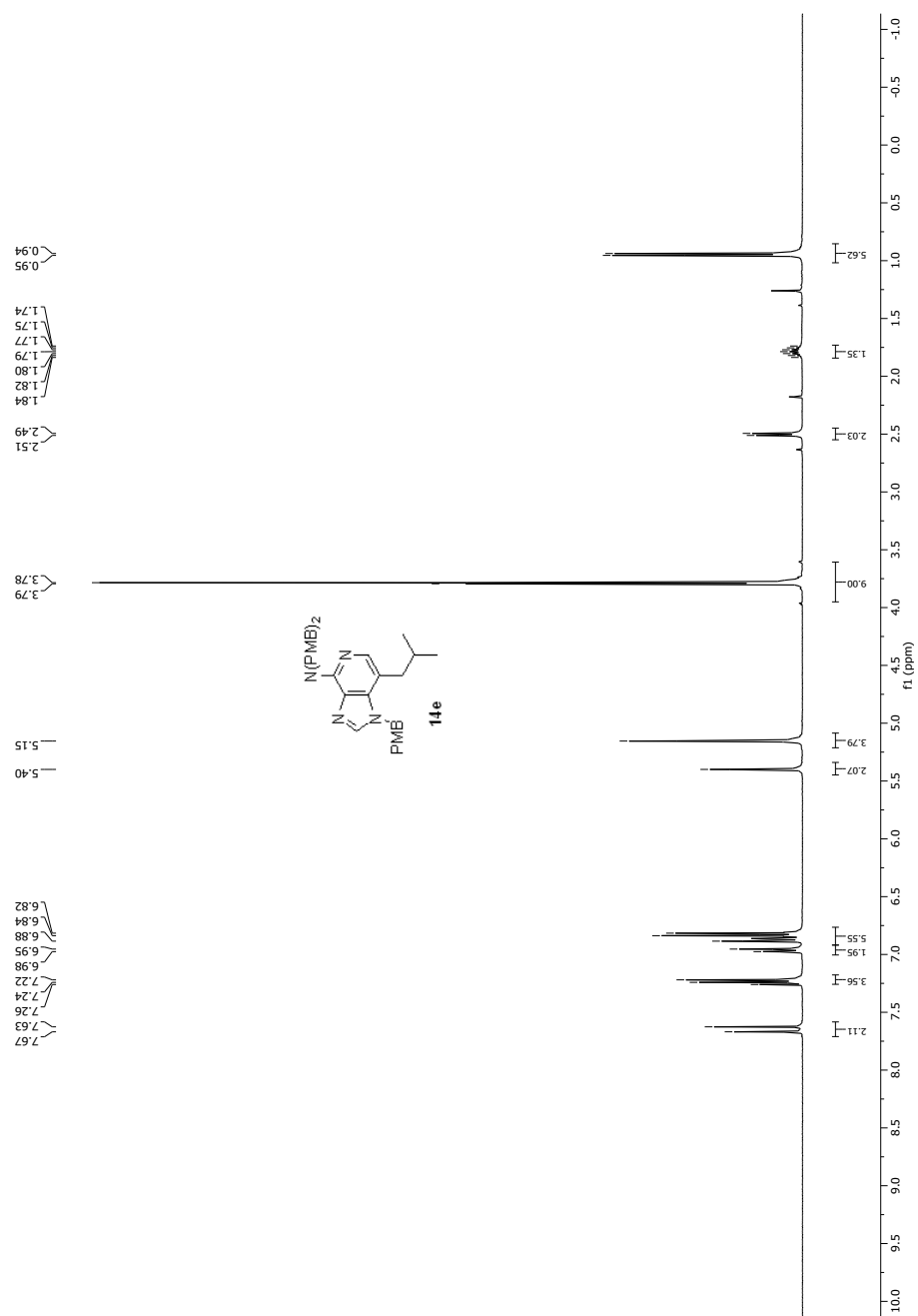
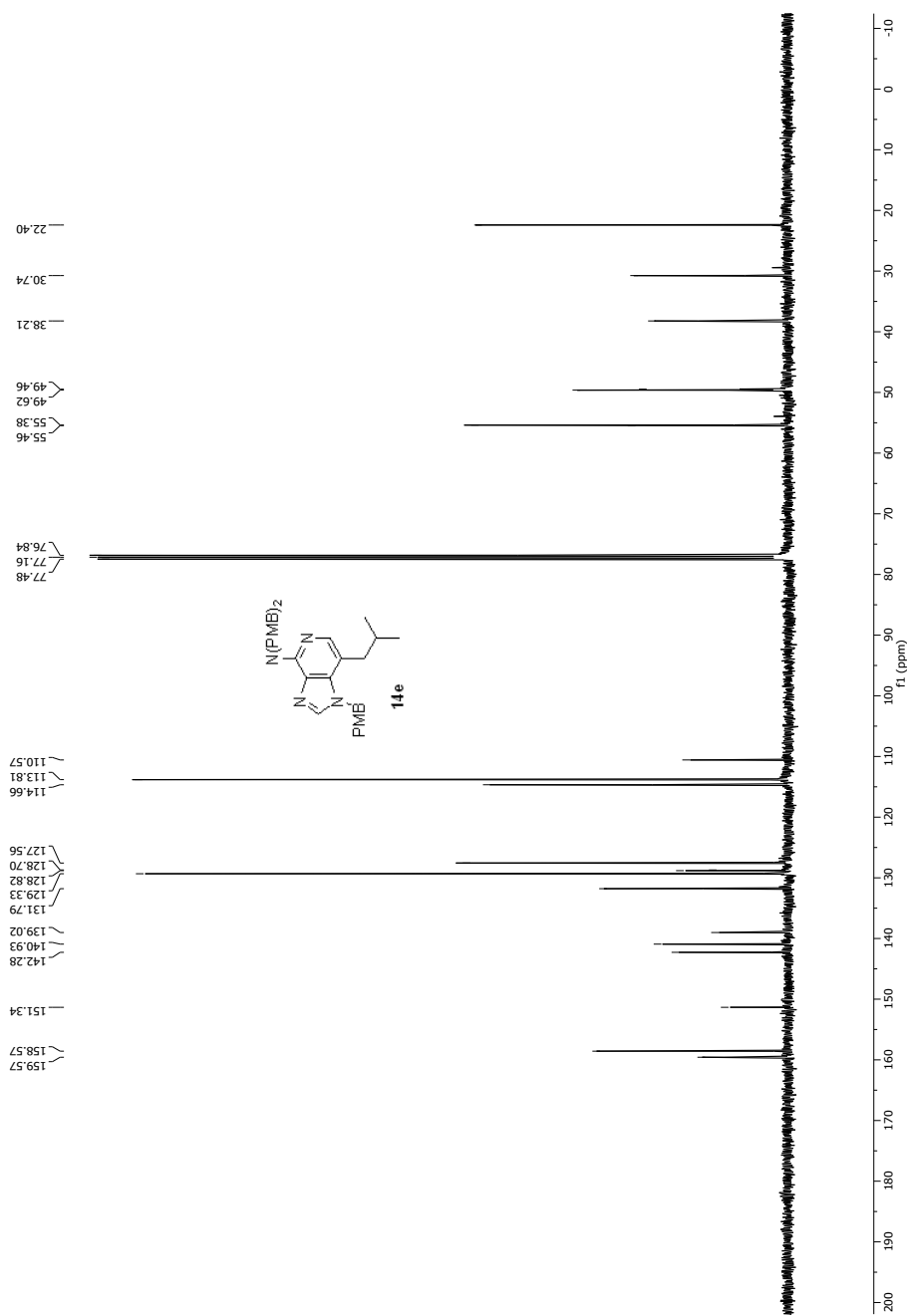


Figure. B33 <sup>13</sup>C NMR spectrum of **14d** (CDCl<sub>3</sub>, 100 MHz).

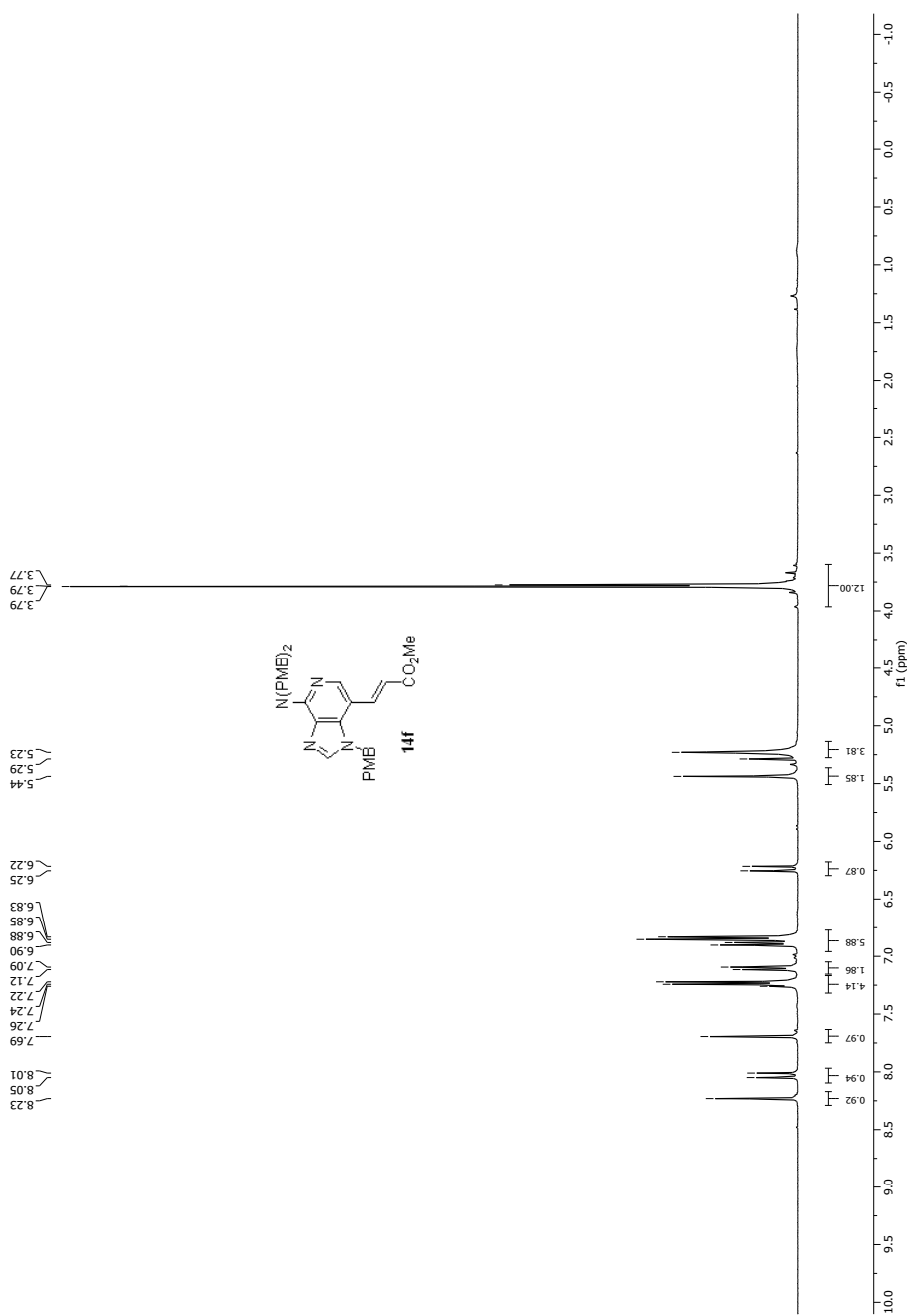




**Figure. B34** <sup>1</sup>H NMR spectrum of **14e** (CDCl<sub>3</sub>, 400 MHz).



**Figure. B35**  $^{13}\text{C}$  NMR spectrum of **14e** ( $\text{CDCl}_3$ , 100 MHz).



**Figure. B36**  $^1\text{H}$  NMR spectrum of **14f** ( $\text{CDCl}_3$ , 400 MHz).

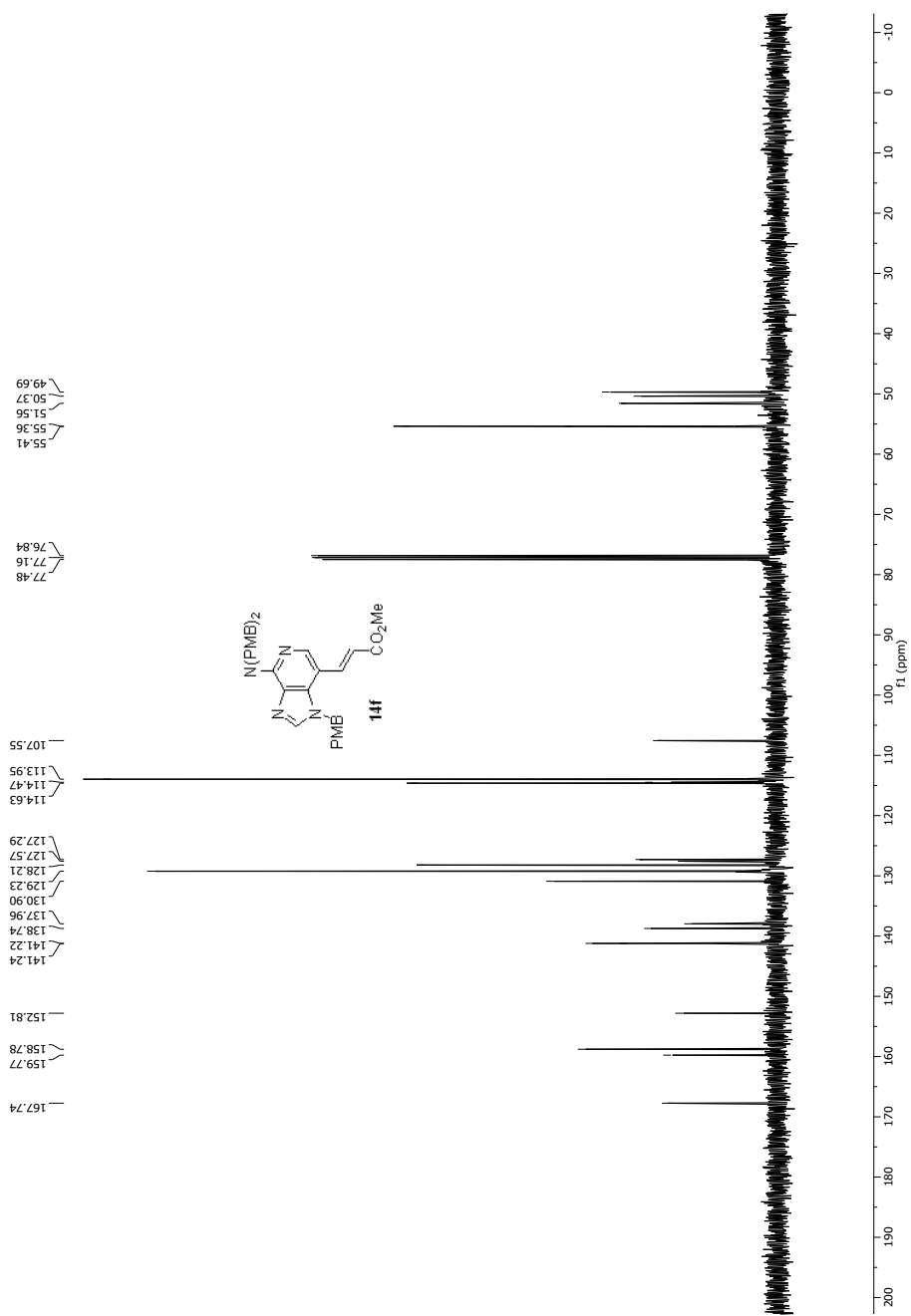
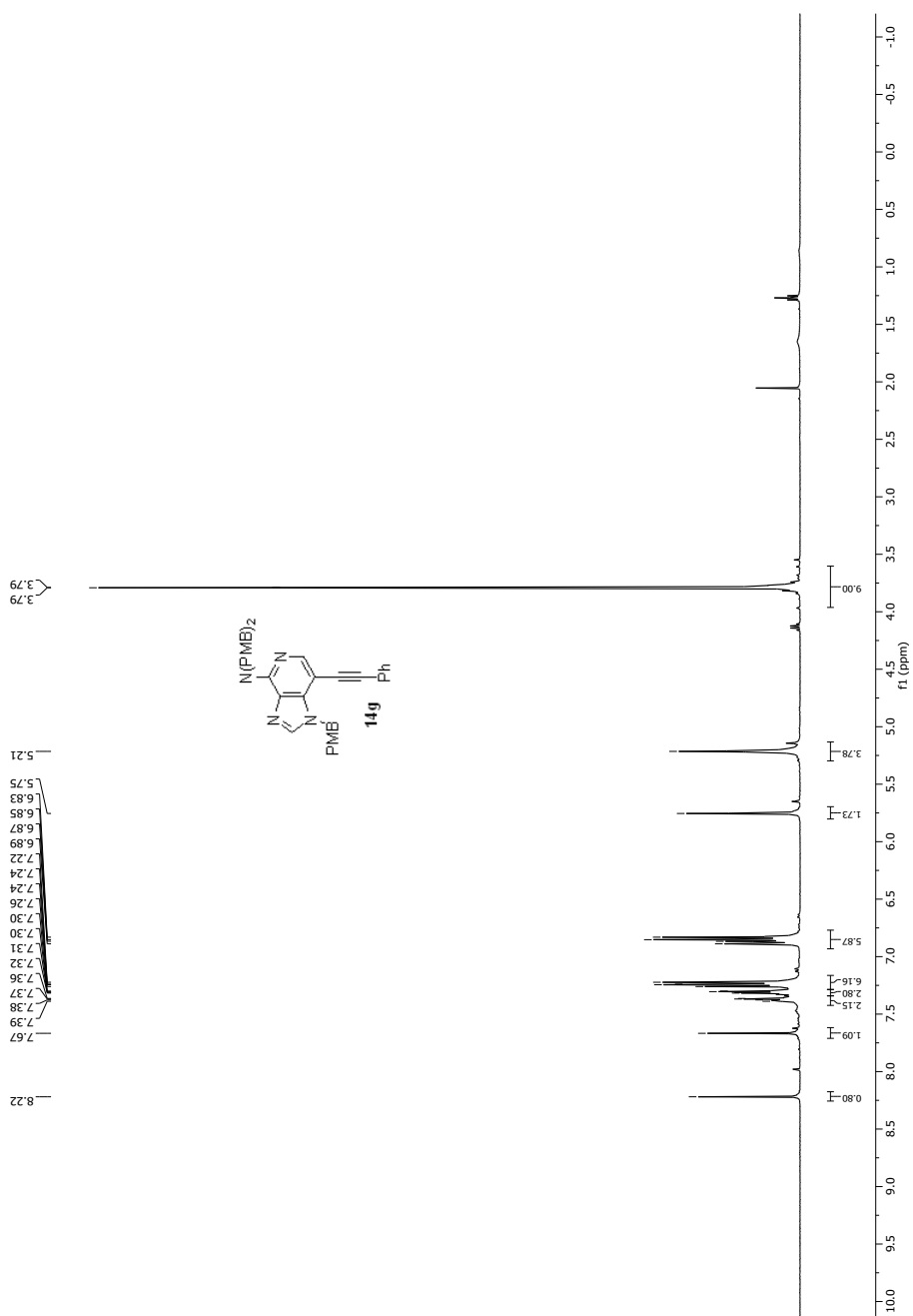
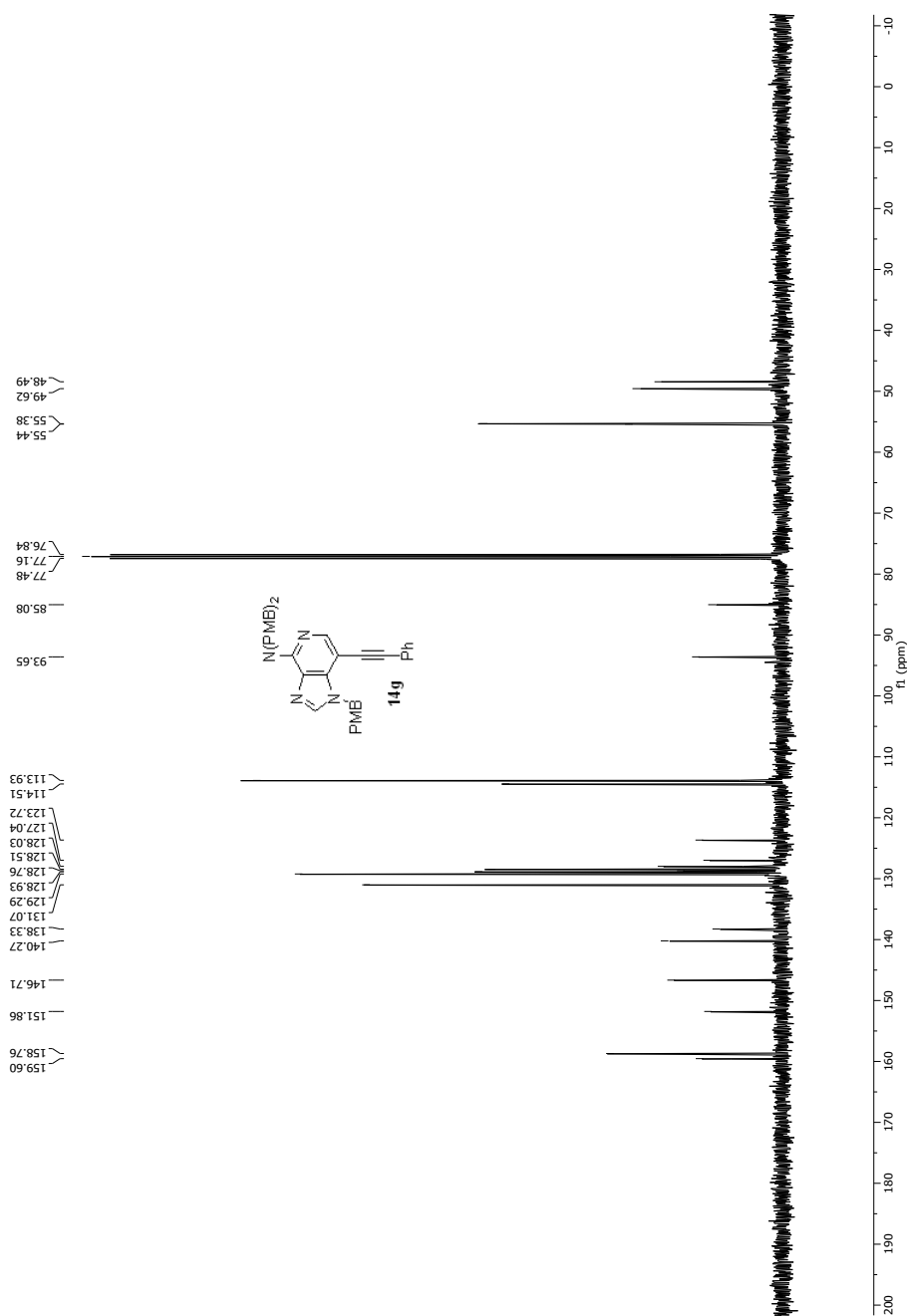


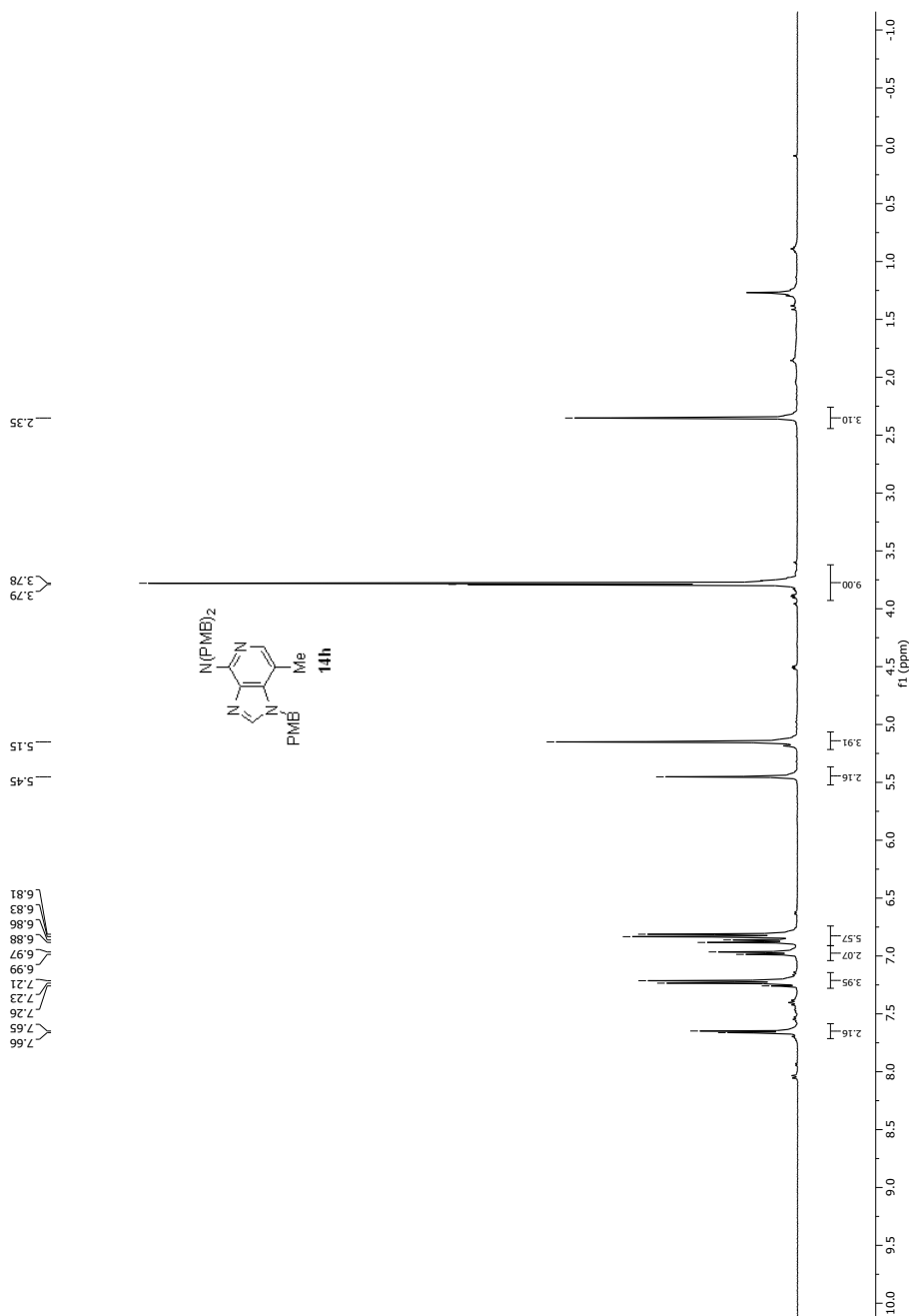
Figure. B37 <sup>13</sup>C NMR spectrum of **14f** (CDCl<sub>3</sub>, 100 MHz).



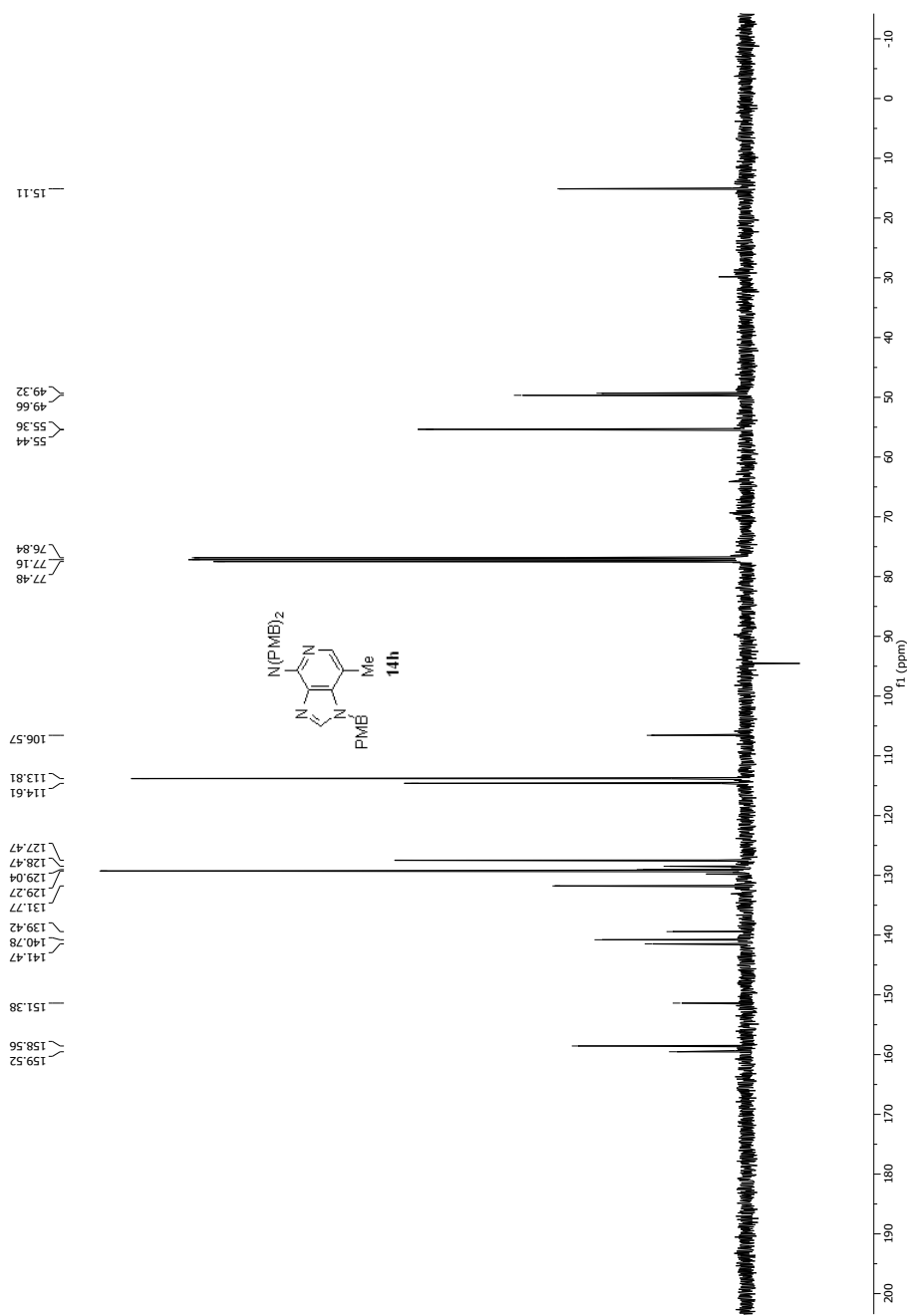
**Figure. B38** <sup>1</sup>H NMR spectrum of **14g** (CDCl<sub>3</sub>, 400 MHz).



**Figure. B39** <sup>13</sup>C NMR spectrum of **14g** (CDCl<sub>3</sub>, 100 MHz).

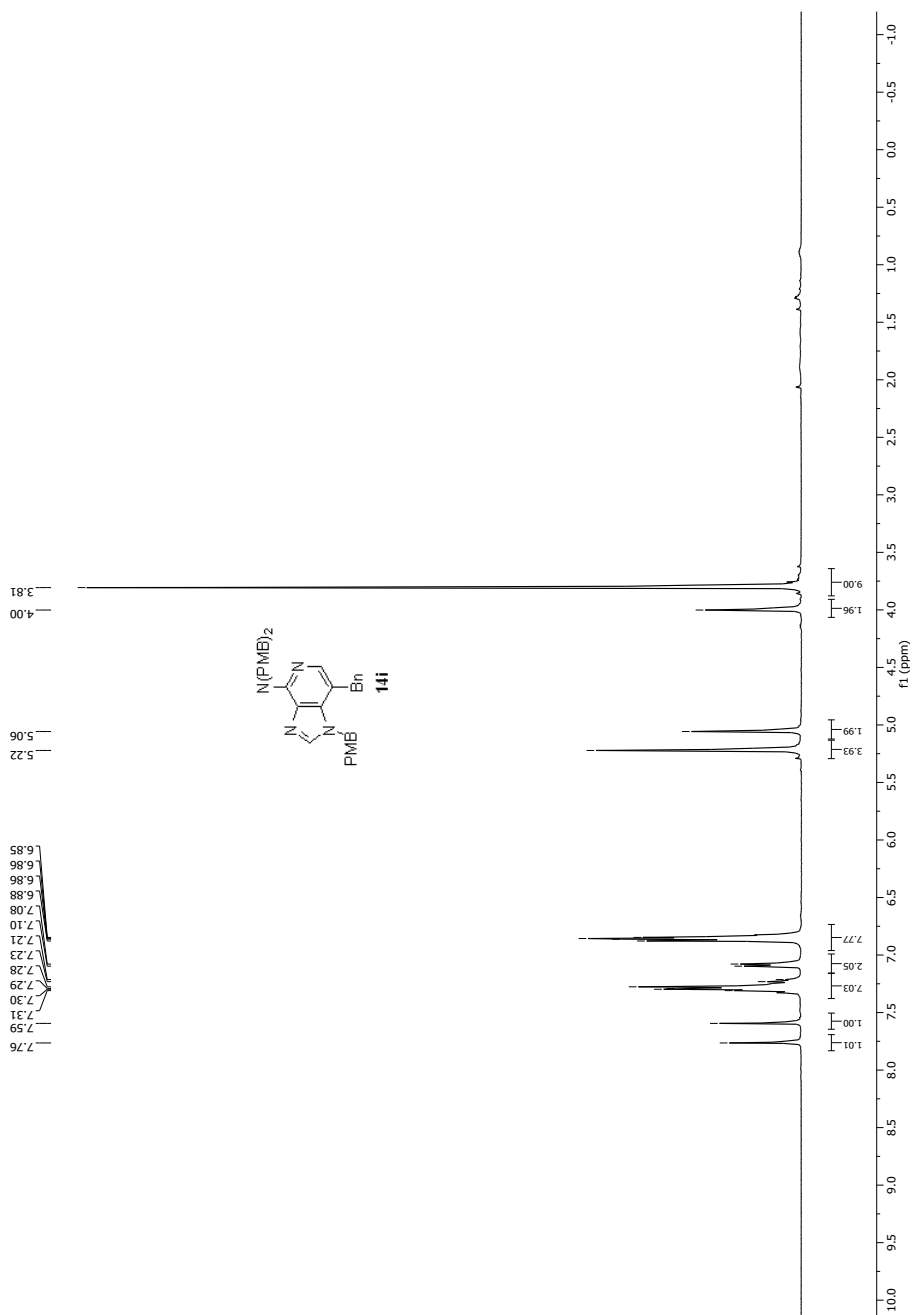


**Figure. B40** <sup>1</sup>H NMR spectrum of **14h** (CDCl<sub>3</sub>, 400 MHz).



**Figure. B41**  $^{13}\text{C}$  NMR spectrum of **14h** ( $\text{CDCl}_3$ , 100 MHz).





**Figure. B42**  $^1\text{H}$  NMR spectrum of **14i** ( $\text{CDCl}_3$ , 400 MHz).

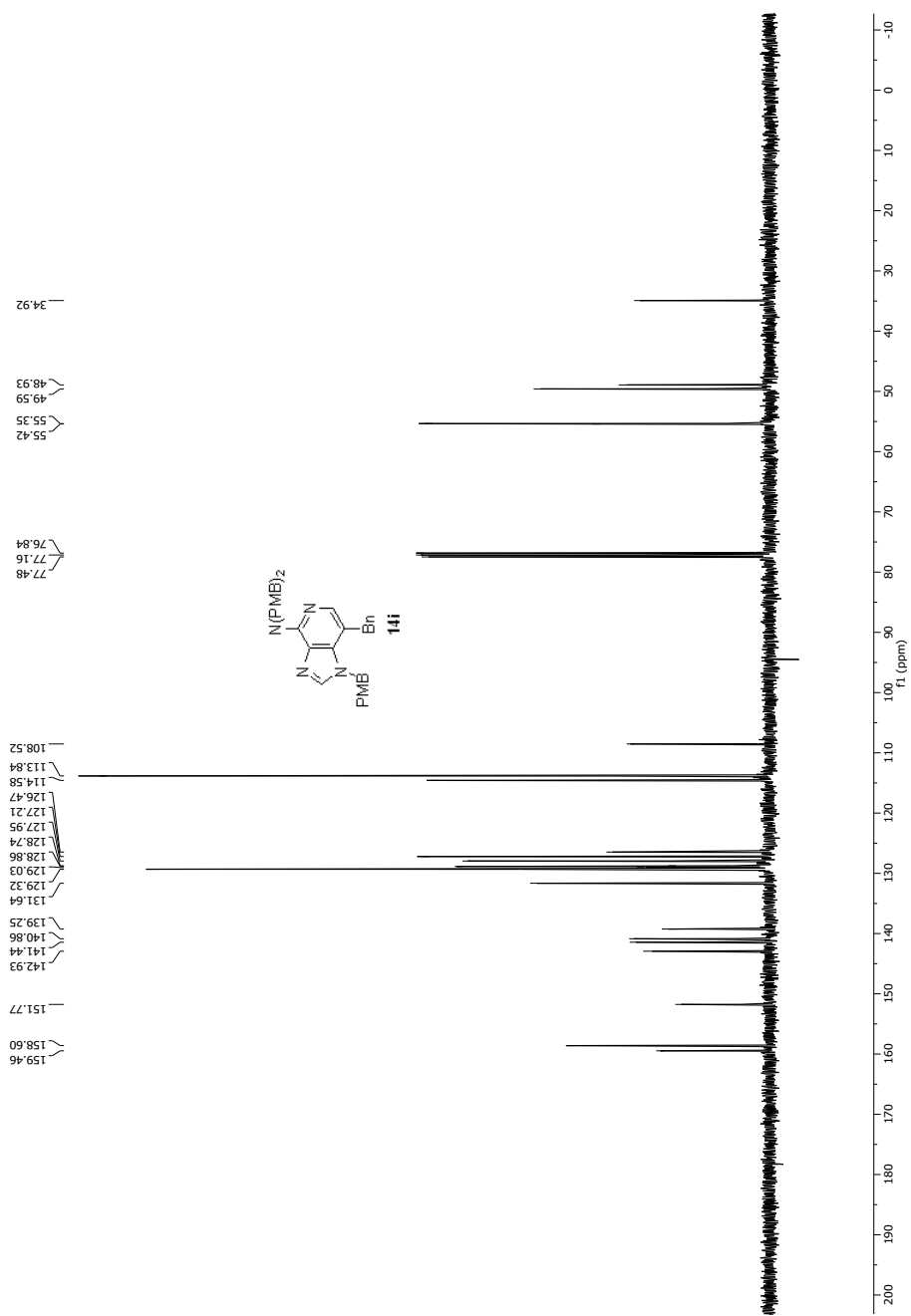
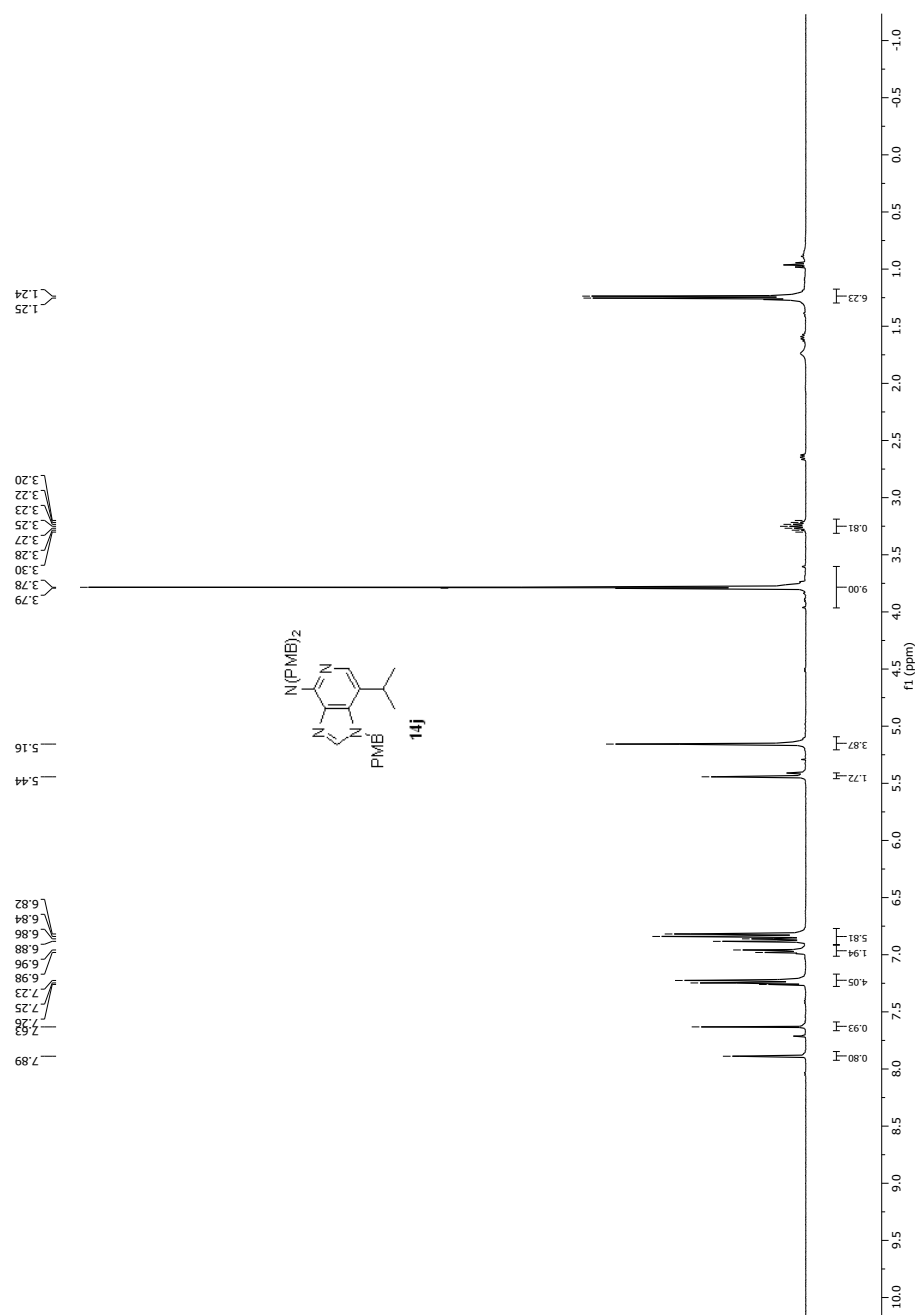


Figure. B44 <sup>13</sup>C NMR spectrum of **14i** (CDCl<sub>3</sub>, 100 MHz).



**Figure. B44**  $^1\text{H}$  NMR spectrum of **14j** ( $\text{CDCl}_3$ , 400 MHz).

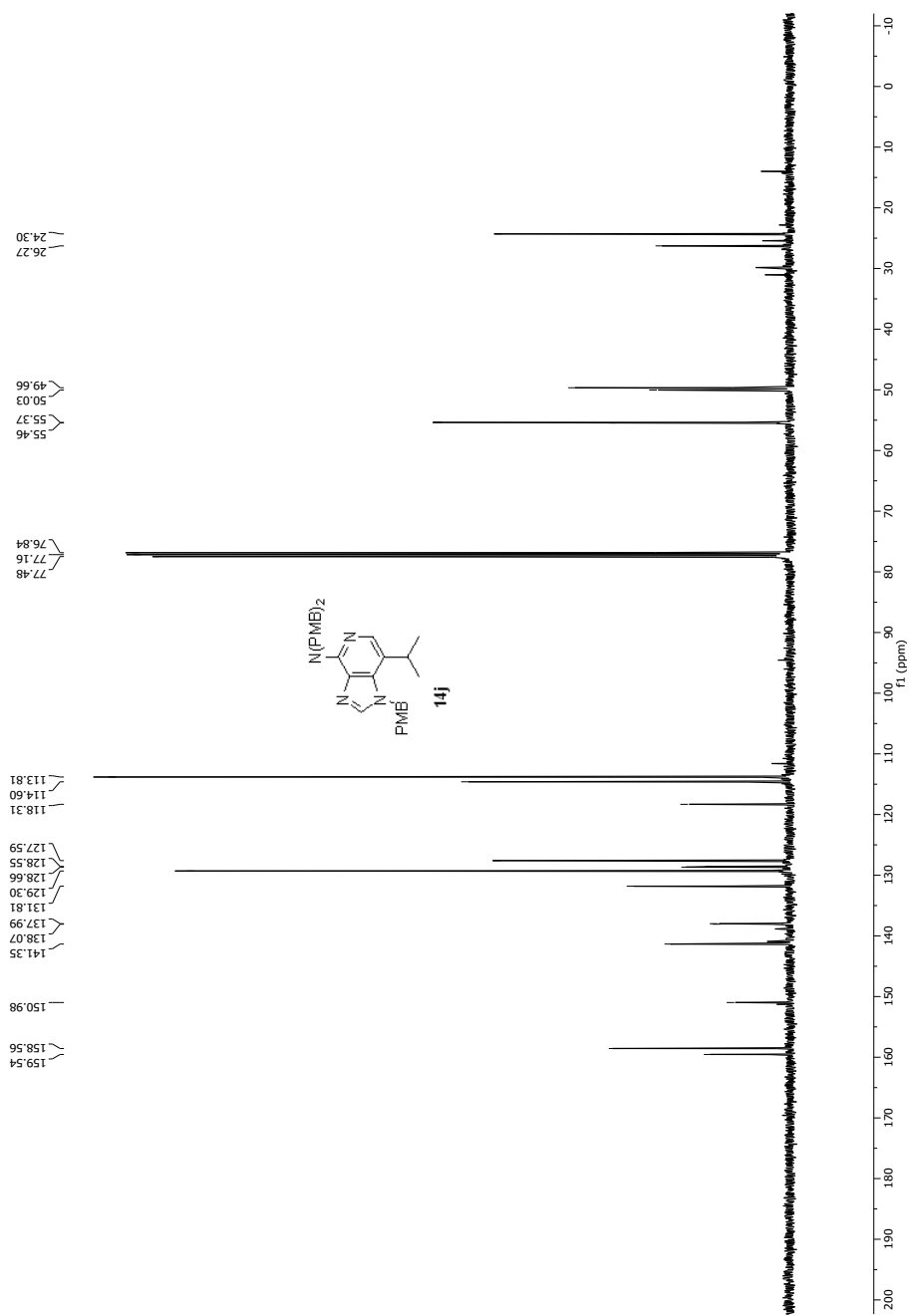
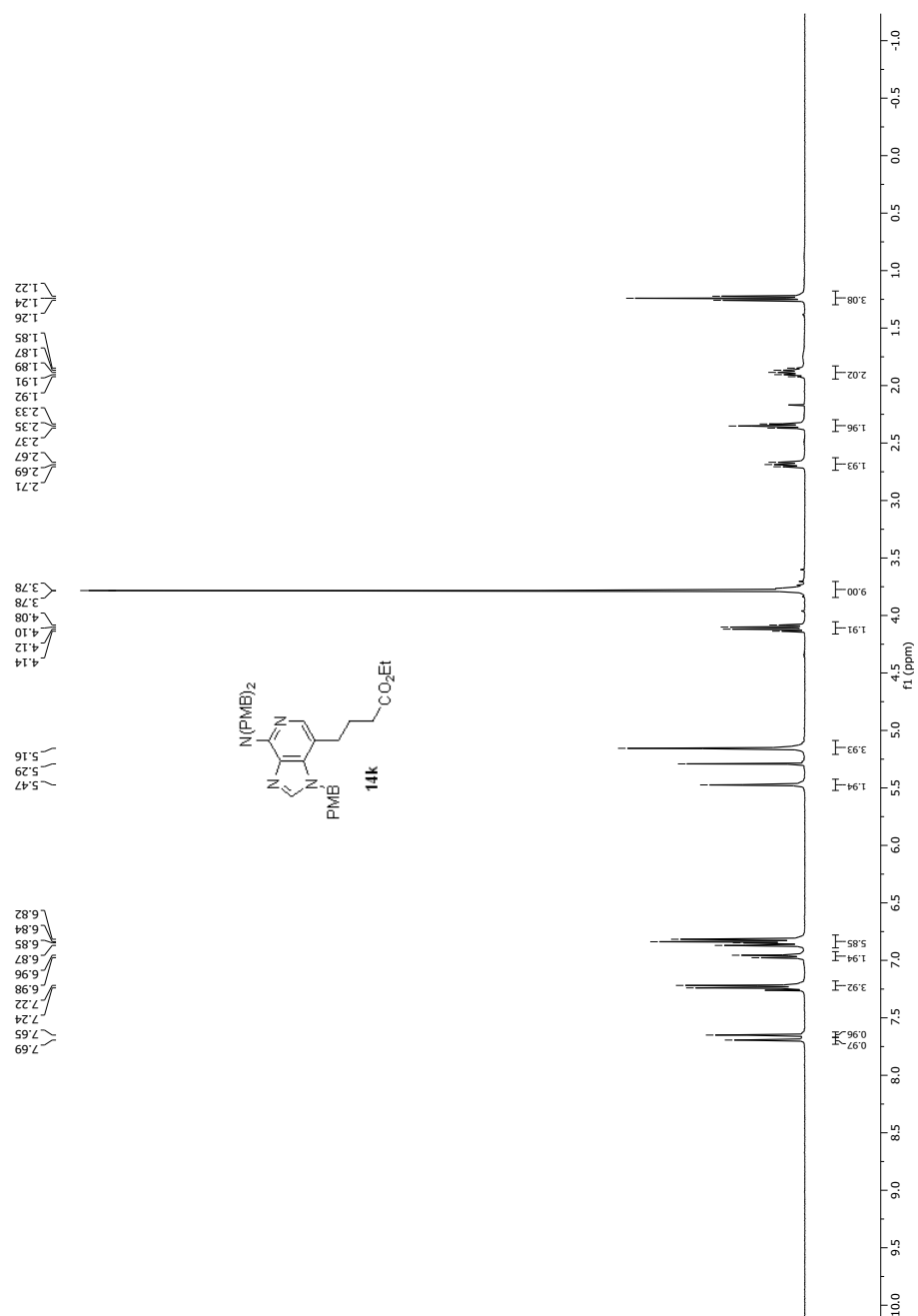


Figure. B45 <sup>13</sup>C NMR spectrum of **14j** (CDCl<sub>3</sub>, 100 MHz).



**Figure. B46** <sup>1</sup>H NMR spectrum of **14k** (CDCl<sub>3</sub>, 400 MHz).

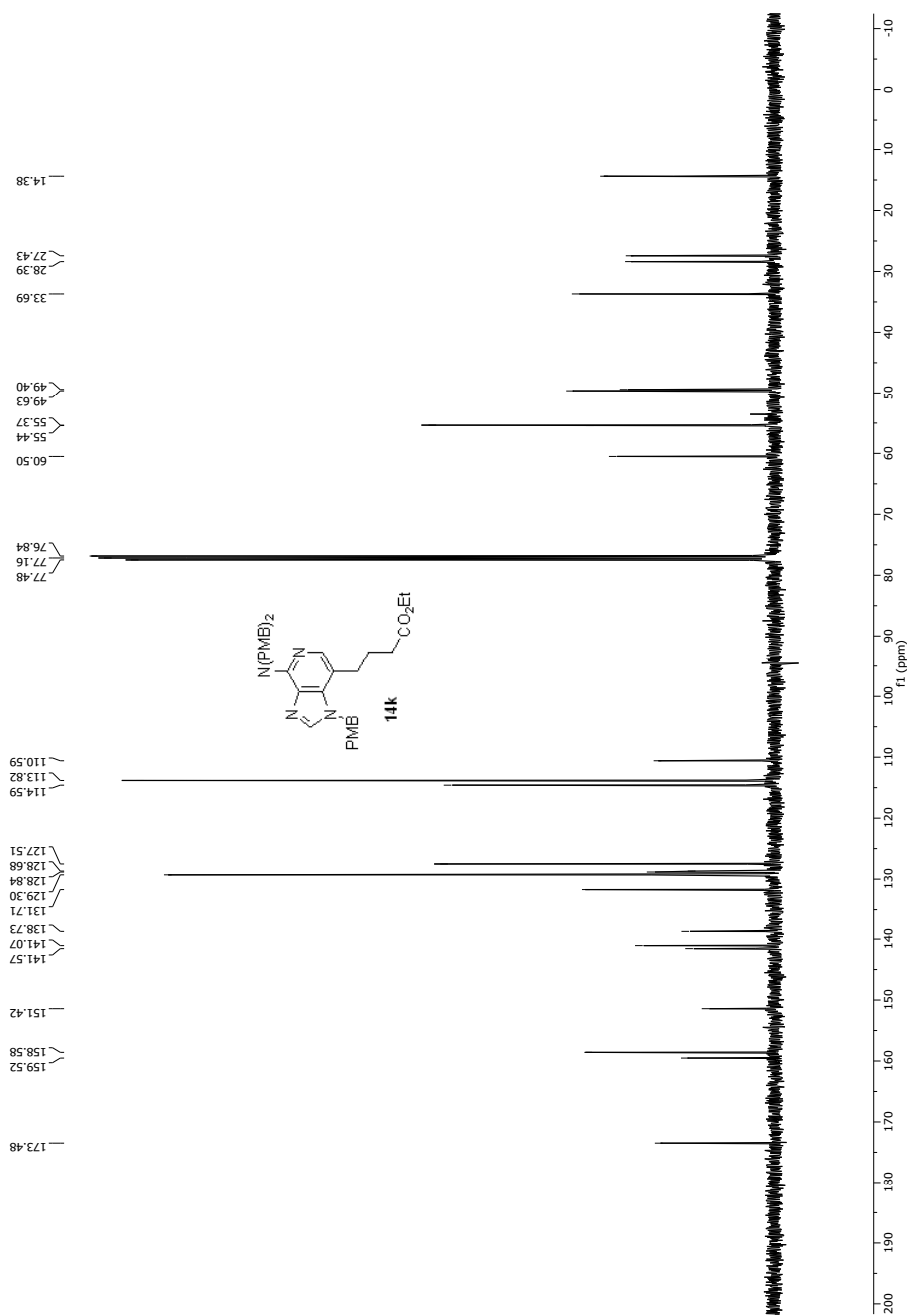
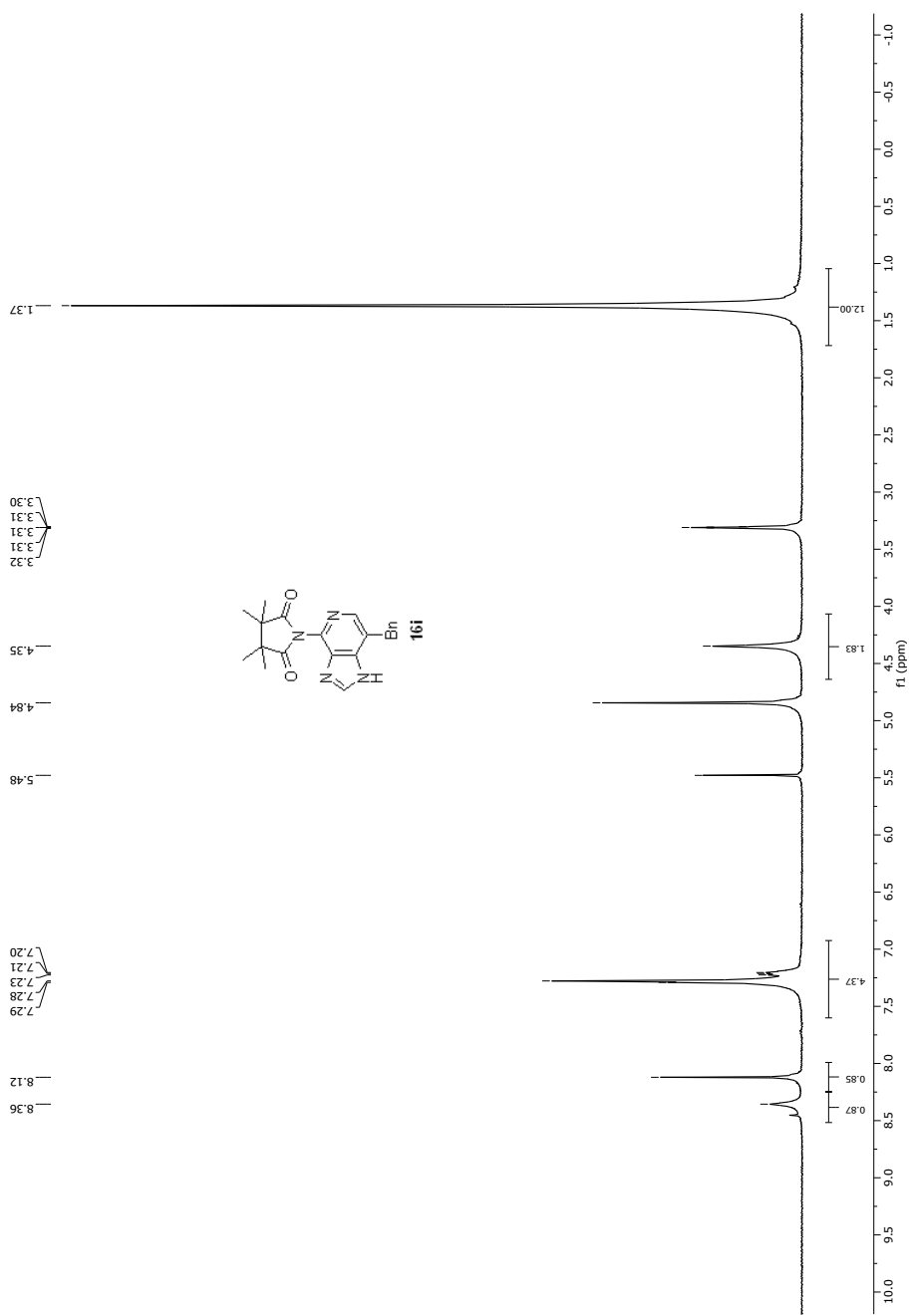
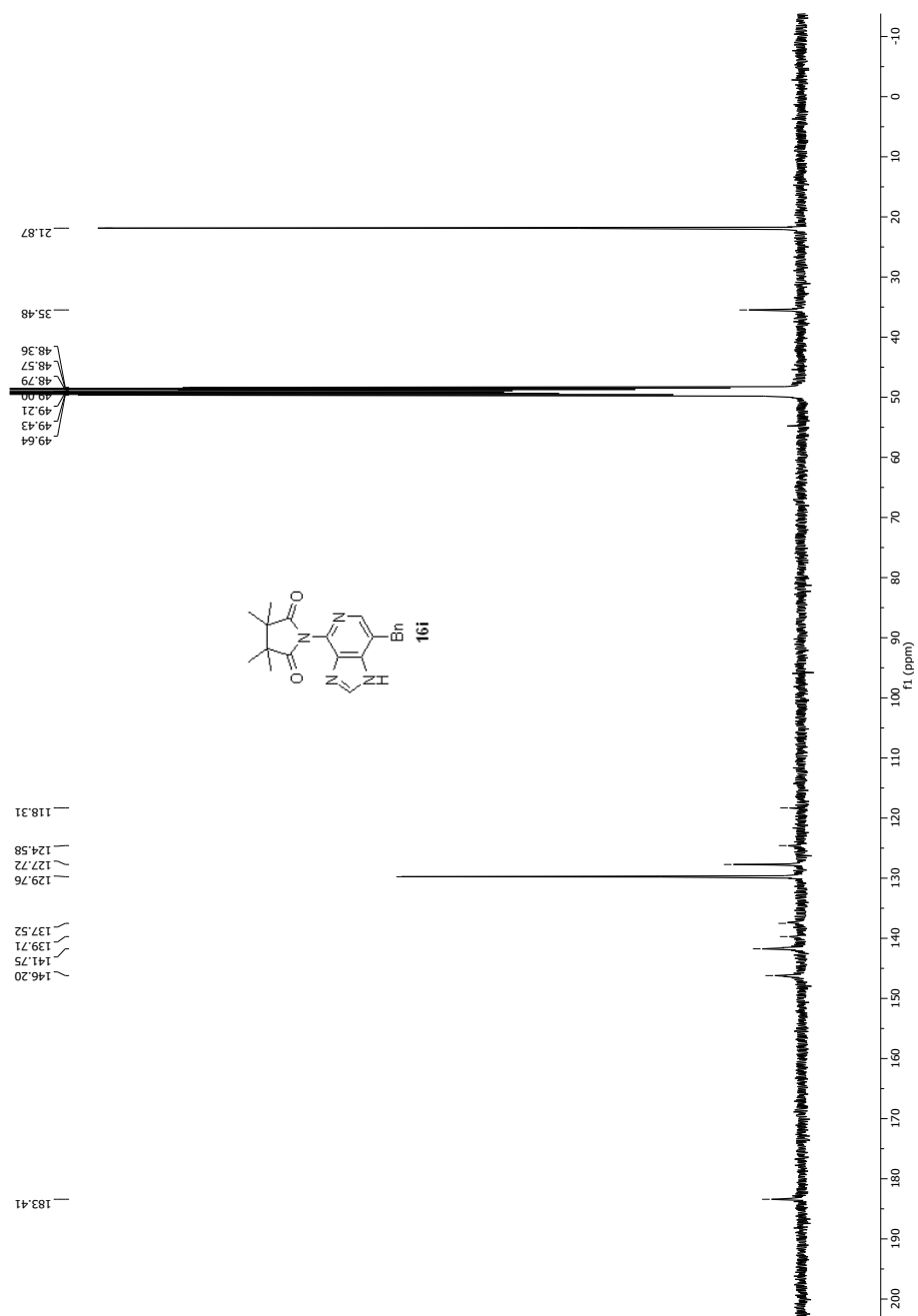


Figure. B47 <sup>13</sup>C NMR spectrum of 14k (CDCl<sub>3</sub>, 100 MHz).

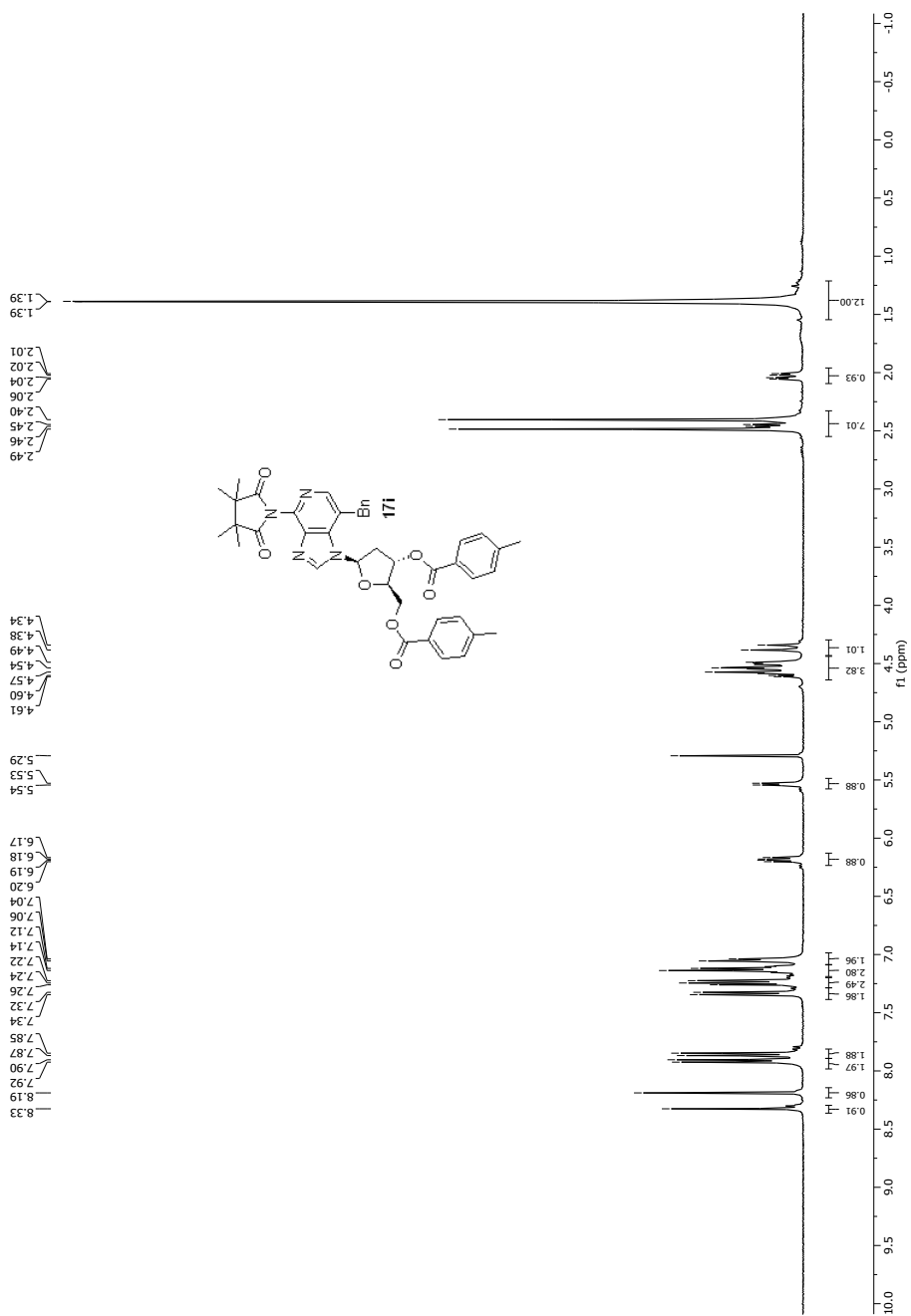


**Figure. B48** <sup>1</sup>H NMR spectrum of **16i** (CD<sub>3</sub>OD, 400 MHz).



**Figure. B49**  $^{13}\text{C}$  NMR spectrum of **16i** ( $\text{CD}_3\text{OD}$ , 100 MHz).





**Figure. B50**  $^1\text{H}$  NMR spectrum of **17i** (CDCl<sub>3</sub>, 400 MHz).

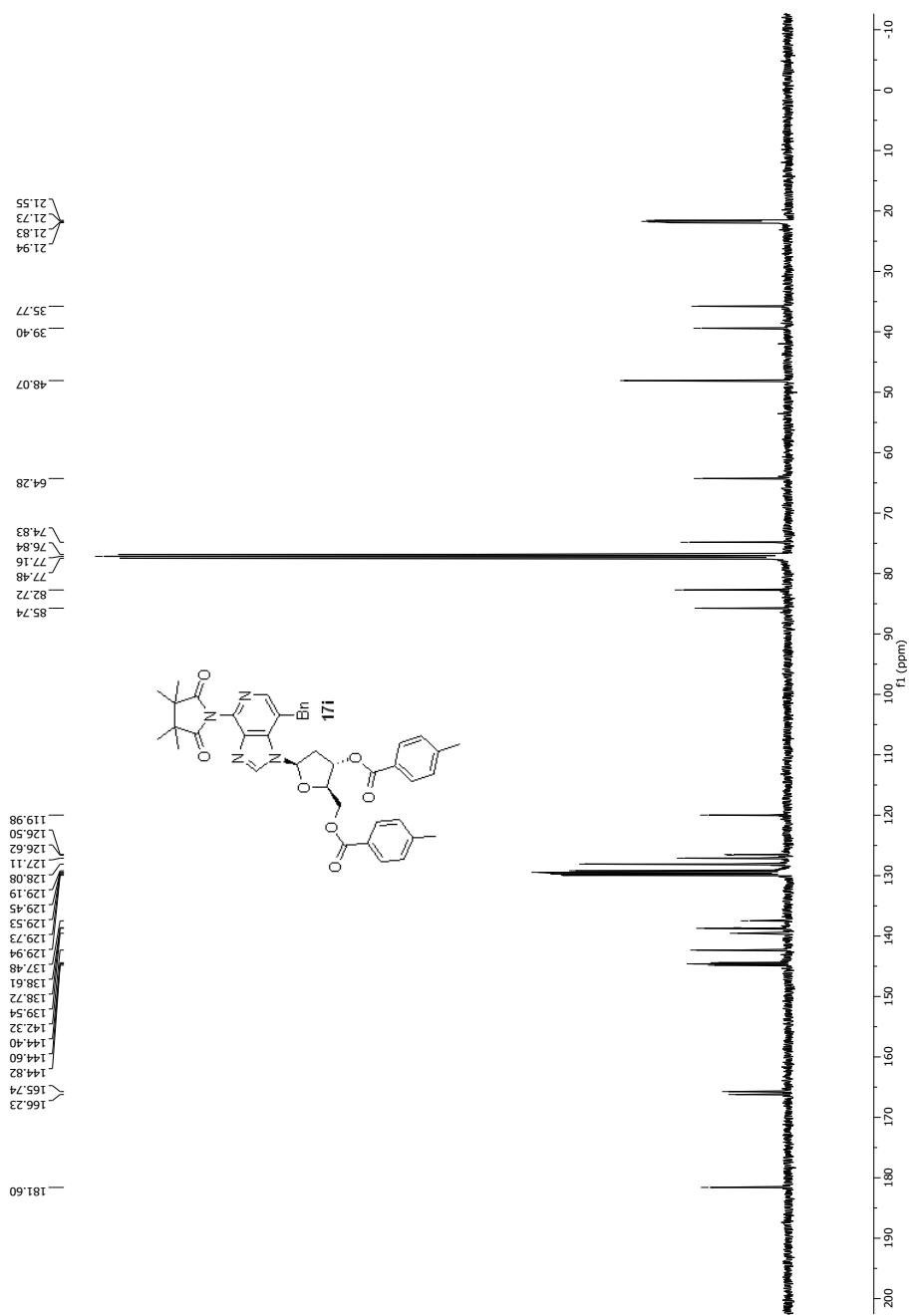
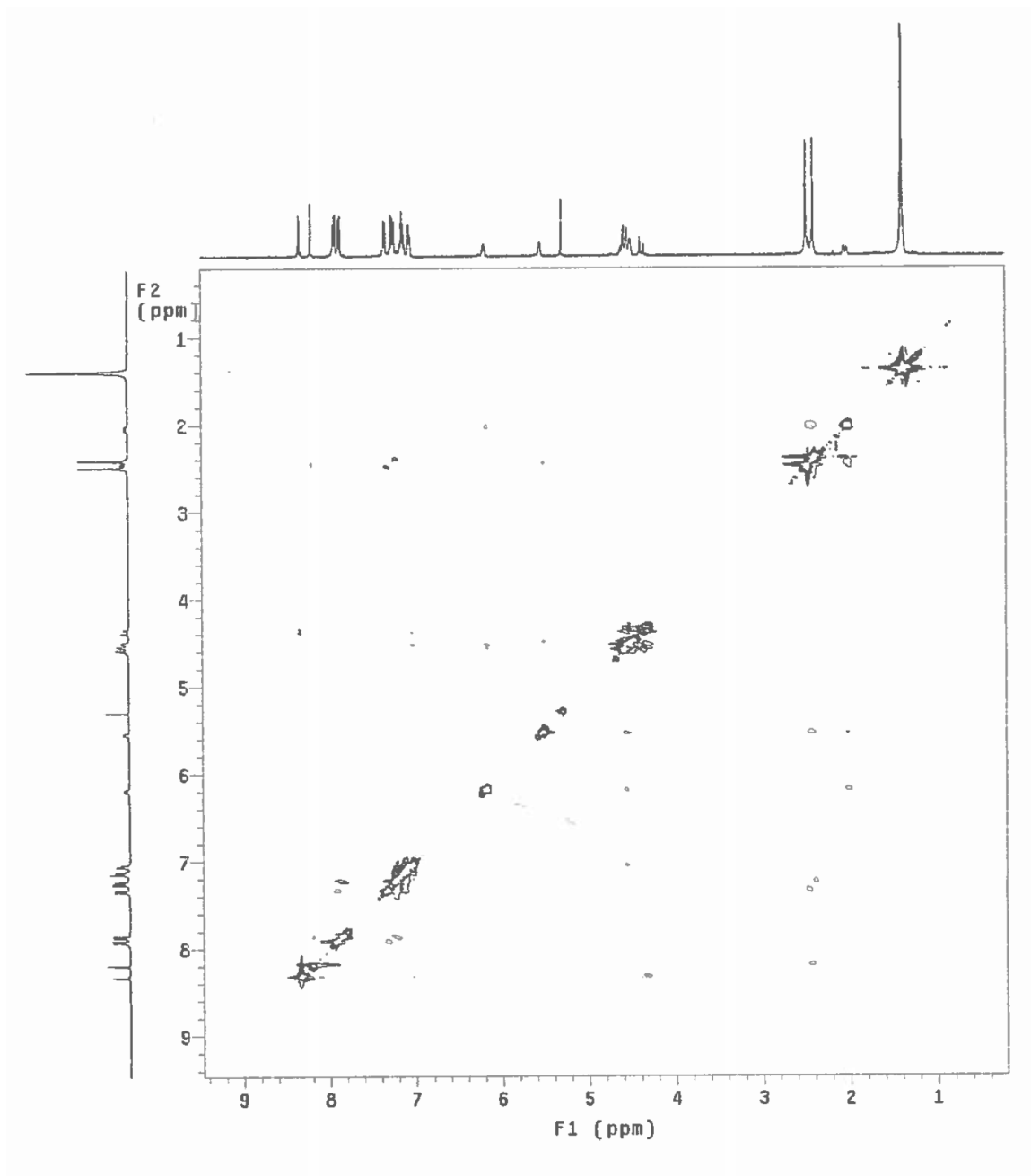
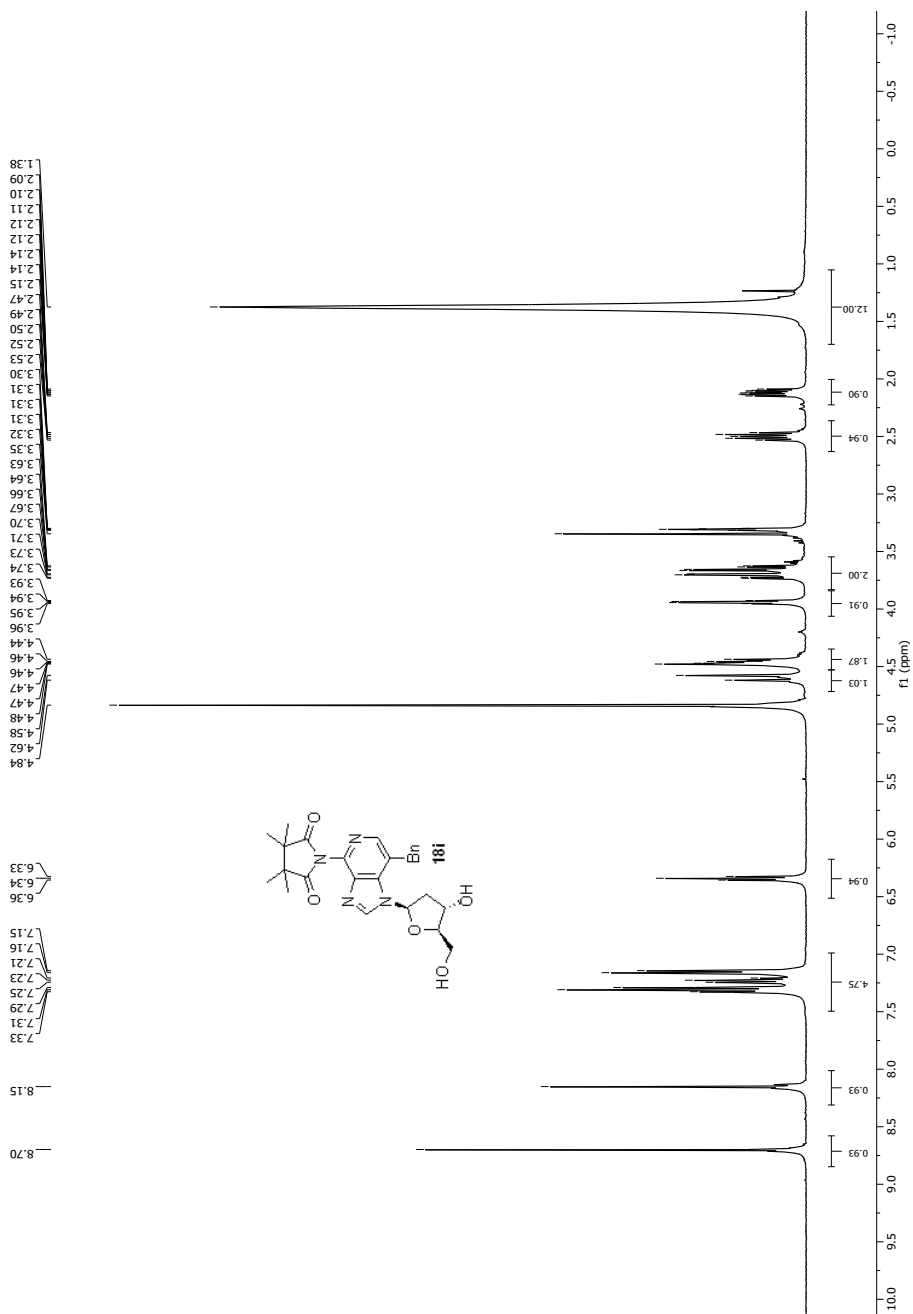


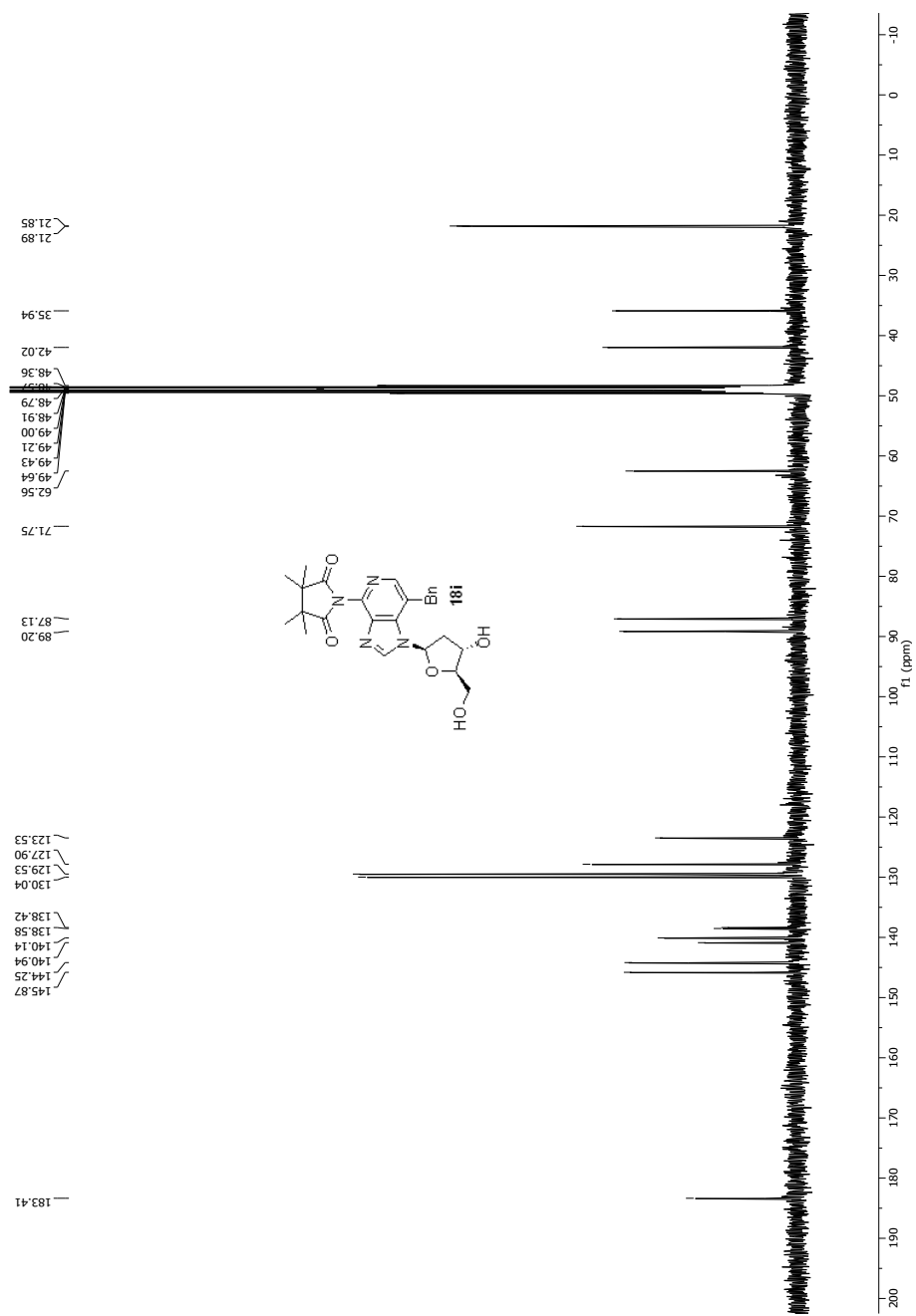
Figure. B51  $^{13}\text{C}$  NMR spectrum of **17i** ( $\text{CDCl}_3$ , 100 MHz).



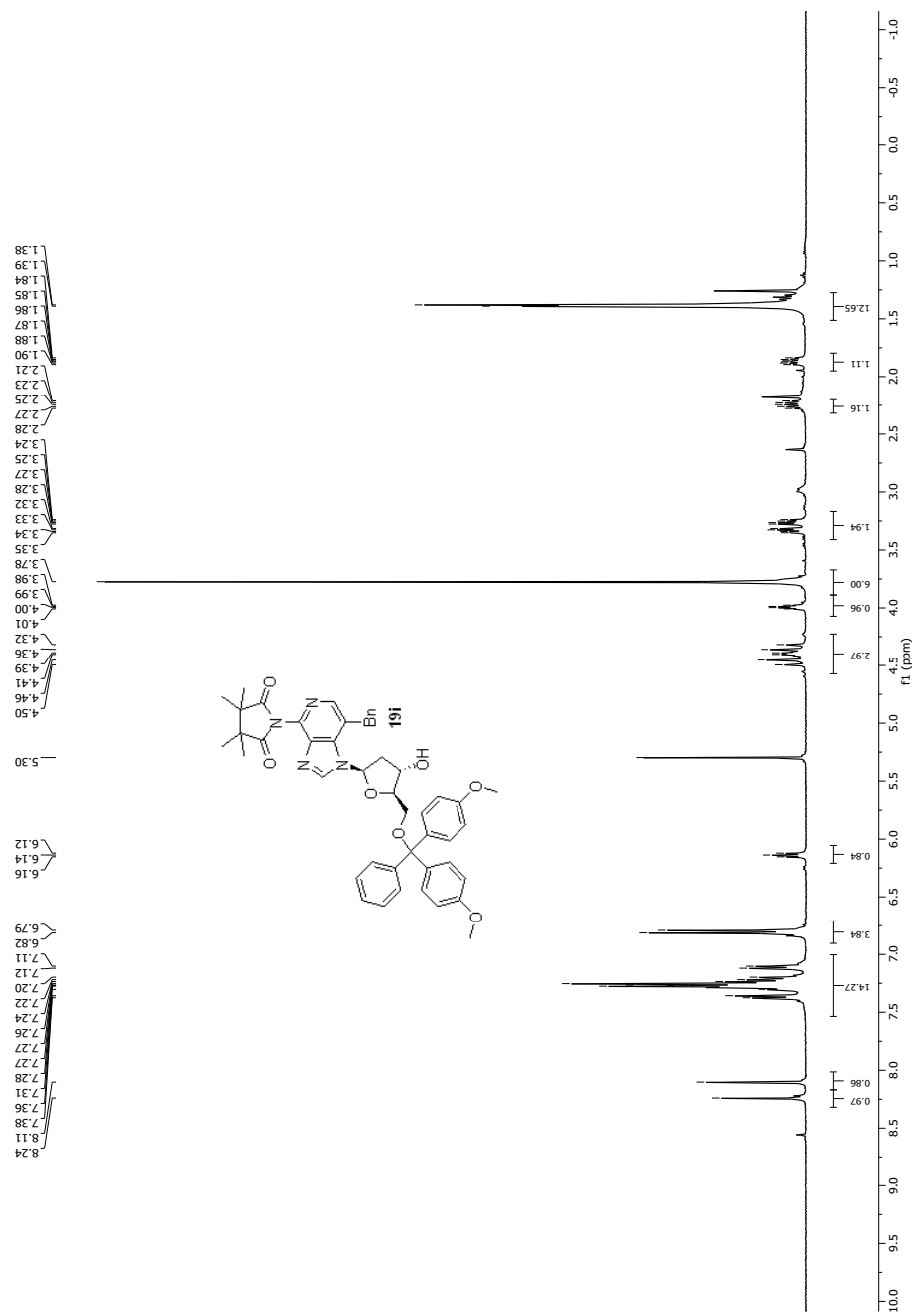
**Figure. B52**  $^1\text{H}$ - $^1\text{H}$  NOESY spectrum of **17i** ( $\text{CDCl}_3$ , 400 MHz).



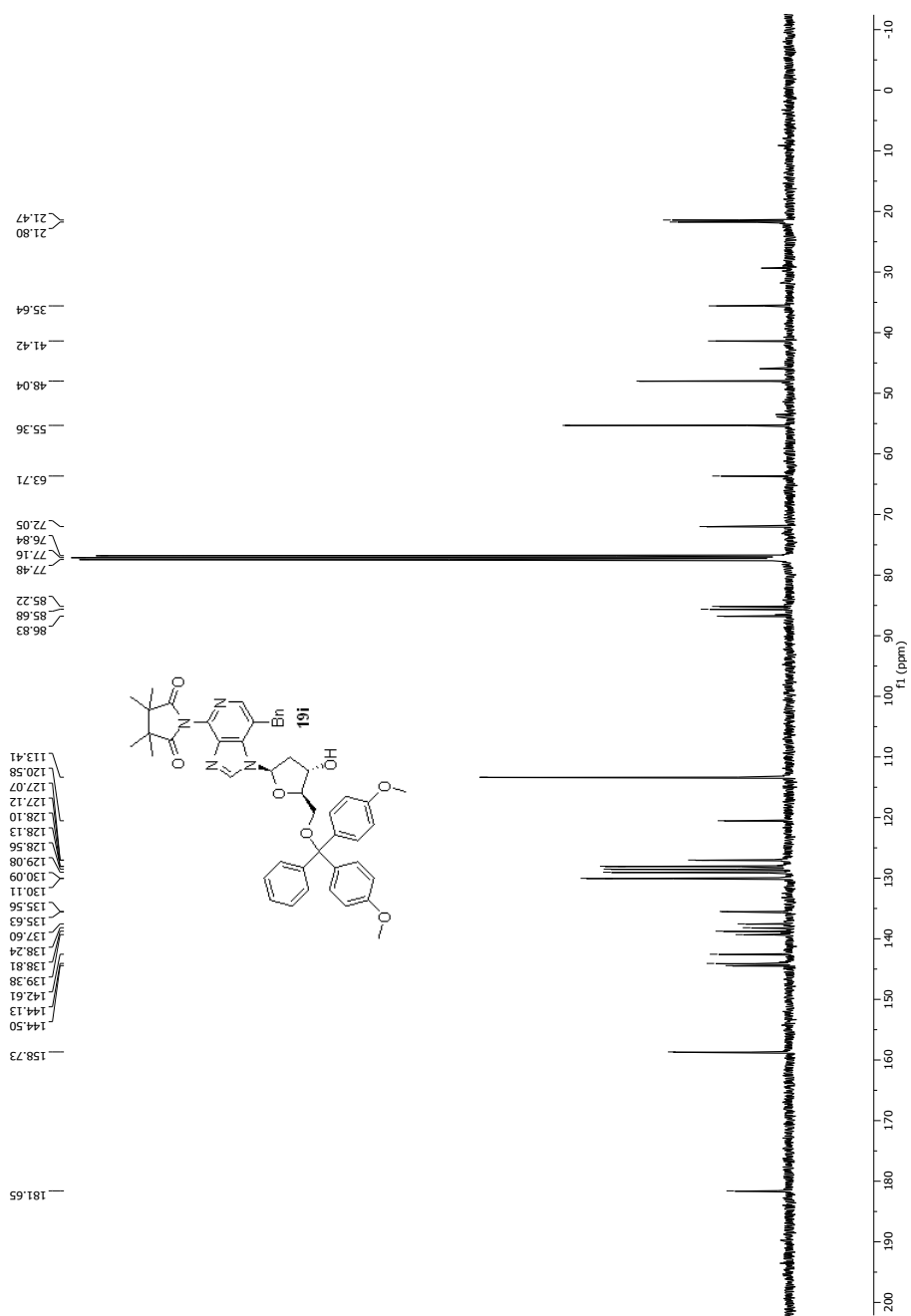
**Figure. B53** <sup>1</sup>H NMR spectrum of **18i** (CD<sub>3</sub>OD, 400 MHz).



**Figure. B54**  $^{13}\text{C}$  NMR spectrum of **18i** ( $\text{CD}_3\text{OD}$ , 100 MHz).



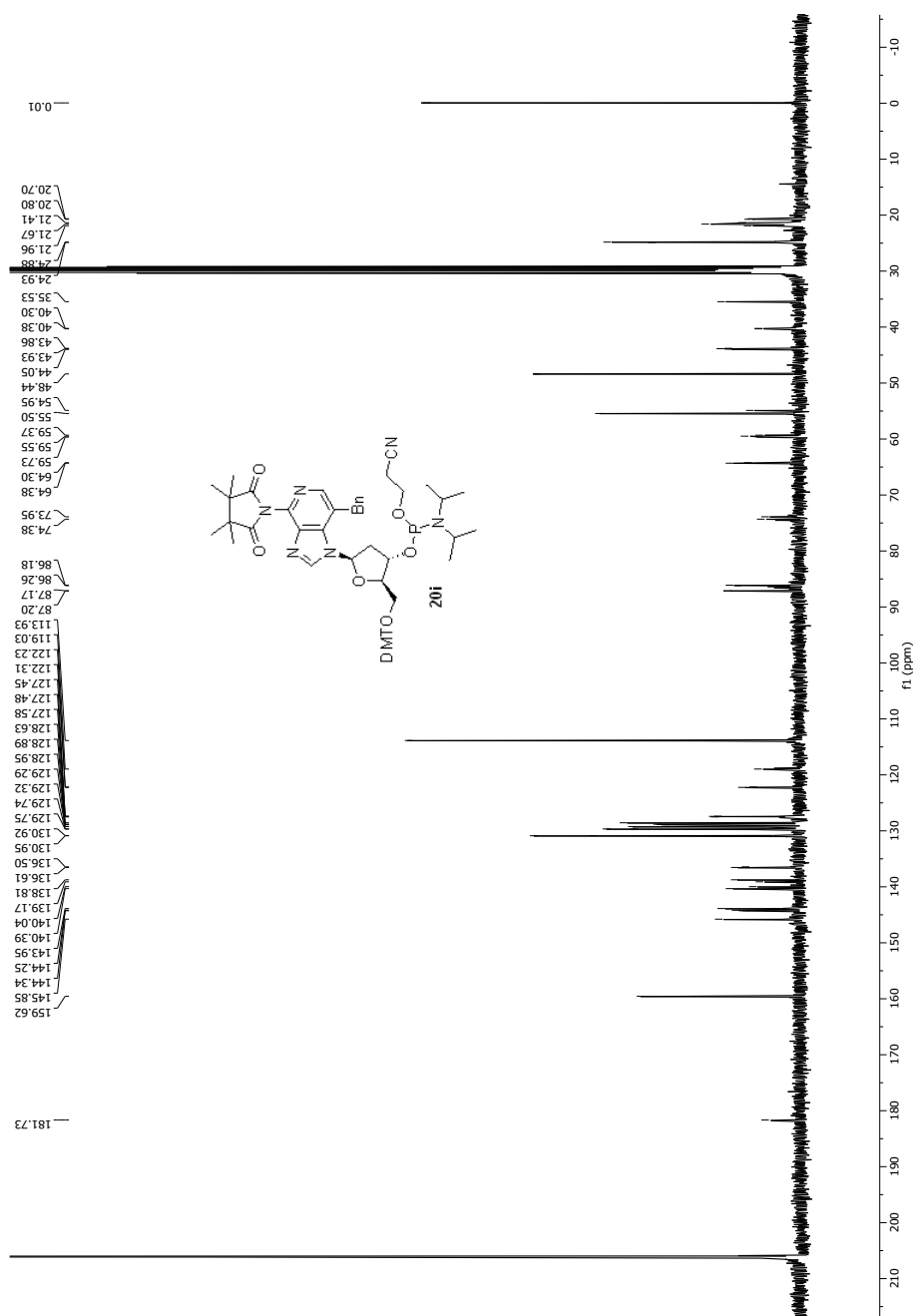
**Figure. B55** <sup>1</sup>H NMR spectrum of **19i** (CDCl<sub>3</sub>, 400 MHz).



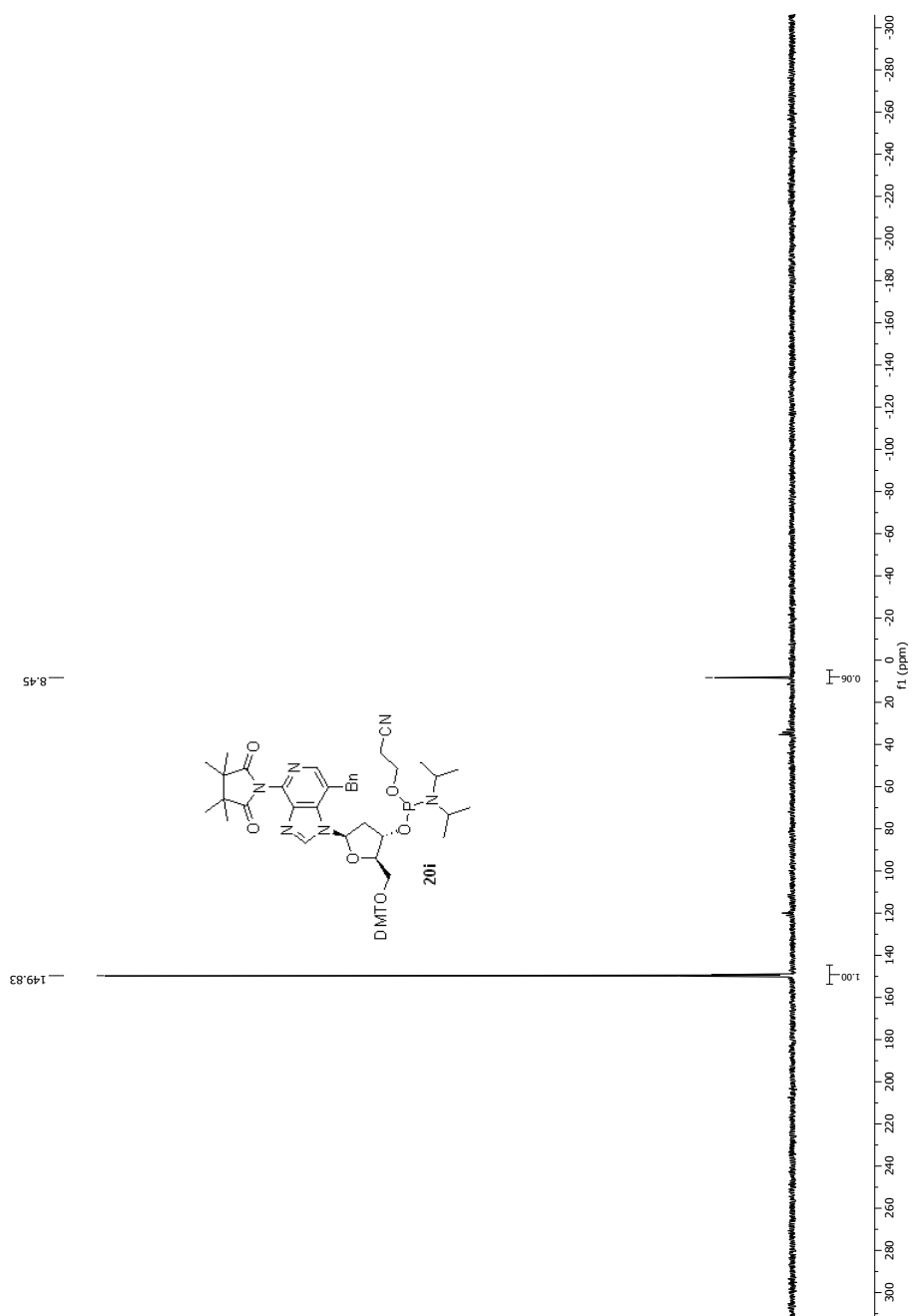
**Figure. B56** <sup>13</sup>C NMR spectrum of **19i** (CDCl<sub>3</sub>, 100 MHz).



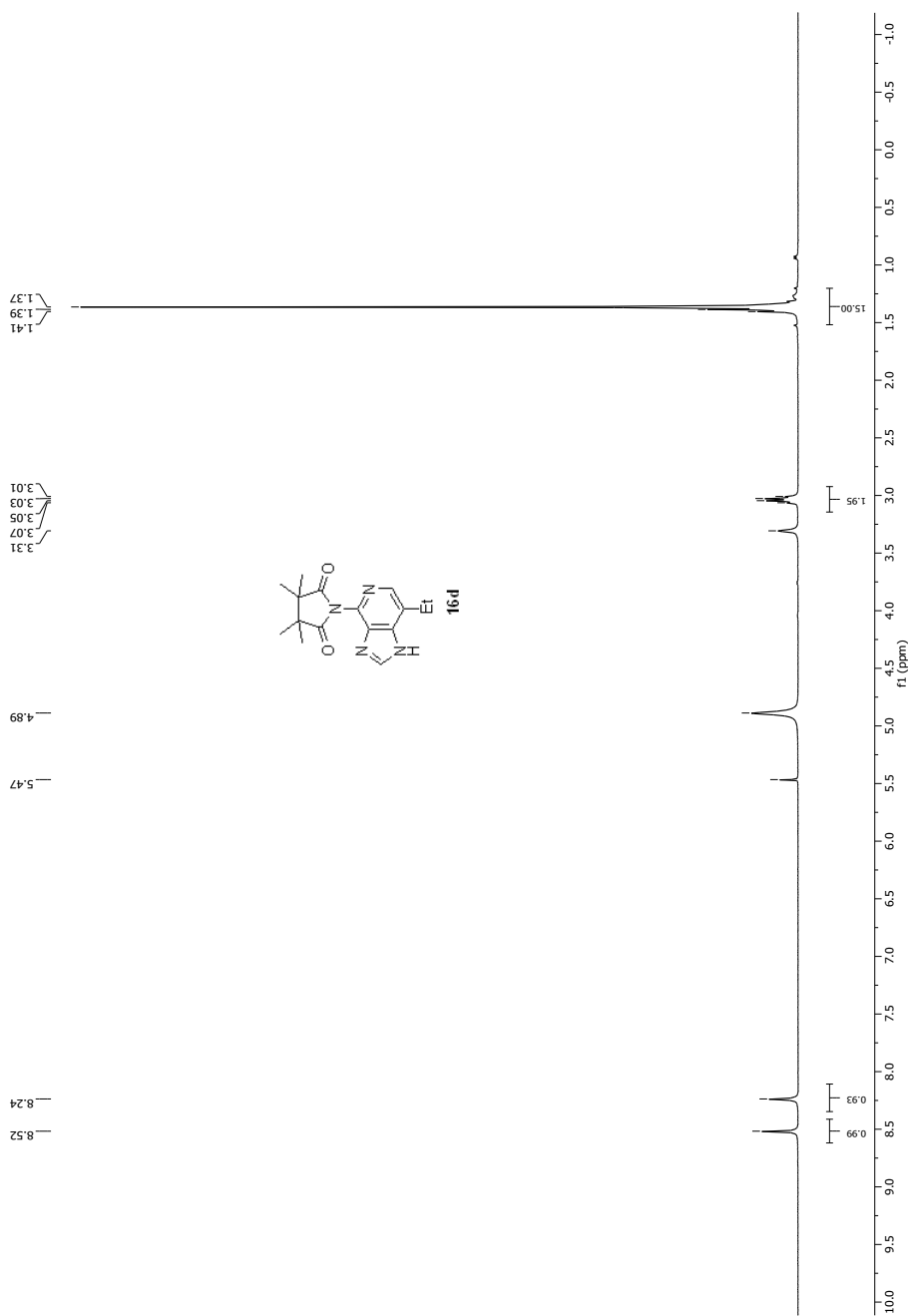




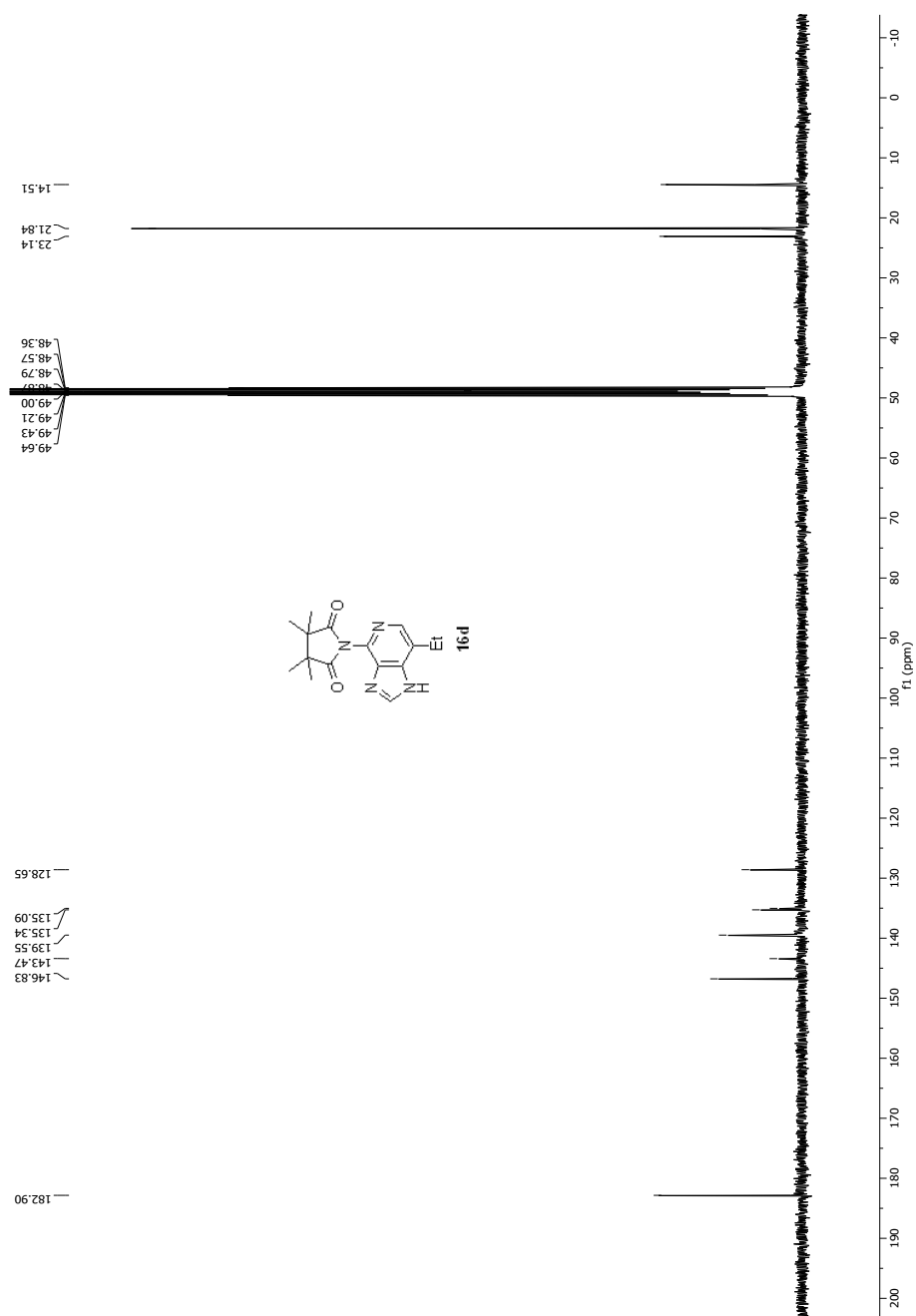
**Figure. B58**  $^{13}\text{C}$  NMR spectrum of **20i** (acetone- $\text{d}_6$ , 100 MHz).



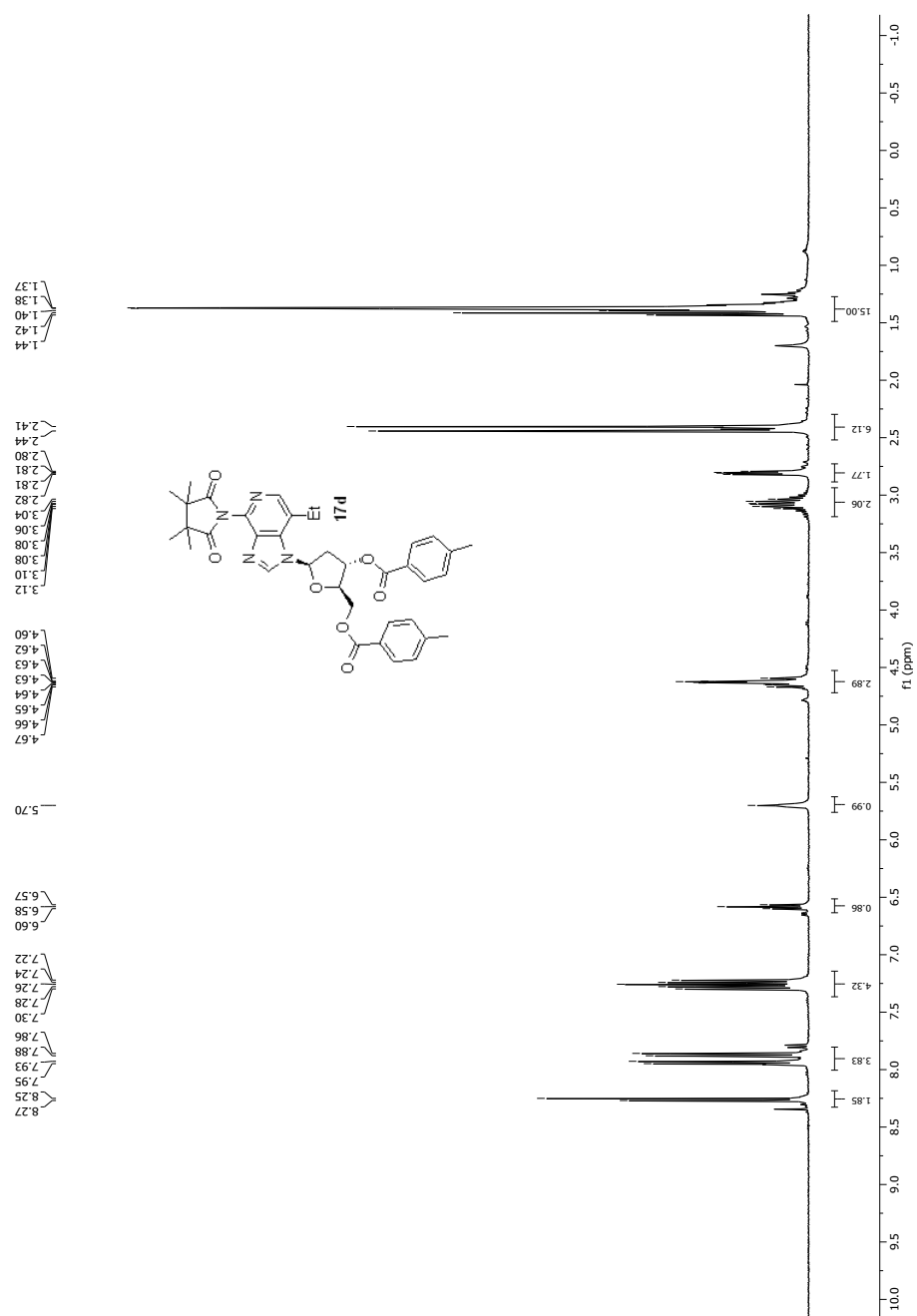
**Figure. B59**  $^{31}\text{P}$  NMR spectrum of **20i** ( $\text{acetone-d}_6$ , 162 MHz).



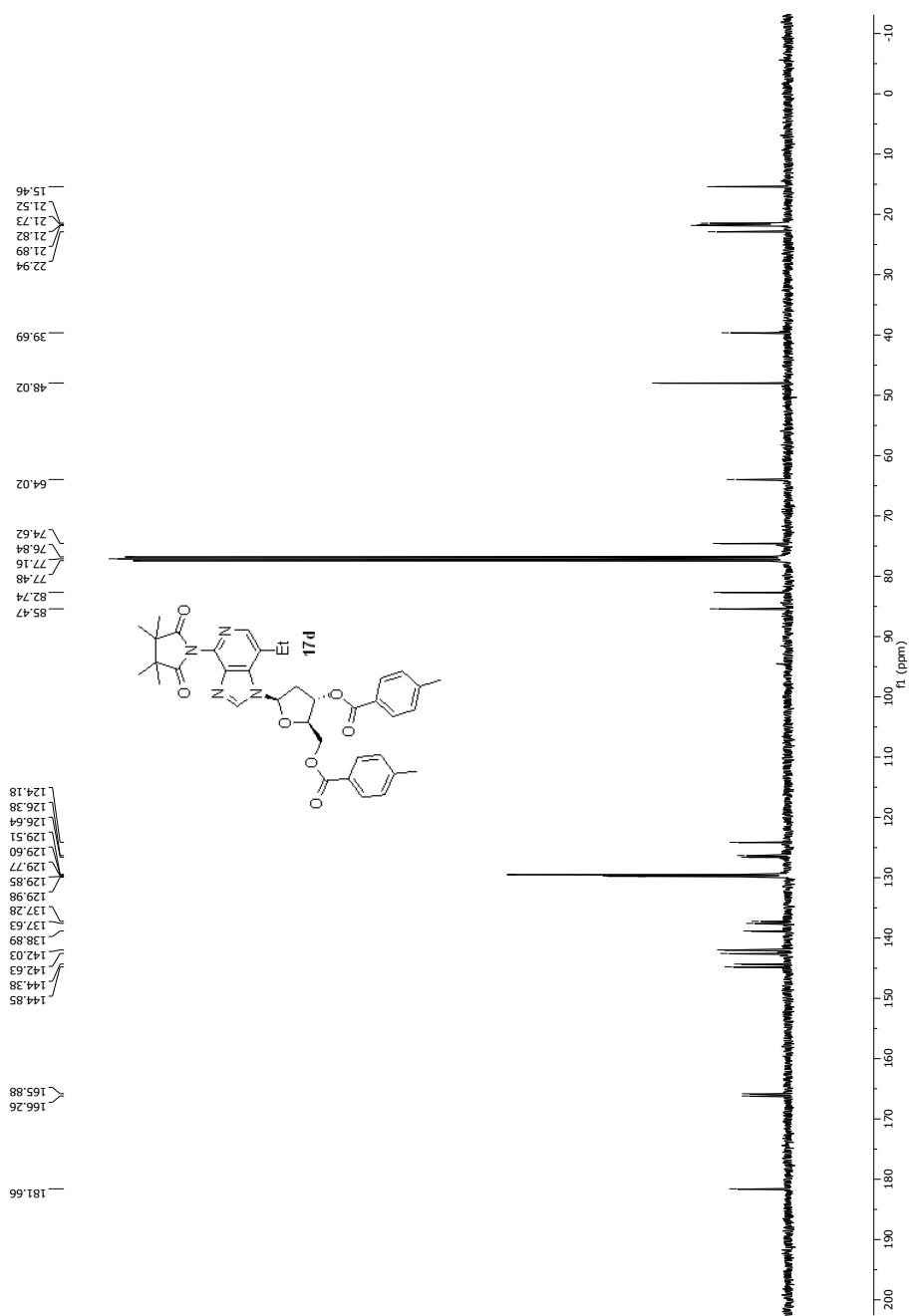
**Figure. B60**  $^1\text{H}$  NMR spectrum of **16d** (CD<sub>3</sub>OD, 400 MHz).



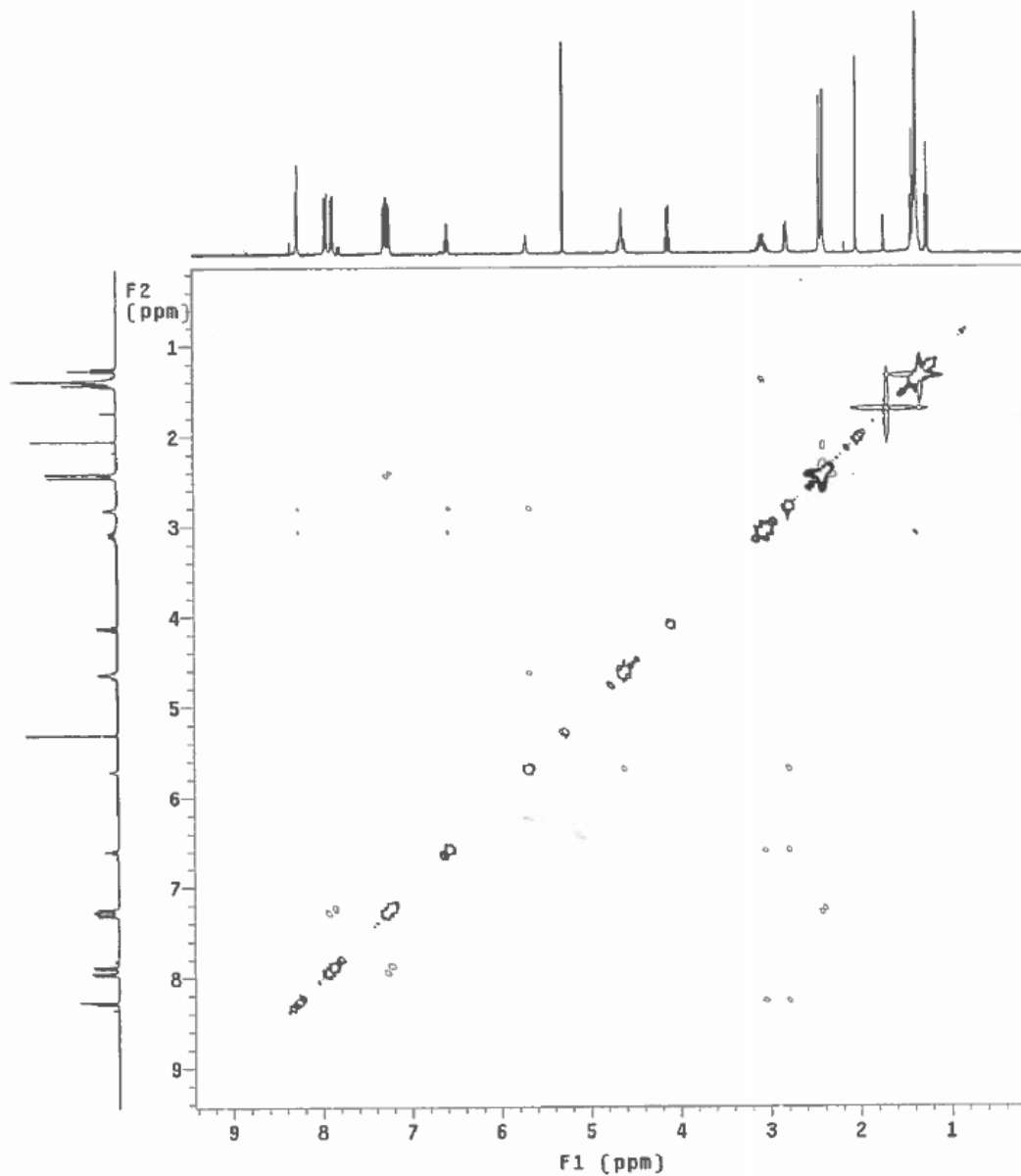
**Figure. B61**  $^{13}\text{C}$  NMR spectrum of **16d** ( $\text{CD}_3\text{OD}$ , 100 MHz).



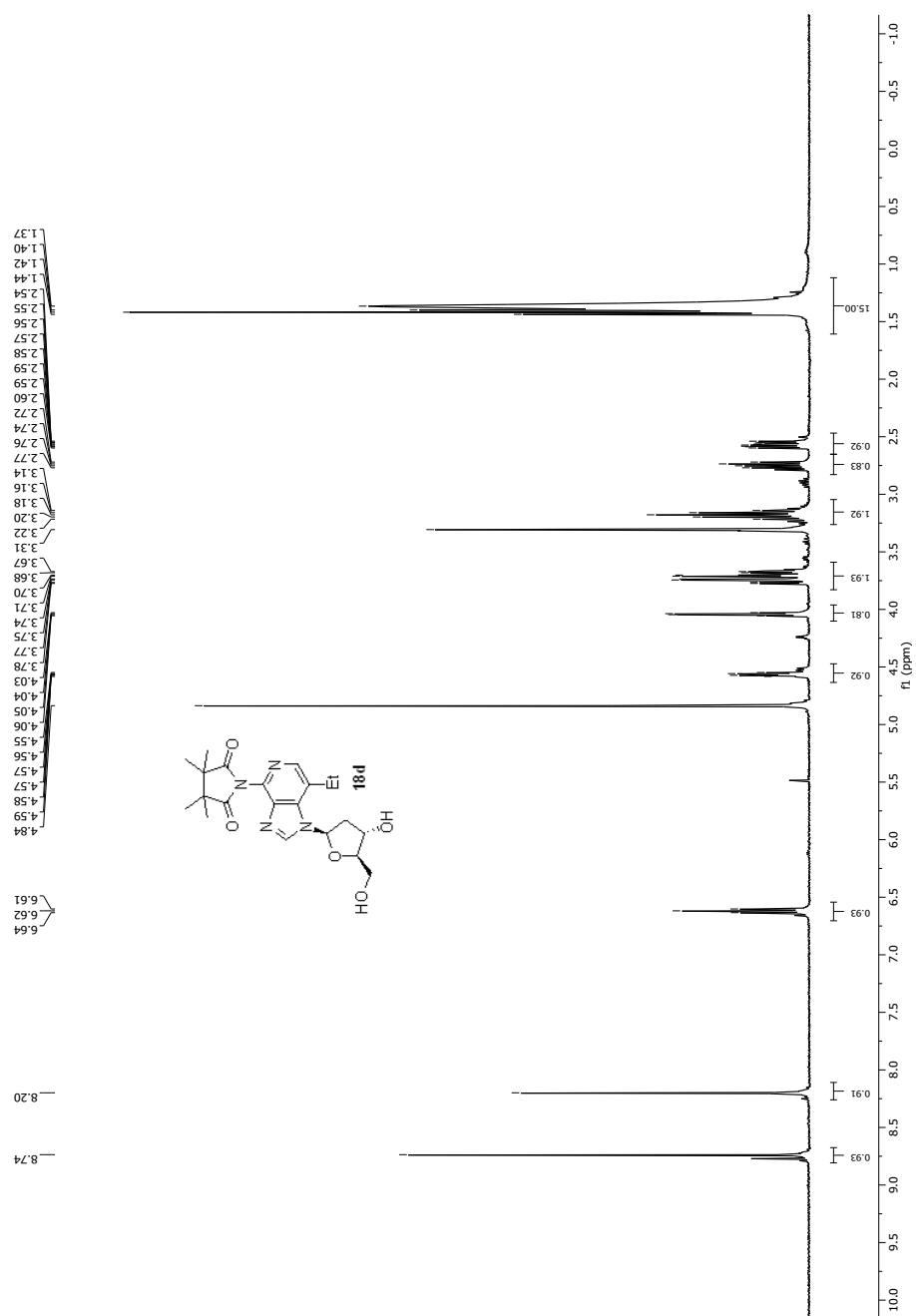
**Figure. B62**  $^1\text{H}$  NMR spectrum of **17d** (CDCl<sub>3</sub>, 400 MHz).



**Figure. B63**  $^{13}\text{C}$  NMR spectrum of **17d** ( $\text{CDCl}_3$ , 400 MHz).

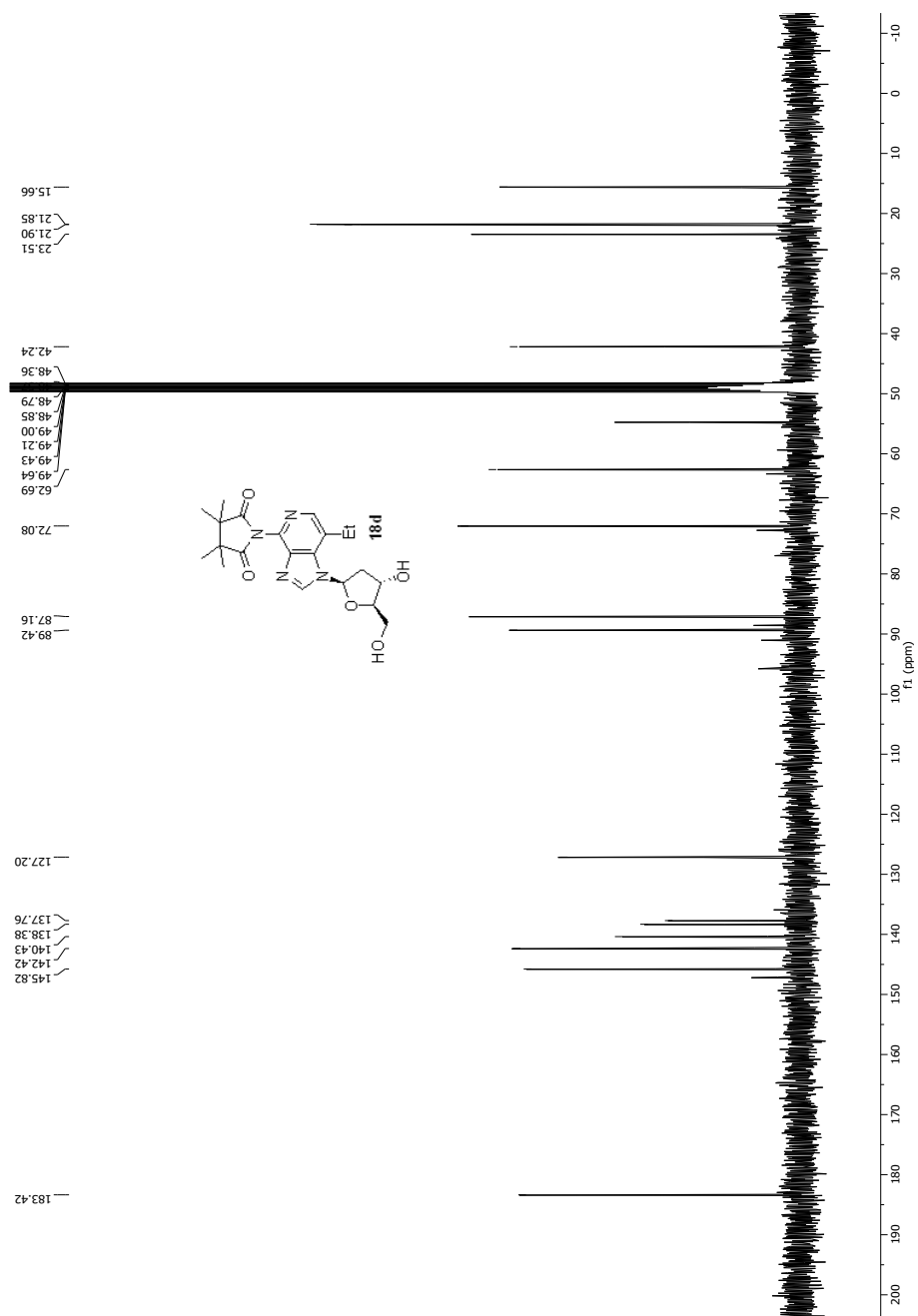


**Figure. B64**  $^1\text{H}$ - $^1\text{H}$  NOESY spectrum of **17d** ( $\text{CDCl}_3$ , 400 MHz).

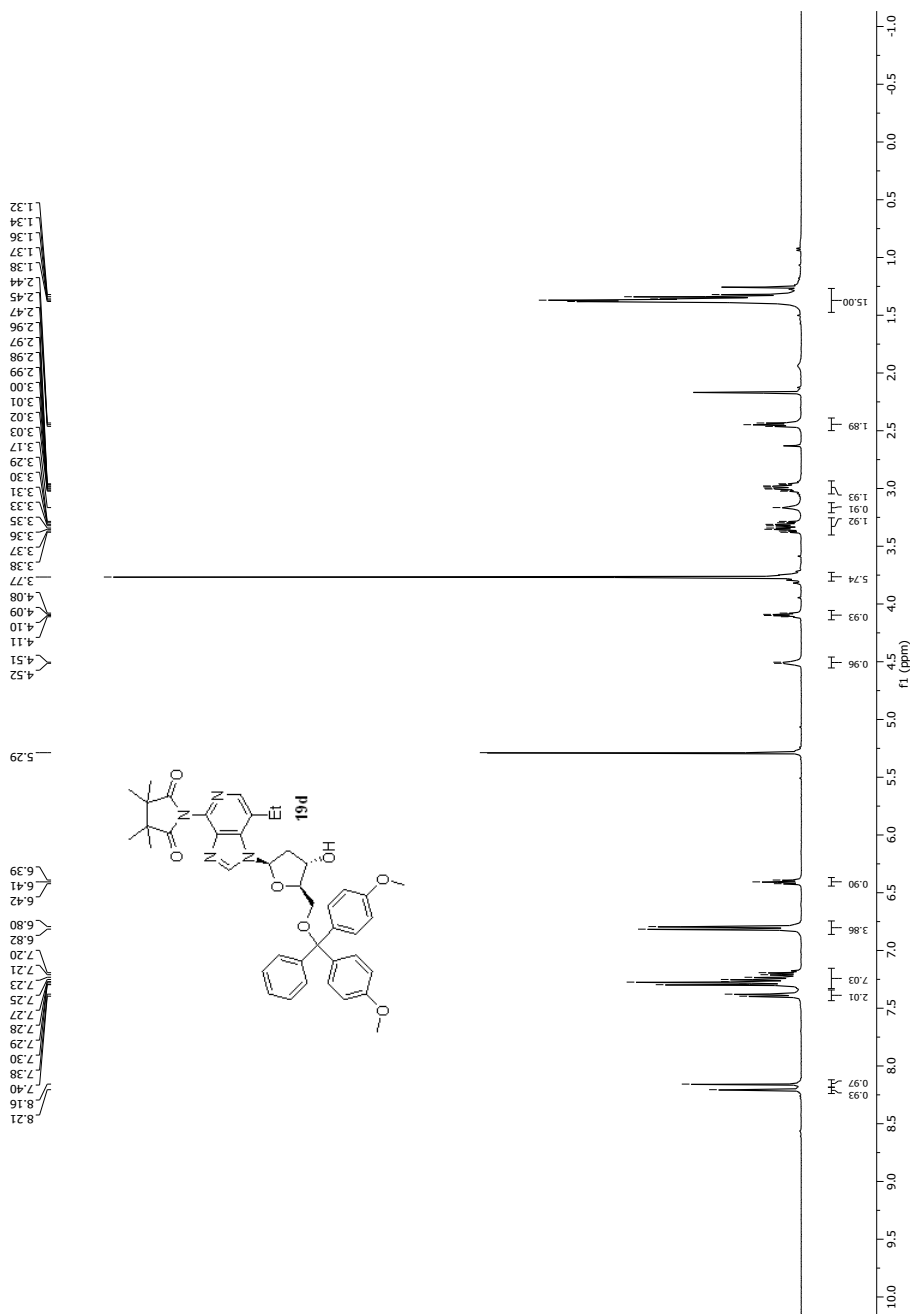


**Figure. B65** <sup>1</sup>H NMR spectrum of **18d** (CD<sub>3</sub>OD, 400 MHz).

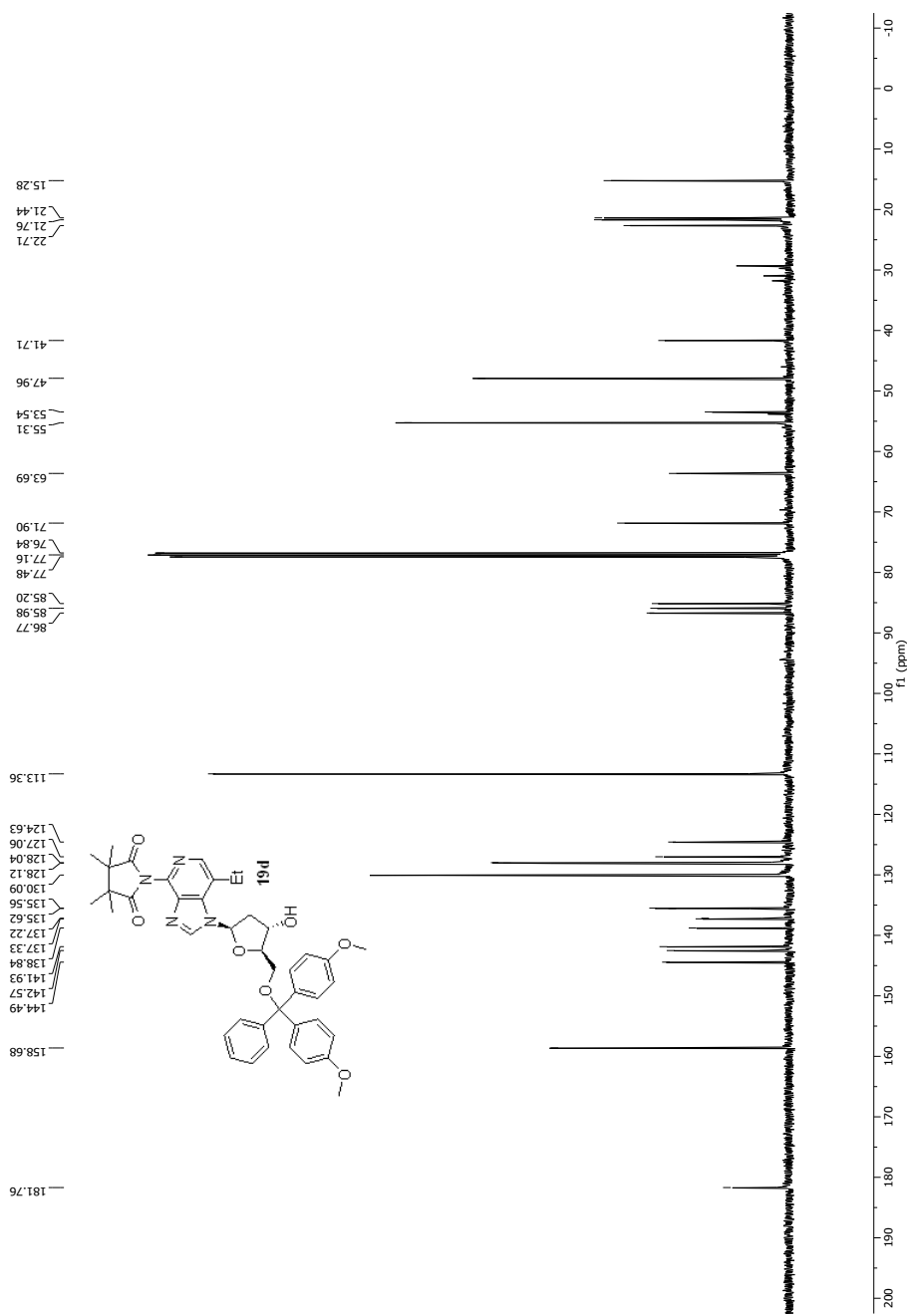




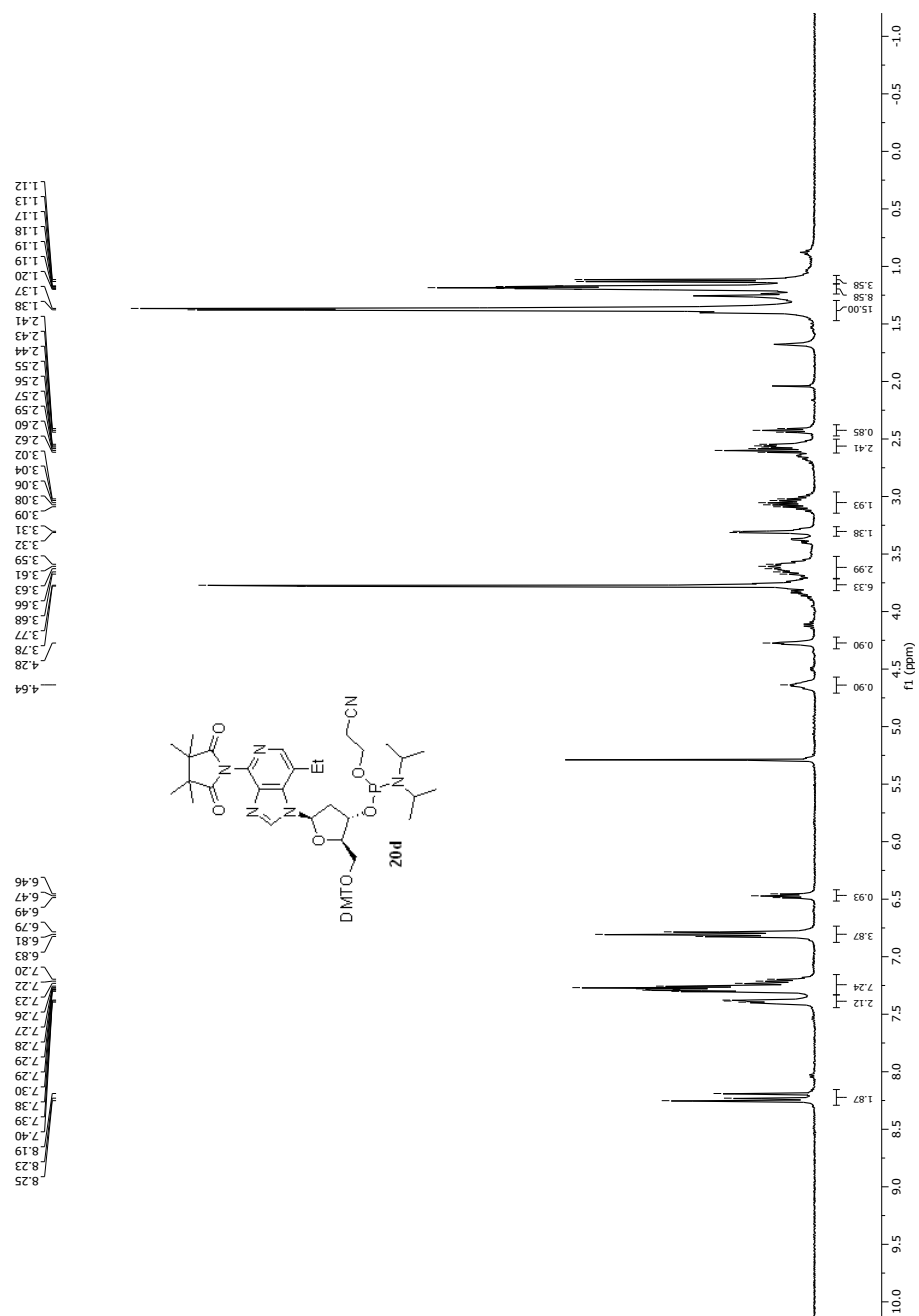
**Figure. B66**  $^{13}\text{C}$  NMR spectrum of **18d** ( $\text{CD}_3\text{OD}$ , 100 MHz).



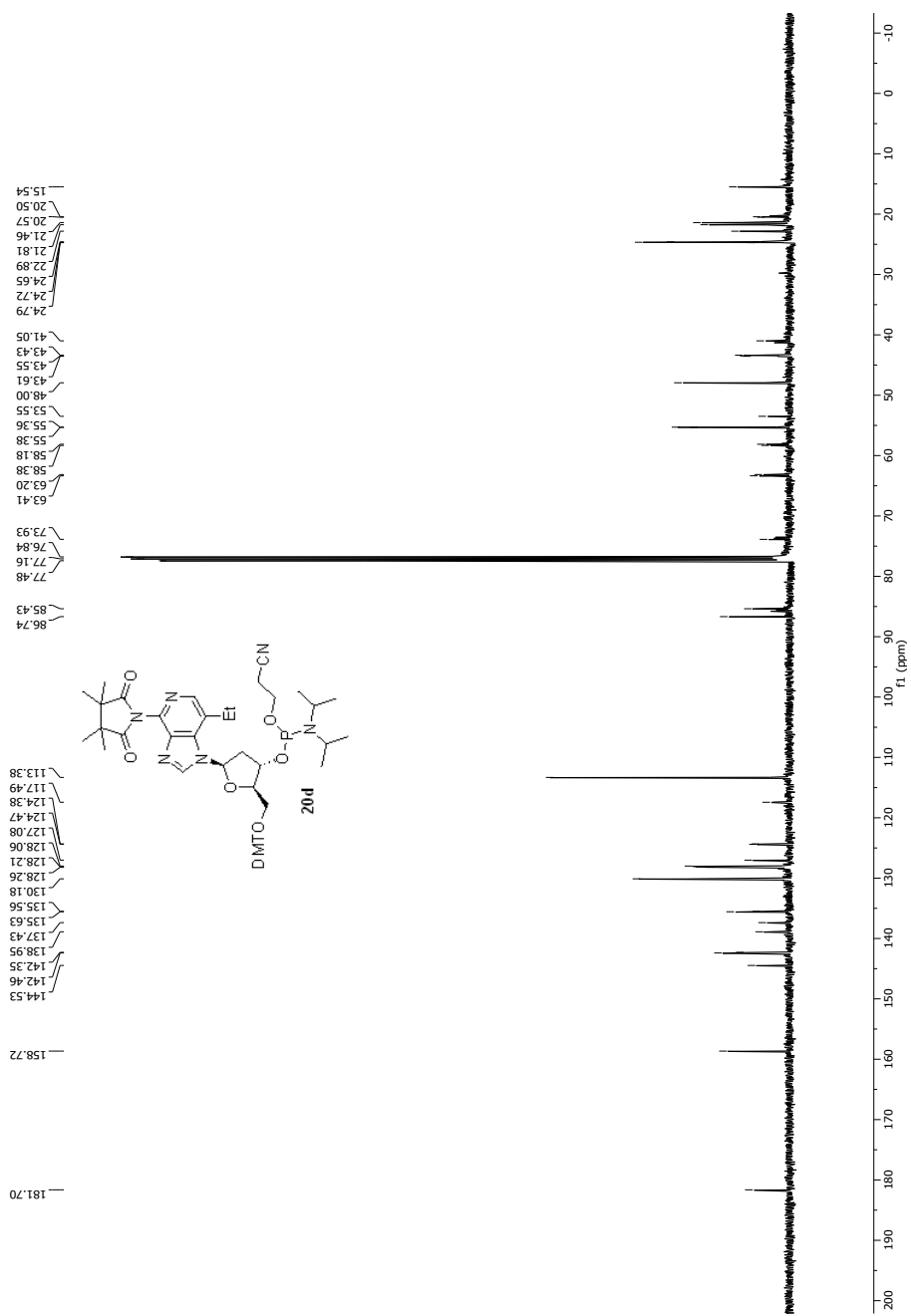
**Figure. B67**  $^1\text{H}$  NMR spectrum of **19d** (CDCl<sub>3</sub>, 400 MHz).



**Figure. B68**  $^{13}\text{C}$  NMR spectrum of **19d** ( $\text{CDCl}_3$ , 100 MHz).



**Figure. B69**  $^1\text{H}$  NMR spectrum of **20d** (CDCl<sub>3</sub>, 400 MHz).



**Figure. B70**  $^{13}\text{C}$  NMR spectrum of **20d** (CDCl<sub>3</sub>, 100 MHz).

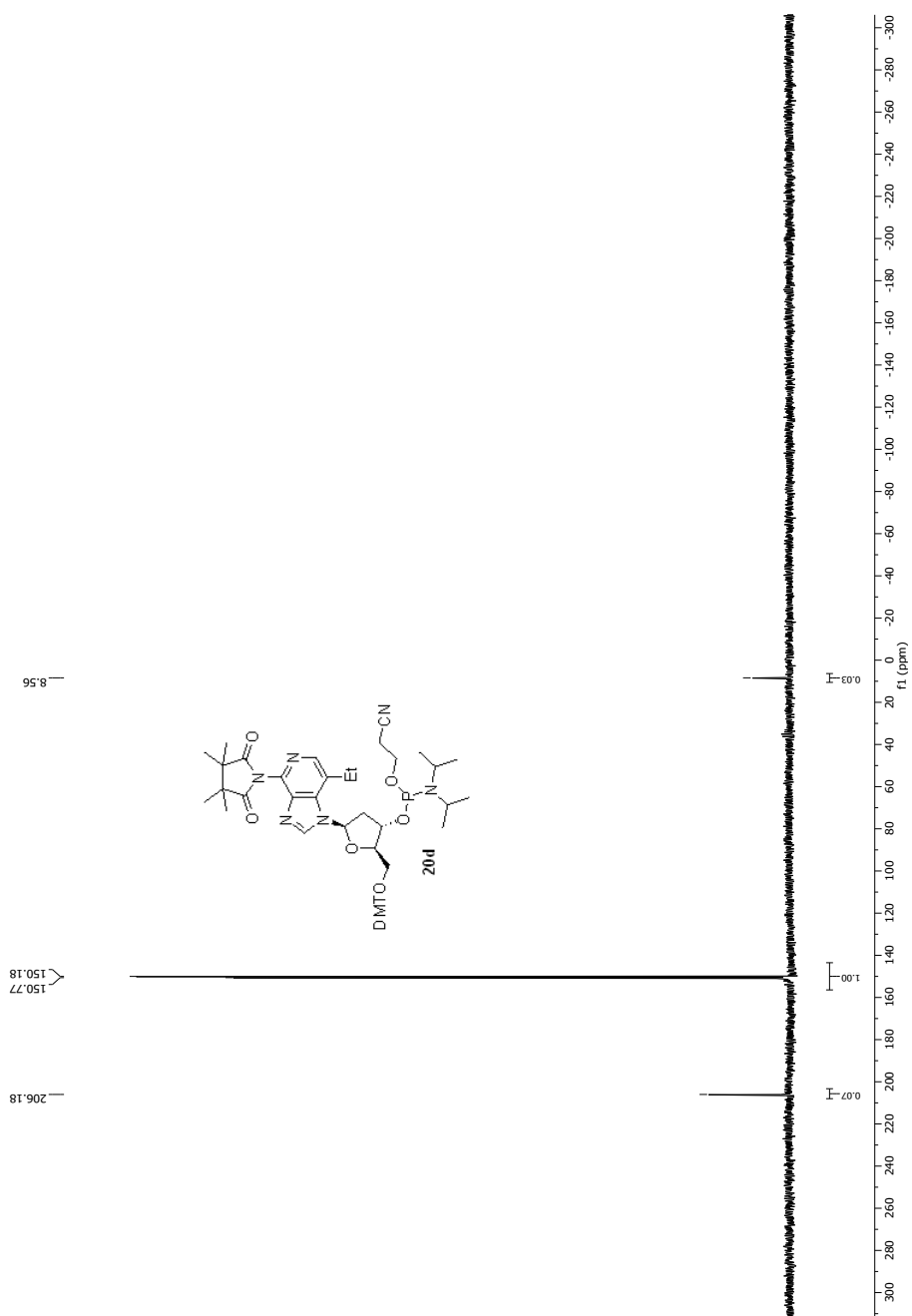
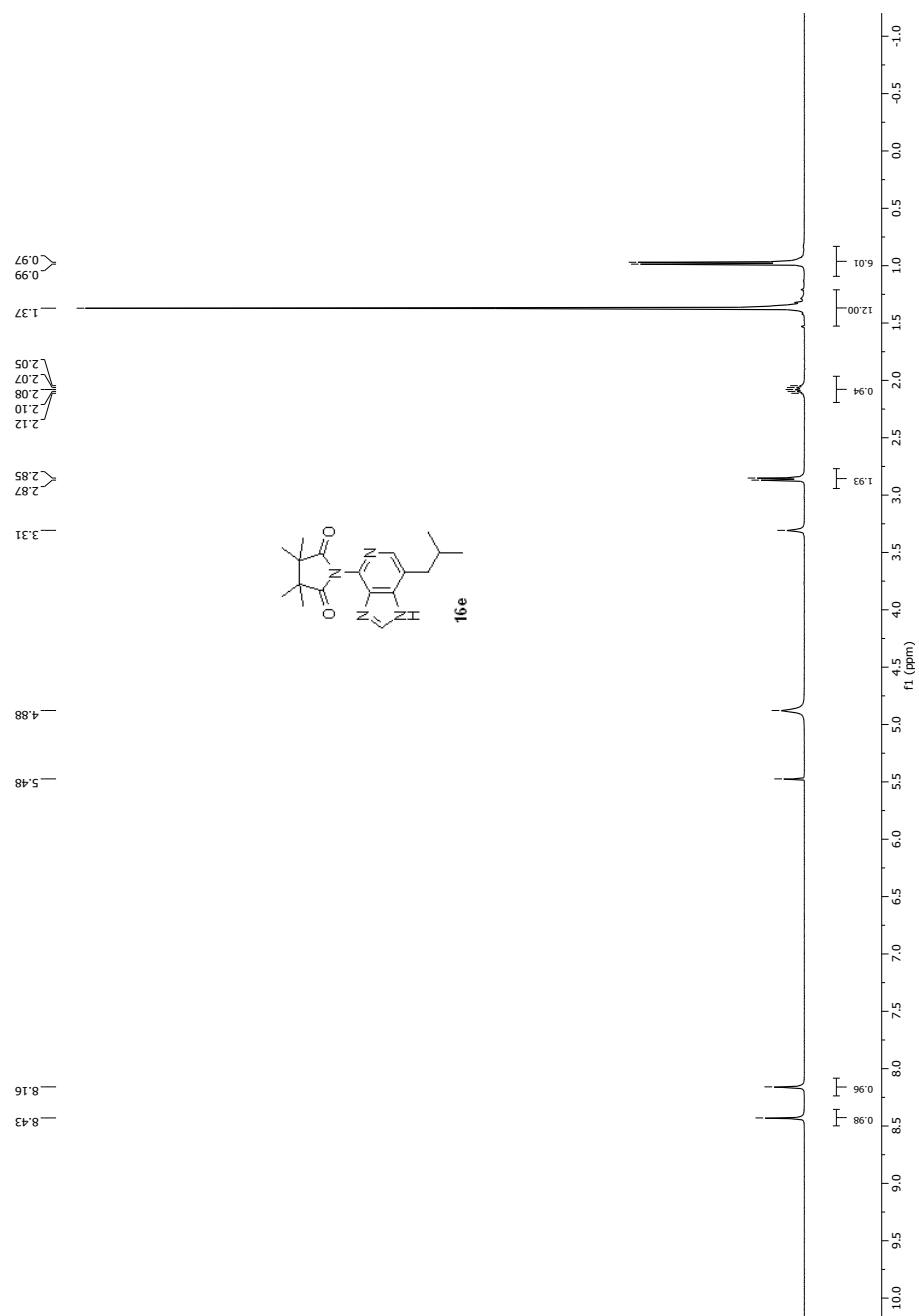
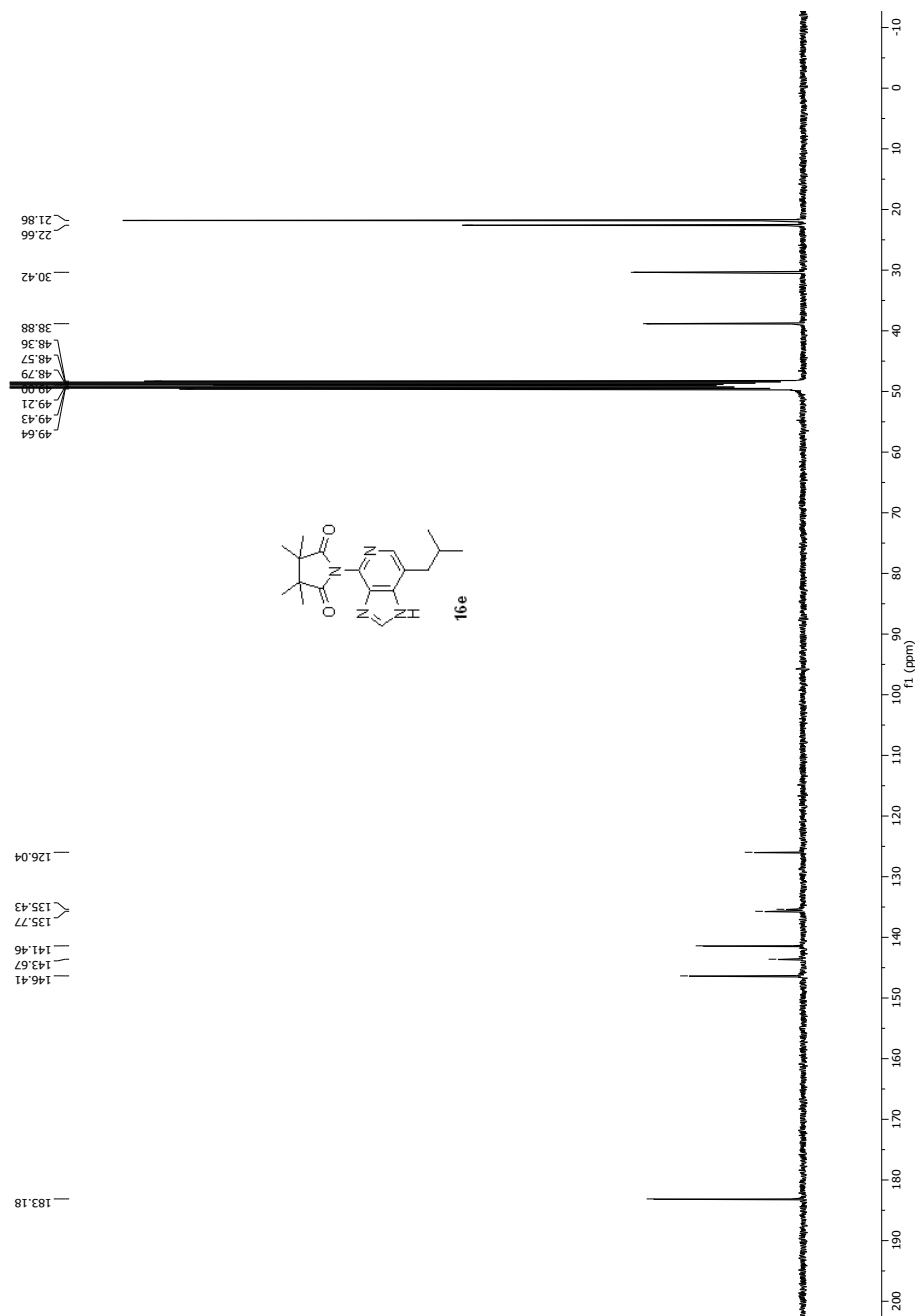


Figure. B71  $^{31}\text{P}$  NMR spectrum of **20d** ( $\text{CDCl}_3$ , 162 MHz).

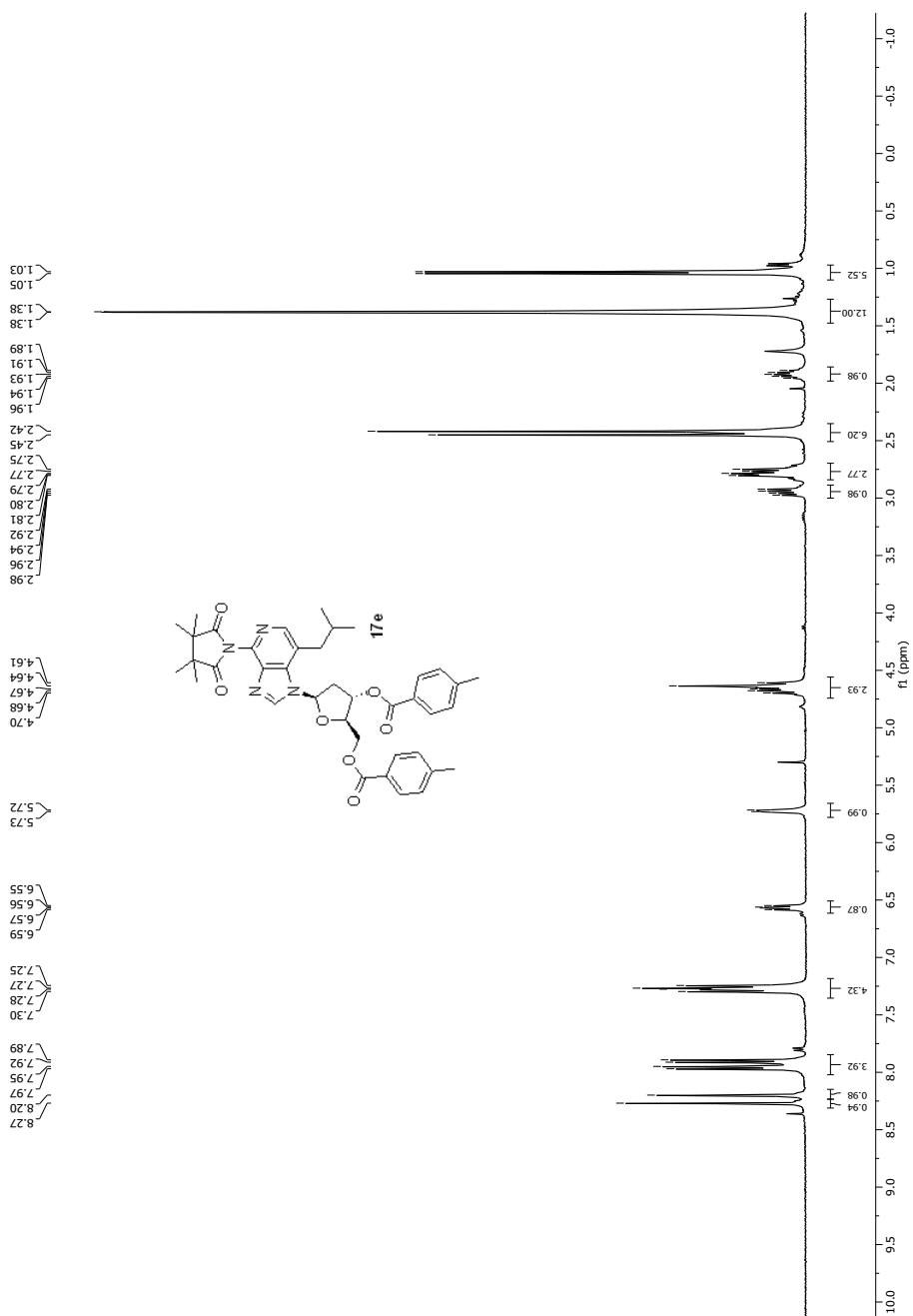


**Figure. B72** <sup>1</sup>H NMR spectrum of **16e** (CD<sub>3</sub>OD, 400 MHz).

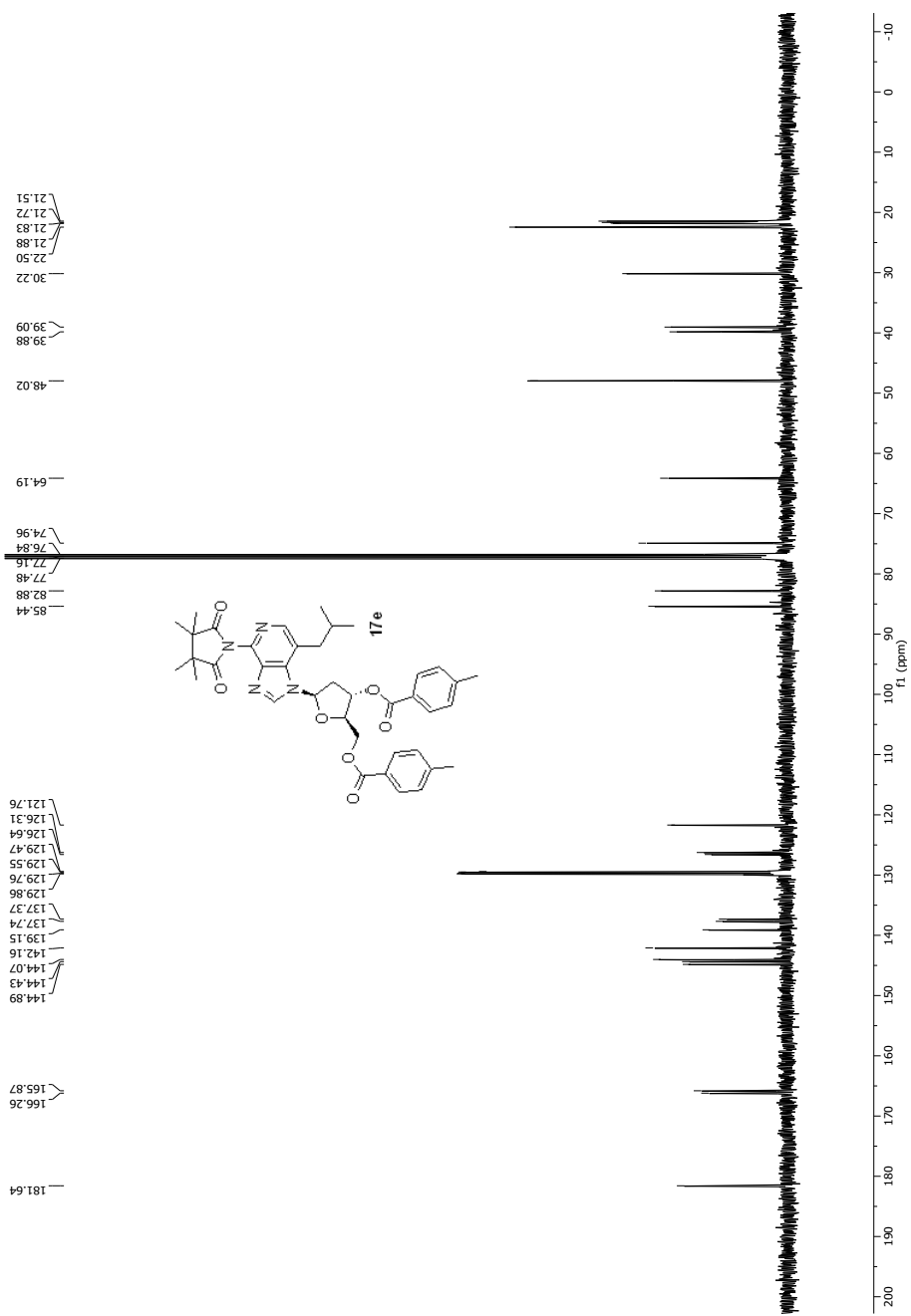


**Figure. B73**  $^{13}\text{C}$  NMR spectrum of **16e** ( $\text{CD}_3\text{OD}$ , 100 MHz).

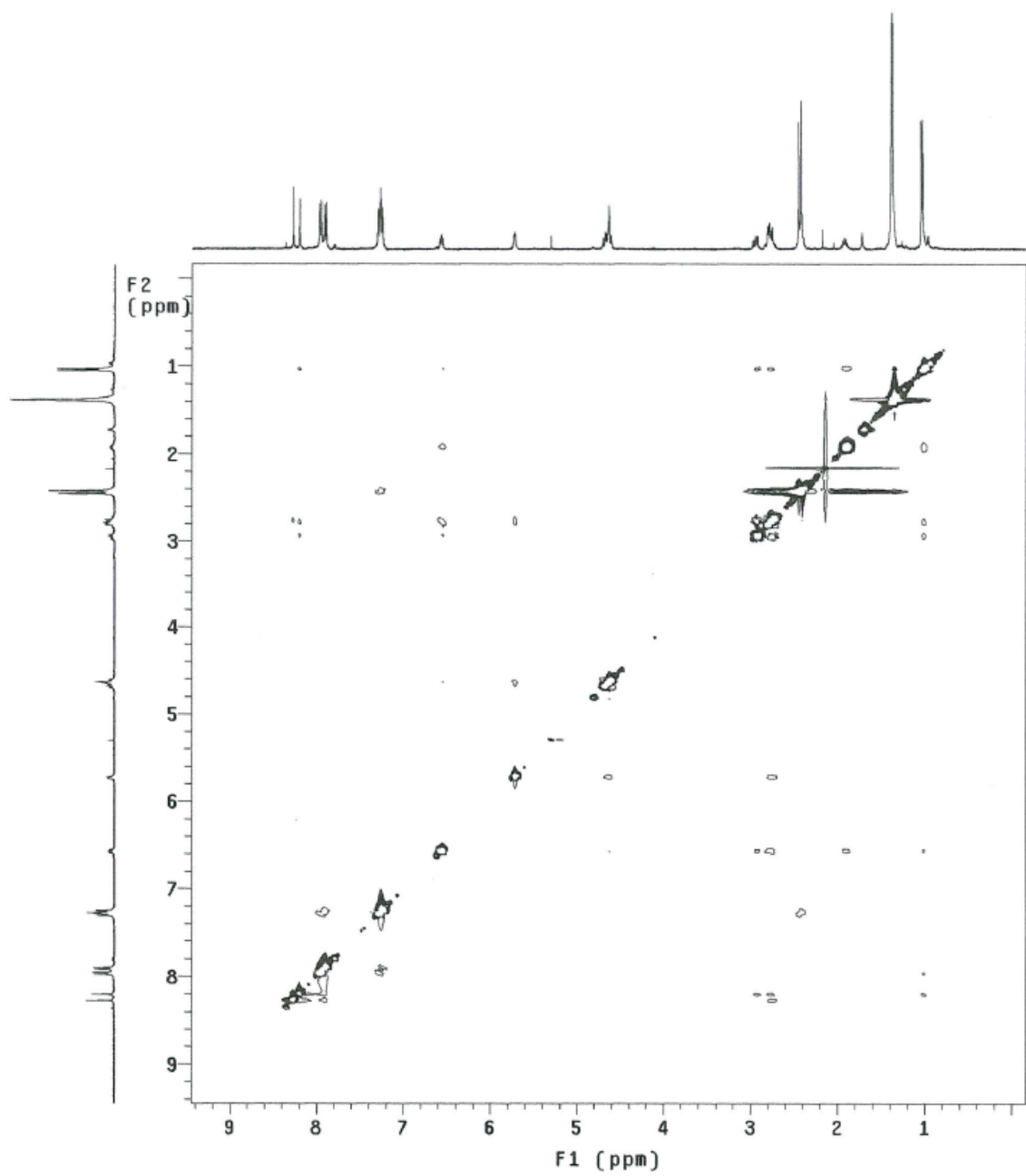




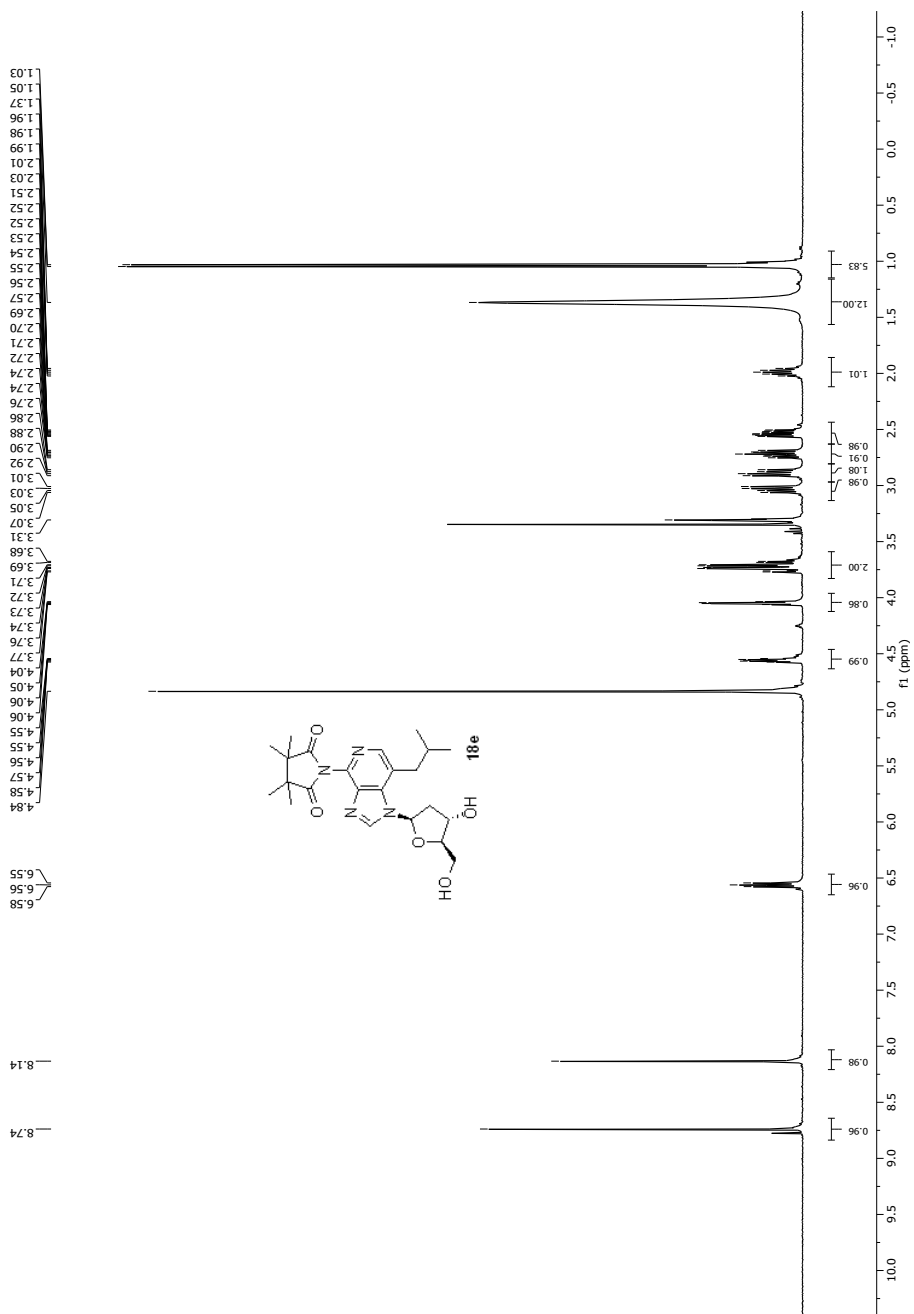
**Figure. B74**  $^1\text{H}$  NMR spectrum of **17e** (CDCl<sub>3</sub>, 400 MHz).



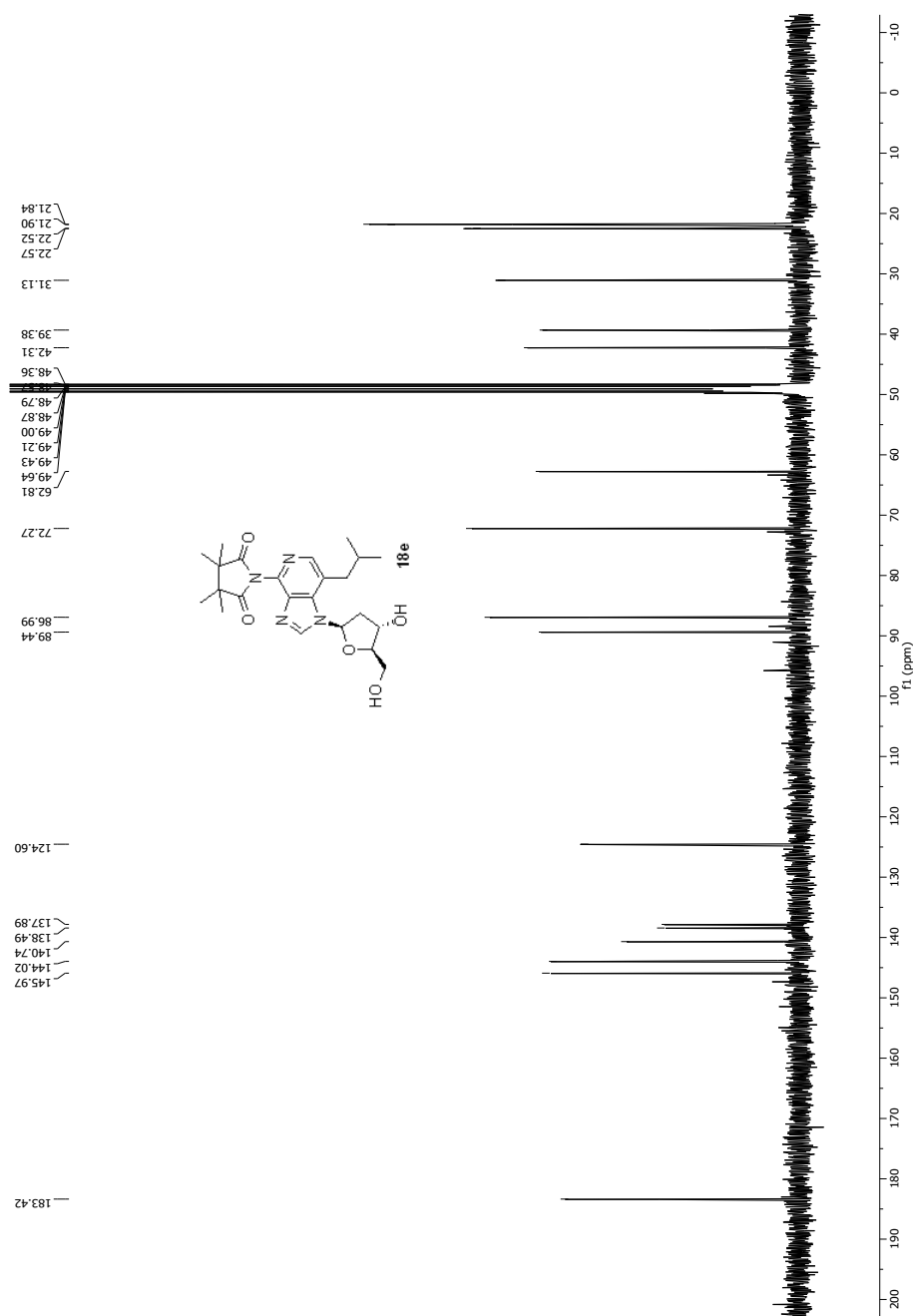
**Figure. B75**  $^{13}\text{C}$  NMR spectrum of **17e** ( $\text{CDCl}_3$ , 100 MHz).



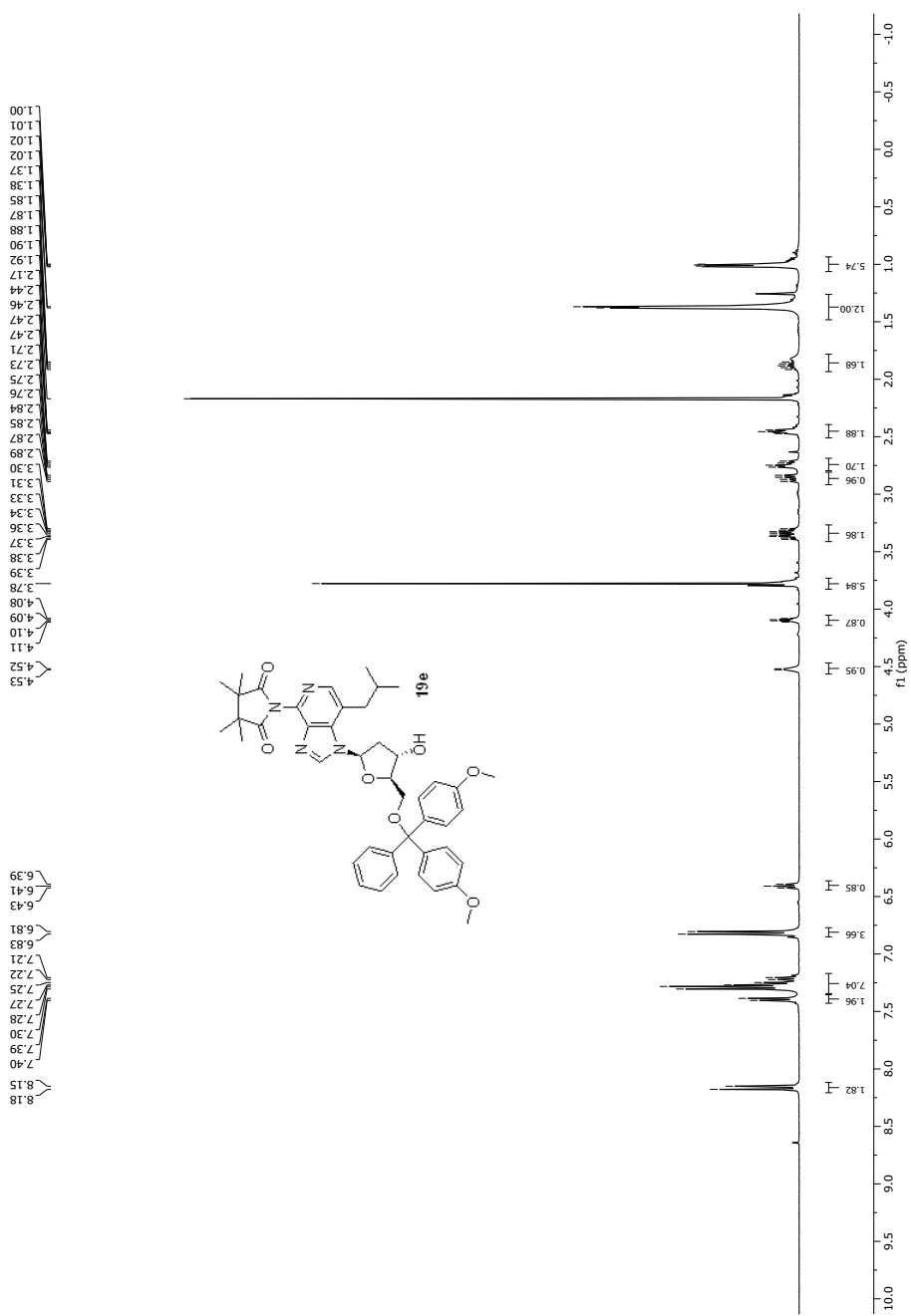
**Figure. B76**  $^1\text{H}$ - $^1\text{H}$  NOESY spectrum of **17e** ( $\text{CDCl}_3$ , 400 MHz).



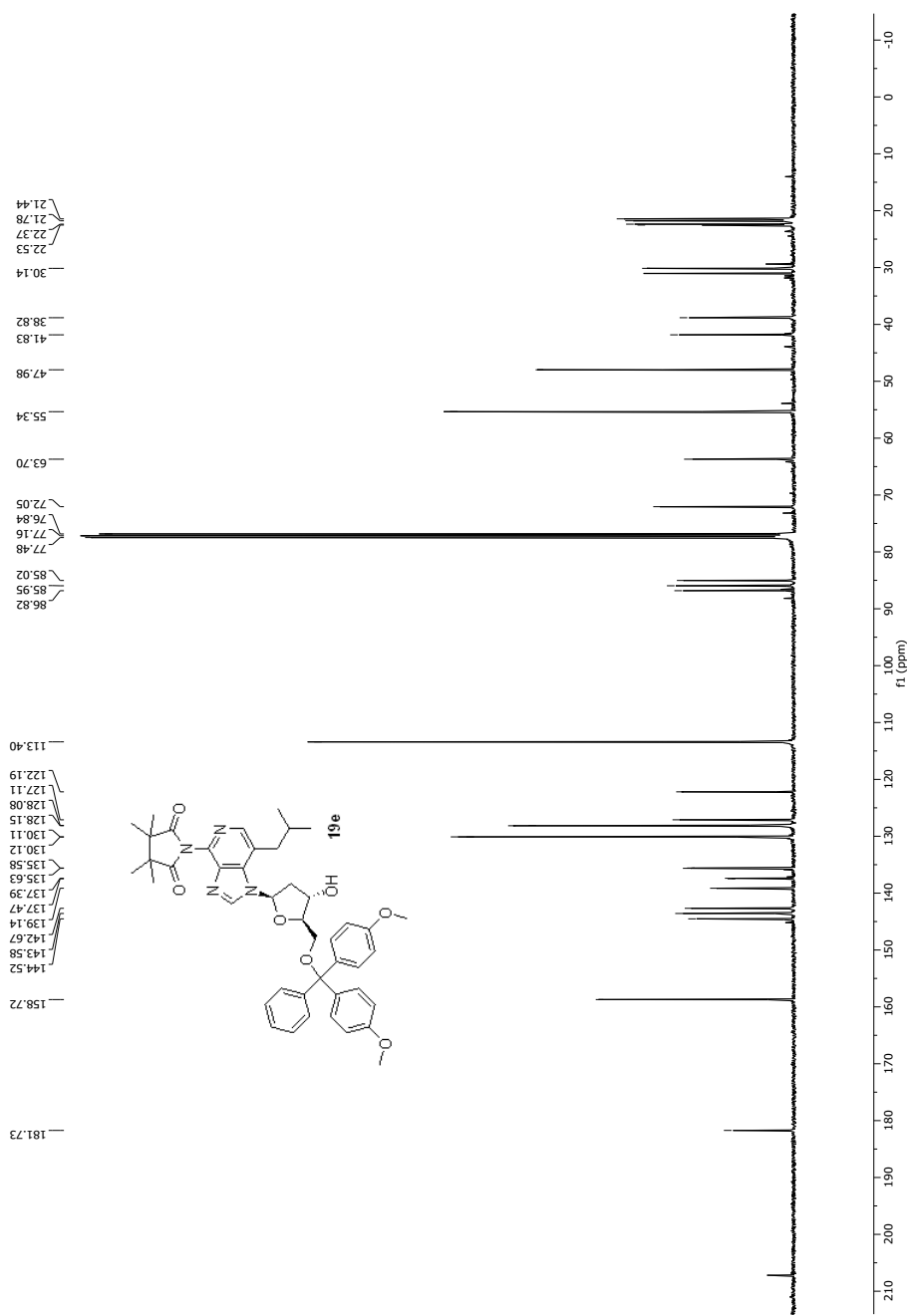
**Figure. B77** <sup>1</sup>H NMR spectrum of **18e** (CD<sub>3</sub>OD, 400 MHz).



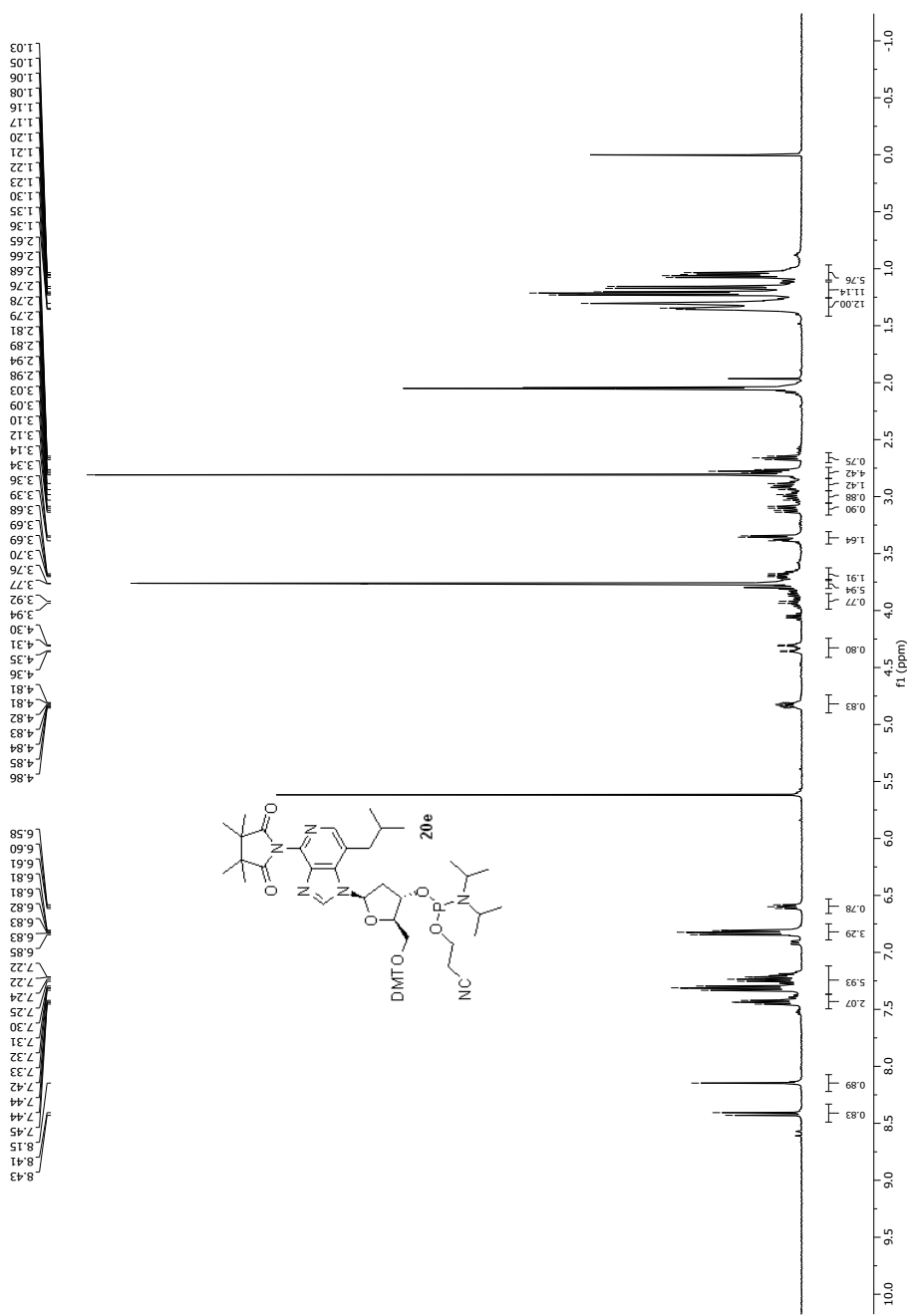
**Figure. B78** <sup>13</sup>C NMR spectrum of **18e** (CD<sub>3</sub>OD, 100 MHz).



**Figure. B79**  $^1\text{H}$  NMR spectrum of **19e** (CDCl<sub>3</sub>, 400 MHz).

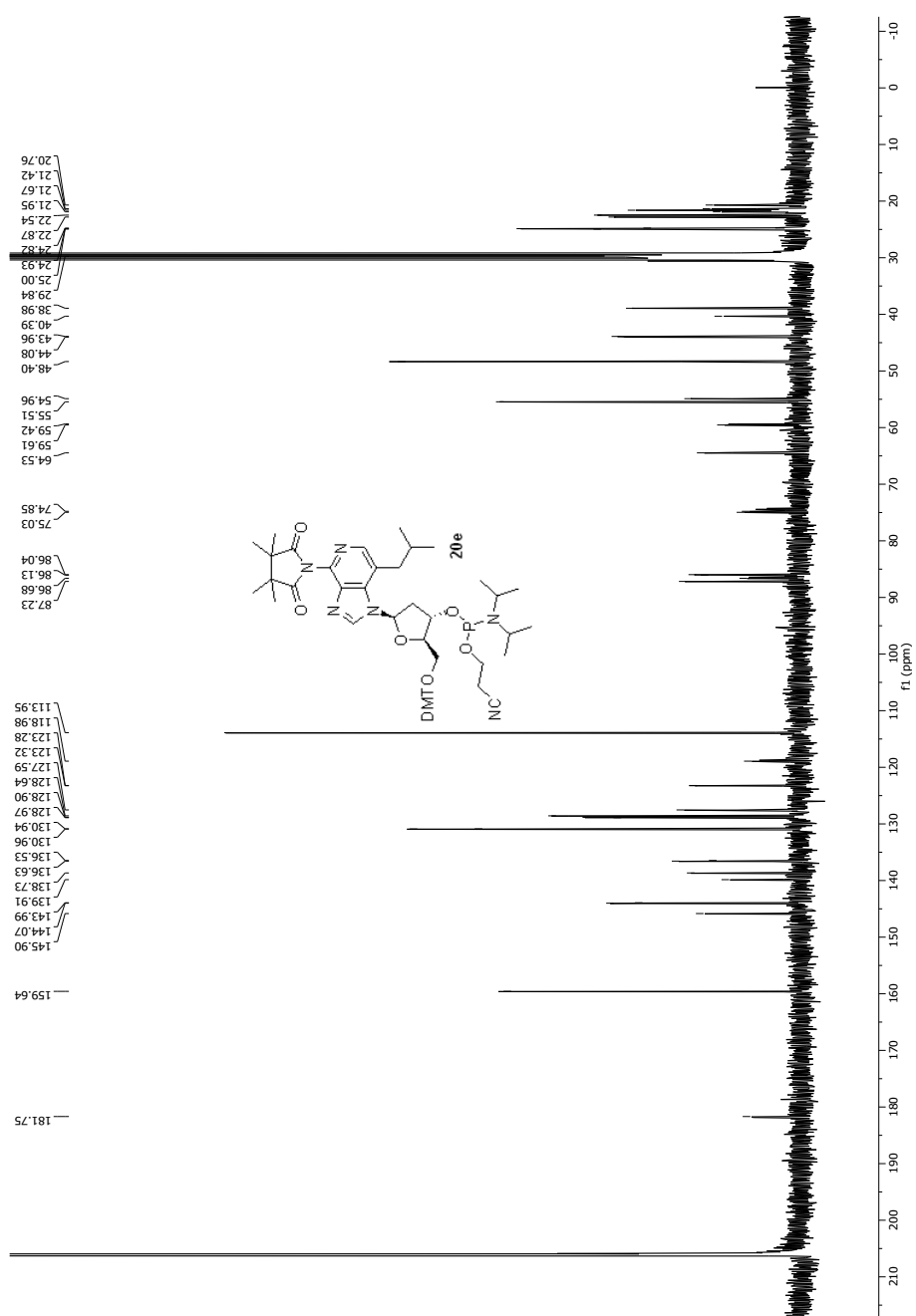


**Figure. B80**  $^{13}\text{C}$  NMR spectrum of **19e** (CDCl<sub>3</sub>, 100 MHz).

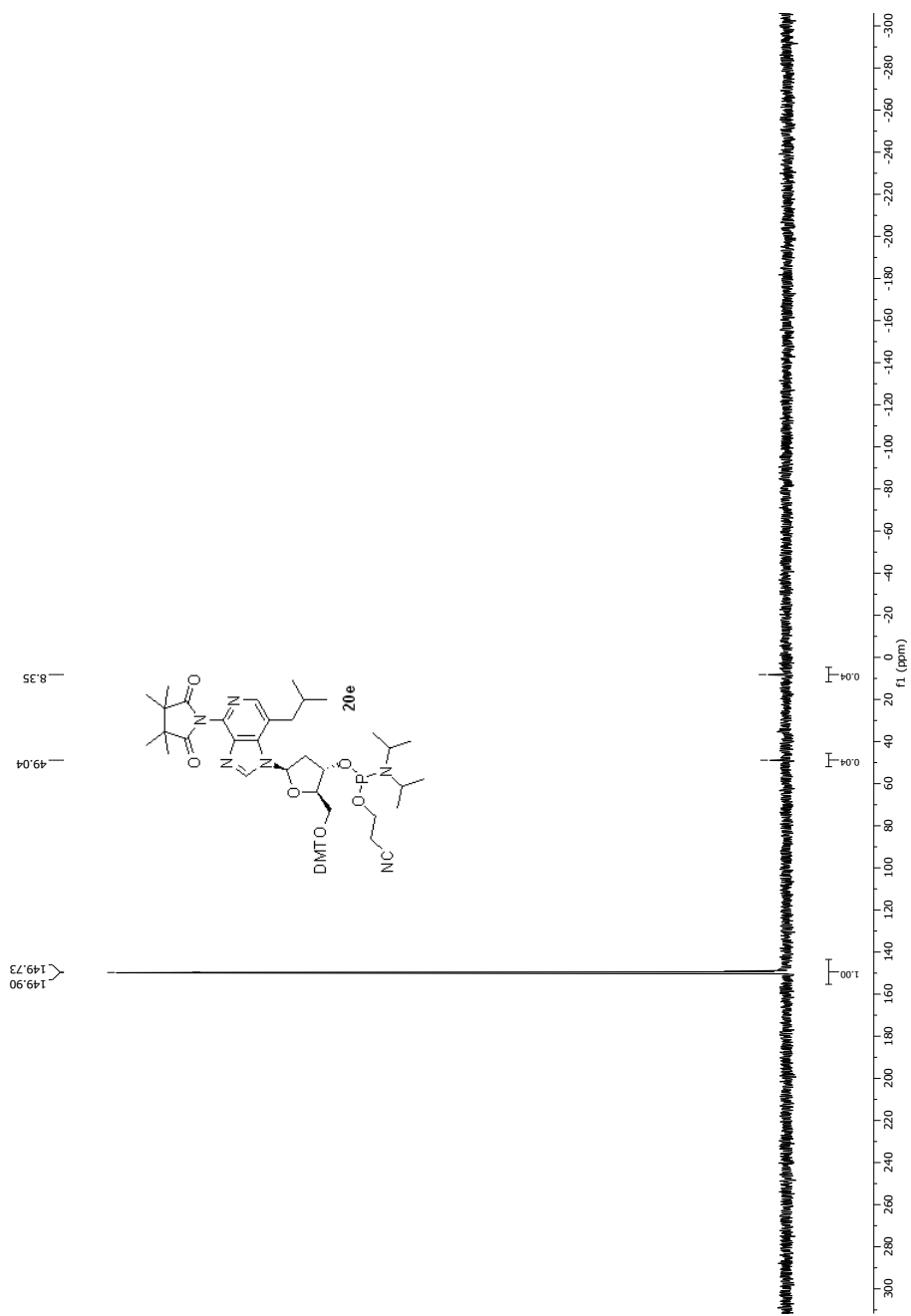


**Figure. B81**  $^1\text{H}$  NMR spectrum of **20e** (acetone- $d_6$ , 400 MHz).

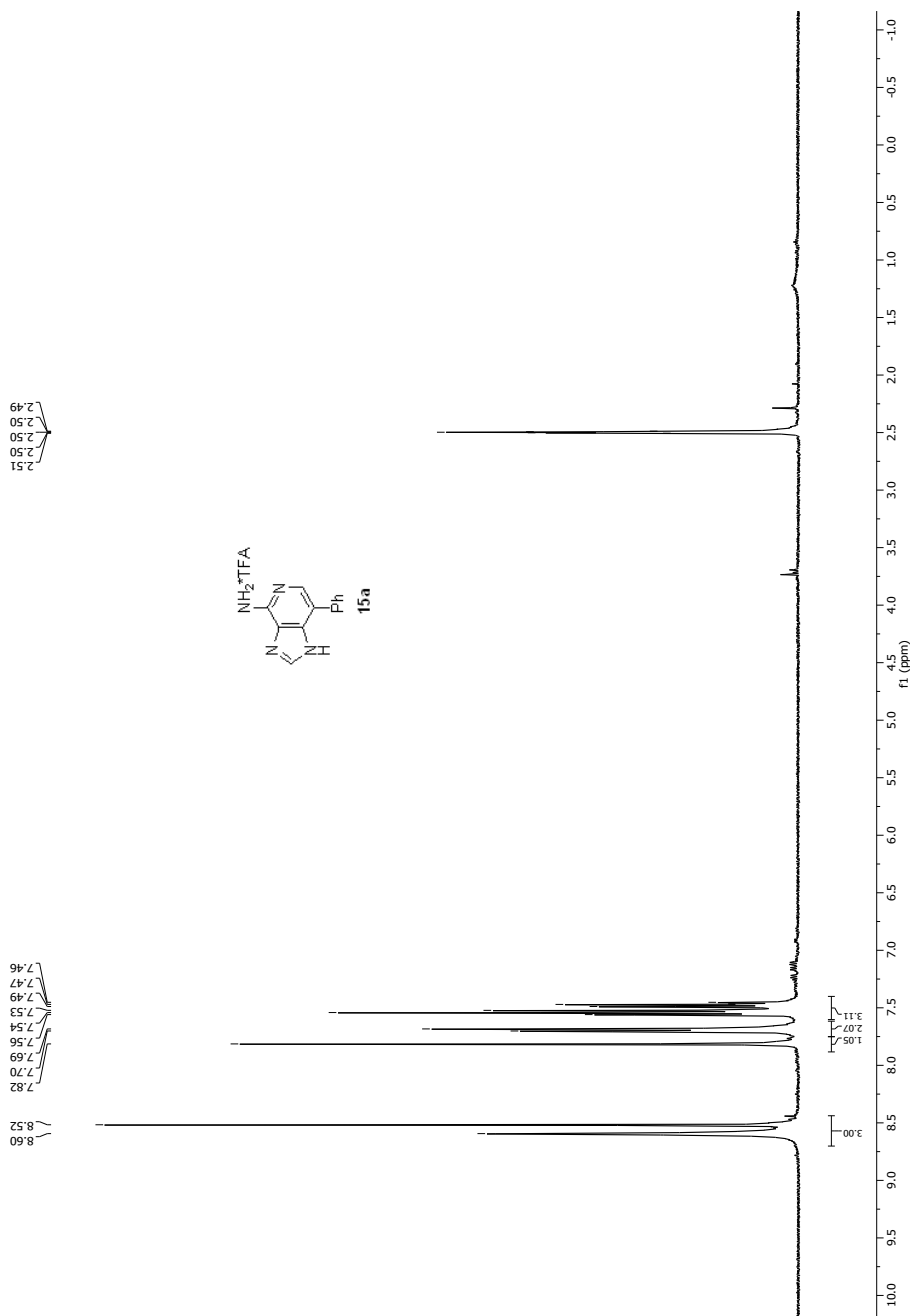




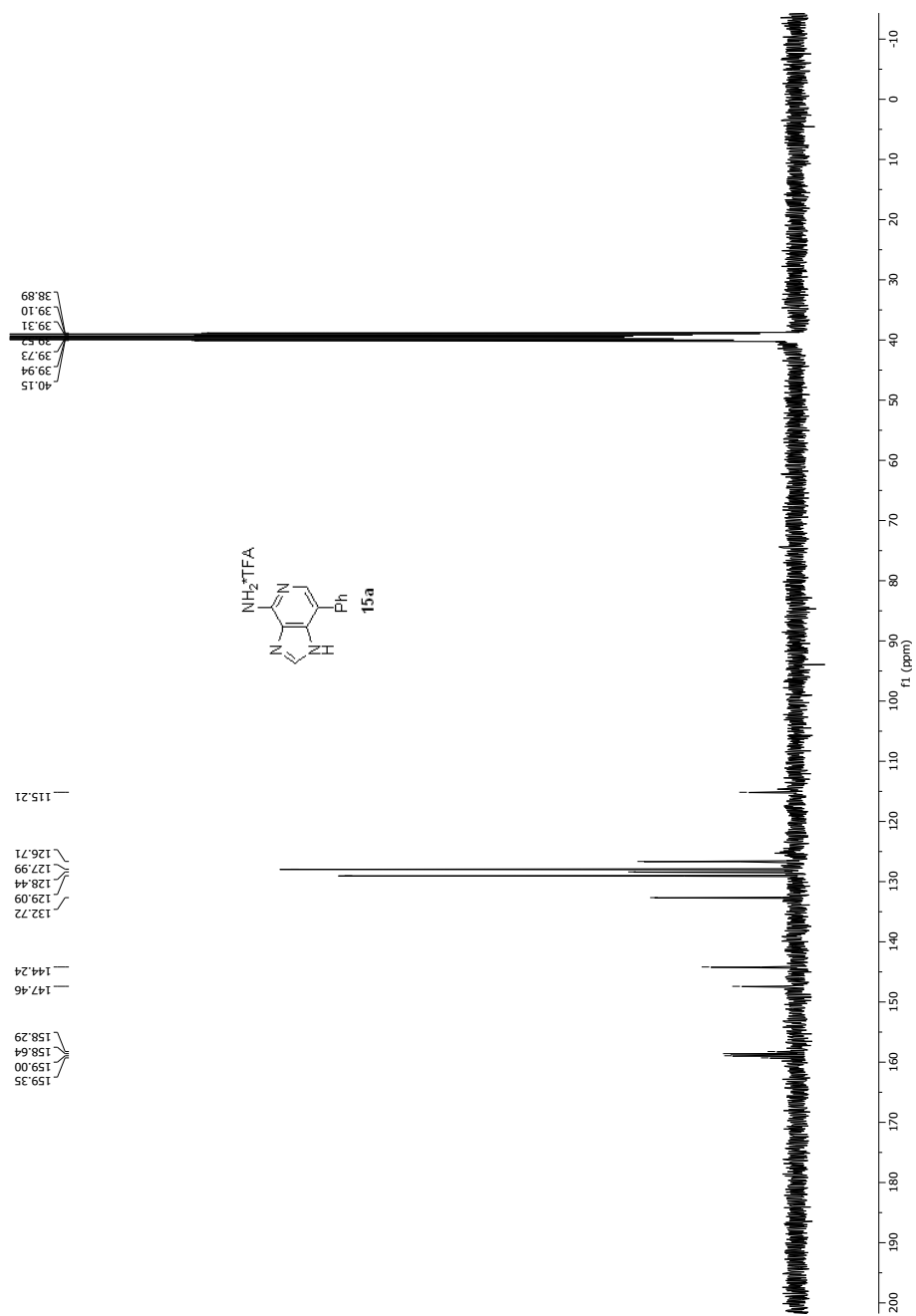
**Figure. B82**  $^{13}\text{C}$  NMR spectrum of **20e** (acetone- $d_6$ , 100 MHz).



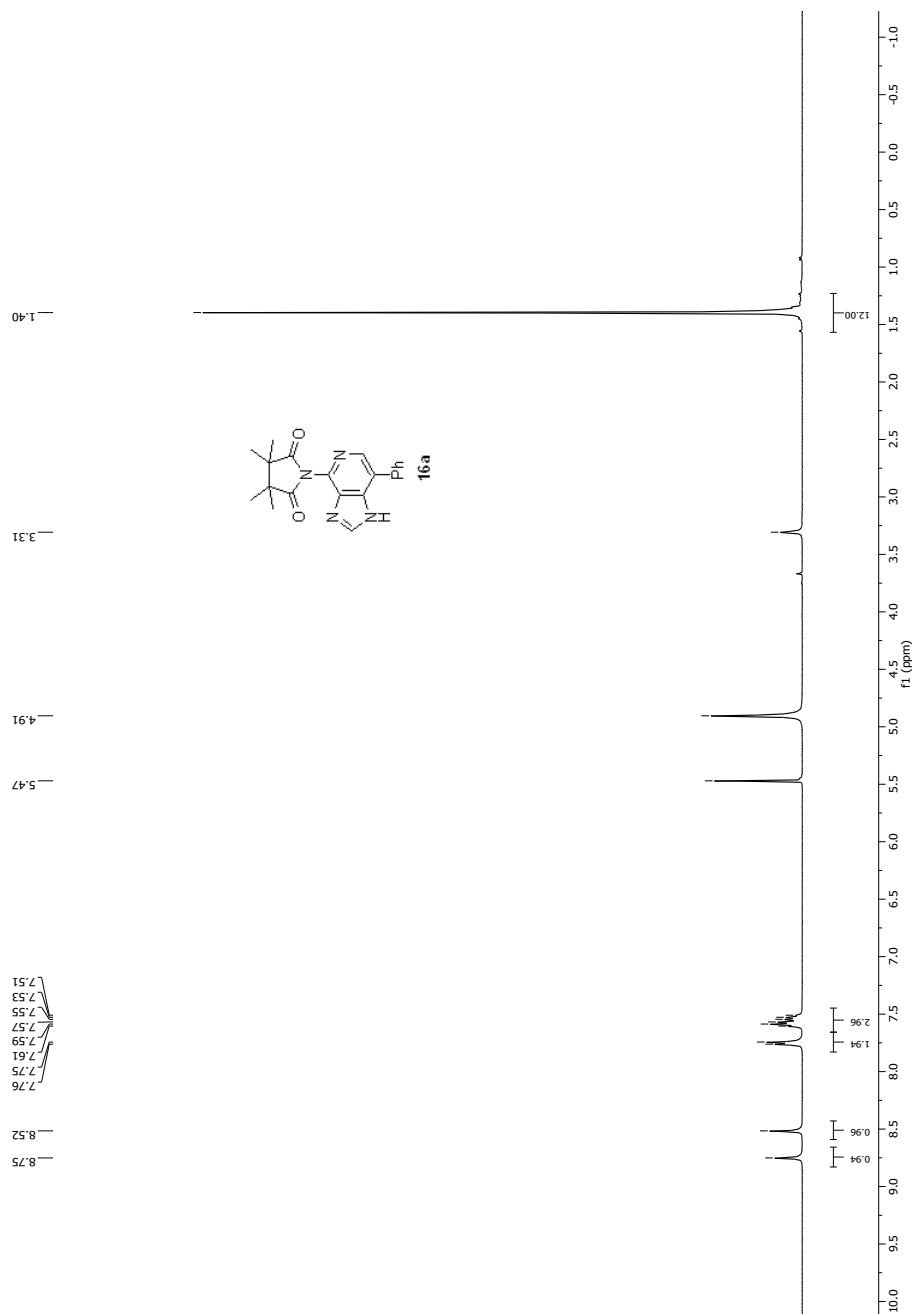
**Figure. B83**  $^{31}\text{P}$  NMR spectrum of **20e** (acetone- $\text{d}_6$ , 162 MHz).



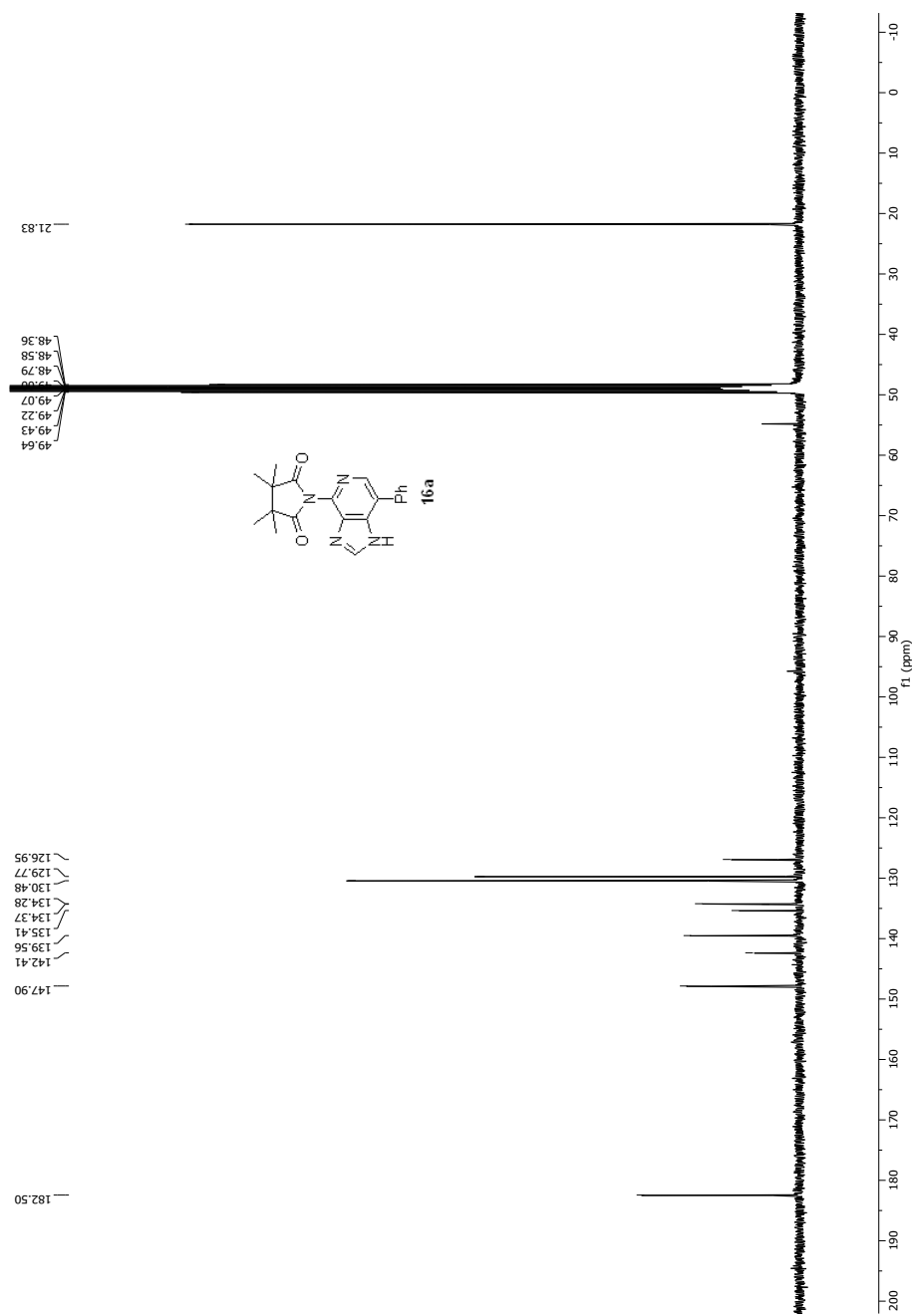
**Figure. B84** <sup>1</sup>H NMR spectrum of **15a** (DMSO-d<sub>6</sub>, 400 MHz).



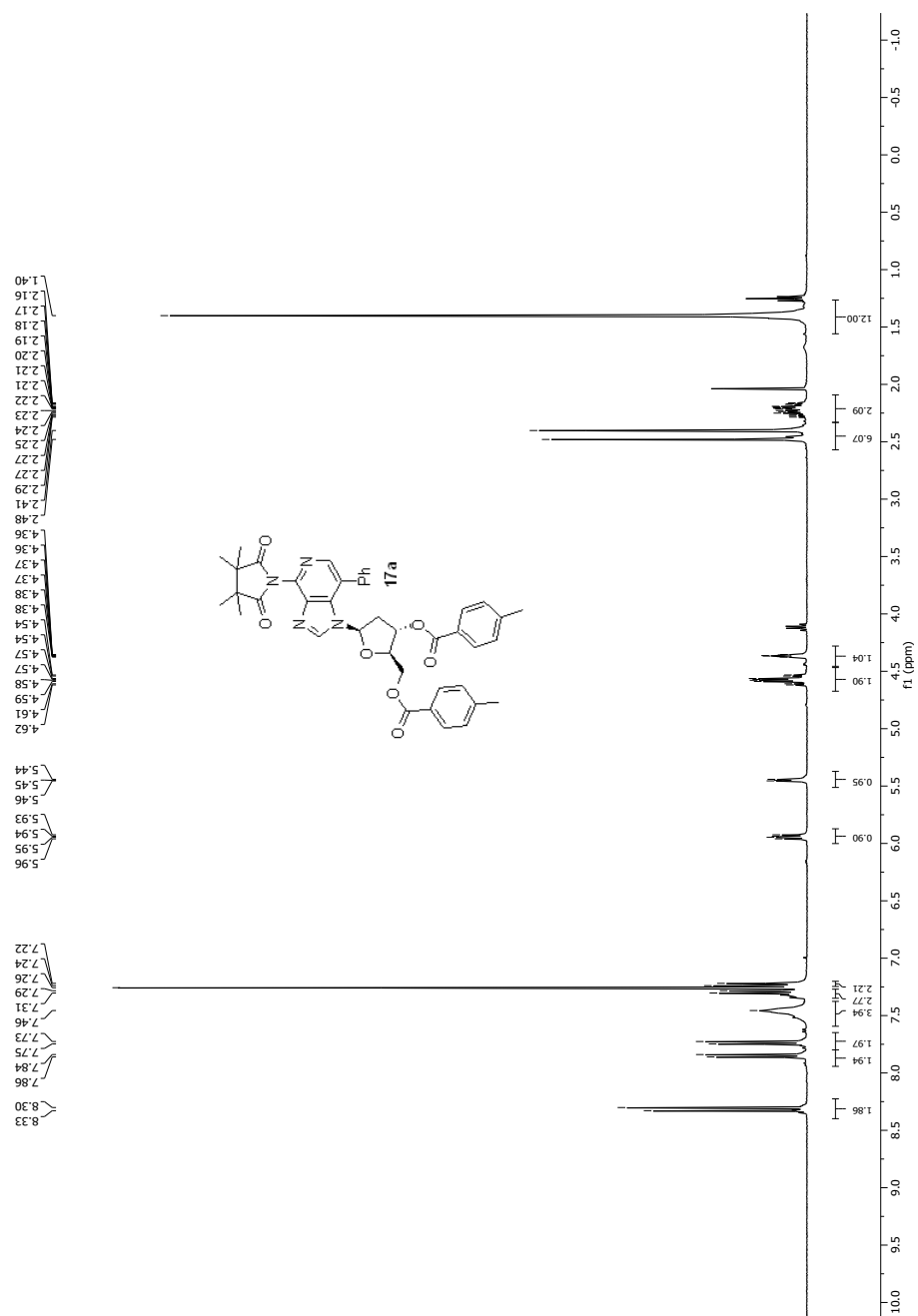
**Figure. B85**  $^{13}\text{C}$  NMR spectrum of **15a** (DMSO- $d_6$ , 100 MHz).



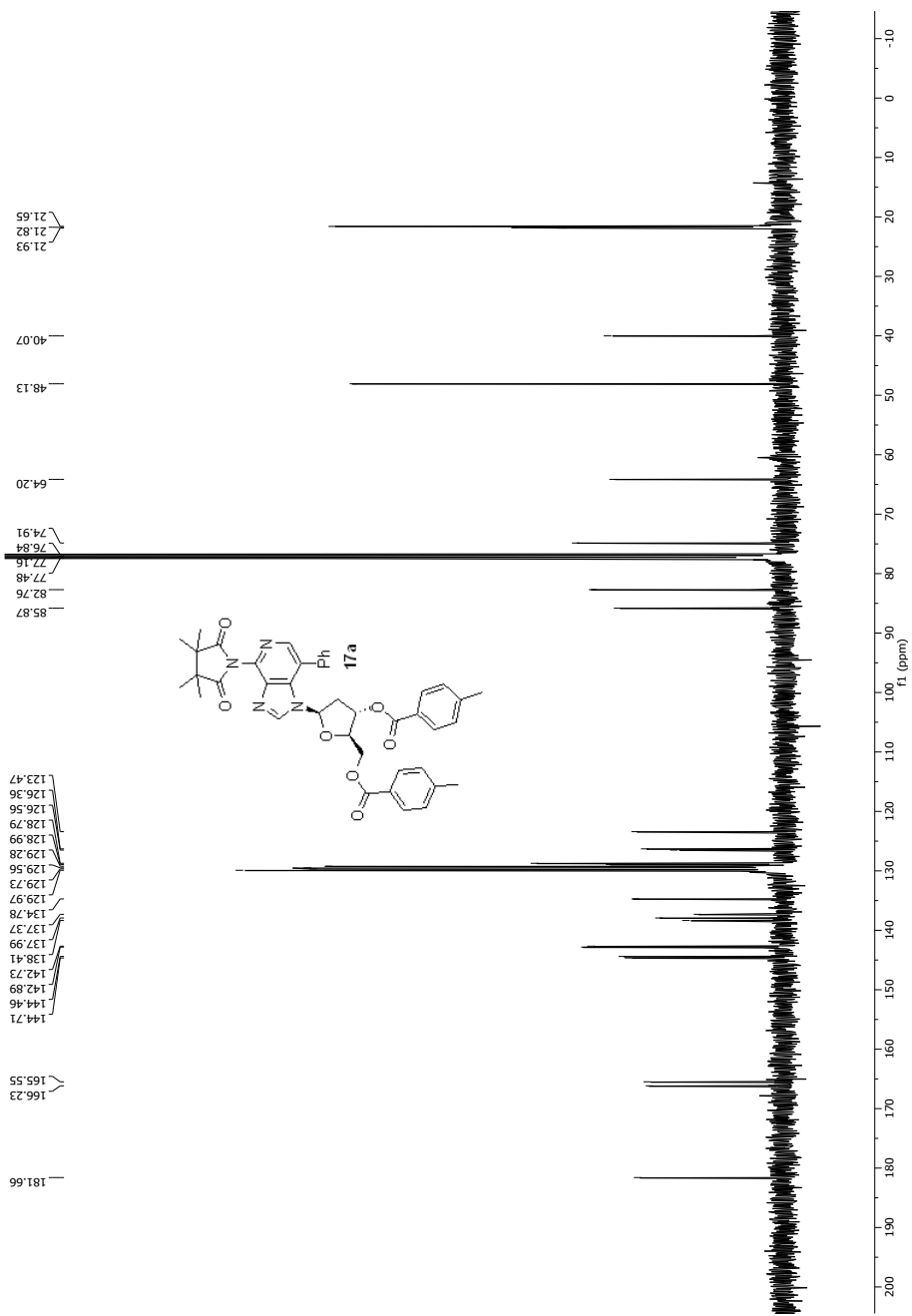
**Figure. B86** <sup>1</sup>H NMR spectrum of **16a** (CD<sub>3</sub>OD, 400 MHz).



**Figure. B87**  $^{13}\text{C}$  NMR spectrum of **16a** ( $\text{CD}_3\text{OD}$ , 100 MHz).

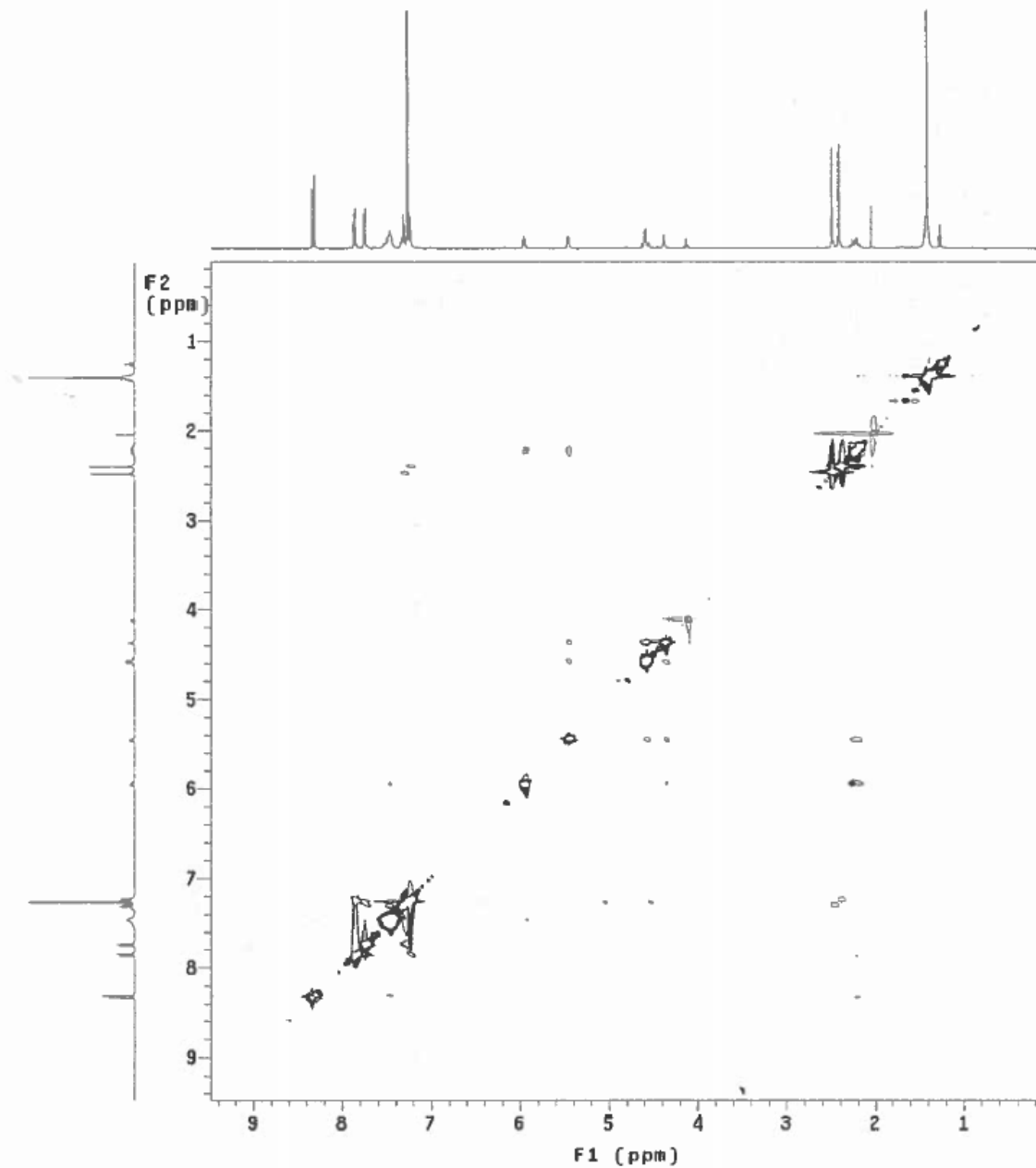


**Figure. B88**  $^1\text{H}$  NMR spectrum of **17a** (CDCl<sub>3</sub>, 400 MHz).



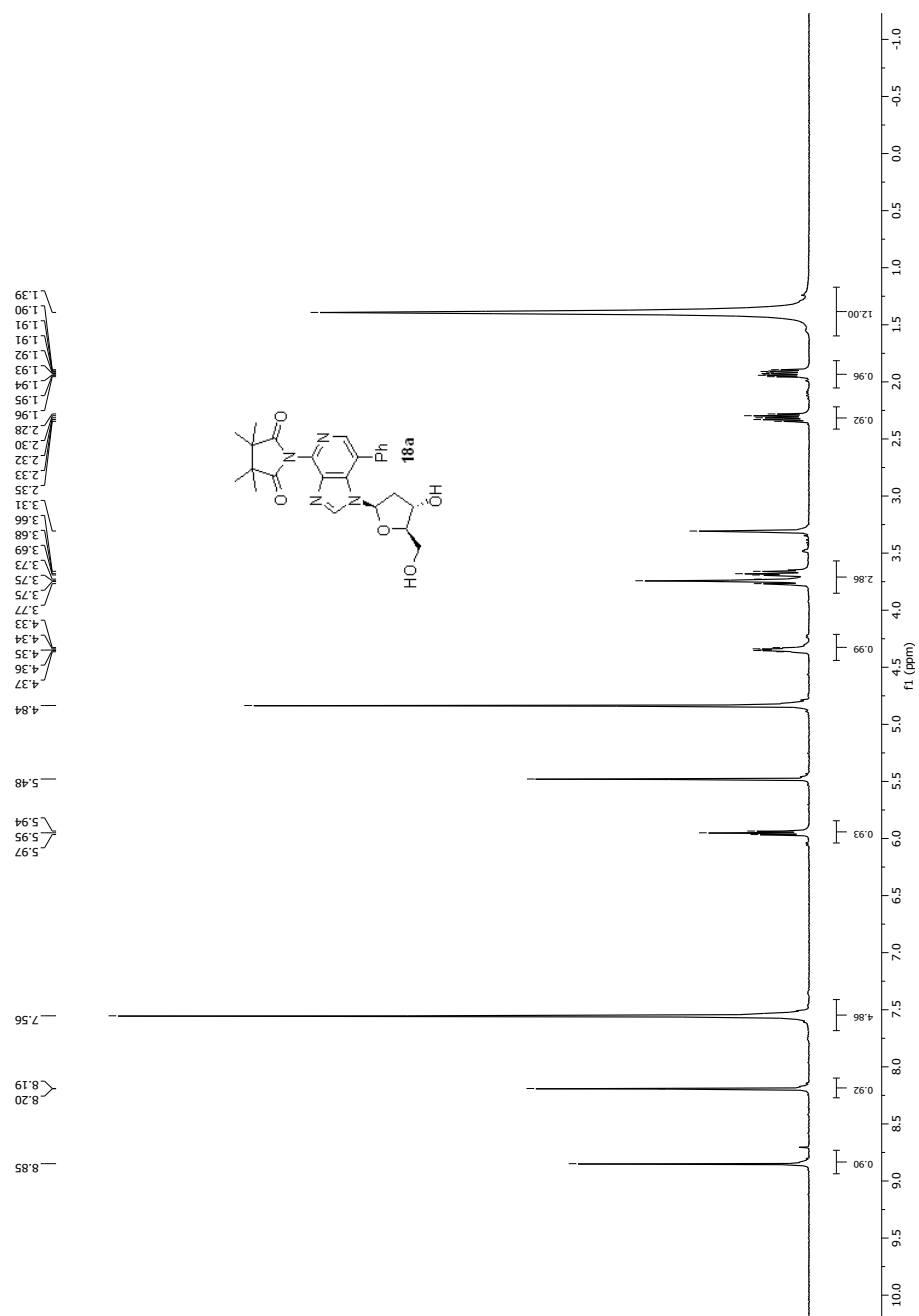
**Figure. B89**  $^{13}\text{C}$  NMR spectrum of **17a** ( $\text{CDCl}_3$ , 100 MHz).



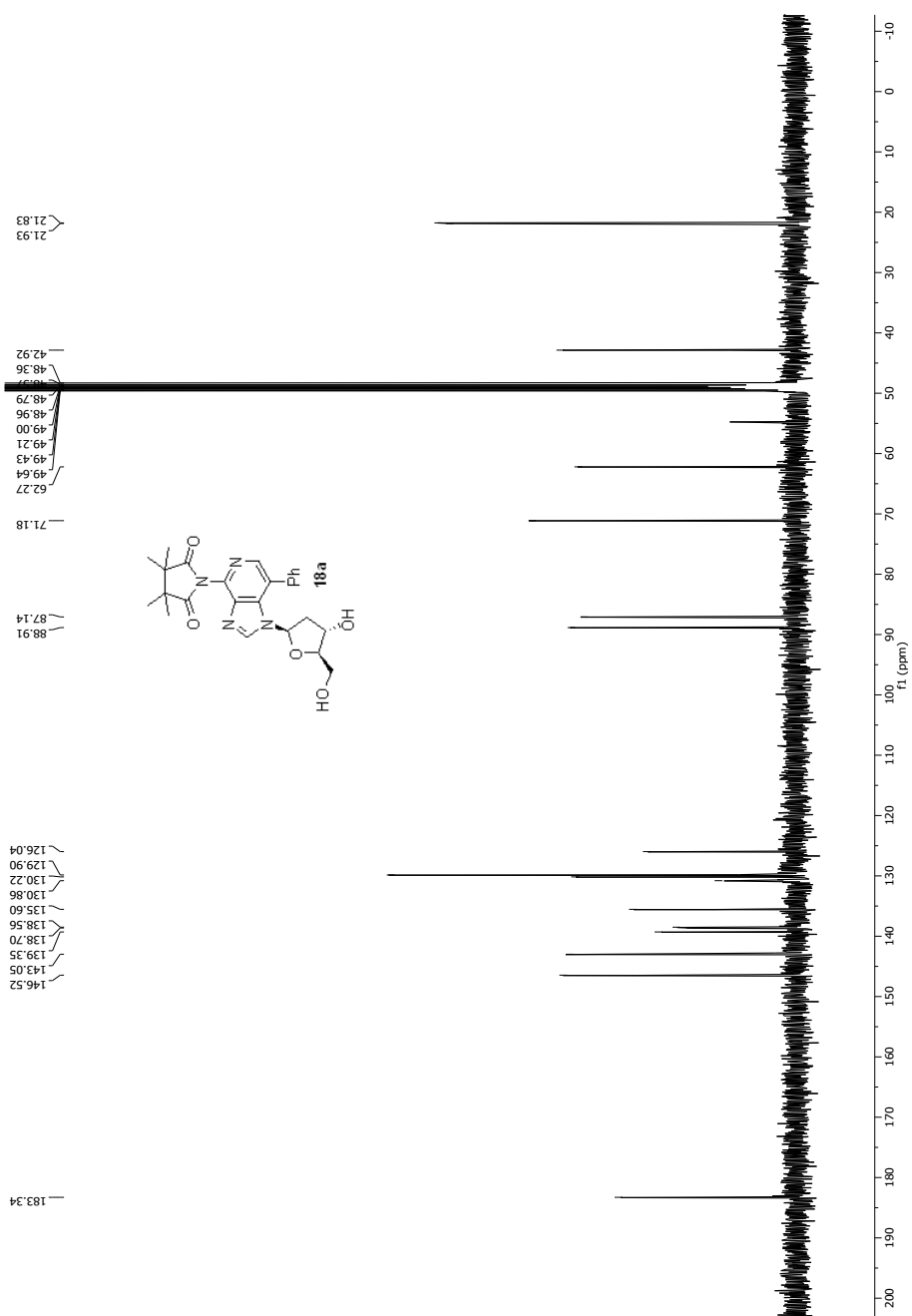


3

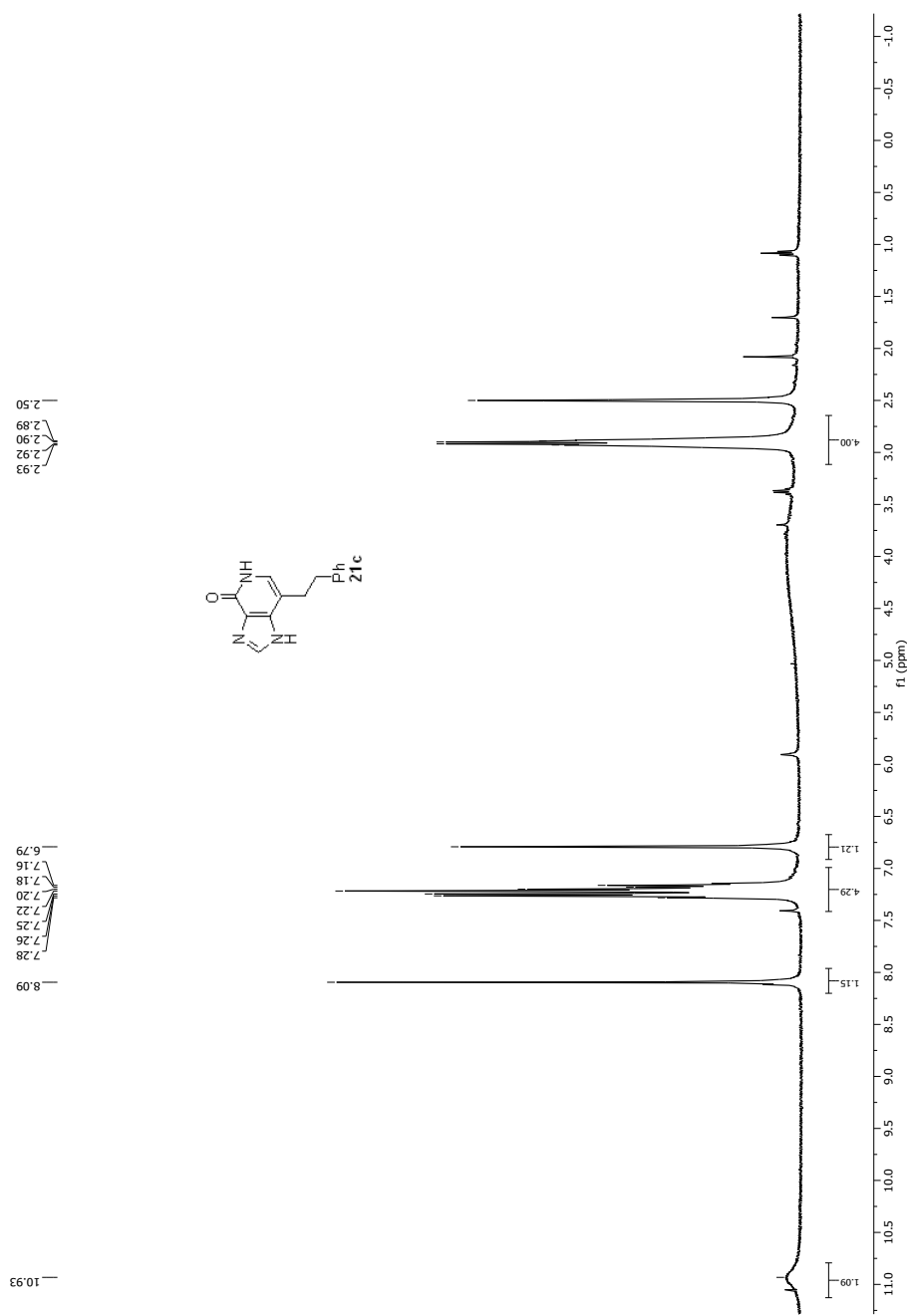
**Figure. B90**  $^1\text{H}$ - $^1\text{H}$  NOESY spectrum of **17a** ( $\text{CDCl}_3$ , 400 MHz).



**Figure. B91** <sup>1</sup>H NMR spectrum of **18a** (CD<sub>3</sub>OD, 400 MHz).



**Figure. B92**  $^{13}\text{C}$  NMR spectrum of **18a** (CD<sub>3</sub>OD, 100 MHz).



**Figure. B93**  $^1\text{H}$  NMR spectrum of **21c** (DMSO- $d_6$ , 400 MHz).

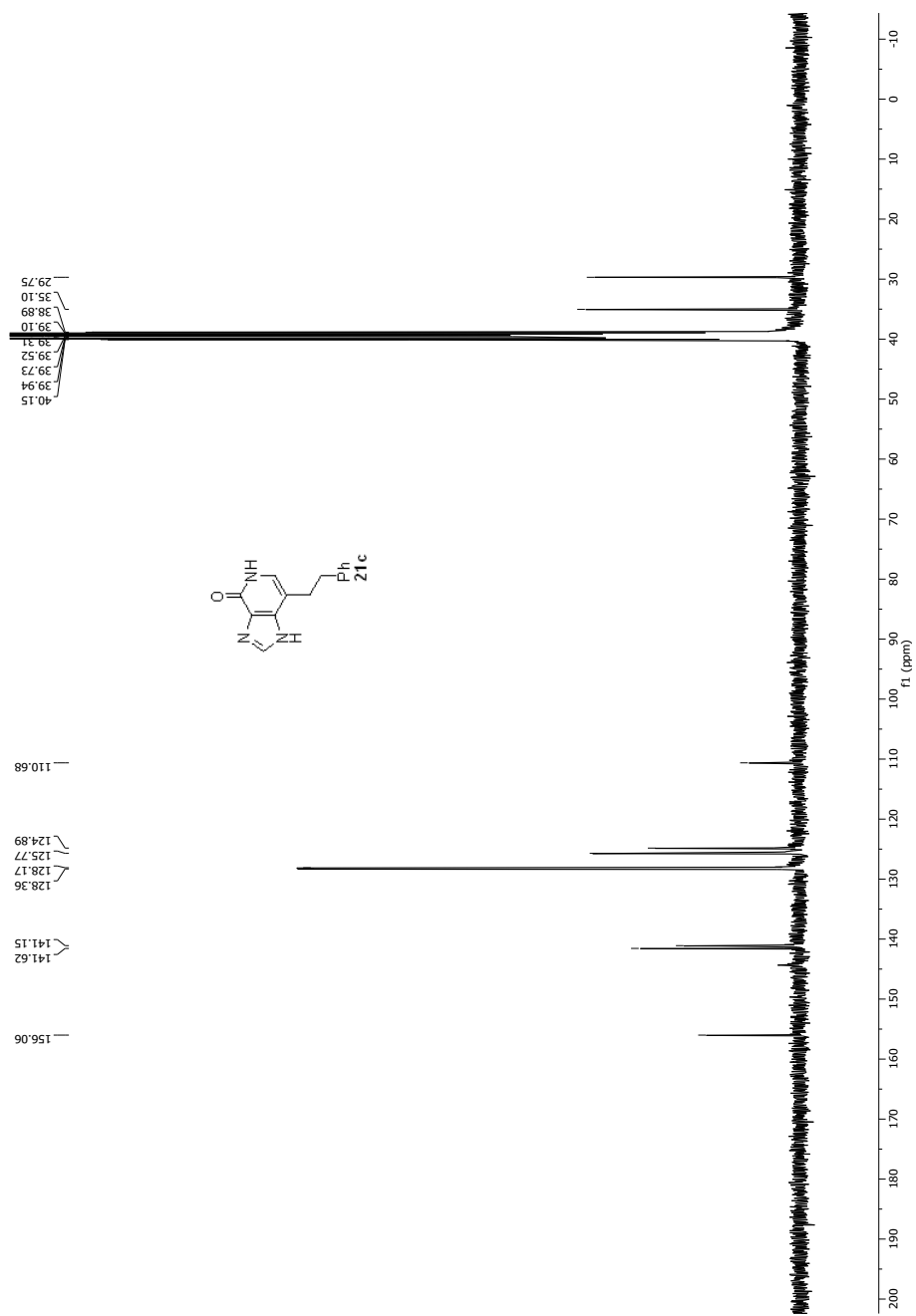
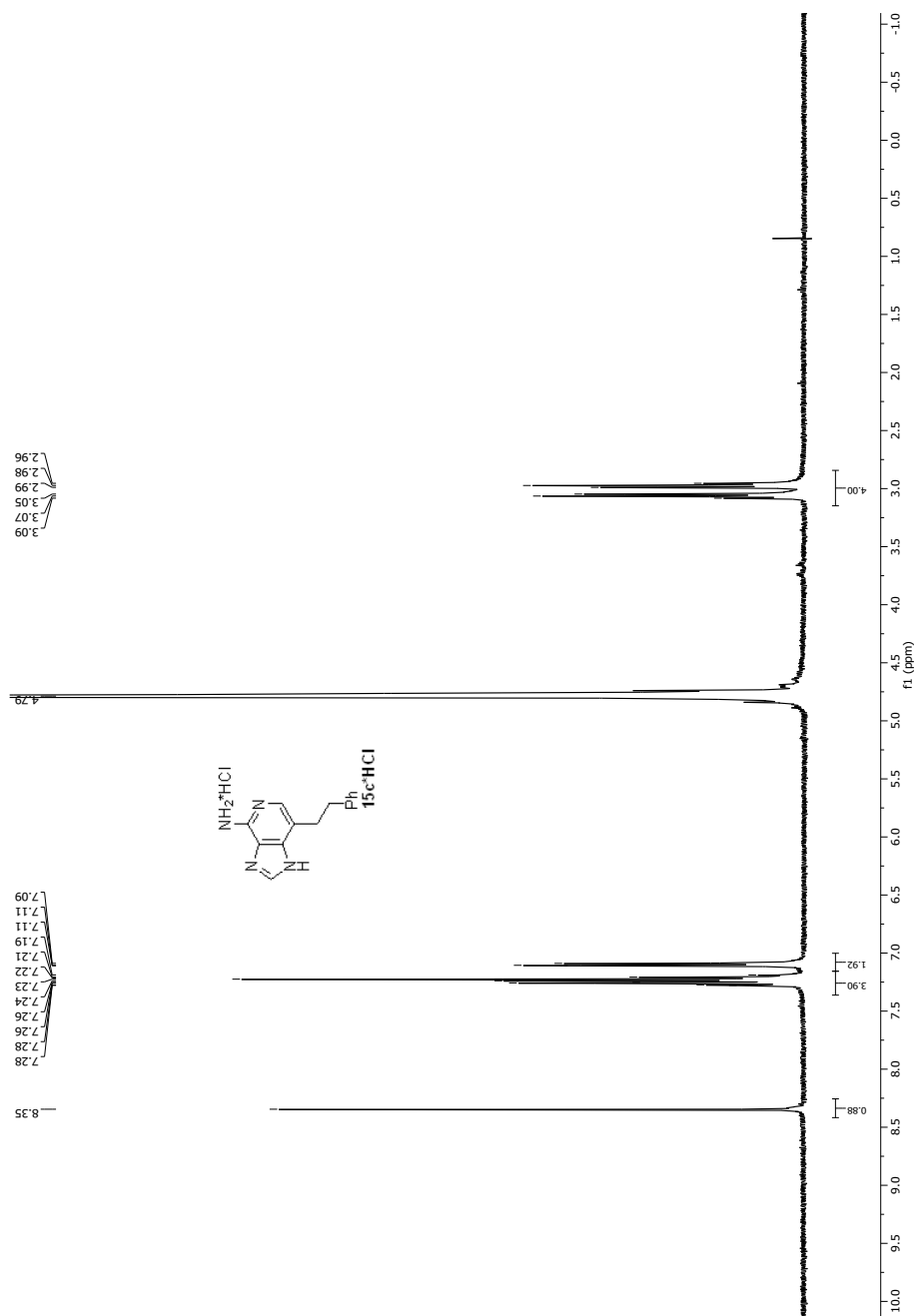
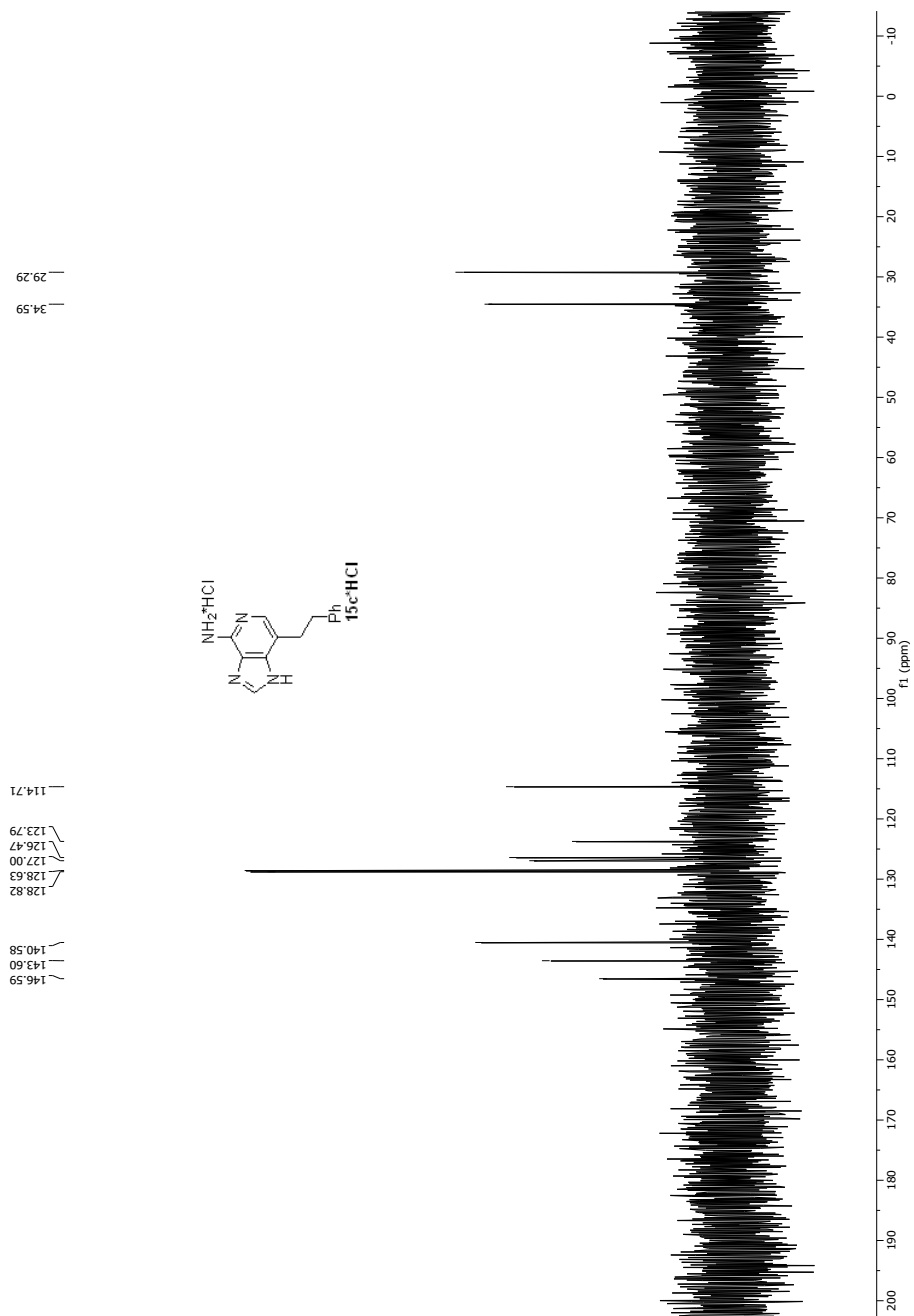


Figure. B94 <sup>13</sup>C NMR spectrum of 21c (DMSO-d<sub>6</sub>, 100 MHz).



**Figure. B95**  $^1\text{H}$  NMR spectrum of  $15\text{c}^*\text{HCl}$  ( $\text{D}_2\text{O}$ , 400 MHz).



**Figure. B96**  $^{13}\text{C}$  NMR spectrum of **15c\*HCl** ( $\text{D}_2\text{O}$ , 100 MHz).